

**DEVELOPMENT OF INTEGRATED
ENVIRONMENTAL CONTROL
SYSTEM DESIGNS FOR AIRCRAFT**

VOLUME I-ECU DESIGN

R.R. Dickmann

M. Conon

S.P. Glover

Distribution limited to U.S. Government agencies only, test and evaluation statement applied April 1972. Other requests for this document must be referred to Air Force Flight Dynamics Laboratory (FEE), Wright-Patterson Air Force Base, Ohio 45433.

FOREWORD

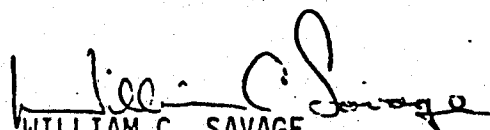
This report presents results developed by the McDonnell Douglas Corporation under Air Force Contract F33615-70-C-1235 "Development of Integrated Environmental Control System Designs for Aircraft". This development program was conducted under the sponsorship of the Air Force Flight Dynamics Laboratory, Project 6146, with Mr. Eugene A. Zara, FEE, as Project Engineer. This report is in four volumes:

- I. ECS Design
- II. ECS Computer Program
- III. IECS Computer Program Users Manual
- IV. Laboratory Demonstration Test

The results presented in this volume on ECS Design were developed by the McDonnell Aircraft Company (MCAIR) and the Douglas Aircraft Company (DAC) of the McDonnell Douglas Corporation. The Program Manager was R. R. Dieckmann (MCAIR); A. C. Watson (DAC) was Associate Program Managers; and S. F. Glover (MCAIR) was ECS Design Group Leader. Other MCAIR contributors were R. L. Crossen, R. N. Johnson, K. C. Li, J. W. Smith, and T. L. Thiele; and other DAC contributors were J. I. Allyn, S. W. Kahn, R. M. Laughlin, and H. J. Meyer, Jr.

Contributions of data from the following manufacturers of ECS systems and components are acknowledged: Abex Corporation; AiResearch Manufacturing Company; Arrowhead Products Division; Barber-Colman Company; Dynamic Air Engineering Inc.; Farr Company; Fairchild Hiller, Stratos-Division; Hamilton Standard; Hydro-Aire Division, Crane Company, Pall Corporation; H. H. Parker Company; Task Corporation, Division of Joy Manufacturing; Vickers Aerospace Division; Vap-Air Division, Vapor Corporation.

This technical report has been reviewed and is approved.



WILLIAM C. SAVAGE
Chief, Environmental Control Branch
Vehicle Equipment Division

ABSTRACT

This report presents the results of a study of environmental control system (ECS) designs for aircraft. The study was performed for the Air Force Flight Dynamics Laboratory. ECS design information is presented for arrangements of components which make up the systems, for performance of the components of the systems, and for penalty factors incurred by an aircraft using these systems. Ten system arrangements for simple and bootstrap air cycles, and vapor cycles are presented. Subsystems which are common to many of these systems are discussed. Typical performances of the many components utilized by these systems are presented. Penalty factors of weight, volume, and relative reliability and cost of these components are related to the design features of these system components.

The ECS design information presented in this volume is included in the digital computer program described in Volume II of this report. The ECS Computer Program will provide system performance, sizing, and penalty factor information. Volume II includes sample problems for the rough performance and sizing analyses of three Air Force aircraft, and the detailed performance and sizing of one Air Force aircraft. Volume III is the IECS Computer Program Users Manual. It contains a complete description of sample problems for rough performance and sizing analyses, and detailed performance analysis. Volume IV presents the laboratory demonstration ECS setup and results, and the computer program setup and results of detailed performance and sizing analyses to represent this ECS.

12

TABLE OF CONTENTS

<u>Section</u>	<u>Page</u>
1. INTRODUCTION	1
1.1 Objectives	1
1.2 Summary	2
1.2.1 ECS Design	2
1.2.2 Computer Program Development	2
1.2.3 Laboratory Demonstration	3
2. SYSTEM DESIGNS	4
2.1 Design Requirements	4
2.1.1 ECS Design Objectives	4
2.1.2 ECS Functions	4
2.1.3 Input Power	5
2.1.4 Heat Sinks	5
2.1.5 Controls	5
2.1.6 System Integration	5
2.1.7 Aircraft Mission Parameters	5
2.2 Environmental Control Systems	7
2.2.1 System and Subsystem Concept	7
2.2.2 Subsystem Schematics	9
2.2.3 System Schematics	25
2.2.4 System Schematic Representation of Inventory Aircraft ECS	44
2.3 Reference Simple Air Cycle System	52
2.3.1 System Operation	52
2.3.2 Components	55
3. COMPONENT DESIGNS	57
3.1 Heat Exchangers	58
3.1.1 General Heat Exchanger Design	58
3.1.2 Single Phase Heat Exchangers	82
3.1.3 Water Boilers	84
3.1.4 Resistance Heaters	86
3.2 Air Cycle Machines	90
3.2.1 General Turbomachine Design	92
3.2.2 Turbines	109
3.2.3 Compressors	114
3.2.4 Fans	118

TABLE OF CONTENTS (CONTINUED)

<u>Section</u>		<u>Page</u>
3.3	Water Separators	119
3.3.1	Efficiency	120
3.3.2	Pressure Drop	124
3.3.3	Weight	127
3.3.4	Volume	127
3.4	Dust Separators	129
3.4.1	Static Separators	129
3.4.2	Self-Cleaning Dust Separators	130
3.5	Fans	135
3.5.1	Fan Performance	135
3.5.2	Fan Sizing	139
3.6	Pump Packages	146
3.6.1	Performance	146
3.6.2	Weight	148
3.6.3	Volume of Pump Packages	153
3.6.4	Example of Pump Package Design	153
3.7	Vapor Cycle Components	154
3.7.1	General Vapor Cycle Component Design	154
3.7.2	Compressors	155
3.7.3	Evaporators and Condensers	157
3.7.4	Refrigerant Charge and Receiver	159
3.7.5	Refrigerants	160
3.7.6	Off-Design Performance	160
3.8	Auxiliary Air Sources	162
3.8.1	Auxiliary Power Units	162
3.8.2	Auxiliary Compressors	169
3.9	Power Drives	171
3.9.1	Electric Motors	171
3.9.2	Hydraulic Motors	175
3.9.3	Pneumatic Drives	176
3.9.4	Shaft	176
3.9.5	Examples of Motor Design	178
3.10	Plumbing	179
3.10.1	Air Ducting	179

TABLE OF CONTENTS (CONTINUED)

<u>Section</u>	<u>Page</u>
3.10.2 Liquid, Refrigerant, and Pneumatic Control Lines	195
3.10.3 Inlets and Outlets	199
3.10.4 Ejectors	211
3.10.5 Valves	219
3.11 Insulation	229
3.11.1 Ducting Insulations	229
3.11.2 Compartment Insulations	241
3.11.3 Fuel Tank Insulations	246
3.11.4 Example Insulation Design	247
3.12 System Controls	249
3.12.1 Temperature Control Systems	249
3.12.2 Pressure Control Systems	265
3.12.3 Water Separator Anti-Ice Control	269
3.12.4 Vapor Cycle Control	270
4. PENALTY FACTORS	271
4.1 Weights	271
4.1.1 Air System Components	273
4.1.2 Liquid Subsystem Components	279
4.1.3 Vapor Cycle Components	281
4.1.4 Auxiliary Air Sources and Power Drives	282
4.1.5 Controls	283
4.2 Reliability	284
4.2.1 Air Systems	284
4.2.2 Liquid Subsystems	285
4.2.3 Vapor Cycle Systems	285
4.2.4 Controls	286
4.2.5 Reliability Index	287
4.3 Cost Factors	290
4.3.1 Development Risk Factors	290
4.3.2 Recurring Cost Factors	296
4.3.3 Logistic Cost Factors	314
5. REFERENCES	316

LIST OF ILLUSTRATIONS

Figure No.

<u>Figure No.</u>	<u>Page</u>
1. Aircraft Mission Parameters	6
2. Open or Closed Loop Simple Air Cycle	8
3. Subsystem 2.1 - Ram Air Heat Sinks	13
4. Subsystem 2.2 - Expendable Water Heat Sinks	14
5. Subsystem 2.3 - Fuel Heat Sinks	15
6. Subsystem 3 - Temperature Regulation of Cooling Air	17
7. Subsystem 4 - Liquid Loop Configurations	20
8. Subsystem 5 - Auxiliary Air Supplies	21
9. Subsystem 6 - Water Separator Configurations	23
10. Subsystem 7 - Condensate Management	24
11. Subsystem 8 - Dust Separators	25
12. Simple Air Cycle	26
13. System S1 - Simple Air Cycle, Open or Closed Loop	27
System S2 - Simple Air Cycle, Open or Closed Loop, with Secondary Heat Transport Loop	29
15. Bootstrap Air Cycle	30
16. System B1 - Bootstrap Air Cycle, Open or Closed Loop	32
17. System B2 - Bootstrap Air Cycle, Open Loop, Regenerative	33
18. System B3 - Bootstrap Air Cycle, Open Loop with High Pressure Water Separator	35
19. System B4 - Simple-Bootstrap Air Cycle, Open Loop	36
20. System B5 - Bootstrap Air Cycle, Open or Closed Loop with Secondary Heat Transport Loop	38
21. Vapor Cycle	39
22. System V1 - Vapor Cycle, Secondary Closed Air Loop	40
23. System V2 - Vapor Cycle, Secondary Open Air Loop with High Pressure Water Separator	42
24. System V3 - Hybrid Vapor Cycle - Air Cycle	43
25. Adapted System S1 - Simple Air Cycle Representing the F-4C Equipment ECS	48
26. Adapted System B1 - Bootstrap Air Cycle Representing the C-9A ECS	50
27. Adapted System V1 - Vapor Cycle Representing the DC-8 ECS	51
28. Reference Simple Air Cycle System	53

<u>Figure No.</u>	<u>Page</u>
29. Typical Cross Flow Heat Exchanger	59
30. General Flow Through a Duct	59
31. Multipass Heat Exchanger	61
32. Typical Performance Data	66
33. Design Pressure Drops for Air Heat Exchangers	68
34. Offset Rectangular Fin Surface $20.06R(D) - 0.100/0.098 - 1/8 (0) - 0.004$	69
35. Offset Rectangular Fin Surface $16.00R(D) - 0.126/0.125 - 1/8 (0) - 0.006$	70
36. Offset Rectangular Fin Surface $24.12R(S) - 0.075/0.075 - 1/9 (0) - 0.004$	71
37. Offset Rectangular Fin Surface $19.35R(S) - 0.0755/0.075 - 1/10 (0) - 0.004$	72
38. Offset Rectangular Fin Surface $12.18R(D) - 0.178/0.174 - 0.178 (0) - 0.004$	73
39. Offset Rectangular Fin Surface $15.76R(D) - 0.153/0.149 - 1/7 (0) - 0.004$	74
40. Offset Rectangular Fin Surface $25.01R(S) - 0.201/0.200 - 1/9 (0) - 0.004$	75
41. Offset Rectangular Fin Surface $15.61R(S) - 0.251/0.250 - 1/8 (0) - 0.004$	76
42. Fin Geometry Selection	77
43. Heat Exchanger Core Volume Comparison	79
44. Triangular Fin Geometry	79
45. Rectangular Fin Geometry	80
46. Rounded Fin Geometry	81
47. Separator Plate Thickness	82
48. Heat Exchanger Weight Comparison	83
49. Typical Boiler Performance	85
50. Typical Resistance Heater	87
51. Plain Triangular Fin Surface $16.96T(D) - 0.126/0.125 - (P) - 0.006$	88
52. Electric Heater Density	89
53. Types of Turbomachinery	91
54. Velocity Triangles for a Generalized Rotor	92
55. Reaction for Generalized Turbomachine	94
56. N _s - D _s Diagram for Centrifugal Compressors	100

	<u>Page</u>	
7.	Ns - η_{ad} Diagram for Centrifugal Compressors	100
58.	Ns - Ds Diagram for Low Pressure Ratio Compressors	101
59.	Ns - Ds Diagram for Centrifugal Turbines	102
60.	Maximum Adiabatic Efficiency for Centrifugal Turbines	103
61.	Ns - Ds Diagram for Axial Turbines	104
62.	Turbomachine Off-Design Performance Comparison	106
63.	Turbomachine Volume	108
64.	Turbomachine Weight	108
65.	Typical Maximum Turbine Adiabatic Efficiencies	111
66.	Typical Turbine Performance Maps	112
67.	ζ - Values as Function of Turbine Pressure Ratio	114
68.	Typical Maximum Compressor Adiabatic Efficiency	116
69.	Typical Compressor Performance	116
70.	Water Separator Efficiencies at High Inlet Entrained Water Content	121
71.	Water Separator Efficiencies at Low Inlet Entrained Water Content	123
72.	Water Separator Wet Pressure Drops	125
73.	Water Separator Dry Pressure Drops	126
74.	Water Separator Weights	127
75.	Water Separator Volumes	128
76.	Weight of Static Dust Separators	131
77.	Volume of Static Dust Separators	132
78.	Weight of High Pressure Dust Separators	133
79.	Axial Fan Static Efficiency	136
80.	General Axial Fan Performance	138
81.	Axial Fan Size Correlation	139
82.	Axial Fan Weights	141
83.	Axial Fan Weights (Hydraulic Motor)	142
84.	Axial Fan Weight (No Motor)	144
85.	Axial Fan Volumes	145
86.	Coolant Pump Efficiency	147
87.	General Coolant Pump Performance	149
88.	General Centrifugal Pump Performance	149
89.	Weight of Coolant Pumps	150

<u>Figure No.</u>		<u>Page</u>
90.	Coolant System Reservoir Weight	151
91.	Weights of Filters for Liquid Coolant Subsystems	152
92.	Vapor Cycle Flow Schematic	155
93.	Typical Performance of Refrigerant Compressor	161
94.	Typical Performance of Evaporator and Condenser	161
95.	APU Fuel Flow Rate Correlation	165
96.	APU Installed Weight Correlation	168
97.	APU Volume Correlation	168
98.	Efficiency of Electric Motors	172
99.	Speed Effects on Weight of a.c. Motors	174
100.	Speed Effects on Weight of d.c. Motors	174
101.	Hydraulic Motor Speeds	177
102.	Hydraulic Motor Weight	177
103.	Schematic of Typical High Pressure Bleed Air Ducting	180
104.	Typical Ducting Performance	184
105.	Schematic of Typical Conditioned Air Distribution Ducting	186
106.	Typical High Pressure Bleed Air Ducting Weight	190
107.	Nominal Wall Thickness of Typical High Pressure Bleed Air Ducting	191
108.	Typical Weight of Low Pressure Ducting	193
109.	Weight of General Low Pressure Ducting	195
110.	Equivalent Length of 90 Degree Bends for Cylindrical Ducts	197
111.	Total Pressure Recovery for Typical Flush Inlet	202
112.	Typical Flush Inlet Pressure Recovery	202
113.	Total Pressure Recovery for Typical Scoop Inlet	204
114.	Typical Scoop Inlet Pressure Recovery	205
115.	Discharge Coefficient for Typical Outlet	209
116.	Performance of Typical Outlets	210
117.	Typical Bleed Air Ejector in a Ram Air Duct	212
118.	Ejector Performance	213
119.	Performance of Typical Aspirator	218
120.	Butterfly Valve Pressure Drop (Fully Opened Position)	221

<u>Figure No.</u>		<u>Page</u>
121.	Pressure Drop of Split-Flapper Check Valves	222
122.	Weights of Pneumatically Actuated Butterfly Valves and Actuators	224
123.	Weights of Electric Motor Driven Butterfly Valves and Actuators	225
124.	Weights of Poppet Valves and Actuators	226
125.	Weights of Split-Flapper Check Valves	228
126.	Bleed Air Duct Insulations	230
127.	Duct Heat Dissipation	233
128.	Bleed Air Duct Radiation Shield Air Gap Insulation Thickness	236
129.	Typical Integral Insulation - Duct Design for Conditioned Air Distribution Duct	239
130.	Compartment Thermal Insulation Designs	242
131.	Typical Temperature Control System	250
132.	Ram Air Heat Sinks Controls for Subsystem 2.1 (2 sheets)	253
133.	Expendable Water Heat Sink Controls for Subsystem 2.2	255
134.	Fuel Heat Sink Controls for Subsystem 2.3	256
135.	Temperature Control of Cooling Air for Subsystem 3 (2 sheets)	257
136.	Liquid Loop Controls for Subsystem 4	259
137.	Auxiliary Air Supply Controls for Subsystem 5	260
138.	Water Separator Controls for Subsystem 6	261
139.	Controller Weight	263
140.	Package Installation Weight	272
141.	Duct Installation Weight	277
142.	Heat Exchanger Costs	299
143.	Turbomachinery Costs	299
144.	Water Separator Costs	300
145.	Axial Fan Costs	302
146.	Air/Refrigerant Heat Exchanger Costs	303
147.	High Pressure Bleed Air Ducting Costs	305
148.	Low Pressure Ducting Costs	305

<u>Figure No.</u>		<u>Page</u>
149.	Butterfly Valve Costs	308
150.	Poppet Valve Costs	309
151.	Split-Flapper Check Valve Costs	310

LIST OF TABLES

<u>Table No.</u>		<u>Page</u>
I	Subsystem 1.1 - High Pressure Air Supply	10
II	Subsystem 1.2 - Auxiliary Compressor Drives	11
III	Inventory Aircraft ECS Data (3 sheets)	45
IV	Size Comparison of Turbomachines	107
V	APU Design Point Data	164
VI	APU Design Point Performances	164
VII	Typical High Pressure Bleed Air Ducting	181
VIII	Summary of Ducting Performance Data	183
IX	Typical Low Pressure Ducting	186
X	Typical Weight of Low Pressure Ducting	193
XI	Typical Control Inputs and Outputs and Weighing Factors	252
XII	Temperature Control Component Weights	263
XIII	Cargo Aircraft Pressure Control Weights	268
XIV	Reliability Index Numbers (2 sheets)	288
XV	Reference Simple Air Cycle System Component List	297
XVI	Temperature Control Component Costs	312
XVII	Cargo Aircraft Pressure Control System Costs	313

NOMENCLATURE AND SYMBOLS

<u>Symbol</u>	<u>Definition</u>
A	Area, in ² (unless ft ² is indicated)
A'	Heat Exchanger Cross Sectional Area, ft ²
A/A	Air to Air
AC	Auxiliary Compressor
AHP	Air Horsepower
APU	Auxiliary Power Unit
B	Number of Single Nozzle Ejector Modules
B1, B2, etc	Bootstrap Air Cycle Systems (See Section 2.2)
BITE	Built-In-Test-Equipment
b	Fin Height, in
C	Product of Flow Rate and Specific Heat (i.e., W_c), Btu/ _p min°F
C	Compressor
C	Control
C _D	Drag Coefficient
CU	Cost Unit, \$20.196 (See Section 4.3)
c	Speed of Sound, ft/sec
c _o	Theoretical Spouting Velocity, ft/sec
c _p	Specific Heat, Btu/lb°F (unless ft lb/lb°R is noted)
D	Diameter, inches (unless ft is noted)
D _s	Specific Diameter
DR	Development Risk (See Section 4.3)
E	Energy, ft lb/lb
E	Ejector
E/E	Electronic/Electrical
ECS	Environmental Control System

Symbol Definition

EHP	Equivalent Horsepower
e	Emissivity
F	Force, lb
F _e	Radiation Factor
F _f	Nozzle Flow Factor (See Section 3.2)
f	Friction Factor
G	Mass Velocity, V'/v
GSE	Ground Support Equipment
g _c	32.2 ft lb/lb sec ²
H	Head, ft lb/lb
HP	Horsepower
HXA, HXL, etc.	Heat Exchanger
h	Film Coefficient, Btu/hr ft ² °R
i	Enthalpy, Btu/lb°F
j	Colburn Modulus
K ₁ , K ₂ , etc.	Constants or Parameters Defined in the Text
K	Pressure Loss Factor (KW ^m form)
K _t	Pressure Loss Coefficient (K _t ρ V' ² /2g _c form)
KW	Kilowatts
k	Thermal Conductivity, Btu/hr ft°R
L	Length, inches (unless ft is noted)
L.G.	Landing Gear
l _e	Effective Fin Length for Conduction, ft. (approximately b/2)
M	Mach Number
MOM	Momentum

<u>Symbol</u>	<u>Definition</u>
N	Rotational Speed, rev/min or rpm
N_p	Number of Flow Passes (See Section 3.1)
N_s	Specific Speed
N_{sl}	Number of Splitter Plates
NIAO	Number of Inputs and Outputs
NTU	Number of Transfer Units
n	Number of Flow Layers for One Fluid (See Section 3.1)
P	Pneumatic Actuator
P	Pressure, lb/in ² or psi (unless psf is noted)
PR	Pressure Ratio, P_{out}/P_{in}
Pr	Prandtl Number
p	Fin Pitch, 1/inch
Q	Volumetric Flow Rate, ft ³ /min or cfm (unless ft ³ /sec is noted)
Q'	Heat Energy, ft lb/lb or Btu/hr
q	Dynamic Pressure, lb/ft ² (psf)
q_{ad}	Adiabatic Head Coefficient
q'	Btu/hr ft ²
R	Gas Constant
Re	Reynolds Number
RI	Reliability Index (See Section 4.2)
r_h	Hydraulic Radius, inches
S	Surface Area, ft ²
St	Stanton Number
SF	Speed Factor (See Section 3.9.1)
SHP _r	Required Shaft Horsepower

	<u>Definition</u>
SW	Switch
S1, S2	Simple Air Cycle Systems (See Section 2.2)
s	Entropy
T	Temperature, °R (unless °F is noted)
T	Turbine
Th	Thrust, lb
TS	Temperature Sensor
t	Thickness, inch
U	Overall Heat Transfer Coefficient, Btu/hr ft ² °R
U'	Blade Velocity, ft/sec
V	Volume, in ³
V'	Fluid Velocity, ft/sec
V2, V3	Vapor Cycle Systems (See Section 2.2)
v	Specific Volume, ft ³ /lb
W	Flow Rate, lb/min
W'	Flow Rate, gal/min
W _{fu}	Fuel Flow Rate, lb/hr
Ws	Work, ft lb/lb
Wt	Weight, lb
W.S.	Water Separator
W _∞	$\rho_{\infty} V_{\infty} A$
W	Width, inches
Z	Altitude, feet

Greek Letters

α	Ratio of Heat Transfer Area to Volume
β	Blade Angle or Ratio of Heat Transfer Area to Volume of One Side
γ	Ratio of Specific Heats
δ	Standard Pressure Ratio, $P/14.70$
Δ	Difference
ϵ	Effectiveness
ϵ_0	Overall Temperature Effectiveness
ϵ_T	Heat Transfer Effectiveness
η	Efficiency
η_P	Polytropic Efficiency of APU Compressor
θ	Temperature Ratio
θ	Time, Hours
κ	Power Ratio
μ	Viscosity
ξ	Effective Length in Flow Direction, inches
π	.3.14159
Π	Dimensionless Analysis Parameter
ρ	Density, lb/ft^3
Σ	Summation
σ	Standard Density Ratio, $\rho/0.0765$
σ	Stefan-Boltzmann Constant, $0.1714 \times 10^{-8} \text{ Btu}/\text{hr ft}^2 (\text{°R})^4$
τ	Shear Stress
ϕ	Angle, Degrees
ψ	Ratio of Free Flow Area to Frontal Area on One Side

Subscripts

ad	Adiabatic
am	Ambient
ave	Average
B	Boiler
b	Bend
bl	Bleed
bu	Bulk
C	Cold or Compartment
c	Compressor or Convective
co	Coolant
cr	Critical
d	Dry or Duct
d	Displacement or Diffuser
E	Entrance
e	Effective
F	Fin
f	Fan
fr	Frontal
g	Gap
H	Hot
HI	High Water Content
IR	Irreversible
i	Inside
is	Isentropic
J	Jet
L	Leakage

Subscripts

l	Local
m or max	Maximum
min	Minimum
NR	Nonrefrigerant
n	No Flow
o	Outside
p	Primary
R	Refrigerant
Re	Requirements
r	Reference, Relative, or Radiative
s	Static or Surface
SP	Separation Plate
s	Secondary
sat	Saturated
T	Total or Tip
Te	Technical
t	Turbine
v	Vertical
w	Wet or Water
x	Exit
x	x direction
y	y direction
∞	Free Stream
1	Inlet (Normally)
2	Outlet (Normally)

Superscripts

m Exponential Constant

o Design Value

* Sonic

SECTION 1

INTRODUCTION

Air Force records on the operation of aircraft in Southeast Asia (SEA) discuss inadequacies of aircraft environmental control systems in SEA, and indicate needs for improving these systems. These records point out that the environmental control systems of some aircraft do not provide adequate cooling while the aircraft are operated on the ground, or during flights at low altitudes. Water has been found in avionic equipment during periods of aircraft maintenance. Pilots have experienced discomfort while using hot air (in the hot, humid environment of SEA) to defog the windshields of some aircraft. Fog, "snow", fumes, or smoke have been discharged from the air diffuser outlets of some aircraft.

Environmental control systems of future aircraft will be required to provide better control of the equipment and crew environments. These systems will have to cool new avionic equipment which dissipate more heat per unit volume than do present avionics. Some future aircraft will operate at speeds of Mach 3 and above, hence the heat loads to be removed by the ECS will be increased due to greater aerodynamic heating rates. Heat sinks other than ram air (e.g. fuel or water) will be needed at these higher speeds because ram air is too hot.

1.1 Objectives

The objective of developing better integrated environmental control system designs for aircraft is to investigate methods which will result in improved avionic equipment reliability and aircraft crew environments. ECS design information and evaluation techniques are needed for developing environmental control systems for future aircraft. General environmental control system design information is needed for evaluating the arrangement of components in a system, and for determining the important characteristics of these components. A digital computer program which contains this information and analyzes the ECS is a needed tool. The ECS computer program developed in this study will provide basic techniques for comparing current, proposed, and advanced ECS designs. This computer program will calculate the performance of an ECS, and will provide data for evaluating the ECS penalties to the aircraft (such as system weight and relative range reduction, cost, and reliability).

The development of advanced environmental control systems must include test programs of the new and improved design concepts. System arrangement problems, and designs of components and system controls, must be defined so that new technology can be developed in these critical areas.

1.2 Summary

The development of integrated ECS designs for aircraft involves investigations of system and component designs, and utilization of available and new technology. This study provides some of the technology for accomplishing these objectives.

The results of the first task of this study - ECS Design - are found in Volume I of this report. A review of ECS controls is presented in Reference 1. The ECS Computer Program is described in Volume II, Volume III is the IECS Computer Program Users Manual, and the Laboratory Demonstration Test ECS is presented in Volume IV.

1.2.1 ECS Design - System flow schematics which are representative of existing conventional and advanced ECS configurations are discussed. Air cycle and vapor cycle environmental control system flow schematics are included for use in fighter, bomber, and cargo aircraft.

Generalized design data for ECS components are presented. These data are based on state-of-the-art experience (i.e., no new component design concepts are considered). The design information is component performance, power required, weight and volume, and relative reliability and cost. Much of the weight, volume, and cost data are empirically correlated with pertinent performance requirements, using presently available ECS component information. These correlations and the component data are presented to indicate the accuracy which may be expected. Standard error of the component weight correlations also are provided. The component performance and design data are part of the computer program. System penalties also can be determined with this computer program. The standard error of the component weights are used to obtain an estimated error of the total system weight (see Section 4.2.2 in Volume II).

1.2.2 Computer Program Development - A digital computer program to calculate ECS performances and penalties was developed for the Air Force CDC 64 computer at Wright-Patterson Air Force Base. This computer program is in the Fortran IV language. It provides for simple or detailed input by the user. The ECS Design information contained in this volume is used in the

computer program. The computer program is set up so that the data analysis techniques in the computer program can be modified easily at a later date.

The performance analysis portion of the computer program is applicable to the system arrangements described in this volume. The system performance analysis methods are described in Volume II on the ECS computer program, hence system performance analysis methods are not presented herein.

The capabilities of the computer program were evaluated by comparing data on ECS of four Air Force aircraft to the calculated results obtained from the computer program. (See Volume II.) Rough sizing analyses were made for the ECS of a fighter, a bomber, and a cargo aircraft (Reference 2). A detailed analysis was made for the ECS of the C-9A Aeromedical Transport.

1.2.3 Laboratory Demonstration - An advanced ECS configuration was assembled, instrumented, and tested at MCAIR, St. Louis. This system consisted primarily of off-the-shelf aircraft ECS components. Tests were performed to simulate ground, loiter, and high velocity operating conditions. System performance was determined with the computer program and is compared with the test results (in Volume IV) to provide further verification of the computer program. Results of the IECS computer program sizing analysis for this ECS also is presented in Volume IV. A demonstration of the laboratory ECS was performed for interested government and industry representatives.

SECTION 2 SYSTEMS DESIGN

Design requirements of the aircraft environmental control systems considered in this study are specified herein. The requirements are discussed in terms of the ECS functions, the thermodynamic boundary conditions of the system, system controls, integration with other aircraft systems, and aircraft mission characteristics. Ten basic ECS flow schematics, and various subsystem options define the assortment of simple air cycle, bootstrap air cycle, and vapor cycle environmental control systems considered in this study. Illustrations of how the ECS of inventory aircraft can be represented by these schematics are included. The system and subsystem schematics show the components for which detail design information is provided in Section 3. A "reference" environmental control system with specific subsystems and controls is presented. It is the basis for the penalty factors discussed in Section 4.

2.1 Design Requirements

The requirements of the environmental control systems conform to specification MIL-E-38453 (USAF) (Reference 3) on environmental control, environmental protection, and engine bleed air systems; to general ECS design objectives; and to specific requirements for ECS functions, sources and forms of input power, heat sinks for final heat rejection, types of system controls, integration with other aircraft systems, and aircraft mission parameters and mission profile limitations.

2.1.1 ECS Design Objectives - Environmental control system designs should provide the desired cooling, heating, and thermal control; and for related auxiliary functions necessary to complete the aircraft missions. Maximum temperature levels should be reduced, and repeated temperature and air flow rate fluctuations should be decreased and eliminated. Less moisture should be delivered to the crew compartments and avionics, and dust should be reduced or eliminated. Higher reliability of avionics will result, thus increasing mission effectiveness and reducing logistics and maintenance costs. The crew will be less fatigued and will operate the aircraft more effectively.

2.1.2 ECS Functions - Environmental control systems provide cooling heating for avionics, other aircraft equipment, and the crew; and maintain temperature control in the crew and equipment compartments. Ventila-

tion and pressurization of compartments are based on personnel and equipment demands. Water and dust removal increases crew comfort and equipment reliability. Emergency provisions for the crew and vital equipment also influence the system designs. Air for defogging and rain removal of transparencies, and ice protection requirements influence system heat loads, temperature control, and bleed air flow rates. Air sources for suit ventilation and pressurization, and pressurization of certain other subsystems (e.g. canopy and door seals, avionics, fuel tanks) must be provided.

2.1.3 Input Power - Input power for the ECS is available from the main engines and from the auxiliary power units (APU), if the latter are used. Various forms of this input power (i.e., bleed air, electrical, hydraulic, and shaft) must be evaluated. Availability and access to a particular form of input power also are criteria in the selection of input power.

2.1.4 Heat Sinks - Air, fuel (JP4), and water are considered as heat sinks in the design of the environmental control systems. The choice of a heat sink influences aircraft performance, and must be included in the aircraft penalty evaluations. Choice of an air heat sink is established by the air temperature encountered during a mission. Fuel used as a heat sink is affected by precooling, insulation (if any), engine fuel temperature limitations, and aircraft mission. Water (as an expendable) is influenced by the ambient pressure as it affects boiling temperature.

2.1.5 Controls - The following types of controls are required: temperature control for crew, avionics, ECS unit, etc.; cabin pressure control for crew and some avionics compartments; control of air flow to crew and avionics subsystems; and humidity control in cockpit and avionics compartments.

2.1.6 Systems Integration - Environmental control system designs should be integrated with the features of other aircraft systems. The engines or an APU provide the input power for the ECS. The use of fuel as a heat sink requires consideration of fuel heat exchangers, fuel leakage, temperature limits, and effects on engine performance. Structure temperature limits may affect ECS heat loads, and compartments and cabins may be insulated for thermal and acoustic reasons.

2.1.7 Aircraft Mission Parameters - The environmental control system must operate when an aircraft is airborne and when it is on the ground. The altitude and speed criteria used in this study are 100,000 feet and Mach 4.0,

pectively, and at dynamic pressures greater than 20 psf and less than 3000 psf. (See Figure 1.) The envelope of these conditions is consistent with current and advanced aircraft operations. This envelope affects the heat loads of the cabin and equipment to be handled by the ECS. Penalty parameters of an ECS are dependent on the aircraft type (i.e., fighter, bomber, or cargo) and its aerodynamic characteristics.

Overall ECS Requirements

● Airborne Operation

- Altitude to 100,000 Feet

- Speeds to Mach 4.0

- Dynamic Pressure: $> 20 \text{ psf}$
 $< 3000 \text{ psf}$

● Ground Operation

- Heat Loads of Cabin and Equipment

- Aircraft Characteristics

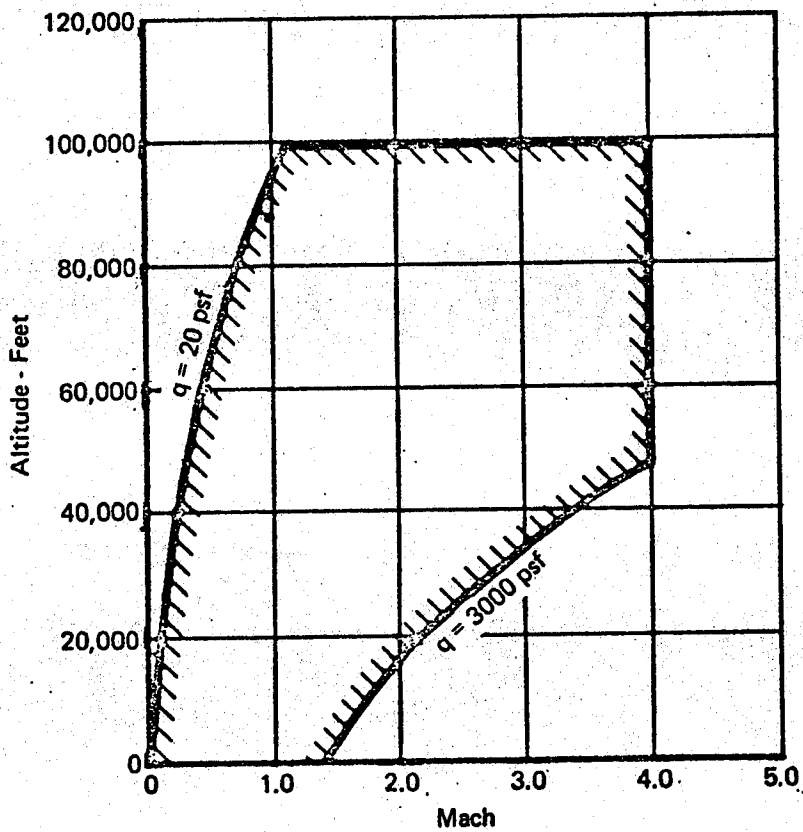


Figure 1 Aircraft Mission Parameters

GP 9416-63

2.2 Environmental Control Systems

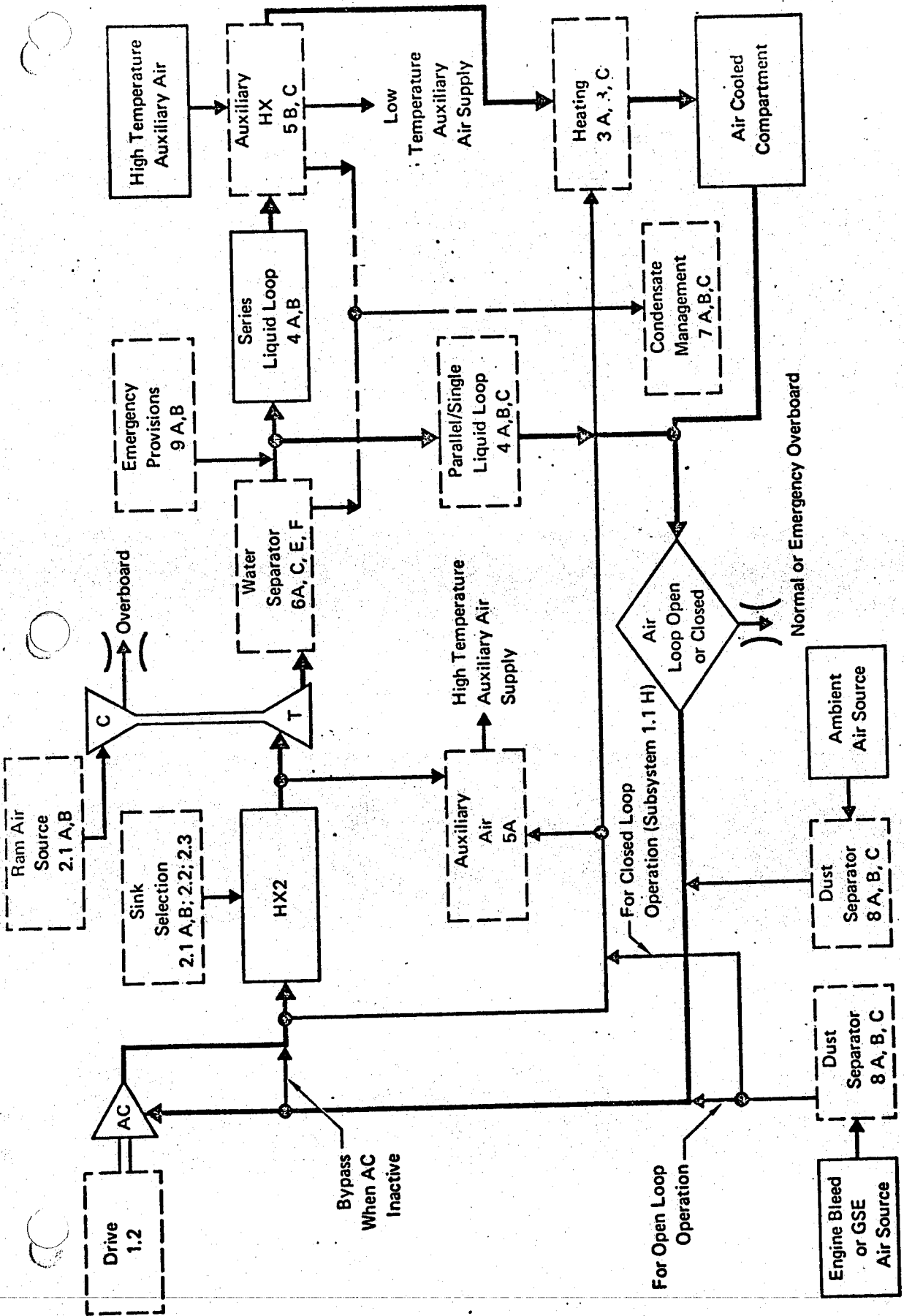
System flow schematics showing the various ECS functions and component arrangements are described in detail. These flow schematics include numerous system and subsystem options which are representative of current and advanced aircraft ECS. A concept to relate subsystem options to system flow schematics is discussed first. The subsystem options are presented next. Then the system flow schematics are described. Examples showing how a number of existing aircraft ECS are represented by these system flow schematics are presented.

2.2.1 System and Subsystem Concept - A system flow schematic for the Open or Closed Loop Simple Air Cycle is presented in Figure 2. This schematic is used to illustrate the way in which schematics are presented in this report. The dashed boxes shown in each system flow schematic include the subsystem name and an alphanumeric identification. These identifications refer to an option illustrated in the subsystem flow schematics. Each system flow schematic contains subsystem options for the use of bleed air sources; heat sinks; water and dust separators; condensate management; auxiliary air; temperature regulation of air and liquid loops; and emergency pressurization, ventilation, and cooling provisions.

Three options for cooling the heat load are considered in each system schematic: (1) one air cooled compartment and one liquid loop, (2) a single air cooled compartment, or (3) a single liquid loop. In the air cycle systems the liquid loop is cooled by air. This liquid loop is in series or in parallel with the air cooled compartment. (The single and parallel liquid loops share the same subsystem options.) The relative locations of the series liquid loop and air cooled compartment are interchangeable. In the vapor cycle systems the option of cooling the liquid loop with air is considered, as well as an option to cool the liquid loop by an independent evaporator in the refrigerant loop.

Heating for temperature regulation in the air loop is shown at a single location in each of the system flow schematics. An optional location for heating in each system is upstream of the liquid loop.

High pressure air is provided to the systems from three power sources: aircraft engine, aircraft APU, or ground support equipment (GSE). The



GP 9416-162

options of high pressure air supply to each system are grouped into two categories. One high pressure air supply category is engine bleed, and the other is auxiliary compressor air. The APU is considered in the auxiliary compressor category, and GSE air is used interchangeably with engine bleed on the ground. The various types of compressor drives are described (in the subsystem section) in conjunction with the three power sources.

Ground conditions, as used in this report, is defined as operation on the ground and operation at low speed airborne conditions, including before and after take-off and landing.

2.2.2 Subsystem Schematics - Various components and fluid flow circuits are arranged into subsystems that are generally applicable to all systems. The subsystem identifications consist of the subsystem number (included in the subsystem description) and a letter labeling the particular subsystem (in the subsystem figure). Flow schematics are not presented for every subsystem. Interrelations also exist between the subsystems. For example, condensate from a water separator may be used to provide additional cooling capacity in a ram air heat sink subsystem.

High Pressure Air Supplies, Subsystem 1.1 - The options of using engine bleed or an auxiliary compressor to provide high pressure air to the systems are listed in Table I. The options are categorized into two groups, open loop or closed loop.

The open loop options include the use of engine or auxiliary air supplied exclusively of one another (A and B), or the use of the two air supplies in combination (C and D). When engine bleed is not used, air for heating is supplied by the auxiliary compressor.

Ground support equipment can be used to supply high pressure air to the system in lieu of engine bleed air during static ground operation (E). Low pressure GSE air may be supplied directly to the ECS distribution system through the emergency ram air duct (F). These options also are available for closed loop systems having a provision to open the loop.

The closed loop options (G and H) include the use of the auxiliary compressor all the time, with ambient air with no engine bleed air, or with engine bleed air to provide make-up and pressurization air at altitude. In option I the auxiliary compressor is used on the ground with the loop closed. However, engine bleed is the primary air supply at altitude

Table I Subsystem 1.1 - High Pressure Air Supply

Open Loop

- A) Engine Bleed All the Time with No Auxiliary Compressor
- B) Auxiliary Compressor All the Time with No Engine Bleed
- C) Auxiliary Compressor on the Ground with No Engine Bleed, Engine Bleed at Altitude with No Auxiliary Compressor
- D) Auxiliary Compressor on the Ground with No Engine Bleed, Boost Compressor Augmenting Engine Bleed at Altitude
- E) Ground Support Equipment High Pressure Air Supply
- F) Ground Support Equipment Low Pressure Air Supply

Closed Loop

- G) Auxiliary Compressor All the Time with No Engine Bleed
- H) Auxiliary Compressor All the Time with Ambient Air on the Ground and Engine Bleed Air at Altitude for Make-Up
- I) Auxiliary Compressor on the Ground with No Engine Bleed in a Closed Loop, Boost Compressor Augmenting Engine Bleed in an Open Loop at Altitude

GP 9416-167

(loop open) with the auxiliary compressor used as a boost compressor when the engine bleed pressure is too low to provide adequate bleed air flows.

All of the open or closed loop options of Subsystem 1.1 which include an auxiliary compressor provide high pressure air to the ECS during ground operation, so that the engines need not operate.

Auxiliary Compressor Drives, Subsystem 1.2 - An auxiliary compressor can be driven by a bleed air turbine, electric motor, hydraulic motor, or shaft. (See Table II.) Power to these drives is supplied by the aircraft engine, or an APU, for airborne or for ground operation. Bleed air and electrical power also are supplied from ground support equipment (GSE hydraulic power is not considered because breaking into the aircraft hydraulic fluid system normally is forbidden). All of the above options are considered in conjunction with an open or closed loop system. The APU also is considered as the auxiliary compressor and a power source in an open loop system. (The APU is not considered as the auxiliary compressor in a closed loop since its inlet air flow rate is several times greater than the bleed air which it supplies to the system.) The compressed APU

Table II Subsystem 1.2 - Auxiliary Compressor Drives

Type of Drive	Power Source			System Type	
	Airborne or Ground		Ground Support Equipment	Open Loop	Closed Loop
	Engine	APU			
Bleed Air Turbine (Pneumatic)	X	X	X	X	X
Electric Motor	X	X	X	X	X
Hydraulic Motor	X	X		X	X
Shaft	X	X		X	X
APU - Used as Auxiliary Compressor		X		X	

GP 9416-166

air not used by the ECS is burned in the turbine drive portion of the APU. The auxiliary compressor drive options are not shown individually in the system schematics, but are selected in accordance with the particular system considered (i.e., the presence of open or closed air loops).

The performance of an APU degrades rapidly with altitude when the APU is utilized to provide bleed air. Altitudes up to 10,000 feet are considered for this option. Shaft, electric, or hydraulic power limitations on an APU occur at higher altitudes.

Heat Sinks - Ram air, aircraft fuel (JP4), and expendable water heat sinks are considered. Ram air is readily available, and is most commonly used at low speeds. However, at higher aircraft speeds other heat sinks become necessary because the ram air is too hot. In these cases fuel and expendable water heat sinks are considered. Where optional heat sinks are indicated in the system flow schematics, one or more heat exchangers may be used in series, each with a different heat sink.

Ram Air Heat Sinks, Subsystem 2.1 - A configuration in which the compressor of a simple air cycle is used to draw air through the primary heat exchanger is shown in Subsystem 2.1A of Figure 3. This eliminates the need for a fan or bleed air ejector for inducing air through the primary heat exchanger for ground operation of the ECS. An optional bypass line

included which may be used at altitude where adequate cooling air flow through the heat exchanger from the ram air effect. Part of the air is still routed to the compressor to load the turbine.

Each version of Subsystem 2.1B indicates direct parallel ram air flow to the compressor and to the heat exchanger at all times. This configuration is applicable to simple air cycles employed at high speeds where the ram air temperature, after passing through the heat exchanger, might exceed compressor design temperature limitations. A fan or bleed air ejector is used to induce cooling air through the heat exchanger for ground and low speed operation. The fan is bypassed at altitude. However, when the bleed air ejector configuration is used, the ram air flows through the same circuit for both active and inactive ejector operation.

The ram air circuits in Subsystem 2.1C are used in bootstrap air cycles and vapor cycles. The fan and bleed air ejector serve the same functions as in Subsystem 2.1B. The fans are driven by hydraulic, electric, or pneumatic motors.

Single ram air exits can be used in each subsystem although multiple exits are shown.

Expendable Water Heat Sinks, Subsystem 2.2 - Water boilers are employed as expendable water heat sinks for air cycle or vapor cycle systems, as illustrated in Figure 4. Use of the bleed air ejector is optional, depending on the required sink temperature versus pressure altitude. Two water boiler versions are employed. One version (Subsystem 2.2A) has an integral storage tank and the other (Subsystem 2.2B) has a separate tank. If space is available, the integral design usually is lighter.

Fuel Heat Sinks, Subsystem 2.3 - Air or refrigerant is cooled by an intermediate transport loop to the aircraft fuel heat sink. (See Figure 5.) The fuel sink can be a fuel line from the tank to the engine or a recirculation loop back to the tank (Subsystem 2.3A), a heat exchanger located in the fuel tank and fuel circulation provided via free convection (Subsystem 2.3B), or a heat exchanger located in the fuel tank and fuel circulated by a pump (Subsystem 2.3C). The fuel bypass in Subsystem 2.3A is a fuel management requirement as a protective measure against excessive fuel temperature and pressure buildup in the fuel system. Protective fuel temperature controls also are considered in Subsystems 2.3B and 2.3C via

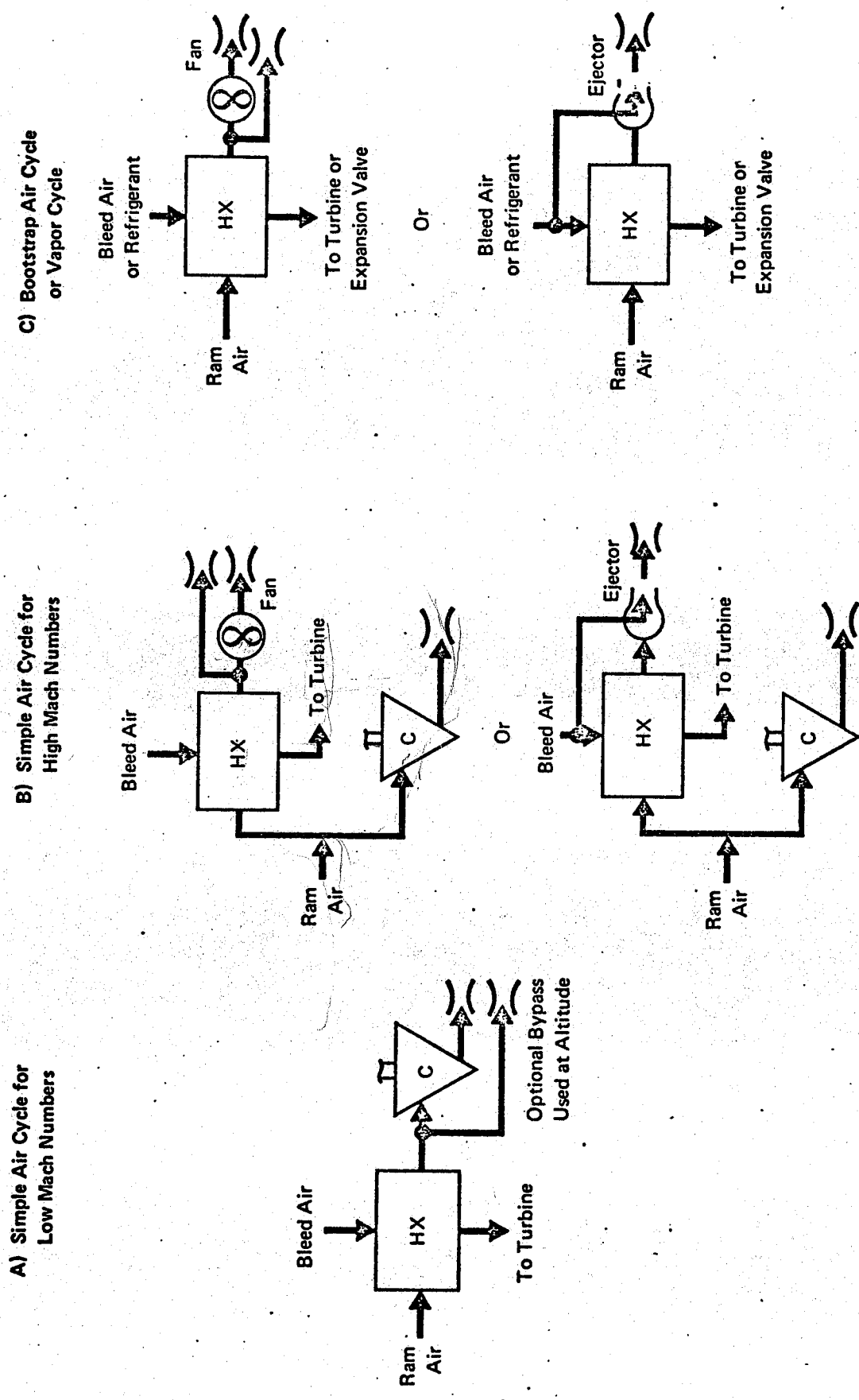
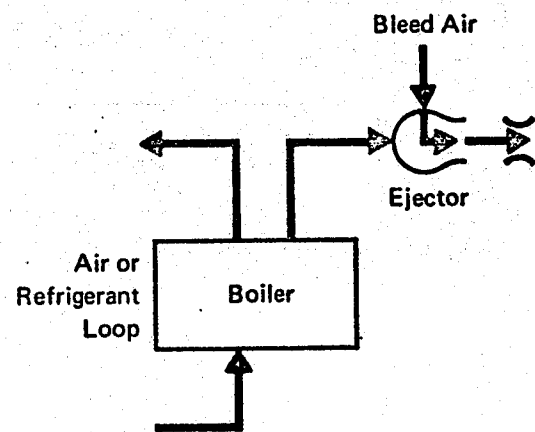


Figure 3 Subsystem 2.1 - Ram Air Heat Sinks

A) Integral Boiler and Reservoir
(with or without Ejector)



B) Separate Boiler and Reservoir
(with or without Ejector)

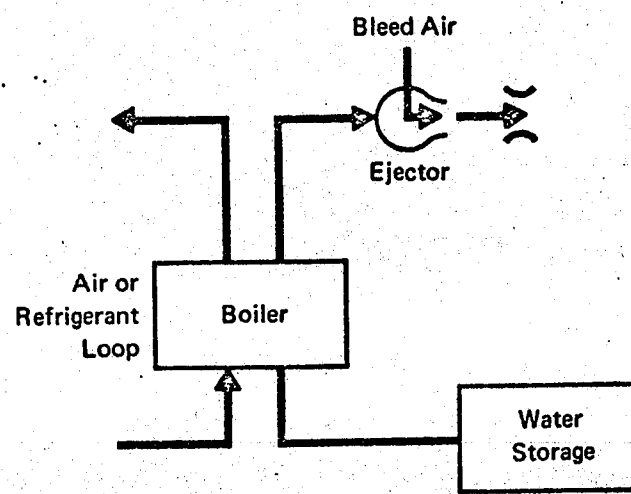


Figure 4 Subsystem 2.2 - Expendable Water Heat Sinks

GP 9416-164

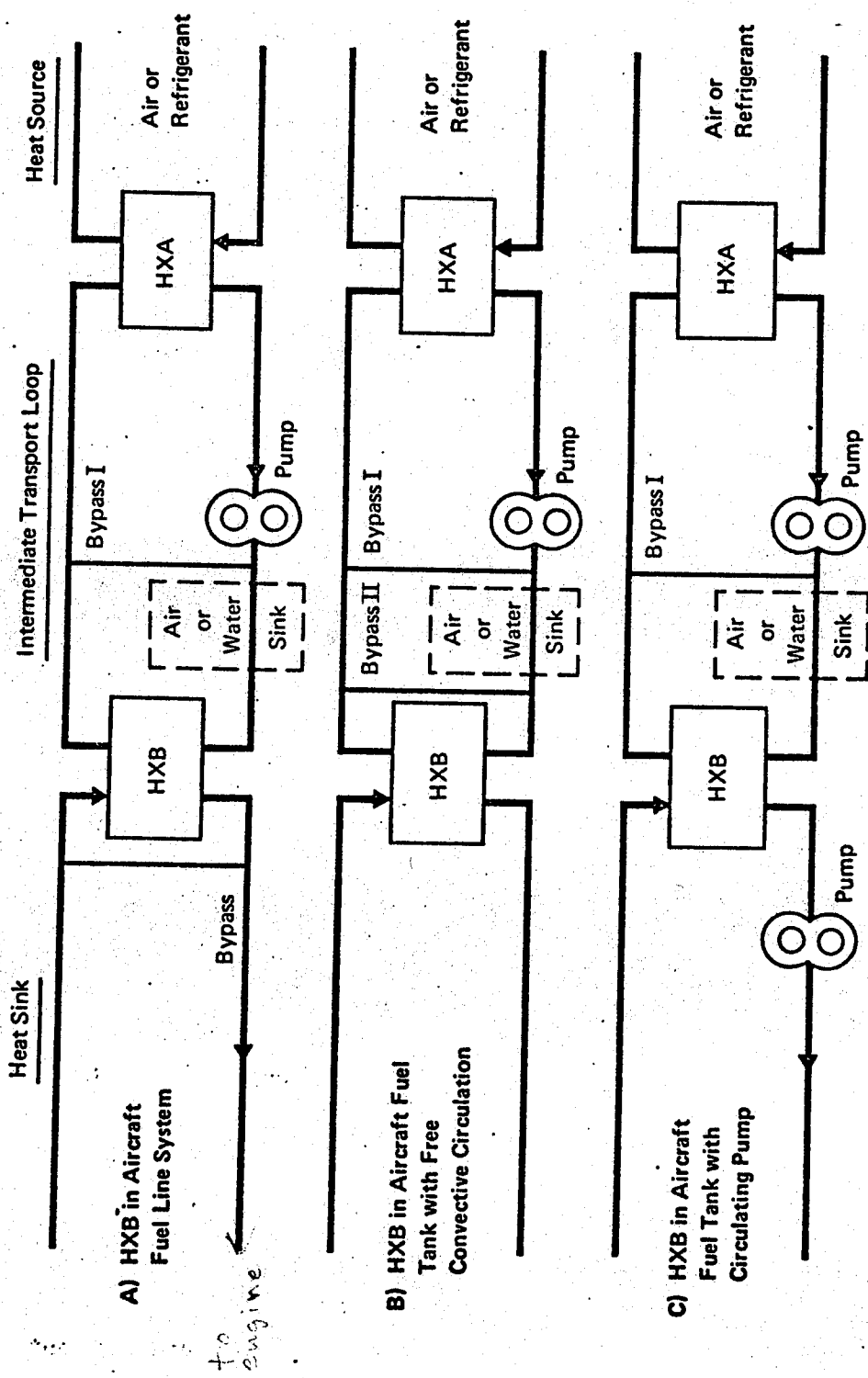


Figure 5 Subsystem 2.3 - Fuel Heat Sinks

plant loop Bypass II and by on/off control of the circulating pump, respectively. Bypass I in each case is for controlling the temperature of the heat source.

The fluid in the intermediate transport loop is a stable liquid which is used to isolate the fuel from the cooling air for safety reasons. It is employed with the vapor cycle for logistic reasons when the fuel tank is remotely located relative to the refrigerant loop. An additional option in each subsystem is direct circulation of the refrigerant through HXB since this does not involve a fire or contamination hazard as does air in a fuel heat exchanger.

The intermediate coolant loop also contains an optional heat sink, shown as dashed lines (any of the options of Subsystems 2.1 or 2.2 may be used). This allows ram air to be used at low speeds, thus conserving the fuel for high speed requirements. Electric, hydraulic, and pneumatic drives are considered for the intermediate loop pump. Engine or APU shaft drives are not considered because the pump load usually is small and pump may be remotely located.

Temperature Regulation of Cooling Air, Subsystem 3 - Optional locations for applying heat to the turbine discharge air for temperature regulation are immediately upstream of the air cooled compartment (shown in the system and subsystem flow schematics) and immediately upstream of the liquid loop. Three optional means of adding heat at either location are considered: mixing with hot bleed air, using a temperature regulation heat exchanger HX1, and heating electrically. (See Figure 6.) Subsystems 3A and 3C each have only one temperature regulation variable. In Subsystem 3A the variable is the bleed air flow, and in Subsystem 3C it is the electrical heater power. The variables for temperature regulation in Subsystem 3B are cold air bypass around or through HX1 (orifice to provide flow split) and flow regulation of the bleed air through HX1.

Temperature regulation by direct mixing of hot bleed air with the refrigerated air is most commonly used. It is the most efficient way of using the hot bleed air. One drawback, however, is that under high moisture conditions the bleed air mix method increases the moisture content

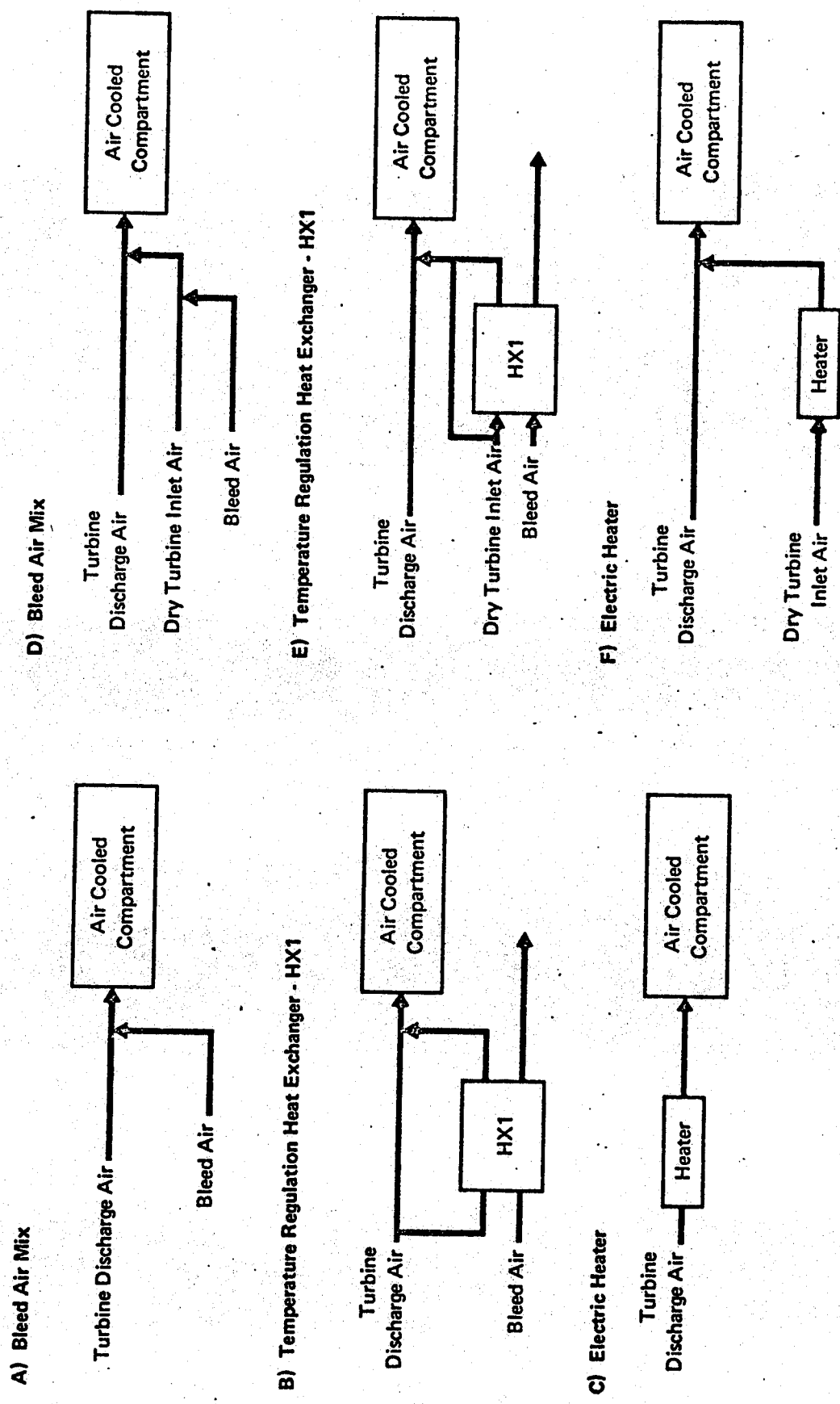


Figure 6 Subsystem 3 - Temperature Regulation of Cooling Air

of the conditioned air to the load, if a water separator is used. Under these conditions a more favorable method of temperature regulation is the use of temperature regulation heat exchanger HXL whereby heat is added with no increase in moisture content to the conditioned air. Electric heaters may be considered when the power load is small, or in areas remote from the bleed air source.

Three subsystems (D, E, and F) are used when a high pressure water separator is utilized upstream of the cooling turbine. In these cases part of the dry turbine inlet air is routed through a turbine bypass line for temperature regulation by direct mixing without increasing the moisture content. Temperature regulation via the turbine bypass air is adequate for most high moisture and high cooling load requirements. However, to broaden the capability of the system when the load requires a large amount of heat, the three methods of adding heat (similar to A, B and C) are included in D, E, and F, respectively. The temperature regulation variables in Subsystem 3D are flow rate regulation of turbine inlet air and of hot bleed air to be mixed with the turbine discharge air, Subsystem 3E variables are turbine inlet air flow through or around HXL (which is mixed with turbine discharge air), and regulation of hot bleed air flow through the opposite side of HXL. Temperature regulation for 3F is similar to that of 3C.

Another method of regulating the temperature of the conditioned air for low cooling loads, where low performance of the turbomachinery is required, is various bypass loops around the turbomachinery components. These bypass loops are considered for the bootstrap systems, in general, and are not shown specifically in all system schematics. Air bypass loops around the evaporators in the vapor cycle systems and the interface heat exchangers in the simple and bootstrap air cycle systems are considered for optional temperature regulation in general, but are not shown in the system schematics.

Liquid Loop Configurations, Subsystem 4 - Loads requiring liquid loops are considered for air and vapor cycle systems. The liquid loop may be cooled by an air loop in either system. In the vapor cycle systems, another option of cooling the liquid loop is the use of a second evaporator which is independent of the one cooling the air loop.

Four combinations of liquid and air loops are considered in the air cycle systems. (See Figure 7.) One air loop and one liquid loop are considered in series or in parallel. A single air loop or a single liquid loop also is considered individually. The various liquid loops and air cooling branches are shown in Subsystems 4A, 4B, and 4C. These subsystem schematics and the system flow schematics illustrate all of the liquid and air loop combinations.

The first three subsystems are for a single or a parallel liquid loop. Each has a different method of temperature regulation. The temperature of the liquid to or from the load can be regulated by a liquid bypass (Subsystem 4A), by an air bypass (Subsystem 4B), or by in-line flow regulation of the cooling air (Subsystem 4C). Two options for series liquid loop subsystems are represented by Subsystems 4A and 4B. The liquid loop subsystem to be used with a vapor cycle evaporator is Subsystem 4D. It has a liquid bypass for temperature regulation. A ram air heat exchanger is included in this loop for emergency cooling. Electric, hydraulic, and pneumatic drives are considered for the liquid coolant pumps. A reservoir is considered in each liquid loop although it is not shown.

Auxiliary Air Supplies, Subsystem 5 - Auxiliary air supply options at two temperature levels are included. (See Figure 8.) The high temperature auxiliary air supply is provided by mixing hot bleed air and precooled bleed air (Subsystem 5A). When lower temperature auxiliary air is required, an auxiliary heat exchanger is included in the cooling air loop to cool the high temperature auxiliary air further. Temperature of the low temperature auxiliary air supply is controlled via an auxiliary air bypass (Subsystem 5B) or a cooling air bypass (Subsystem 5C). More than one auxiliary air supply may be desired, depending on the particular aircraft applications. The auxiliary air temperatures also may vary. Typical uses for auxiliary air are:

Windshield defogging, rain removal, anti-ice and de-ice

Internal ECS anti-ice

Airfoil leading edge anti-ice

Crewman suit pressurization, ventilation, and cooling

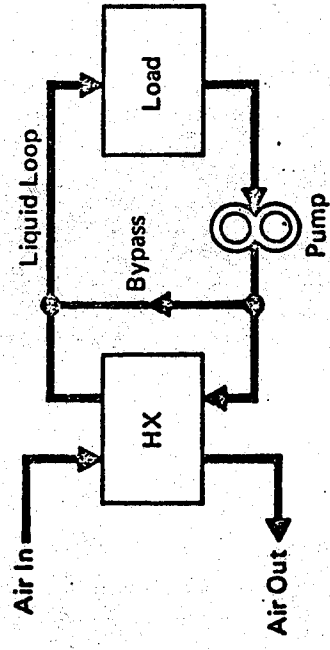
Fuel tank pressurization

Remote equipment pressurization

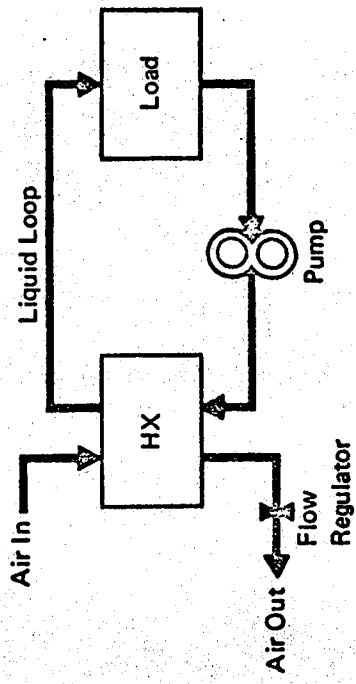
Open or closed loop make-up or heating

Canopy and other seals.

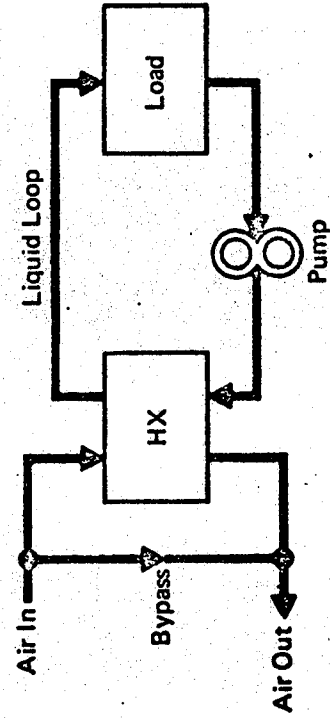
A) Liquid Bypass for Parallel, Series, or Single Liquid Loop



C) In-Line Air Flow Regulator for Parallel, or Single Liquid Loop



B) Air Bypass for Parallel, Series, or Single Liquid Loop



D) Evaporator Liquid Loop

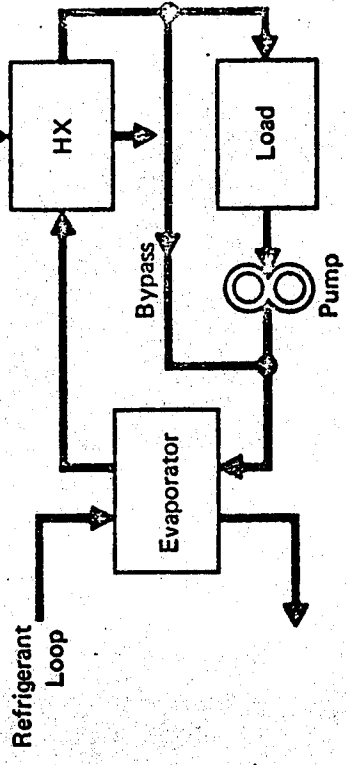


Figure 7 Subsystem 4 - Liquid Loop Configurations

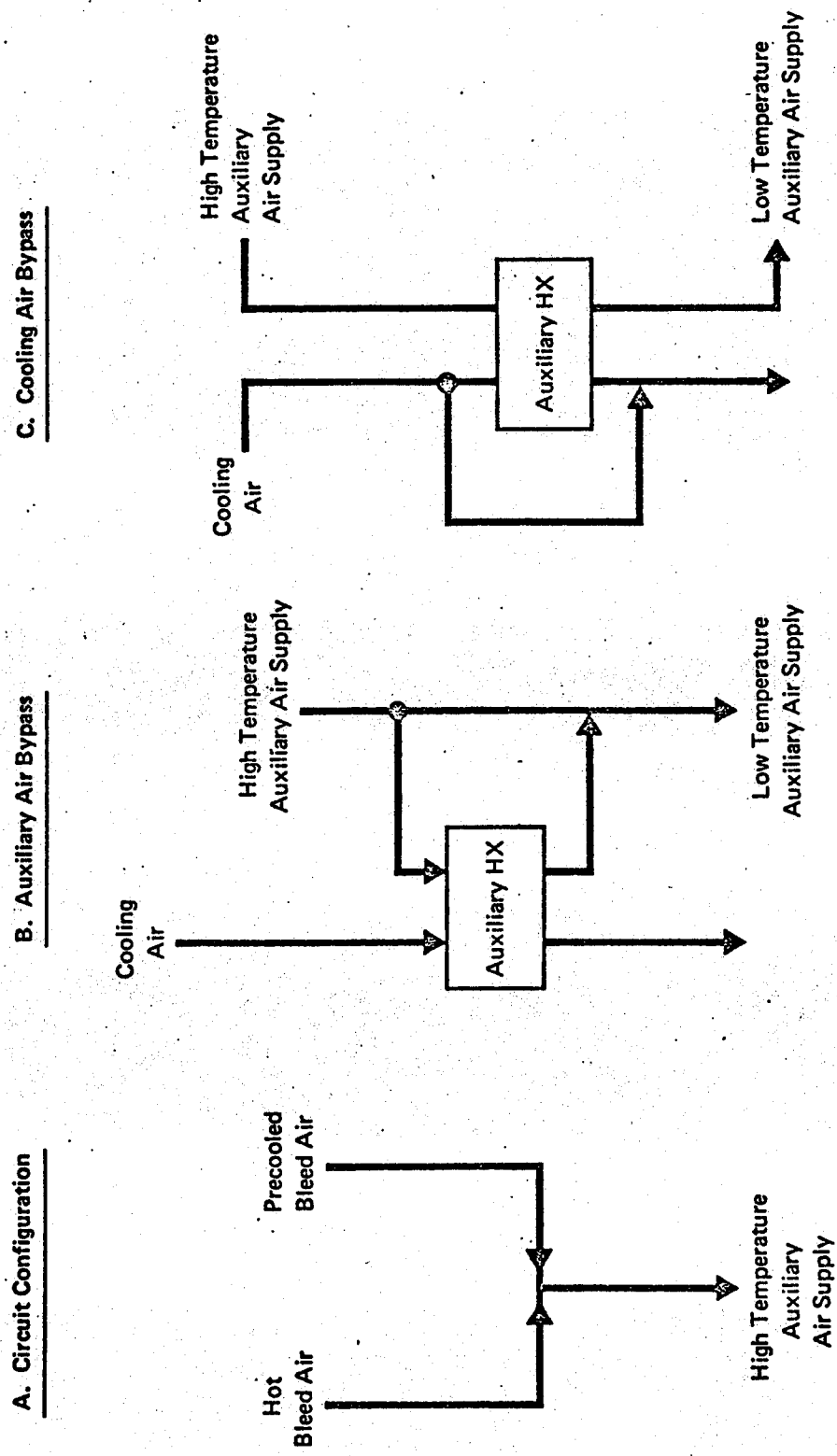


Figure 8 Subsystem 5 - Auxiliary Air Supplies

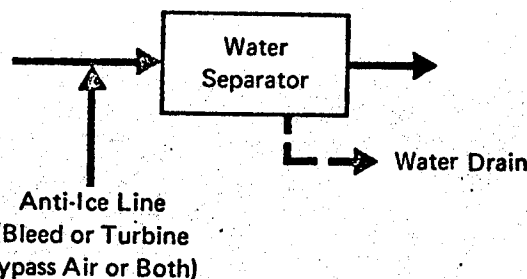
Water Separator Configurations, Subsystem 6 - Both low pressure and high pressure water separators are considered. An altitude bypass line is optional with a low pressure water separator. The anti-ice feature is optional with either type of water separator. (See Figure 9.) At high pressure the capacity of air to hold water in the vapor state is less than at low pressure, and water removal upstream of the turbine inlet may reduce detrimental effects of water on the turbine. Thus, a high pressure water separator upstream of a cooling turbine or a throttling valve is considered. The option to include an anti-ice valve only is included to prevent icing in a downstream heat exchanger or of fluid on the opposite side of the heat exchanger.

The low pressure water separators also have an internal bypass (not shown in the figure) which opens if the separator clogs up, thus allowing passage of adequate ventilating and cooling air.

Condensate Management, Subsystem 7 - Condensate from the various sources shown in the system flow schematics is routed to a common junction. It may be routed to the cooling air sink to increase the ECS cooling capacity or may be dumped overboard. (See Figure 10.) The condensate usually is routed to the ram air side of the secondary heat exchanger. Gravity feed (Subsystem 7A) may be adequate for some aircraft where freezing is no problem. If freezing is apt to occur (due to operating altitude or geographical mission requirements) warm air can be mixed with the water near the discharge port as shown in Subsystem 7B. A pumping device (Subsystem 7C) is required when the discharge pressure is higher than the condensate pressure.

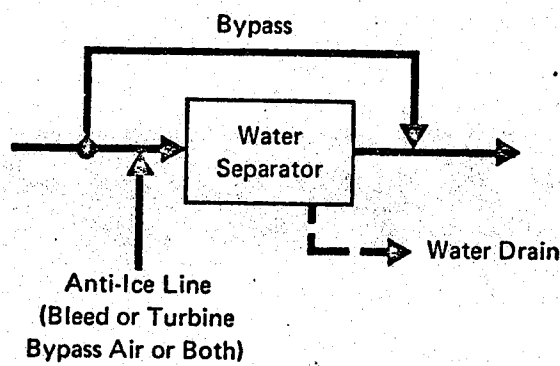
Dust Separators, Subsystem 8 - Dust separators are considered at each of the two air inlets to the ECS. One separator functions to clean ambient air to the auxiliary compressor intake and the other to clean engine bleed air to the system. Dust separators (filters) also are considered in closed air loops to remove dust, although this is not shown in the system flow schematics. Two types of dust separators are considered. They are static and self-cleaning centrifugal types. The performance penalty for using a static dust separator is pressure loss in the filtered air. A different penalty is associated with the centrifugal type separator. This a scavenge air flow loss to provide the self-cleaning capability. When air pressure is not high enough, high pressure air is used in a small

**A) Water Separator (No High Altitude Bypass)
with Anti-Ice Line**



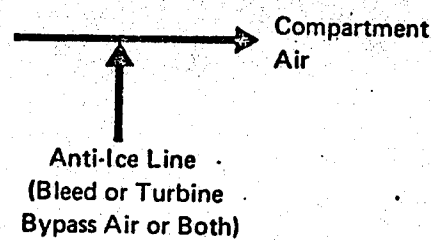
B) Same as A without Anti-Ice Line

**C) Water Separator (High Altitude Bypass)
with Anti-Ice Line**



D) Same as C without Anti-Ice Line

E) Anti-Ice Only



F) No Water Separation or Ice Control

Figure 9 Subsystem 6 - Water Separator Configurations

GP 9416-173

Gravity Feed

Water from
All Sources

Cooling Air Sink
or Overboard

B) Gravity Feed with Warm Air Mix

Water from
All Sources

Warm Air Mix
to Prevent
Freezing

Cooling Air Sink
or Overboard

c) Forced Ejection

Water from
All Sources

Bleed
Air

Aspirator

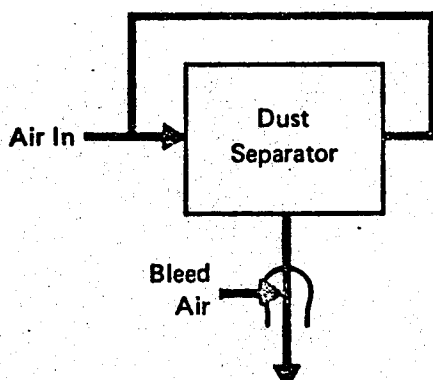
Cooling Air Sink
or Overboard

Figure 10 Subsystem 7 - Condensate Management

ector. Three options (See Figure 11) at each location are a separator with altitude bypass (Subsystem 8A), a separator without altitude bypass (Subsystem 8B), and no separator (Subsystem 8C). The bypass may also function when the separator becomes very dirty or clogged up. The limiting pressure drop which requires the bypass to be opened is a system requirement. When dust is removed from all air sources to the system, better ECS reliability and performance is expected, as well as improved equipment reliability and crew comfort.

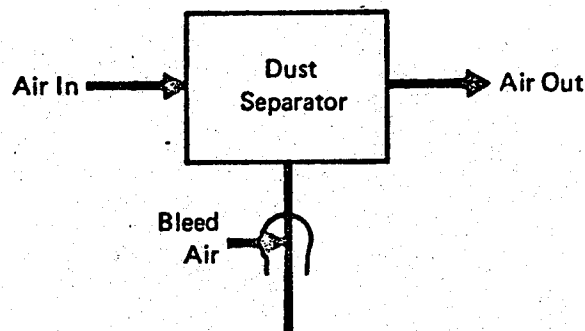
Emergency Provisions, Subsystem 9 - Means of providing emergency pressurization, ventilation, and cooling are included. Subsystem 9A is ram air for ventilation and pressurization (depending on aircraft speed) without any cooling. Subsystem 9B is the same as 9A with an integral water boiler (Subsystem 2.2A, Figure 4) for cooling. Either of these subsystems is connected to the regular environmental control system distribution ducting which is equipped with an overboard valve if the system is closed. These subsystems may be used simultaneously with the regular environmental control system for emergencies (such as a hole in the canopy) or may function alone if the regular ECS is defective.

A) With Bypass



Scavenge Air and
Bleed Air Overboard
for Centrifugal
Type Separators

B) Without Bypass



Scavenge Air and
Bleed Air Overboard
for Centrifugal
Type Separators

C) No Dust Separator

Figure 11 Subsystem 8 - Dust Separators

GP 9416-171

Additional methods for providing ventilation and pressurization to the crewmen (independent of the ECS) are cryogenic oxygen, high pressure oxygen, or self-contained oxygen systems. These systems are used in various applications for normal or emergency conditions.

2.2.3 System Schematics - Flow schematics of each system are presented. They are grouped by system type: simple air cycles, bootstrap air cycles, and vapor cycles. The alphanumeric identification of each system is indicated in the corresponding title (i.e., S1 and S2 for simple air cycles; B1, B2, etc., for bootstrap air cycles; and V1, V2, etc., for vapor cycles). Each system type is discussed in general, followed by a description of the corresponding system schematics. There are ten basic systems with various subsystem options. The operations of the systems are discussed for both altitude and ground conditions. In each system flow schematic a heavy solid line indicates the main flow paths of the air or refrigerant loops, and phantom lines represent condensate flow. Only one inlet air source (ambient, engine bleed, or GSE) is available to each system at any one time.

2.2.3.1 Simple Air Cycles - The simple air cycle refrigeration system consists of two air circuits through the turbomachinery, as shown in Figure 12. High pressure bleed air is expanded through the turbine to provide cooling air to the various loads. Work from the cooling turbine is absorbed by the compressor. The turbine and compressor are on a common shaft. The compressor transfers the work to the ram air which flows through the ram air circuit.

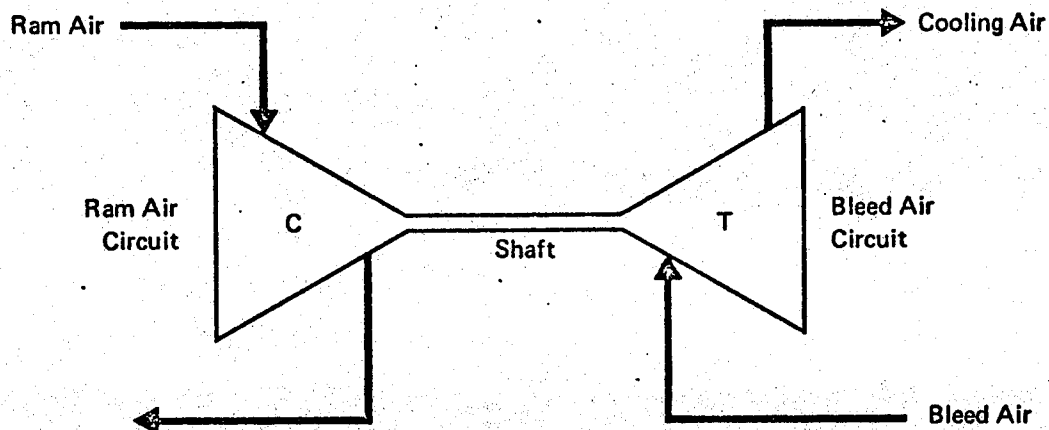


Figure 12 Simple Air Cycle

GP 9416-174

The open loop simple air cycle is more representative of current aircraft whereas a closed loop is more advanced. Closed loops provide more efficient water and dust separation. In addition to these closed loop advantages, a secondary closed loop cooled by an air to air heat exchanger and having a circulating fan also provides a more uniform air flow rate. The regenerators, and the expendable water and fuel heat sinks are methods to provide capacity at higher speeds. Other features of the simple air cycle systems are the use of temperature regeneration heat exchanger (HXI) and the various applications of the auxiliary compressor.

Simple Air Cycle, Open or Closed Loop, System S1 - This simple air cycle system flow schematic (shown in Figure 13) can be designed to function as an open loop, a closed loop, or a combination open and closed loop system (as discussed for the various auxiliary compressor and engine

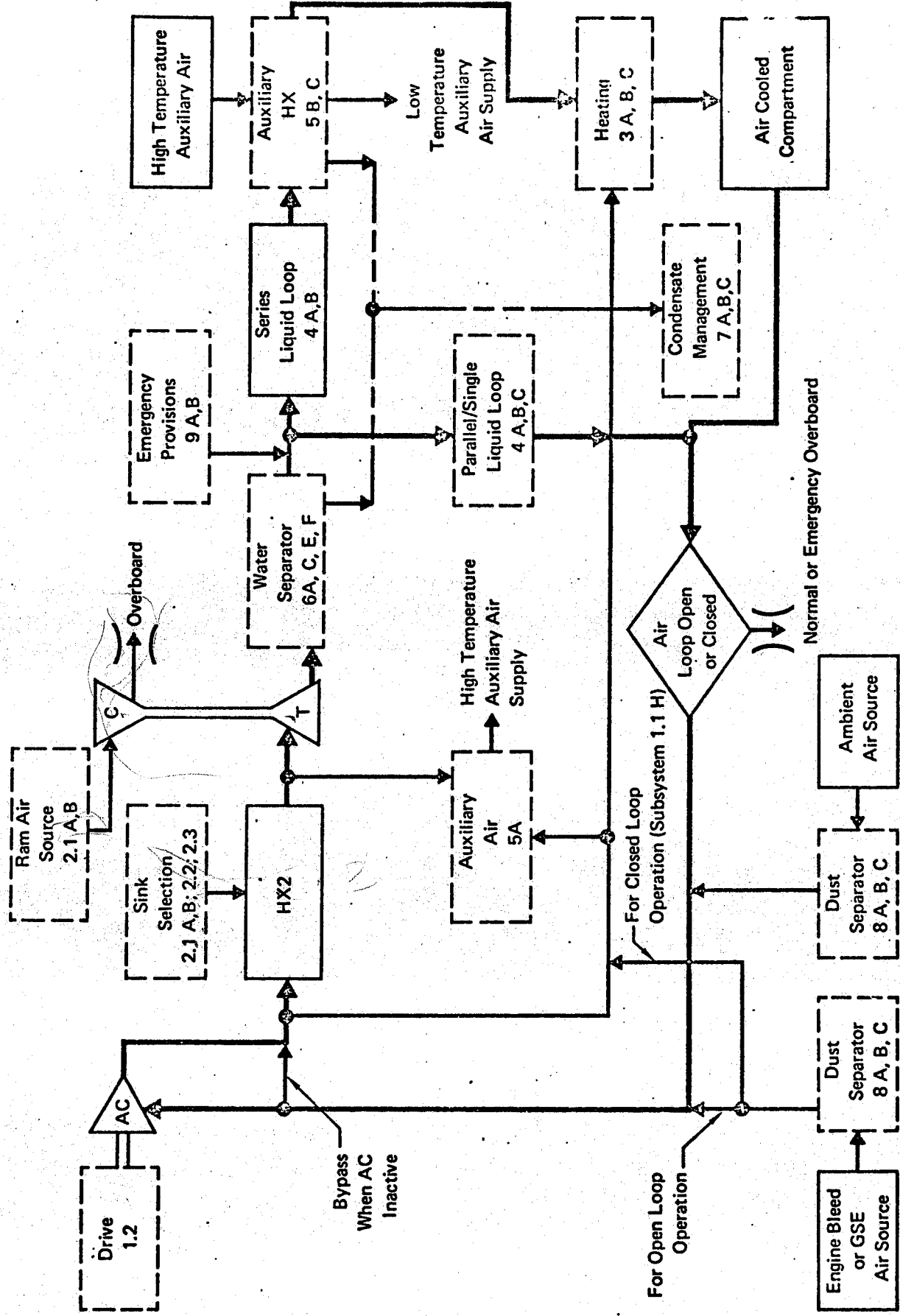


Figure 13 System S1 - Simple Air Cycle, Open or Closed Loop

GP 9416-162

bleed air supply options in Subsystem 1.1). The heavy solid lines show the primary air flow paths for open or closed loop operation with an active auxiliary compressor. This flow path applies when engine bleed air or ambient air is supplied to a system which has an active auxiliary compressor. When the auxiliary compressor is inactive, the bypass is employed. Note the two different engine bleed air inlets for open or closed loop operation.

The high pressure air is precooled in HX2, and cooled further by expansion through the turbine. The turbine discharge air is dried as it passes through the water separator, and then the air flow splits if a parallel liquid loop is being used. If a parallel liquid loop is used, part of the air goes through the parallel loop, and the remainder is heated by the auxiliary heat exchanger to regulate the air temperature before it flows to the air cooled compartment. Discharge air from the air cooled compartment and the parallel loop may be dumped overboard or recirculated, in accordance with the closed or open loop option.

The water separator options with anti-ice are selected since the turbine discharge air can be below freezing. The anti-ice feature, when the separator is not used, is included to prevent possible icing in a downstream heat exchanger. Three heating options are considered at each optional location. The location not shown is in the parallel liquid loop branch.

Simple Air Cycle, Open or Closed Loop, with Secondary Heat Transport Loop, System S2 - This system employs a simple air cycle in the primary cooling air loop. (See Figure 14.) The cooling load is serviced by a secondary air heat transport loop which includes a circulating fan with optional electric, pneumatic, or hydraulic drives. Heat is transferred from the heat transport loop to the primary cooling loop via the interface heat exchanger (HX4). The primary cooling loop may be an open or closed loop employing all of the high pressure air supply options of Subsystem 1.1. The precooler heat exchanger is included to cool bleed air for pressurization to the secondary loop when engine bleed is used. When the auxiliary compressor is employed without engine bleed at altitude, pressurization to

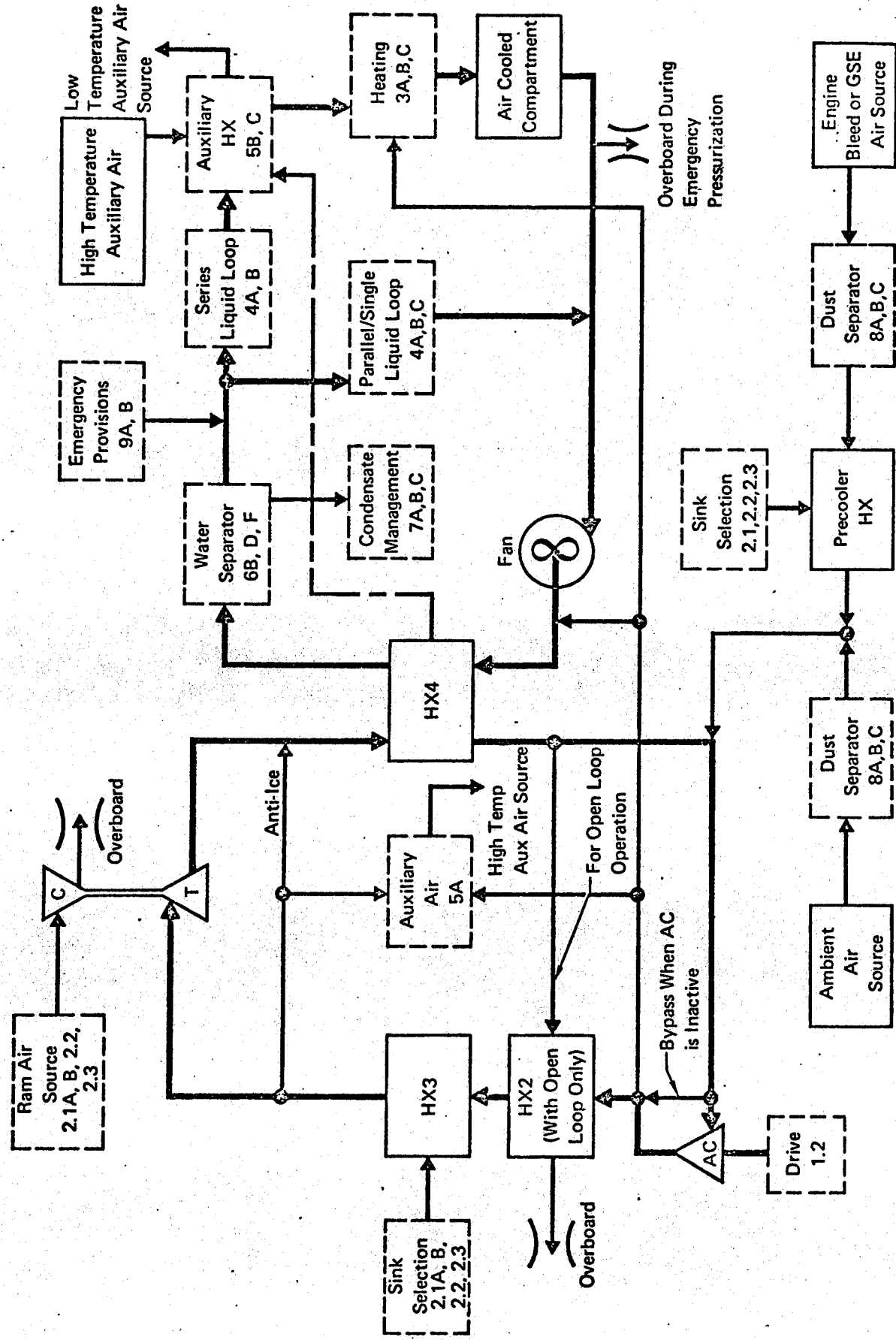


Figure 14 System S2 - Simple Air Cycle, Open or Closed Loop, with Secondary Heat Transport Loop

GP 9416-161

the secondary loop is supplied directly from the auxiliary compressor which normally is not as hot as engine bleed air.

Heat exchanger HX2 is utilized as a regenerator during open loop operation of the primary loop to take advantage of the cooling capacity of the exhaust air from HX4. The locations of HX2 and HX3 are interchangeable. The optional locations provide a more efficient system depending on the type of heat sink utilized at HX3. For example, if a ram air heat sink is used, potential cooling capacity is greater if HX3 precedes HX2. However, if an expendable water heat sink is used, the reverse locations may be desirable to conserve water.

Bleed air is added at the turbine exit to prevent icing at the entrance of HX4. The water separator options in the secondary loop do not need the anti-icing feature, since anti-icing in the primary loop ensures temperatures above freezing in the secondary loop.

2.2.3.2 Bootstrap Air Cycles - The bootstrap air cycle system employs a single air circuit through the turbomachinery, as shown in Figure 15.

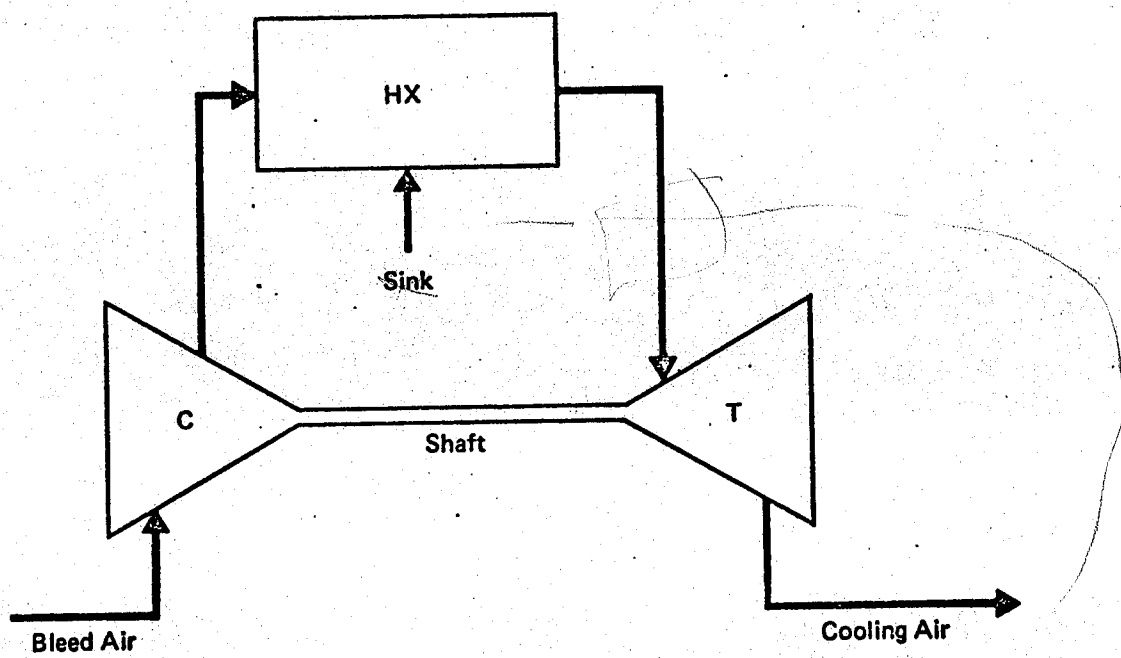


Figure 15 Bootstrap Air Cycle

GP 9416-175

Bleed air is routed through the compressor where shaft power is converted into an increase in air temperature and pressure. Next the air is circulated through one or more heat exchangers where the temperature is reduced. Then the air is expanded through the cooling turbine. The turbine provides power through the common shaft to the compressor. The turbine discharge air pressure is related to the pressure requirements of the loads. The bootstrap air cycle has an advantage over the simple air cycle in that bleed air at a lower pressure can be used to provide adequate pressurization and cooling.

The open loop option of System B1 is most representative of current aircraft. The closed loop, the secondary closed loop, and the regenerative open loop are typical of systems being developed, or of advanced concepts. The closed loops provide more efficient water and dust separation, and a more uniform flow rate (especially the secondary closed loop systems). Another feature used in one of the bootstrap systems is the application of a high pressure water separator.

Bootstrap Air Cycle, Open or Closed Loop, System B1 - This bootstrap air cycle system represents an open, closed, or combination open and closed system. (See Figure 16.) The various open and closed loop options and associated high pressure air supply options are indicated in Subsystem 1.1. The subsystem options of this bootstrap air cycle system are the same as those of Simple Air Cycle System S1, except for the selection of the appropriate ram air sink options.

Bootstrap Air Cycle, Open Loop, Regenerative, System B2 - This system includes the options of regenerative air source and location of the regenerative heat exchanger. (See Figure 17.) The two optional sources of regenerative air are water separator discharge air or exhaust air from the air cooled circuits. The regenerator also can be located upstream of the compressor. An additional option at each location is to reverse the relative locations of the regenerator with HX2 or HX3. These different relative locations can provide greater system capacity and more discrete use of the expendable water or fuel sink depending on the heat sinks selected for HX2 and HX3. All of the open loop high pressure air supply options in Subsystem 1.1 are applicable to System B2.

Bootstrap Air Cycle, Open Loop, With High Pressure Water Separator, System B3 - This open loop bootstrap system employs a high pressure water

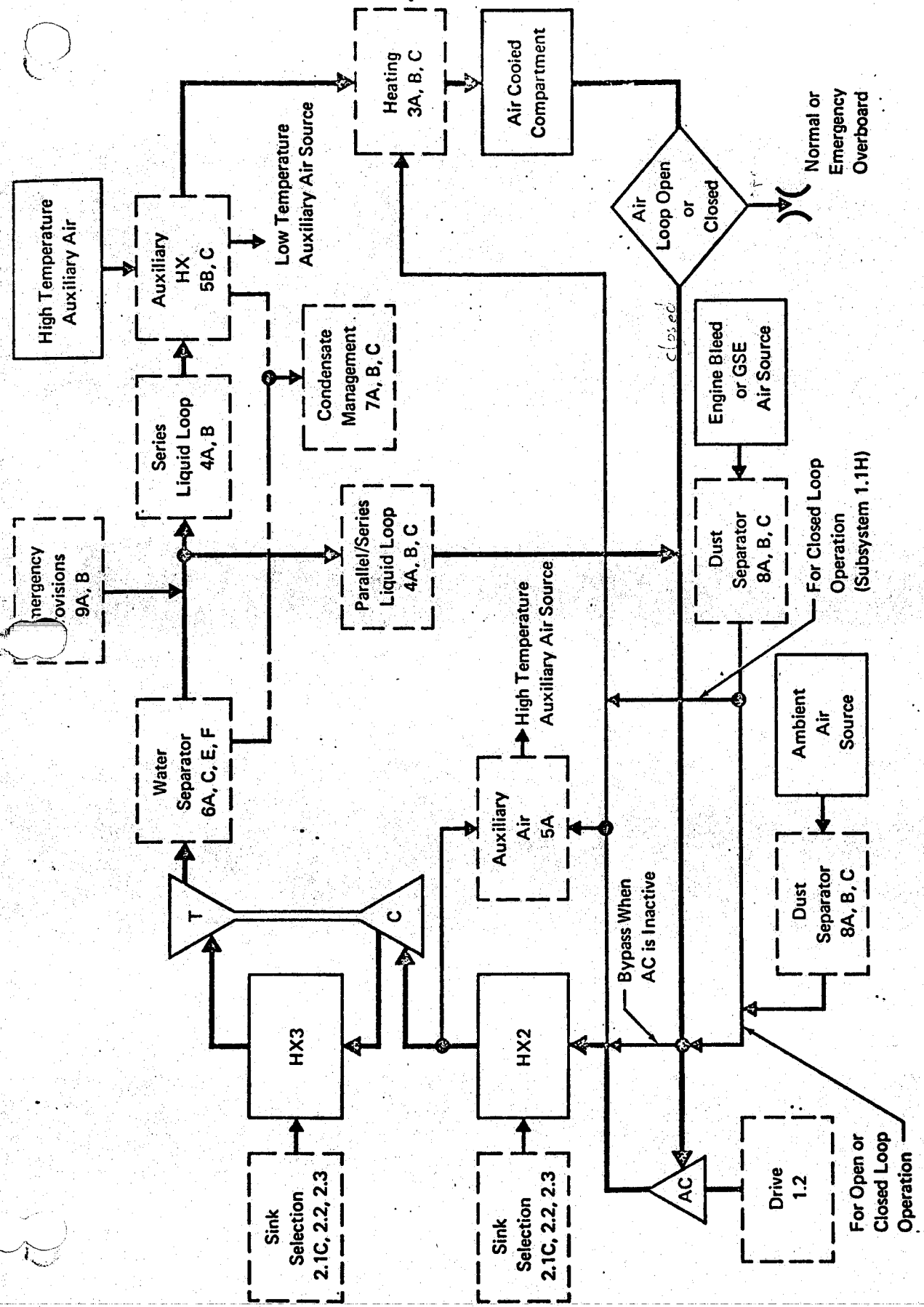


Figure 16 System B1 - Bootstrap Air Cycle, Open or Closed Loop

GP 9416-170

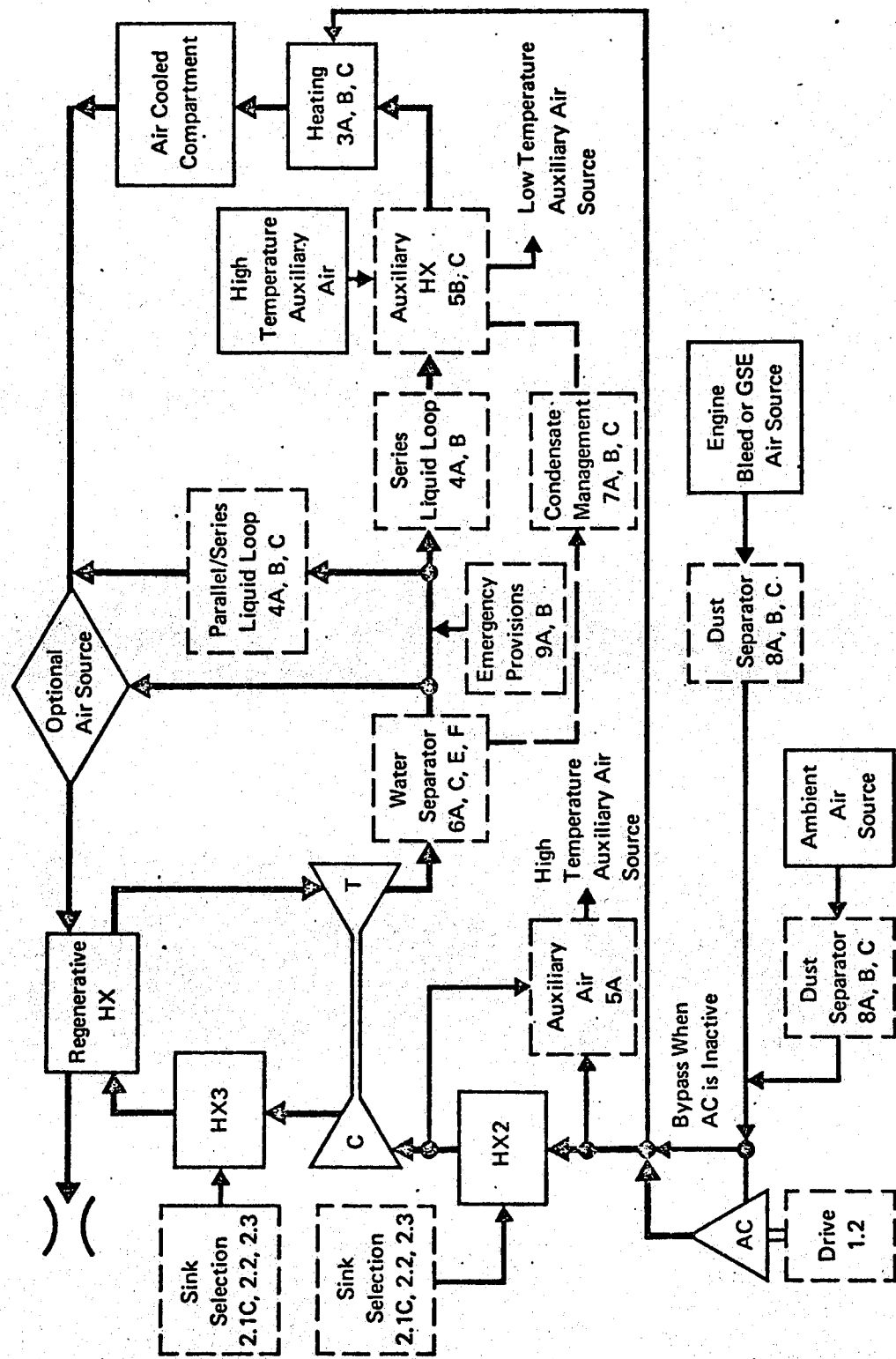


Figure 17 System B2 Bootstrap Air Cycle, Open Loop, Regenerative

ator, uses the turbine discharge air to cool air in the high pressure water separator (HX2), and uses the cooling loop discharge air for regeneration. (See Figure 18.) The open loop options of Subsystem 1.1 can be used to supply high pressure air to the system. Using the turbine discharge air to cool air in the high pressure water separator improves the water removal capability. Anti-icing is included in the water separator options (HX2 can be used as a regular heat exchanger for Subsystem option 6F), and at the turbine discharge. The bypass around HX2 is used to provide adequate cooling (when necessary).

Dry air for heating is taken from the water separator exit. Since this air has passed through the water separator it can be mixed with the turbine discharge cooling air for temperature regulation without increasing the water content. The options of utilizing this air source and hot bleed air or an electric heater for temperature regulation are shown in the appropriate subsystems. Options for the cooling loop discharge air are:

(1) overboard dump, (2) regeneration at HX3, or (3) regeneration at HX4.

indicated heat sinks at HX3 and HX4 are used when the regeneration option is not exercised or in conjunction with the regenerator (i.e., two heat exchangers in series).

An optional location for the high pressure water separator is between HX3 and the turbine. HX2 could be eliminated and dry heating air for temperature regulation would be taken from the line between the water separator and the turbine. In this location the pressure would be higher and thus the water removal capability may be comparable even though fewer components are used. The remainder of the system schematic and subsystem options would remain the same.

Simple-Bootstrap Air Cycle, Open Loop, System B4 - This system employs a three wheel air cycle machine. It has characteristics of a simple air cycle for ground operation and of a bootstrap air cycle for airborne operation. (See Figure 19.) The primary bleed air open loop is shown in heavy solid lines; the ram air lines are dashed. For ground operation, the fan circulates ram air through the primary and secondary heat exchangers (HX2 and HX3). The compressor is inactive at this time, and the bleed air flow-through HX2 bypasses the compressor. At altitude the fan becomes inactive and the ram air flows through the bypass around the fan to HX2 and HX3. At altitude, when the cooling load requires use of the turbomachinery, this sys-

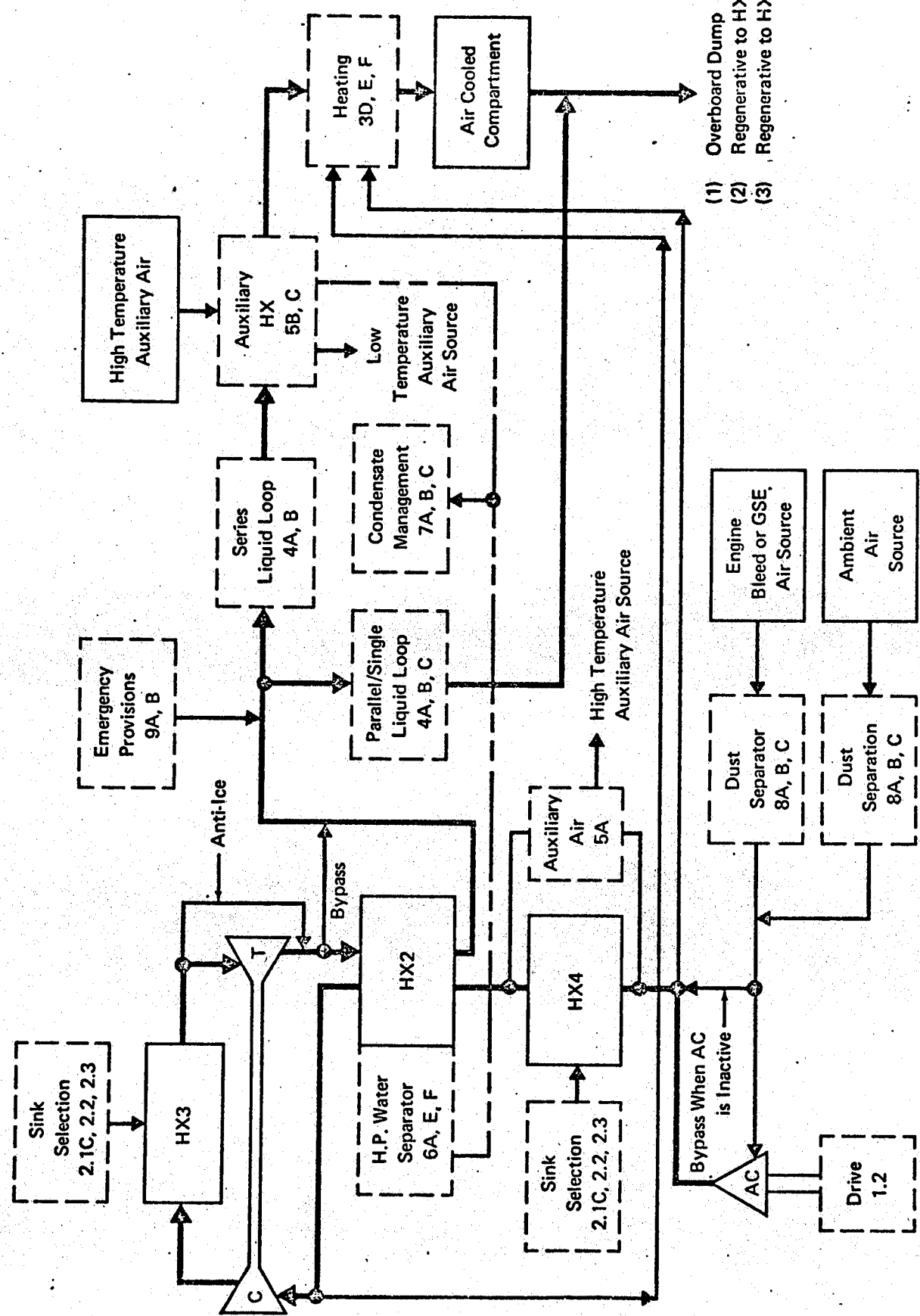
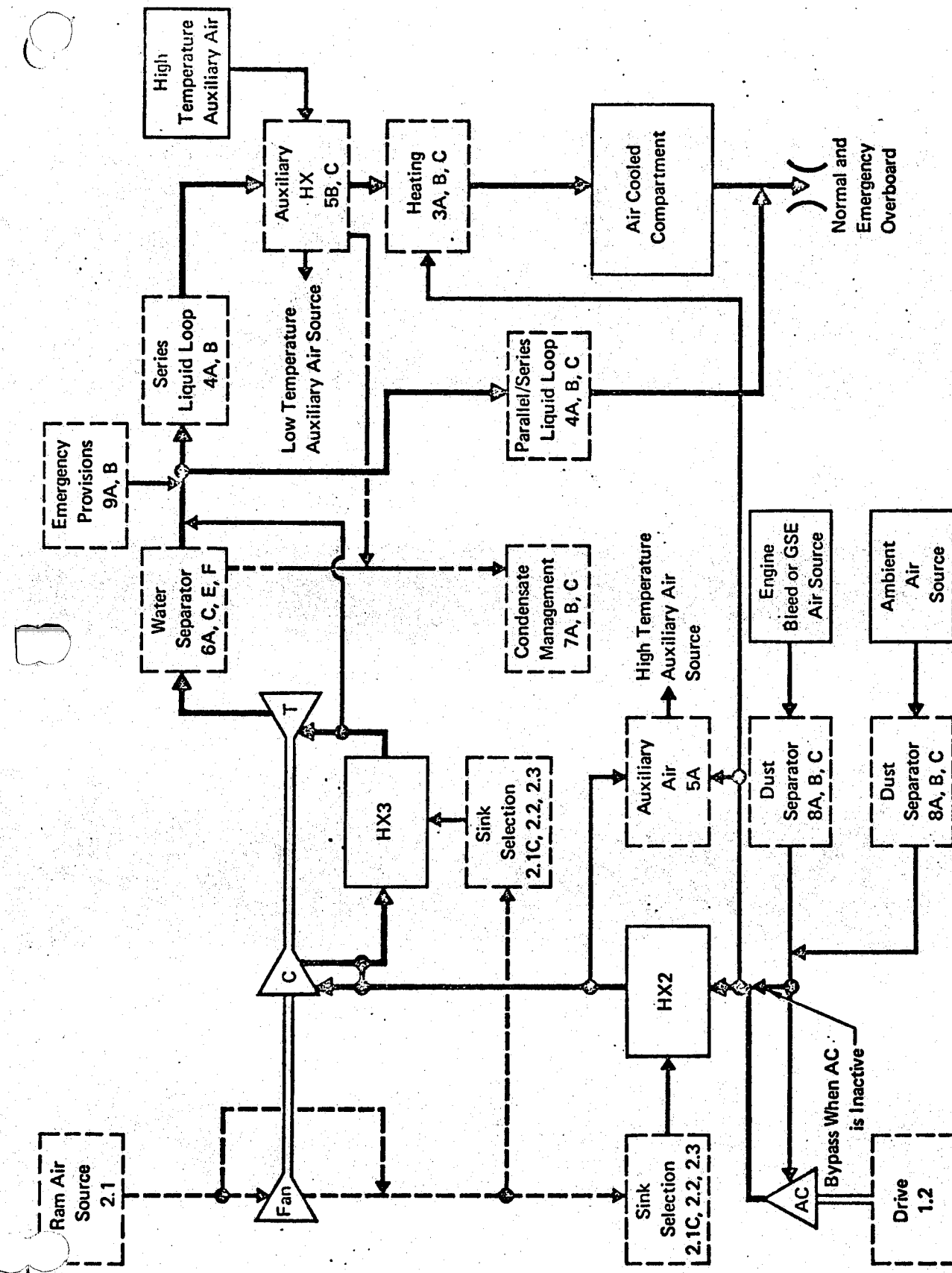


Figure 18 System B3 - Bootstrap Air Cycle, Open Loop with High Pressure Water Separator

Figure 19 System B4 - Simple - Bootstrap Air Cycle, Open Loop



tem functions the same as the open loop option of System Bl. When the cooling load is small, or when heating is required, another option is included. The turbomachinery may be bypassed by using the compressor and turbine bypass lines. This option conserves bleed air and increases the life of the turbomachinery. The system flow schematic and subsystem options, including high pressure air supply, are equivalent to those of the open loop option of System Bl with the exception of the fan and the bypass loops around the turbomachinery components.

Bootstrap Air Cycle, Open or Closed Loop, with Secondary Heat Transport Loop, System B5 - This system employs a bootstrap air cycle in the primary cooling loop, as shown in Figure 20. Heat is transferred from the closed secondary air heat transport loop to the primary loop by an interface heat exchanger (HX4). The primary and secondary loops are denoted by heavy solid lines. All of the air supply options of Subsystem 1.1 are applicable. This bootstrap system parallels that of the simple air cycle System S2, except for the appropriate ram air heat sink options.

2.2.3.3 Vapor Cycles - The basic vapor cycle refrigeration subsystem consists of a compressor, condenser, receiver, expansion valve, evaporator, and associated plumbing. (See Figure 21.) The refrigerant flows at high pressure from the compressor discharge through the condenser and receiver to the expansion valve, where it is throttled to low pressure. Low pressure refrigerant flows through the evaporator to the compressor inlet. Phase changes take place in the condenser, at the expansion valve, and in the evaporator.

The lines from the condenser to the expansion valve carry liquid refrigerant at a temperature a few degrees below saturation temperature. The liquid flashes into a two phase mixture at the expansion valve and evaporates completely in the evaporator as heat is absorbed from the heat source. The refrigerant is slightly superheated and it remains in a vapor state throughout the compression process. At the condenser the vapor condenses to a liquid giving up its latent heat to the heat sink. The receiver is a reservoir containing liquid refrigerant and a vapor space.

A single open or closed air loop serviced by one evaporator, is most representative of current aircraft applications. Dual evaporators, with one servicing a liquid cooling loop, is an advanced system design.

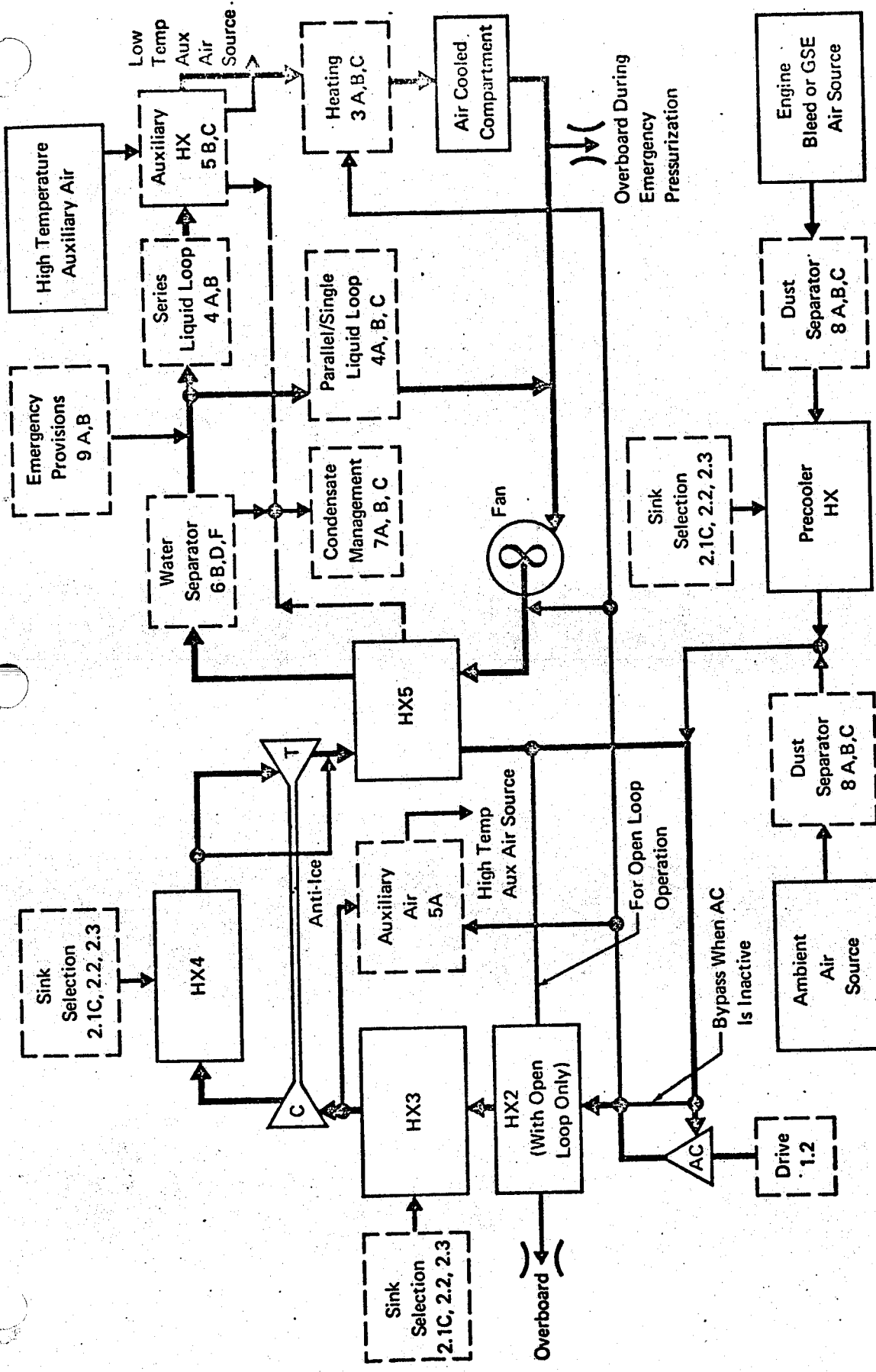


Figure 20 System B5 –
Bootstrap Air Cycle, Open or Closed Loop
with Secondary Heat Transport Loop

GP 9416-183

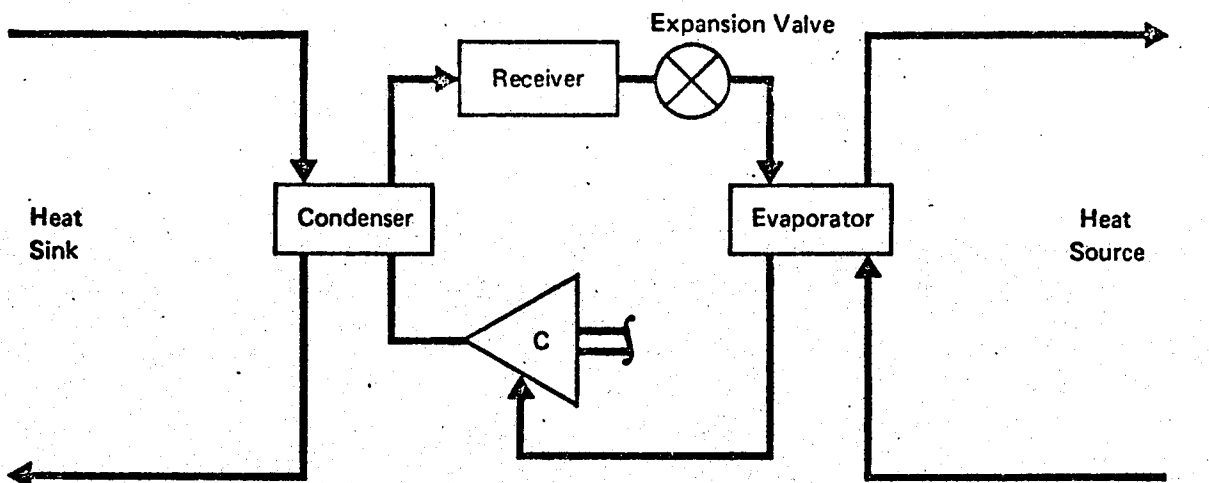


Figure 21 Vapor Cycle

GP 9416-159

Vapor Cycle, Secondary Closed Air Loop, System VI - This system consists of a primary vapor cycle loop which cools an air loop and an optional liquid loop. (See Figure 22.) The primary flow paths in the refrigerant and air loops are denoted by heavy solid lines. The optional liquid loop is shown in Subsystem 4D. Heat is transferred from the secondary air loop and optional liquid loop to two parallel evaporators (in the refrigerant loop), and regulated at independent pressures to provide the desired heat sink temperatures for the air and liquid loops, respectively. The ultimate heat sinks (ram air, expendable water, and fuel) denoted for the condenser are the heat sinks discussed in Subsystems 2.1C, 2.2 and 2.3. The refrigerant compressor may be driven by any of the auxiliary drive options listed in Subsystem 1.2 for closed loop systems.

The secondary closed air loop in this system parallels the simple air cycle System S2 and the bootstrap air cycle System B5. The refrigerant temperature in the evaporator is regulated to prevent freezing of the water on the air side, thus the water separator options do not include anti-icing. The fan which provides recirculation of the cooling air may be driven by an electric, pneumatic, or hydraulic motor.

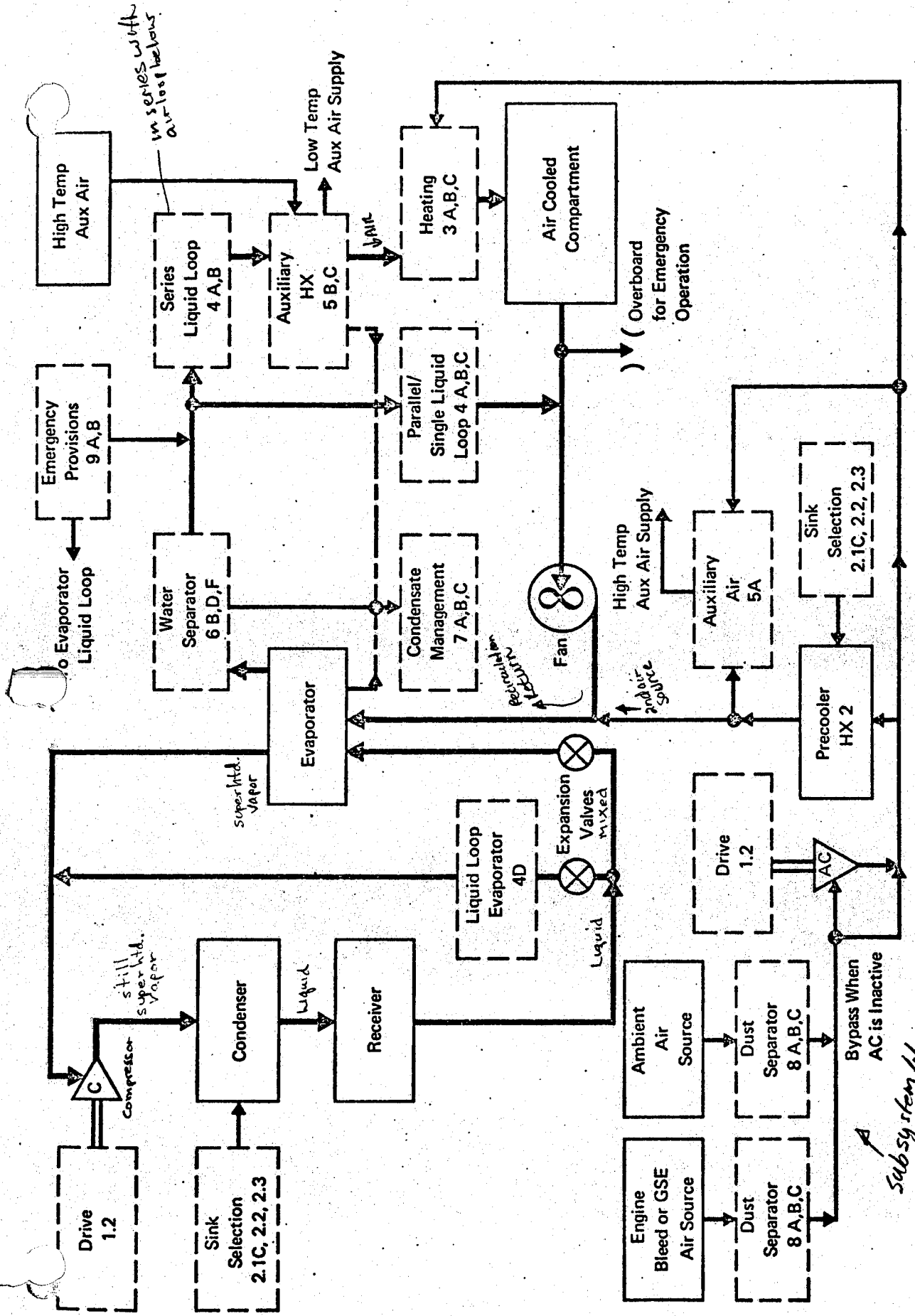


Figure 22 System V1 - Vapor Cycle, Secondary Closed Air Loop

GP 9416-156

High pressure air is supplied to the system by the open loop options of Subsystem 1.1. The precooler HX2 is employed to cool the high temperature auxiliary air supply and the make-up air to the closed loop. Use of the precooler allows the vapor cycle loop to be designed for a lower capacity (i.e., the vapor cycle loop does not have to cool the high temperature auxiliary air supply). The auxiliary air supply requirements can be quite large compared to that of the closed air loop.

Vapor Cycle, Secondary Open Air Loop with High Pressure Water Separator, System V2 - This system is composed of a vapor cycle loop with two parallel evaporators which cool an optional liquid loop and an open air loop independently. (See Figure 23.) The refrigerant loop functions the same as in System V1. Air is supplied to the system as indicated by the open loop options of Subsystem 1.1. The advantage of the precooler (HX2) is the same as in the previous system. The highlight of this system is the application of the high pressure water separator. The water separator located in the air side of the evaporator, where the temperature is low and where high pressure is maintained by the throttling valve, will have excellent water removal capability. As the cooling air passes through the throttling valve, the pressure is reduced to equipment and cabin requirements. After passing through the cooling circuits the air is dumped overboard.

Hybrid Vapor Cycle - Air Cycle, System V3 - This system has a vapor cycle loop which is identical to the two previous vapor cycle systems except for the refrigerant compressor drive. (See Figure 24.) This drive is a cooling turbine in the air loop which shares the air loop cooling load with one of the evaporators. Thus the title, Hybrid Vapor Cycle - Air Cycle, is appropriate. The air loop is supplied by the options of Subsystem 1.1. Air is precooled by HX2 and further cooled in the evaporator where condensate is removed at high pressure. Additional cooling occurs as the air is expanded through the turbine. The air then is circulated through the cooling circuits and dumped overboard, or recirculated in the closed loop version.

The high pressure water separator does not include the anti-ice feature since the inlet air is regulated above freezing via the refrigerant loop control. However, anti-ice is included at the turbine discharge to

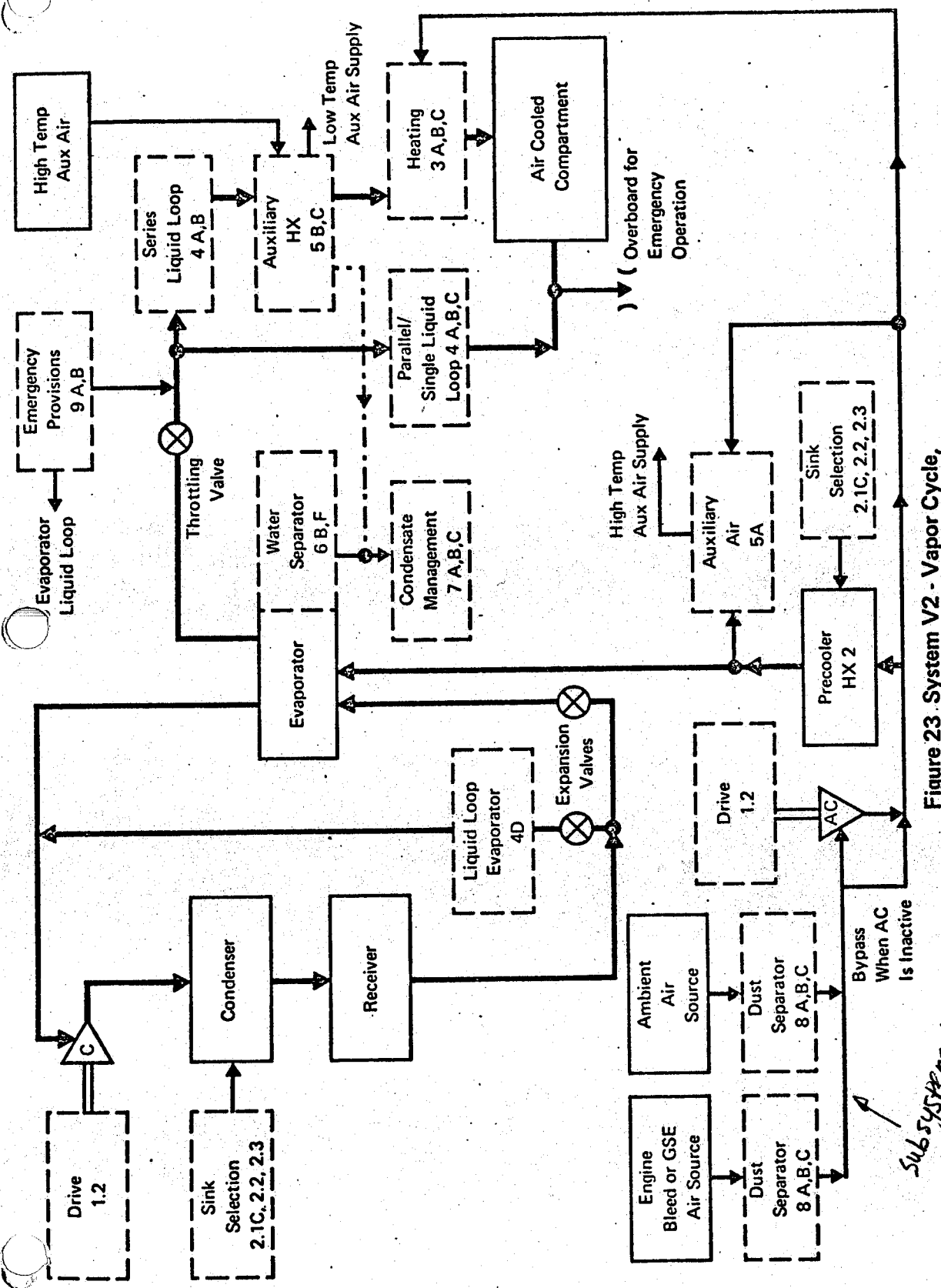


Figure 23 System V2 - Vapor Cycle
Secondary Open Air Loop with High Pressure Water Separator

GP 9416-153

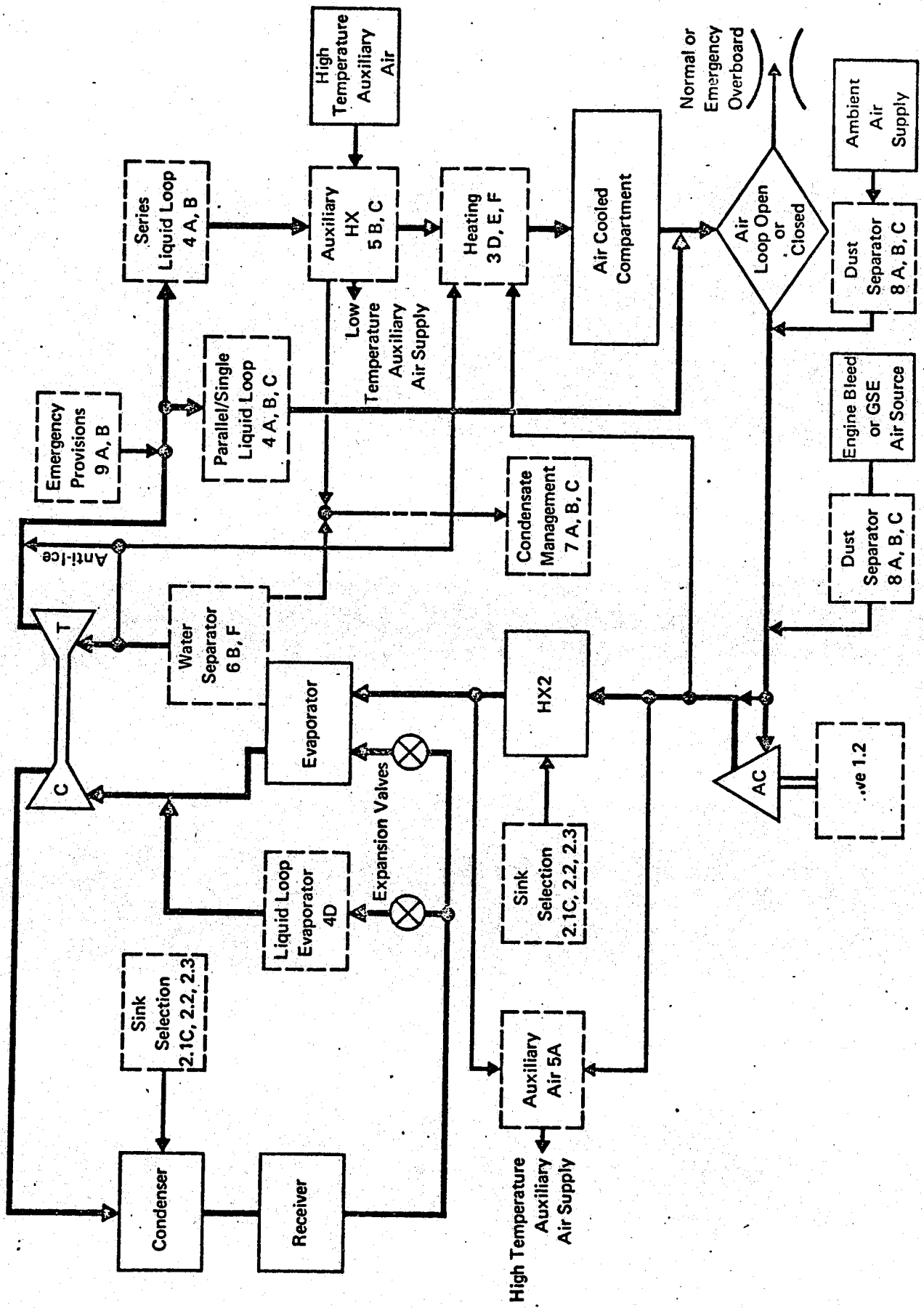


Figure 24 System V3 - Hybrid Vapor Cycle-Air Cycle

prevent icing in the duct or in a downstream heat exchanger. Since water removal occurs upstream of the cooling turbine, the air is dry at this point, and thus, it can be used for temperature regulation of the cooling air as indicated by the heating options.

2.2.4 System Schematic Representation of Inventory Aircraft ECS - The capability of the previously discussed system flow schematics to represent actual aircraft ECS is discussed. The simple air cycle System S1, the bootstrap air cycle System B1, and the vapor cycle System V1 represent the majority of the aircraft ECS investigated. Table III, Sheet 1 includes aircraft ECS that are related in detail to these three systems. A tabulation of other aircraft having ECS represented by the above three systems, and bootstrap air cycle systems B2 and B4 is shown in Sheets 2 and 3 of Table III to show the scope of the investigation. The above five system flow schematics and the remaining five system flow schematics (more typical of advanced systems) provide reasonable alternatives for ECS design selection over the speed-altitude-dynamic pressure flight envelope discussed in Section 2.1.

Adapted System S1 - The open loop version of the simple air cycle represents the F-4C equipment ECS by deleting the unnecessary circuitry and subsystems of System S1, and then selecting the appropriate subsystem options. (See Figure 25.) The F-4C equipment ECS does not contain a water or a dust separator, an ambient air source, a series liquid loop, an auxiliary compressor, or an auxiliary heat exchanger. Hence, these subsystems are deleted from System S1. Selection of the appropriate subsystem options adapts System S1 to represent the F-4C equipment ECS. The subsystems selections are as follows: the engines, or GSE, supply high pressure air to the system; ram air is used as the heat sink at HX2; a parallel liquid loop, which has heating provisions for regulating the temperature of the air servicing the liquid loop to the AWG-9 radar system is used; the same heating option also is provided for the air cooled compartments (these heat loads are considered as one heat load, and air is supplied at a weighted average temperature); auxiliary air is obtained downstream of HX2; GSE refrigerated air is supplied through the emergency ram air duct with the ECS inoperative; ram air is provided for emergency cooling.

This page is blank

Table III Inventory Aircraft ECS Data

Sheet 1

Aircraft	Schematic Application		Zone	Air Source	Sinks	Ice Protection	Components			ECS Performance		Remarks
	No.	Description					Liquid Loop	Water Separator	Ground Operation	Maximum Cooling Capacity (Btu/Hr)		
F-4C	S1	Open Simple Cycle	Equipment	Manifolded Engine Bleed	Ram Air	Supplied from Cabin System for Windshield	Parallel Type for Radar Cooling	None	Ground Cart	45,000	Auxiliary air supplied downstream of primary HX. Hot bleed air is supplied to ram air ejector.	
F-111A	S1	Open Simple Cycle	All	Manifolded Engine Bleed	Water and Ram Air	Windshield Rain Removal, Cowl and Spike	None	With Anti-Ice	Ground Cart	85,000	Two auxiliary HXs (A/A other A/Water). Miscellaneous cooling and pressurization. Water boiler in series with primary HX.	
C-141	S1	Open Simple Cycle (2 Systems)	All	2 Stage Engine Bleed or APU (Manifolded)	Ram Air	Wing Leading Edge	None	With Anti-Ice	APU or Ground Cart	148,000	Both units operate at same level. Conditioned air manifolded. Temperature control with bleed air mix.	
C-9A	B1	Open Bootstrap (2 Systems)	All	2 Stage Engine Bleed or APU (Manifolded)	Ram Air	Wing Leading Edge, Cowl, Empennage	None	With Anti-Ice	APU or Ground Cart	144,000	Both units operate at same level. Conditioned air manifolded. Temperature control with bleed air mix.	
F-111D	B1	Open Bootstrap	All	Manifolded Engine Bleed	Water and Ram Air	Windshield Rain Removal, Cowl and Spike	None	With Anti-Ice	Ground Cart	68,000 (Estimate)	Two auxiliary HXs (A/A other A/Water). Miscellaneous cooling and pressurization. Water boiler in series with secondary HX..	
C-5A	B1	Open Bootstrap (2 Systems)	All	2 Stage Engine Bleed or 2 APUs (Manifolded)	Ram Air	Wing Leading Edge	None	With Anti-Ice	APUs or Ground Cart	309,000	Both units operate at same level. Conditioned air manifolded. Temperature control with bleed air mix.	
F-15	B2	Open Bootstrap - Regenerative	All	Engine Bleed (Manifolded)	Ram Air	Windshield Rain Removal	Series Type for Forward Elec. Cooling	With Anti-Ice	Ground Cart	N.A.	Turbine discharge air used in regenerator.	
DC-8	V1	Open Vapor Cycle (2 Systems)	All	Boosted Ram	Ram Air	Wing Leading Edge, Cowl, Empennage, Windshield - Rain Removal	None	Without Anti-Ice	APU or Ground Cart	324,000	Three turbocompressors supply cabin air.	
RC-135C	V1	Closed Vapor System	Electronics Bay	100% Recirculation	Ram Air	Wing Leading Edge - Air Supplied from Pneumatic System	Parallel Type within Elec. Package	None	Only when Hydraulic Power Available	76,800	100% recirculation with hydraulic driven fan. Cabin system provides pressurization.	
XB-70	-	Closed Hybrid Cycle	All	100% Recirculation Bleed Makeup	Water Ammonia	Windshield Rain Removal	None	Water Trap	Ground Cart	360,000	Ammonia used as expendable heat sink. Cabin and E/E loads on parallel air loops. Vapor cycle uses water as heat sink. Water boiler cools emergency ram air.	

Table III Inventory Aircraft ECS Data

Sheet 2

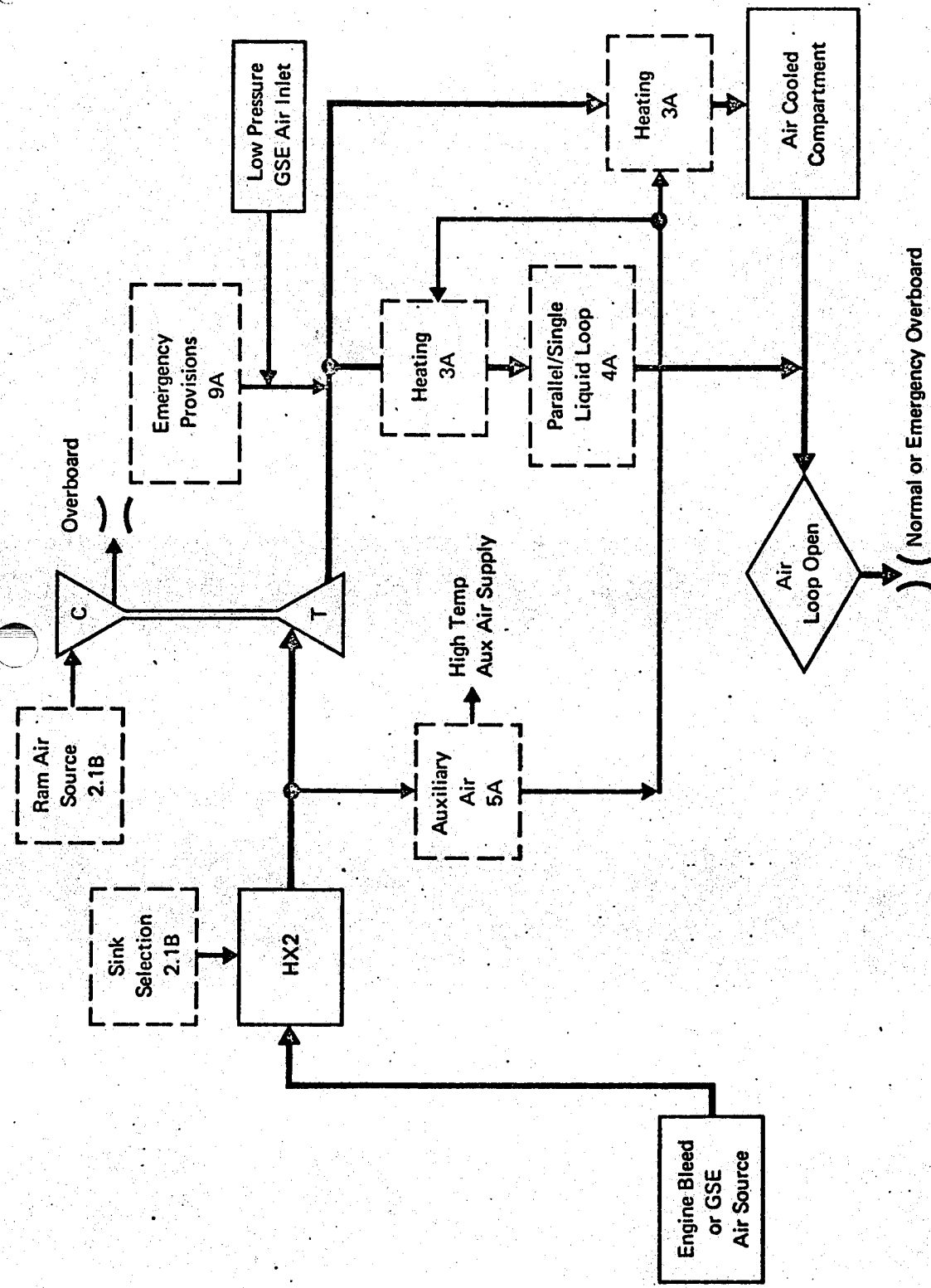
Aircraft No.	Description	Zone	Air Source	Sinks	Components			ECS Performance		Remarks
					Ice Protection	Liquid Loop	Water Separator	Ground Operation	Maximum Cooling Capacity (Btu/Hr)	
F-4C	B1 Open Bootstrap	Cabin	Manifolded Engine Bleed	Ram Air	Windshield Rain Removal	None	Retrofit	Ground Cart	42,000	Rain removal air uses bleed mixed with primary HX exit air. W.S. added on retrofit contract.
A-7D	B1 Open Bootstrap	All	Engine Bleed	Ram Air	Windshield Rain Removal	None	With Anti-Ice	Ground Cart	N.A.	Low pressure bleed used for rain removal air.
F-14	B1 Open Bootstrap	All	Manifolded Engine Bleed	Ram Air	Windshield Rain Removal	Parallel Type for E/E Cooling	With Anti-Ice	Ground Cart	N.A.	Liquid loop used in addition to air for E/E cooling.
F-5	S1 Open Simple Cycle	All	Manifolded Engine Bleed	Ram Air	Windshield Rain Removal	None	With Anti-Ice	Ground Cart	39,000	E/E cooled with cabin exhaust air.
F-101A	S1 Open Simple Cycle	All	Manifolded Engine Bleed	Ram Air	Windshield Rain Removal	None	None	Ground Cart	21,000	E/E cooled with ram air.
F-101B	S1 Open Simple Cycle (2 Systems)	Cabin/ Equipment	Manifolded Engine Bleed	Ram Air	Windshield Rain Removal	None	None	Ground Cart	34,500	Cabin air is filtered. Both units share same primary HX.
F-105	S1 Open Simple Cycle (2 Systems)	Cabin/ Equipment	Engine Bleed	Ram Air	Windshield Rain Removal	None	None	Ground Cart	35,400	Equipment 35,400
F-104	S1 Open Simple Cycle	All	Manifolded Engine Bleed	Water Ram Air	Windshield Rain Removal	None	With Anti-Ice	Ground Cart	24,700	Ground blower used for E/E cooling.
F-106	S1 Open Simple Cycle	All	Manifolded Engine Bleed	Ram Air	Windshield Rain Removal	None	With Anti-Ice	Ground Cart	27,500	Precooler external to ECS pack. Water boiler in series with primary HX.
A-37	S1 Open Simple Cycle.	All	Manifolded Engine Bleed	Ram Air	Windshield Defogging	None	With Anti-Ice	With Engines Only	36,900	E/E cooling on parallel air loop.
S-3A	S1 Open Simple Cycle	All	Manifolded Engine Bleed	Ram Air	Wing Leading Edge	None	With Anti-Ice	Ground Cart	N.A.	A very simple system.
P-1127	B1 Open Bootstrap Cabin		Engine Bleed	Ram Air	Windshield Defogging	None	With Anti-Ice	APU or Ground Cart	18 lb/min	Cabin exhaust used for E/E cooling.
	S1 Open Simple Equipment				None		None		30 lb/min	Ram air cooling for forward E/E. Ground blowers for E/E coolers.
										Single stage bleed air supply. All air is filtered.

GP 9416-186

Table III Inventory Aircraft ECS Data
Sheet 3

Aircraft	No.	Description	Zone	Air Source	Sinks	Components			ECS Performance		Remarks
						Ice Protection	Liquid Loop	Water Separator	Ground Operation	Maximum Cooling Capacity (Btu/Hr)	
C-133	S1	Open Simple Cycle (2 Systems)	All	Manifolded Engine Bleed	Ram Air	Wing Leading Edge and Empennage	None	With Anti-Ice	Ground Cart	113,000	Two-stage operation of precoolers. Precooled air to ECS units.
C-140	S1	Open Simple Cycle (2 Systems)	All	Manifolded Engine Bleed	Ram Air	Windshield Defogging	None	With Anti-Ice	Ground Cart	25,000	Commercial version has vapor cycle unit for ground operation.
B-52H	S1	Open Simple Cycle (2 Systems)	Forward Cabin	Manifolded Engine Bleed	Ram Air	Nacelles and Wing Leading Edge	None	With Anti-Ice	Ground Cart	57,600	Cabin air is filtered. Precooler with ejector in pod.
B-58	B1	Open Bootstrap (2 Systems)	All	Manifolded Engine Bleed	Water	Nacelles and Ram Air	None	With Anti-Ice	Ground Cart	165,200	Only inboard engines supply bleed air. Water boiler in series with secondary A/A HX.
KC-135	B1	Open Bootstrap	Main and Crew Cabin	Manifolded Engine Bleed	Ram Air	Wing Leading Edge	None	With Anti-Ice	Ground Cart	128,000 (Estimate)	Mid-stage bleed air.
2707 (SST)	B2	Open Simple-Bootstrap Regenerative	All	Manifolded Engine Bleed	Ram Air Fuel	Forebody Defogging	Series Type	With Anti-Ice	APU or Ground Cart	675,000 (Estimate)	Regenerative HX in series with primary HXs. Liquid loop between fuel and air. Four systems basic - 3 systems on prototype. Ram air is alternate sink for liquid loop.
DC-10	B4	Open Simple-Bootstrap (3 Systems)	All	2 Stage Engine Bleed or APU (Manifolded)	Ram Air	Wing Leading Edge	None	With Anti-Ice	APU or Ground Cart	218,000	Three-wheel cooling turbine. All systems operate at same level. Temperature control with bleed air mix (all zones).
747	B4	Open Simple-Bootstrap (3 Systems)	All	2 Stage Engine Bleed or APU (Manifolded)	Ram Air	Wing Leading Edge	None	With Anti-Ice	APU or Ground Cart	315,000	Three-wheel cooling turbine. All systems operate at same level. Temperature control with bleed air mix (all zones).
Cessna 500	B4	Open Simple-Bootstrap	All	Manifolded Engine Bleed	Ram Air	Windshield Defogging	None	With Anti-Ice	With Engines Only	24,000	Bleed air used for temperature control.
L-1011	B4	Open Simple-Bootstrap (3 Systems)	All	Manifolded Engine Bleed	Ram Air	Wing Leading Edge	None	With Anti-Ice	APU or Ground Cart	N.A.	Three-wheel cooling turbine. All systems operate at same level. Temperature control with bleed air mix (all zones).
880	V1	Open Vapor Cycle Recirculating (2 Systems)	All	Boosted Ram	Ram Air	Wing Leading Edge	None	None	Ground Cart	215,000 (Estimate)	Two turbo compressors boost ram for two vapor cycle units. Optional electrical or pneumatic drive.
B-52	V1	Closed Vapor Cycle	Missile	Manifolded Engine Bleed	Ram Air	None	None	None	L.P. Ground Cart	N.A.	Bleed air used for makeup in closed loop.

Figure 25 Adapted System S1 - Simple Air Cycle Representing the F-4C Equipment ECS



Other aircraft that utilize simple air cycle ECS (such as the F-111A and the C-141) can be represented by System S1 by following the above deletion and subsystem selection procedure. These aircraft ECS depict the flexibility of System S1, since they contain several components not used on the F-4C. For example, the F-111A has a water boiler (Subsystem 2.2A without bleed air ejector), a water separator (Subsystem 6A), and auxiliary heat exchanger (Subsystem 5). The C-141 uses two parallel systems and an APU which supplies bleed air for ground operation.

Adapted System B1 - Bootstrap air cycle System B1 represents the C-9A ECS. Unnecessary subsystems and circuitry are deleted, and selection of the appropriate options from the remaining subsystems are shown in Figure 26. Deletion of the liquid loop, the auxiliary heat exchanger, the dust separator, the ambient air source, and the auxiliary compressor generates the system flow schematic for the C-9A ECS. Ram air is used as the heat sink (Subsystem 2.1C with fan) for each of the two identical C-9A systems provides agreement with the actual system. Auxiliary air is obtained upstream of HX2 (Subsystem 5A). Heating of the air cooled compartment is provided by mixing bleed air with conditioned air. Condensate from the water separator is drained overboard. Engine bleed or APU air is supplied for ground or altitude operation, with a provision for using GSE air supply in the emergency ram air ducting. These subsystem selections make System B1 representative of the C-9A.

There are many aircraft which use a bootstrap air cycle ECS, most of which can be adapted to System B1. The F-111D and C-5A can be represented by System B1 when the proper deletions and subsystems are considered, as was done for the C-9A. These aircraft use the same components as employed in the C-9A ECS. The F-111D also has a water boiler (Subsystem 2.2A) and an auxiliary heat exchanger (Subsystem 5). The C-5A uses two identical systems with two APU's.

Adapted System V1 - Vapor cycle ECS, such as System V1, have had more application on commercial than on military aircraft. Therefore, vapor cycle System V1 is adapted to the DC-8 ECS configuration by deleting unnecessary circuits and subsystems, and selecting the appropriate options of the remaining subsystems (shown in Figure 27). The DC-8 was one of the two proposed Air Force AWACS aircraft, hence the DC-8

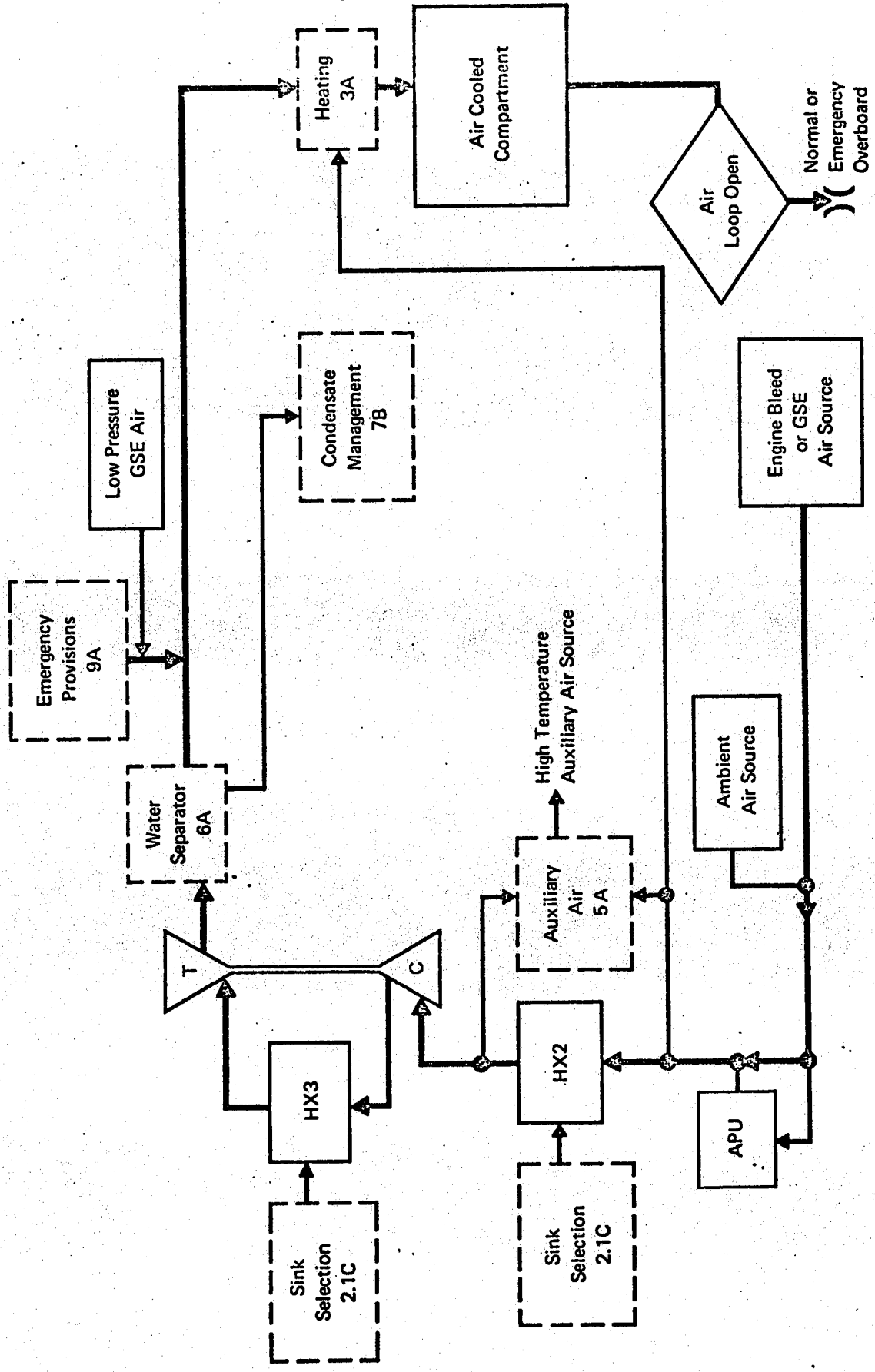


Figure 26 Adapted System B1 - Bootstrap Air Cycle Representing the C-9A ECS

GP 9416-154

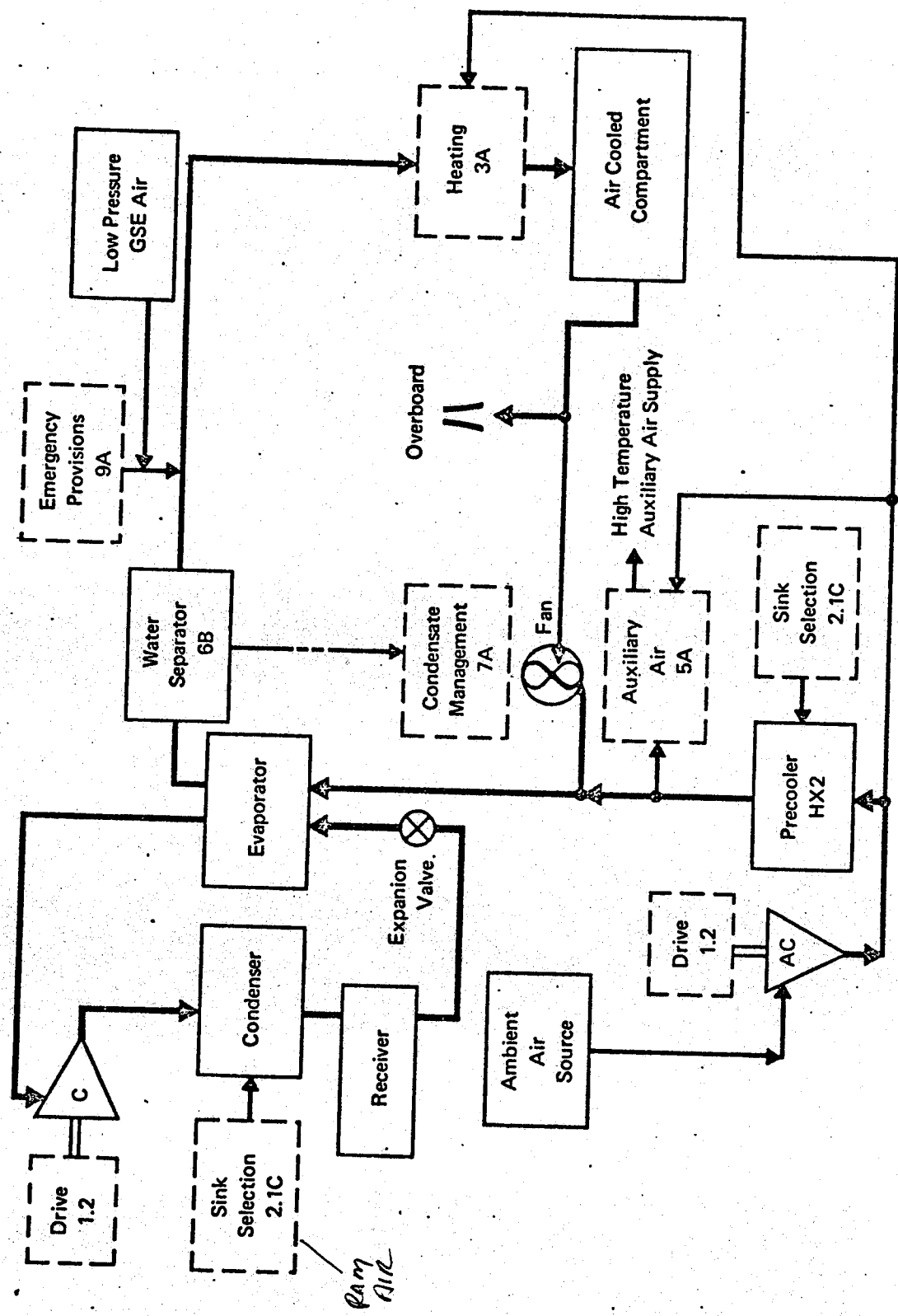


Figure 27 Adapted System V1-Vapor Cycle Representing the DC-8 ECS

ECS represents a possible military application. The DC-8 ECS configuration is obtained by deleting the dust separator, the liquid loop (in the air or refrigerant loop), and the auxiliary heat exchanger from System VI. This system is made representative of the DC-8 ECS by selecting the appropriate subsystem options shown. These subsystem options are: use of air turbine driven auxiliary air and Freon compressors, use of ram air as the heat sink, draining the condensate into the ram air to increase its heat sink capability, heating is provided for the air cooled compartment by mixing auxiliary compressor air with conditioned air. Use of ambient air as the air source completes the adaptation required to make System VI representative of the DC-8 ECS.

The RC-135 also uses a vapor cycle for equipment cooling. Subsystem options considered in the DC-8 ECS are used on the RC-135 ECS with the exception of the auxiliary air compressor. The RC-135 air loop is closed and includes parallel liquid loops for electronic equipment cooling. Make-up air is supplied from the cabin bootstrap ECS. The B-52 has a vapor cycle system which utilizes two parallel evaporators to cool missiles.

2.3 Reference Simple Air Cycle System

A flow schematic showing both components and controls is described in this section. This "reference" system is the base for the relative reliability and cost data presented in Section 4.

The Reference Simple Air Cycle System provides conditioned air to an air cooled load of a fighter aircraft. A flow schematic is shown in Figure 28.

2.3.1 System Operation - Bleed air is extracted from the jet engine compressors and is ducted to the simple air cycle system. Appropriate check and shutoff valves are in this duct. The bleed air is cooled by an air to air heat exchanger (7), passes through a pressure regulating and shutoff valve (12), expands through a turbine (14), and flows through the water separator (23) to the load. Some of the bleed air may bypass the turbine to mix with cold turbine discharge air, hence prevent freezing of liquid water which is delivered by the turbine. Bleed air from upstream of the turbine may be mixed with water separator exit air to provide air at a temperature determined by the temperature control system.

The air temperature is controlled to a dual temperature schedule which is switched at an altitude of 25,000 feet. Below 25,000 feet an

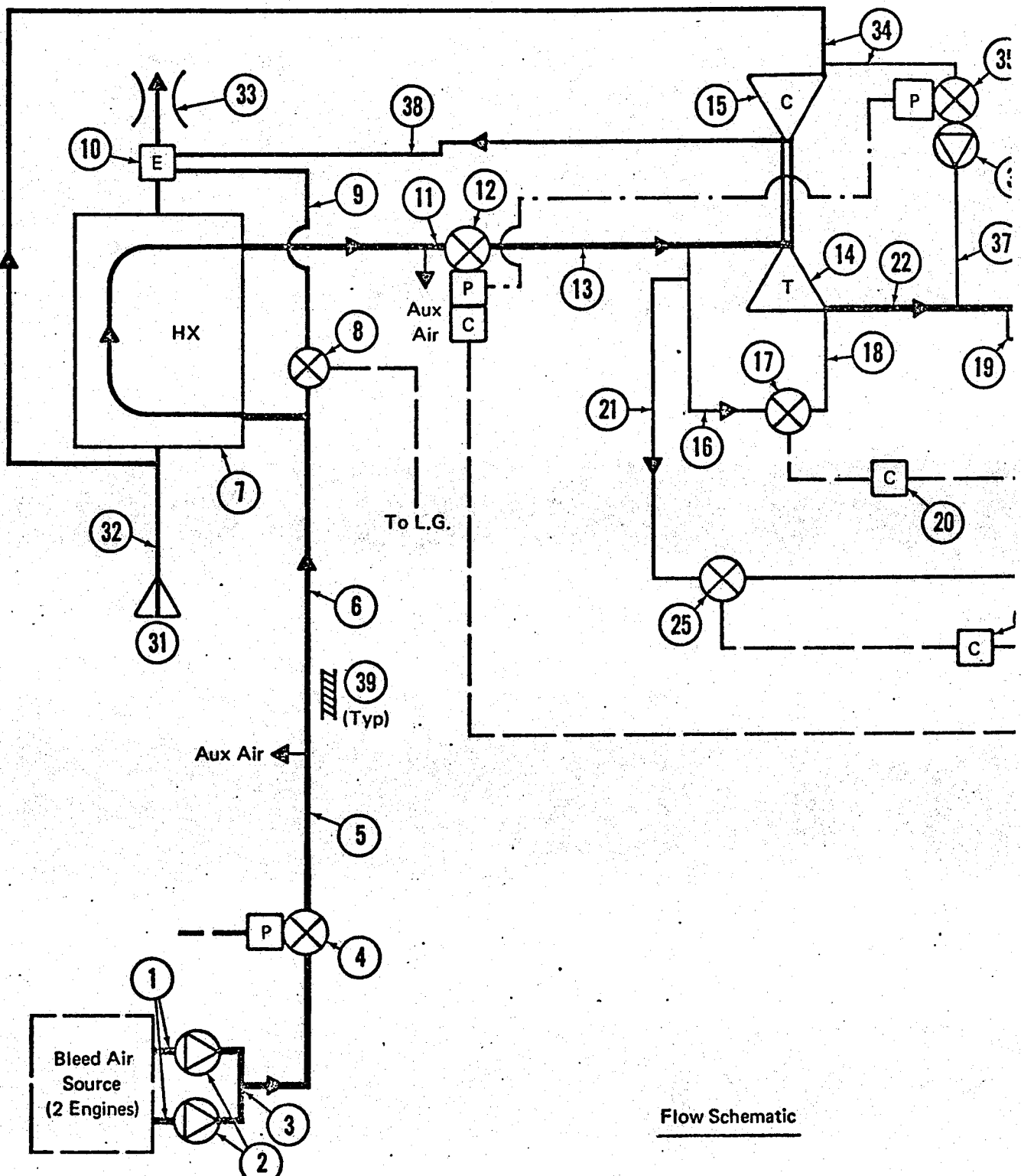
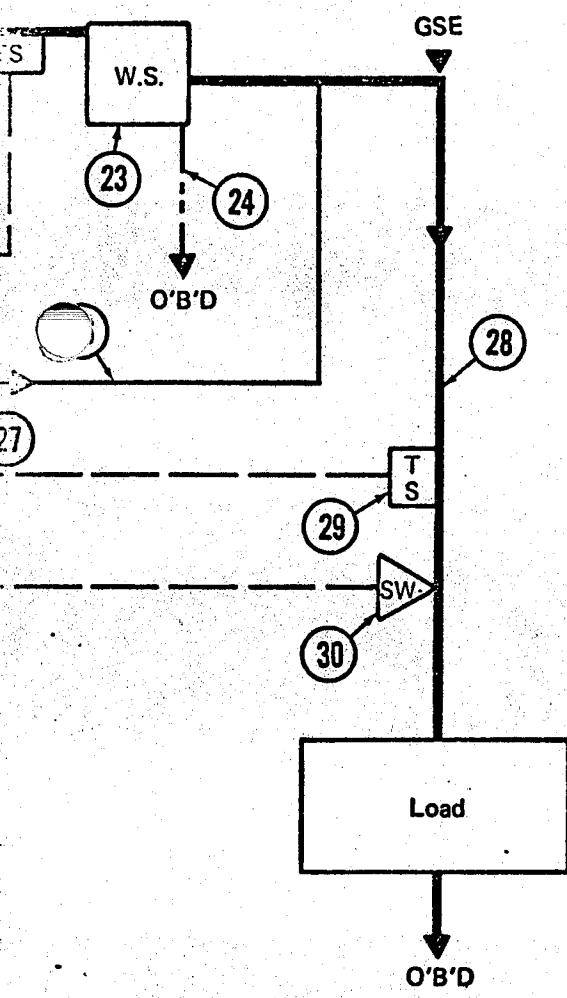


Figure 28 Reference Simple Air Cycle System

Component List

Nomenclature:

— Air Flow (Main Flow Heavy)
 - - - Pneumatic Control
 - - - Water
 - - - Electrical



Item	Name
1	Duct (2), Engine Manifold
2	Valve (2), Check, Bleed Air
3	Duct, Wye, Bleed Air
4	Valve, Shutoff, Bleed Air
5	Duct, Bleed Air (with "T")
6	Duct, Bleed Air (with "T")
7	Heat Exchanger, Air to Air
8	Valve, Shutoff, Ejector
9	Duct, Ejector, Bleed Air
10	Ejector Compressor Air/Bleed Air
11	Duct, Heat Exchanger Outlet, Bleed Air
12	Valve, Pressure Regulating and Shutoff
13	Duct, "T" Section
14	Turbine
15	Compressor
16	Duct, "T" Section
17	Valve, Modulating, Anti-Ice
18	Duct, "T" Section and Mixing Muff
19	Sensor, Temperature, Anti-Ice
20	Controller, Temperature, Anti-Ice
21	Duct, Bypass, Temperature Control
22	Duct, Water Separator Inlet with "T" Section
23	Water Separator
24	Line, Water Drain
25	Valve, Bypass, Hot Air
26	Duct, Bypass, Hot Air
27	Controller, Temperature
28	Duct, Conditioned Air
29	Sensor, Temperature
30	Switch, Limit, Temperature
31	Inlet, Ram Air
32	Diffuser, Ram Air
33	Outlet, Ram Air
34	Duct, Bypass, Ram Air, with "T" Section
35	Valve, Shutoff, Emergency, Ram Air
36	Valve, Check, Ram Air
37	Duct, Ram Air
38	Duct, Outlet, Compressor
39	Insulation, Bleed Air Duct

65°F delivery temperature is obtained, and above 25,000 feet a 40°F delivery temperature is obtained. This is accomplished via operation of the bypass valve (25). The anti-ice control (20) for the water separator controls to 35°F below 25,000 feet. The shutoff function of valve (12) is dependent on a signal from the temperature limit switch (30). Nominally 35 pounds of air per minute flow to the air cooled load below 25,000 feet.

Bleed air for auxiliary air use is obtained upstream of the air to air heat exchanger (7), and between the air to air heat exchanger and the pressure regulator and shutoff valve (12). A maximum of 480 pounds per minute is obtained at the former location (sea level condition), and five pounds per minute at the latter location.

Ram air enters the external scoop inlet (31). Part of this air is ducted through the air to air heat exchanger and then flows through the ejector (10) prior to discharge overboard through the ram air outlet and part of the ram air is ducted to the compressor. The ejector induces ram air flow through the heat exchanger, particularly at low ram air pressures during static operations.

2.3.2 Components - Further descriptions of several components are presented.

Air to Air Heat Exchanger (7) - This heat exchanger is a stainless steel two-pass cross-flow plate-fin type.

Pressure Regulating and Shutoff Valve (12) - This is a stainless steel butterfly valve. It is positioned by a pneumatic actuator to limit the downstream pressure to a maximum of 105 psig. It also may be closed when the integral solenoid is de-energized.

Turbine - Compressor (14-15) - The turbine and compressor are radial flow designs. Work of expanding the bleed air is transmitted to the compressor via a common shaft. This work is absorbed by the ram air as it is compressed. The turbine exhaust contains a "muff" in which hot bleed air is mixed with cold turbine discharge air for control of the air temperature to the water separator. Maximum pressure ratio across the turbine is approximately 12. Maximum pressure ratio of the compressor is 1.2.

Water Separator (23) - The water separator contains a coalescer (to enlarge the very small water droplets in the turbine discharge air at high

humidity conditions), swirl vanes (which cause the large water droplets to move outward), and a collector section (to remove the water). It contains an internal relief valve.

Ejector (10) - A dual compressor air/bleed air multi-nozzle ejector is located in the heat exchanger outlet. The shutoff valve (8) in the bleed air line is closed by a signal indicating that the landing gear are retracted.

Ram Air Shutoff Valve (35) - This is a pneumatically actuated normally closed valve. The actuation pressure is obtained from the pressure regulating and shutoff valve (12).

SECTION 3

COMPONENT DESIGNS

Detail design information necessary to obtain the performance, weight, and volume, of the various components that comprise the environmental control system designs, are presented. Weight and volume are presented for system controls. Typical system controls for the systems of Section 2 are illustrated. Transient performance of system controls is not presented since the component design information is to be utilized for steady state performance analyses only.

The analytical methods for determining component performance, weight and volume, are based on state-of-the-art component data and standard design practices. These methods reflect knowledge of currently operating aircraft and of some aircraft in the development phase. Each of the component analysis methods are compatible with its use in the ECS computer program. The performance analysis methods of each component are presented first, followed by sizing and weight analyses. The performance data that are used in the sizing and weight analyses are flow rate and the state properties: temperature, pressure, and humidity (for air) of the working fluids.

Data for the following components are presented:

Heat Exchangers (Air, Liquid, Water)

Air Cycle Machines (Turbines, Compressors, Fans)

Water Separators

Dust Separators

Fans (Constant Speed)

Pump Packages (for Liquid Coolant Loops)

Vapor Cycle Components (Compressors, Evaporators, Condensers)

Auxiliary Air Sources (APU's and Compressors)

Power Drives

Plumbing (Ducting, Inlets, Outlets, Ejectors, Valves)

Insulation

System Controls (Temperature, Pressure)

3.1 Heat Exchangers

Development of compact heat transfer surfaces during the past 15 years has provided heat exchanger designs that satisfy the stringent performance and installation requirements of environmental control systems. This investigation into heat exchanger design involves determining component performance, volume, and weight. The heat transfer between two fluid streams separated by a known boundary (heat transfer surface), and the fluid friction between each fluid and the heat transfer surface are described. Both single and two phase fluid flow are considered. Single phase flow refers to heat transfer between two air streams, an air and a liquid stream, two liquid streams, or air and an electric heater. Two phase flow refers to a phase change on one side only, such as in a water boiler. For the case of condensing liquids, as in a high pressure water separator, a single phase analysis approach with consideration for the subtraction of water in the overall energy balance is used.

Analysis methods to determine performance are presented by describing the heat transfer and pressure effects of the heat exchanger with respect to flow rates. Heat transfer surface performance is specified by the use of effectiveness maps. Pressure drop versus flow rate data are generated for each side of the heat exchanger.

The core volume is based on that arrangement of the required heat transfer area which also satisfies the imposed pressure drop restrictions. Volume is described by the dimensions of the core. Weight is determined from the density of the particular core construction technique and materials used. Examples for heat exchanger sizing are found in Volumes II, III, and IV.

3.1.1 General Heat Exchanger Design - Heat exchanger design involves definition of the friction of the fluid streams, definition of the heat transfer between the streams, and definition of the volume and weight of given heat transfer surfaces that satisfy the defined heat transfer and fluid friction conditions. The heat exchanger core design is considered to be cross flow utilizing plate fin construction, as shown in Figure 29. This design is used most often for heat exchanger designs in all types of aircraft ECS. Figure 29 shows the fluid flowing from left to right. The cross flow fluid is normal to the page through the cross-hatched areas. A view of the cross flow section of the heat exchanger also could be represented by Figure 29.

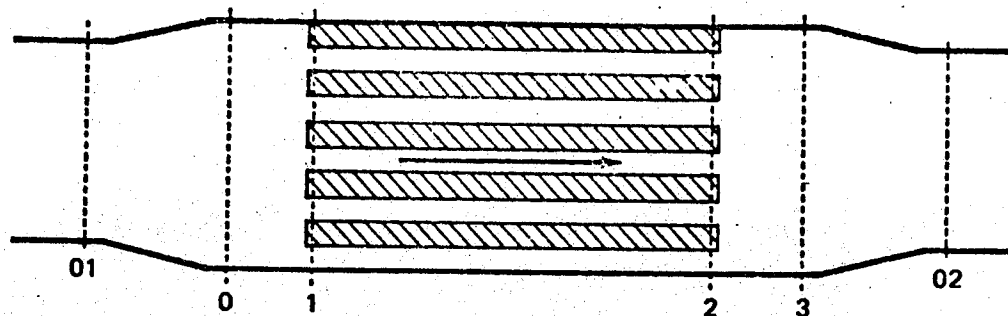


Figure 29 Typical Cross Flow Heat Exchanger

GP 9416-106

Heat transfer occurs between the two fluids within the heat exchanger core, locations 1 to 2. Pressure drops are considered through the heat exchanger (locations 0 to 3) and through the headers (locations 01 to 0 and 3 to 02).

Two equations governing the overall pressure drop in the exchanger are developed, beginning with a force-momentum balance on the fluid in a single heat exchanger duct. Then end effects are added. After some simplifications are made, the equations are denoted as being two of five basic heat exchanger equations. The approach presented is derived from Reference 4.

Consider a constant area duct of arbitrary cross-sectional area (A') and total surface area inside the duct (A). (See Figure 30.) A force balance is made assuming steady flow conditions, with $\frac{d}{d\theta}$ denoting derivative with respect to time. (P has units of lb/ft^2 .)

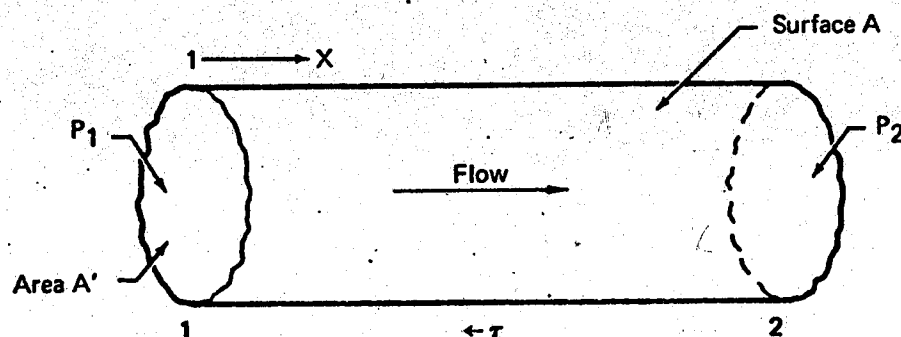


Figure 30 General Flow Through A Duct

GP 9416-123

$$\Sigma F_x = \frac{d \text{ MOM}_x}{d\theta} \quad (1)$$

$$\Sigma F_x = (P_1 - P_2)A' - \tau A \quad (2)$$

$$\frac{d \text{ MOM}_x}{d\theta} = G(v'_2 - v'_1)A' \quad (\text{where } G = \frac{V'}{v}) \quad (3)$$

$$(P_1 - P_2)A' - \tau A = \frac{G}{g_c} (v'_2 - v'_1)A' \quad (4)$$

$$\Delta P = \tau \frac{A}{A'} + \frac{G}{g_c} (v'_2 - v'_1) \quad (5)$$

The shear stress is related to the friction factor (f):

$$\tau = f \rho \frac{(V')^2}{2g_c} \quad (6)$$

hence:

$$\Delta P = \left[\frac{1}{2} \rho (V')^2 \frac{A}{A'} f + G(v'_2 - v'_1) \right] \frac{1}{g_c} \quad (7)$$

v' - fluid velocity

An overall surface shear stress is considered and a uniform wall heat flux is assumed. An average velocity, $V'_{ave} = \frac{V'_1 + V'_2}{2}$, also is used.

$$\rho (V'_{ave})^2 = G V'_{ave} = G \frac{V'_1 + V'_2}{2} = G \frac{Gv_1 + Gv_2}{2} = G^2 v'_{ave} \quad (8)$$

Likewise:

$$G(v'_2 - v'_1) = G(Gv_2 - Gv_1) = G^2(v_2 - v_1) \quad (9)$$

Substituting into Equation (7):

$$\Delta P = \left[\frac{1}{2} f G^2 v'_{ave} \frac{A}{A'} + G^2 (v_2 - v_1) \right] \frac{1}{g_c} \quad (10)$$

Consider a multipass heat exchanger made of ducts as shown in Figure 31.

For the hot fluid, neglecting the plate and fin thickness, the free flow cross-sectional area is: $A'_{H,fr} = \frac{n_H b_{TH} L_C}{N_{PH}}$

$$A'_{H,fr} = \frac{n_H b_{TH} L_C}{N_{PH}} \quad (11)$$

$n_H = \# \text{ flow layers of hot fluid}$
 $b_T = \text{fin height}$
 $L_C = \text{width}$
 $N_p = \# \text{ flow passes}$

where n is number of flow layers for one fluid and N_p is number of flow passes for one fluid. The total frontal area (A_{frH}) is:

$$A_{frH} = \frac{L_C L_n}{N_{PH}} = \frac{A_{eH}}{N_{PH}} \quad (12)$$

frontal
 flow path
 of hot fluid

$\beta = \frac{\text{total heat transfer area of one side}}{\text{volume between plates of the side}}$

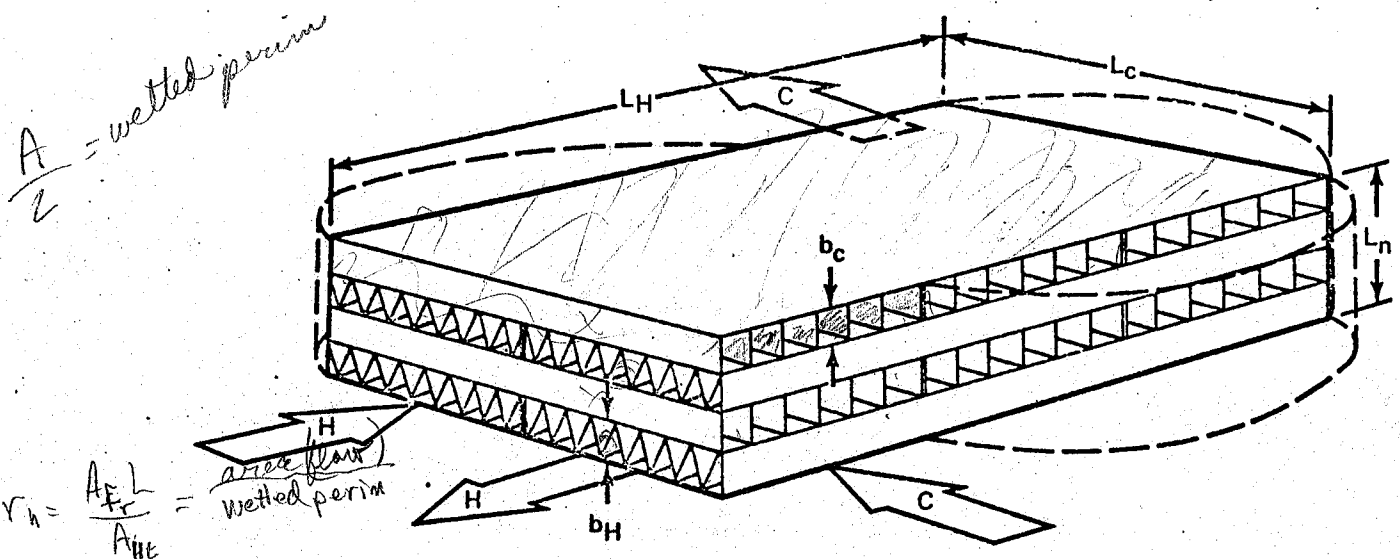


Figure 31 Multipass Heat Exchanger

GP 9416-122

Define the nondimensional area ratio ψ_H :

$$\text{same as } \psi_H = \frac{A'_H}{A_{frH}} = \frac{b_{TH} \beta_H r_{H} H}{b_{TH} + b_{TC} + 2t_{SP}} = \frac{\text{free flow area}}{\text{total frontal area}} = \frac{\% \text{ flow area}}{\text{plate thickness}} \quad (13)$$

Similar expressions are obtained for the cold fluid ducts.

The pressure changes between points 0 and 01 and between points 02 and 3 in Figure 29 are due to area changes alone. Assuming constant local density, these pressure changes can be written as:

$$\Delta P_E = P_0 - P_{01} = \frac{1}{2g_c} \rho_0 \left[(v'_{01})^2 - (v'_{00})^2 \right] = \frac{1}{2g_c} \rho_{01} (v'_{01})^2 \left(1 - \frac{(v'_{00})^2}{(v'_{01})^2} \right) \quad (14)$$

$$P_X = P_{02} - P_3 = \frac{1}{2g_c} \rho_2 \left[(v'_{02})^2 - (v'_{03})^2 \right] = - \frac{1}{2g_c} \rho_{02} (v'_{02})^2 \left(1 - \frac{(v'_{03})^2}{(v'_{02})^2} \right) \quad (15)$$

For continuity:

$$\frac{v'_{00}}{v'_{01}} = \frac{A'}{A_{fr}} = \frac{V'_{01}}{V'_{02}} = \psi \quad (\text{hot or cold fluid}) \quad (16)$$

hence:

$$\Delta P_E = \frac{1}{2g_c} \rho_{01} (v'_{01})^2 (1 - \psi^2) \quad \text{and} \quad \Delta P_X = - \frac{1}{2g_c} \rho_{02} (v'_{02})^2 (1 - \psi^2) \quad (17)$$

Irreversible pressure changes also occur in the entrance and exit.

$$\Delta P_{IRE} = K_{tE} \frac{1}{2g_c} p_1 (v'_1)^2 \text{ and } \Delta P_{IRX} = K_{tX} \frac{1}{2g_c} p_2 (v'_2)^2. \quad (18)$$

irreversible entrance *irreversible exit*

The total entrance and exit pressure change is:

$$\begin{aligned} \Delta P_{EX} &= \Delta P_E + \Delta P_{IRE} + \Delta P_{IRX} + \Delta P_X \\ &= \frac{1}{2g_c} p_1 (v'_1)^2 (1 - \psi^2 + K_{tE}) - \frac{1}{2g_c} p_2 (v'_2)^2 (1 - \psi^2 - K_{tX}) \end{aligned} \quad (19)$$

or in terms of G and v :

$$\Delta P_{EX} = \frac{1}{2g_c} G^2 v_1 [(1 - \psi^2 + K_{tE}) - (1 - \psi^2 - K_{tX}) \frac{v_2}{v_1}] \quad (20)$$

The overall pressure drop is:

$$\Delta P = \frac{1}{2g_c} G^2 v_1 \left[(1 - \psi^2 + K_{tE}) + f \frac{v_{ave}}{v_1} \frac{A'}{A} + 2 \left(\frac{v_2}{v_1} - 1 \right) - (1 - \psi^2 - K_{tX}) \frac{v_2}{v_1} \right] \quad (21)$$

eq. 10 *shear area*
open flow area = A'

where A' and A now represent the combined areas for all ducts on one flow side. Entrance and exit effects are small compared to the core pressure drop, hence K_{tE} and K_{tX} may be neglected. (See Reference 5.) Additional arrangement yields:

$$\Delta P = \frac{1}{2g_c} G^2 v_1 \left[\frac{1}{2} f \frac{A}{A'} \left(\frac{v_2}{v_1} + 1 \right) + \left(\frac{v_2}{v_1} - 1 \right) (1 + \psi^2) \right] \quad (22)$$

Dividing by $\frac{1}{2g_c} G^2 v_1 (1 + \psi^2)$:

$$\frac{2\Delta P g_c}{G^2 v_1 (1 + \psi^2)} = \frac{1}{2} \left[f \frac{A}{(1 + \psi^2) A'} \left(\frac{v_2}{v_1} + 1 \right) \right] + \frac{v_2}{v_1} - 1 \quad (23)$$

$r_H = \frac{A}{A'} L N_p$

The hydraulic radius (r_h) is defined as follows:

$$\frac{L}{r_h} = \frac{A' N_p}{A} \quad r_h = \frac{A' L}{A} N_p \quad \frac{D_H}{4} \quad \begin{matrix} A' - \text{cross section open flow area, each flow path?} \\ A - \text{shear area, each flow path?} \\ L - \text{length} \end{matrix} \quad (24)$$

and the Reynolds number is:

$$Re = 4r_h G/\mu = 4r_h \frac{\rho V_{el}}{\mu}$$

Equation (23) is rewritten to introduce r_h and Re :

$$\frac{32 r_h^2 \Delta P g_c}{Re^2 \mu^2 v_1 (1 + \psi^2)} = \frac{L f N_p}{2r_h (1 + \psi^2)} \left(\frac{v_2}{v_1} + 1 \right) + \frac{v_2}{v_1} - 1 \quad (26)$$

This pressure drop for the hot fluid and for the cold fluid represents two of the five basic heat exchanger equations.

Heat Transfer - It is assumed that the flow from position 01 to position 1 and from position 2 to position 02 (Figure 29) is isothermal, and the thermal resistance of the plate separating the hot and cold fluids is negligible. The two fluids have temperatures T_H and T_C , surface areas A_H and A_C , heat transfer coefficients h_H and h_C , total surface temperature effectiveness ϵ_{OH} and ϵ_{OC} , and the separation plate temperature (T_{SP}) is uniform throughout the plate thickness at any location. These facts are used to find the overall heat transfer coefficient (U).

The energy balance equations for each fluid, and for the overall system are:

$$Q'_H = h_H A_H (T_H - T_{SP}) \epsilon_{OH} \quad \text{heat energy overall eff. hot side} \quad (27)$$

$$Q'_C = h_C A_C (T_{SP} - T_C) \epsilon_{OC} \quad \text{separation plate} \quad (28)$$

$$Q'_W = (UA) (T_H - T_C) \quad \text{overall YES} \quad (29)$$

Combining these equations:

$$T_H - T_C = \frac{Q'_W}{(UA)} = \frac{Q'_H}{h_H A_H \epsilon_{OH}} + \frac{Q'_C}{h_C A_C \epsilon_{OC}} = (T_H - T_{SP}) + (T_{SP} - T_C) \quad (30)$$

For steady state heat transfer, $Q'_W = Q'_H = Q'_C$, and:

$$\frac{1}{(UA)} = \frac{1}{h_H A_H \epsilon_{OH}} + \frac{1}{h_C A_C \epsilon_{OC}} \quad (31)$$

The Number of Transfer Units is defined as:

$$NTU = \frac{(UA)}{(W_c)_p \min} \quad (UA) = (UA)_{cold} = (UA)_{hot} \quad (32)$$

This expression is a non-dimensional form of the "heat transfer size" of the heat exchanger. Using this definition, Equation (31) is rewritten:

$$\frac{1}{(NTU) (W_c)_p \min} = \frac{1}{h_H A_H \epsilon_{OH}} + \frac{1}{h_C A_C \epsilon_{OC}} \quad (33)$$

The heat exchanger effectiveness is defined as:

$$\epsilon = \frac{(W_c)_H (T_{H1} - T_{H2})}{(W_c)_p \min (T_{H1} - T_{C1})} = \frac{(W_c)_C (T_{C2} - T_{C1})}{(W_c)_p \min (T_{H1} - T_{C1})} \quad (34)$$

This is a general heat transfer effectiveness and is not a "temperature effectiveness," where $(W_c)_H$ or $(W_c)_C$ would equal $(W_c)_p \min$.

The overall fin effectiveness is defined by:

$$\epsilon_{OF} = 1 - \frac{A_F}{A} (1 - \epsilon_F) \quad \begin{matrix} A_F & \text{FIN area} \\ \text{Overall fin area} & \text{Heat transfer area FIN} \end{matrix} \quad (35)$$

re:

$$\epsilon_F = \frac{\tanh ml_e}{ml_e}$$

$$m^2 = \frac{2h}{kt} (1 + \frac{t}{\xi})$$

W A = ft X 1bm of fluid/sec

BTU of sec

(36)

uninterrupted flow length Lm

(37)

See Reference 5 for further explanation.

The Stanton number (h/Gc_p) is combined with the Reynolds number to obtain an expression for the film coefficient:

$$h/Gc_p = h/\rho v c_p$$

$$Re St = j Re$$

$$h = St Gc_p = St_c p \text{Re } \mu / 4r_h = \frac{c_p \mu}{4r_h} (\text{Re } St)$$

$$\rightarrow eq 52 P 73. (38)$$

This expression is substituted into Equation (33):

$$\frac{1}{UA} = \frac{1}{(NTU)(W_{cp})_{\min}} = \frac{4r_{hH}}{\epsilon_{OH}^c p H^\mu H^{\alpha_H} (\text{Re } St)_H} + \frac{4r_{hC}}{\epsilon_{OC}^c p C^\mu C^{\alpha_C} (\text{Re } St)_C}$$

$$St = \frac{h}{\rho c_p V \phi}$$

$$St = j (Pr^{2/3})$$

$$h = St \rho c_p V \phi$$

$$h = j \rho c_p V \phi$$

The ratio of heat transfer area to volume is defined as a

$$a = \frac{A}{V} = \frac{A}{A' \frac{LN_P}{fr} \frac{1}{LN_P}} = \frac{A}{A'} \frac{A'}{A' fr} \frac{1}{LN_P} = \frac{A}{A'} \frac{\psi}{LN_P}$$

*A' fr see 13 for
frontal area*

$$A = a A' \frac{L}{\psi} N_P$$

(41)

This is substituted into Equation (39):

$$\frac{1}{(NTU)(W_{cp})_{\min}} = \frac{4r_{hH} \psi_H}{N_{PH} \epsilon_{OH}^c p H^\mu H^{\alpha_H} (\text{Re } St)_H} + \frac{4r_{hC} \psi_C}{N_{PC} \epsilon_{OC}^c p C^\mu C^{\alpha_C} (\text{Re } St)_C} \quad (42)$$

Rearranging:

$$\frac{A' L N_{PH}}{(NTU)(W_{cp})_{\min} \psi_H} = \frac{4r_{hH}}{\epsilon_{OH}^c p H^\mu H^{\alpha_H} (\text{Re } St)_H} + \frac{4r_{hC}}{\epsilon_{OC}^c p C^\mu C^{\alpha_C} (\text{Re } St)_C} \frac{A' L \psi_N_{PH}}{A' L \psi_N_{PC}} \quad (43)$$

Using the definition of ψ , the latter portion of the right hand term is unity:

$$\frac{A' L N_{PH}}{A' L \psi_N_{PC}} = \frac{L_H}{L_C} \frac{L_C L_n}{L_H L_n} = 1$$

Therefore, Equation (43) reduces to:

$$\frac{A' L N_{PH}}{(NTU)(W_{cp})_{\min} \psi_H} = \frac{4r_{hH}}{\epsilon_{OH}^c p H^\mu H^{\alpha_H} (\text{Re } St)_H} + \frac{4r_{hC}}{\epsilon_{OC}^c p C^\mu C^{\alpha_C} (\text{Re } St)_C} \quad (44)$$

The Reynolds number for the hot fluid is rewritten to include the no flow length (L_n) to obtain the third of the five basic heat exchanger equations.

$$Re_H = \frac{4r_{hH}G_H}{\mu_H} = \frac{4r_{hH}W}{\mu_H A'_H}$$

(45)

$$Re_H = \frac{4r_{hH}W_H N_{PH}}{\mu_H L_C L_n \psi_H}$$

(46)

Equation (44) is rearranged to obtain the fourth of the five basic heat exchanger equations used in the calculation procedure.

$$\frac{r_{hH} W_H L_N_{PH}}{(NTU)(W_c)} = \frac{r_{hH}}{\epsilon_{OH}^c \mu_{pH} \epsilon_{H}^c (Re St)_H} + \frac{r_{hC}}{\epsilon_{OC}^c \mu_{pC} \epsilon_{C}^c (Re St)_C}$$

(47)

Overall Energy Balance - The heat balance between the two fluids is:

$$W_C c_{pC} \Delta T_C = -W_H c_{pH} \Delta T_H$$

(48)

Recalling the expression for Reynolds number:

$$\Delta T_C = - \frac{Re_H \mu_H A'_H}{Re_C \mu_C A'_C} \frac{4r_{hC} c_{pH}}{4r_{hH} c_{pC}} \Delta T_H$$

(49)

But:

$$\frac{A'_H}{A'_C} = \frac{A'_H}{A'_C} \frac{L_n L_C L_H}{L_n L_C L_H} = \frac{N_{PC} L_A f_{rC} A'_H}{N_{PH} L_A f_{rH} A'_C} = \frac{L_C \psi_H N_{PC}}{L_H \psi_C N_{PH}}$$

(50)

Therefore the temperature changes of the hot and cold fluids are related as follows:

$$\Delta T_C = - \frac{Re_H \mu_H L_C \psi_H r_{hC} c_{pH} N_{PC}}{Re_C \mu_C L_H \psi_C r_{hH} c_{pC} N_{PH}} \Delta T_H$$

(51)

This is the last of the basic equations used to calculate heat exchanger performance and size. If a cold fluid Reynolds number is calculated similar to Equation (46), the Re_C is used as the last equation instead of Equation (51).

Performance - Performance analysis of heat exchangers requires effectiveness maps. (See Figure 32A.) These maps are derived from test data. Derived maps are based on a heat transfer surface size which satisfies a unique design condition. Explanation of the derivation procedure is contained in the following section on size. If the inlet fluid conditions are known (and assuming no fluid loss through the heat exchanger core), the exit

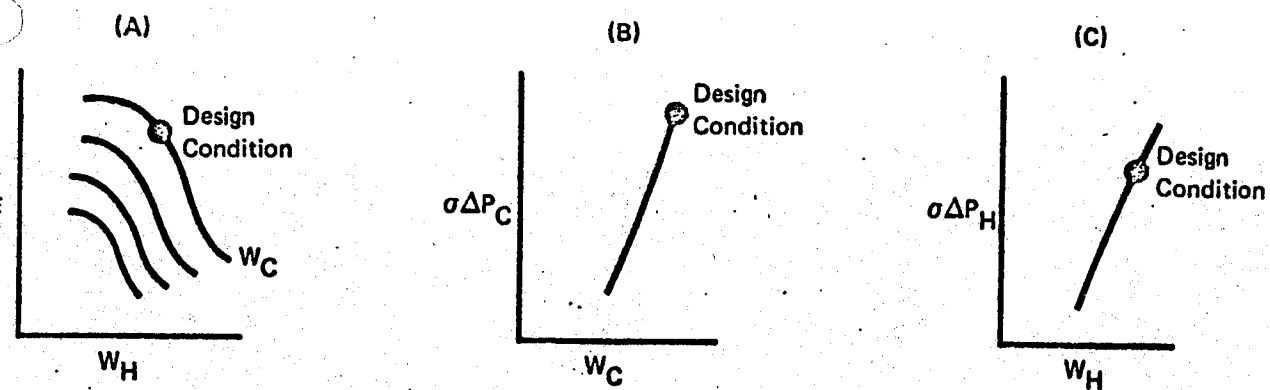


Figure 32 Typical Performance Data

GP 9416-101

temperatures are determined with Equation (34). Consideration of fluid loss or gain due to water condensation or addition of water to an air stream is made with an energy balance. Variations in the heat transfer coefficient to account for the water are not included.

The flow friction characteristics for each fluid side normally are presented as $\sigma\Delta P$ versus flow rate. (See Figures 32B and 32C.) The pressure drop data are derived from information about the core geometry or from actual test data.

Derivation of the heat exchanger performance is based on knowledge of the core geometry performance. This information is often not available, hence estimates of reasonable performance are required. Assuming a constant heat transfer effectiveness implies a variable surface area. Thus, any performance calculation based on an assumed effectiveness is an implied design condition and is only valid for that condition.

Selection of the appropriate design effectiveness is subjective. Both the limitations on available volume and the range of desired performance affect the effectiveness to be selected. Typical ECS heat exchanger designs have an effectiveness of 80%, considering the above conditions: (This effectiveness is on the minimum heat capacity ($W_{C_p \text{ min}}$) side.) Varying this value, for a fixed flow condition, directly affects the volume. Similarly, the range of desired performance to maintain high effectiveness is related to volume. Therefore, an effectiveness of 80% is reasonable. (See also Reference 6.)

Design values of pressure drop per pass are based on the inlet pressure. (See Figure 33.) These values are representative of design conditions for the air side of air to air or air to liquid heat exchangers. These data are not to be confused with the ΔP versus flow rate performance map data indicated in Figure 32. (References 6 through 9 contain performance data for actual heat exchangers.)

Size - The size of a heat exchanger is determined from the known design conditions for the selected heat transfer surface fin geometry. A typical fin surface geometry is described below. The second row of numbers refer to the tabulated definitions which follow.

25.01R(S)-0.201/0.200-1/9(0)-0.004(A1)

1 2 3 4 5 6 7 8 9

1. Number of fins per inch.
2. Type of fin cross section in the flow direction.
(R = rectangular, T = triangular, U = U-shape).
3. Fin sandwich construction (SD = single-double, S = single, D = double, T = triple).
4. Fin height before stacking and brazing, b, inch.
5. Distance between plates after stacking and brazing the fins, measured in the test core, inch.
6. Effective fin length in the flow direction (ξ), inch.
(Not used for plain surface.)
7. Type of surface (L = louvered, O = offset, P = plain, S = strip).
8. Fin metal thickness (t), inch.
9. Fin material [(Al) = aluminum, (SS) = stainless steel, (Ni) = nickel].

With the core fin geometry and design performance conditions known, the core volume is determined by an iterative approach. The unknowns are the core dimensions: L_H , L_C , and L_n .

Several typical fin geometry designations (from References 5 and 10) are:

20.06R(D) - 0.100/0.098 - 1/8 (0) - 0.004

16.00R(D) - 0.126/0.125 - 1/8 (0) - 0.006

24.12R(S) - 0.075/0.075 - 1/9 (0) - 0.004

19.35R(S) - 0.0755/0.075 - 1/10 (0) - 0.004

12.18R(D) - 0.178/0.174 - 0.178 (0) - 0.004

15.75R(D) - 0.153/0.149 - 1/7 (0) - 0.004

25.01R(S) - 0.201/0.20 - 1/9 (0) - 0.004

15.61R(S) - 0.251/0.250 - 1/8 (0) - 0.004

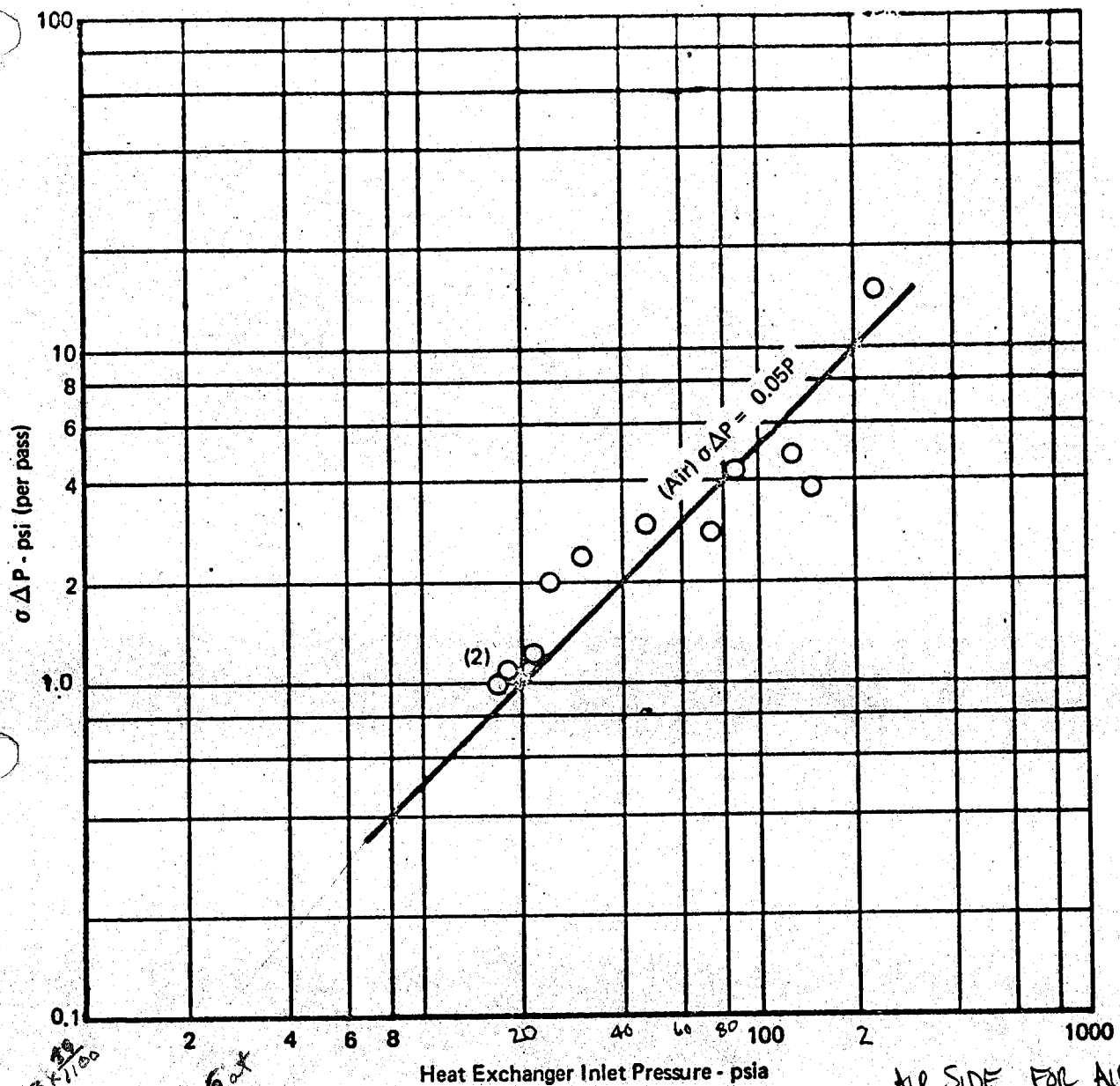


Figure 33 Design Pressure Drops for Air Heat Exchangers

GP 9416-120

Friction factors (f) and Colburn moduli (j) for each of these fin surfaces are found in Figures 34 through 41.

Fin selection is based on the ability of a specific geometry to satisfy the heat transfer and flow friction requirements in a minimum volume. Therefore, it is desirable to relate fin geometry to these requirements. The five fin geometries are related to design pressure in Figure 42 to reflect current heat exchanger fin applications.

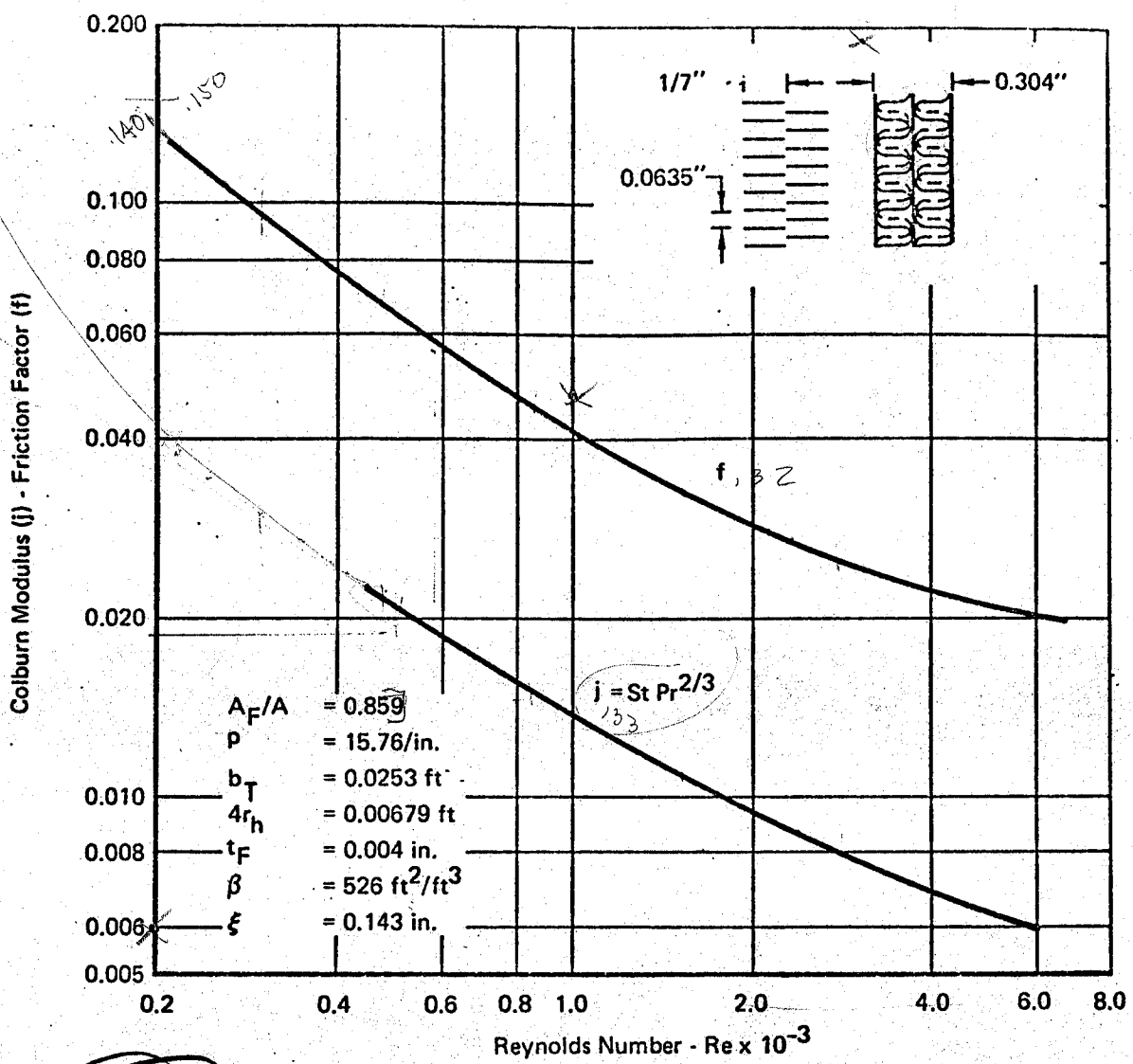


Figure 39 Offset Rectangular Fin Surface

$$15.76 R(D) - 0.153/0.149 - 1/7 (0) - 0.004$$

GP 9416-128

$$\begin{aligned}
 P_F &= \frac{t_F p \rho_{\text{metal}} (b + \frac{1}{p} + t_F [2\pi - 9])}{b} \\
 &= .004 \text{ in.} \times \frac{15.76}{1 \text{ in.}} (.152 \text{ in.} + \frac{1 \text{ in.}}{15.76} + .004 \text{ in.}[2\pi - 9]) \rho_{\text{metal}} \\
 &= .152 \text{ in.}
 \end{aligned}$$

1/2
Kays
+
London

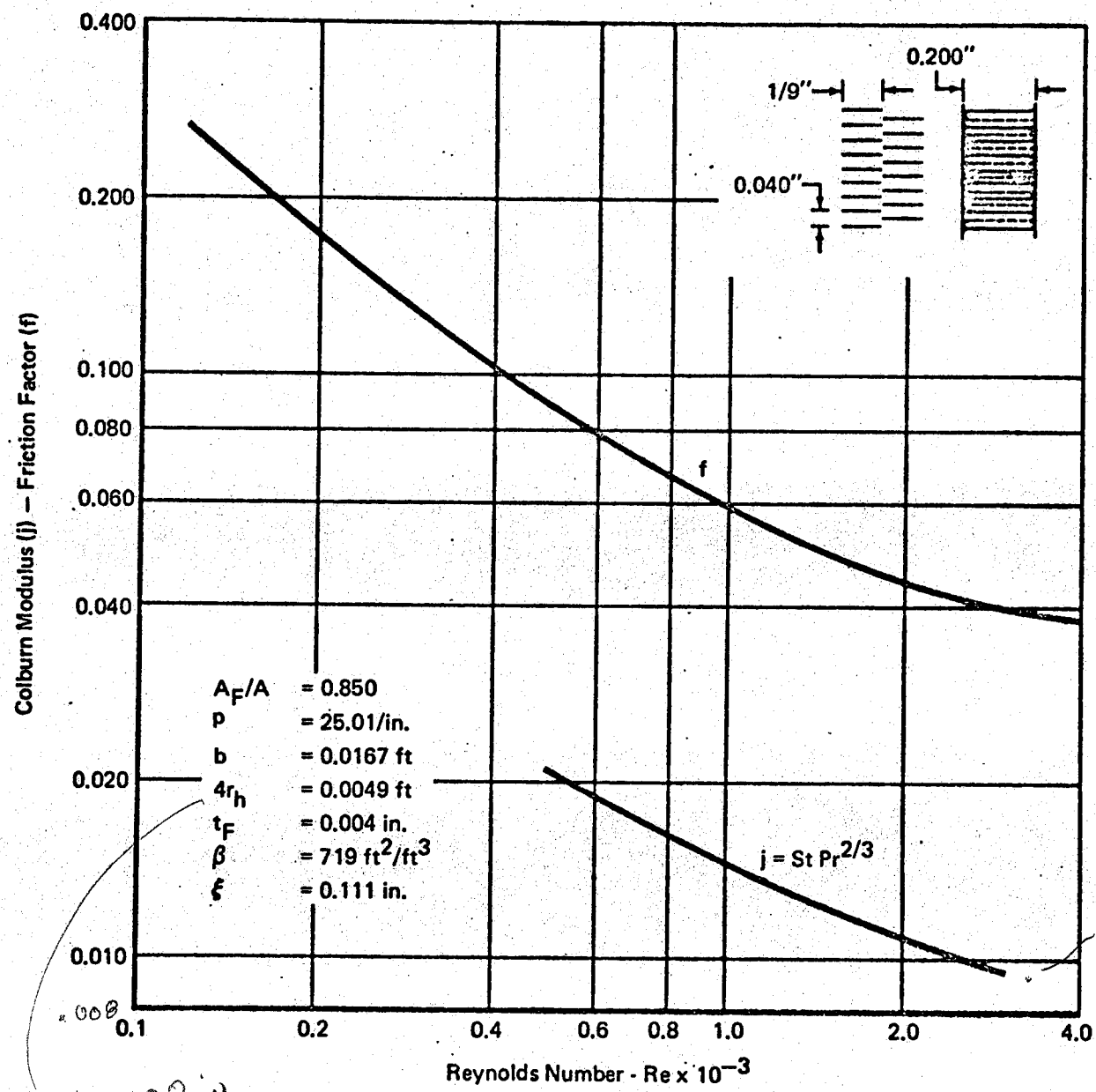


Figure 40 Offset Rectangular Fin Surface
 $25.01R(S) - 0.201/0.200 - 1/9(O) - 0.004$

GP 9416-127

-2

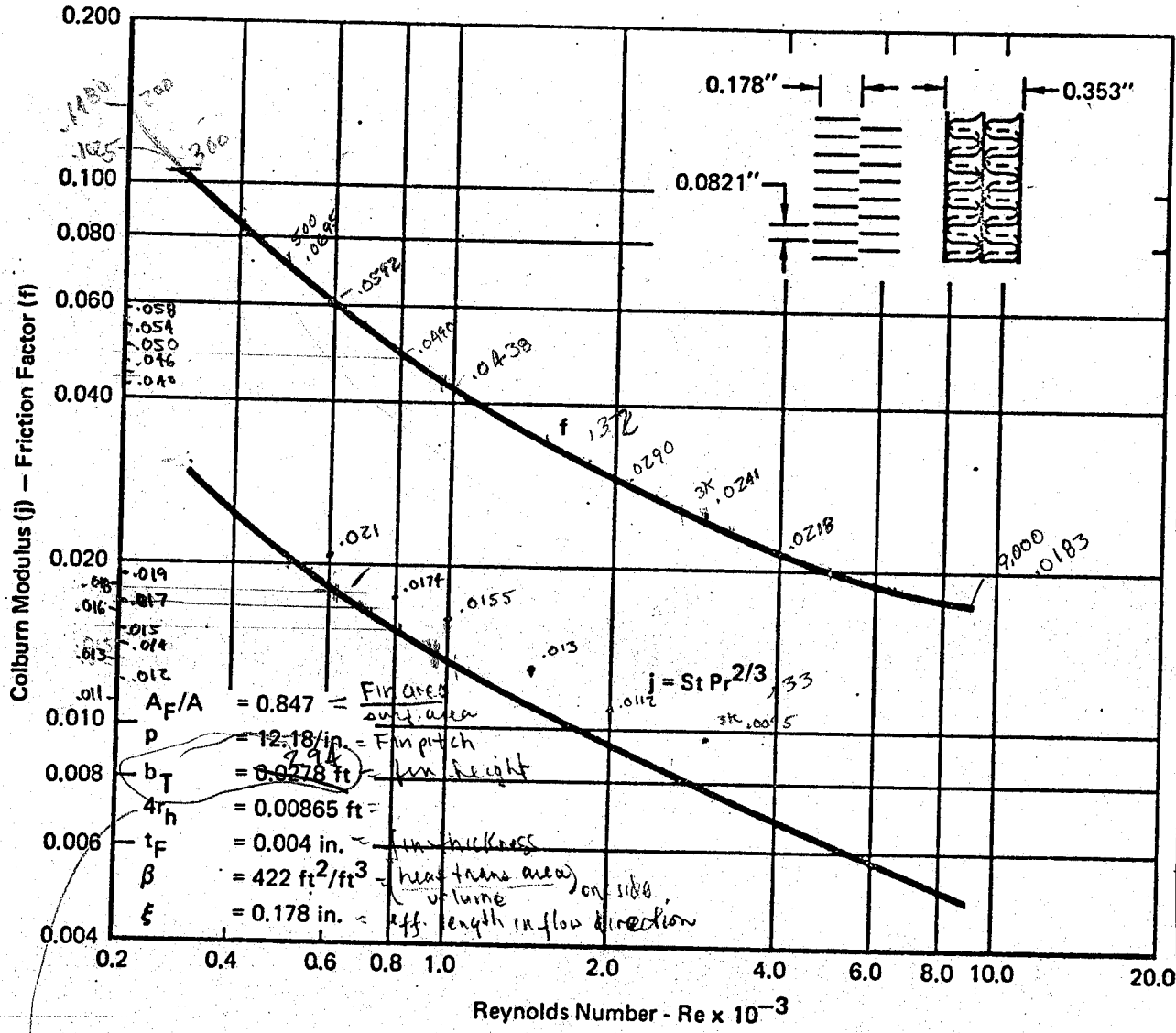


Figure 38 Offset Rectangular Fin Surface
 $12.18R(D) - 0.178/0.174 - 0.178(O) - 0.004$

GP 9416-129

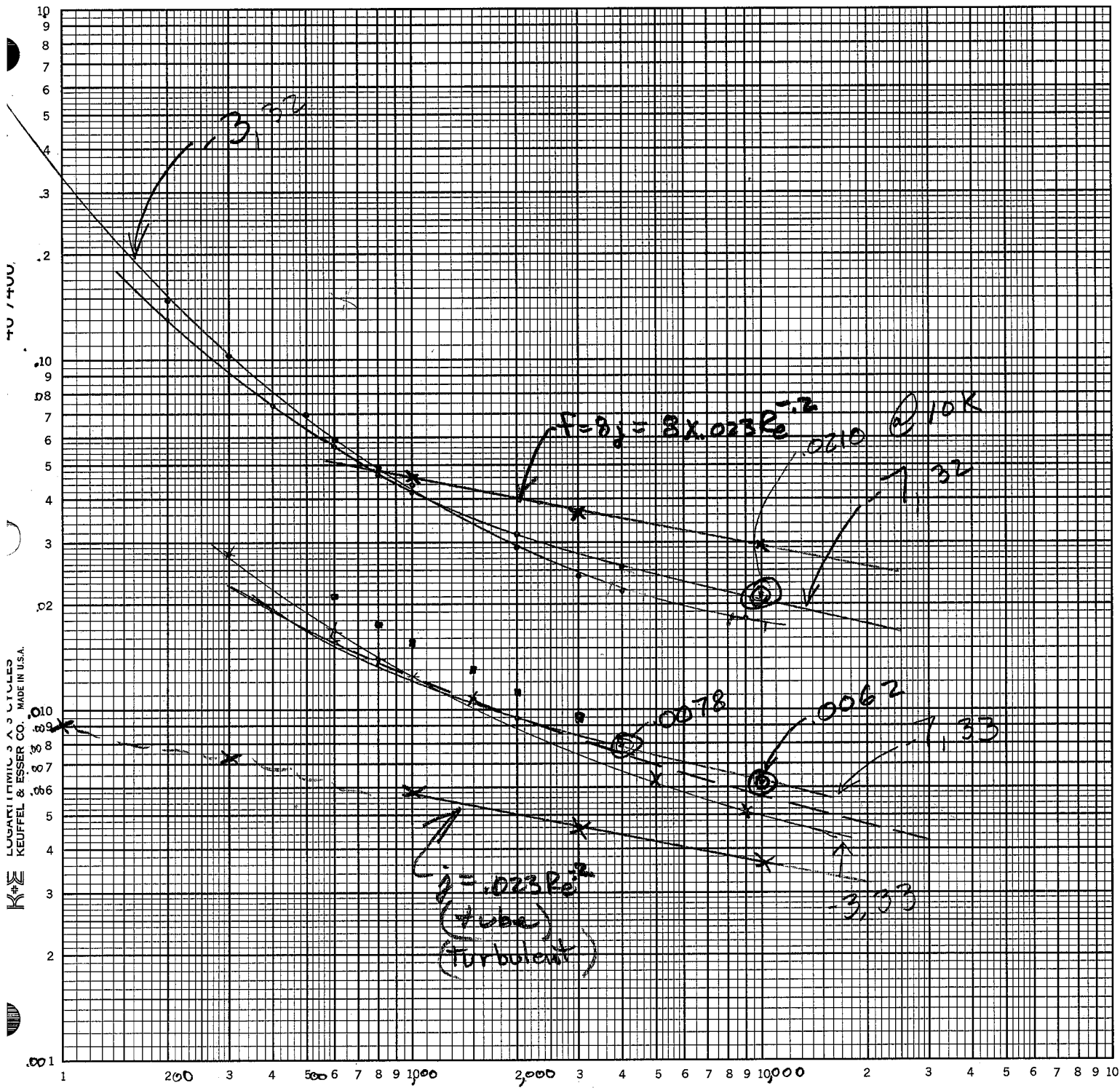
Fin: -731
 P 166 + 199 Kays
 + 227 London

$$f_c = \frac{b_{Tc} \beta_c r_{hc}^{3/8}}{b_{Tc} + b_{Th} + 2t_{sp}}$$

$$= \frac{0.0294 \times 422 \times 0.00865}{0.0294 \times 0.00625 + 0.001}$$

$\frac{12 \times 0.294}{353} = 1.18$	$\frac{V_h \text{ in}}{353 \text{ in}^2} = 1.18$
$\frac{(f+2/f)^3}{(f+2/f+3)^2} / 12 = 1.18$	$\frac{\text{unit flow}}{\text{length}} = 1.18$
$C_{Fin} = 0.004 \frac{\text{in}^2/\text{in}^3}{353 \times 1.18} = 0.000004$	1.18

-7 fin
-3 fin
p. 73A



Re

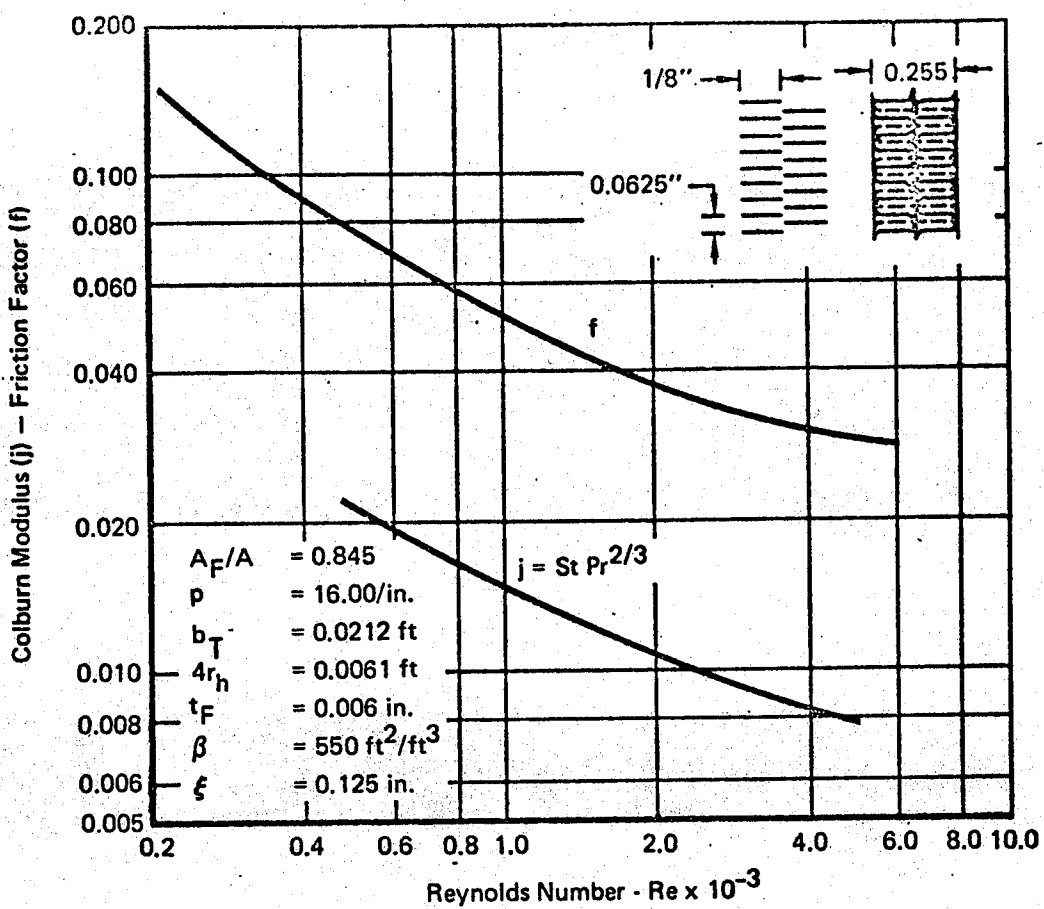


Figure 35 Offset Rectangular Fin Surface

16.00R(D) - 0.126/0.125 - 1/8(O) - 0.006

GP 9416-130

-4

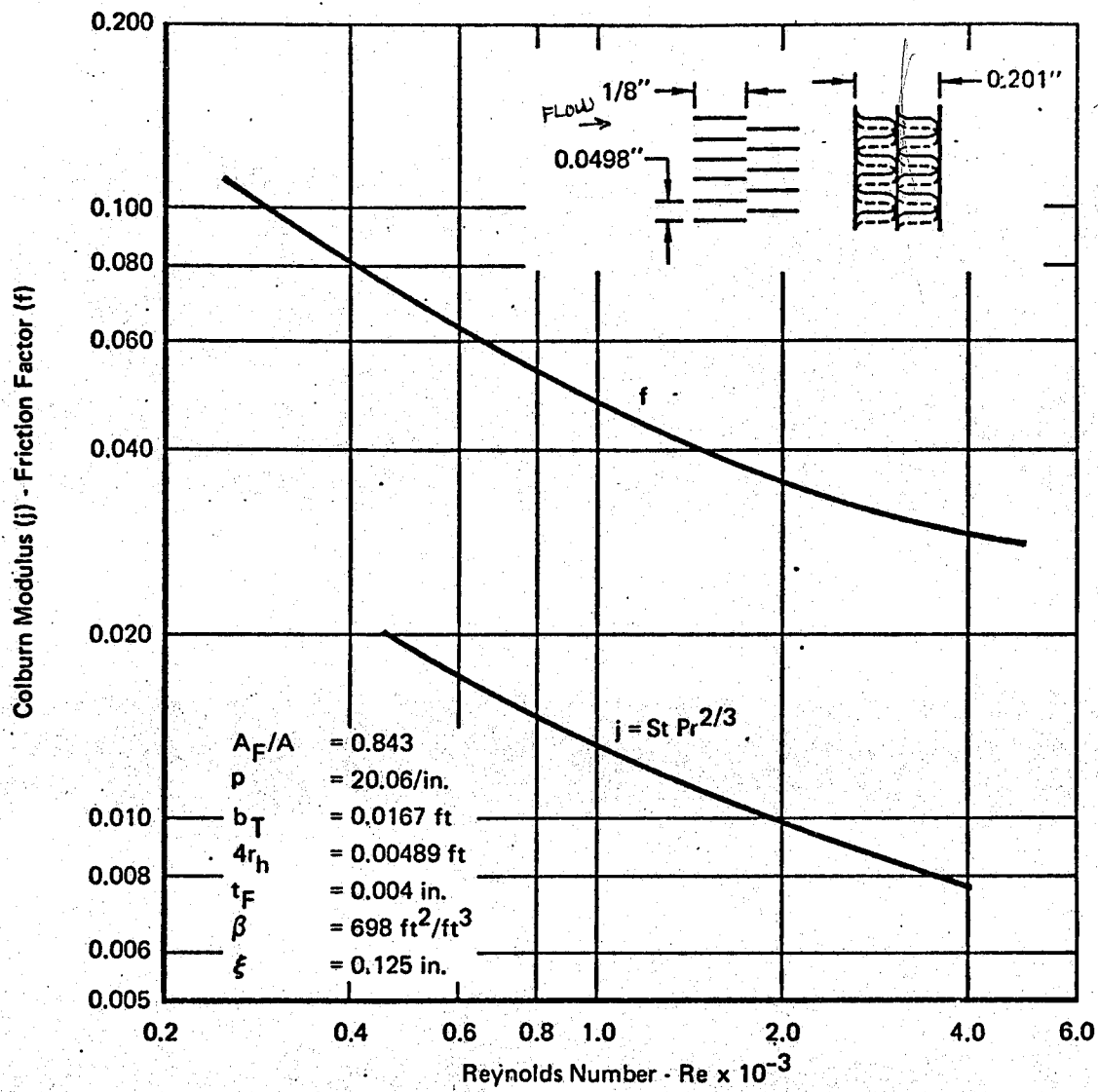


Figure 34 Offset Rectangular Fin Surface

$$20.06 R(D) - 0.100/0.098 - 1/8 (0) - 0.004$$

FINNS
 1.0" 0.0498"
 20.06 FINNS/in.
 dist. bet. plate
 fin height
 fin length
 offset thickness
 FIN AREA
 HX SURF AREA

$$j = \text{Colburn Modulus} = St \cdot Pr^{2/3} = \frac{h_c D_h}{K} \cdot \frac{Pr^{2/3}}{Re \cdot Pr}$$

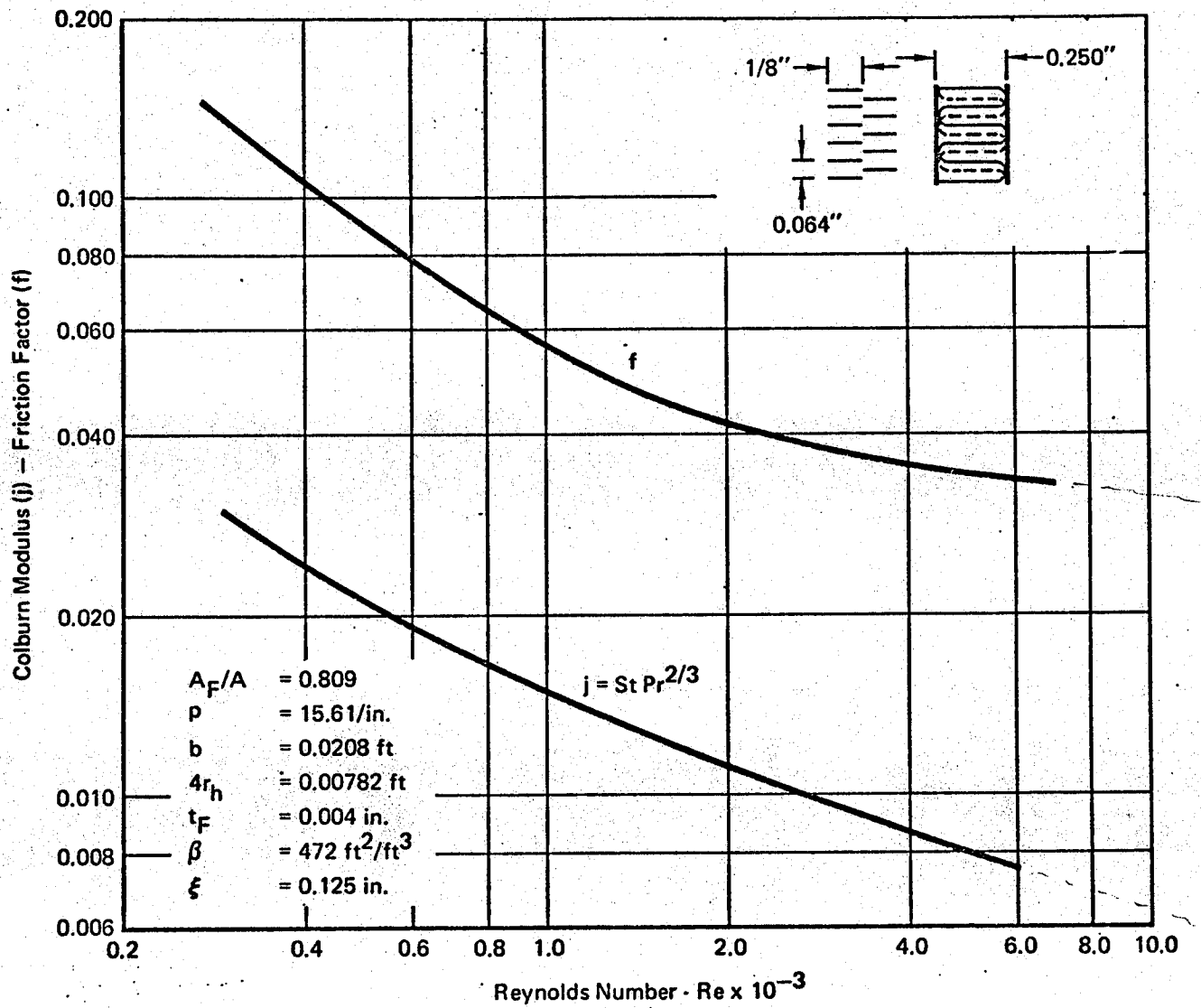


Figure 41 Offset Rectangular Fin Surface

15.61R(S) — 0.251/0.250 — 1/8(O) — 0.004

GP 9416-132

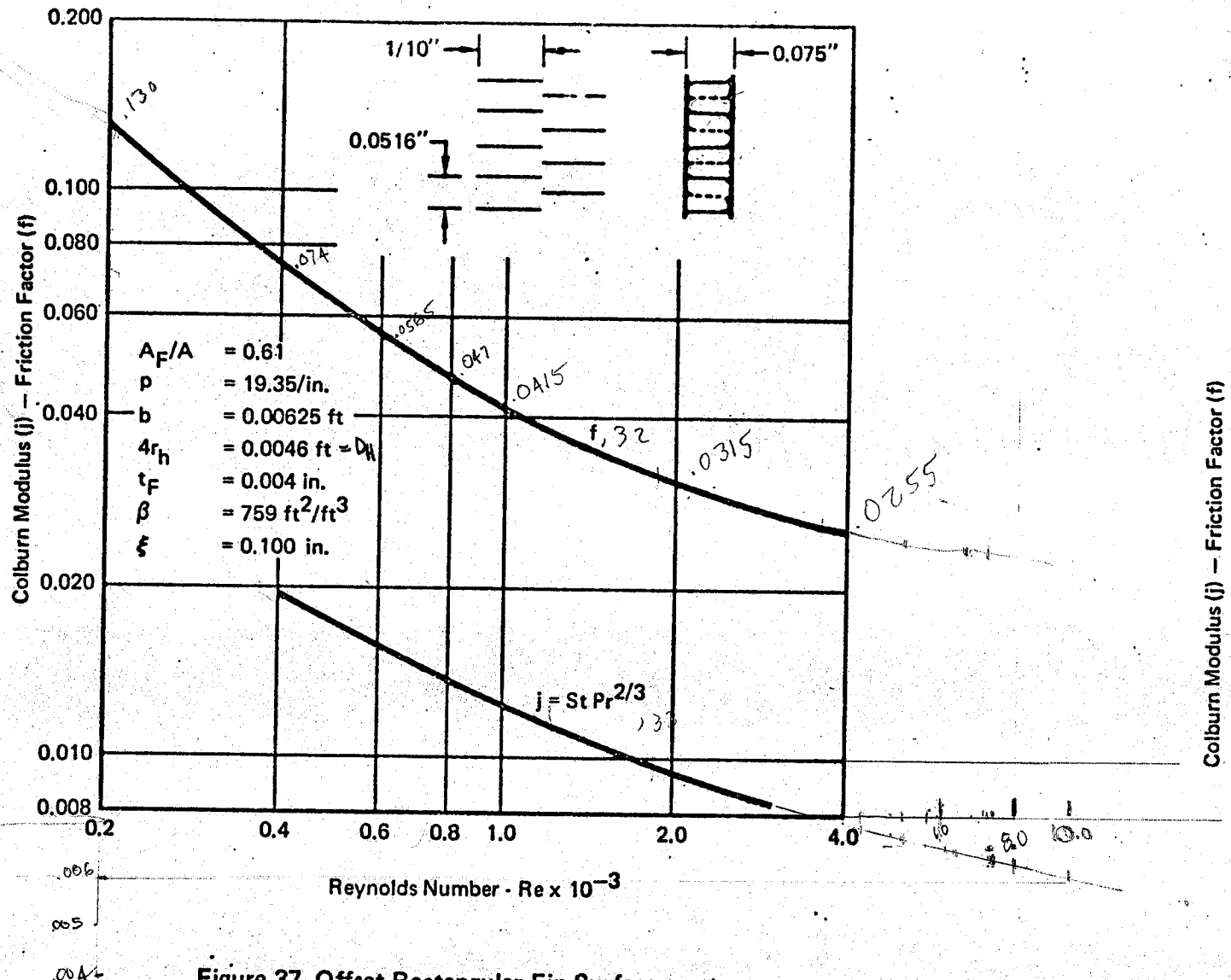


Figure 37 Offset Rectangular Fin Surface
 $19.35R(S) - 0.0755/0.0750 - 1/10(O) - 0.004$

GP 9416-135

-7

$$\varphi_n = \frac{b_{TH} \beta_n r_{nh}}{b_{TH} + b_{TC} + 2t_{SP}} = \frac{.00625 (759) (.00115)}{.00625 + .0278 + .001} = .1488$$

free flow
 $\frac{\text{type } 3}{A_{\text{total frontal}}}$

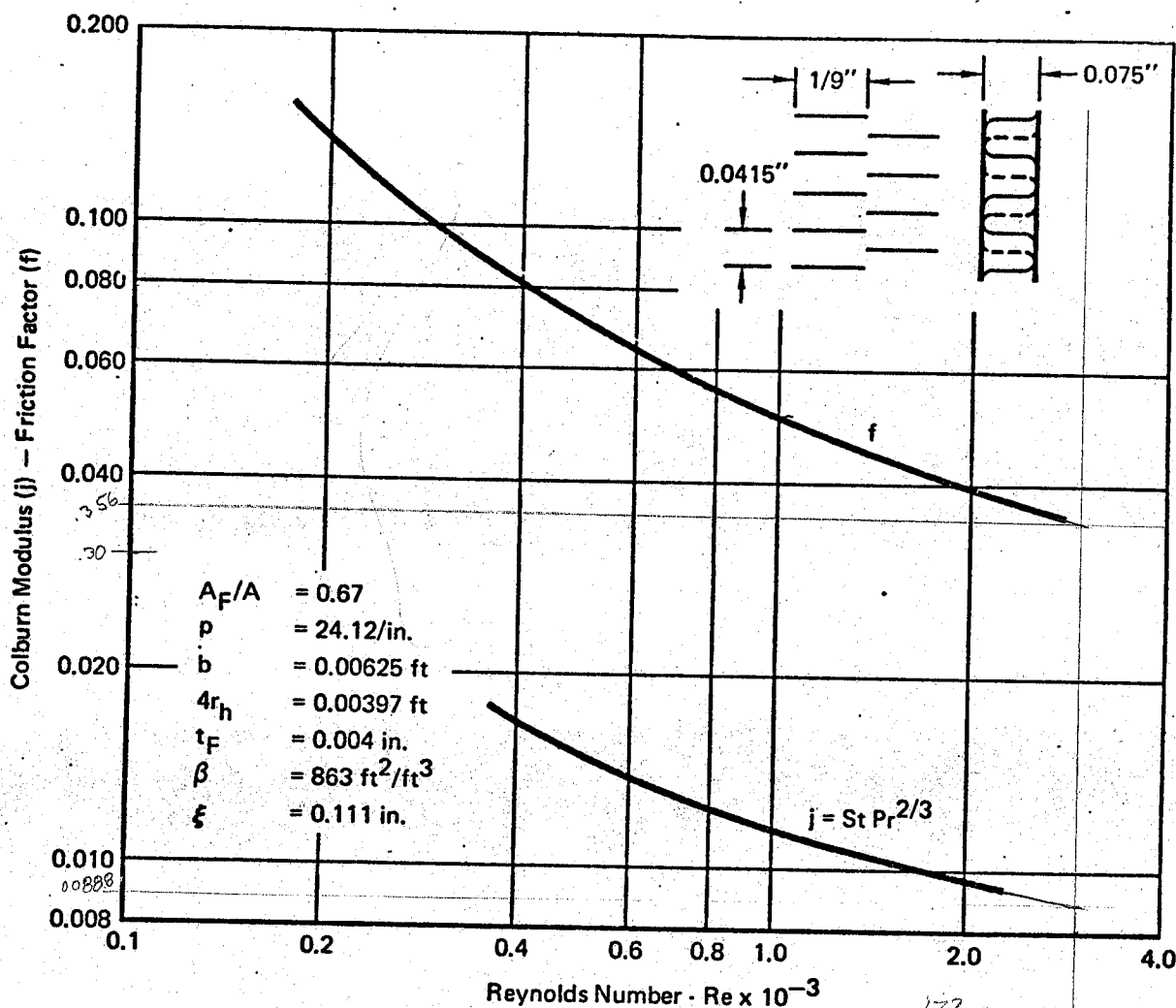


Figure 36 Offset Rectangular Fin Surface

$24.12R(S) - 0.075/0.075 - 1/9(O) - 0.004$

GP 9416-134

(8)

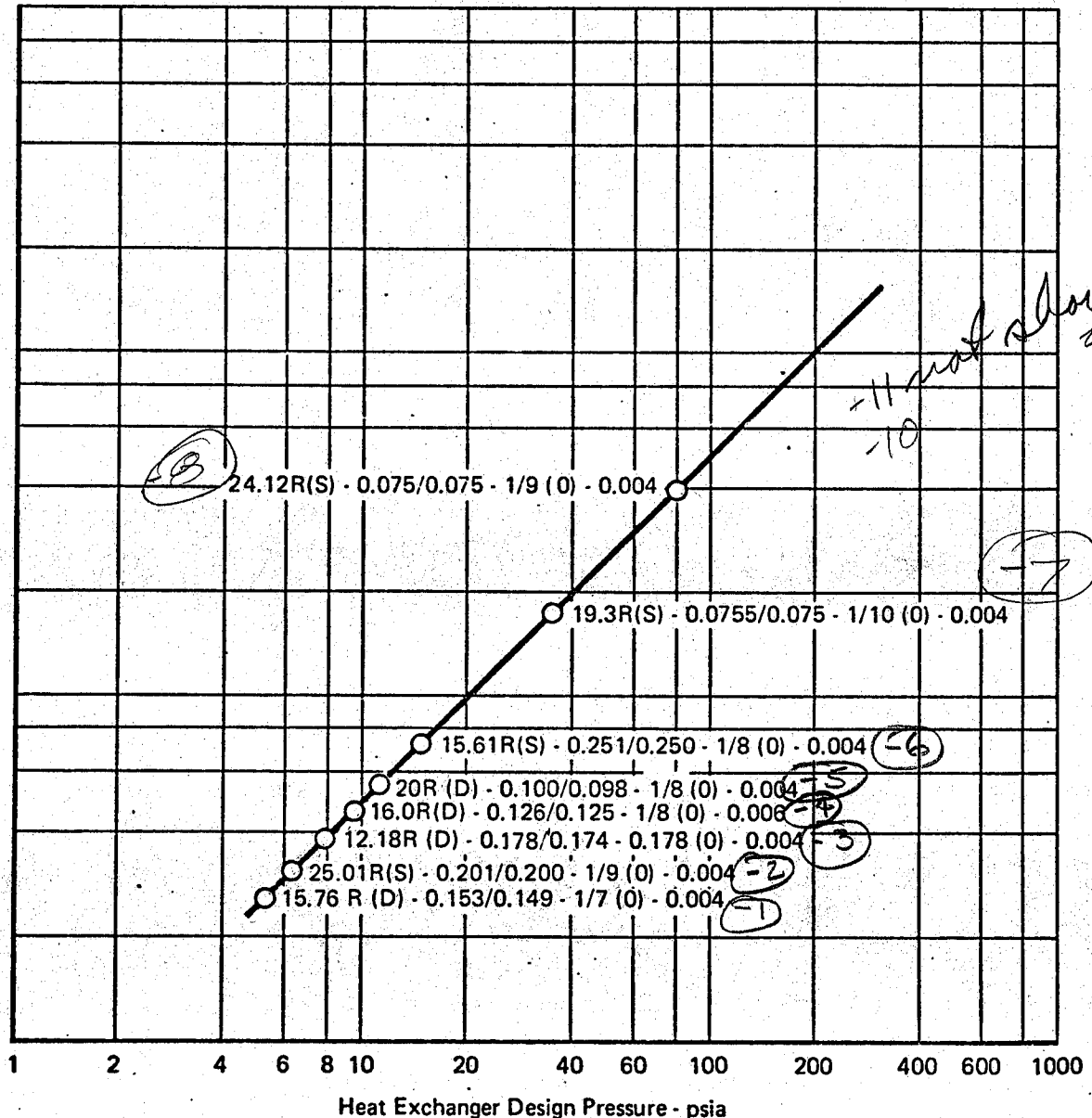


Figure 42 Fin Geometry Selection

GP 9416-179

-8 BLEED PRE
-10 BLEED SEC

Core performance (for assumed or known dimensions) is determined as follows:

Reynolds Number is obtained from Equation (46).

The Colburn modulus ($j = St Pr^{2/3}$) is determined for this

Reynolds number. (Figure 34 is an example of such data.) Prandtl number is known from the fluid properties, therefore:

$$Re St = j Re Pr^{-2/3} \quad (52)$$

This product is obtained for both sides.

Overall temperature effectiveness of the selected fin surface is determined with Equation (35). $\epsilon_{oF} = 1 - \frac{A_F}{K} (1 - \epsilon_F)$

Number of heat transfer units (NTU) is determined with Equation (47).

Heat transfer effectiveness (ϵ_T) is based on the core geometry. The following equation is for a cross flow design with both fluids mixed. Reference 10 contains NTU versus ϵ_T for other designs.

$$\epsilon_T = \frac{NTU}{\frac{NTU}{1 - e^{-NTU}} + \frac{(C_{min}/C_{max}) NTU}{1 - e^{-(C_{min}/C_{max}) NTU}} - 1} \quad (53)$$

Pressure drop is obtained from Equation (26). An iterative procedure is used if the dimensions are assumed.

Weight and Volume - The number of hot and cold flow layers are:

$$n_H = \frac{L_n - b_{TC} - 2t_{SP}}{(b_{TH} + b_{TC} + 2t_{SP})} \quad \text{and} \quad n_C = n_H + 1 \quad (54)$$

Hence, the volumes of each side are:

$$V_H = n_H L_C L_H [b_{TH} - N_{SL} t_{SP}] \quad \text{and} \quad V_C = n_C L_C L_H [b_{TC} - N_{SL} t_{SP}] \quad (55)$$

Figure 43 demonstrates results of comparing calculated and known volumes of several heat exchangers.

The bulk fin densities are used to determine the total weight of the hot and of the cold fins.

$$Wt_{FH} = \rho_{FH} V_H \quad \text{and} \quad Wt_{FC} = \rho_{FC} V_C \quad (56)$$

Bulk fin densities are determined by calculating the fin metal weight in a cubic inch of fin volume. Equations for bulk densities of three common fin shapes are presented.

The unit length (flattened) of a triangular fin (Figure 44) is:

$$L = s + \frac{\pi r \phi}{180} \quad (57)$$

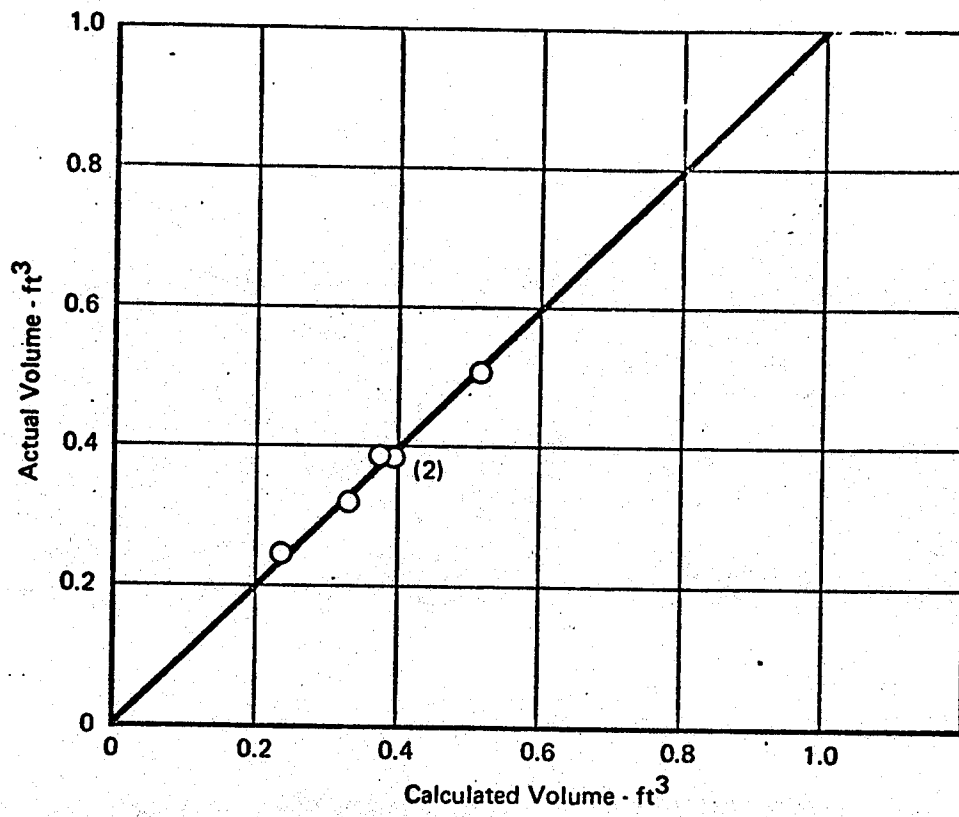


Figure 43 Heat Exchanger Core Volume Comparison

GP 9416-198

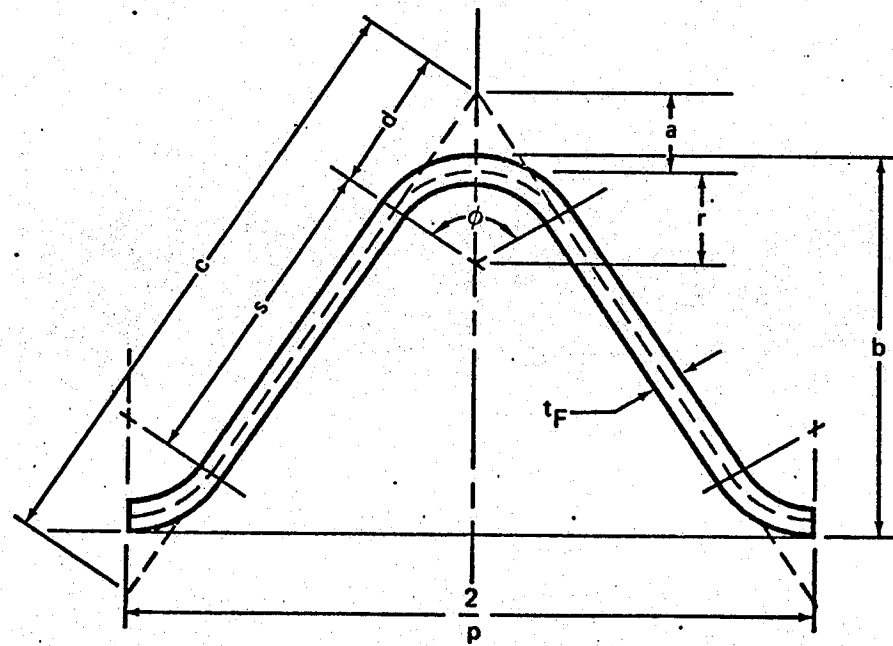


Figure 44 Triangular Fin Geometry

GP 9418-118

here:

$$c = [(b + 2a)^2 + (\frac{1}{p})^2]^{1/2}$$

$$s = c - 2d$$

$$d = rp(b + 2a)$$

$$r = 3t_F$$

$$\phi = 2 \cos^{-1} \left(\frac{r}{a+r} \right)$$

$$a = \frac{2rp^2 b - 1 + \sqrt{1+p^2 b^2 - 4rp^2 b}}{\frac{1}{r} - 4rp^2}$$

The weight of the fin contained in a cubic inch is:

$$\rho_F = \frac{p t_F \rho_{\text{metal}} L}{b} \quad (58)$$

The unit length (flattened) of a rectangular fin (figure 45) is:

$$L = b + \frac{1}{p} - 9t_F + 2\pi t_F \quad (59)$$

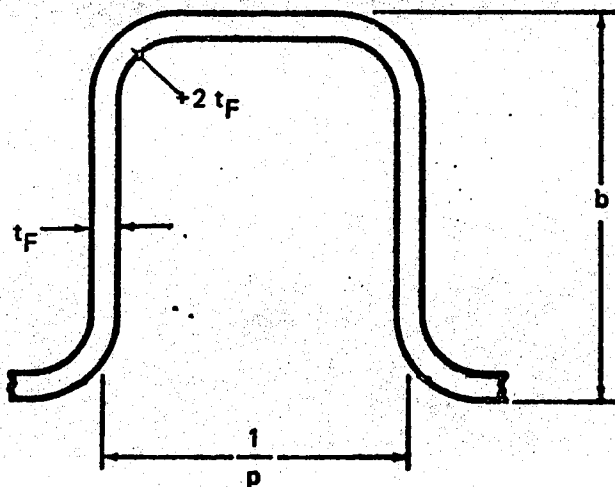


Figure 45 Rectangular Fin Geometry

GP 8416-117

The weight of fin contained in a cubic inch is:

$$\rho_F = \frac{t_F p \rho_{\text{metal}} (b + \frac{1}{p} + t_F (2\pi - 9))}{b} \quad (60)$$

Fin length (flattened) of a rounded fin (Figure 46) is:

$$L = b - t_F + \frac{1}{p} \left(\frac{\pi}{2} - 1 \right) \quad (61)$$

Weight of the fin contained in a cubic inch is.

$$\rho_F = \frac{\rho_{\text{metal}} L}{b} \quad (62)$$

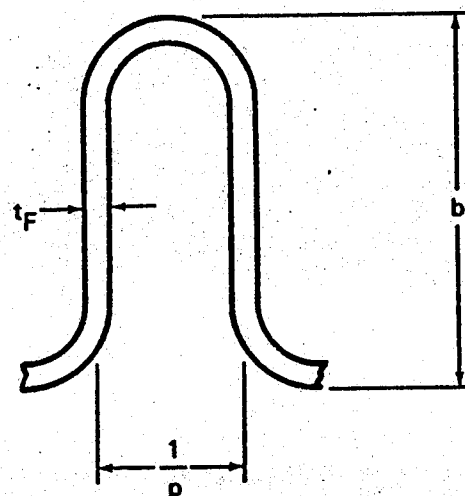


Figure 46 Rounded Fin Geometry

GP 9416-116

Aluminum separator plates (i.e., tube sheet) are made from braze sheet stock, typically 0.012 to 0.016 inch thick. Steel and nickel separator plate thicknesses are found in Figure 47. Separator plate density is found in the following table:

Material		
Aluminum #12 Braze Sheet	Steel (1095)	Nickel (A286)
0.1 lb/in ²	0.283 lb/in ³	0.289 lb/in ³

Brazing allowances are made for steel and nickel separation plates by adding a 0.001 inch coating of commercially pure nickel (0.322 lb/in³) to both sides of the plate. No increase in the aluminum plate thickness is accounted for.

The core weight is the sum of the weights of the fins and the separation plates.

$$W_{\text{core}} = W_{\text{FH}} + W_{\text{FC}} + \rho_{\text{metal}} (n_H + n_C + 1) L_C L_H t_{\text{SP}} \quad (63)$$

An additional term is added if the fin geometry contains a splitter plate.

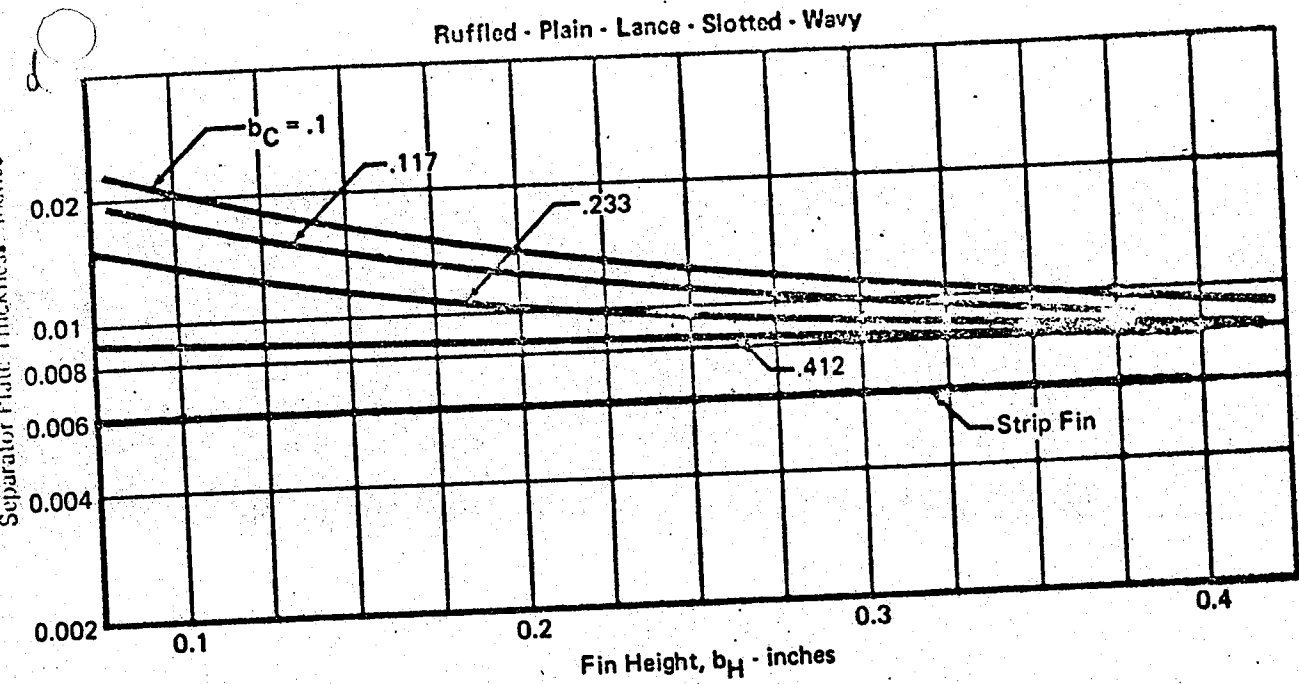


Figure 47 Separator Plate Thickness

OR 8416-102

Wrap-up weight, which includes an allowance for headers and supports, is estimated by:

$$W_t = K_1 W_{t,core} (V_{core})^{-0.118} \quad (\text{from Reference 6}) \quad (64)$$

For complex headers $K_1 = 3.23$, but for simple headers K_1 may be as low as 2.615. Actual header weight is determined from the surface area, thickness, and material density of the header. Use of this approach, instead of Equation (64), should include a factor for brazing and supports (e.g., 8%). Calculations of several heat exchanger weights, using actual fin geometries and estimated design conditions with Equation (64), are compared to actual weights in Figure 48. The standard error is 12.0%. Heat exchangers with simple headers weigh up to 21% less than those with complex headers.

3.1.2 Single Phase Heat Exchangers - The types of single-phase heat exchangers considered are: air to air, air to liquid, and liquid to liquid. Plate-fin construction and cross flow arrangements (Figure 31) are typical for all of the above types. Several recent designs are counter flow arrangements.

Performance - A heat transfer effectiveness of 80% at the design condition is achievable for most heat exchangers. Without size or weight

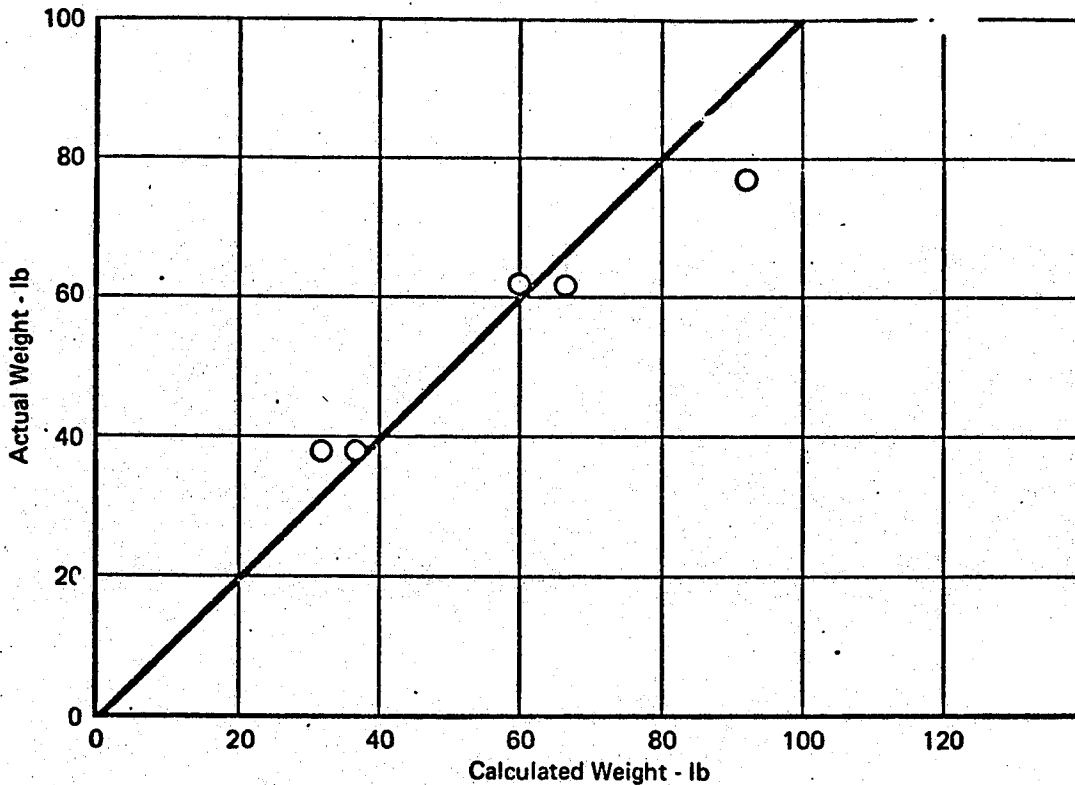


Figure 48 Heat Exchanger Weight Comparison

GP 9416-199

limitations higher effectivenesses can be obtained. Peculiar envelope restrictions often reduce the effectiveness.

The air side pressure drop at the design condition increases as the inlet pressure increases, as is shown in Figure 33. Data points shown in this figure are for the bleed air, ram air, or conditioned air sides of several current heat exchangers. A typical air side design pressure drop per pass as a function of inlet air pressure (Figure 33) is:

$$(\Delta P)_{\text{air design}} = 0.05P_{\text{in}} \quad (65)$$

A typical liquid side design pressure drop per pass is:

$$(\Delta P)_{\text{liquid design}} = 2.0 \text{ psi (per pass)} \quad (66)$$

Pressure drops per pass vary from about 1 psi for water or glycol water to about 3 psi for silicate and fluoro-type coolants. The liquid sides of heat exchangers typically are multipass cross flow designs.

Off-design performance of a heat exchanger is obtained by following the information presented in Section 3.1.1.

Water may be added to or condensed from an air stream. In either case no modification of the heat transfer coefficient is made. Calculation of the

overall energy balance is modified to account for the water evaporated or condensed. For either case the enthalpy of the air-vapor-liquid mixture (per pound of dry air) is:

$$i = c_{p, \text{air}} T_{\text{air}} + \frac{(W_i)_{\text{vapor}}}{W_{\text{air}}} + \frac{(W_i)_{\text{liquid}}}{W_{\text{air}}} \quad (67)$$

The air temperature in Equation (67) is determined iteratively by equating the enthalpy of the mixture to the enthalpy out of the heat exchanger:

$$i_2 = i_1 + (\Delta i) \quad (68)$$

The enthalpy change (Δi) in the heat exchanger may be positive or negative (i.e., heat added or heat removed).

Weight and Volume - The weight and volume calculation technique described in Section 3.1.1 is used.

3.1.3 Water Boilers - Boilers are used to extend the capability of the available ram air heat sink. Use of water as the expendable liquid is very common (e.g., F-111 and B-58). Other liquids, such as ammonia, have been used but are not considered in this study. Typical boiler construction is a fully immersed plate-fin core.

Performance - Boiling of the water occurs at the water/heat transfer surface interface through pool boiling. The temperature effectiveness considers the water at a constant temperature (T_{sat}).

$$\epsilon = \frac{T_{\text{in, air}} - T_{\text{out, air}}}{T_{\text{in, air}} - T_{\text{sat, water}}} \quad \text{air side} \quad (69)$$

Effectiveness maps are used in a modified form incorporating the ambient pressure effects on T_{sat} . Figure 49 is typical water boiler effectiveness data. Water flow rate is based on free convection only. Forced convection is not considered typical design practice. Air side pressure drop is determined in the same manner as for single phase heat exchangers.

Size - The single phase core sizing procedures are used to size the boiler side core. The total mass of water available is:

$$W_{\text{water}} = (\text{BR}) (\theta) \quad (70)$$

where:

BR = Boiling rate, obtained from heat load

θ = Time

Total volume of an integral boiler is:

$$V_B = V_{\text{core}} + \frac{W_{\text{water}}}{\rho} \quad (71)$$

where:

V_B = Boiler volume

V_{core} = Core volume

Wt_{water} = Mass of water

ρ = Water density at T_{sat}

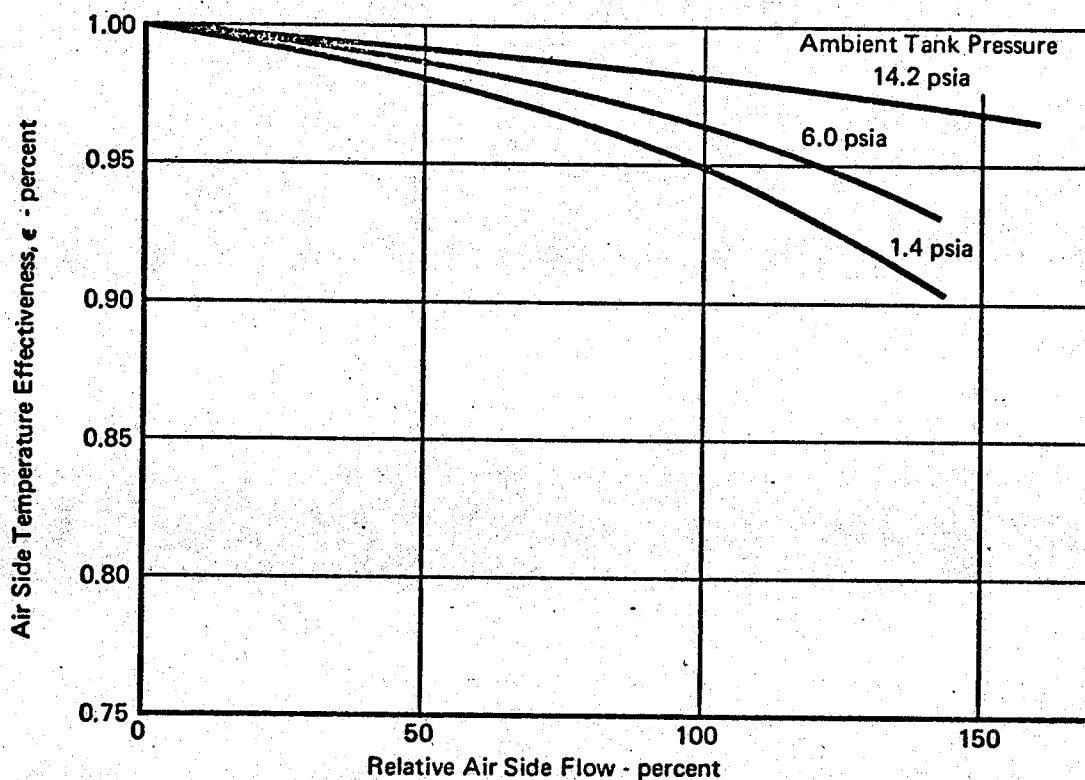


Figure 49 Typical Boiler Performance

GP 9416-141

Weight - The combined weight of the core, the water, and the integral container is the boiler weight. The container is assumed cubic in shape, and made of aluminum or steel, as desired. Material gage is held constant at 0.050 with 100% of the container metal weight allowed for stiffeners and supporting structure. Therefore, the container weight is:

$$Wt_{container} = 2(6 V_B^{2/3} t_{metal} \rho_{metal}) \quad (72)$$

For water boilers with a separate storage tank the heat exchanger is weighted dry (see Section 3.1.1) and the tank is sized to hold all the water. The tank is considered as a cylinder with hemispherical ends and a length to diameter ratio of 2. Therefore, knowing the volume of water required, the

corresponding surface area is:

$$A = 2\pi \left(\frac{12V}{5\pi}\right)^{2/3}$$

The container is considered to be made of 0.050 aluminum weighing 0.1 lb/in³. Therefore, container weight is equal to 0.005 A(pounds). Adding a 100% of the metal weight to account for stiffening and supports yields:

$$Wt_{water\ tank} = 0.01 A + Wt_{water} \quad (73)$$

This approximates the weight and volume of water storage tanks for boilers. If the tank is integral with the surrounding structure the effects of the water on the system weight must be evaluated separately.

3.1.4 Resistance Heaters - Construction of resistance heaters (electric heaters) consists of a finned heat transfer surface on the air side and a resistance material coating on the element plates. Protection from overheating is provided by a thermal protector for each heater element. Figure 50 illustrates a typical resistance heater construction. Only single pass configurations are considered typical.

Performance - Resistance heaters normally are insulated, hence all energy supplied to the heater element is absorbed by the air stream. The exit temperature is:

$$T_X = \frac{Q'}{Wc_p, \text{air}} + T_{in} \quad (74)$$

Pressure drop is based on ΔP versus flow rate obtained by the same procedure as for any heat exchanger. (See Section 3.1.1.) Typical fin geometry is: $16.96T(D) - 0.126/0.125 - (P) - 0.006(AL)$. Figure 51 represents the friction factor versus Reynolds number for this fin.

Size - Resistance heater size is based on the maximum input power condition. Using a value of $25 \text{ KW}/\text{ft}^3$ as a power density typical of heater construction a core volume is obtained directly. This volume is considered to have a face area normal to the air stream (A), and a flow length (L). The variables L and A are varied until they satisfy the overall volume requirement and the pressure drop requirement.

Weight - Weight is calculated from an average core density obtained from Figure 52. This weight represents the total weight of fins, electrical hardware, and required supports. The heater is considered immersed in the air duct, and header weight is not assumed part of the heater.

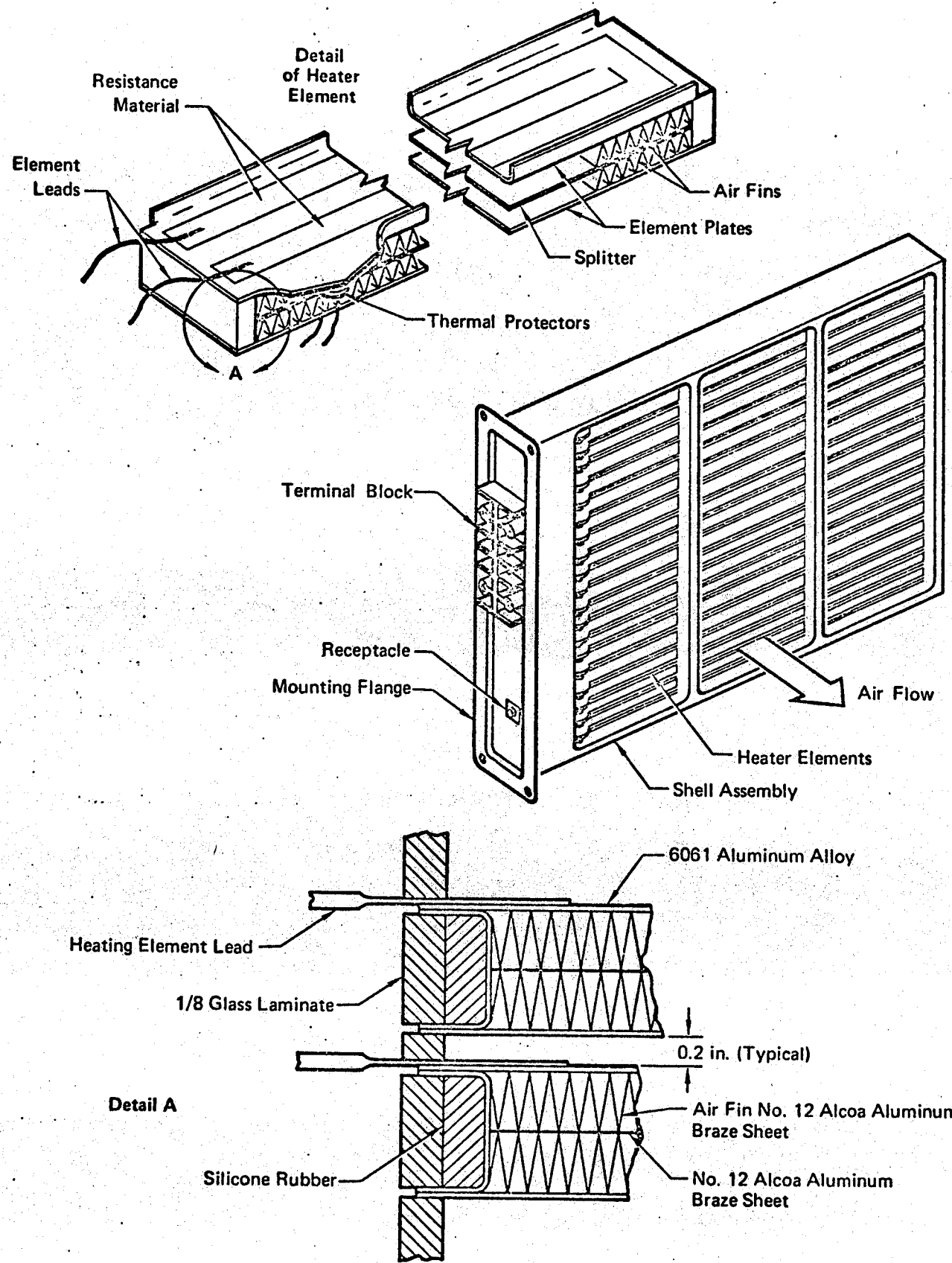


Figure 50 Typical Resistance Heater

GP 9416-187

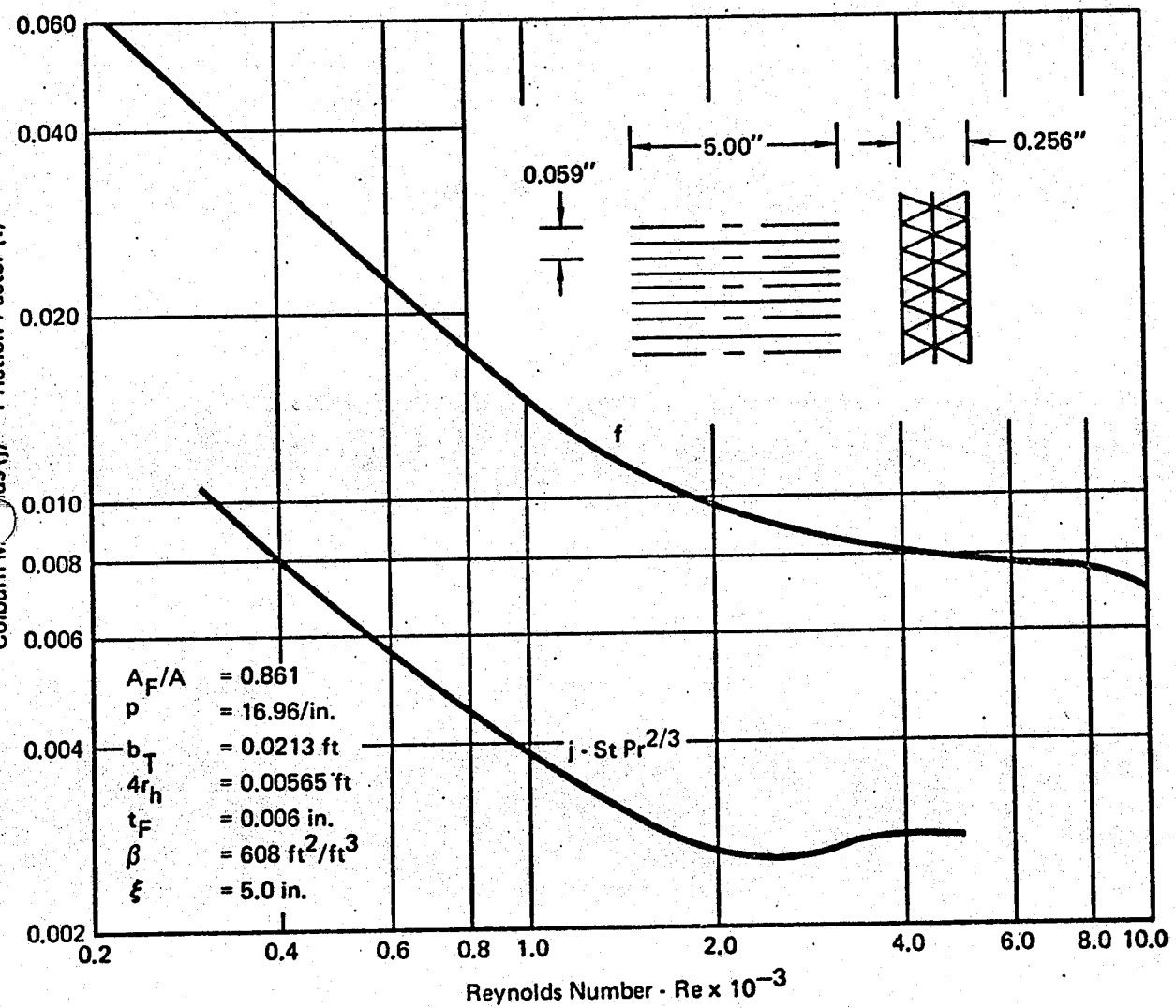


Figure 51 Plain Triangular Fin Surface

$$16.96T(D) - 0.126/0.125 - (P) - 0.006$$

GP 9416-133

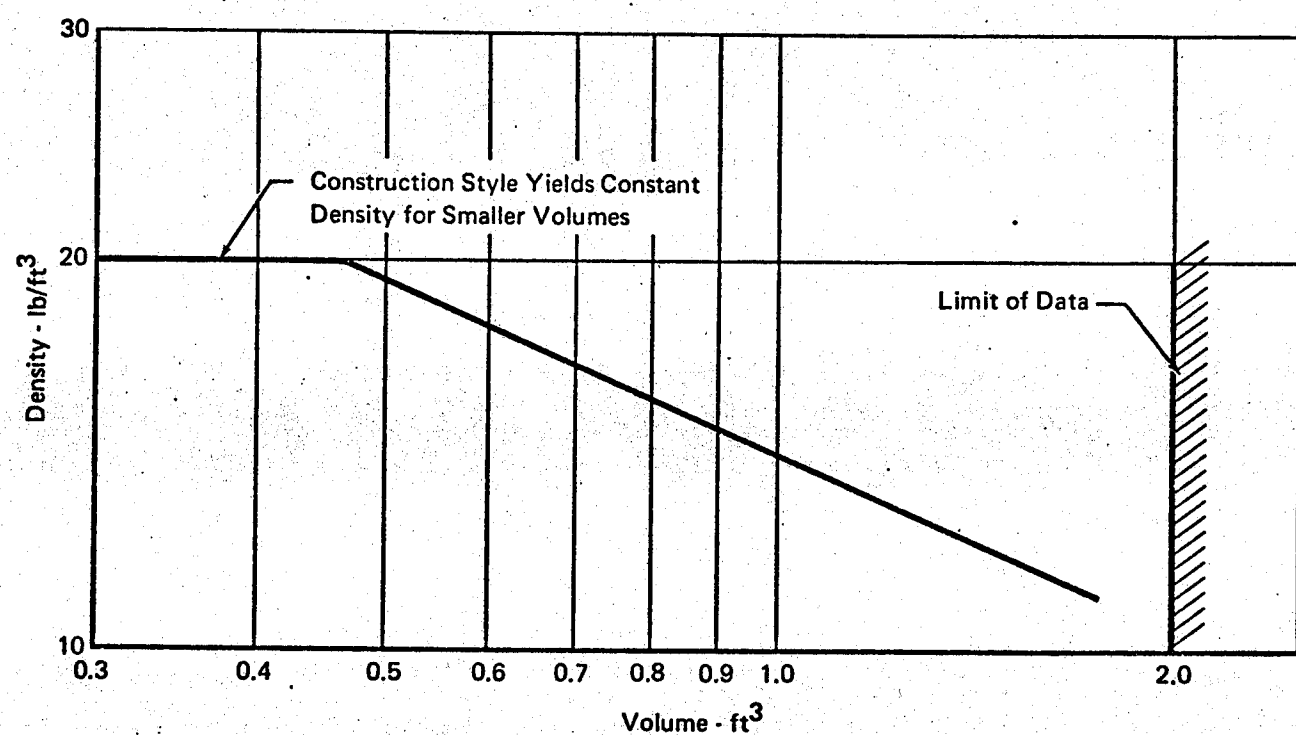


Figure 52 Electric Heater Density

GP 9416-140

3.2 Air Cycle Machines

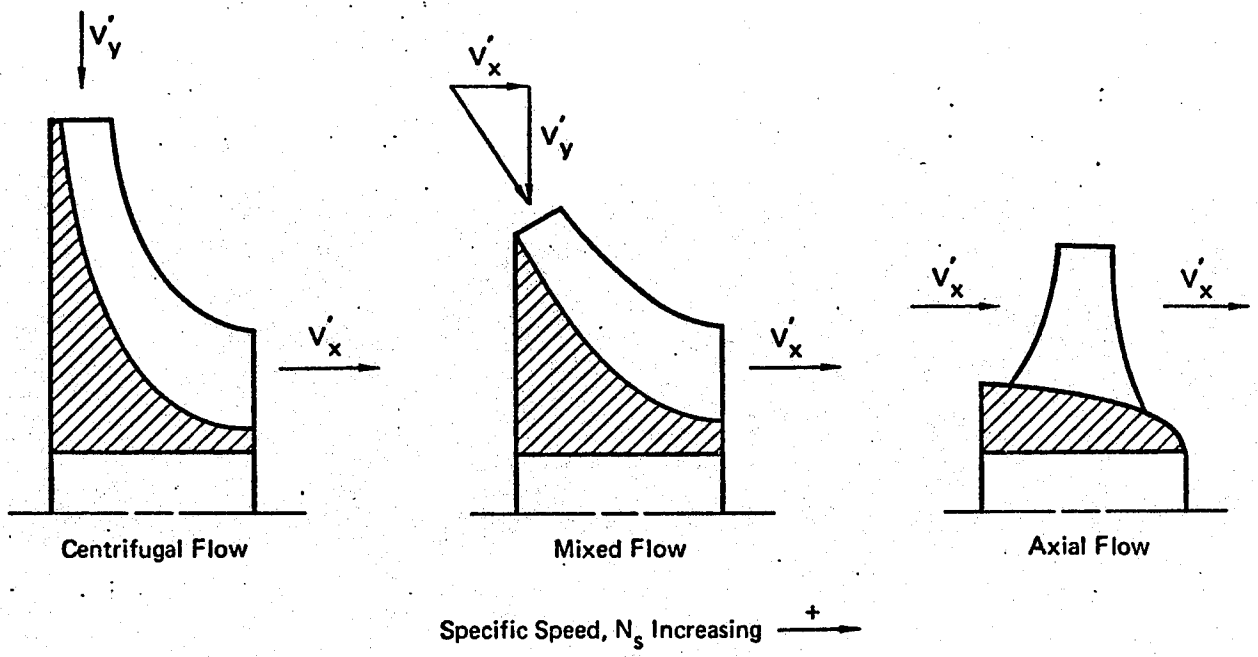
Machines which produce a pressure rise (head) or power using rotative elements, without fixed displacement, are generally classified as turbomachines. Head or pressure producing turbomachines are called pumps, fans, or compressors. Power producing turbomachines are called turbines. All types of turbomachines involve energy transfer between the fluid stream and the rotor. The resultant pressure effects are dependent on the geometry of the rotor and the nature of the energy transfer. Three rotor geometries are commonly used: centrifugal, mixed flow, and axial. (See Figure 53.) Centrifugal rotors generally are used to develop high heads for low flow at moderate to high speed operation. Mixed flow rotors are applied to moderate speed, high flow conditions requiring a low head. Axial rotors are used when high speed and high flow are desired with a low head.

Most aircraft ECS use the centrifugal turbomachine geometry. Therefore, the majority of the design data presented herein are for this rotor geometry. The analysis method is general and is adaptable to any rotor geometry if appropriate design data are utilized. Additional data are included for mixed and axial processes.

Selection of a rotor geometry implies an overall similitude approach to determine the performance-size relationships for that geometry. Utilizing dimensionless groupings of pertinent variables to express geometric, kinematic, and dynamic quantities enables one to compare the physical nature of various turbomachines. Therefore, if two turbomachines are operated such that all the dimensionless groups are equal, the same physical conditions are said to exist. Equality of the physical conditions implies: (1) kinematic similitude, where the velocity ratios are the same throughout the entire process; (2) dynamic similitude, where the ratios of the forces between the rotor and the fluid are the same; and (3) geometric similitude, where the various dimension ratios are everywhere the same.

Application of the turbomachine elements are directed to three basic air cycles found in aircraft ECS. These cycles are Bootstrap (Figure 15), Simple (Figure 12), and Simple-Bootstrap (Figure 19).

Simple air cycle turbomachines have a radial or axial turbine loaded by a radial or axial compressor. The compressor selection is based on the flow and head demands of the ram air circuit. Axial compressors typically are used for high flow rates at low head to provide an adequate ram air heat sink.



Note: Velocities are reversed for compression processes.

Figure 53 Types of Turbomachinery

GP 9416-195

Radial compressor designs are preferred where only a load for the turbine is desired. Bootstrap air cycle turbomachines are radial compressor designs driven by an axial or a radial turbine. The radial design is dominant. Simple-bootstrap air cycle turbomachines have three wheels on the same shaft. The turbine and compressor wheel designs are radial while the fan is axial (based on the four which have been designed).

3.2.1 General Turbomachine Design - Relationships between performance and size is accomplished by describing the compression and expansion processes in dimensionless terms.

3.2.1.1 Energy Transfer - Development of dimensionless groups, for expressing similarity conditions, is dependent on understanding the nature of the energy transfer between the rotor and the fluid. The energy equation for a general turbomachine process leads to the Euler turbine equation (Reference 11):

$$E = \frac{1}{2g_c} [(v'_1)^2 - v'_{r1}^2] + (u'_1)^2 - u'_{r2}^2 + (v'_{r2})^2 - (v'_{r1})^2 \quad (75)$$

The terms of the equation represent the fluid velocity components shown in Figure 54. (An outward flow radial compressor is shown, but the general relations also apply to a turbine if the flow directions are reversed.)

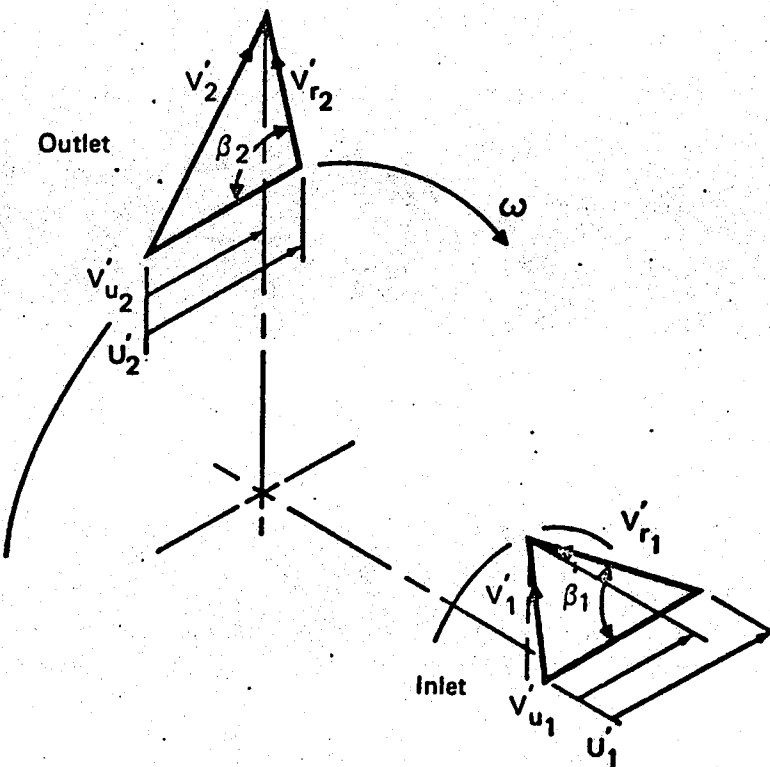


Figure 54 Velocity Triangles for a Generalized Rotor

The following terms represent the various components of total energy (E).

$(v'_1^2 - v'_2^2)$ represents the absolute change in kinetic energy of the fluid. It is the dynamic component of the total energy.

$(U'_1^2 - U'_2^2)$ describes the change in centrifugal energy developed in rotating an element of fluid from one radius of rotation to another.

$(v'_{r_2}^2 - v'_{r_1}^2)$ represents the change in the relative velocity between the rotor and the fluid.

Both $(U'_1^2 - U'_2^2)$ and $(v'_{r_2}^2 - v'_{r_1}^2)$ describe the change in the static component of the total energy. Each of these terms varies with the type of rotor design and the thermodynamic process involved.

The ratio of static energy to total energy is termed reaction (Ψ).

$$\Psi = \frac{1}{2g_c} \frac{(U'_1^2 - U'_2^2) + (v'_{r_2}^2 - v'_{r_1}^2)}{E} \quad (76)$$

The reaction of a particular turbomachine indicates the nature of the fluid energy at the exit condition. If $\Psi = 0$, the entire energy change (less losses) is due to the change in fluid velocity, with the inlet static head remaining constant throughout the process. The other extreme is $\Psi = 1$, with the exit dynamic energy equal to the inlet dynamic energy, and the energy change is due to static head only. Changes occur in all three components of total energy in actual processes, thus reaction is between 0 and 1. Rotor geometry and blade angle affect the energy transfer. Of the three basic rotor geometries mentioned, the centrifugal design (Figure 53) has the widest use in ECS turbomachinery. A nominal design for a centrifugal compressor rotor is an exit blade speed equal to twice the inlet blade speed (i.e., $U'_2 = 2U'_1$) and an inlet blade angle of 45° ($\beta_1 = 45^\circ$). The outlet blade angle is allowed to vary, hence the reaction (Ψ) is a function of outlet blade angle only:

$$\Psi = \frac{2 + \cot \beta_2}{4} \quad (77)$$

This relation is shown in Figure 55. With appropriate change in nomenclature, the result applies to a centrifugal turbine rotor also. The balance of this report deals with the centrifugal style of rotor.

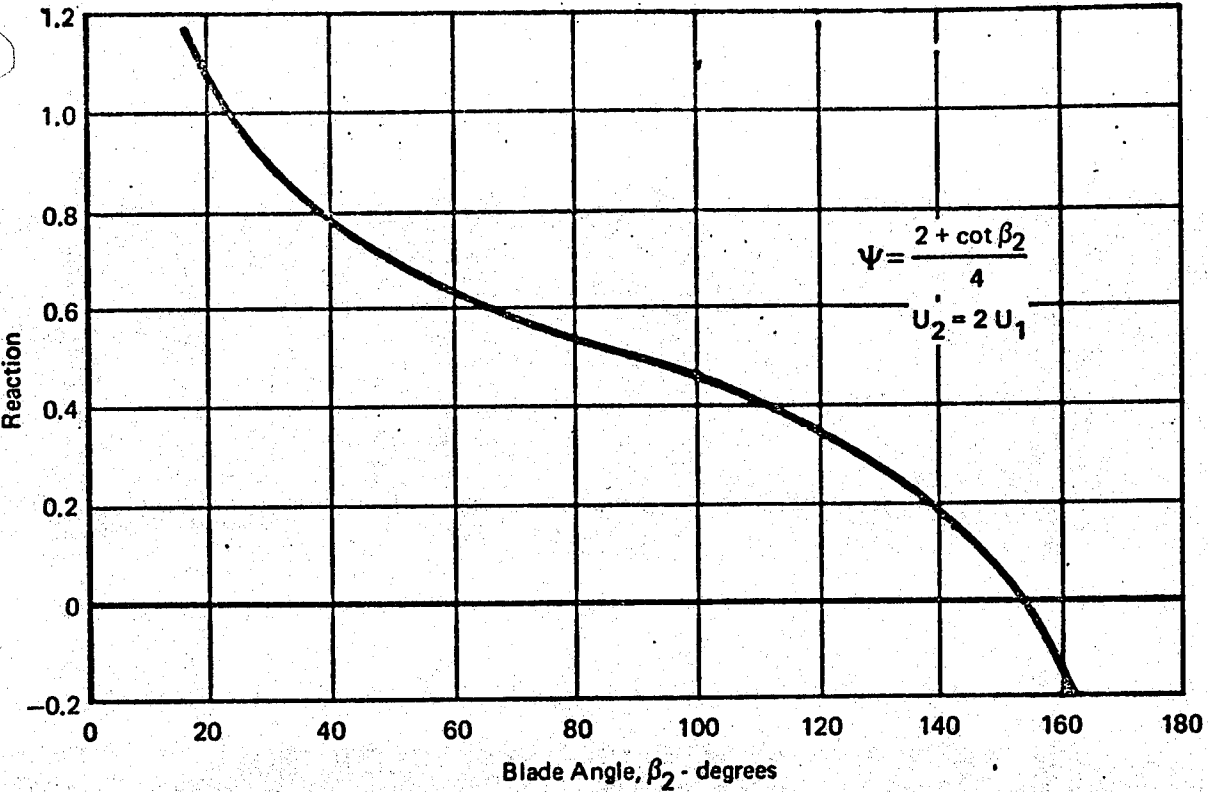


Figure 55 Reaction for Generalized Turbomachine

The change in the thermodynamic state of the fluid is related to the shaft work by:

$$W_s = c_p (T_1 - T_2) + \frac{V_1^2 - V_2^2}{2g_c} + Q' \quad (78)$$

The shaft work also can be related to the total temperature (T_T):

$$W_s = c_p (T_{T1} - T_{T2}) + Q' \quad (79)$$

The above equation represents the energy transfer incurred in the process.

Equating the Euler turbine equation to shaft work yields:

$$\frac{1}{2g_c} \left[(V_1^2 - V_2^2) + (U_1^2 - U_2^2) + V_{r2}^2 - V_{r1}^2 \right] = c_p (T_{T1} - T_{T2}) + Q' \quad (80)$$

This equation form relates the dynamic statement of energy transfer to the thermodynamic statement. If the process is adiabatic then the heat energy (Q') equals zero. Therefore, energy, as described by the Euler Equation, is equated to the change in temperature of the fluid.

The compression or expansion process of an actual turbomachine is not isentropic. The adiabatic efficiency is the ratio of the changes of enthalpy the isentropic and actual compression or expansion processes. For air as an ideal gas, the isentropic enthalpy change is related to the pressure ratio across the turbomachine. Thus, for a compressor, the adiabatic

efficiency is:

$$\eta_{ad,c} = \frac{T_{in} \left[\frac{y-1}{(PR)^{\frac{y}{\gamma}} - 1} \right]}{T_{out} - T_{in}} \quad (81)$$

where:

$$PR = \frac{P_{out}}{P_{in}}$$

The adiabatic efficiency of a turbine is:

$$\eta_{ad,t} = \frac{T_{in} - T_{out}}{T_{in} \left[\frac{1-(PR)}{\frac{y-1}{y}} \right]} \quad (82)$$

3.2.1.2 Dimensional Analysis - Applying dimensional analysis techniques to the general fluid flow problem encountered in an examination of the behavior of rotors is most useful in the analysis of the operating characteristics. Relationships between head, flow, size, and speed are of interest for any turbomachine. The variables H , Q , N , and D can be grouped into two dimensionless terms (noted here as Π).

$$\Pi_1 = \frac{Q}{ND^3} \text{ and } \Pi_2 = \frac{H}{D^2 N^2} \quad \text{if } \frac{Q^2}{ND^3} \times \frac{1}{D^2 N^2} = \text{ft}^2/\text{sec}^3 \times \frac{1}{g} = \text{ft}$$

Significance is given to these two Π 's by inspection of the properties involved (other relations between other variables also can be obtained, as is discussed in Reference 11).

Π_1 is termed capacity coefficient. It relates the flow rate in dimensionless terms. Also, since Q is proportional to $V'D^2$:

$$\Pi_1 = \frac{Q}{ND^3} \text{ which is proportional to } \frac{V}{ND} \quad (83)$$

The quantity ND (with D as the rotor diameter) represents the blade tip speed. Thus, for a fixed value of Π_1 , a relationship between fluid velocity and blade velocity is expressed. If Π_1 has the same value for two conditions of Q , N , and D , the velocity triangles for those conditions are similar (i.e., kinematic similarity is expressed).

Π_2 is termed the head coefficient. It represents the head in dimensionless terms. Since ND is proportional to U :

$$\Pi_2 = \frac{H_{ad}}{(U')^2 / g_c} \quad (84)$$

is a ratio of fluid head (total energy) to kinetic energy of the rotor.

as Π_2 expresses conditions of dynamic similarity.

Derivation of other similarity parameters as a function of Π_1 and Π_2 is presented in the following sections. These parameters are used in conjunction with generalized design data to obtain sizing criteria - the wheel diameter and the rotational speed.

Specific Speed - The terms developed in the previous section are combined to eliminate the characteristic dimension D.

$$\text{Cut noise } N^{20\%} \Pi_3 = \frac{(\Pi_1)^{1/2}}{(\Pi_2)^{3/4}} = \frac{(NQ)^{1/2}}{H^{3/4}} \quad \left(\frac{Q}{ND^3} \right)^{1/2} = \frac{\cancel{H^{3/4}}}{\cancel{(D^3 N^2)}} \quad \frac{Q^{1/2} D^{3/2} N^{3/4}}{H^{3/4}} \quad (85)$$

This Π_3 term is referred to as specific speed (N_s). It expresses all values of N, Q, and H which lead to similar flow conditions in geometrically similar turbomachines. (Q is $\text{ft}^3/\text{sec.}$)

$$N_s = \frac{(NQ)^{1/2}}{H^{3/4}} g H \quad (86)$$

N_s is evaluated at a best efficiency condition for design purposes.

Specific Diameter - The Π terms are combined to eliminate rotational speed (N), yielding specific diameter (D_s). (Q is $\text{ft}^3/\text{sec.}$)

$$\Pi_4 = \frac{(\Pi_2)^{1/4}}{(\Pi_1)^{1/2}} = \frac{DH^{1/4}}{Q^{1/2}} \quad H \approx \text{feet} \quad (87)$$

$$D_s = \frac{DH^{1/4}}{Q^{1/2}} \quad 100 = \frac{100}{(100)^{1/2}} \quad 10 = \frac{D}{(80)^{1/2}} \quad (88)$$

The variables D, Q, and H describe a range of geometrically similar turbomachines independent of the rotational speed.

Adiabatic Head Coefficient - The adiabatic head coefficient ($q_{ad,c}$), which represents the conditions of dynamic similarity, is used in describing compression processes. Using Equations (86) and (88) for N_s and D_s , respectively, the adiabatic head coefficient is rewritten as:

$$q_{ad,c} = \Pi_2 = \frac{3600 g_c}{D_s^2 N_s^2 \pi^2} \quad (89)$$

Expansion processes are represented by inverting Π_2 . The tip speed of the

$$\begin{aligned} N &= 100 \\ Q &= 100 \\ N_s h &= 100^0 \\ Q &= 80 \\ N &= 111.8 \end{aligned}$$

turbine wheel (U'_1) is proportioned to DN. A theoretical nozzle spouting velocity (c_o) is defined, which is proportioned to the inlet head (H). The ratio of tip speed to theoretical spouting velocity (turbine velocity ratio) is proportional to the square root of the reciprocal of N_s^2 .

$$\frac{U'_1}{c_o} \alpha(\pi_2)^{-1/2} = \frac{DN}{\sqrt{H}} \quad (90)$$

or

$$\frac{U'_1}{c_o} = (\alpha_{ad})^{-1/2}$$

$$\pi_2 = \frac{3600 g_c}{D_s^2 N_s^2 \pi^2}$$

Therefore:

$$\frac{U'_1}{c_o} = \frac{\pi D_s N_s}{60(g_c)^{1/2}}$$

$$\frac{1}{\pi_2^{1/2}} = \frac{D_s N_s \pi}{60 \sqrt{g_c}} \quad (91)$$

or

$$\frac{U'_1}{c_o} = \frac{U'_1}{60 \sqrt{g_c H_{ad,t}}}$$

(92)

Mach Number - Relationships between the Mach number based on the peripheral component of fluid velocity, and the maximum efficiency achievable in compression processes are established in References 11 and 12. The reference Mach number is defined as:

$$M^* = \frac{U'_2}{c_{in}^*} = \frac{U'_2}{\left(\frac{2\gamma}{\gamma+1} g_c R T_{in} \right)^{1/2}} \quad (93)$$

Solving Equation (84) for U'_2 yields:

$$U'_2 = \left(\frac{g_c H_{ad}}{\alpha_{ad}} \right)^{1/2} \quad (94)$$

The adiabatic head is defined as:

$$H_{ad,c} = \frac{\gamma R T_{in}}{\gamma-1} \left[\left(\frac{P_{out}}{P_{in}} \right)^{\frac{\gamma-1}{\gamma}} - 1 \right] \quad (95)$$

Substituting into the above equation for M^* yields:

$$M^* = \left[\frac{\left(\frac{P_{out}}{P_{in}} \right)^{\frac{\gamma-1}{\gamma}} - 1}{2 \frac{\gamma-1}{\gamma+1} q_{ad,c}} \right]^{1/2} \quad (96)$$

This relationship is used to compare a given compression process to an optimum process having the same inlet conditions.

Power - The energy required to raise a given flow to a specific head per unit time is power. Introducing specific speed (from Equation (86)) into this equation yields:

$$HP = \frac{\rho H_{ad}}{550} \left(\frac{N_s H_{ad}}{N} \right)^{3/4} \quad (97)$$

The efficiency is used to obtain power for real compression and expansion processes. Hence the power required by a compressor is:

$$HP_c = \frac{\rho_{in} Q_{in} H_{ad,c}}{550 \eta_{ad,c}} = \frac{\rho_{in}}{550 \eta_{ad,c}} \left(\frac{N_s H_{ad,c}}{N} \right)^{5/4} \quad (98)$$

and the power produced by a turbine is:

$$HP_t = \frac{\rho_{out} Q_{out} H_{ad,t} \eta_{ad,t}}{550} = \frac{\eta_{ad,t} \rho_{out}}{550} \left(\frac{N_s H_{ad,t}}{N} \right)^{5/4} \quad (99)$$

The power output of a turbine must be balanced by the power required by the compressor of a simple or a bootstrap air cycle machine. This is expressed as a power ratio (κ):

$$\kappa = \frac{\frac{HP_c}{c}}{\frac{HP_t}{t}} = \frac{\frac{(W_c p \Delta T)_c}{c}}{\frac{(W_c p \Delta T)_t}{t}} \quad (100)$$

To account for frictional losses and leakage $0.95 \leq \kappa \leq 0.98$. If a three-wheel turbomachine for a simple-bootstrap air cycle system is considered:

$$\kappa = \frac{\frac{HP_c + HP_f}{c}}{\frac{HP_t}{t}} = \frac{\frac{(W_c p \Delta T)_c + (W_c p \Delta T)_f}{c}}{\frac{(W_c p \Delta T)_t}{t}} \quad (101)$$

and typically $0.95 \leq \kappa \leq 0.98$.

3.2.1.3 Generalized Design Diagrams - Similarity relations for the design of turbomachines are discussed in Reference 12. Generalized design diagrams which relate specific speed (N_s), specific diameter (D_s), and efficiency (η) are derived in this reference for several types of

turbomachines. N_s - D_s diagrams for compressors and turbines are presented in this section.

The N_s - D_s generalized design diagram for centrifugal (radial) compressors is shown in Figure 56. This figure is calculated for a Mach number (M^*) of 1.5, a pressure ratio of 3, and a high Reynolds number. In the low specific speed regime the efficiency is reduced as a function M^* , as is shown in Figure 57. The pressure ratio effect is included in the reference M^* . (See Equation 96.) At high specific speeds the inlet Mach number becomes a limiting criterion if the pressure ratio is greater than 4. Smaller efficiencies than are given in Figure 56 are obtained at lower Reynolds numbers (see Reference 12), but a Reynolds number correction is not utilized herein.

The generalized N_s - D_s diagram for low pressure ratio compressors (e.g., axial) is shown in Figure 58 (from Reference 12). This figure is based on large Reynolds numbers. The efficiency values quoted in Figure 58 represent average values (i.e., they are not limiting values).

The generalized N_s - D_s design diagram for centrifugal (radial) turbines is given in Reference 12. (See Figure 59.) This figure is calculated for a pressure ratio (P_{in}/P_{out}) of 6 and high Reynolds number. At pressure ratios other than 6, the change in efficiency is expressed by the relation:

$$\eta_{r_{PR=6}} - \eta_{r_{PR=6}} = (5 \times 10^{-9}) N_s^{3/2} D_s^{5/2} \left[\left(\frac{P_{in}}{P_{out}} \right)^{\frac{1}{Y}} - \left(\frac{P_{in}}{P_{out}} \right)^{\frac{1}{Y}} \right] \quad (102)$$

where the reference condition is a pressure ratio of 6. A useful item of information obtained from Figure 59 is the maximum adiabatic efficiency for a specified velocity ratio (U'_1/c_0) which is presented in Figure 60.

The generalized N_s - D_s diagram for axial turbines is given in Figure 61. This figure is based on a reaction turbine having a large Reynolds number. The axial turbine geometry ratio indicated in Figure 61 describes optimum values. (See Reference 13.) *P.R. limit for axial turbines = ?*

These turbomachine N_s - D_s diagrams are representative of good design. They express relationships by which turbomachine sizing and performance data are obtained.

3.2.1.4 Performance - These general turbine and compressor data are related to specific component data. Use of the generalized N_s - D_s diagrams for evaluating component off-design performance is compared to actual

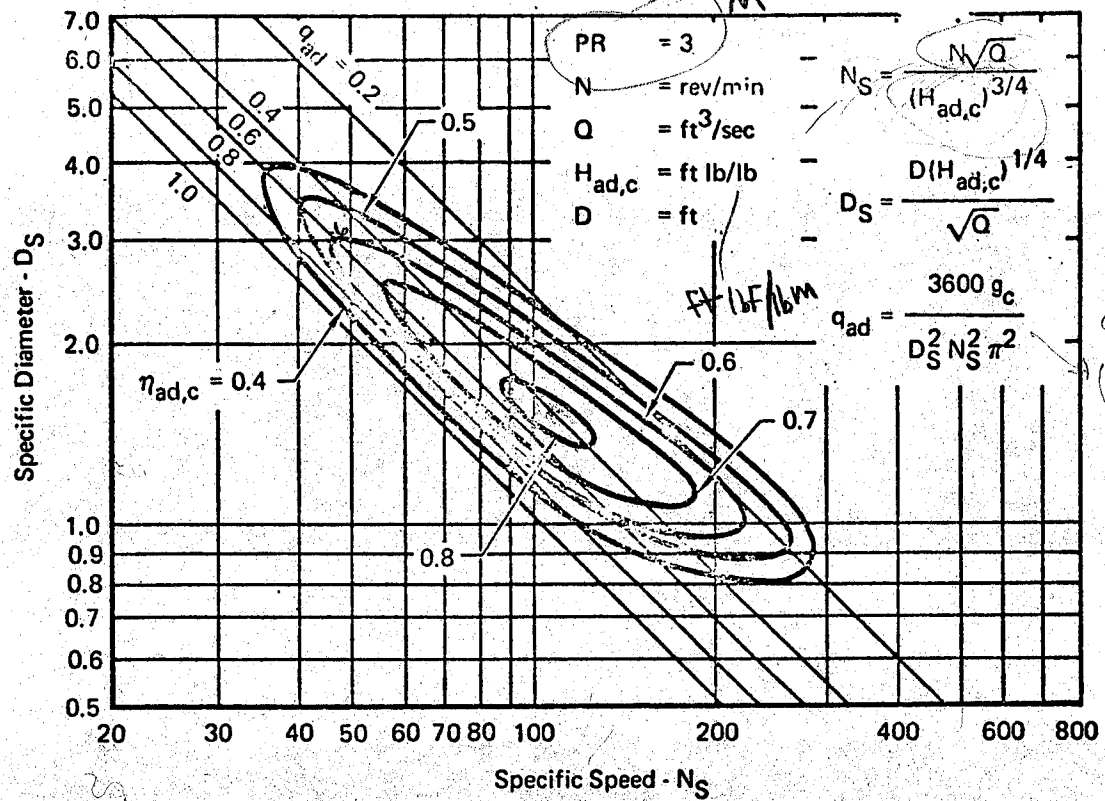


Figure 56 N_s - D_s Diagram for Centrifugal Compressors

GP 9416-55

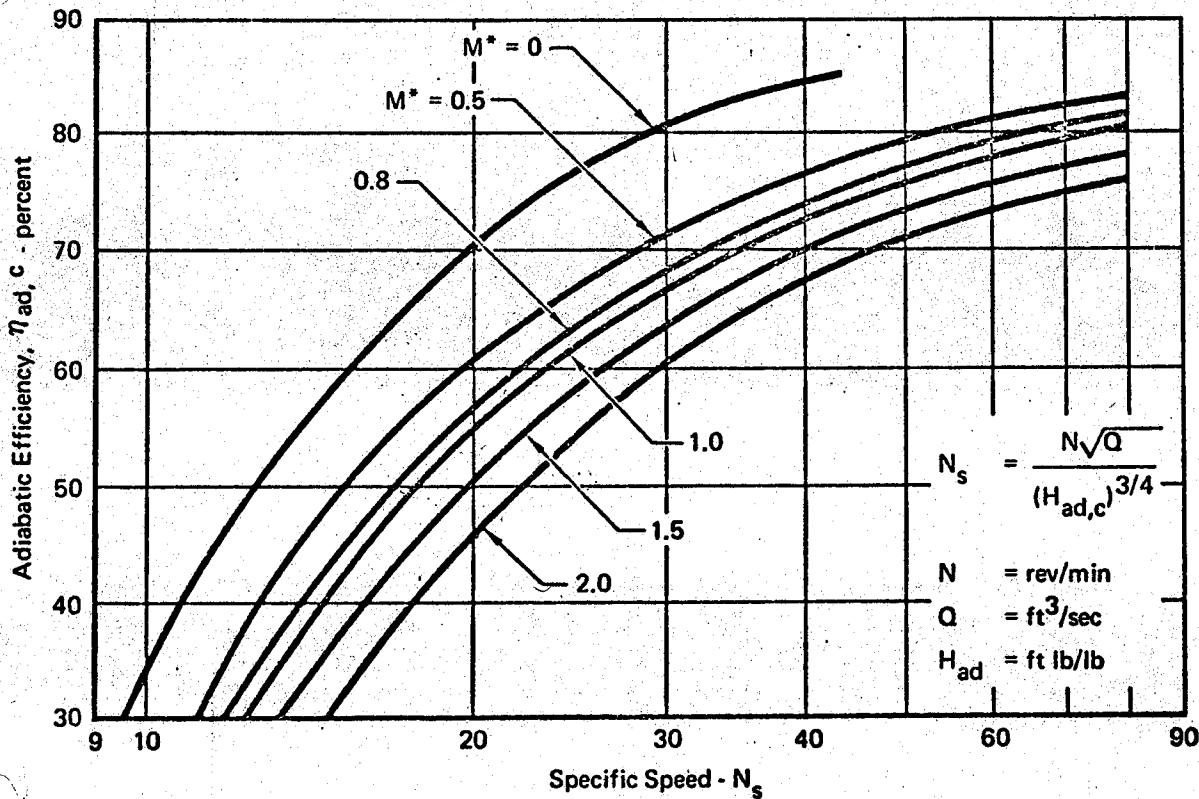


Figure 57 N_s - η_{ad} Diagram for Centrifugal Compressors

GP 9416-54

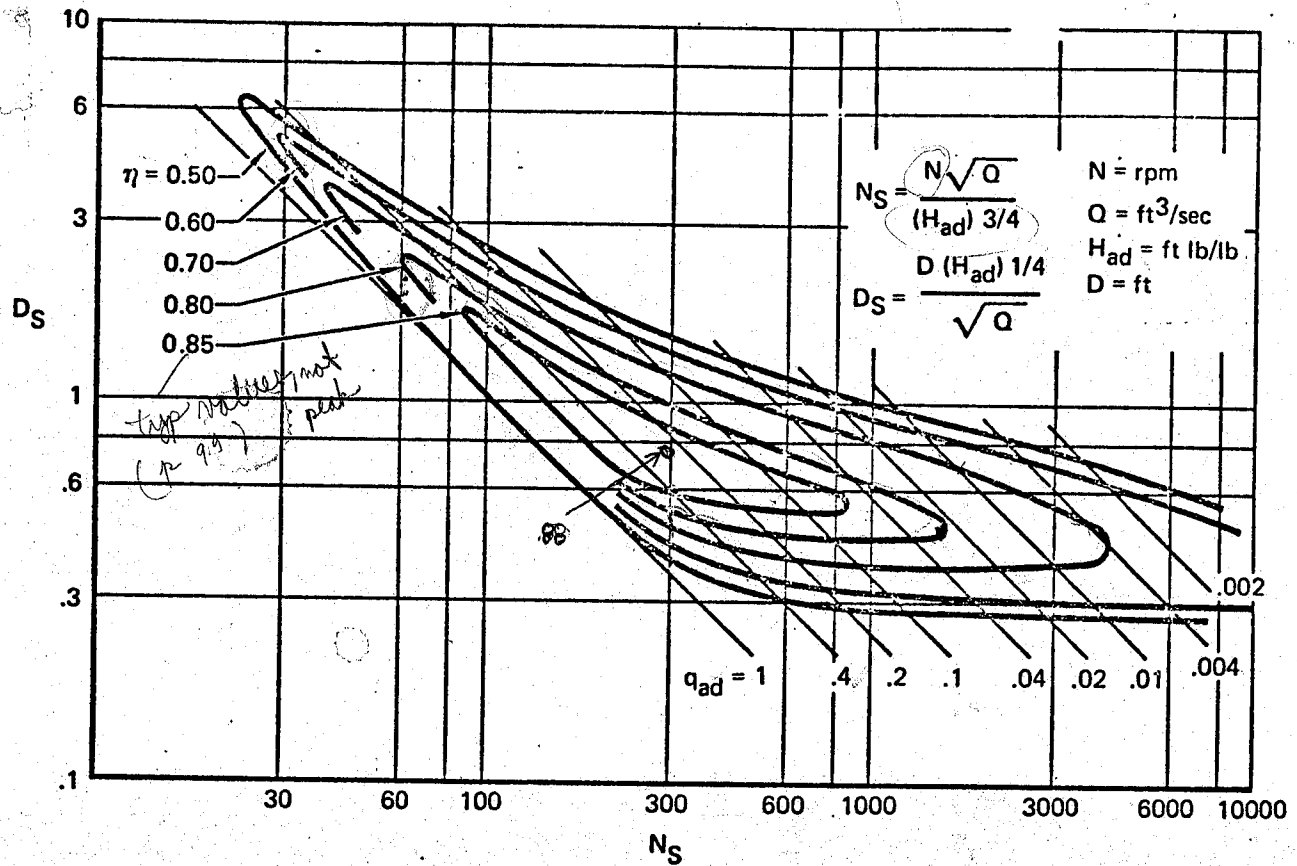


Figure 58 N_s - D_s Diagram for Low Pressure Ratio Compressors

GP 9416-191

(axial)

also low PR fans
(see p 118)

53.3 for air

$$H_{ad} = \frac{k}{\alpha-1} R \Delta T$$

$$= \frac{ft/lbf}{lbm^{0.8} R} \times 0R = \frac{ft/lbf}{lbm}$$

$$R_{He} =$$

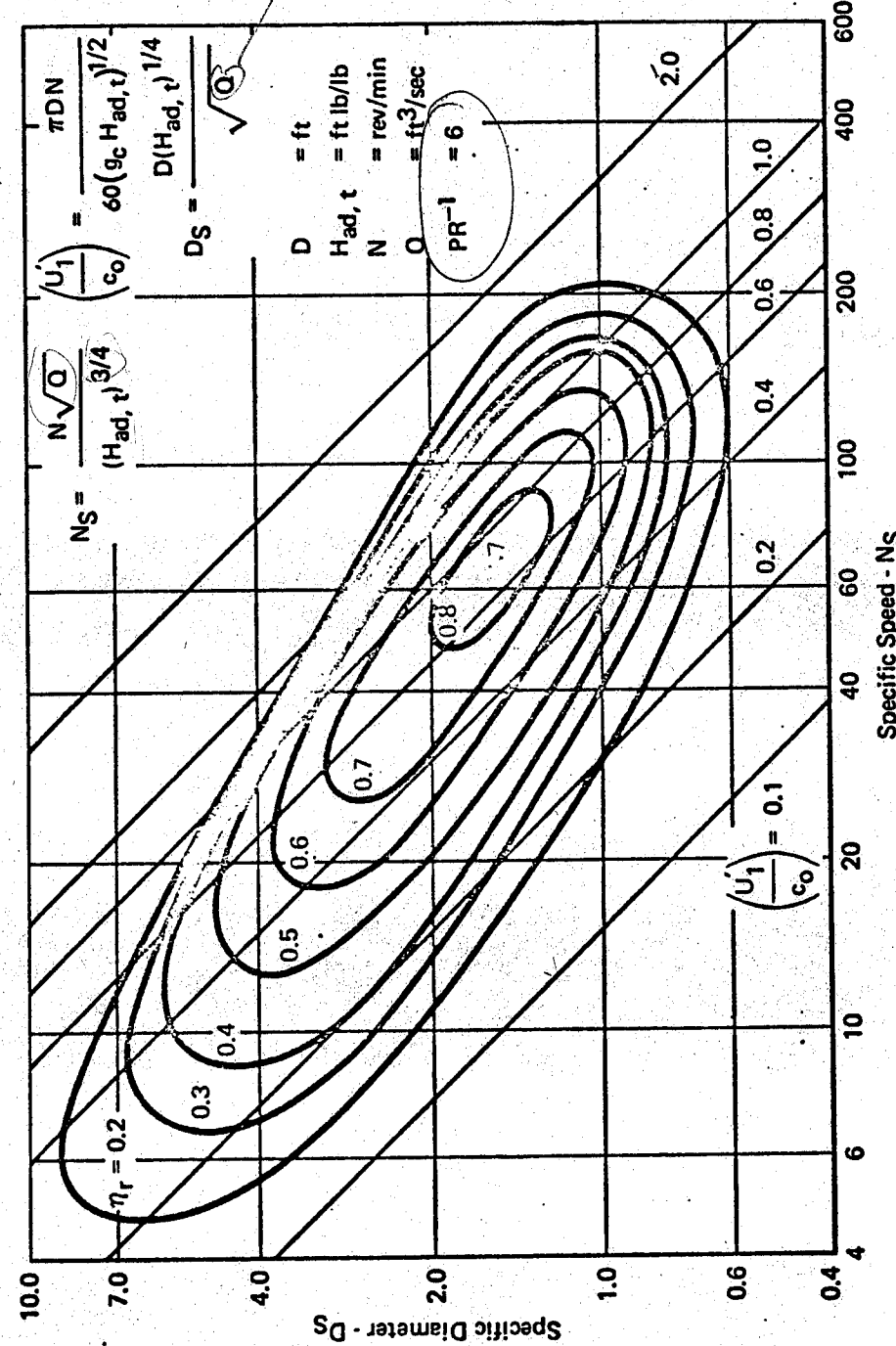


Figure 59 N_s - D_s Diagram for Centrifugal Turbines

GP 9416-53

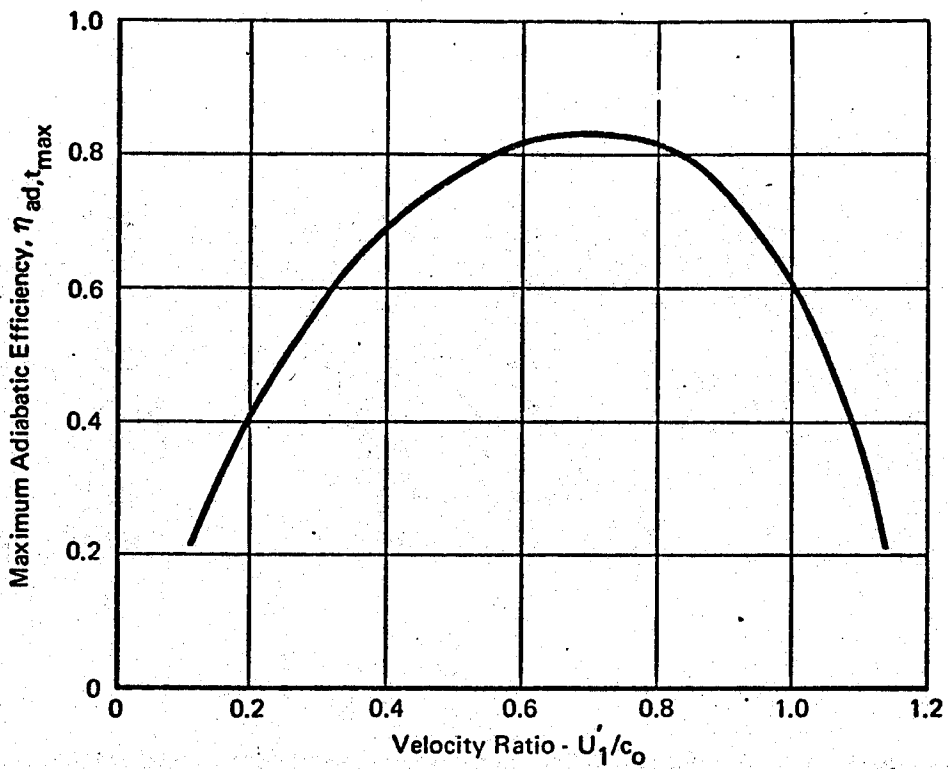


Figure 60 Maximum Adiabatic Efficiency for Centrifugal Turbines

GP 9416-56

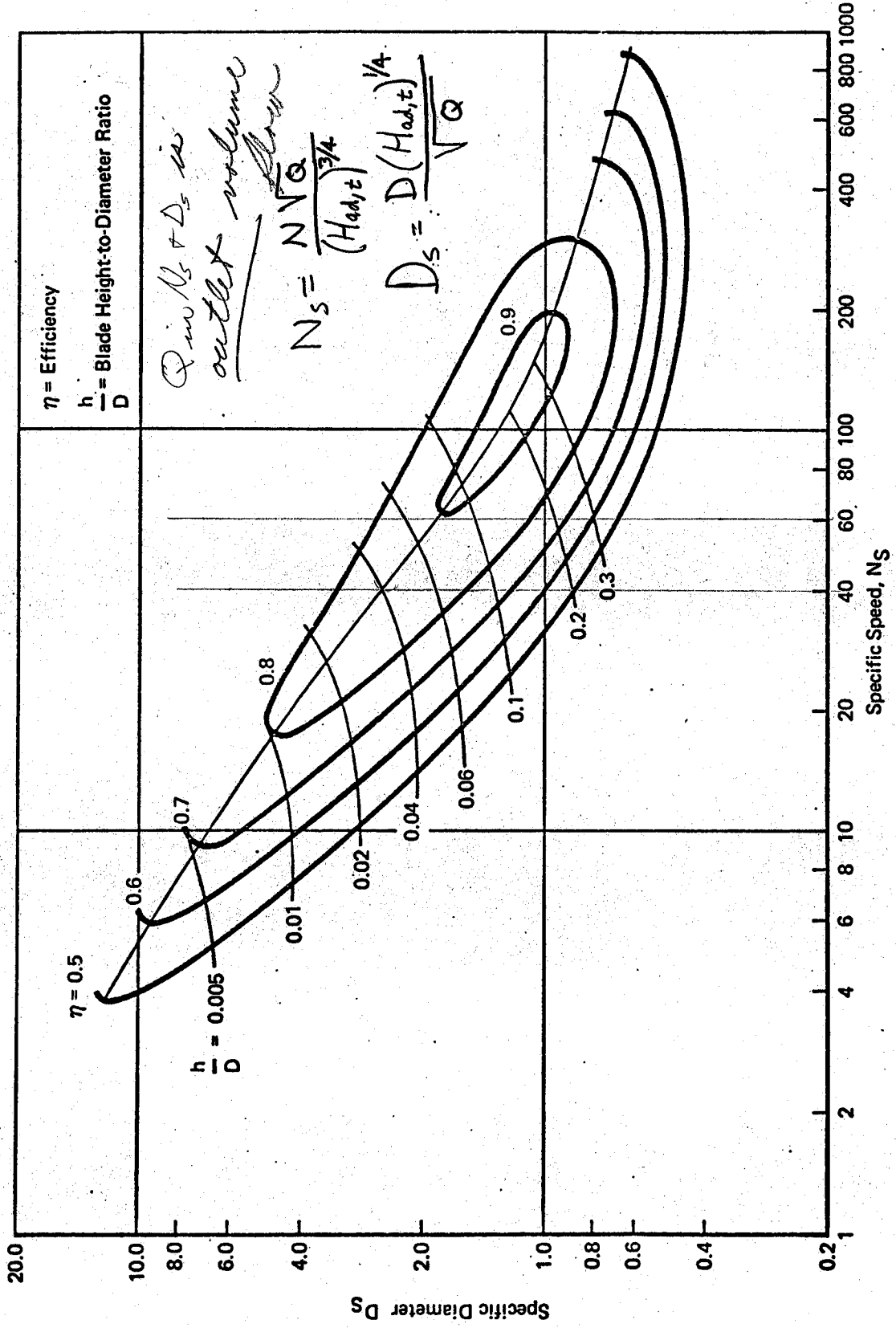


Figure 61 N_s - D_s Diagram for Axial Turbines

GP 9416:192

performance in Figure 62. This figure shows calculated efficiencies compared to known efficiencies for several operating conditions and wheel geometries.

3.2.1.5 Size - The sizing approach for turbines, compressors, and fans is evaluated by comparing calculated wheel diameters to the known diameters. Table IV presents this comparison using speed as an indicator of the design condition. An estimate of the wheel diameter, based on the exterior component dimensions, is given for several turbomachines since the actual diameter is not known.

The volume of a compressor or turbine wheel and its housing nominally might be considered to be proportional to the wheel diameter cubed. Since the turbomachine (i.e., compressor and turbine, and fan if applicable) is an integral unit, its total volume can be determined. Assuming the cubic relationship, the volume of a single wheel and housing was determined. A correlation of these data indicated that the volume is better represented as being proportional to the fourth power of the wheel diameter. By proportioning the total volume according to D^4 , Figure 63 is obtained, with the correlation:

$$V = \frac{2}{3} D^4 \quad (103)$$

Figure 63 includes data from three-wheel turbomachines. The volume of the fan of these machines is relatively large. When this fan is considered to be 75% of the total volume, the compressor and turbine volumes correlate with those of two-wheel turbomachines. The volumes of these fans are approximately four times as large as for other turbomachines.

3.2.1.6 Weight - The weight of turbomachines was found to be proportional to the square of the wheel diameter, as suggested by Balje in Reference 12. The constant of proportionality suggested by Balje (for 100% admission turbines) was found to be low. The weight of a single wheel and housing was determined by ratioing the total turbomachine weight according to the square of the wheel diameter. (See Figure 64.) The resulting correlation is:

$$Wt = 0.40 D^2 \quad (104)$$

The standard error of this correlation is 12.2%. The fans of three-wheel turbomachines have been included in Figure 64. Reference 14 suggests that weight is proportional to diameter cubed, but this correlation did not fit the data for the full range of weights considered. Since Equation (104) describes the weight of a single wheel and housing, the total turbomachine

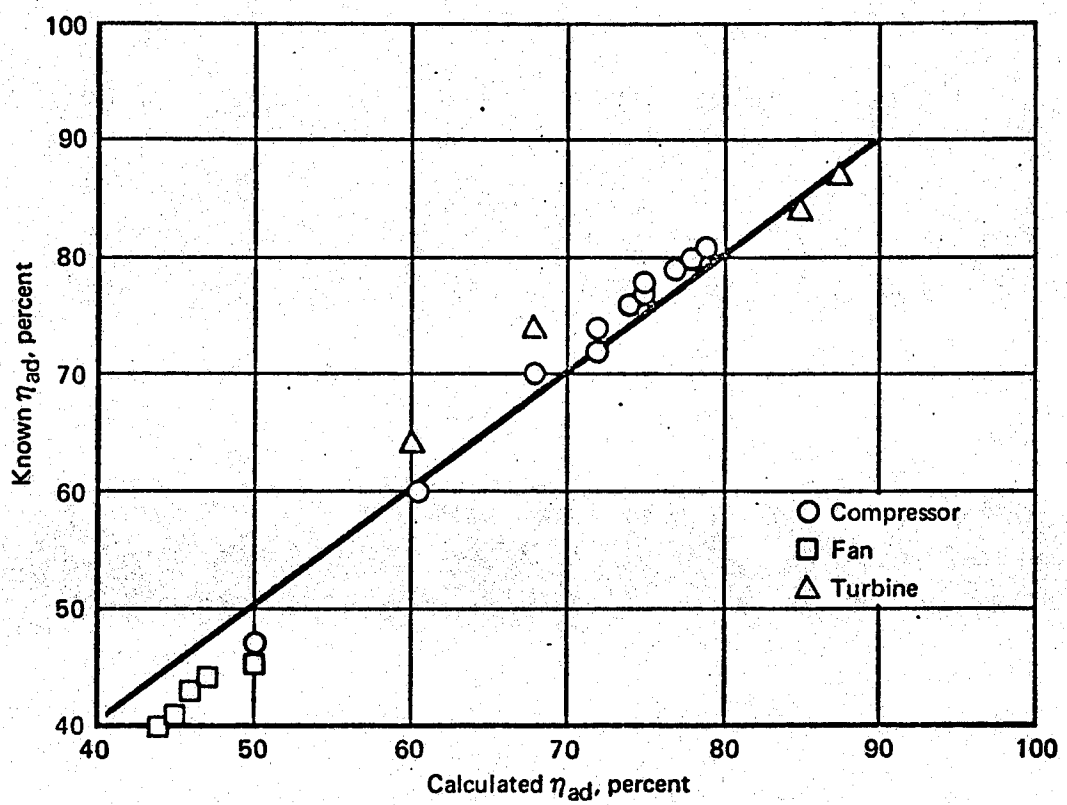


Figure 62 Turbomachine Off-Design Performance Comparison

GP 9416-211

Table IV. Size Comparison of Turbomachines

Wheel Type			Known Diameter (ft)	Calculated Diameter (ft)	Speed Basis (rpm)
Turb.	Comp.	Fan			
X	X		0.358	0.355	60,000
			0.333	0.347	60,000
O	O		0.290 → 0.250	0.286	86,000
			0.350 → 0.290	0.301	86,000
X	X	X	0.449	0.454	60,000
			0.466	0.476	60,000
			0.500	0.508	60,000
O		O	0.290 → 0.250	0.273	89,000
			0.340 → 0.308	0.320	89,000
O			0.450 → 0.360	0.444	70,000
O			0.380 → 0.350	0.346	82,000
O			0.450 → 0.390	0.446	82,000

X = Known Diameter

O = Estimated Diameter Range

GP 9416-197

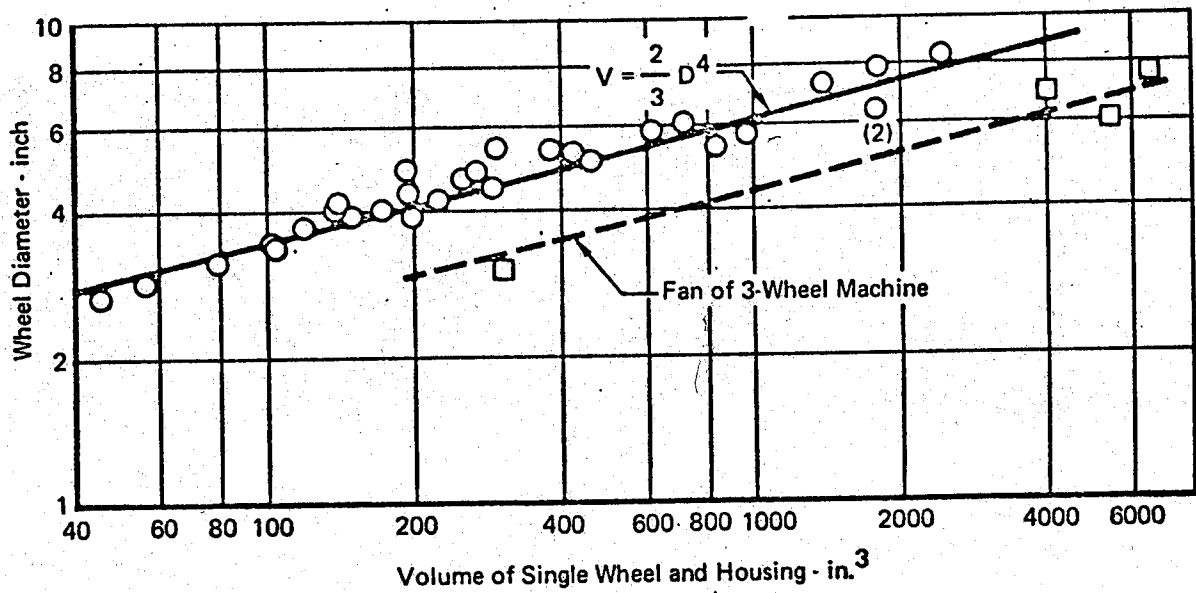


Figure 63 Turbomachine Volume

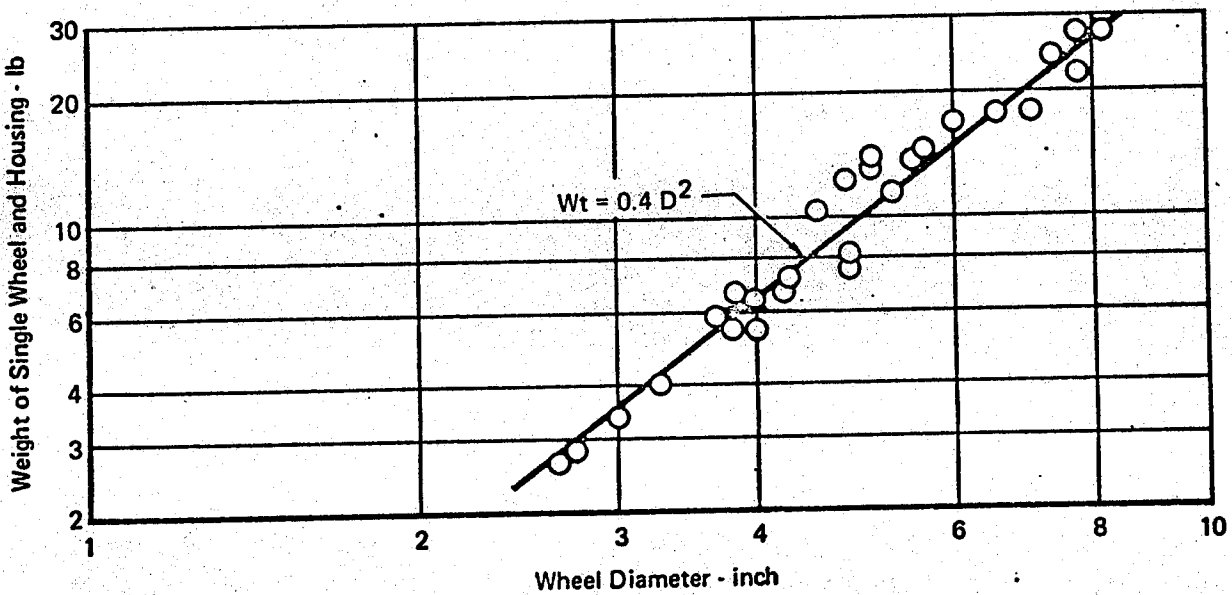


Figure 64 Turbomachine Weight

weight is the sum of the individual wheel weights.

Examples to determine the weights of air cycle turbomachines in the C-5A, F-111A, and B-52H (based on performance data from Reference 2) are described in Volume II.

3.2.2 Turbines - Expansion of the working fluid (e.g., air) is achieved by extracting work from the fluid, thus lowering the static components of total energy. Values for the reaction (Ψ) are typically 0.5 for most ECS applications. Figure 55 shows that this requires a blade angle of 90° for centrifugal turbine.

Inspection of the Euler turbine equation shows that directing the fluid flow inward takes the maximum advantage of the centrifugal energy term, since $U_1'^2$ must be greater than $U_2'^2$. Values of N_s and D_s are dependent upon which flow volume (inlet or exhaust) is used. For reaction turbines greater significance is given to the exhaust flow since it controls the exhaust triangle. The inlet velocity triangle has little influence since velocity is near critical. Geometry is dominant for the inlet velocity triangle.

Turbines are utilized for two purposes in the majority of ECS applications: (1) as a device for lowering the temperature and pressure of a fluid by extracting energy; and (2) as a device to power another component such as a fan or a refrigerant compressor. The first application is more restrictive since it involves both the matching of the turbine power output to a compressor demand or load and meeting a cooling requirement.

Turbine Performance - Performance calculations are defined implicitly and explicitly. Implicit performance analyses use typical values for efficiency and pressure ratio without knowing the turbine geometry. Therefore, each implicit performance condition has a unique size associated with it. Explicit performance analyses are based on actual or preliminary turbine designs. Specific performance map data are used to describe the relationships between pressure ratio, speed, and flow rates.

Implicit performance is based on a typical value of turbine efficiency. Figure 65 suggests that a maximum efficiency of 76 percent is typical for ECS turbines. Therefore, exit temperature of the turbine is determined without specifying speed. Maximum turbine efficiencies of 87% for radial turbines and 90% for axial turbines are suggested by Rohlik (Reference 15) and Balje' (Reference 12). Establishing typical designs based on these efficiencies is not recommended. However, these maximum efficiencies illustrate what is

possible if optimum designs are used. Turbine pressure ratios vary a large amount (Figure 65). A mean value of six is indicated.

Explicit turbine performance is based on knowledge of the turbine inlet conditions, the desired pressure ratio, and the turbine geometry. Basically two performance formats are used:

1. Turbine pressure ratio versus turbine nozzle flow factor for a range of corrected speeds. Figure 66a is an example of a typical map.
2. Turbine adiabatic efficiency versus turbine velocity ratio for a range of pressure ratios. Figure 66b is an example of a typical map.

Isentropic temperature drop is:

$$\Delta T_{is,t} = T_{in} \left[1 - \left(\frac{P_{out}}{P_{in}} \right)^{\frac{\gamma-1}{\gamma}} \right] \quad (105)$$

Nozzle flow factor (F_f) is:

$$F_f = \frac{W \sqrt{T_{in}}}{31.84 P_{in} A_e} \quad (106)$$

A_e is the turbine effective nozzle area. The rotational speed is obtained from Figure 66a, and the turbine velocity ratio (U'/c_o) is found with Equation (92). Efficiency is obtained from Figure 66b for the known pressure ratio. Exit temperature then is calculated:

$$T_{out} = T_{in} - n_{ad,t} \Delta T_{is,t} \quad (107)$$

Turbine Size - Calculation of the wheel diameter is based on the energy states of the fluid entering and leaving the turbine. Limitations on the wheel size are imposed to reflect stress considerations. Wood (Reference 16) suggests a maximum tip speed of 2000 ft/sec and a maximum rotational speed of 60,000 rev/min as good design objectives. The previously derived dimensionless groups (Section 3.2.1) are organized into a technique to establish turbine diameter and design speed consistent with the design conditions imposed.

Adiabatic efficiency is determined from Equation (82). Adiabatic head is determined by multiplying Equation (105) by $(\gamma R / (\gamma - 1))$. The exhaust conditions (dry air rated) are used to determine the volumetric flow rate (ft^3/sec):

$$Q = \frac{WRT_{out}}{60P_{out}} \quad (P_{out} \text{ is psf}) \quad (108)$$

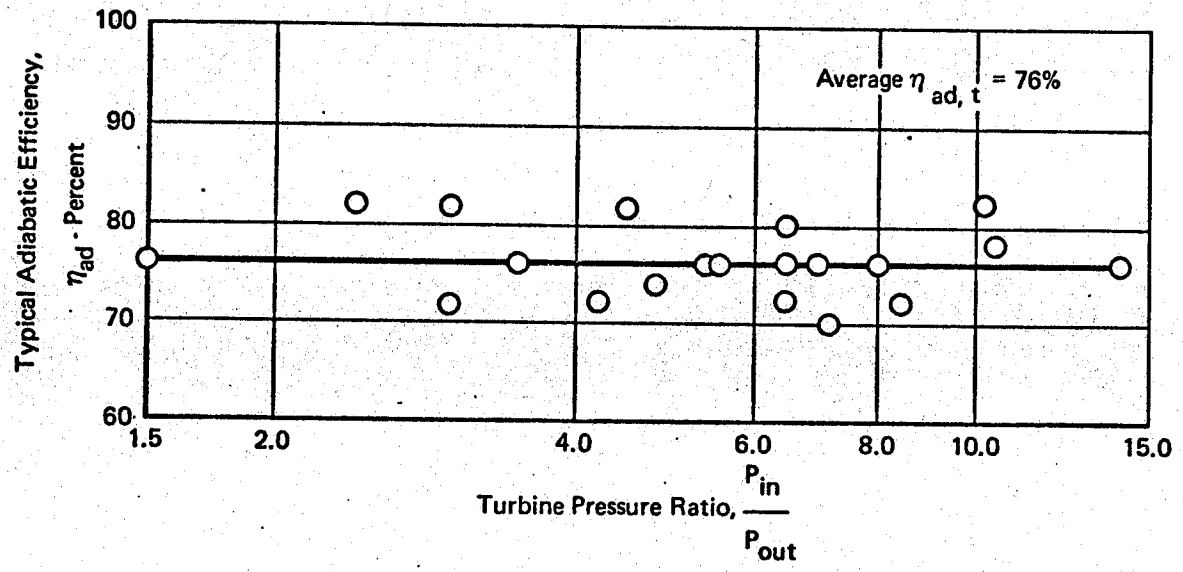


Figure 65 Typical Maximum Turbine Adiabatic Efficiencies

GP 9416-209

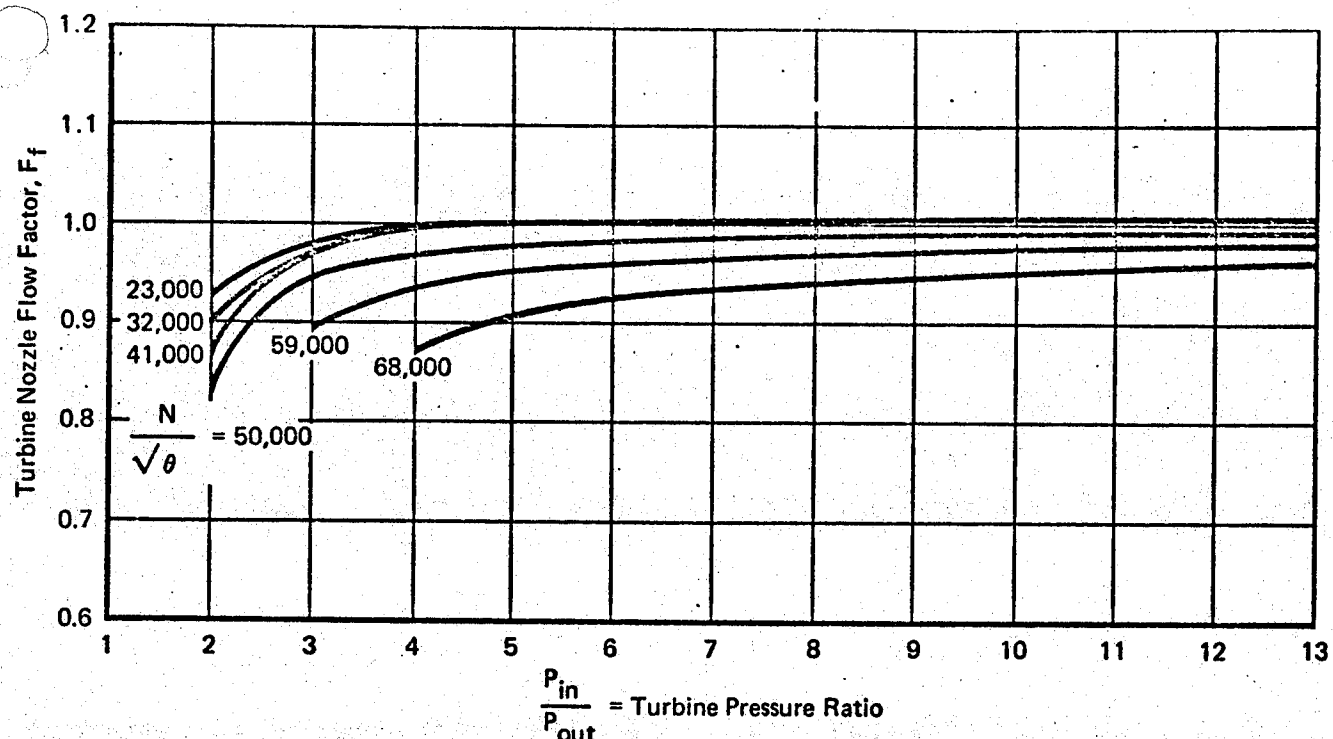


Figure 66a Typical Turbine Performance Maps

GP 9416-137

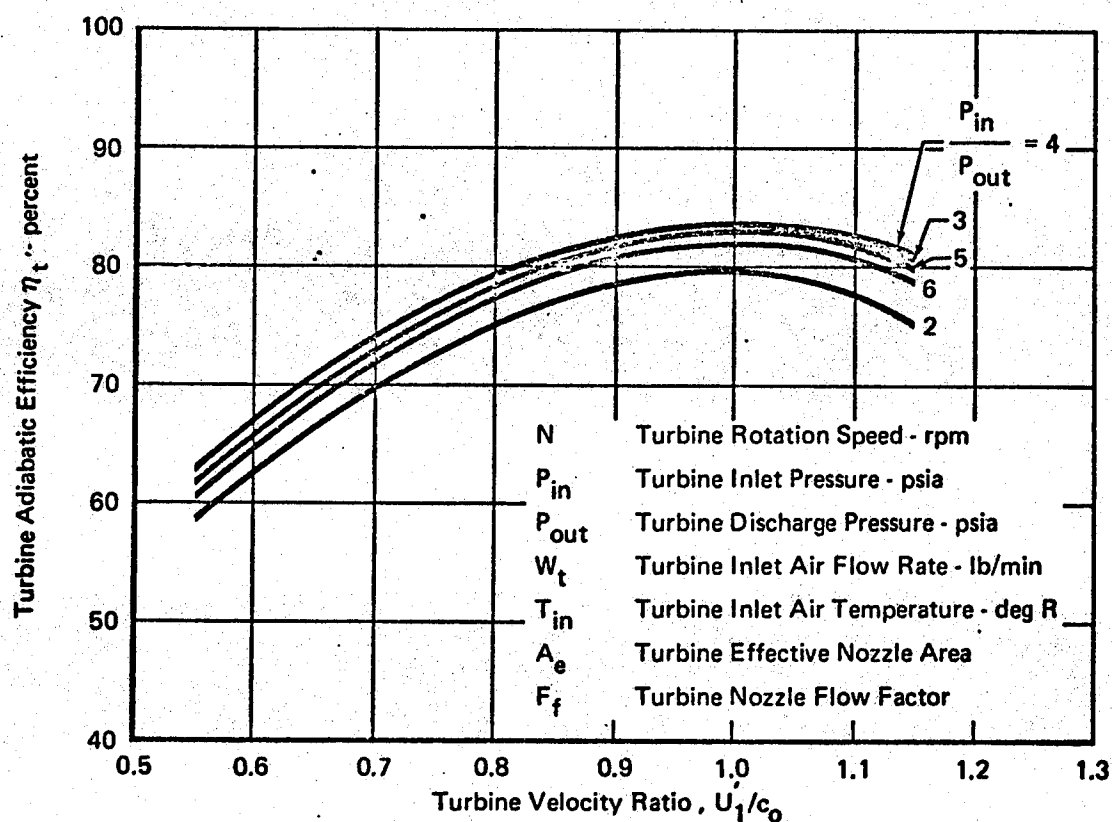


Figure 66b Typical Turbine Performance Maps

GP 9416-136

The specific speed is calculated if the rotational speed is a limiting factor or if the rotational speed is known for the compressor which is driven by the turbine.

D_s is determined from Figure 59 or 61 using the given value for $n_{ad,t}$ and the calculated N_s . (The largest value of D_s is selected initially.) Hence the wheel diameter is determined with Equation (88). Tip speed (U'_1) normally is less than or equal to 2000 ft/sec. If $U'_1 > 2000$ ft/sec, the rotational speed is reduced, and a new value for N_s is determined until $U'_1 \leq 2000$ ft/sec. (This may involve resizing the compressor to maintain common rotational speed.) The velocity ratio is determined from Equation (92) if the limiting tip speed is specified. For this velocity ratio the maximum adiabatic efficiency is obtained from Figure 60. If the adiabatic efficiency obtained from the input data is greater than that obtained from Figure 60, the tip speed is changed to increase the maximum efficiency (obtained from Figure 60) to that of the input data. This involves resizing the compressor for a different speed.

Output power is obtained from Equation (99). The turbine power is compared to the compressor power using Equations (100) and (101). The turbine effective nozzle area (A_e) is required to generate the performance map set for a specific turbine. The specific diameter is an indicator of effective nozzle area. (See Reference 12.)

$$D_s = \frac{\zeta}{\sqrt{A_e/D^2}} \quad (109)$$

where ζ is a function of turbine pressure ratio. Values for ζ are obtained from Figure 67.¹¹⁴ Therefore, A_e is known for the design condition.

For a given nozzle area, the flow factor is obtained in terms of flow rate, temperature, and pressure. By sequentially varying the flow rate, speed, and pressure ratio, while holding diameter constant, the corresponding values of flow factor, velocity factor, and efficiency are calculated from the generalized $N_s - D_s$ diagrams. The resultant data are arranged into the map format of Figure 66 for use in performance calculations. Since these data are based on the generalized $N_s - D_s$ diagrams, operating conditions significantly different from the design condition should be viewed with caution. Knowing the flow rate and the wheel diameter, the volume and weight are determined from Equations (103) and (104), respectively.

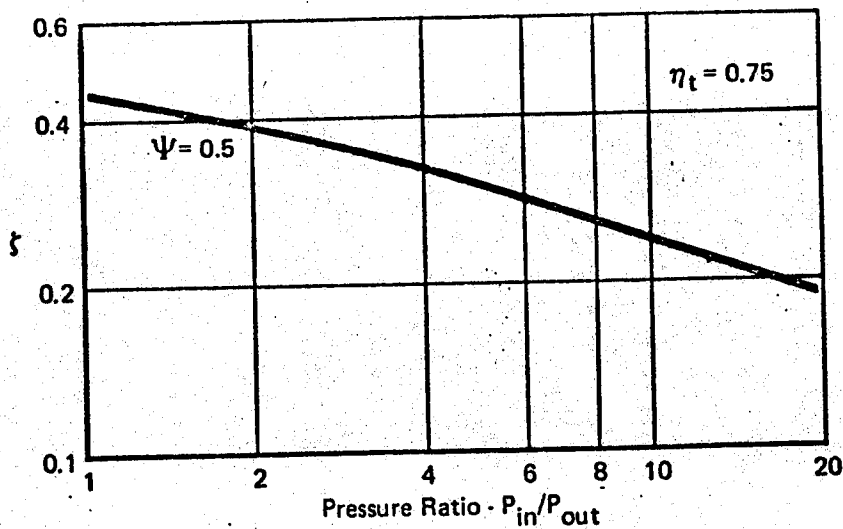


Figure 67 ζ -Values as Function of Turbine Pressure Ratio

GP 9416-148

3.2.3 Compressors - An increase in the static component of total head is provided by a compressor. A rotor design having a reaction (Ψ) greater than or equal to 0.5 is favored. (See Figure 55.) For centrifugal compressors a reaction of 0.5 is assumed with a blade angle (β_2) of 90°. In more detailed studies β is adjusted to the demand for static head.

Flow through a centrifugal rotor is directed outward to take advantage of the centrifugal energy term in the Euler turbine equation. The choice of the inlet or the exit flow condition for evaluating N_s and D_s is important. Since the compressor inlet flow controls the inlet velocity triangle, and the exit velocity triangle is fixed by the wheel geometry, the volumetric flow at the inlet is used.

There are three major applications of compressors: (1) loading a turbine in a simple air cycle system (Figure 12); (2) increasing the energy level of the working fluid for efficient use of a heat sink in a bootstrap air cycle system (Figure 15); and (3) providing pressurized air to the ECS (e.g., a boost compressor).

Compressor Performance - The evaluation of compressor performance is implicit or explicit. Data relating pressure ratio, speed, and flow rate to efficiency are used to calculate performance. An implicit statement of performance describes typical design efficiencies without relating them to a specific geometry or wheel size... Explicit performance data describe

efficiencies that correspond to an actual or initial compressor design.

Implicit compressor performance is established by selecting a typical efficiency and pressure ratio. Figure 68 suggests that a maximum efficiency ($n_{ad,c}$) of 64% is typical for ECS compressors. Exit temperature is calculated without specifying speed. A maximum compressor efficiency of 85% is suggested as an upper limit by Balje (Reference 12). Use of efficiencies higher than 64% for establishing typical designs is not recommended. An 85% efficiency is achievable if good design practices which incorporate optimum geometry are used. Bootstrap air cycle compressors typically operate at a pressure ratio of 1.8. Simple air cycle compressors typically have a pressure ratio of 1.2 at low altitudes and 1.8 at high altitudes.

Explicit compressor performance calculations are dependent upon knowing the inlet conditions (pressure, temperature, and flow rate) and a desired pressure ratio.

Isentropic temperature rise is:

$$\Delta T_{is,c} = T_{in,c} \left[\left(\frac{P_{out}}{P_{in}} \right)^{\frac{y-1}{y}} - 1 \right] \quad (110)$$

Corrected speed ($N/\sqrt{\theta}$) is obtained from Figure 69, hence speed is calculated.

Adiabatic efficiency also is obtained from Figure 69. Therefore, exit temperature is:

$$T_{out} = T_{in} + \frac{\Delta T_{is,c}}{n_{ad,c}} \quad (111)$$

Compressor Size - The inlet and exit energy states of the fluid entering and leaving the compressor allows the wheel diameter to be calculated. Since the compressor wheel design is limited by the centrifugal stress, a limiting value of tip speed (1500 ft/sec) is imposed.

The following analysis provides a technique to determine wheel diameter and rotational speed of a compressor when the inlet and exit states and the flow rate are specified. The analysis technique relates these known data through the dimensionless parameters and the generalized design diagram. Iteration may be required in order to meet the limiting design conditions.

Adiabatic efficiency is obtained from Equation (81). The adiabatic head is calculated with Equation (95). The compressor volumetric flow at inlet conditions is used. Determination of a specific speed consistent with

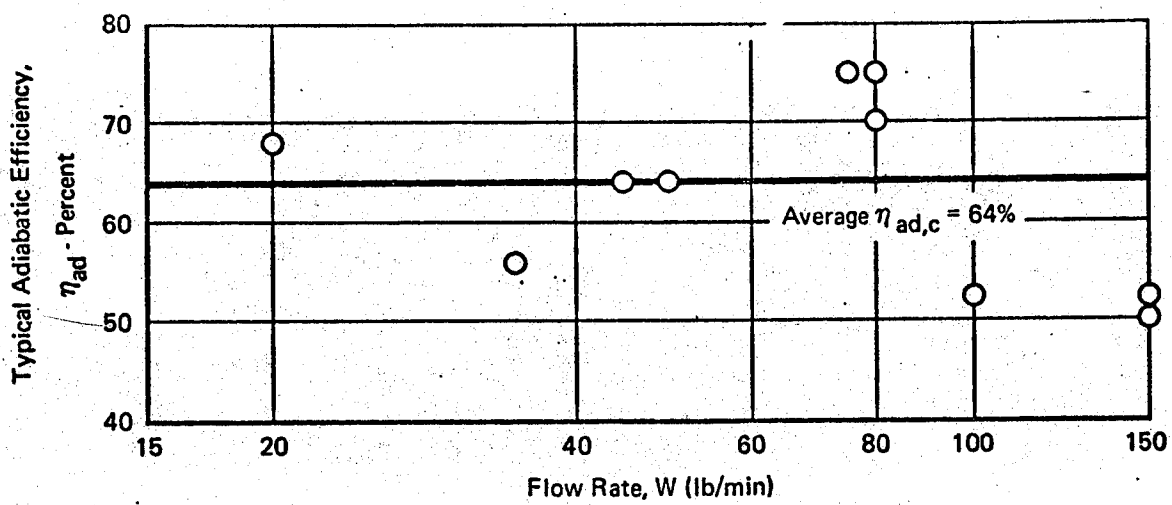


Figure 68 Typical Maximum Compressor Adiabatic Efficiency

GP 9416-210

Compressor Pressure Ratio

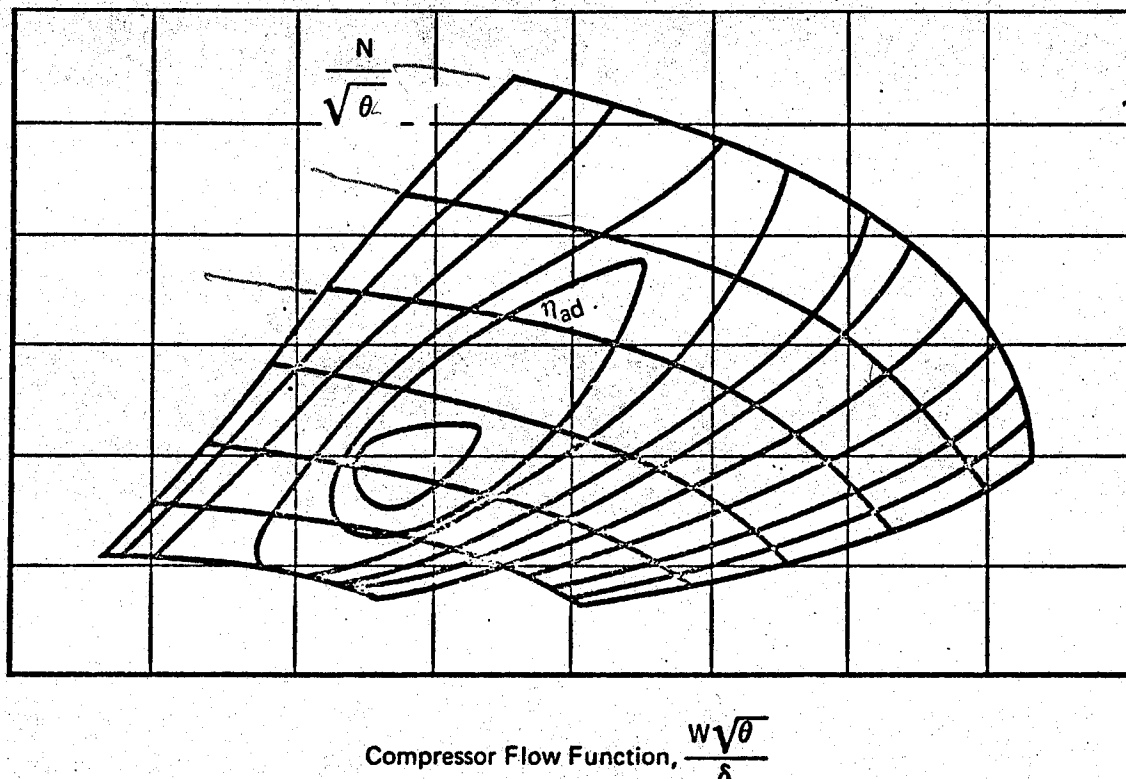


Figure 69 Typical Compressor Performance

GP 9416-131

the efficiency is dependent on the limiting design condition of the compressor. If the rotational speed is the limiting design factor, the specific speed is utilized. (See Equation 86.) If tip speed is the limiting design factor, the product of specific speed and specific diameter are utilized for the compressor design.

The adiabatic efficiency and the specific speed are used to obtain a corresponding value of D_s from Figures 56 or 58 when rotational speed is the limiting design factor. Selection of the smallest value of D_s is recommended for the initial iteration. Equation (88) is solved for D . The rotational speed and the diameter are used to determine tip speed (U'_2). If $U'_2 \leq 1500$ ft/sec, then the design is within a realistic range. However, if $U'_2 > 1500$ ft/sec, the rotational speed must be restricted, and a lower value is assumed for specific speed. This lower value for specific speed is used to determine a corresponding value of D_s , and another check of the tip speed is made. If $U'_2 \leq 1500$ ft/sec is still not obtainable, the rotational speed is reduced until $U'_2 \leq 1500$ ft/sec.

An alternate approach is used if the tip speed (U'_2) is the limiting design factor. A $(D_s N_s)$ product is obtained for the limiting tip speed:

$$D_s N_s = \frac{60 U'_2}{\pi (H_{ad,c})^{1/2}} \quad (112)$$

This product and the adiabatic efficiency are used to obtain D_s and N_s . This is done iteratively by selecting values of N_s and D_s from the proper efficiency curve in the $N_s - D_s$ diagrams (Figure 56 or 58). The rotational speed then is calculated using Equation (86) to ensure that it is not unreasonable. The head coefficient is calculated from Equation (89). The reference Mach number is calculated with Equation (96). This reference Mach number and the specific speed are used to determine if the adiabatic efficiency is realistic. If the adiabatic efficiency is greater than that obtained from Figure 57, a new specific speed must be assumed so that the low efficiency limit at low specific speeds is not exceeded. The required power is obtained from Equation (98).

Off design data for the sized compressor are based on the $N_s - D_s$ diagram of Figure 56 or 58. The flow rate and pressure ratio are sequentially varied while holding the inlet temperature and diameter constant in order to calculate efficiency and speed. The data are arranged in the format of Figure 69.

Caution should be used if conditions vary significantly from the design condition since variations in inlet temperature are not accounted for. Knowing the design flow rate and wheel diameter, volume and weight are calculated using Equations (103) and (104), respectively.

3.2.4 Fans - Low pressure ratio compressors ($PR \leq 1.2$) are commonly called fans. The fan provides a load for the turbine and circulation of ram air in simple and simple-bootstrap air cycles. Therefore, a maximum flow is produced by a relatively low head. This results in a wheel design of high specific speed. Axial blade designs fit this requirement and are considered typical of current ECS applications. The $N_s - D_s$ values of Figure 58 represent the similarity criteria of low pressure ratio axial compressors. Mixed flow blade designs are found in several simple cycle units and can be considered typical.

Fan Performance - The compressor performance analysis procedure is used to determine the fan exit temperature for a known pressure ratio. The basis for the analysis is an implicit or explicit statement of the nature of the data used to determine the fan exit conditions. Implicit data describes typical performance of fans without specifying a geometry. Higher efficiencies are obtainable as suggested by Figure 58, but these values are not considered typical of ECS fan applications. Explicit data, in the form of Figure 69,¹⁶ describe a fan of known geometry.

Fan Size - The characteristic wheel diameter and off-design performance map are determined in the same manner as for compressors. The $N_s - D_s$ diagram of Figure 58 is used to describe low pressure ratio axial wheel designs. Knowing the design flow rate and wheel diameter volume and weight are calculated using Equations (103) and (104), respectively.

3.3 Water Separators

Design data for performance analyses of water separators include their efficiency in removing entrained liquid water, and the pressure drop of the air (with or without entrained water) as it flows through the water separator. Heat exchangers designed to condense a very large percentage of the water vapor in air may be classed as water separators. These "water separators" are discussed on page 84. Water collectors which remove liquid water from walls of air ducts are included as part of the overall duct performance in Section 3.10.

The cold air which is discharged from the expansion turbine of an environmental control system during operation in humid conditions contains very small water droplets. If this water-laden, misty air is allowed to flow into the aircraft cockpit it will obscure instruments and controls. It may collect on the windshield or canopy, thus reducing pilot visibility during critical periods of the mission. Humid, uncomfortable conditions in the cockpit and cabin also are produced. Collection of this water in electronic equipment compartments reduces the reliability of the equipment. Liquid water which might form on cargo may cause damage later when the cargo is used.

The water droplets which are discharged from an expansion turbine are nominally 1/2 micron in diameter. These droplets will double in diameter approximately five feet downstream from the turbine discharge. (A more complete discussion of droplet sizes in expansion turbine discharges is presented in Reference 17.) Removal of liquid water, by existing aircraft water separators, is accomplished by creating an inertial force on the water droplets which is different than the air flow. The most common means is a centrifugal force produced by spiral or vortex flow inducers (vanes or louvers). The efficiency of removing the liquid water increase as the droplet size is increased. This is accomplished with a fine metallic screen or supported synthetic fabric (the new designs) upstream of the vortex generators. Flat, conical, and cylindrical shapes are used for these coalescers. The larger water droplets then are swirled and collected on the circumferential surface of the separator and removed.

The efficiency of removing water increases as the air flow rate and liquid water content of the air through the separator increase. At a constant liquid water content, the efficiency reaches a maximum (at an air flow

rate designated as W_m), and then decreases as the air flow rate is increased further. This maximum air flow rate (W_m) normally occurs at the maximum aircraft velocity at sea level. Separator efficiency, air flow pressure drop, weight, and volume are correlated via the air flow rate at maximum collection efficiency. Correlations of efficiency are made for high liquid water contents (approximately 100 grains of entrained water per pound of dry air and greater) and low liquid water content (approximately 50 grains per pound of dry air). The correlations at high water contents are representative of efficiencies when the environmental control system is operated with the maximum specific humidity of 154 grains of water per pound of dry air, as specified in Reference 18. Correlations of the air pressure drop through the separators are made for wet and for dry (i.e., no entrained liquid water) air flows.

A more detailed investigation for the development of an improved water separator concept is found in Reference 19. Experimental efficiencies and pressure drops as a function of air velocity are correlated to theoretical techniques. Data trends in this reference are the same as are reported herein.

Data on water separators manufactured by several companies are utilized to develop the information presented herein. (See References 2, 6, 8, 20, and 21.)

3.3.1 Efficiency - The efficiency of a water separator is the ratio of liquid water removed by the separator to the entrained liquid water entering the separator. Efficiencies of water separators when the inlet entrained water content is high (approximately 90 to 180 grains of liquid water per pound of dry air) are shown in Figure 70. The efficiencies are presented as a function of air flow rate relative to the reference air flow (W_m). (This air flow rate ratio is designated as W_r .) A parabolic equation is assumed to be representative of the mean separator efficiency data (in Figure 70) as a function of the air flow rate ratio. The maximum value of this mean efficiency occurs at W_r equal one. Use of the method of least squares results in the following parabolic equation for average separation efficiency at high inlet water conditions:

$$\eta_{HI} = 41.3 + 78.7 \left(W_r - \frac{1}{2} W_r^2 \right) \quad (113)$$

here: η = separation efficiency, percent

$W_r = W/W_m$, air flow ratio.

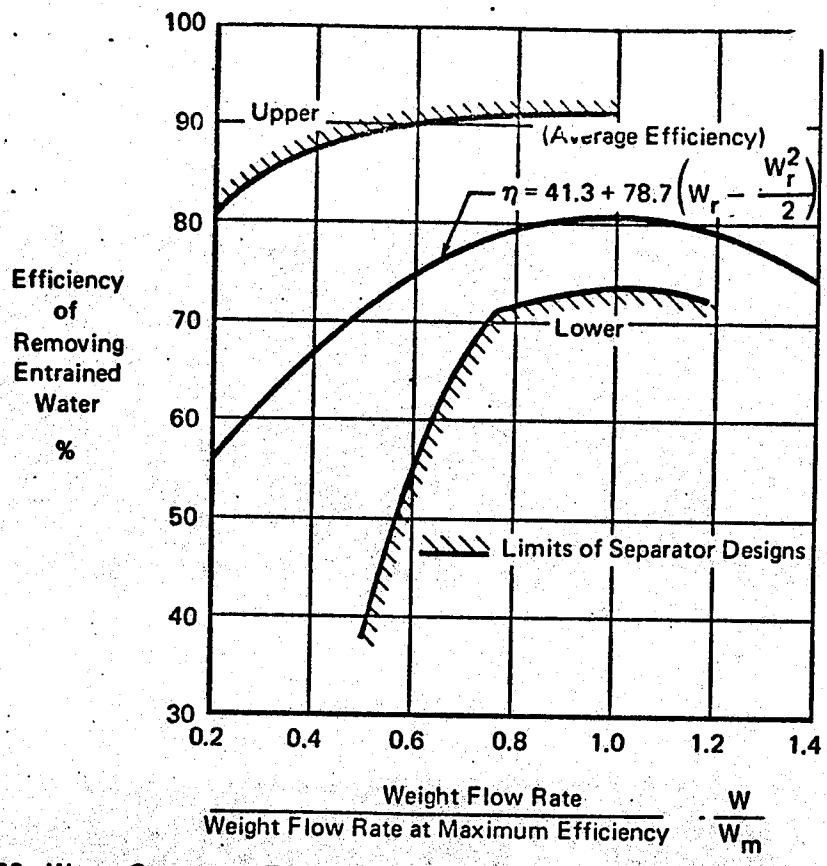


Figure 70 Water Separator Efficiencies at High Inlet Entrained Water Content

GP 9416-23

At $W_r = 1.0$ the average efficiency is 80.7%. The standard error of the above equation is 16.5% (based on the 27 water separators considered).

Sufficient data are not available to correlate the separation efficiency as a function of the inlet water content. Therefore, separation efficiencies at lower water contents are correlated using the same approach as is described above, and the same W_m . The following equation provides a correlation at lower inlet water conditions (approximately 50 to 80 grains of liquid water per pound of dry air):

$$\eta_{LO} = 36.6 + 78.0 \left(W_r - \frac{1}{2} W_r^2 \right) \quad (114)$$

where: η = separation efficiency, percent

$W_r = W/W_m$, air flow ratio.

These efficiencies are shown in Figure 71. At $W_r = 1.0$ the average efficiency is 75.6%. The standard error of the efficiency equation for low inlet water content is 15.9%, based on 13 water separator efficiencies.

Two Air Force Military Specifications designate water separator efficiency requirements. MIL-E-38453(USAF) (Reference 3) states: "All air cycle cooling systems shall have a water separator which removes at least 85 percent of the entrained moisture from the turbine discharge air for the conditions of maximum sea level airflow rate with an ambient moisture level in the range of 154-182 grains of water per pound of dry air. At all lower airflow and humidity conditions, the maximum allowable entrained moisture content in the cooling air shall not exceed that quantity resulting from the above design condition." Specification MIL-A-83116(USAF) (Reference 22) states: "All air cycle subsystems shall have provisions which will assure that the maximum quantity of entrained moisture in the subsystem discharge air does not exceed the values shown below for all possible subsystem airflow rates:

Subsystem Inlet Air Total Moisture Content - Grains/Lb of Dry Air	Maximum Allowable Quantity of Entrained Moisture in Subsystem Discharge Air - Grains/Lb of Dry Air
---	---

0 - 154	H_{Sat} at $40^{\circ}\text{F} \leq 35 \text{ gr/lb}$	$18 = .15(154 - 35)$
155 - 182		$22 = .15(182 - 35)$

The separation efficiency of both referenced specifications (References 3 and 22) thus is greater than the average of existing water separators.

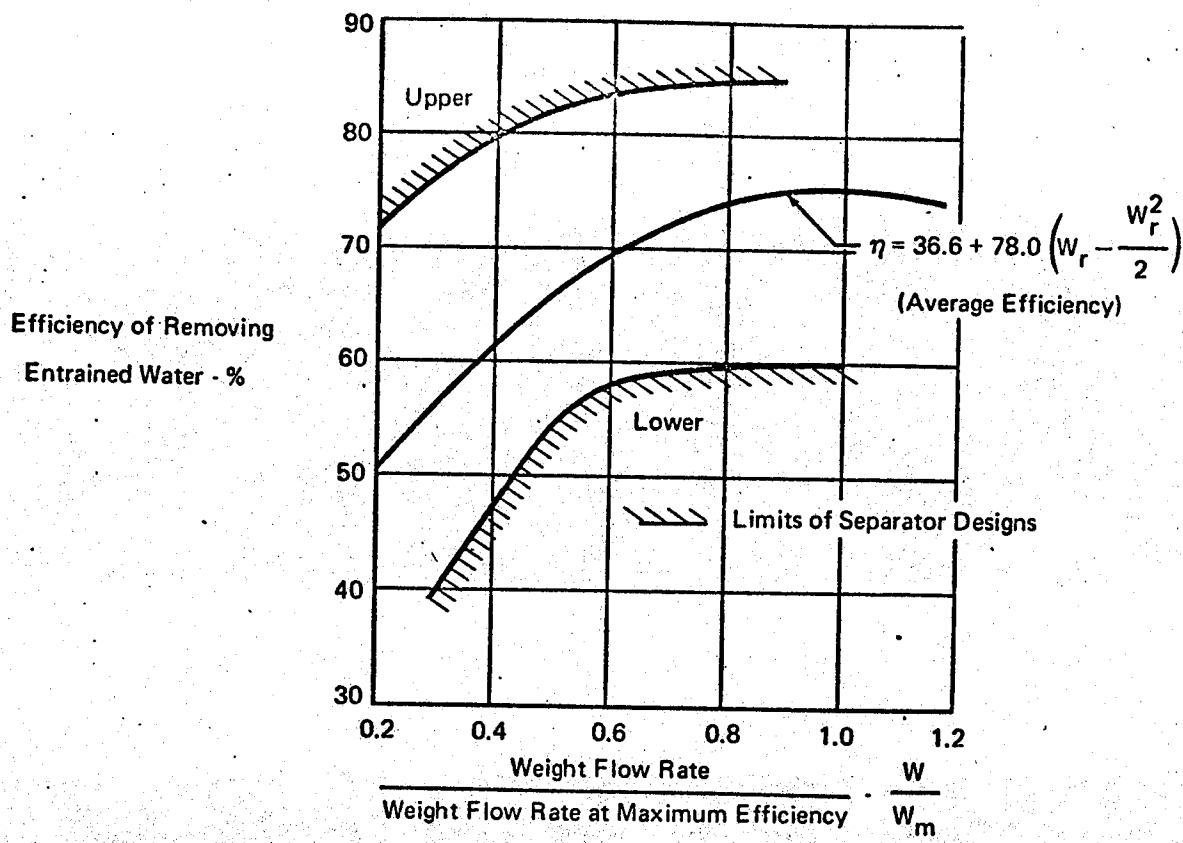


Figure 71 Water Separator Efficiencies at Low Inlet Entrained Water Content

GP 9416-22

3.3.2 Pressure Drop - The pressure drop of the air flow through a water separator is greater when the separator is wet than when it is dry. The available data indicate that the wet pressure drop is almost independent of the entering entrained liquid water content. Apparently this is because the coalescer is saturated at low entrained moisture conditions.

Relatively large differences in the pressure drop at maximum separation efficiency are typical of available separators. All separator pressure drops are discussed relative to a standard inlet air density of 0.0765 lb/ft^3 . The wet and the dry pressure drops are divided into two groups. Pressure drop data of the separators are expressed by the equation: $\sigma\Delta P = KW^m$. Some separator pressure drops do not fit this form (e.g., the pressure drop varies linearly with air flow rate).

The separator wet pressure drops are divided into a group of 13 separators and a group of 6 separators. Average values of "m" for each of these groups were determined, and a least squares determination of the constant "K" was obtained. The resulting equations are (see Figure 72):

$$\sigma\Delta P_{LO,W} = 1.83 (W/W_m)^{1.56} \quad (115)$$

(This equation has a standard error of 21.7% for the 13 water separators.)

$$\sigma\Delta P_{HI,W} = 3.15 (W/W_m)^{1.46} \quad (116)$$

(Standard error for the 6 separators is 14.5%).

The separator dry pressure drops are divided into a group of 8 separators and group of 7 separators. The correlation equations are (see Figure 73):

$$\sigma\Delta P_{LO,D} = 0.825 (W/W_m)^{1.80} \quad (117)$$

(with a standard error of 8.9%); and

$$\sigma\Delta P_{HI,D} = 1.47 (W/W_m)^{1.92} \quad (118)$$

(standard error of 28.0%).

These groupings are not consistent (e.g., some separators had wet pressure drops in the high group, and dry pressure drops in the low group). No relation between separation efficiency and pressure drop is readily obtainable. The more recently designed water separators have a wet pressure drop which is 2.2 psi or less at the air flow rate for maximum separation efficiency. These more recent separators do not have appreciably improved efficiencies.

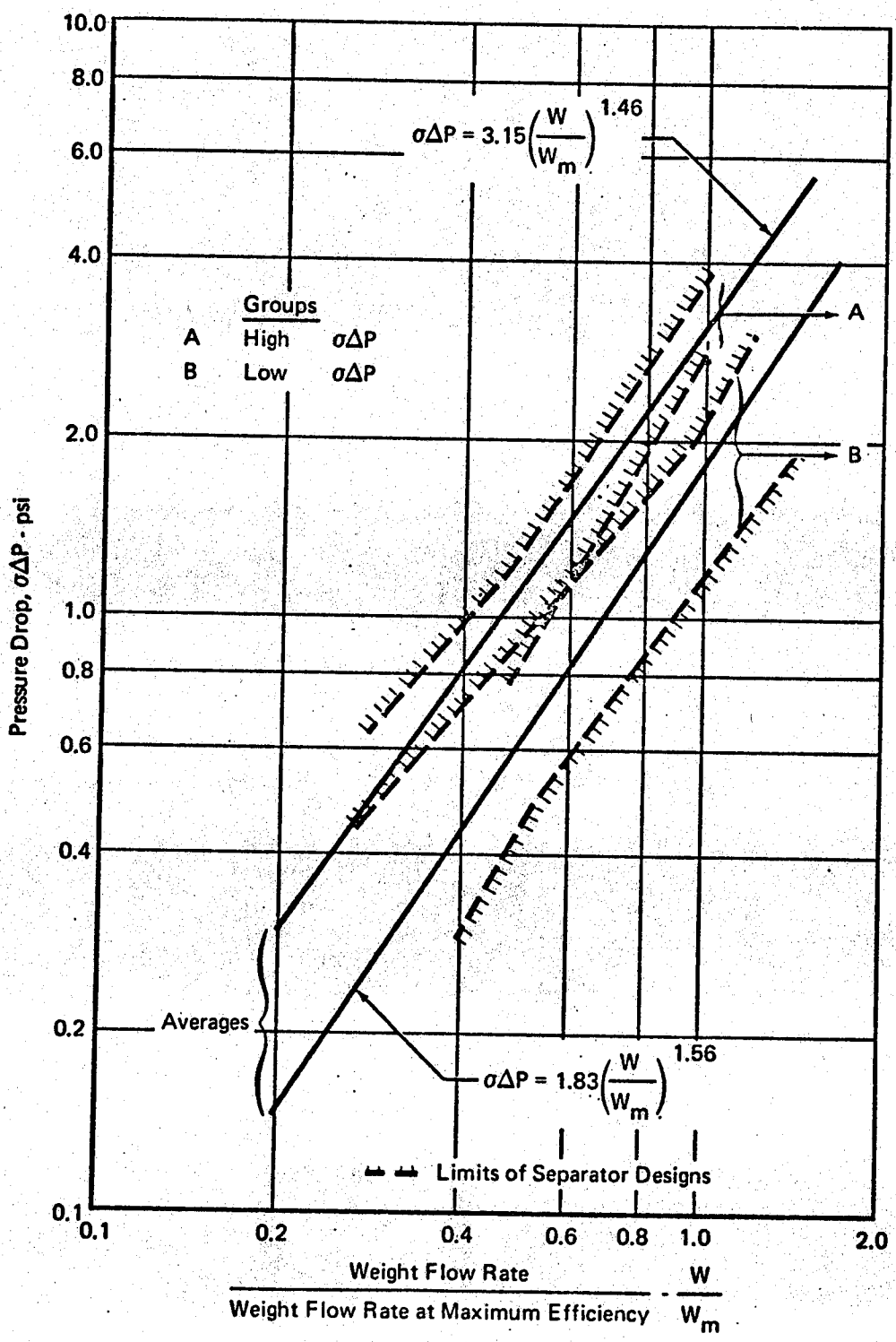


Figure 72 Water Separator Wet Pressure Drops

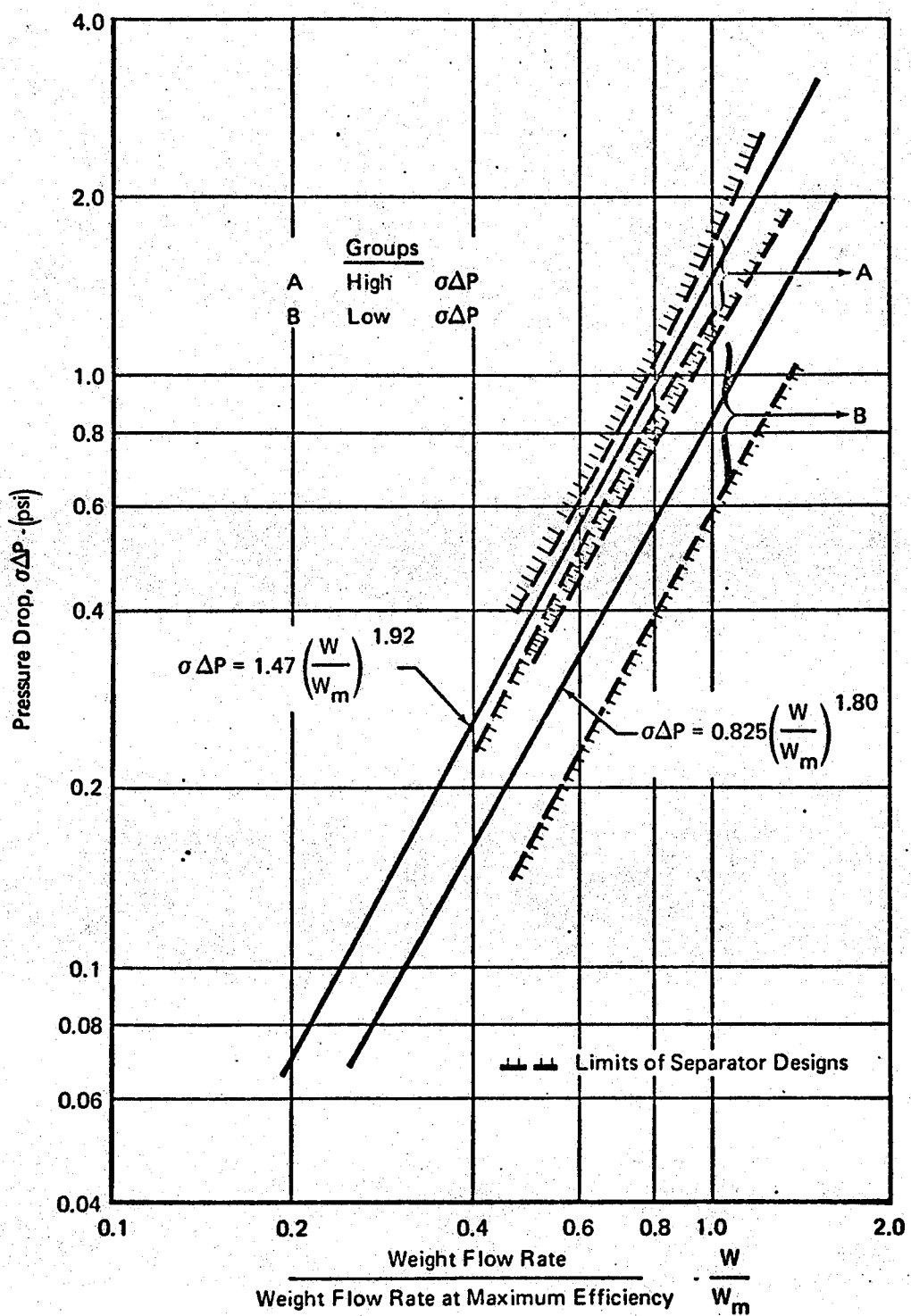


Figure 73 Water Separator Dry Pressure Drops

GP 9416-25

3.3.3 Weight - The weights of 28 water separators (with internal relief valves, nominally) are correlated by the equation:

$$Wt = 0.0936 W_m \quad (119)$$

This correlation is illustrated in Figure 74. The equation has a standard error of 17.3% for the water separators considered. This correlation equation was determined empirically by noting a linear relation between weight and W_m , and obtaining the constant (0.0936) by the method of least squares.

3.3.4 Volume - The volumes of 26 water separators (which normally include an internal relief valve which opens if the separator freezes or becomes clogged) are correlated by the equation:

$$V = 2.11 W_m^{1.5} \quad (120)$$

This correlation is illustrated in Figure 75. This equation has a standard error of 21.4% for the water separators considered. The correlation equation was determined empirically by determining that the volume is proportional to the 1.5 power of W_m (approximately), and obtaining the constant (2.11) by the method of least squares. Note that the relation between weight and volume is typical of a hollow container, which is a general characteristic of water separators.

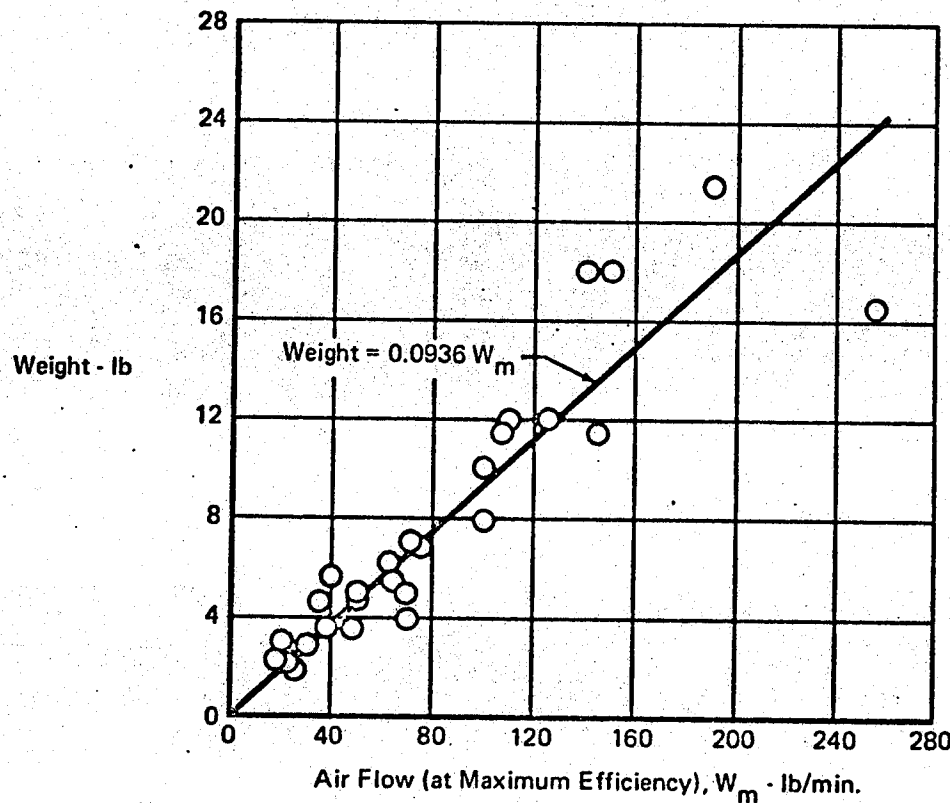


Figure 74 Water Separator Weights

GP 9416-21

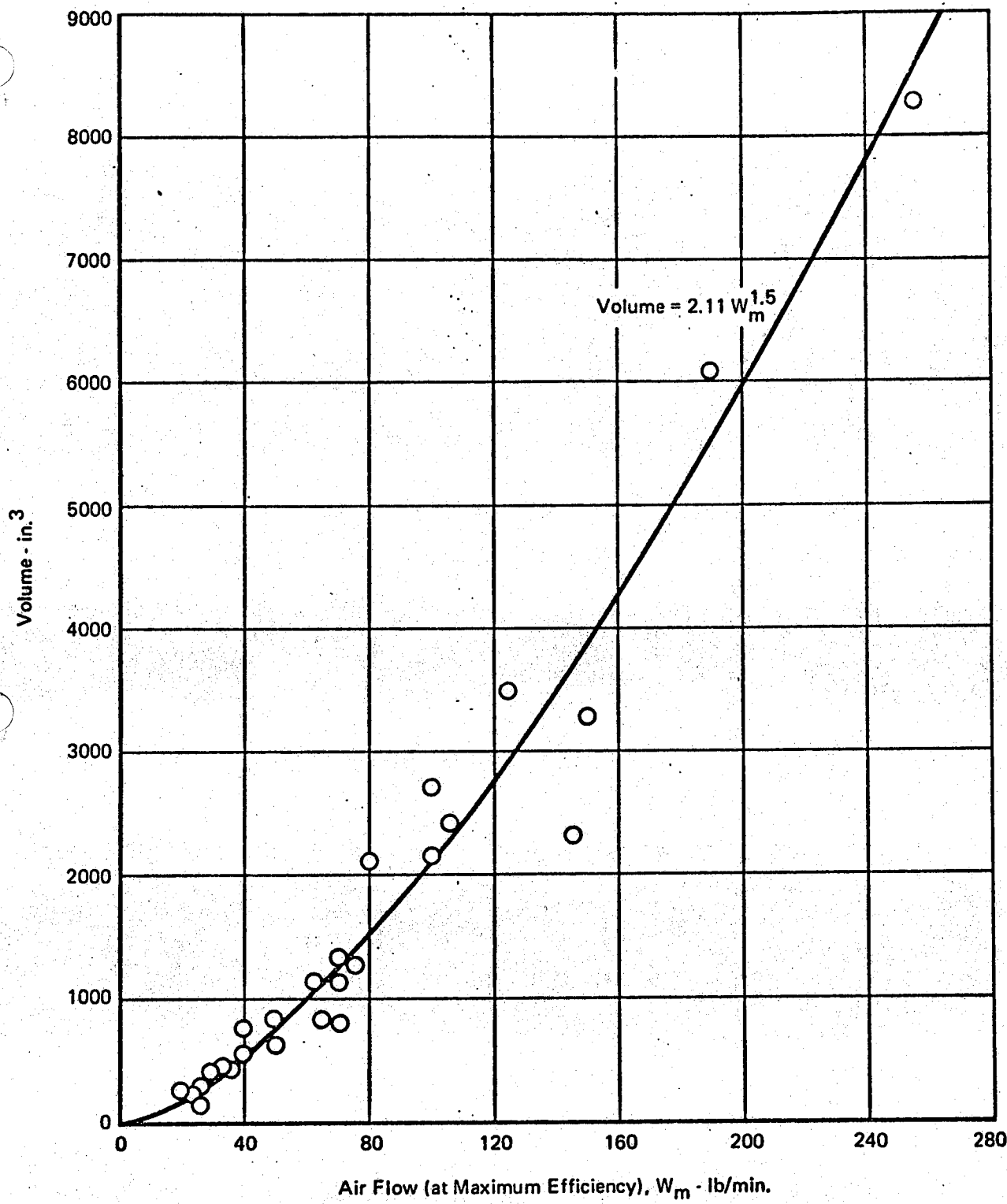


Figure 75 Water Separator Volumes

GP 9416-20

3.4 Dust Separators

A dust separator is a device located in an air system to control contamination by trapping or separating particles entrained in the flow. These contaminants are detrimental to ECS reliability and to pilot comfort. Two types of separators are considered: static separators (filters) and centrifugal self-cleaning dust separators. They can be used in a high pressure bleed line, in low pressure distribution lines and compartments, or upstream of an ambient air inlet (e.g., to an auxiliary compressor or an auxiliary power unit). The performance, weight, and volume correlations for each type of separator are described in the following sections.

3.4.1 Static Separators - The filtration of a static separator is accomplished by impingement and retention of solid contaminants on a filtration medium having a matrix of pores or openings. The filtration medium is made of stainless steel. Fabric and paper filters are not desirable in aircraft application since electro-static buildup may cause a fire (especially if oil is accumulated) in case of electric arcing. Frequent cleaning or replacement is required to maintain the designed performance since a static separator has no self-cleaning feature. Two different filter constructions are considered. One has a rectangular frame with filtration medium up to 2 inches thick. The second is a tee-type construction (relative to the duct installation) having a cylindrical housing. The rectangular filters are for low pressure applications and tee-shape filters are used in high pressure bleed lines.

Performance of Static Separators - The performance of a dust separator is expressed in terms of efficiency and pressure drop. The efficiency is the ratio of the weight of particles trapped to the weight of particles introduced. It depends on the size of the smallest particle which the filter design is to separate from the main air stream. Efficiencies vary from 80% to 98% for particles larger than 5 microns. For coarser particles (larger than 15 microns), the efficiency is close to 100%.

The pressure drop across the filters is expressed in terms of pressure loss coefficient (K_t).

$$\Delta P = K_t \frac{\rho(v')^2}{2g_c} \quad (121)$$

$$\Delta P = \frac{K_t}{2} (k P M^2) \quad (122)$$

Values of K_t are approximately 0.10 and 6.9 for tee-type and rectangular type filters, respectively. Thus, knowing the upstream pressure and pressure loss coefficient, ΔP is calculated by assuming a typical value of upstream Mach number. (See Section 3.10.) If the duct diameter is known, the following equation is utilized for more accurate pressure drop evaluations.

$$\Delta P = (1.008 \times 10^{-3}) K_t \frac{W^2}{\rho D^4} \quad (123)$$

The above equation results from a combination of the equation defining K_t and the continuity equation. Hydraulic diameters are used for rectangular type filters.

Weight and Volume of Static Separators - Weight data for several static separators are shown in Figure 76 in terms of the maximum design flow rate. (See References 23 and 24.) The mean value is represented by the following equation, which has a standard error of 4%:

$$W_t = 0.195 W_m^{0.79} \quad (124)$$

The volume correlation for tee-type separators is (see Figure 77):

$$V = 7.3 W_t^{1.28} \quad (125)$$

The volume of rectangular shaped filters is not considered since they are inside the ducting.

3.4.2 Self-Cleaning Dust Separators - Self-cleaning dust separators operate on the same principle as is used for the "collector" section of water separators. The dust-laden air is accelerated by imparting a centrifugal force to it, and the greater inertia of the dust particles causes them to accumulate, leaving a nearly clean portion of air flow. In most dust separators, a vane of some configuration is used to accelerate the air. A portion of the entering air is removed from the separator with the dirt. This is referred to as the "scavenge" air flow.

Performance of High Pressure Dust Separators - An "orifice" is required to limit the amount of scavenge air flow in a high pressure dust separator, since the internal pressure is greater than ambient. This scavenge air flow is 4% to 10% of the inlet air flow. Higher scavenge air flows probably

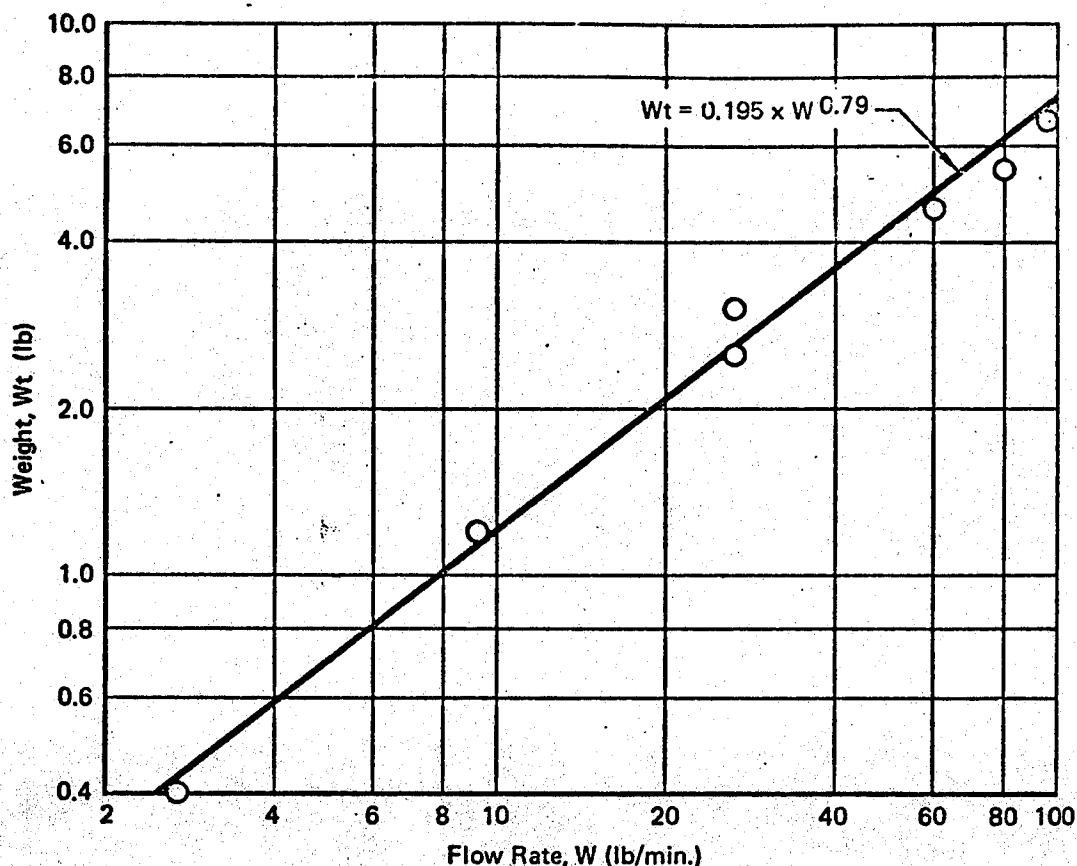


Figure 76 Weight of Static Dust Separators

GP 9416-86

increase the removal efficiency of dust removal. Typical efficiencies are 92% to 99% of coarse dirt (> 25 microns), and 80% to 90% of finer dirt particles (> 5 microns).

The maximum pressure drop of three known high pressure dust separators is from 2.7% to 3.15% of the inlet total pressure at their design flow rates. Hence, a design pressure drop of 3% of inlet total pressure seems to be typical. The pressure drop at other flow rates follows (very nearly) the relation:

$$\Delta P = K W^{1.9} \quad (126)$$

This equation is used for off-design evaluations, after the design condition has been determined.

Weight and Size of High Pressure Dust Separators - The weights of four high pressure dust separators are indicated in Figure 78 as a function of their design flow rates. A least mean squared linear fit to these four data points results in the following equation:

$$Wt = 0.5 + 0.0346W \quad (127)$$

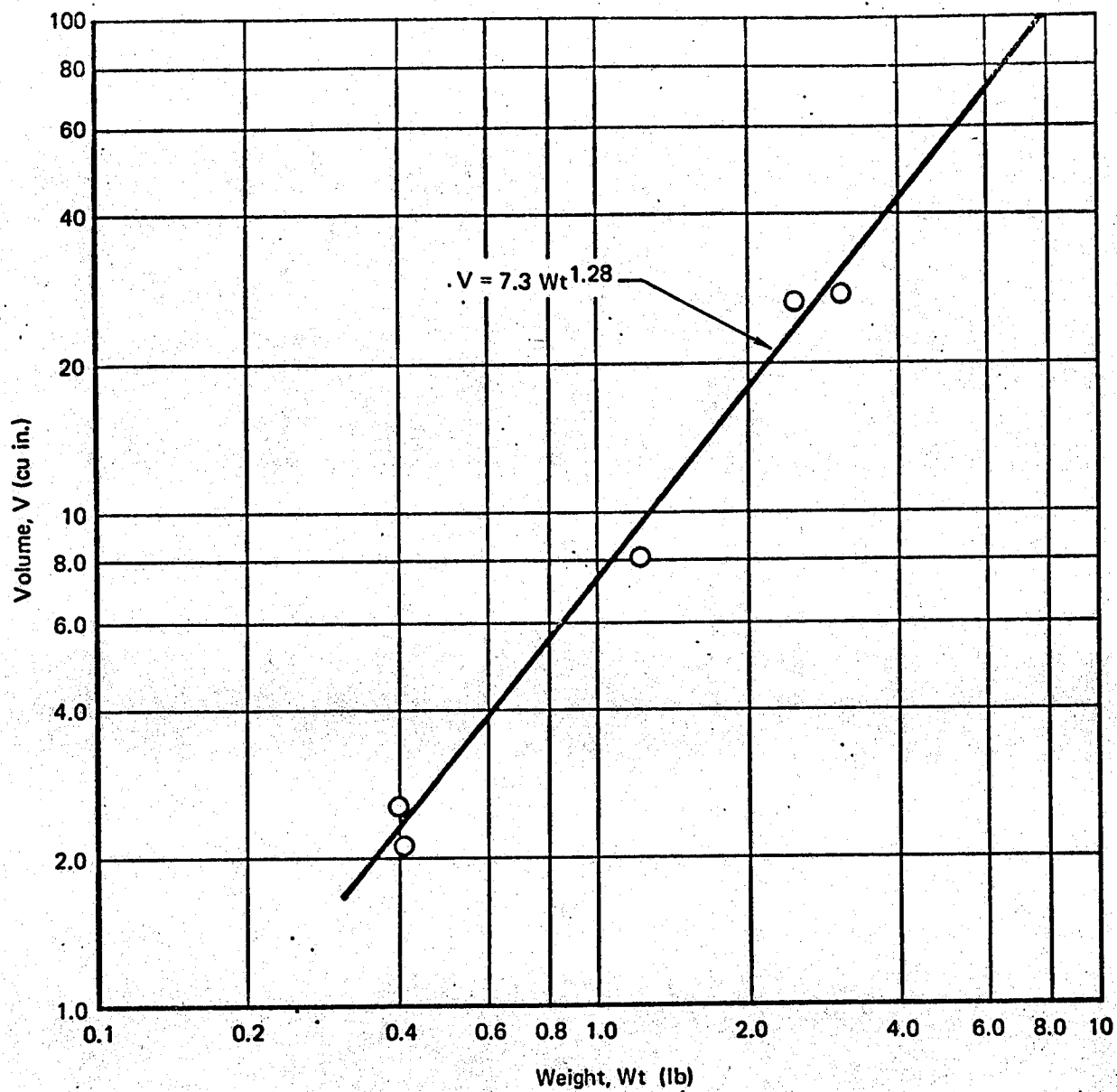


Figure 77 Volume of Static Dust Separators

GP 9416-85

For the four separators depicted, this equation has a standard error of 12.25%.

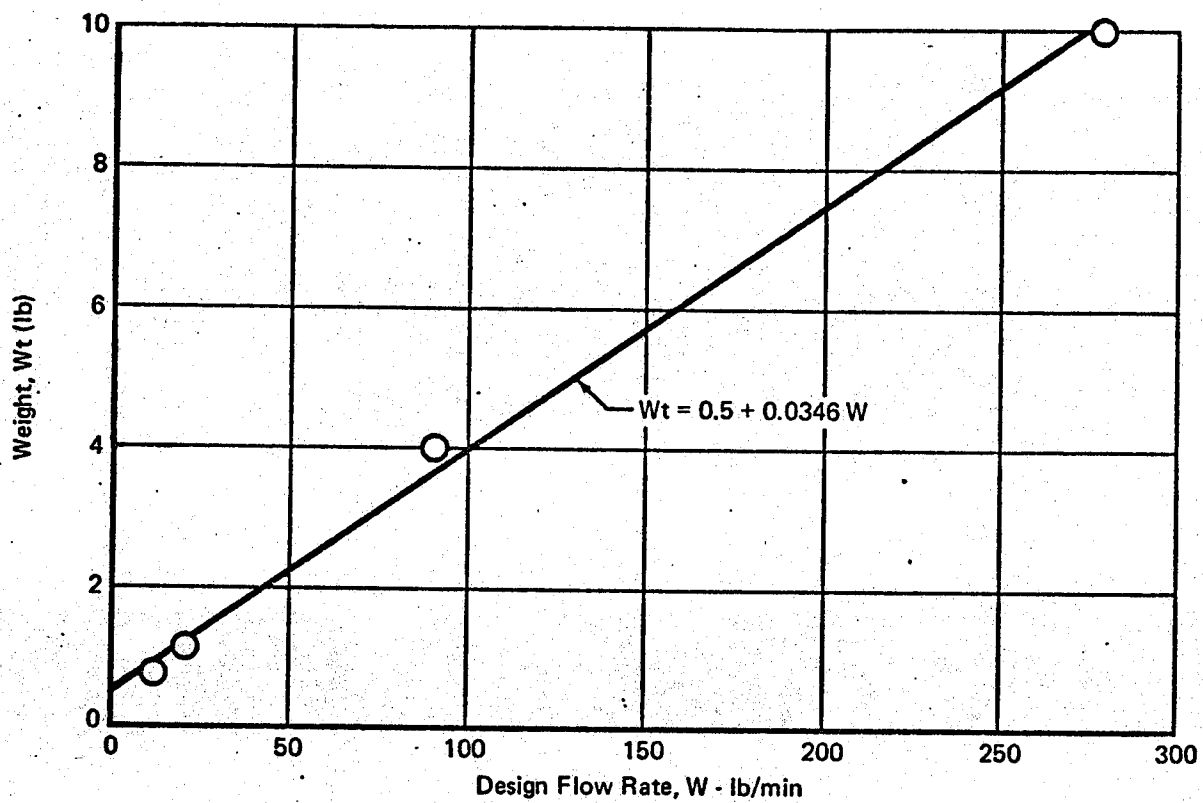


Figure 78 Weight of High Pressure Dust Separators

GP 9416-29

The relation between weight and overall size (volume) of these separators is assumed to be that of a shell-type construction. Therefore, volume is proportional to the 1.5 power of weight. The least mean squared equation is:

$$V = 19 Wt^{1.5} \quad (128)$$

This relation overestimates the size of the smaller units.

Performance of Ambient Pressure Dust Separators - The dirty scavenge air must be pumped out of a self-cleaning dust separator which operates with an ambient pressure inlet. A scavenge air flow rate of 10% of the inlet air flow still provides adequate dust separation. A bleed air ejector using approximately 1% bleed air to scavenge air flow rate is typical.

General discussions and evaluations of several ambient inlet dust separators are found in References 25 through 28. The average pressure drop of the thirteen separators described in these references is 0.18 psi at "design".

flow rates. Not all of these separators are designed for aircraft, nor do they have the same configuration. Self-cleaning dust separators with pressure drops as low as 0.04 psi are available. These are single-inlet axial flow designs having a large number of vanes, or a number of small-tube dust separators in parallel. (See References 28 and 29.) Lower weight single-inlet axial flow designs with fewer vanes have higher pressure drops (to approximately 0.4 psi) to achieve the same efficiency. The higher pressure drops are the result of higher velocities to obtain adequate dust separation efficiencies.

Pressure drops at off-design conditions are correlated by Equation (126).

Weight and Volume of Ambient Dust Separators - A typical multiple-tube design (Reference 28) has an 8 cfm flow rate per small tube (approximate). This design concept is constructed of plastic or aluminum (or both). Simple scaling of this separator results in the following weight and size estimates:

$$Wt = 0.00264Q \quad (129)$$

and:

$$V = 0.15Q \quad (130)$$

A single inlet design might consist of an aluminum or plastic (or both) version of the high pressure design. Its weight is approximated by:

$$Wt = 0.18 + (9.3 \times 10^{-4})Q \quad (131)$$

and volume by:

$$V = 92 Wt^{1.5} \quad (132)$$

Separators also are staged as a single unit to increase the dust removal efficiency. The weight of these units is higher (approximately 3/4 more) and the volume is nearly double that of a single-stage unit.

3.5 Fans

Separate fans (i.e., not driven by the air cycle machine turbine) are used to circulate air in secondary closed air loops or between aircraft compartments, and to provide ambient air flow to air cooled heat sinks or heat loads during static aircraft operations. Axial flow fans driven by electric motors are used in almost all of these applications. A few mixed or centrifugal flow fans are used, but the data available for these types is insufficient for further evaluations.

More than 75 axial fans are considered in developing the fan performance and sizing data, including fans having several types of drives. Approximately 50 percent of these fans are used in operational aircraft. The remaining fans may be used in aircraft, but additional specific information about their application is not known. The fans considered herein deliver at least 100 cubic feet per minute (at standard conditions). Smaller fans (e.g., which may be used to cool individual electronic units) are not considered.

Earlier studies provide the general format to evaluate fans for use in aircraft environmental control systems. Numerous fans are considered in previous studies (References 6 and 30) and both theoretical and empirical correlations of fan design data are included in these references. The data presented in this report validate or improve these correlations with more recent fan data (e.g., References 31 through 34) for fans which deliver at least 100 cubic feet per minute.

3.5.1 Fan Performance - The design performance requirements of a fan are the air flow rate and pressure drop in the air loop. The power to drive the fan is related to the fan efficiency and the type of drive used. It should be noted that the inefficiencies represent additional heat loads. The efficiencies of various drives are found in Section 3.9.

The pressure rise provided by fans must be matched to the pressure drop of the air circuit. A pressure rise of 0.5 psi is typical if the circuit contains a heat exchanger (0.75 psi maximum). If the circuit does not contain a heat exchanger a pressure rise of 0.3 psi is typical (minimum of 0.1 psi).

Fan Efficiency - The most common method of defining fan overall efficiency is based on the static pressure rise provided by the fan. This overall efficiency is called the static efficiency (η_S).

$$\eta_S = \frac{\text{fluid power}}{\text{input power}}$$

(133)

or

$$\eta_S = 3.24 \frac{Q(\Delta P_S / \sigma)}{\text{watts in}}$$

Reference 30 indicates that the maximum static efficiency of a fan type (e.g., axial) is related to the specific speed. Specific speed is:

$$N_S = \frac{N \sqrt{Q}}{\left(\frac{\Delta P_{St}}{\sigma}\right)^{0.75}}$$

CFM
IN. H₂O

(134)

where: ΔP_S is inches H₂O.

No relational trend between maximum static efficiency and specific speed is obtained for a number of the a.c. electric motor driven fans considered.

(See Figure 79.) The design flow rate and pressure rise provided by a fan generally are selected at the point of maximum static efficiency. Values for maximum static efficiency vary between 20 and 80 percent for a wide range of specific speed values. The average value of maximum static efficiency is approximately 60 percent. Several other approaches for developing a relation for static efficiency were attempted (e.g., as a function of specific speed and specific diameter, or of fluid power output), but no correlation is indicated.

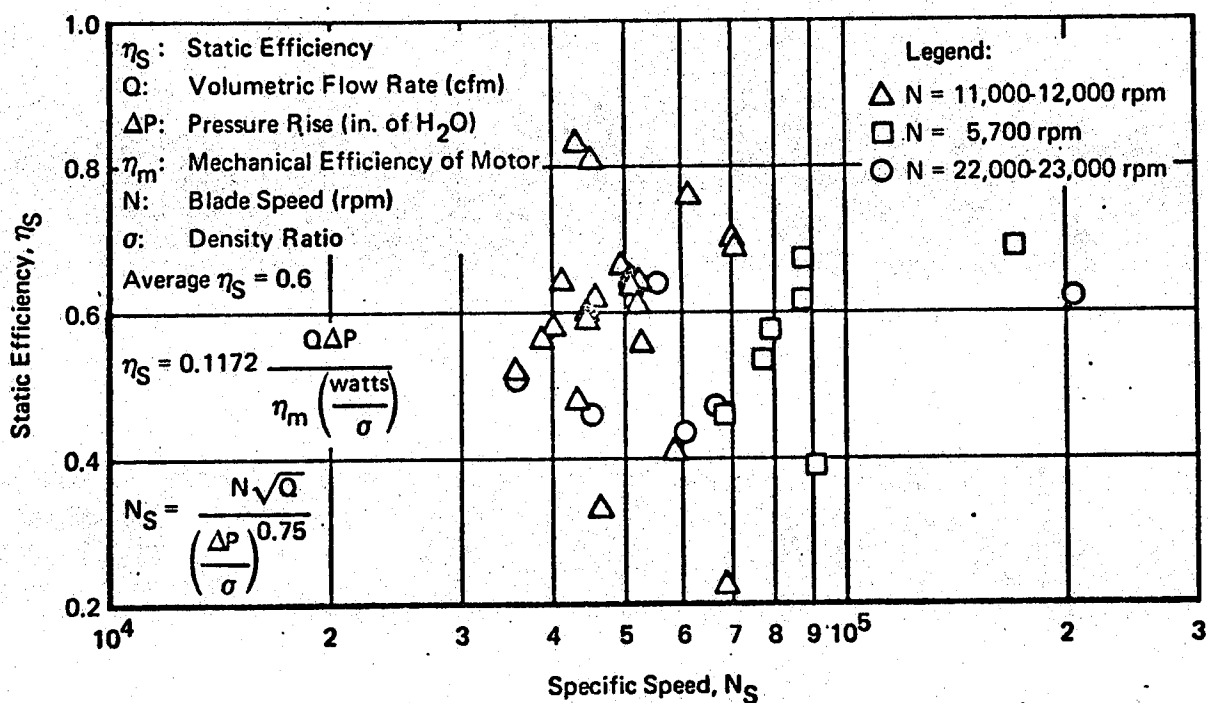


Figure 79 Axial Fan Static Efficiency

GP 9416-16

Fan Off-Design Performance - Fan performance at flow rates other than at the point of maximum efficiency is empirically correlated. This is accomplished by approximating a fan performance curve (pressure rise versus flow rate) by a second order polynomial. This polynomial is of the form:

$$\frac{Q}{Q_{\Delta P=0}} = 1.0 + K_1 \left(\frac{\Delta P}{(\Delta P)_{n_{max}}} \right) + K_2 \left(\frac{\Delta P}{(\Delta P)_{n_{max}}} \right)^2 \quad (135)$$

where the constants K_1 and K_2 are to be determined, and:

$Q_{\Delta P=0}$ is the flow rate with no pressure rise

$(\Delta P)_{n_{max}}$ is the pressure rise at maximum static efficiency (i.e., approximate design point.)

This polynomial is normalized using data of several fans. The constants K_1 and K_2 are calculated from data for 25 fans. The final equation:

$$\frac{Q}{Q_{\Delta P=0}} = 1.0 - 0.224 \left(\frac{P}{(\Delta P)_{n_{max}}} \right) - 0.123 \left(\frac{\Delta P}{(\Delta P)_{n_{max}}} \right)^2 \quad (136)$$

has a standard error of 4.7% for the performance points shown in Figure 80. Fan stall may be encountered with $\Delta P/(\Delta P)_{n_{max}}$ ratios greater than approximately 1.1 (or $Q/Q_{\Delta P=0}$ ratios less than approximately 0.6). Therefore, this equation should be considered invalid for $\Delta P/(\Delta P)_{n_{max}}$ ratios in this region.

The fan power requirements and efficiencies at these off design conditions are estimated by a rule-of-thumb approximation: a 20 percent reduction in power is required (from the design point) at a flow rate which is 30 percent greater than the design flow rate.

Fan performance at other than standard air densities is generalized such that the pressure rise and power requirements are proportional to air density at constant volumetric flow rates. Similarly, if a given fan is driven at a different speed, the following fan laws apply (Reference 30):

$$Q/N = \text{constant},$$

$$\frac{\Delta P_S}{\sigma N^2} = \text{constant},$$

$$\frac{\text{power}}{\sigma N^3} = \text{constant}.$$

Due to motor output or blade characteristics, these generalizations are not universally true.

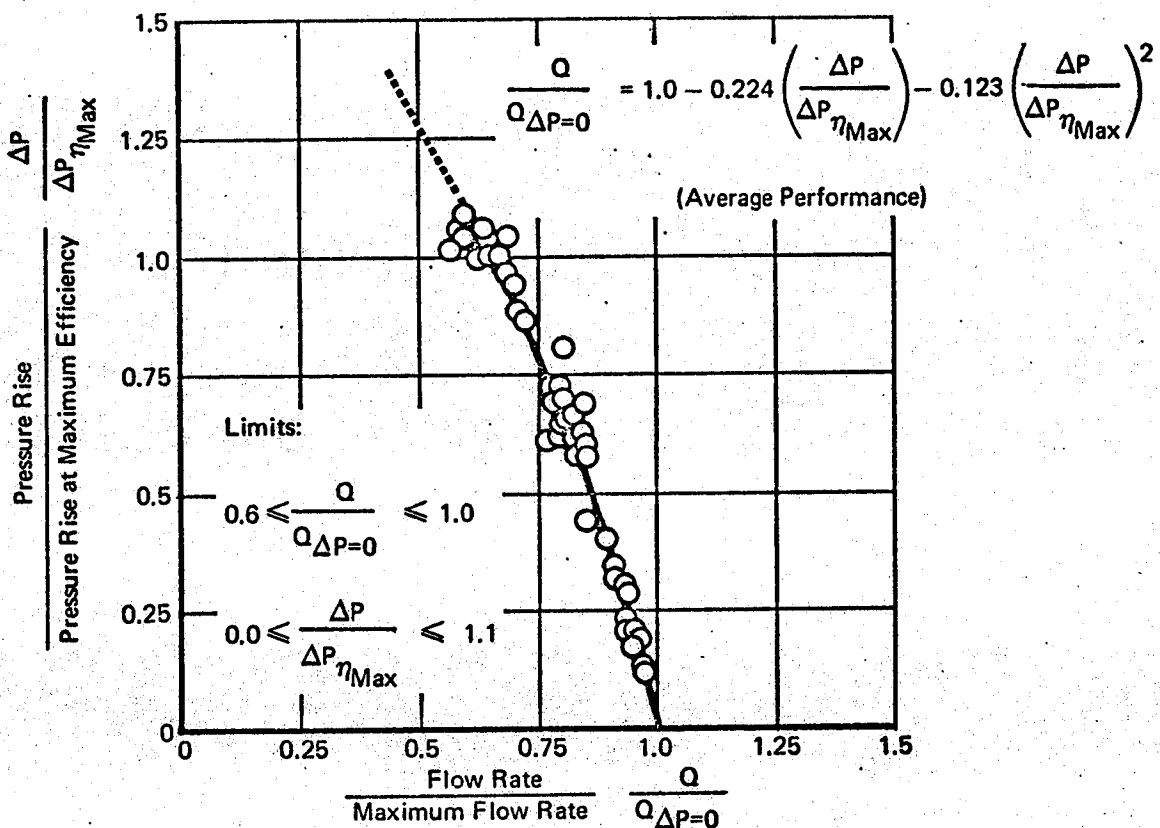


Figure 80 General Axial Fan Performance

GP 9416-15

3.5.2 Fan Sizing - The sizes of axial fans are related to the design volumetric flow rate (i.e., the flow rate at maximum fan efficiency) and the fan speed. Fan weights and volumes are correlated to fan size and type of drive.

Fan Size - Blade Tip Diameter - Correlation of the blade tip diameter data is related to the basic fan flow law, found in Reference 30. This is:

$$D_T = K_1 \left(\frac{Q}{N} \right)^{1/3} \quad (137)$$

Using vendor data for fans having several types of drives, the constant (K_1) of this equation is calculated for each fan. Within a 9% standard error, the average value of the constant is 1.40. Thus, given the required volumetric flow rate and desired blade speed, the tip diameter is estimated by:

$$D_T = 1.40 \left(\frac{Q}{N} \right)^{1/3} \quad (138)$$

where: D_T = feet.

Figure 81 shows this correlation.

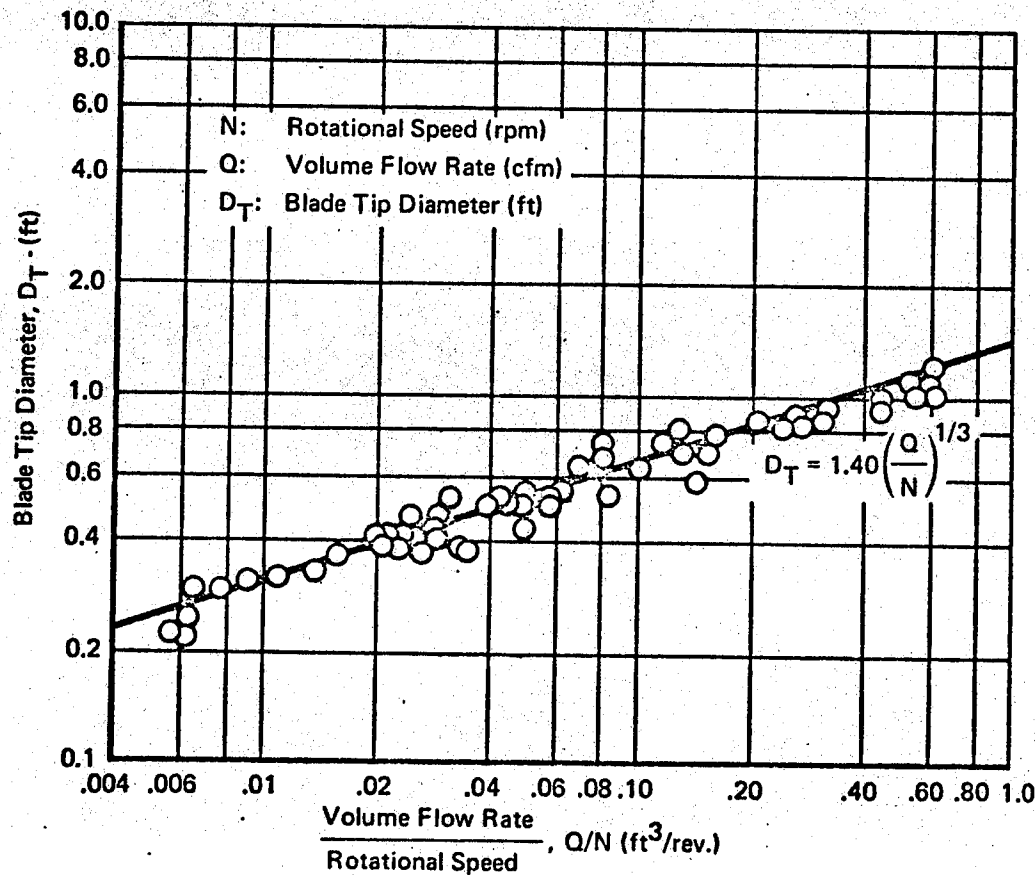


Figure 81 Axial Fan Size Correlation

GP 9416-19

The size of a fan is shown to be dependent on the required volumetric flow rate and the rotational speed of its drive. Fan noise increases as the fan speed is increased. The noise produced by an eight pole 400 Hz a.c. motor generally is considered tolerable. Higher speed motors are used for fans in remote locations. Pneumatic and hydraulic motors are noisy, hence they are recommended for remote locations. Use of higher motor speeds do result in lighter weight fans, as is shown in the next section.

Fan Weight - The total weight of a fan is given in Reference 6 as $0.0352 D_T^3$, D_T being in inches. This is merely the total volume equation (given in Reference 6) multiplied by a bulk density of 0.0271 lb/in^3 . However, this equation provides a poor correlation of the fan data considered herein.

Two empirical relations for the weights of a fan and electric motor (a.c. or d.c.) are presented. Using the method of least squares, two equations fit the fan data. These equations are:

$$Wt = 0.3D_T^{1.92} \quad (139)$$

and:

$$Wt = 0.26 D_T^2 \quad (140)$$

These equations for correlating weight and tip diameter are illustrated in Figure 82. With these equations, the total weight is within a standard error of 25%. It should be noted that these equations are for aluminum fans. For magnesium fans, approximately:

$$Wt(\text{Magnesium}) = 5/6 Wt(\text{Aluminum}) \quad (141)$$

Also note that no weight difference is indicated for a.c. or d.c. motor drives. Examples to determine the weight of several fans used in the C-5A are found in Volume II.

Fewer hydraulic motor driven fans have been used in aircraft ECS. A correlation for the weight of several fans with hydraulic motors is shown in Figure 83. The correlation equation is:

$$Wt = 0.178 D_T^{2.0} \quad (142)$$

The standard error of this equation is 10.9%. Comparison of hydraulic and electric motor driven fans indicates that hydraulic motor driven fans are lighter. However, this result should not be extrapolated to smaller fan sizes because small hydraulic motors are heavier than small electric motors.

Also, it should be remembered that hydraulic motors are noisy.

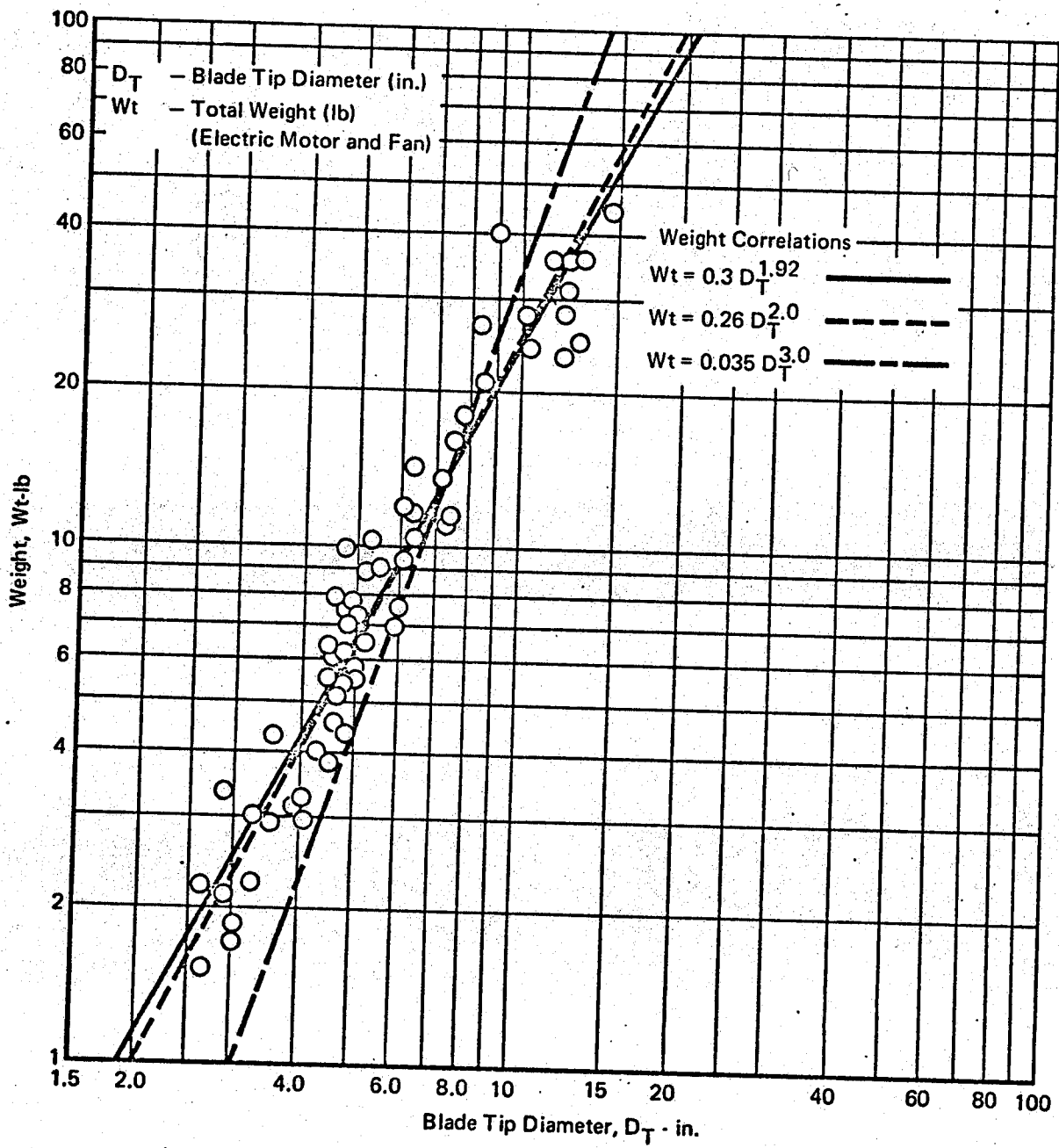


Figure 82 Axial Fan Weights

GP 9416-17

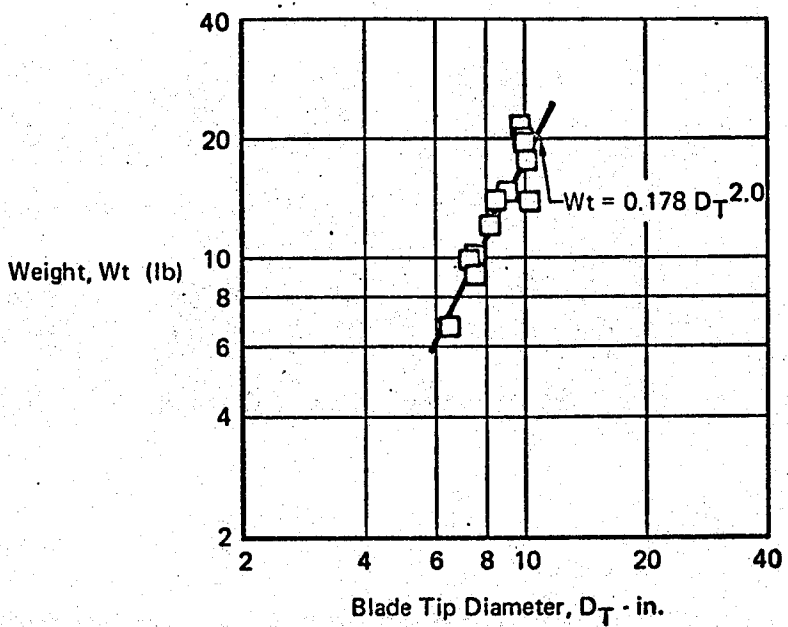


Figure 83 Axial Fan Weights
(Hydraulic Motor)

GP 9416-36

The weights of several externally driven fans (belt or shaft) are shown in Figure 84. A correlating equation also is shown:

$$W_t = 0.109 D_T^{2.0} \quad (143)$$

This equation has a standard error of 19.9% for the fan data shown in the figure.

A few bleed air turbine driven fans have been manufactured. Axial turbine blades are mounted on the outside diameter ring of the fan blades. No correlation of the weight of bleed air turbine driven fans could be obtained. An approximate method is to add two turbine blade heights to the blade tip diameter, and to use the weight equation for externally driven fans with this "effective blade tip diameter."

Fan Volume - An equation for total fan volume as a function of blade tip diameter is $V = 1.3 D_T^3$ (Reference 6). This equation is obtained by making the following assumptions.

1) $L = 1.15 D_T$

2) $D_o = 1.2 D_T$

This equation for volume is very close to the equation:

$$V = 1.1 D_T^{2.93}, D_T - \text{ft} \quad (144)$$

which was formulated empirically using the method of least squares with actual volume data for fans with electric motors. The similarity between these two equations is seen in Figure 85. Both equations provide fair approximation of total volume, with a standard error of 35%. The main reason for the large deviation is the wide variation of length with tip diameter. This equation also provides an adequate estimate of the volume of hydraulic motor driven fans.

Externally driven fan volumes do not include an additional volume for the hydraulic or electrical motor drive. The bulk volume of these fans is approximately two-thirds the volume of a fan and motor. The volume of a turbine driven fan is approximated as an externally driven fan with an effective blade tip diameter (see above).

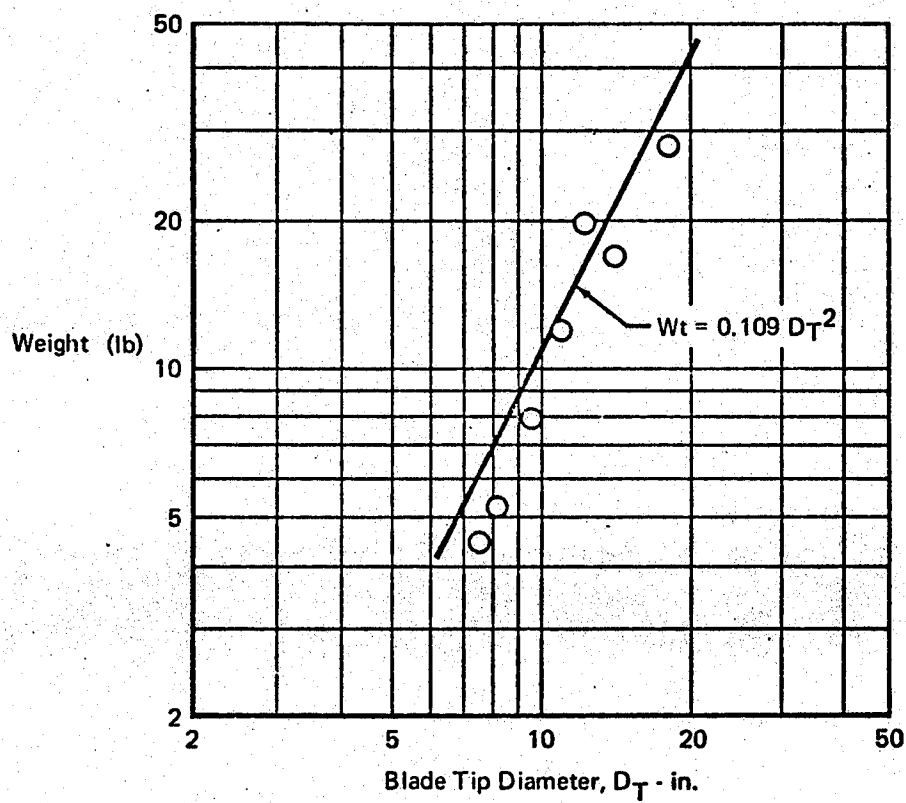


Figure 84 Axial Fan Weight (No Motor)

GP 9416-18

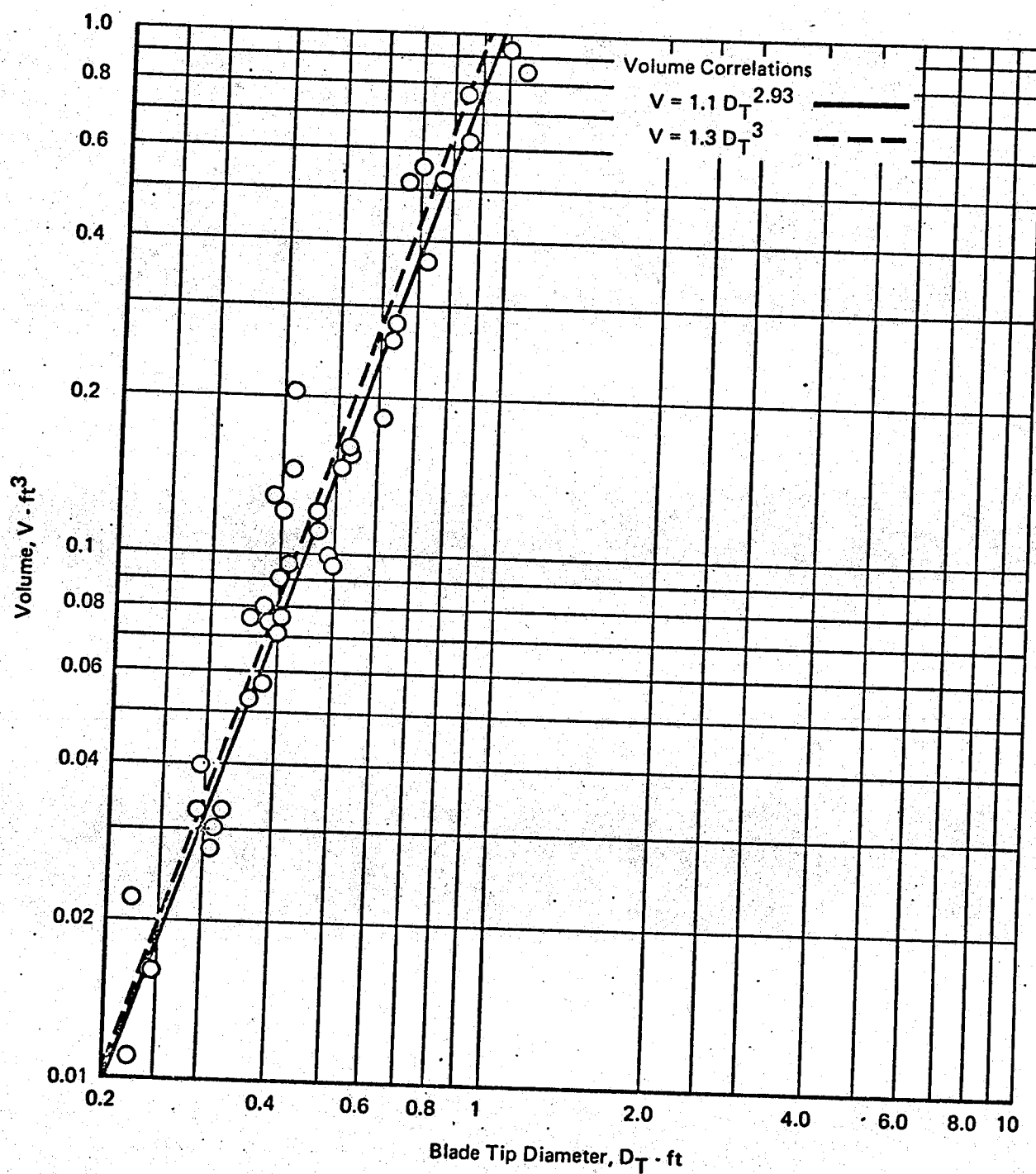


Figure 85 Axial Fan Volumes

GP 9416-37

3.6 Pump Packages

Liquid pumps are used to transfer liquid coolant from the liquid cooled heat load to the basic ECS system (i.e., air cycle or vapor cycle), which serves as the heat sink for the closed liquid loop subsystem, or from the basic ECS system to the fuel cooled heat sink. The liquid pump is located upstream of the heat sink so that the coldest liquid is delivered to the "load."

The pump package (as considered herein) includes the pump, motor (electrical motors are used almost exclusively), liquid accumulator or reservoir (to compensate for liquid density change for the range of temperature encountered), relief and bypass valves, and other packaging items, such as interconnecting liquid passages or tubing, fill and disconnect fittings, etc.

Most pumps used in aircraft ECS liquid loops are vane or gear type positive displacement pumps. Characteristics of these two types appear to be indistinguishable. Some centrifugal pumps are used and some information on centrifugal pumps is presented. In general, centrifugal pumps are used for liquid flow rates greater than are required in many aircraft liquid cooled loads (e.g., 10 to 20 gallons per minute or greater). The vane or gear pumps are used with relief (or bypass) valves. Nominal rotational speed for vane or gear pumps is approximately 5700 rpm, although positive displacement vane pumps operating at 11,000 rpm are not uncommon. Centrifugal pumps normally are operated at 11,000 or 23,000 rpm (approximately). The data used herein are taken from References 35 and 36, and other miscellaneous vendor documents.

3.6.1 Performance - The design point performance requirement of a liquid coolant pump is determined by the flow rate required to cool the liquid heat load, and the liquid pressure drop of the liquid loop (i.e., the load and the liquid loop components). A nominal pressure drop of 5 psi is typical of filters used in many liquid loop subsystems. Heat exchanger pressure drops are nominally 2 psi per pass. (See Section 3.1.2.) A typical pressure drop for liquid lines is 0.06 psi per inch of length. (See Section 3.10.2.) The flow rate and pressure rise define the fluid power requirements of the pump. Power to drive the pump is determined by the pump efficiency.

Pump Efficiency - The efficiency of vane and gear pumps (often defined as overall efficiency) is:

$$\eta = \frac{\text{Fluid Power Out}}{\text{Shaft Power In}} = \frac{(\Delta P)W}{1714(\text{HP})} \quad (145)$$

Reference 30 indicates the overall efficiency of positive displacement pumps increases as outlet pressure is increased. Figure 86 shows the efficiencies of 17 vane and gear pumps as a function of pump pressure rise. (The efficiencies shown in Figure 86 are determined from liquid flow rate, pressure rise, and electric motor power input. The shaft power input to the pump is calculated with the electric motor efficiency data found in Section 3.9.1.) A correlation of pump efficiency as a function of pump pressure rise is indicated in Figure 86. This equation for pump efficiency is:

$$\eta = 1 - \frac{4.8}{(\Delta P)^{1/2}} \quad (146)$$

Insufficient data on aircraft centrifugal coolant pumps are available to obtain a correlation of their efficiency characteristics.

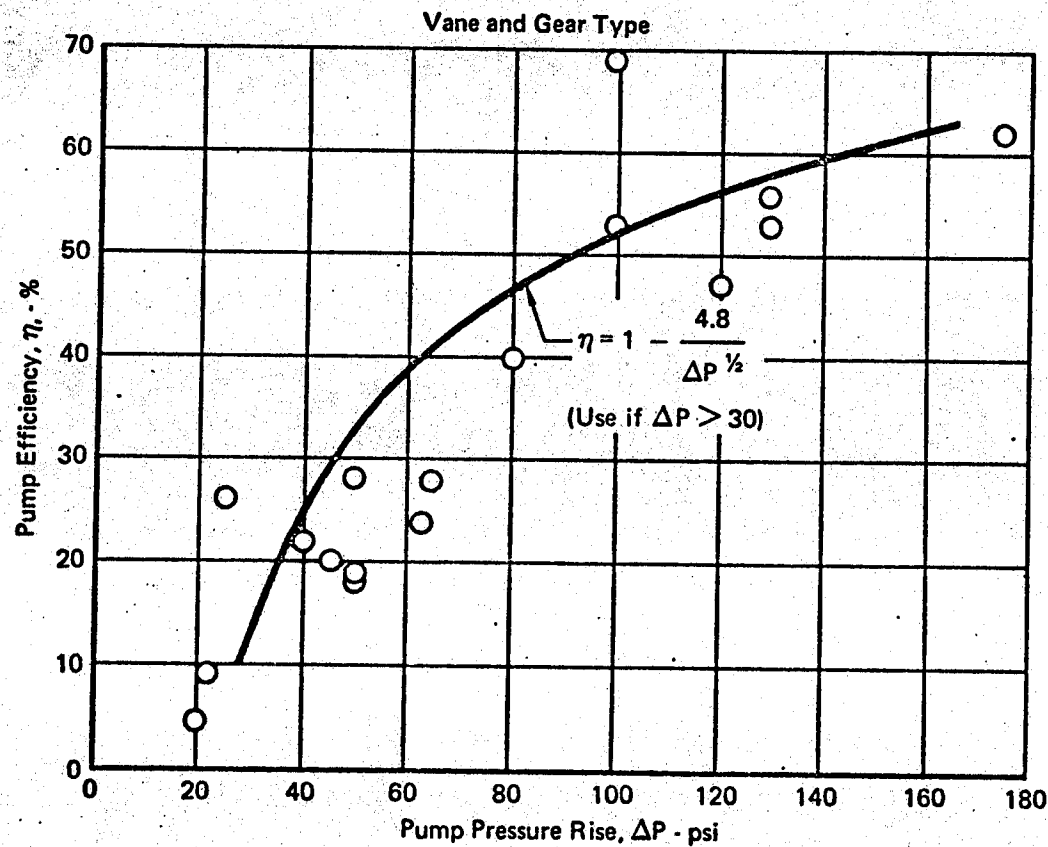


Figure 86 Coolant Pump Efficiency

GP 9416-196

Performance Curves - The design and off-design performance characteristics (i.e., pressure rise versus flow rate) are correlated on a relative basis. The bases used herein differ slightly for vane and gear pumps, and for centrifugal pumps. Vane and gear pumps are operated with relief valves, hence the pressure rise at which this relief valve opens is used as a reference. For centrifugal pumps the maximum pressure rise is used. For both types of pumps (positive displacement and centrifugal) the maximum flow rate is used as the other reference.

Upper and lower limits of the relative pressure rise versus relative flow rate of several vane and gear pumps are shown in Figure 87. The average relative flow rate at which the relief valve opens on ten pumps is 0.85, as is indicated in the figure. Manufacturers' designated design pressure rises very slightly from that of the relief valve opening (relative ΔP from 0.8 to 1.1 for eight pumps), but have an average almost that of the relief valve opening (actually a relative ΔP of 0.97). The average value of the maximum pressure rise of these pumps is 25% greater than that at which the relief valve opens. These data are used to obtain the average off-design performance curve of vane or gear type pumps shown in Figure 87.

Envelopes of the relative performance of a few centrifugal pumps are shown in Figure 88. The indicated manufacturers' design points fall between relative pressure rises of 0.6 and 0.75.

3.6.2 Weight - A liquid coolant pump package, as installed in an aircraft, often includes the pump, motor, relief valve (if applicable), filter, liquid reservoir, and other miscellaneous valves, fitting, and interconnecting liquid passages or tubing. (Liquid to air heat exchangers and fans also are included to form a liquid cooling package. These liquid cooling packages are not included in this section.) The weights of several of the components included in a pump package are discussed individually, and a packaging weight factor (which includes the small miscellaneous items) also is determined.

Weight of Pump and Motor - The weight of positive displacement pumps is expected to increase as the displacement volume per revolution increases. (See Reference 30.) The electric motor drives of liquid coolant pumps normally are integral with the pumps. The weights of coolant pumps and motors (and relief valves of vane and gear pumps) versus displacement volume per revolution are shown in Figure 89. Since the motors of pumps having small displacement volumes per revolution weigh more than the pumps, an average

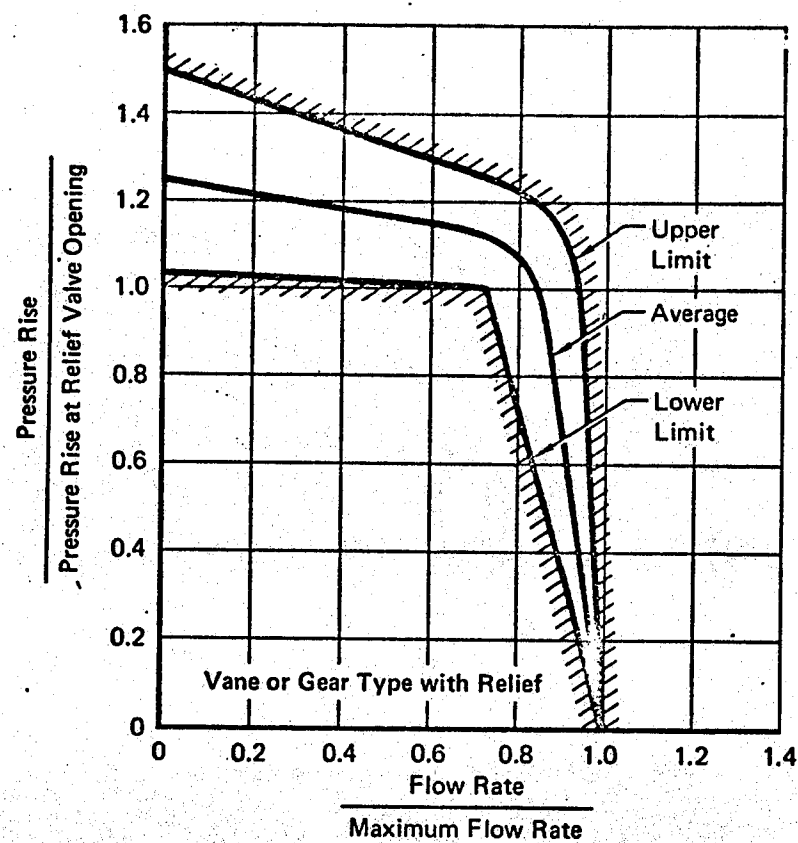


Figure 87 General Coolant Pump Performance

GP 9416-26

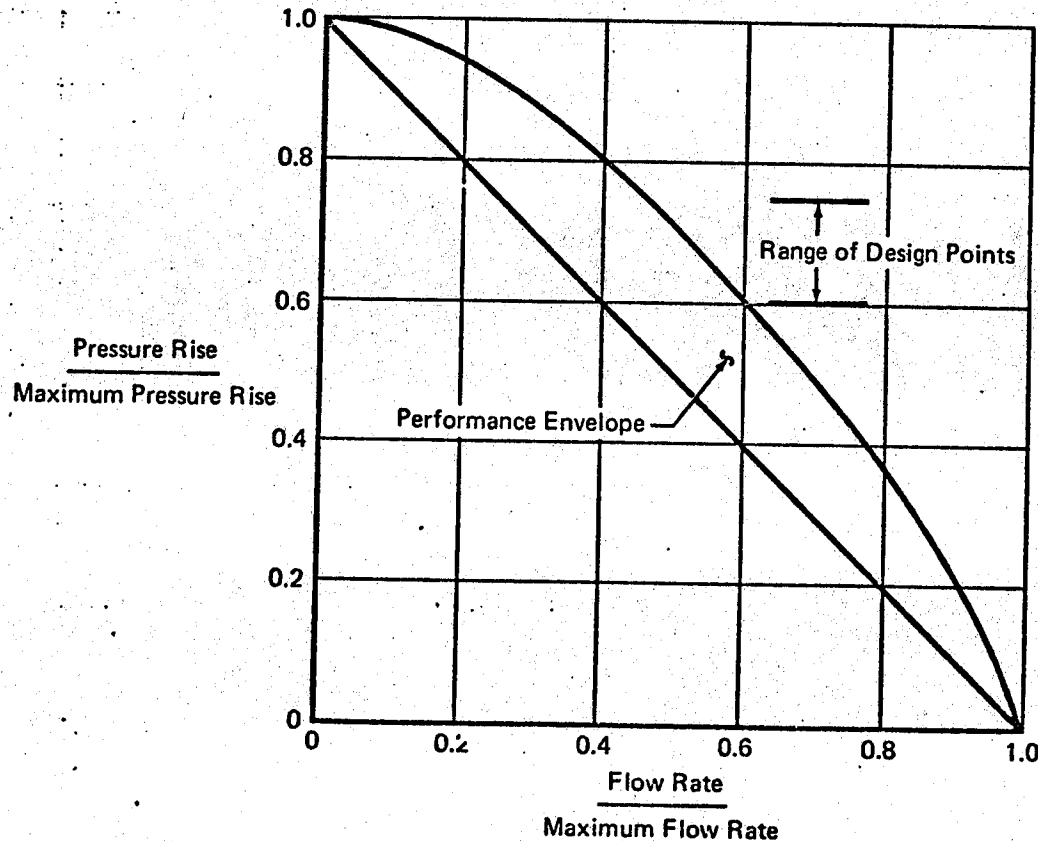


Figure 88 General Centrifugal Pump Performance

GP 9416-30

motor plus pump weight of 2.1 pounds is shown. For vane and gear pumps having displacement volumes greater than $0.088 \text{ in}^3/\text{rev}$, the average weight is assumed to increase as displacement volume per revolution is increased. Using least mean squares techniques, the weight of vane and gear pumps having displacement volumes per revolution greater than $0.088 \text{ in}^3/\text{rev}$ is:

$$\text{Weight (vane or gear)} = 10.63 \left(\frac{1728Q}{N} \right)^{2/3} \quad (147)$$

Use of this approach predicts the weights of the 23 pumps considered with a standard error of 19%. The weights of four centrifugal pumps are shown in Figure 89. The least mean squares relation between the weight of the three larger centrifugal pumps and their displacement volume per revolution is:

$$\text{Weight (centrifugal)} = 22.92 \left(\frac{1728Q}{N} \right)^{2/3} \quad (148)$$

for displacement volumes per revolution greater than $0.028 \text{ in}^3/\text{rev}$.

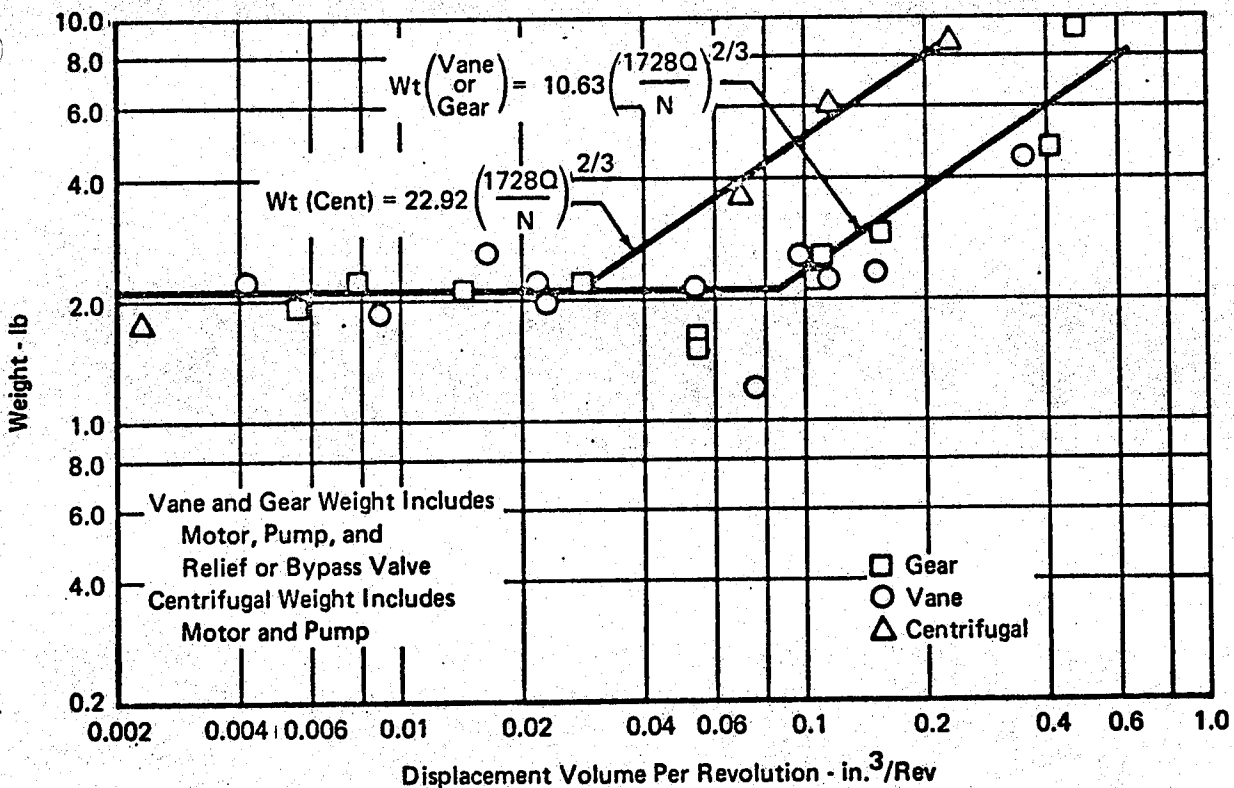


Figure 89 | Weight of Coolant Pumps

GP 9416-35

Weight of Liquid Subsystem Reservoirs - The volumetric displacement of accumulators or reservoirs is determined by the volumetric change of the total amount of liquid in the liquid loop subsystem. A low temperature of -65°F normally is used. The upper temperature depends on the allowable liquid temperature from the liquid heat load, and the aircraft environment. A maximum temperature of 250°F is indicative for use in Mach 2 plus fighters. Higher maximum temperatures would be used for faster aircraft. A margin normally is added in determining the volumetric displacement requirements of the reservoir. A gas pressurization source is needed to compensate for liquid displacement.

Individual reservoirs are less common than reservoirs which are integral in a pump package. The weights and fluid displacements of a few reservoirs is shown in Figure 90. Since the reservoir is basically a shell construction, the weight should be proportional to the 2/3 power of displacement volume. A least mean squares fit for the data points shown in Figure 90 results in the following equation for liquid reservoir weights:

$$Wt_{reser.} = 0.131 V_d^{2/3} \quad (149)$$

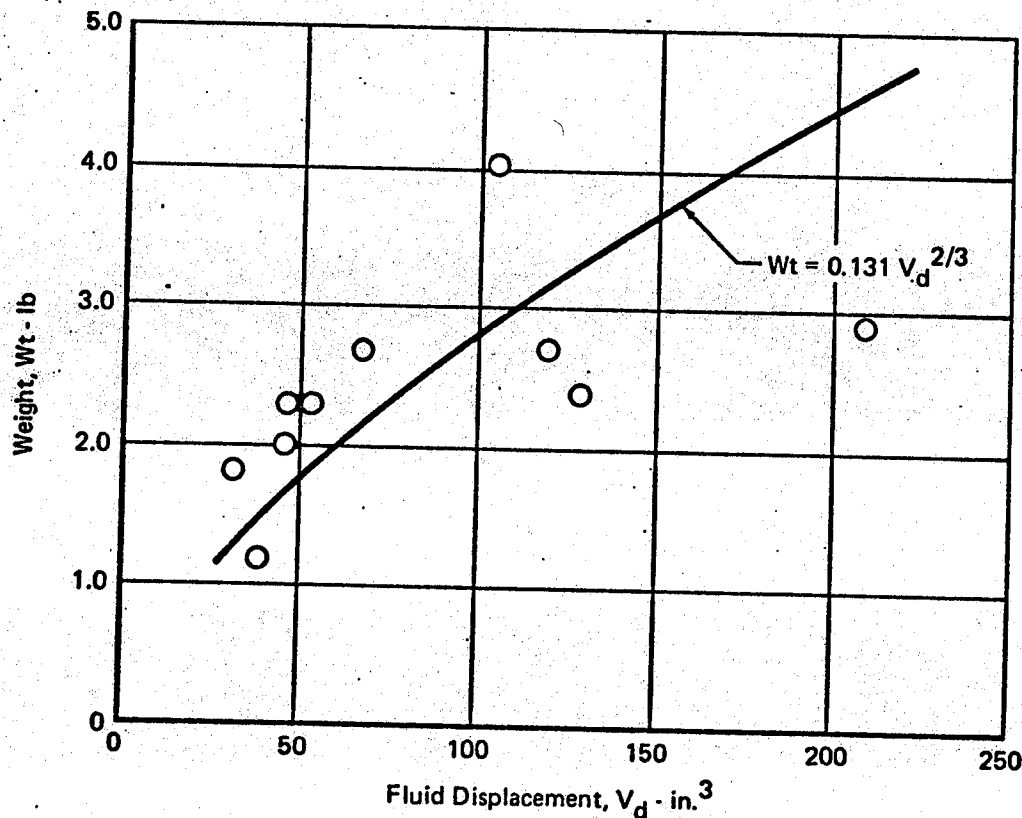


Figure 90 · Coolant System Reservoir Weight

GP 9416-27

Equation (149) predicts the weights of the ten reservoirs with a standard error of 29%.

Weight of Liquid Subsystem Filters - Filters in liquid loop subsystems are often included in the pump package. The size and weight of the filters increase as the volumetric flow rate of liquid coolant increases. The weights of several liquid filters are shown in Figure 91. (Some of the filter weights used in Reference 14 are included.) A least mean squares relation for the weights of liquid subsystem filters is:

$$W_{filters} = 0.55 + 0.128 (W') \quad (150)$$

The standard error of this correlation is 21%.

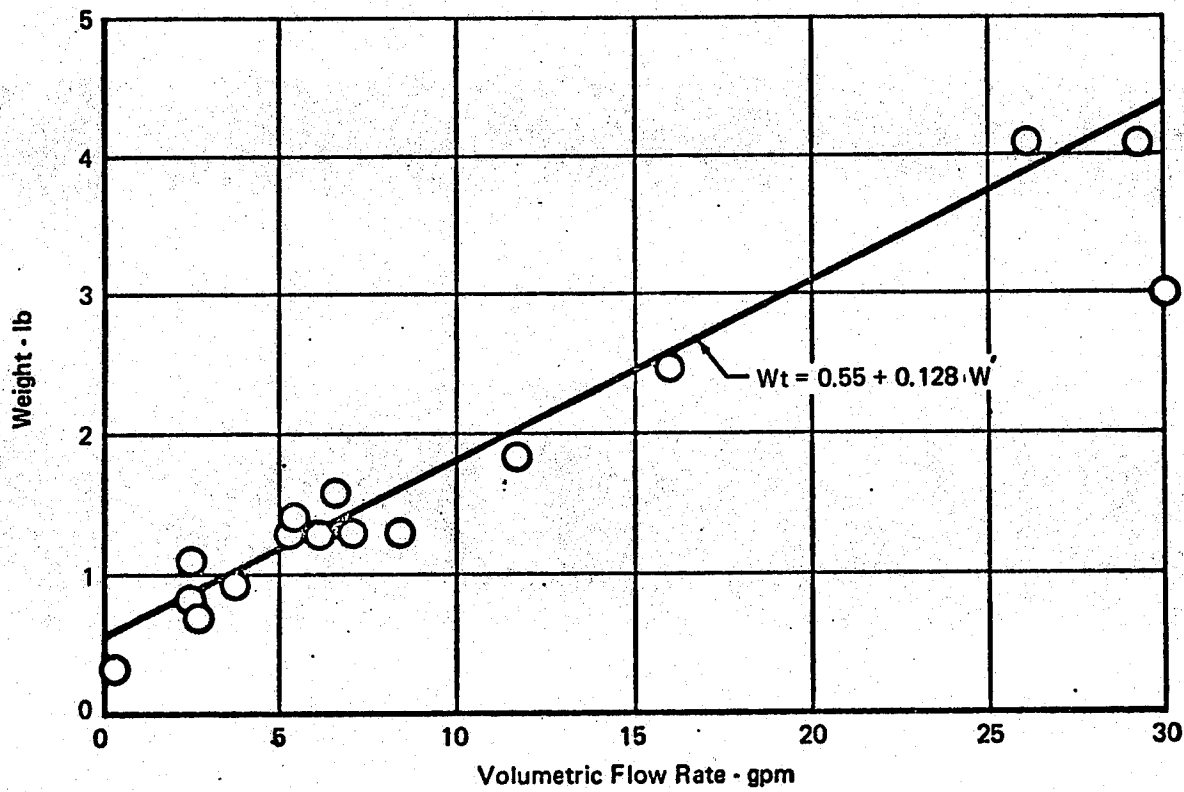


Figure 91 Weights of Filters for Liquid Coolant Subsystems

GP 9416-28

Weight of Pump Packages - Liquid loop subsystem pumps often are assembled, or packaged, with several other components used in the liquid loop subsystem. These components may include the electric motor, a reservoir, a bypass or relief valve, a filter, a temperature control valve, interconnecting liquid flow passages or lines, and disconnect and fill fittings. A sum of the appropriate component weights as presented previously in this section should underpredict the weight of pump packages, since the small miscellaneous items (lines, fill valves, etc.) are not determined on an individual basis. A comparison of the calculated weights of several pump packages (for which the contents are known) and the actual pump package weights (which includes the miscellaneous items) indicates that the total pump package weight is 10% to 15% greater than the calculated sum of the weight of the major components of the pump package.

3.6.3 Volume of Pump Packages - The size, or volume, of pump packages (rather than of individual components) is discussed herein. The volume, of course, is dependent on the reservoir size. The volume is related to the pump package weight (i.e., bulk density). The bulk density of several pump packages considered (exclusive of liquid cooling subsystems which include a heat exchanger, and possibly a fan) varied from 38 to 67 pounds per cubic foot. The pumps considered have estimated displacement volumes per revolution from $0.01 \text{ in}^3/\text{rev}$ to $0.12 \text{ in}^3/\text{rev}$. The estimated reservoir sizes vary from 15 to 100 cubic inches (data were not available on all packages considered). The average bulk density, of the nine pump packages considered, is 52.3 pounds per cubic foot. The standard error of this average bulk density is 23.6%.

3.6.4 Example of Pump Package Design - An example is presented to illustrate pump package design based on the previous information. The pump package contains a vane pump and motor, relief valve, reservoir, filter, and temperature control valve. It provides 6.0 gpm at a $\Delta P = 30 \text{ psi}$. The pump is driven by a 4-pole 400 cps a.c. motor (speed of 11800 rpm), and the reservoir volume is 300 in^3 .

$$\text{Pump efficiency (Eq. 146): } n = 1 - \frac{4.8}{(30)^{1/2}} = 12.3\%$$

$$\text{Power required (Eq. 145): } = \frac{(30)(6.0)}{(1714)(0.123)} = 0.854 \text{ hp}$$

$$\text{Displacement volume} = \frac{(1728)(6.0)(0.1337)}{11800} = 0.117 \frac{\text{in}^3}{\text{rev}}$$

Pump weight (Eq. 147): $W_t = 10.63 (0.117)^{2/3} = 2.54 \text{ lb}$
(includes motor and relief valve).

Reservoir weight (Eq. 149): $W_t = 0.131 (300)^{2/3} = 5.87 \text{ lb}$

Filter weight (Eq. 150): $W_t = 0.55 + 0.128(6) = 1.32 \text{ lb}$

Temperature control valve weight = 1.1 lb (See Section 4.1.2)

Pump package weight = 1.1 (2.54 + 5.87 + 1.32 + 1.1) = 11.91 lb.

3.7 Vapor Cycle Components

A vapor cycle refrigeration system basically consists of a compressor, a condenser, a receiver, one or more evaporators, and an expansion valve. A system flow schematic is found in Figure 92. The evaporators and the condenser are heat transfer components. The receiver is a separate component which is not a part of the condenser. The following discussion is based on data from some of the existing cargo aircraft vapor cycle systems.

3.7.1 General Vapor Cycle Component Design - The design of components for a vapor cycle is dependent on the heat load and heat sink characteristics, and parameters which describe conditions in the refrigerant loop. Ordinarily, these refrigerant loop considerations are selected from prior experience. Refrigerant loop considerations include:

- (1) No refrigerant flows through the bypass line at the system design point. The bypass line is one method to provide compressor surge control. (See Figure 92.)
- (2) A reasonable value for evaporator pressure drop is 10% of the evaporator pressure.
- (3) The efficiency of a turbine driven compressor should include an allowance for oil cooling.
- (4) An electric motor driven compressor should be sized for a 10% increase in the refrigerant flow to allow for cooling.
- (5) The enthalpy entering the evaporator is nominally the enthalpy of saturated liquid at a few degrees below the condensing temperature.
- (6) The pressure at the compressor inlet nominally is about 4% below that at the evaporator exit.
- (7) The pressure at the condenser inlet nominally is about 4% below that at the compressor discharge.

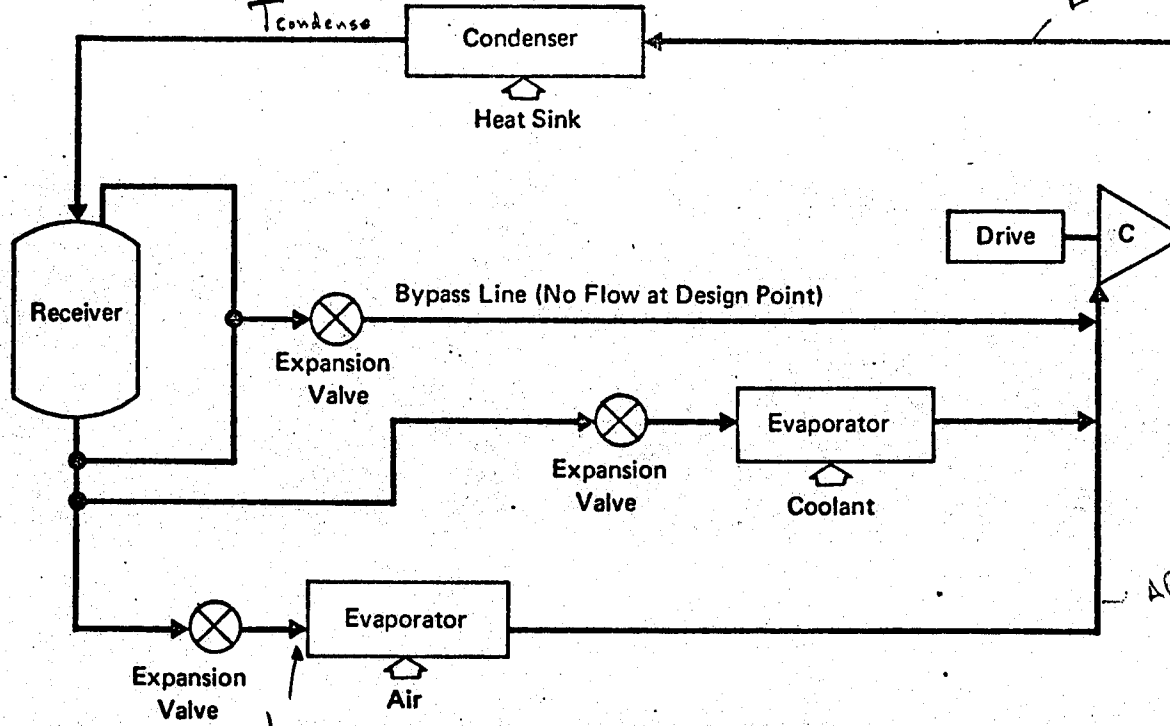


Figure 92 Vapor Cycle Flow Schematic

GP 9416-47

- (8) The evaporating temperature and the condensing temperature affect the sizes of the components and the compressor power, and selection of these temperatures should be carefully considered.

3.7.2 Compressors - Aircraft refrigerant compressors are centrifugal or rotary designs. Current design practice is to integrate the centrifugal compressor and the power drive into a single frame and bearing package. An integrated drive for rotary compressors also is common, but not universal. Three manufacturers are building refrigerant compressors for aircraft in current production. Two manufacturers build centrifugal units and one builds rotary machines. Centrifugal compressors driven by an electric motor operate at a nominal speed of 24,000 rpm. Centrifugal compressors driven by an air turbine are not operated above 80,000 rpm. Rotary compressors also may operate at a nominal speed of 24,000 rpm.

3.7.2.1 Centrifugal Compressors - The compressor used on one current aircraft is a high speed, air turbine driven, single stage compressor for refrigerant R-12. It is used in a cooling system which has a rated capacity of 15 tons and the rated shaft speed is 80,000 rpm.

One basic a.c. electric motor driven compressor design is used with modifications on several aircraft. It is a two stage centrifugal compressor for refrigerant R-114 and is designed for a 10 ton system. The shaft speed is 23,300 rpm. Compressors driven by a.c. electric motors for aircraft are constructed as sealed units without external shaft seals. Refrigerant circulates through the motor to cool it.

The efficiency of the high speed compressor is 61% at its design point. The efficiency of a comparably sized two-stage compressor is 71%. Both machines have higher efficiencies at part load. A modification of the procedure in Section 3.2 is used to estimate design point efficiency. This modified method predicts an efficiency of 77% for the high speed compressor and of 70% for a two-stage unit. The procedure for estimating design point efficiency is as follows: (1) Calculate specific speed, as in Section 3.2; (2) Obtain the specific diameter from Figure 56 at the point of best efficiency; (3) Calculate the rotor diameter, and then the rotor tip speed; (4) Calculate the tip Mach number, which is defined as the ratio of tip speed to the speed of sound at inlet conditions; (5) Using the tip Mach number instead of the M^* of Section 3.2, enter Figure 57 and determine the adiabatic efficiency. This completes the calculation of efficiency for a single stage. If the compressor is a two-stage machine the efficiency is calculated for the first stage using half the overall head, and two percentage points are subtracted to obtain the overall isentropic efficiency.

Weight - The integrated turbo-compressor package described above weighs 12.6 pounds. The 10-ton capacity electric motor driven compressor described above weighs 33.5 pounds, with an estimated 11 pounds for compressor weight. The weight of a centrifugal compressor is estimated by adding 50% to the weight of the power drive unit. (Power drive weights are presented in Section 3.9.)

Volume - The volume of a centrifugal compressor is estimated by adding 50% to the volume of the power drive motor or 30% to the volume of the power drive turbine.

3.7.2.2 Rotary Compressors - Rotary compressors used for aircraft refrigeration systems are of the Lysholm design.

Rotary compressors at the 10-ton capacity level weigh more than comparable centrifugal machines, and exhibit similar efficiencies. For smaller systems the rotary machines scale down with little deterioration of efficiency,

improving their position relative to centrifugal machines. Generally speaking, rotary machines are considered for low capacities or unusually high heads.

3.7.3 Evaporators and Condensers - The procedure for sizing evaporators and condensers is applicable to a plate-fin geometry. Tube-plate heat exchangers have certain advantages and disadvantages. Uniform flow division of refrigerant to several tubes is more readily accomplished than is distributed along the span of several plates. The tubes can be folded back in a multi-pass arrangement to achieve slightly better effectiveness. However, plate-fin designs usually are more compact and typically have lower refrigerant side pressure drop.

A plate-fin geometry which is suitable for evaporators and condensers which exchange heat with air follows:

air side: $15.75R(D) - 0.153/0.149 - 1/7 (0) - .004(A_1)$; (See Figure 39.)

refrigerant side: $16R(S) - 0.10 - 1/8 (0) - .006$ (Close to -4)
separator plate: 0.016 thick Dist bet. Plates FIN LENGTH offset fin thickness (12.5 sep)

This refrigerant side surface is suitable for R-12, R-11, and R-114. The following data are calculated for this fin geometry:

Core density is 0.0185 lb/in^3 (bulk fin densities are obtained with the methods of Section 3.1),

refrigerant flow area is 19.3% of the total face area on the refrigerant side, and $\frac{A_r}{A_{fr}}$

air flow area is 62% of the total face area on the air side. $\frac{A_a}{A_{fr}}$

The fin data of Section 3.1 also may be used, including use of liquid instead of air.

Air to Refrigerant Heat Exchanger Performance - The air side performance of air cooled condensers and air cooling evaporators is obtained from the techniques of Section 3.1. The temperature on the refrigerant side is assumed to be equal to the condensing or evaporating temperature.

For evaporators: $h = 150 \text{ Btu/hr.ft}^{2^\circ\text{F}}$, } refrigerant side

For condensers: $h = 200 \text{ Btu/hr.ft}^{2^\circ\text{F}}$.

For both condensers and evaporators the pressure drop is:

$$P = f \frac{L}{r_h} \frac{\rho(v')^2}{2g_c} \quad w \frac{f L}{D} q \quad (151)$$

where:

f = 0.05 for the refrigerant (typical)

L = one half of passage length

ρ = Density of saturated vapor

v' = Velocity of flow assuming all fluid is saturated vapor.

The desuperheat factor is the ratio of the desuperheating heat transfer to the total heat rejection in the condenser. An evaporator air side pressure drop of 0.15 psia is typical. This pressure drop is typical of the selected fin geometry. It also requires low fan power. A typical condenser air side pressure drop is 0.22 psi for ground static conditions. Use Figure 33 if an altitude condition is being considered.

Evaporator Sizing - The system considered here does not include a separate superheater. Some superheat is desirable at the evaporator exit for definition of an expansion valve control point, and to avoid liquid in the compressor. Since superheating in the evaporator is an inefficient use of an evaporator surface, it is desirable to keep the amount of superheat small. A superheat of 10°F is suggested at the evaporator exit when the refrigerant is R-12 or R-11, and 20°F for R-114.

The following procedure for sizing evaporators is suggested:

(a) Select an evaporating temperature 12°F below exit air temperature.

The evaporating temperature is the saturation temperature of the refrigerant at the pressure in the evaporator.

(b) Calculate temperature effectiveness (η) from Equation (69). $\epsilon = \frac{(T_{in} - T_{out})_{air}}{T_{in,air} - T_{sat,H_2O}}$

(c) Assume nonrefrigerant side core flow length (L_s) and core height (L_n).

(d) Estimate the refrigerant side core flow length (L_R):

$$L_R = 3.0 + 0.6 \sqrt{\frac{L_s L_n}{R}}$$
 (152)

(e) Calculate nonrefrigerant side pressure drop (See Equation 26).

(f) Calculate NTU:

$$NTU = \frac{L_s L_n L}{(W_c p)_{NR} \left[\left(\frac{4 r_h^2 Pr^{2/3}}{c_p \mu Re j \psi (\eta)} \right)_{NR} + \left(\frac{r_h}{h \psi} \right)_R \right] R k}$$
 (153)

(g) Calculate temperature effectiveness:

$$\epsilon = 1 - e^{-\frac{NTU}{R - r_{refrig}}} \quad \text{cross flow}$$
 (154)

(h) Iterate by varying L_s and L_n to obtain consistent values of pressure drop on the nonrefrigerant side and temperature effectiveness.

Condenser Sizing - A condensing temperature at the design point which is 8°F higher than the temperature of the heat sink fluid leaving the condenser is suggested. The condensing temperature is assumed as the saturation temperature of the refrigerant at the pressure in the condenser.

The procedure for sizing the evaporator is used, except that the refrigerant side core flow length is estimated as:

$$L_R = 6.0 + 0.4 \sqrt{\frac{E}{R} L_n} \quad (155)$$

If the air cooled condenser is sized at a ground static condition, the cooling air flow to give a 40°F temperature rise in the air passing through the condenser is chosen.

Weight and Volume - Evaporator and condenser weight are calculated with the methods of Section 3.1. An examination of the weights of four assembled condensers and evaporators for aircraft and several condensers and evaporators for ground installations indicates that a reasonable allowance for the end strips and headers of evaporators and condensers is 60% of the calculated core weight. Use of Equation (64) also is satisfactory. Volumes for evaporators or condensers are calculated from the face area times the air side length.

3.7.4 Refrigerant Charge and Receiver - The refrigerant charge is estimated (for preliminary sizing of a system) as 1.15 pounds per ton of refrigeration plus 0.04 pounds per ton of refrigeration per foot of separation of the evaporator and condenser. A more accurate determination is based on the volumes of components. It is assumed that liquid is 20% of the evaporator volume and 40% of the condenser volume. An estimate of the amount of fluid in the plumbing is related to the compressor capacity. This estimate (cubic feet of liquid in the plumbing) is 0.2% of the volumetric flow rate (cfm) of vapor at the compressor inlet. After summing up the volume allowances for the condenser, the evaporator, and the plumbing, 50% is added to obtain the refrigerant charge.

The receiver contains liquid and vapor in equilibrium. Subcooling the expansion valve can be obtained by locating the evaporator below the receiver, by incorporating the receiver into the condenser, or by adding a separate subcooler in the line between the receiver and the expansion valve. Subcooling at the receiver is zero. Subcooling at the condenser exit to allow for pressure drop in the line between the condenser and the receiver is assumed to be 2°F.

Receiver bulk density is estimated as 0.01 lb/in^3 . Receiver volume is approximately 20% more than the refrigerant charge volume.

3.7.5 Refrigerants - Refrigerants R-11, R-12, R-114 are typical for aircraft vapor cycle systems. These refrigerants are non-toxic, and provide a range of thermodynamic properties. Several equations are required to describe the thermodynamic properties of a refrigerant, but the same set of equations are used for all refrigerants. Each refrigerant requires its own data file of empirical constants. The empirical equations and constants come from publications of the DuPont Company and papers written by consultants for duPont, principally J. J. Martin. (See References 37 through 39.) The original authors used these equations and constants to prepare the published tables of refrigerant properties. Note that if the compressor discharge temperature is greater than 280°F, there is a possibility of thermal breakdown of the refrigerant.

3.7.6 Off-Design Performance - The compressor inlet conditions are assumed to be nearly constant at off-design conditions. A suitable set of parameters for mapping compressor performance is volumetric flow (Q), shaft speed (N), pressure ratio (P_{out}/P_{in}), and isentropic efficiency (η). The assumption of nearly constant inlet conditions is adequate for many applications. A map of the performance of a typical compressor is shown in Figure 93.

The performances of an evaporator or condenser are dependent upon the flow rate of the heat source fluid or the heat sink fluid (respectively). This is because the heat transfer rate on the evaporating or condensing side of this component is relatively large. Hence the temperature effectiveness of either an evaporator or a condenser is typically a function of this fluid flow rate only. (See Figure 94.)

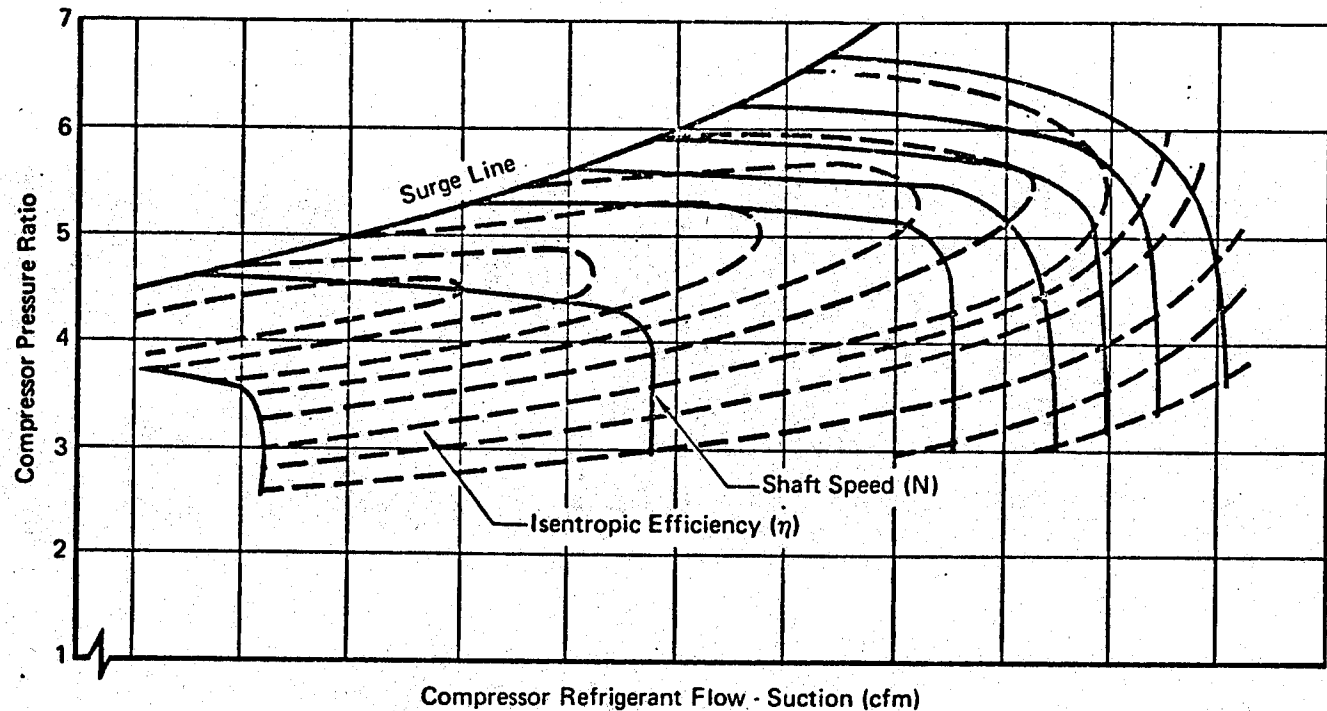


Figure 93 Typical Performance of Refrigerant Compressor

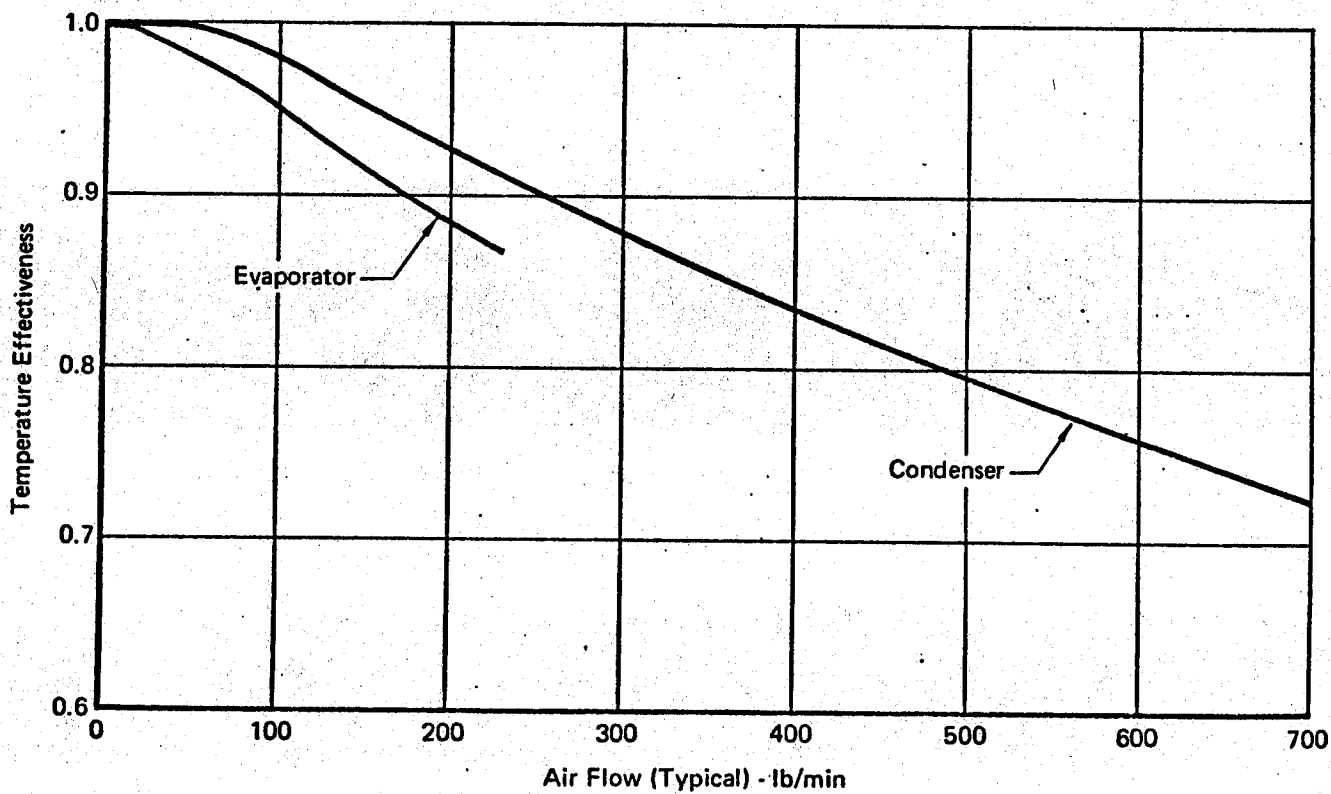


Figure 94 Typical Performance of Evaporator and Condenser

3.8 Auxiliary Air Sources

The most common source of high pressure air to operate the aircraft refrigeration equipment is engine bleed air. Auxiliary air sources used in lieu of engine bleed air are an auxiliary power unit (APU) or an auxiliary compressor. An APU is a small gas turbine unit integrally connected to an air compressor. The compressor inlet is ambient air. Part of the compressed air is mixed with fuel which burns in the combustor, and then expands through the turbine to provide power to drive the compressor. Part of the compressed air is bled off the compressor and utilized as an air source for the ECS. Shaft power extracted from an APU also is discussed in this section.

An auxiliary compressor as an individual unit may be utilized as the only source of high pressure ECS air, or used in conjunction with engine bleed air. In the latter case it is known as a boost compressor. The primary difference in the two applications is the required pressure ratio. Either auxiliary compressor is powered by various types of drives (i.e., electrical, hydraulic, pneumatic, or shaft).

Another auxiliary air source is ground support equipment (GSE) which supplies high pressure air or low pressure conditioned air. Air sources provided by GSE are not considered as part of the aircraft ECS. Air sources provided by GSE are applicable only to ground static operating conditions, whereas the other auxiliary air sources are applicable to ground and air-borne operating conditions.

3.8.1 Auxiliary Power Units - An auxiliary power unit (APU) is a relatively small gas generator that provides a secondary source of shaft horsepower or bleed air flow, or both, to an aircraft environmental control system. It also is an onboard primary source of power that enables the pilot to start his main engines without the need of GSE. A design investigation of APU's for future fighters is found in Reference 40.

The design point conditions of an APU are ambient conditions (altitude, temperature, etc.) and bleed air and shaft horsepower characteristics. The required simultaneous correlating equations to define the design point fuel flow rate, size, and weight are presented. These results are based on empirical correlations of existing APU's. The important correlating parameter is the equivalent horsepower (EHP). APU bleed airflow rates, fuel flow rates, bleed air pressures and temperatures at off-design conditions are defined relative to the design point performance.

Design Point - The design point is selected as a sea level static, 103°F day, standard pressure ambient condition. Design point data on APU's considered in this study are listed in Table V. The design performances of these APU's are shown in Tables V and VI.

The equivalent horsepower is the sum of the required shaft horsepower and the air horsepower. The air horsepower is defined as the amount of energy that could be obtained by expanding the available bleed airflow through a hypothetical 100% efficient turbine. The EHP is calculated at the design point only. The equation for EHP is:

$$EHP = SHP_r + (c_p)(T_{bl} - T_e) (w_{bl}^o) \left(\frac{1}{42.42} \right) \quad (156)$$

where:

$$T_e = \frac{T_{bl}}{\frac{\gamma-1}{\gamma}} \quad (PR) \quad (157)$$

A representative bleed air temperature (T_{bl}) is 890°R and a representative bleed air pressure ratio is 3.19. Using these values, T_e equals 638°R. Typically $c_p = 0.243 \frac{\text{Btu}}{\text{lb}^\circ\text{R}}$ and $\gamma = 1.40$. The installed bleed air pressure ratio is:

$$PR = \frac{P_{bl}}{P_{in}} = \frac{P_{bl}}{P_{am} - (K_1)(P_{am})} \quad (158)$$

where:

$$K_1 = \frac{P_{am} - P_{in}}{P_{am}} \quad (159)$$

A typical value of K_1 is 0.02. The bleed air temperature at the design point is:

$$T_{bl} = T_{am}^o (PR)^{\frac{n_p}{n_p - 1}} \quad (160)$$

Typical values of the polytropic efficiency (n_p) are $n_p = 0.830$ for $PR < 3.0$, and $n_p = 0.770$ for $3.0 \leq PR \leq 5.0$. It is assumed that each compressor stage of the APU has a constant polytropic efficiency. The maximum bleed air pressure ratio is 5.0. The fuel flow rate of an installed APU that has simultaneous bleed air and shaft horsepower extraction, or bleed air extraction only is:

$$w_{fu}^o = [(-1.158 \times 10^{-3})(EHP) + 1.501] (EHP) \quad (161)$$

Table V APU Design Point Data

APU	Bleed Air* Flow (lb/min)	Bleed Air* Press. (psia)	Bleed Air* Temp. (°R)	Fuel Flow* Rate (lb/hr)	Bare Weight (lb)	Installed Weight (lb)	Bare Rect. Vol. (ft ³)	SHP* _r	AHP*	EHP
A	85.5	46.1	890	230	323	832	20.4	60	124	184
B	89.0	46.1	887	240	285	716	18.3	50	127	177
C	500.0	43.9	893	990	558	1402	93.3	63	686	749
D Initial	385	41.0	803	440	601	1464	32.2	142	457	599
D Growth	422	45.6	828	493	601	1464	32.2	189	561	750
E	—	—	—	131	118	296	6.84	96	—	96
F	—	—	—	143	144	362	9.375	154	—	154
G	—	—	—	286	340	853	21.1	345	—	345
H	—	—	—	82	89.2	224	5.09	56	—	56
I	—	—	—	94	97	244	6.31	75	—	75

* Installed Values

GP 9416-125

Table VI APU Design Point Performances

APU	W _{fu} ⁰ /EHP (lb/hr/HP)	EHP/Wt* (HP/lb)	EHP/V (HP/ft ³)
A	1.25	0.221	9.03
B	1.35	0.247	9.68
C	1.32	0.534	8.04
D Initial	0.735	0.409	18.6
D Growth	0.657	0.512	23.3
E	1.36	0.324	14.05
F	0.93	0.425	16.4
G	0.83	0.405	16.3
H	1.46	0.250	11.0
I	1.25	0.308	11.9

* Installed Values

GP 9416-126

A correlation of this equation with fuel flow rate data is shown in Figure 95 (up to EHP of approximately 850). This equation has a standard error of 49%. The installed fuel flow rate of an APU that has shaft horsepower extraction only is:

$$W_{fu}^o = [(-2.43 \times 10^{-3})(EHP) + 1.55] (EHP) \quad (162)$$

Equation (162) is correlated with fuel flow rate data of several APU's in Figure 95 (up to an EHP of 350). The standard error of Equation (162) is 20.1%.

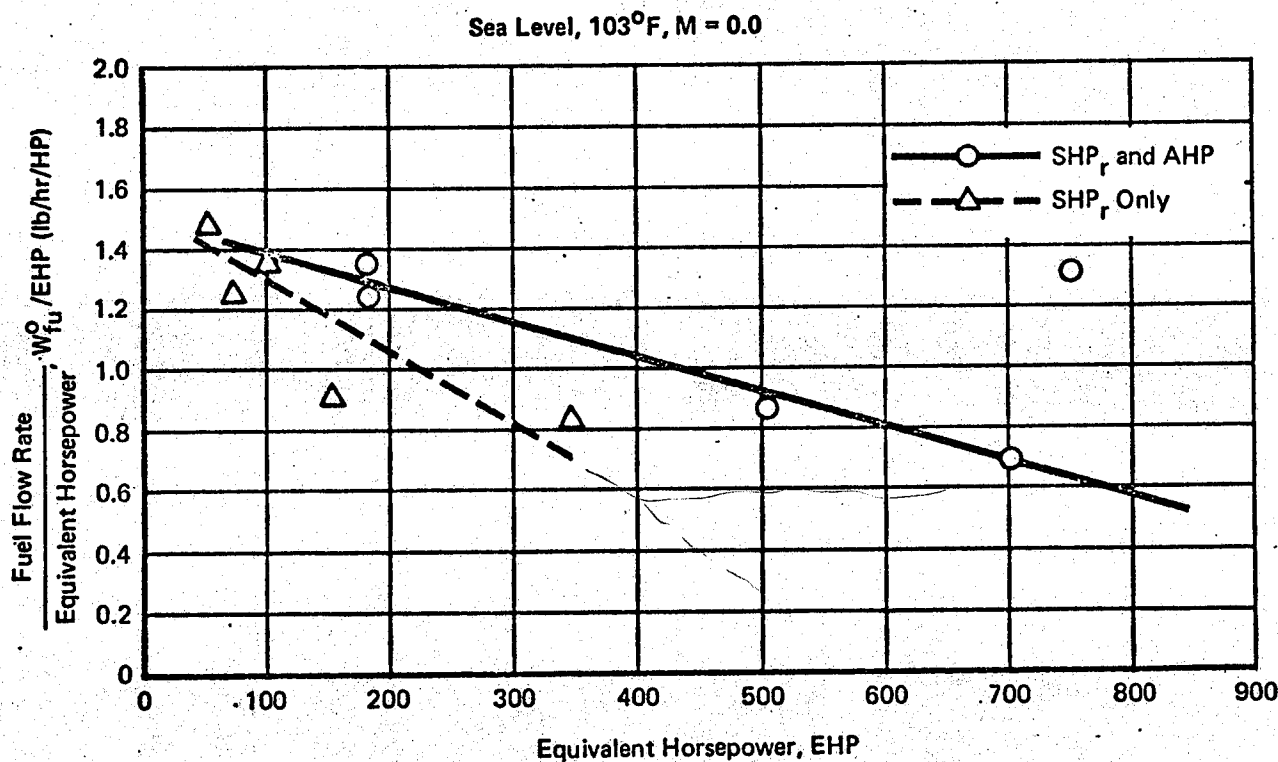


Figure 95 APU Fuel Flow Rate Correlation

GP 9416-38

Off-Design - Off-design conditions occur at various field elevations and ambient temperatures, and in flight. A flush inlet total pressure (from Section 3.10) and the total temperature are used in the equations which follow when off-design performance in flight is determined. The shaft horsepower required at the design point equals the shaft horsepower requirement at an off-design condition.

The bleed air pressure ratio that is assumed or calculated at the design point stays essentially constant at an off-design condition. The off-design

installed bleed air temperature is:

$$\frac{0.286}{n_p} T_{bl} = T_{am} (\text{PR}) \quad (163)$$

Compressor polytropic efficiency is estimated as before. The bleed air flow rate at off-design is based on the bleed air flow requirement at the design point.

$$W_{bl} = W_{bl}^o \delta + K_1 \delta (T_{am} - T_{am}^o) \quad (164)$$

The quantity "K₁" is defined as:

$$K_1 = \frac{\Delta W_{bl}/\delta}{\Delta T_{am}} \quad (165)$$

It is a function of $\text{SHP}_{r/\delta}$.

$$K_1 = -0.542 - (0.001233)(\text{SHP}_{r/\delta}) + (5.625 \times 10^{-6}) (\text{SHP}_{r/\delta})^2 - (1.042 \times 10^{-8}) (\text{SHP}_{r/\delta})^3 \quad (166)$$

Equation (166) is valid up to a $\text{SHP}_{r/\delta}$ of 200. If it is necessary to calculate K₁ for a value of $\text{SHP}_{r/\delta}$ greater than 200, the value of K₁ for $\text{SHP}_{r/\delta} = 200$ is used. Equation (166) is valid up to altitudes of 10,000 feet. The off-design fuel flow rate also is related to the fuel flow rate at the design point. The fuel flow rate at the design point is calculated from Equation (161) or (162). The fuel flow rate at off-design is:

$$W_{fu} = W_{fu}^o \delta + K_2 \delta (T_{am} - T_{am}^o) \quad (167)$$

The quantity "K₂" is defined as:

$$K_2 = \frac{\Delta W_f/\delta}{\Delta T_{am}} \quad (168)$$

where:

$$K_2 = -0.561 - (0.001692)(\text{SHP}_{r/\delta}) + (9.375 \times 10^{-6}) (\text{SHP}_{r/\delta})^2 - (2.083 \times 10^{-8}) (\text{SHP}_{r/\delta})^3 \quad (169)$$

Equation (169) is valid up to a value of $\text{SHP}_{r/\delta}$ of 200. To calculate K₂ for a $\text{SHP}_{r/\delta}$ greater than 200 use the value of K₂ calculated with $\text{SHP}_{r/\delta}$ equal to 200. Equation (169) is valid up to altitudes of 10,000 feet.

The problem might arise where only the bleed air and shaft horsepower requirements at off-design conditions are known. These off-design requirements need to be related back to the design point in order to calculate the

design point bleed airflow, fuel flow rate, shaft horsepower requirement, bare rectangular volume, and installed weight. The shaft horsepower requirement at off-design equals the shaft horsepower requirement at the design point. With the bleed air requirement at off-design given (W_{bl}), the design point bleed airflow rate is calculated from Equation (164). With the design point bleed airflow rate and the shaft horsepower requirement, the equivalent horsepower at the design point is calculated from Equation (156). Equation (161) is used to calculate the design point installed fuel flow rate.

Weight - The installed weight of an APU that has simultaneous bleed air and shaft horsepower extraction is:

$$W_t = \frac{EHP}{(4.215 \times 10^{-4}) (EHP) + 0.159} \quad (170)$$

This equation also is accurate in predicting the installed weight of an APU that has bleed air extraction only. The standard error of Equation (170) is 7.2% (up to an EHP of approximately 850).

The installed weight of an APU that has shaft horsepower extraction only is:

$$W_t = \frac{EHP}{(6.29 \times 10^{-4}) (EHP) + 0.253} \quad (171)$$

Equation (171) has a standard error of 12.9% (up to an EHP of about 350). (See Figure 96.) In order to obtain bare APU weight from installed APU weight, a factor of 0.398 is used. This factor is obtained by comparing installed and basic APU weight data. Installed weight includes ducting, gearing, controls, and installation factors.

Volume - The bare rectangular volume (ft^3) of an APU that has simultaneous bleed air and shaft horsepower extraction is:

$$V = \frac{EHP}{(0.0232) (EHP) + 5.1} \quad (172)$$

This equation also predicts the basic volume of an APU that has bleed air extraction only. Equation (172) is correlated to an EHP of 850 in Figure 97. The basic rectangular volume of an APU that has only shaft horsepower extraction is:

$$V = \frac{EHP}{(0.01714) (EHP) + 11.8} \quad (173)$$

Sea Level, 103°F, M¹ = 0.0

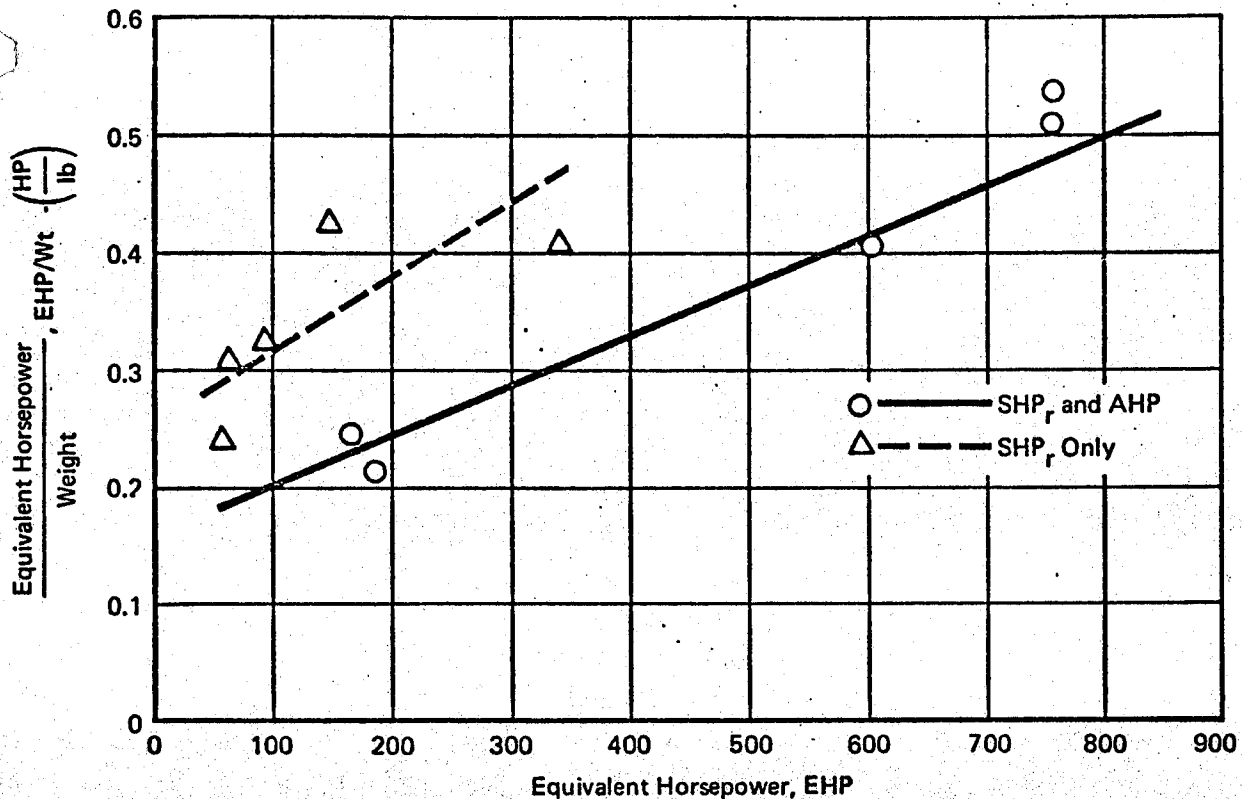


Figure 96 APU Installed Weight Correlation

GP 9416-40

Sea Level, 103°F, M¹ = 0.0

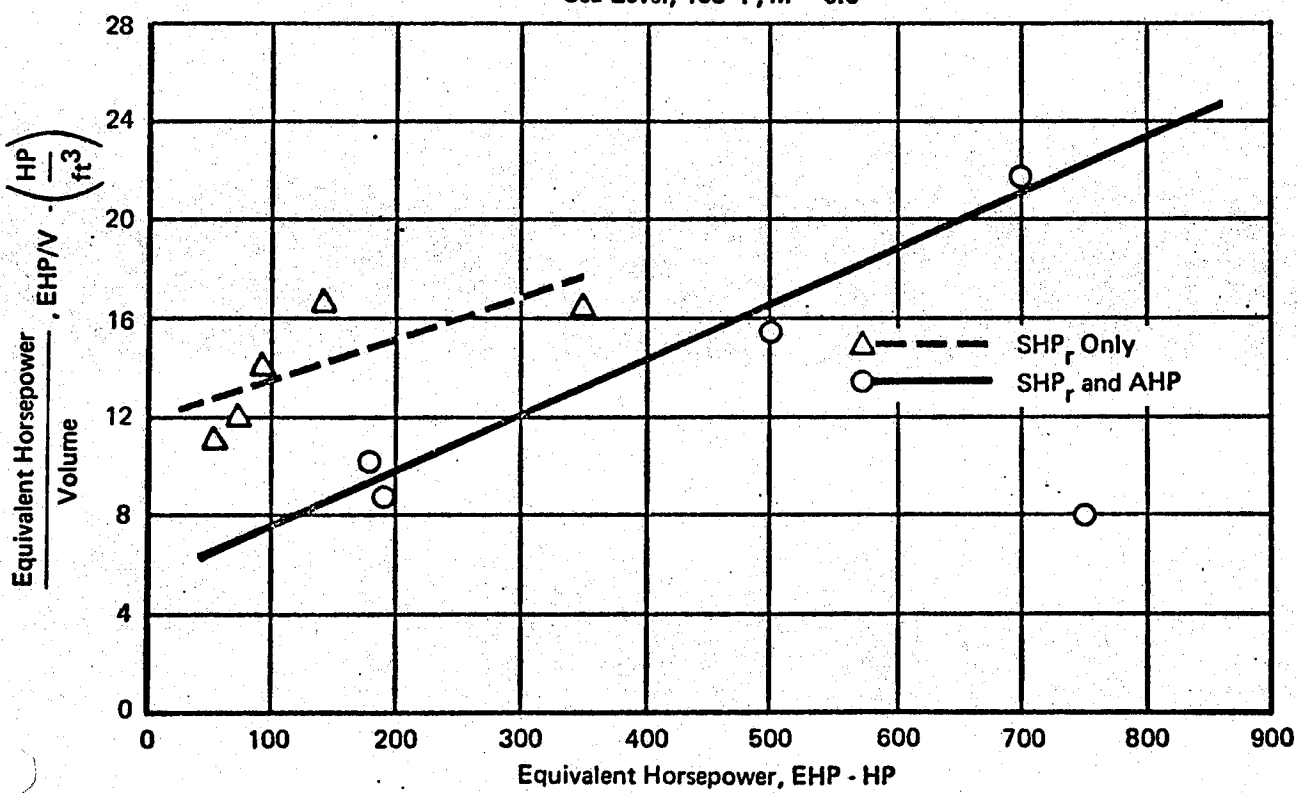


Figure 97 APU Volume Correlation

GP 9416-39

This equation is considered up to an EHP of 350, as is shown in Figure 97.

Example - The following example indicates how the previous information is used. Assume an APU having the following features at sea level hot day conditions is desired:

$$\text{Bleed Pressure } (P_{bl}) = 50 \text{ psig}$$

$$\text{Bleed Flow } (W_{bl}^o) = 50 \text{ lb/min}$$

$$\text{Shaft Horsepower (SHP)} = 80 \text{ HP}$$

The inlet pressure (P_{in}) is obtained from Equation (159).

$$P_{in} = 0.98 P_{am} = (0.98)(14.7) = 14.4 \text{ psia}$$

The installed bleed air pressure ratio is:

$$PR = \frac{50 + 14.7}{14.4} = 4.5$$

Bleed air temperature (Equation 160):

$$\frac{0.286}{0.770}$$

$$T_{bl} = 563 (4.5) = 984^\circ\text{R}$$

Effective inlet temperature (Equation 157):

$$T_e = \frac{984}{(4.5)^{0.286}} = 640^\circ\text{R}$$

Equivalent horsepower (Equation 156):

$$\text{EHP} = 80 + (0.243)(984-640) \left(\frac{50}{42.42} \right) = 178.5 \text{ HP}$$

Fuel flow rate (Equation 161):

$$W_{fu}^o = [(-0.001158)(178.5) + 1.50] (178.5) = 231 \text{ lb/hr}$$

Installed weight (Equation 170):

$$W_t = \frac{178.5}{(0.0004215)(178.5) + 0.159} = 762 \text{ lb}$$

3.8.2 Auxiliary Compressors - Auxiliary compressors provide air flow and pressure requirements to supplement the primary air supply system (i.e., engine bleed) as a boost compressor, or as an independent air supply. Selection of compression process having a reaction of 0.5 or greater is made. (Reaction is described in Section 3.2.) Both radial and axial wheel designs of suitable reaction are used. Radial designs are considered typical in this report. (See Figure 56 for the generalized N_s - D_s diagram.) Application of auxiliary compressors involves a drive and a coupling. The various drives

are evaluated in Section 3.9. Couplings or other disconnect methods are applied to shaft drives only.

Performance - Analysis of the compressor performance is made using the methods described in Section 3.2.3. Speed is selected according to the tip speed limit of 1500 ft/sec. However, the speed limitations of the various drives must be considered. For components which require gearing to satisfy the overall performance requirements, an additional 2% to 3% power loss is typical.

Size - The characteristic wheel diameter (D) is determined with the methods found in Section 3.2.3. Figure 56 is used as the generalized N_s - D_s diagram to describe auxiliary compressors. Map data in the format of Figure 69 is derived to provide off-design analyses capability for the sized component. Knowing the characteristic wheel diameter and the flow rate, the volume and weight are determined from Equations (103) and (104), respectively.

3.9 Power Drives

Electric, hydraulic, pneumatic, and shaft types of power drives are discussed. Direct and alternating current electric motors, high pressure piston type hydraulic motors, centrifugal pneumatic motors (turbines), and two types of shaft power drives are considered. Shaft power is obtained directly from an aircraft engine or an APU pad. Applications for these power drives are auxiliary compressors, vapor cycle compressors, liquid pumps, fans, etc., as indicated in Section 2. Further investigations and developments of aircraft power systems are discussed in Reference 41.

3.9.1 Electric Motors - Electric motors are the most common type of power drive for environmental control system components. Alternating current (a.c.) motors are more prevalent (i.e., 400 Hz, 115/200 volt), although some 27 volt d.c. motors have been used.

Performance - Electric motor performance variables to be considered are motor speed, power, and efficiency. The required motor speed is influenced by the component being driven. For 400 Hz a.c. motors, speed also must be related to the number of poles in the motor (i.e., two poles provide speeds near 24,000 rpm, four poles provide speeds near 12,000 rpm, etc.).

Efficiencies of about 50 a.c. and d.c. electric motors are shown in Figure 98. No trend is apparent to indicate different efficiencies between a.c. and d.c. motors. Alternating current motors generally are used when outputs above 0.2 HP are required (large d.c. motors weigh more for the same power output). A nominal curve relating efficiency and power output is presented in Reference 42. This curve fits the data rather well, and is approximated by the following equation:

$$\eta = 1 - \frac{0.281}{(HP)^{0.169}} \quad \text{for } 100 \text{ HP, } \eta = 87.1\% + 4\% \text{ for } 23 \text{ K RPM} \quad (174)$$

The data indicate that speed has a minor effect on efficiency, the trend being toward very slightly higher efficiencies at higher speeds. The motor speeds used in Figure 98 vary from 2500 rpm to 23,000 rpm. A majority of these motors have speeds between 5500 rpm and 11,500 rpm. A nominal approach is to assume that the efficiency from Equation (174) applies to 7500 rpm, that the efficiency is 2% greater or less than this value for 11,500 rpm and 5500 rpm (respectively), and 4% greater at 23,000 rpm.

Weight - The weight of an electric motor is primarily dependent on power output and rotational speed. Correlations to obtain weight are based on the

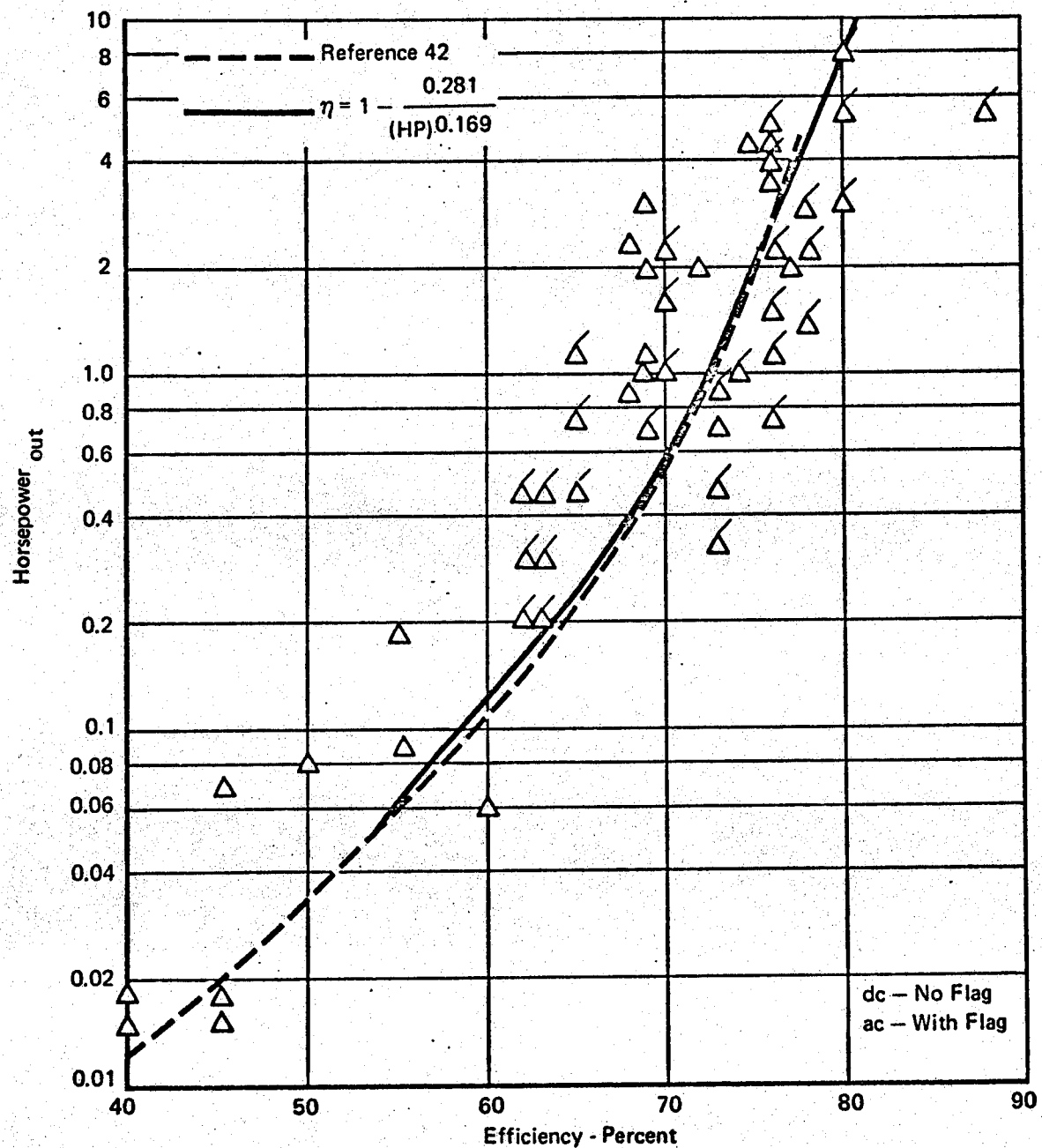


Figure 98 Efficiency of Electric Motors

GP 9416-208

assumption that power and speed are independent factors.

The lowest weight of an a.c. motor is approximately two pounds. Using weight data of a.c. motors, an equation relating the weight and power of a.c. motors having a speed of 10,000 rpm is obtained:

$$\begin{aligned} \text{Wt}_{\text{a.c.}} &= 2.0 + 2.3 (\text{HP})^{5/6} \\ &\quad 10,000 \text{ rpm} \end{aligned} \quad (175)$$

Using 10,000 rpm as the reference speed, a "speed factor" effect on a.c. motor weight is shown in Figure 99. The least mean squares equation for this a.c. motor speed factor (SF) is, very nearly:

$$\text{SF}_{\text{a.c.}} = (\text{N} \times 10^{-4})^{-1.25} = 1. @ N = 10,000 \quad (176)$$

Hence, the weight of an a.c. motor is approximated by:

$$\text{Wt}_{\text{a.c.}} = 2.0 + 2.3 (\text{HP})^{5/6} (\text{N} \times 10^{-4})^{-1.25} \quad W = 2 + 2.3 (45)^{5/6} (2.3)^{-1.25} = 21.4 \quad (177) (6) = .11$$

The standard error of this equation, for the 36 a.c. motors considered, is 11.1%.

A similar approach is used to obtain an equation for the weight of d.c. motors. The minimum weight is estimated at 1.5 pounds. For d.c. motors having a rotational speed of 10,000 rpm:

$$\begin{aligned} \text{Wt}_{\text{d.c.}} &= 1.5 + 2.3 (\text{HP})^{5/6} \\ &\quad 10,000 \text{ rpm} \end{aligned} \quad (178)$$

The speed factor data for d.c. motors are shown in Figure 100, including the speed factor equation obtained by a least mean squares analysis. Very nearly, the d.c. motor speed factor effect is:

$$\text{SF}_{\text{d.c.}} = \frac{5}{3} (\text{N} \times 10^{-4})^{-1.25} \quad (179)$$

Hence the estimated weight of a d.c. motor is:

$$\text{Wt}_{\text{d.c.}} = 1.5 + 3.83 (\text{HP})^{5/6} (\text{N} \times 10^{-4})^{-1.25} \quad (180)$$

The standard error of this equation, for the 21 d.c. motors considered, is 25.9%.

Volume - The volume of an electric motor is determined from the bulk density of the motor. Since the motors have little void volume, (i.e., the

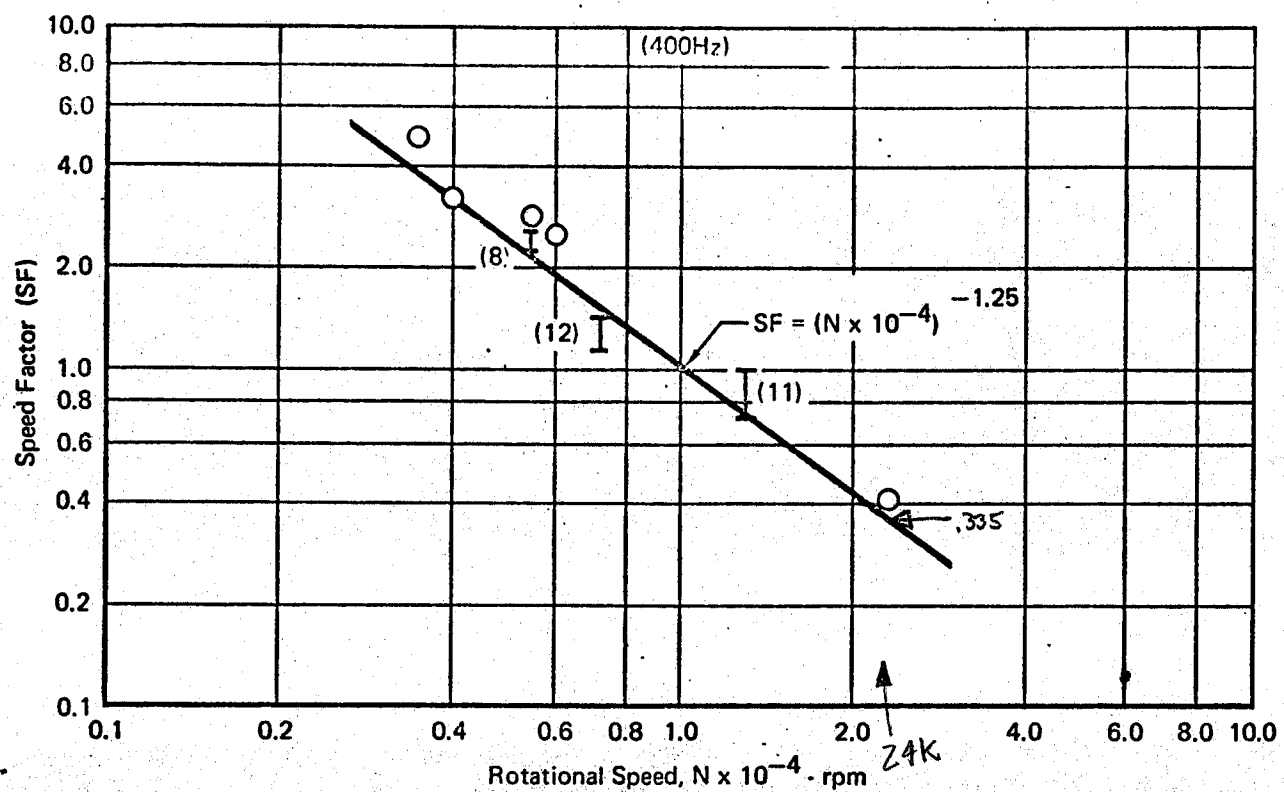


Figure 99 Speed Effects on Weight of a.c. Motors

GP 9416-212

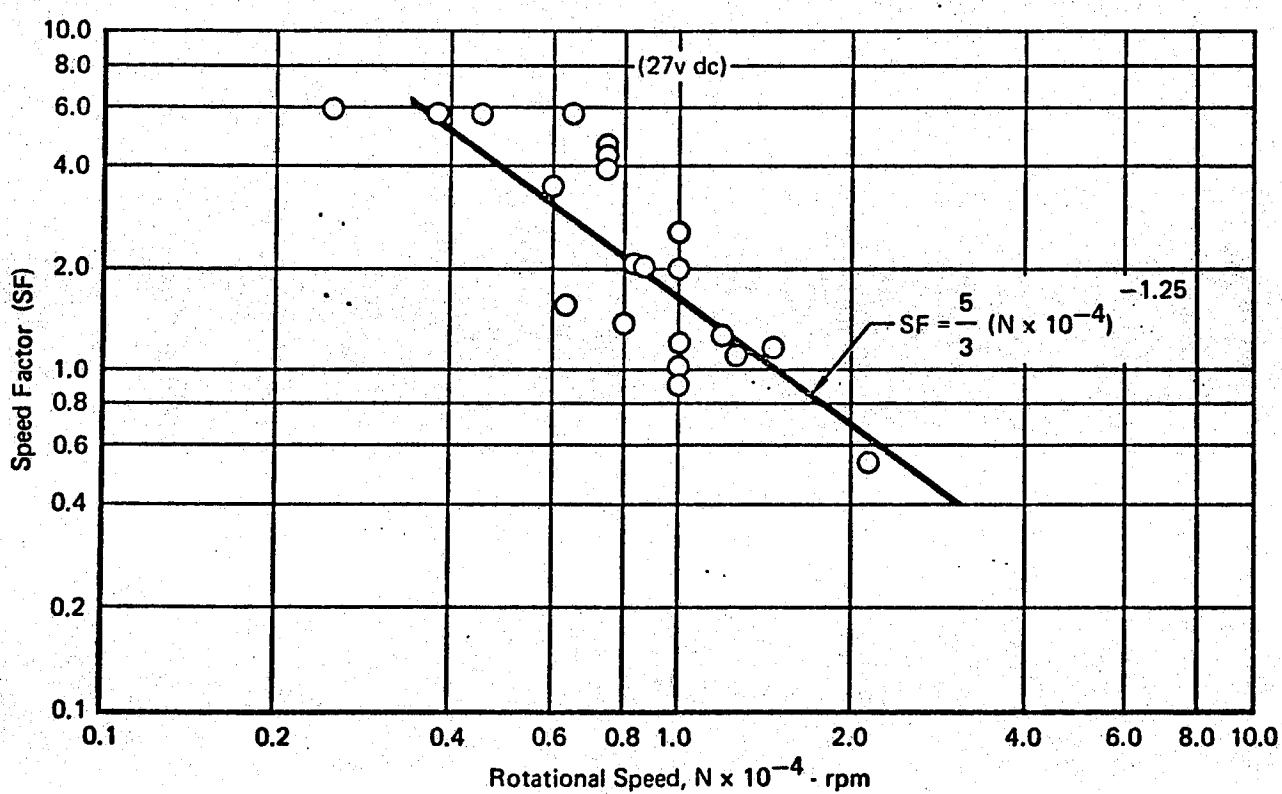


Figure 100 Speed Effects on Weight of d.c. Motors

GP 9416-213

motor consists of windings, rotor, and stator frame) the bulk density is approximately independent of speed and power. The average bulk density of the motors considered for the weight correlation is 0.10 lb/in^3 .

3.9.2 Hydraulic Motors - Hydraulic motor designs are essentially the same as hydraulic pump designs. These motors utilize the high pressure (2500 psi to 3000 psi) fluid available from a utility (or primary) hydraulic system.

Two types of motors are used. The bent-axis motor has pistons and cylinder block set at an angle to the drive shaft. The pistons translate sequentially (valve action) to rotate the drive shaft. An inline-motor has axial pistons. As the pistons translate an angled plate on the shaft is rotated.

Hydraulic motor vendors provide product lines of incrementally sized hydraulic motors for use with MIL-H-5606 hydraulic fluid: (See References 43 to 45.) These motors are used for many other applications in addition to ECS use. Overall performance and weight data are considered for all of these designs in the following sections. Motors from these basic product lines generally are modified to meet particular individual requirements. The following correlations are based on hydraulic motors used to drive fans, compressors, and pumps.

Performance - The fluid power input to a hydraulic motor is determined by the power requirement of the driven component and the motor efficiency. The average efficiency of 16 typical hydraulic motors used for ECS is 82%. These motors have speeds from 2400 rpm to 12,500 rpm, and power outputs from 1.2 HP to 16 HP. Basic hydraulic pumps (i.e., without modifications for specific uses) have slightly higher efficiencies.

The operating speed of hydraulic motors decreases as the motor size (displacement volume per revolution) increases. (See Reference 30.) This is shown in Figure 101. The upper and lower limits of this figure are representative of various types of designs from several vendors. Two hydraulic motor speed levels are indicated by the data in this figure. Motors operated at the higher speed (average is nearly 12,500 rpm) are considered to be typical of motors which drive the ECS component directly. Motors operated at the lower speeds drive higher speed ECS components through a gear train. Four of these motor designs are connected to gear trains.

Weight - The weights of hydraulic motors varies according to the application and the motor type. Inline motor designs are lighter than bent-axis designs for less than eight horsepower. (See Reference 41.) The range of hydraulic motor weights as a function of size (displacement volume per revolution - $\text{in}^3/\text{rev.}$) is indicated in Figure 102. The weights of 14 motors used for ECS type components also are indicated. Four of these motor weights include gearing. A least mean squares weight correlation for ten of these motors (without gears) is:

$$Wt = 11.37 \times (1728Q/N)^{1/2} \quad (181)$$

(The average weight of the four motors plus gears is approximately 50% greater.) The standard error of this correlation is 20%, for the 14 hydraulic motors considered.

3.9.3 Pneumatic Drives - Pneumatic power drives are used to drive auxiliary compressors, fans, pumps or other components as indicated in Section 2.2. The pneumatic drive is considered to be an axial or a radial turbine. The selection of the wheel design is based on the design value of specific speed, with high specific speeds ($N_s > 110$) indicating axial designs. Figures 59 and 61 are the appropriate generalized $N_s - D_s$ diagrams for radial and axial wheel designs, respectively.

Performance - The power to meet the load requirement is based on the performance procedures outlined in Section 3.2.2. The same limitations on tip speed are applied.

Size - Calculation of the characteristic wheel diameter also is based on the method described in Section 3.2.2. Off-design performance analysis capability, for the sized component, is provided by deriving the turbine performance map set in the format of Figure 66. The map derivation procedure is outlined in Section 3.2.2. Volume and weight are determined from Equations (103) and (104), respectively.

3.9.4 Shaft - Shaft power is supplied from a non-ECS component (i.e., engine) or an APU pad to drive an auxiliary compressor. APU shaft power is considered in Section 3.8.1. The nature of engine shaft power makes it difficult to access a direct performance weight other than in the form of aircraft penalties (i.e., fuel, range, payload, etc.). The speed of the shaft is assumed to be equal to the engine speed. Speed-multiplying gearing is accounted for in Section 3.8.2 on auxiliary compressors. Use of a shaft also involves a coupling or clutch. Comparison of the compressor weight to

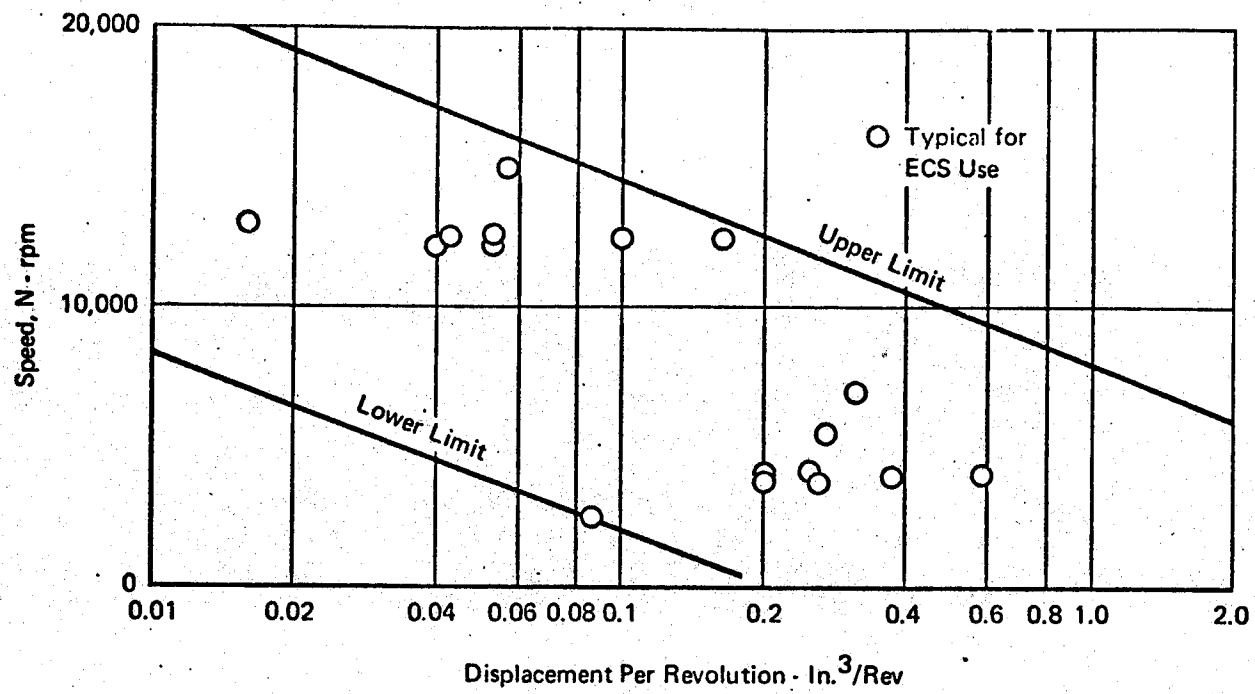


Figure 101 Hydraulic Motor Speeds

GP 9416-41

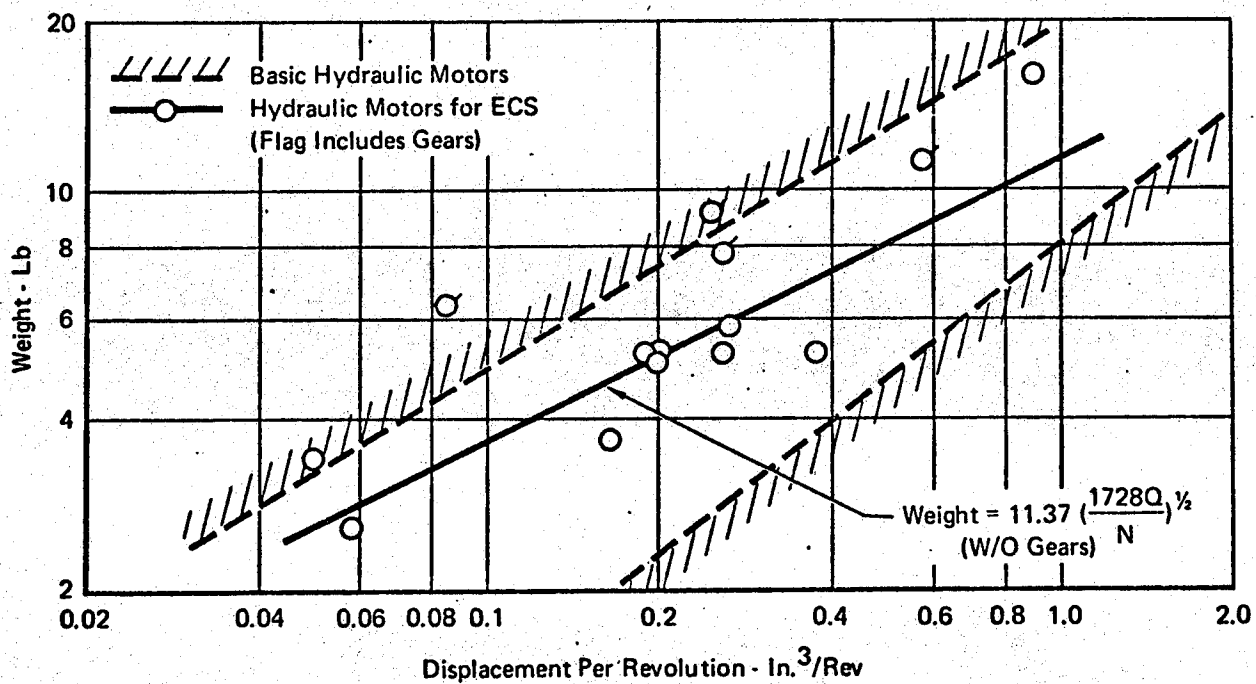


Figure 102 Hydraulic Motor Weight

GP 9416-5

the associated clutch weight, for two commercial aircraft auxiliary compressors, shows that clutch and gearing weight is nearly equal to the compressor weight. Therefore, the clutch weight is set equal to the calculated compressor weight.

3.9.5 Examples of Motor Design - The following examples illustrate use of the previous information to determine the weights of an electric and a hydraulic motor. The motors are to provide 0.75 HP at 11,800 rpm.

Electric Motor Efficiency (Equation 174):

$$n = 1 - \frac{0.281}{(0.75)^{0.169}} = 70.5\%$$

$$\text{Power input} = \frac{0.75}{0.705} = 1.064 \text{ HP or } 793 \text{ watts.}$$

Weight of 400 Hz a.c. motor (Equation 177):

$$Wt = 2.0 + 2.3(0.75)^{5/6} (1.18)^{-1.25} = 3.47 \text{ lb}$$

The hydraulic motor uses a normal 2800 psi hydraulic system pressure differential, and it has an efficiency of 82%.

$$\text{Power input} = \frac{0.75}{0.82} = 0.915 \text{ HP}$$

$$\text{Flow required: } W' = \frac{1714 \text{ HP}}{n(\Delta P)} = \frac{(1714)(0.75)}{(0.82)(2800)} = 0.56 \text{ gpm}$$

$$\text{Displacement/revolution} = \frac{(1728)(0.56)(0.1337)}{11800} = 0.011 \text{ in}^3/\text{rev}$$

$$\text{Weight (Equation 181): } Wt = (11.37)(0.011)^{1/2} = 1.19 \text{ lb.}$$

3.10 Plumbing

Components which are associated with ECS plumbing are discussed in this section. These components include ducting, lines, ram air inlets and outlets, ejectors, and valves. A bleed air ejector often is utilized to induce air flow through the ram air circuit during static operations. Other ejector applications, such as pumping water or steam, are included. Various types of valves are discussed. These valves are located at numerous points within an ECS. They regulate the fluid flow through the plumbing. Example designs for plumbing components are presented in Volumes II, III, and IV.

3.10.1 Air Ducting - Duct design requirements are found in Reference 3. The ducts must be designed with strength and flexibility to withstand the various loads imposed on them, including contraction and expansion due to relative temperature levels. Compensators are installed (particularly in high pressure ducts) to allow for dimensional changes. Straight circular ducts with no discontinuities are considered as ideal design goals to curtail noise.

Two levels of analysis detail are presented. The first requires the least amount of detail concerning the ducting geometry, and is based on typical aircraft ducting. If more geometry data are known (e.g. duct length, diameter, number and size of bends, etc.), a more detailed method is used. Duct volume basically is length times nominal cross section area. Weight determination is based on the typical data regardless of which method is used to determine performance. The total ducting weight is more accurate than the weights of individual sections of ducting which compromise a typical length of ducting.

3.10.1.1 Performance from Typical Data - Several sections of typical ducting are used as a basis to derive a technique for determining overall ducting pressure drops.

High Pressure Ducting - Typical geometry of a section of high pressure ducting is defined in Figure 103 and Table VII. Individual pieces of the duct sections are identified by item number. The pressure drop for each of the two duct sections of Figure 103 is described by:

$$\Delta P = K W^2 \quad (182)$$

where K is a pressure loss factor. A pressure loss factor per unit length is determined from the known pressure loss factors and lengths for each

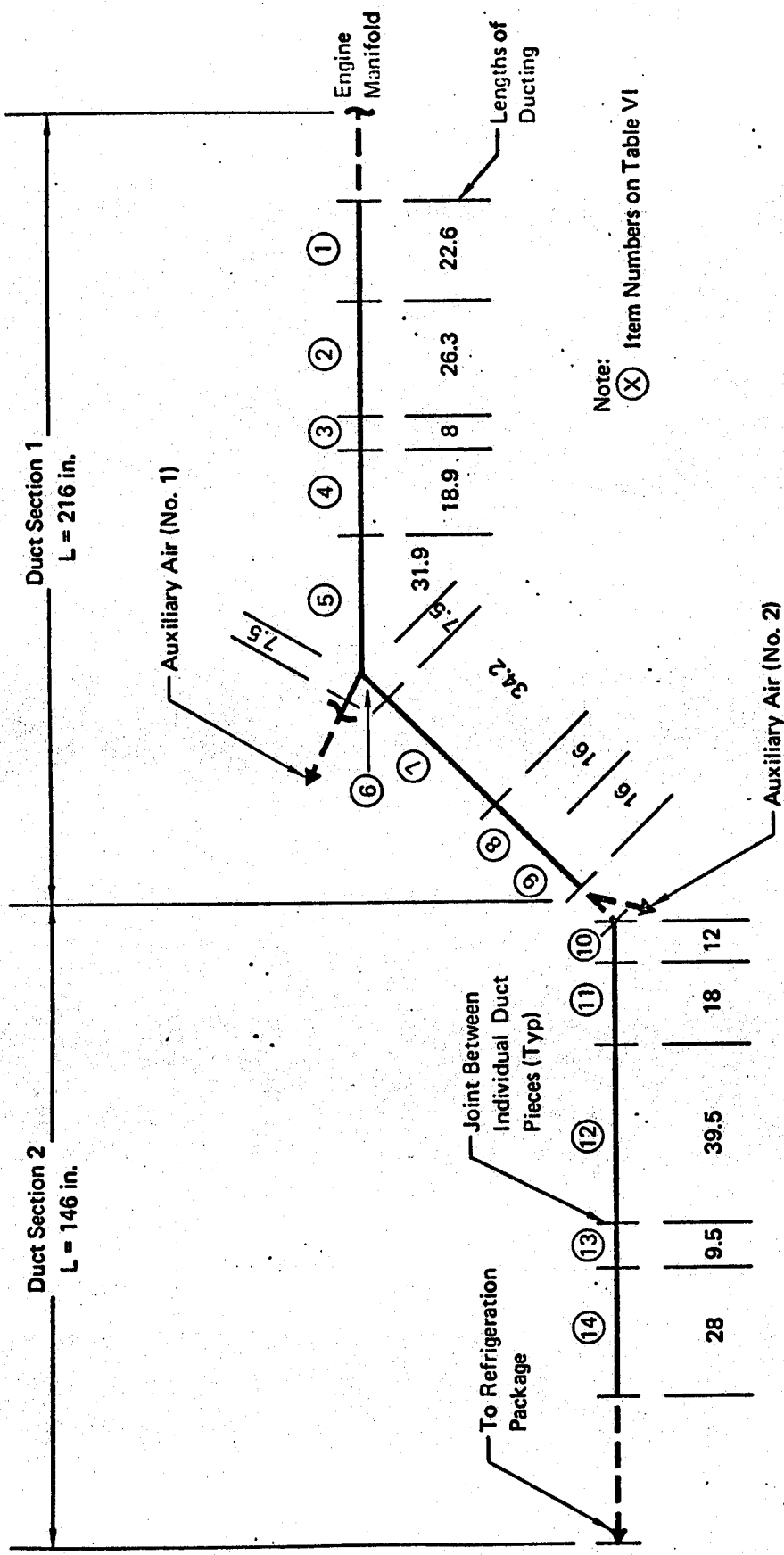


Figure 103 Schematic of Typical High Pressure Bleed Air Ducting

GP 9416-107

Table VII Typical High Pressure Bleed Air Ducting

Item No.	Diam D~In.	Weight Wt-Lb	Length L~In.	Wall Thickness t~In.	Average Wt/(Lt) Lb/in. ²	Component Description
1	4.5	21.37	22.6	0.032		90° elbow with two gimbal (universal) joints
2	4.5	5.17	26.3	0.032		Straight with attached mounting bracket
3	4.5	8.27	8.0	0.032		Gimbal joint
4	4.5	4.22	18.9	0.032		Straight with attached mounting bracket
5	4.5	5.12	31.0	0.032		Straight (Portion of No. 5 and No. 6)
		44.15	106.8		12.92	
6	4.0	5.00	15.0	0.032		Wye (Portion of No. 5 and No. 6)
7	4.0	13.05	34.2	0.032		Double 90° elbow section with two pin joints
8	4.0	2.57	16.0	0.032		Straight (Portion of No. 8 and No. 9)
		20.62	65.2		9.88	
9	3.5	2.3	16.0	0.032		Portion of No. 8 and No. 9 with two bends and attached mounting brackets
10	2.5	3.52	12.0	0.025		Pin joint, mounting bracket and axial adjustment compensator
11	2.5	1.62	18.0	0.016		Straight with bend and mounting bracket
12	2.5	1.53	39.5	0.016		Straight with mounting bracket
13	2.5	7.81**	9.5	0.016		Straight with axial, thermal compensator and axial adjustment compensator
14	2.0		28.0	0.016		Straight with axial, thermal compensator and axial adjustment compensator
		16.78	113.0	0.0202*	7.35	

* This is an average thickness weighted in accordance with surface area and corresponding thickness of each individual part, items 9 through 14.

** Total for Items 13 and 14

GP 9416-52

section. The various duct diameters of each section are converted to an effective diameter as follows. The pressure drop equation may be expressed as:

$$\Delta P = K_t \frac{\rho V^2}{2g_c} \quad (183)$$

where $K_t = 4f L/D$. By using the continuity equation and representing the area in terms of duct diameter, it is found that:

$$K_t \text{ is proportional to } \frac{1}{D^5} \text{ (assuming } f \text{ is a weak function of } Re) \quad (184)$$

Bends (or sudden changes in diameter) are accounted for by adding a K_t for these bends or diameter changes. When bends and other discontinuities are most significant in calculating pressure losses throughout the duct system (as experience shows to be the case) the representative K factor in Equation (182) is more nearly approximated by:

$$K_t \text{ is proportional to } \frac{1}{D^4} \text{ (assuming the bend } K_t \text{ is a weak function of } Re) \quad (185)$$

To calculate the effective diameter (D_e) of each of the two duct sections in Figure 103, the pieces with different diameters are weighted in accordance with their corresponding lengths as follows:

$$\frac{1}{D_e^4} = \left[\frac{L_1}{D_1^4} + \frac{L_2}{D_2^4} + \dots \frac{L_n}{D_n^4} \right] (\sum L_i)^{-1}$$

or:

$$D_e = \left[\frac{\sum L_i}{\frac{L_1}{D_1^4} + \frac{L_2}{D_2^4} + \dots + \frac{L_n}{D_n^4}} \right]^{1/4} \quad (186)$$

Pressure loss factors per unit length (K/L) are tabulated in Table VIII and plotted versus effective diameter in Figure 104. Pressure loss factors of other ducts yet to be discussed also are shown in the table and in the figure.

Table VIII Summary of Ducting Performance Data

Duct Section No. (Fig.)	Type of Ducting	Duct Length, L - in.	K/L	Effective Diameter, D_e - in.
			$\frac{\text{lb Min}^2}{\text{in.}^3 \text{lb}^2}$	
1 (Fig. 103)	High Pressure Bleed	216	7.46×10^{-8}	4.15
2 (Fig. 103)	High Pressure Bleed	146	6.72×10^{-6}	2.22
-	High Pressure Bleed	21.75	6.92×10^{-6}	3.64
-	Refrigeration Package Discharge	-	2.94×10^{-6}	3.0
-	Refrigeration Package Inlet	36.5	1.24×10^{-5}	2.0
-	Refrigeration Package, Pressure Regulator to Heat Exchanger	43.2	2.04×10^{-5}	2.0
-	Refrigeration Package, Compressor to Sec. Heat Exchanger	32	7.51×10^{-5}	1.5
-	Refrigeration Package, Heat Exchanger to Turbine	37	6.33×10^{-5}	1.75
1 (Fig. 105)	Distribution to Heat Load No. 1 Tee	86.1	6.19×10^{-5}	1.75
2 (Fig. 105)	Heat Load No. 1 Tee to Heat Load No. 2 Tee	11.8	6.53×10^{-5}	1.75
3 (Fig. 105)	Heat Load No. 2 Tee to Heat Load No. 3	58.7	1.03×10^{-4}	1.75
-	Ram Air	86	4.85×10^{-9}	10.3
-	Ram Air Diffuser	26.5	3.71×10^{-7}	3.59

GP 9416-49

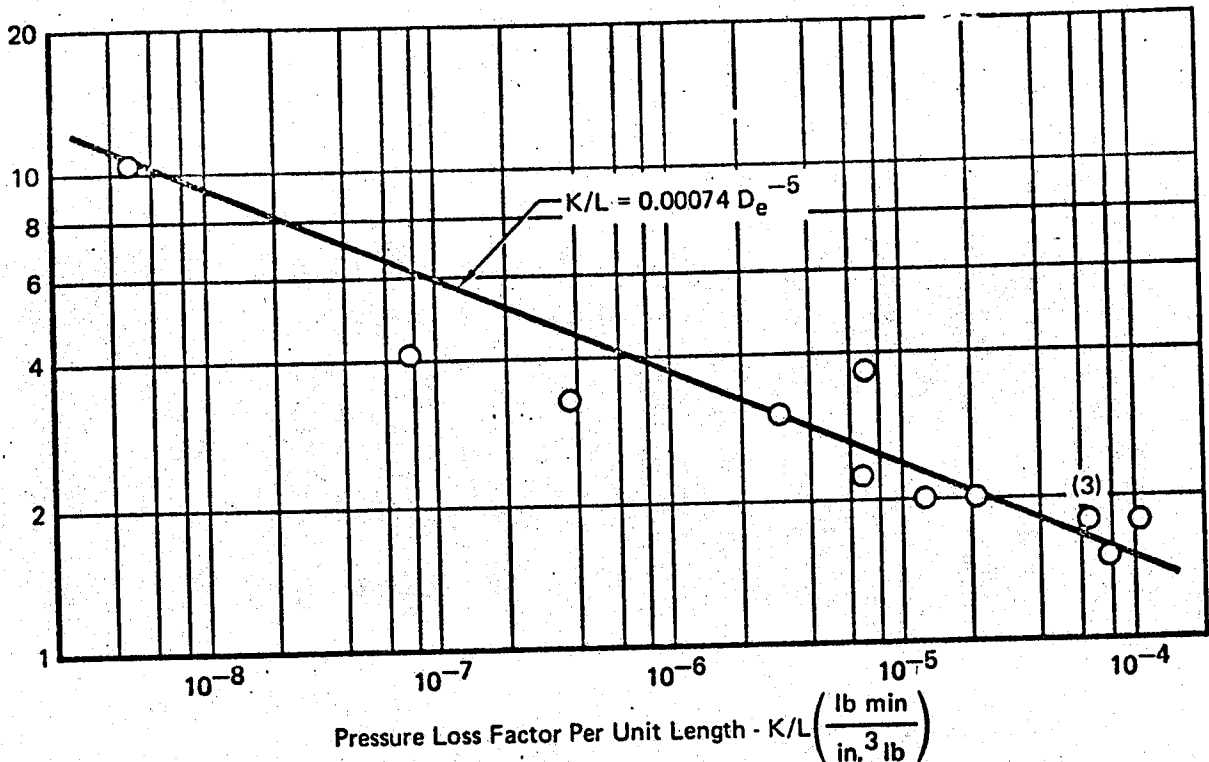


Figure 104 Typical Ducting Performance

GP 9416-108

Refrigeration Package Ducting - The refrigeration package contains the components necessary to reduce the temperature and pressure of the high temperature, high pressure air supply to the temperature, pressure, and moisture content required by the heat loads. Various pieces of ducting are used to connect all of the components, and to connect the package to the high pressure air supply and to the distribution ducting. Most of these ducts are relatively short (compared to high pressure air supply and low pressure distribution ducting), and usually do not contain special bellows type thermal compensators (found in the high pressure air supply ducting) or flexible low pressure ducting. Due to the compact packaging of the components, the ducts commonly have complex shapes (e.g. numerous bends and changes in cross-sectional shape and area).

Various sections of interconnecting ducting are included in Table VIII. Techniques similar to those described in the previous section are used to obtain pressure loss factors (K/L) and effective diameters (D_e). Results are plotted in Figure 104.

Conditioned Air Distribution Ducting - A typical section of distribution ducting from the refrigeration package to air cooled heat loads is considered for this analysis. Table IX lists each individual part by item number, uninstalled lengths and component description. (Weight data are discussed in subsequent sections.) Figure 105 is a schematic representation of the ducting. The installed lengths of the individual pieces of ducting and the particular sections utilized to calculate pressure loss factors (K/L) and effective diameters (D_e) are indicated. The previously described procedure is used to obtain these data.

Ram Air Circuit Ducting - A typical ram air duct has a 160° U-shaped bend with a minimum radius of curvature equal to one duct diameter. The bend is followed by a diffuser section and then a straight section. It has a total length of 86 inches. The cross section varies from a circular shape to an elliptical shape at the other end. The pressure loss factor is based on test data. A second ram air ducting section (approximately 26.5 inches long) is primarily a diffuser with a slight bend. The pressure drop of this section is known in the form of Equation (182). The effective diameter for each of these ram air ducts is found by the method used in the previous section. The data are tabulated in Table VIII and plotted in Figure 104.

Typical Pressure Drop Data - There is considerable scatter in the pressure loss data depicted in Figure 104. Attempts to correlate the data as a function of use (e.g. high pressure ducting, refrigeration or low pressure ducting) do not indicate well defined trends. The best curve fit to all of the data seems to be:

$$\frac{K}{L} = 0.00074 D_e^{-5}. \quad (187)$$

A pressure loss factor (K/L) which is inversely proportional to diameter to the fifth power is not expected since losses due to bends and other discontinuities usually are most significant. The pressure loss coefficient (K_t) for discontinuities is assumed to be a weak function of Reynolds number. However, considering the data as a whole, the correlation in Figure 104 indicates that K_t is inversely proportional to Re and to D_e which results in K being proportional to D_e^{-5} . Reference 30 indicates that the K_t of a 90°

Table IX Typical Low Pressure Ducting

Item No.	Material*	Total Length (in.)	Wall Thickness (in.)	Weight (lb)	Component Description
1	FG	10.5	0.040	0.80**	Wye fiberglass section.
	FX	16.75	—		Two rubber flex tubes.
2	AL	18.05	0.035	0.33	Aluminum tubing, 1.75 OD with several small bends.
3	AL	31.70	0.035	0.57	Same as above.
4	FG	47.30	0.040	1.45	Fiberglass tee section to Heat Load No. 1, odd shape.
5	AL	18.18	0.035	0.30	Aluminum tubing, S-shaped.
	AL	5.6	0.035	0.08	Aluminum tubing to Heat Load No. 3.
6	FX	7.9	—	0.22	90° rubber flex tube, 1.75 ID.
7	AL	19.74	0.035	0.41	Aluminum tube with welded on mounting plate, nearly straight, 1.75 OD.
8	FX	8.50	—	0.24	Rubber flex tube, 1.75 ID.
9	AL	11.9	0.035	0.49	Aluminum tubing parts (1.75 OD), some flattened and welded together, odd shape.
10	FX	6.9	—	0.18	90° bend rubber flex tube, 1.75 ID.
	AL	5.0	0.035	0.10	Aluminum tubing 1.75 OD.

*FG — Fiberglass Duct

**Total for all portions.

AL — Aluminum Duct

FX — Rubber Flexible Duct

GP 9416-51

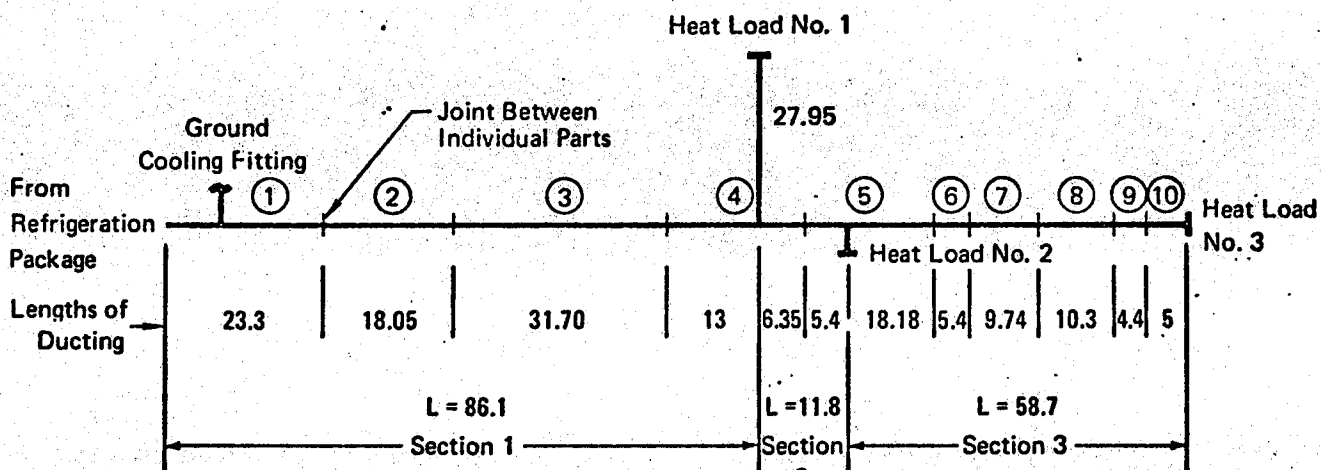


Figure 105 Schematic of Typical Conditioned Air Distribution Ducting

GP 9416-109

bend (with an optimum radius of curvature to duct diameter ratio of 3) is inversely proportional to effective diameter at Reynolds numbers of approximately 1.5×10^5 . Thus, the correlation in Figure 104 is in agreement with this accepted reference.

Pressure Drop Calculation Procedure - The flow rate and upstream pressure and temperature are known. If the duct length and diameter are available, the pressure loss factor is obtained from the typical duct performance data in Equation (187). This value of K is substituted into Equation (182) to obtain the duct pressure drop.

The pressure drop may be estimated as a function of inlet pressure and Mach number if only the duct lengths is known. A less accurate correlation of the typical duct performance data in Figure 104, represented by the following equation, is used.

$$\frac{K}{L} = 0.00014 D_e^{-4} \quad (188)$$

Using the continuity equation, the duct diameter is:

$$D = (3.056 W/\rho M \sqrt{\gamma R g_c T})^{1/2} \quad (189)$$

Substituting D into Equation (188), and solving for K/L yields:

$$K/L = 0.00216 \gamma g_c \rho P M^2 / W^2 \quad (190)$$

Substituting the above equation into Equation (182), the pressure drop is:

$$\Delta P = L (0.00216 \rho_{std} \gamma g_c) P M^2 \quad (191)$$

A typical duct Mach number is 0.15 for most ECS ducting (e.g. except cargo distribution ducting). To maintain an acceptable limit on noise level, a better Mach number for cargo distribution ducting is 0.05.

Heat transfer through the duct walls is not considered in the above pressure drop evaluations.

3.10.1.2 Detailed Performance - More accurate calculation methods are used when more detail concerning the ducting geometry (i.e. length, diameter, cross-sectional shape, bends, diffusers, etc.) are available.

$$\sigma \Delta P = 0.02 \left(4f \frac{L}{D} + K_1 K_{t90} \right) \frac{w^2}{\rho_{std} g_c A^2} \quad (192)$$

The first term in the parenthesis accounts for frictional losses and the latter for turning losses. K_{t90} is a pressure loss coefficient for 90° bends, and K_1 is a correction factor for bends other than 90°. Pressure loss data from Reference 30 are utilized for ducting with circular, elliptical, and rectangular cross sections. The friction factor and K_{t90} are determined as a function of Reynolds number. Figures 1A-10 through 1A-23 of Reference 30, with the exceptions of Figures 1A-15 and 1A-21, illustrate the detail that is involved in analyzing the above type of bends. Figures 1A-15 and 1A-21 are for mitered bends which are not commonly used. Pressure loss data for expansions, contractions, and diffusers also are found in the same reference. The requirements for duct insulation and heat transfer through insulated and bare duct walls are discussed in Section 3.11.

Equivalent friction factors for typical ducting may be obtained by combining Equations (182), (192), and (187) or (188). If Equation (187) is used, the equivalent friction factor is 0.01404, and if Equation (188) is used, the equivalent friction factor is 0.00265D.

3.10.1.3 Weight Analysis - Duct weight analyses are divided into two parts: for high pressure bleed air ducting, and for low pressure and ram air ducting.

High Pressure Air Ducting - Duct weight data are obtained from a typical aircraft. The various duct parts are made primarily of 19-9DL steel. (See Table VII.) The nominal operating pressure and temperature are: 340 psig and 980°F, respectively. These ducts are designed for proof and burst pressure of approximately 2 and 3.3 times the nominal operating pressure, and for various typical axial and bending loads. The above multiplying factors for proof and burst pressure are standard practice for current aircraft. For new aircraft designs the multiplying factors are 2 and 4 for proof and burst pressures, respectively. (See Reference 46.) However, these newer ducts probably weigh the same, considering improvements in materials and thermal compensators.

Various tolerance compensators are required to allow for relative dimensional changes between the aircraft structure (mounting hard points) and the ducting (due to thermal expansion and fabrication tolerances). The Component Description column of Table VII indicates which pieces of ducting contain tolerance compensators. *MP/81*

The Wall Thickness column in Table VII gives the nominal thicknesses of the plain straight sections of the ducts (i.e. no bends or discontinuities). This is a good indicator of the effective thickness (t_e) which accounts for the thicker sections at discontinuities and duct components (e.g. thermal compensators). The effective thickness is calculated as follows:

$$t_e = \frac{Wt}{DL\rho} \quad (193)$$

where: ρ is density of steel. The ratio t_e/t remains nearly constant. (The third group in Table VII includes ducts with different diameters and some with different nominal thicknesses. An average diameter of 2.5 inches and an average thickness of 0.202 inches, determined as a weighted average of duct wall area, are used.) The maximum variation of t_e/t is 15%. This occurs between the average values for ducts in the 4.5 inch and 2.5 inch groups. A weight parameter, for each of the three groups, is calculated as follows:

$$\frac{Wt}{(Lt)} = \frac{\Sigma Wt}{(\Sigma L)t} \quad (194)$$

This parameter is listed in Table VII and plotted versus diameter in Figure 106.

The above weight parameter provides an option of specifying the wall thickness as well as the duct length. As an aid in determining a wall thickness, Figure 107 shows a minimum wall thickness for handling and installation of high pressure ducting (Reference 46) and the wall thicknesses of the typical ducting. If the operating pressure and temperature are less than that of the typical ducting (340 psia, 980°F) then some value between the typical curve and the minimum thickness curve may be selected. A greater thickness may be selected for higher temperatures and pressures.

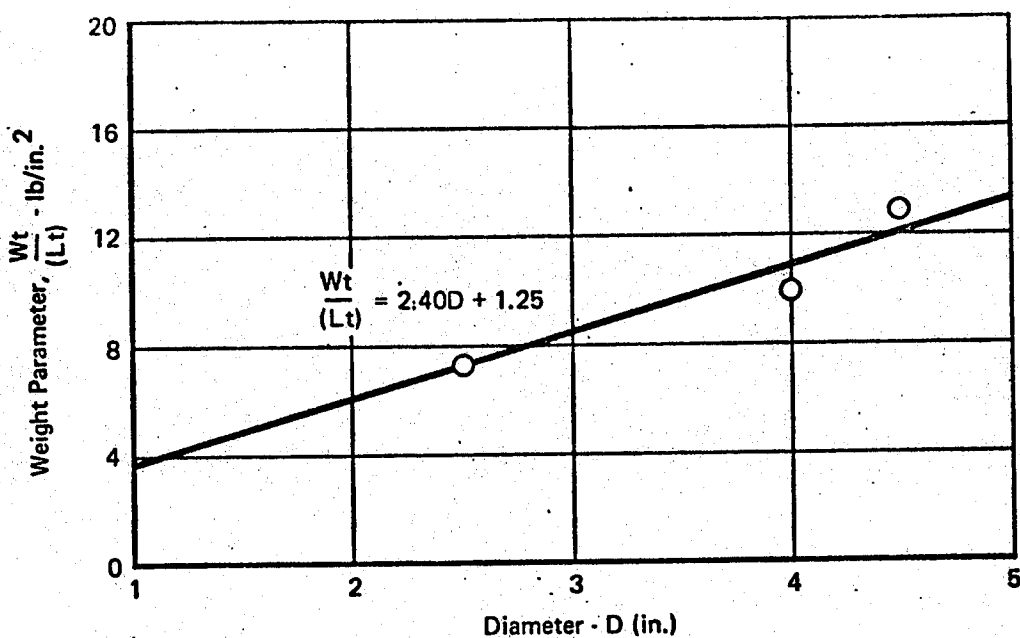


Figure 106 Typical High Pressure Bleed Air Ducting Weight

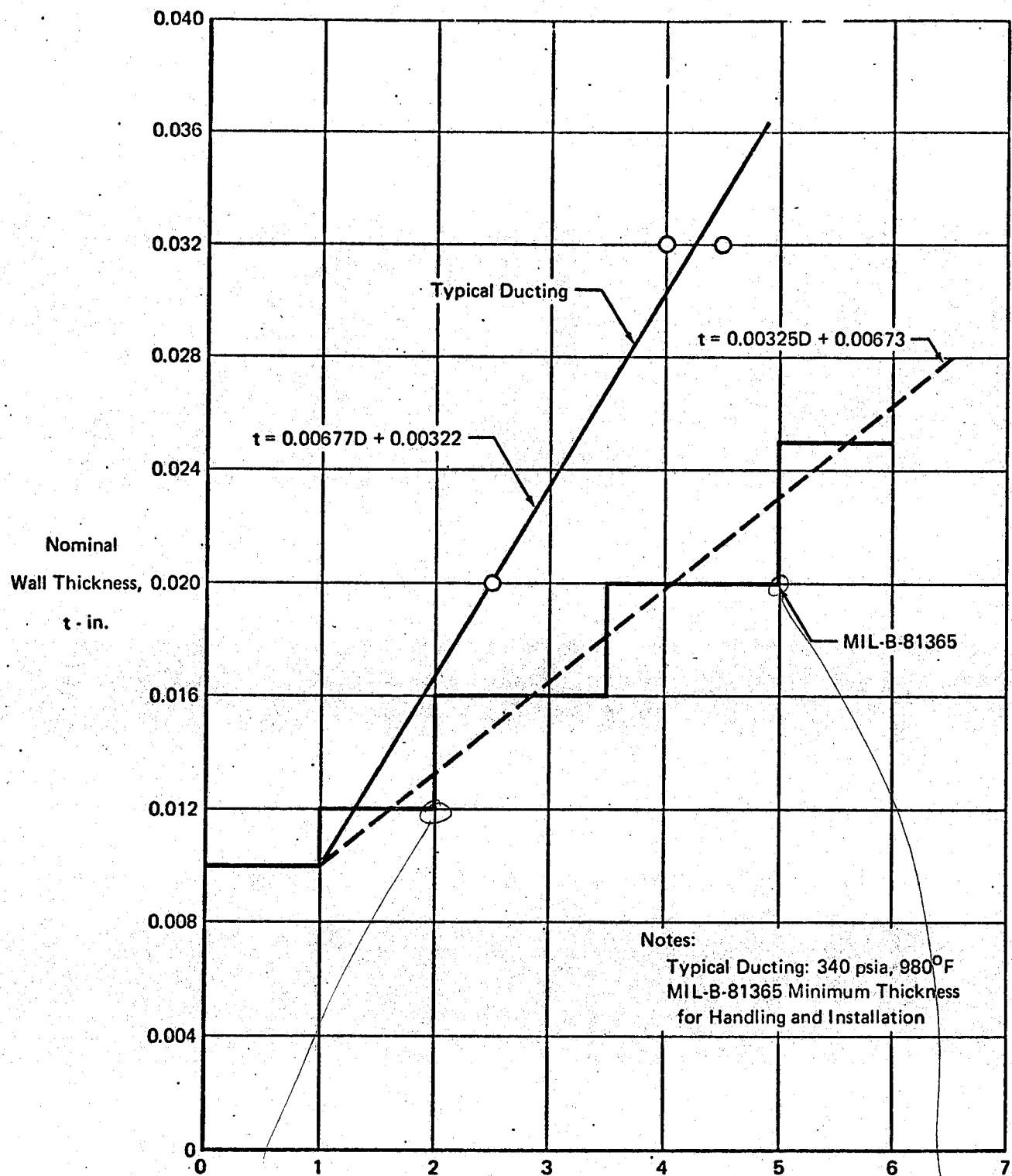
GP 9416-110

The equation for ducting weight, based on data in Figure 106, is:

$$Wt = Lt (2.40D + 1.25) \quad (195)$$

The accuracy of this equation relative to the three duct sections of Table VII is $\pm 6.7\%$. However, because only three data points were used to obtain Equation (195), its error is estimated as 15%. If the bleed air duct is made of tubing, (this is likely to be the case for diameters of 1.0 inch and less) the weight equation for low pressure aluminum ducting (which is discussed later), is used in lieu of the above equation. The low pressure aluminum ducting weight equation is corrected with a density ratio for materials other than aluminum.

Refrigeration Package Ducting - The weight of ducting between the components within a refrigeration package is less than the weight of the high pressure ducting. The average $Wt/(Lt)$ for these ducts is approximately 70% of that for the high pressure ducts. This is based on an average duct diameter of 2.35 inches. It is assumed the trend is the same for other duct diameters.



$$\Delta P_2'' = PR_f = 340 \frac{1.0}{.010} = 34,000 \text{ psi}$$

$$\Delta P_5'' = PR_f = 340 \frac{2.5}{.020} \Rightarrow$$

$\Delta P = 42,500 \text{ psi}$
 Design max
 @ 980°F, steel

Figure 107 Nominal Wall Thickness of Typical High Pressure Bleed Air Ducting

GP 9416-111

Low Pressure Ducting - A section of distribution ducting is selected as typical low pressure ducting. This ducting is made up of a variety of materials - reinforced rubber flexible ducting, aluminum tubular and weldment assemblies, and fiberglass layup ducts. Table IX lists the individual pieces of ducting.

The flexible ducts are used to absorb any relative dimensional changes between the ducting and airframe due to temperature changes. Aluminum tubular ducting nominally is used where the envelope requirements do not require excessive bending, cutting, or welding. Where the envelope requires more complex geometry, fiberglass ducting is utilized.

The working pressure in the ducting is low (i.e. about 5 psig). Thus, the wall thickness of the ducting is not a function of pressure. The maximum temperature limit is 300°F. The ducting is designed to withstand this temperature and loads due to vibration, handling, installation, etc. The typical distribution ducting has a nearly constant diameter of 1.75 inches for its entire length. The individual ducts in Table IX are scaled up to larger diameters to obtain typical ducting weight correlations.

The aluminum tubing weight is based on a constant wall thickness of 0.035 inch for duct diameters up to 5 inches, and a wall thickness of 0.042 inch for a duct having a diameter of 5 inches or greater (which is standard MCAIR design practice). A multiplying factor is applied to obtain the weight of a finished duct part. Use of this factor assumes that integral mounting brackets, coupling flanges, etc. increase at the same rate as the product of diameter and wall thickness.

The weights of all of the aluminum ducts are summed and divided by the product of the summed lengths times the wall thickness. This is done for each of the three diameters (see Table X) and is plotted versus diameter. (See Figure 108.) The typical weight of aluminum ducting is:

$$\frac{Wt}{(Lt)} = 0.34D \quad \dots \quad (196)$$

For materials with different densities, the weight is corrected by using a density ratio. The above equation is based on a density of 0.098 lb/in³.

A similar procedure is used to determine a typical weight parameter versus equivalent diameter for the two fiberglass ducts listed in Table IX.

Table X Typical Weight of Low Pressure Ducting

Duct Type	Diameter (in.)	ΣWt (lb)	ΣL (in.)	$\Sigma Wt/\Sigma L$ (lb/in.)	t (in.)	$\Sigma Wt/\Sigma L t$ (lb/in. ²)
Aluminum	1.75	2.18	105.2	0.0207	0.035	0.592
	3.50	4.40	105.2	0.0418	0.035	1.193
	5.00	7.55	105.2	0.0717	0.042	1.71
Fiberglass	1.75	1.612	57.8	0.028	0.04	0.70
	3.50	3.22	57.8	0.056	0.04	1.39
	5.00	4.61	57.8	0.080	0.04	2.00
Flexible Rubber	1.75	1.048	40.1	0.0261	—	—
	3.50	2.095	40.1	0.0522	—	—
	5.00	2.99	40.1	0.0745	—	—

GP 9416-50

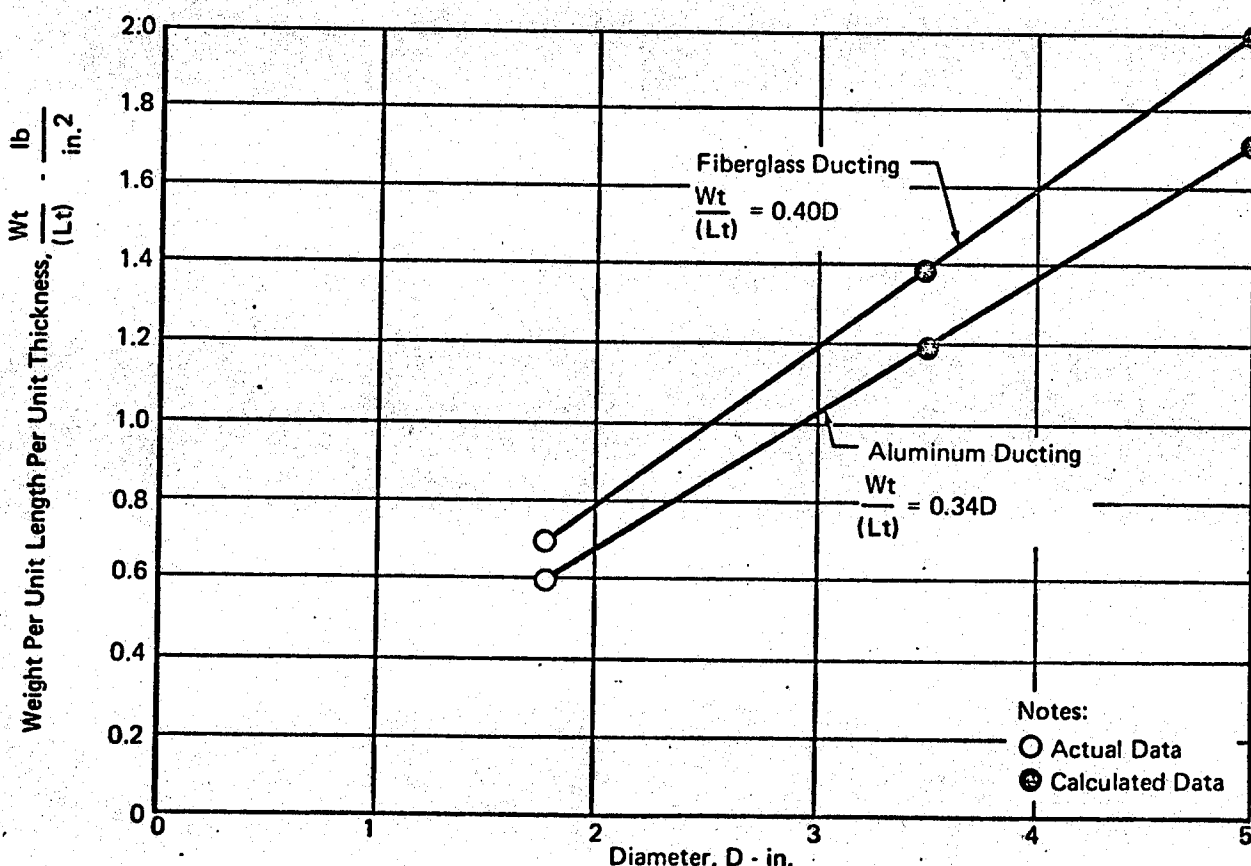


Figure 108 Typical Weight of Low Pressure Ducting

GP 9416-112

Equivalent diameters to indicate the cross-sectional dimensions of a non-circular duct increase at the same rate as the diameter of a circular duct. The thickness used in the weight parameter is the nominal thickness found in the straight sections. This thickness is used since the actual part weight is used in scaling up the weights of larger duct sizes. Thus the weight of thicker sections, where larger stress concentrations occur, are accounted for in the total weight. The wall thickness remains the same for the increased duct diameters. After increasing the weight of each fiberglass duct directly as a function of effective diameter (constant wall thickness), typical weight parameters are calculated in the same manner as for the aluminum ducting. (See Table X and Figure 108.) The weight parameter is:

$$Wt/(Lt) = 0.40D \quad (197)$$

The weight of flexible ducting is based on a weight factor (w_{FX}) of 0.0149 lb/in. ID/inch length. This correlates with actual weights of the flexible ducts with a maximum error of 6.5%.

The typical distribution ducting is a combination of aluminum, fiber-glass, and flexible ducting. A weight per unit length for each type of ducting is determined, then the summation is weighted for the total length. This correlation is shown in Figure 109. It is represented by the following equations:

$$Wt = (0.0137)DL, D < 3.5; \quad (198)$$

and:

$$Wt = (0.0179D - 0.0147)L, D > 3.5. \quad (199)$$

The accuracy of this correlation is estimated as 15%.

Other Ducting Weight Considerations - The methods to predict weight of high pressure bleed air ducting are generally applicable to all current types of aircraft. The use of steel is common in most current aircraft due to the high temperature of the high pressure air supply to the refrigeration package. In some cases where the temperature is not too high (e.g. approximately 800°F), titanium ducting is being used. This results in some reduction in weight.

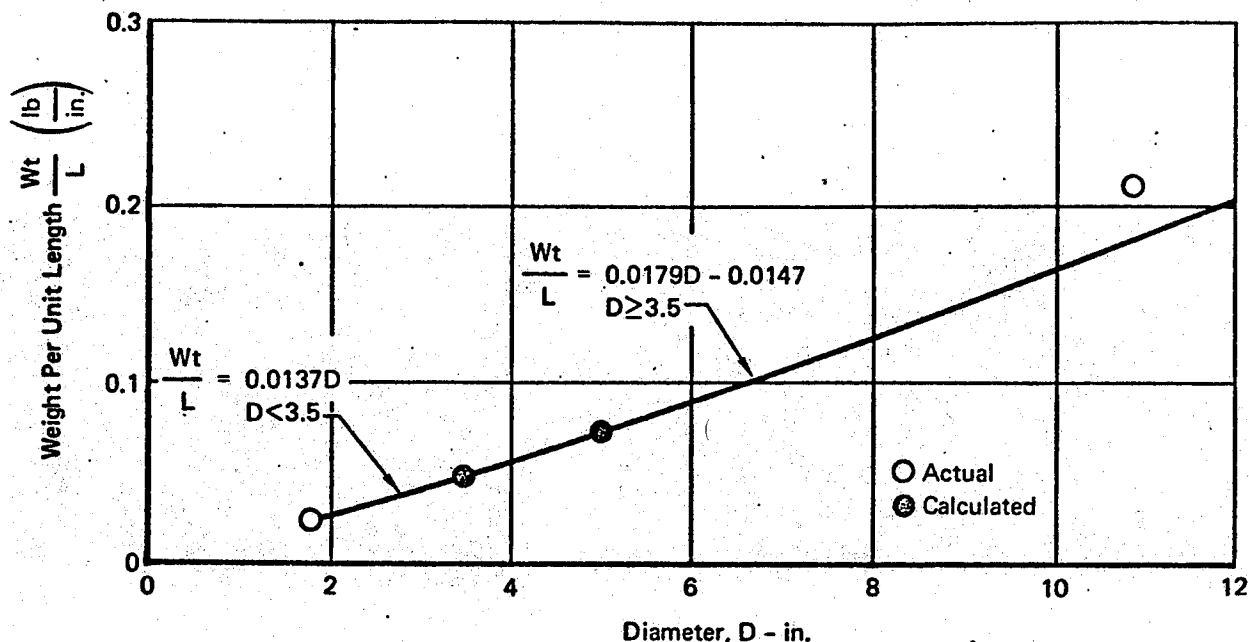


Figure 109 Weight of General Low Pressure Ducting

The methods of calculating the weight of low pressure ducting are applicable to all types of aircraft for the ram air circuits and the low pressure distribution circuits. The aluminum ducting weight correlation is more typical of an all aluminum ducting circuit than is the fiberglass duct weight correlation for an all fiberglass ducting circuit. This is because fiberglass ducting is used primarily for complex geometries.

3.10.2 Liquid, Refrigerant, and Pneumatic Control Lines - Plumbing for the liquid cooling loops, for the water heat sink or condensate water, for the vapor cycle refrigerant, and for the sensing and control lines of a pneumatic type control system generally are made of standard size aluminum or steel tubing.

Liquid Coolant Lines - Three levels of detail for calculating coolant line pressure losses are presented. The first requires the least known geometry and flow data, while the latter ones require more. In the first method, only the line length is required. The effective length (L_e) is:

$$L_e = K_1 L \quad (200)$$

where: $K_1 = 1.3$ when $L \geq 120$ in.

$K_1 = 2.0$ when $L < 120$ in.

The effective length is the length of a straight section of tubing which has the same pressure drop as an actual coolant line which contains bends, fittings, etc. A typical value of $\Delta P/L_e$ is 0.06 psi/inch. If the line diameter is known, the Equation (182) form is used as:

$$\Delta P = 0.0324 \frac{f L_e}{\rho g_c D_i^5} W^2 \quad (201)$$

The friction factor is a function of Reynolds number for laminar flow.

For turbulent flow wall roughness effects also are included. The friction factor for drawn tubing utilized in most liquid loops has a wall roughness very close to that of a "smooth pipe" as defined in the Moody graph of Reference 47.

A detailed analysis method for determining coolant line pressure drop is based on knowing the geometry of the various bends and straight sections of the tubing. The same pressure drop equation is used, and all terms are determined the same way except for L_e/D_i . The term L_b/D_i for a 90° bend is obtained from Figure 110 as a function of relative radius (r/D). (See Reference 48.) For bends other than 90° , L_b/D_i is determined from Figure 110 in conjunction with the following equation:

$$\frac{L_b}{D_i} = R_T + (n-1)(R_L + \frac{R_b}{2}) \quad (202)$$

where: n = portion of 90° bend (can be less or greater than one)

R_T = total resistance due to one 90° bend,

R_L = resistance due to length of one 90° bend,

R_b = bend resistance due to one 90° bend.

The L_b/D_i for the bends is added directly to L/D_i for the straight sections to find the total effective length to diameter ratio. There are many types of fittings. An additional pressure drop for fittings is added as an L_e . Coolant tubing usually is made of aluminum, which has a specific weight (ρ_{AL}) of $169 \text{ lb}/\text{ft}^3$. The weight of any coolant line tubing is:

$$Wt = 0.3071 (D_o - t)t L \frac{\rho}{\rho_{AL}} \quad (203)$$

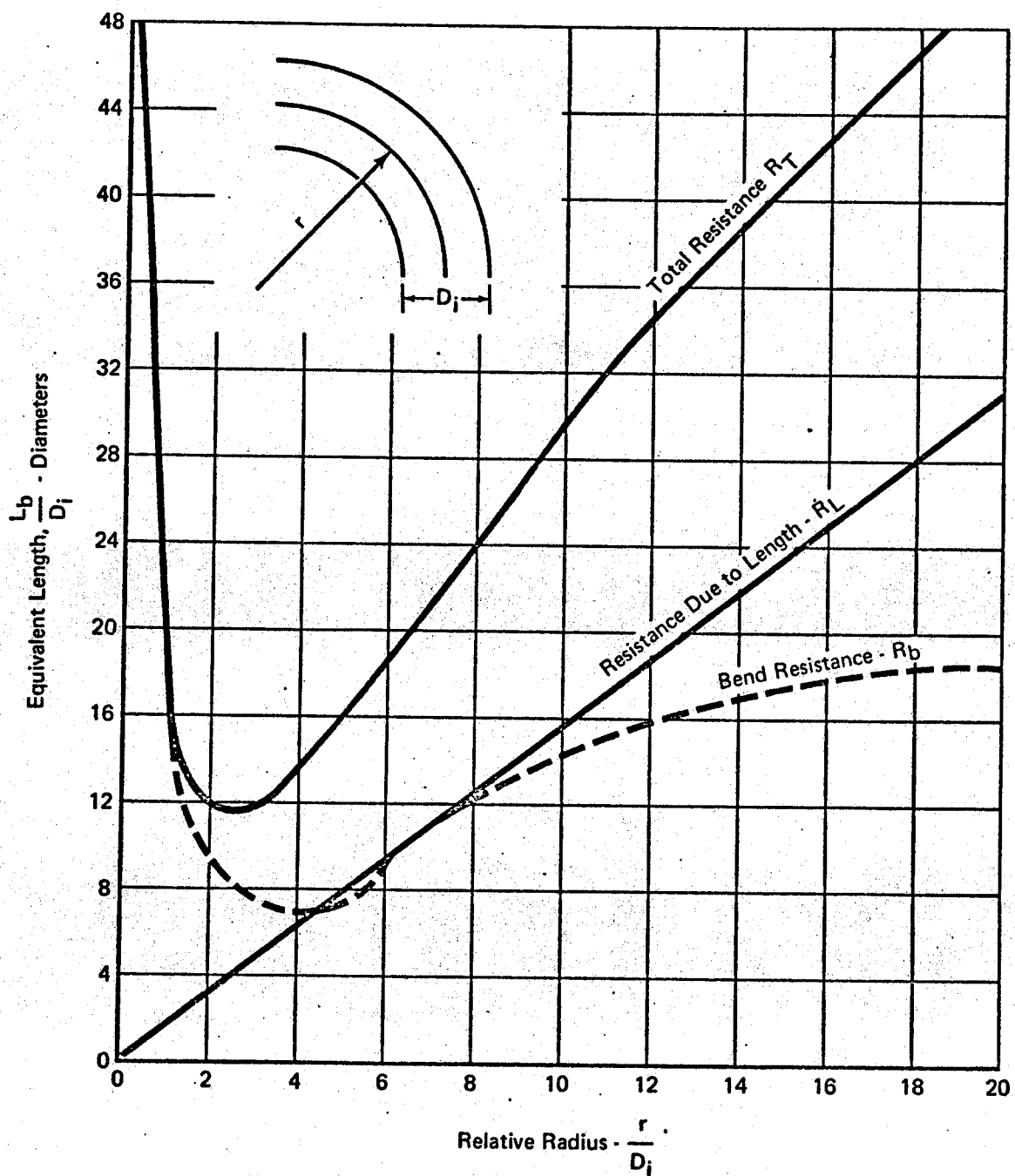


Figure 110 Equivalent Length of 90 Degree Bends for Cylindrical Ducts

GP 9416-114

where a typical wall thickness of 0.028 is used for both aluminum and steel alloys. Weights of line fittings are added if known. Weight of the coolant within the lines is:

$$Wt = \frac{\pi}{4} D_i^2 L \rho_{co} \quad (204)$$

where ρ_{co} is specific weight of the coolant.

Water Lines - Water lines are considered for condensate management and circulation of water from a separate water boiler reservoir to the water boiler. The minimum diameter of water separator drainage line is 3/8 inch (Reference 22). This requirement is necessary to alleviate clogging of the line with various types of debris common to open systems. This requirement also is assumed applicable to the water boiler reservoir line.

A larger line diameter may be required for water lines between a water boiler and separate reservoir, or a gravity water drain line. The following sizing procedure is used. The pressure level at each end of these water lines is known, thus, the diameter is determined from the following equation:

$$\Delta P = 0.0324 \frac{f}{\rho g_c} \frac{L_e}{D_i} \frac{W^2}{D_i^4} - \frac{\rho L_v}{144} \quad (205)$$

The first term accounts for the frictional line losses. The effective length (L_e) is determined the same way as is indicated in the coolant line section. The last term on the right hand side of the equation accounts for differences in elevation between the inlet and outlet. An iterative method of solution for diameter is required. A diameter is assumed, the velocity is determined from the continuity equation, and the friction factor is calculated from Reference 47.

The minimum 3/8 inch line size is used when an aspirator or ejector is utilized to pump the condensate to a higher pressure level. The procedure for calculating the pressure drop is the same as is used for the coolant lines where the diameter is known. Determination of weight for all water lines is the same as outlined in the coolant line section.

Vapor Cycle Refrigerant Plumbing - The size of the refrigerant lines depends upon the refrigerant being used, the allowable pressure drop, the required flow, and the distance between components. Self sealing disconnects and flexible hoses are used in the vicinity of components that require removal or replacement. Allowances for line pressure drops are made on a simplified level in Section 3.7.

The weight of the refrigerant lines is approximately ten percent of the basic vapor cycle system weight (i.e. bare uninstalled weight of the drive/compressor, evaporator, condenser, and receiver) plus one percent per foot of separation between the evaporator and condenser. If the separation distance is unknown, typical values of 10 and 5 feet may be used for cargo and fighter type aircraft, respectively. The above weight accounts for the throttling valve, fittings, flexible and rigid lines, self sealing disconnects, etc.

Pneumatic Control Lines - Pneumatic control lines are considered for air and vapor cycle systems. Sense lines are typically 5/16 or 3/8 inch O.D. Smaller lines usually are not used in order to prevent frozen condensate from blocking the line. The 5/16 O.D. is used more often and is considered the reference size for this study, but the 3/8 O.D. would be used in applications where it is necessary to prevent misconnection of a sense line or where the line pressure drop could affect the performance. Transient performance of the control systems is not considered in the performance analyses, hence pressure drops in the sense lines are not presented. The typical wall thicknesses and equations for coolant lines are used to obtain tubing weight. Common practice is to limit aluminum lines to 200°F. If the length is not known, three feet is typical.

3.10.3 Inlets and Outlets - Four types of inlets commonly used for ECS are considered. They are: scoop inlets, flush inlets, inlets on engine ducts, and nose inlets. The selection of inlet types for a specific aircraft is the result of a compromise between pressure recoveries and drag penalties. Nose and scoop inlets generally provide higher pressure recoveries than flush inlets. However, flush inlets have less drag penalties than nose and scoop inlets. A survey of about twenty aircraft shows that no trend is apparent to categorize the types of inlets according to the types of aircraft, except that inlets on engine ducts are used on

aircraft that maintain sustained flight at high speed (e.g. Mach 3.0).

However, inlets on engine ducts are not used exclusively for Mach 3 aircraft.

Approaches for the prediction of pressure recoveries and drag penalties and for sizing and weight estimation of ram air inlets are presented. The performance characteristics of outlets in terms of typical discharge coefficients are presented. Sizing and weight predictions of outlets when a bleed air ejector is employed in the system are discussed as part of the ejector discussion in Section 3.10.4. If a fan rather than a bleed air ejector is used in a ram air circuit, the sizing and weight correlations are approximated by an outlet model which is considered typical.

A number of documents discuss the pressure recovery and mass flow rate ratio for scoop and flush type inlets (See References 30, 49, 50, and 51.) Reference 49 is a theoretical approach to determine the flow rate ratio and pressure recovery for attached and for detached scoop inlets. A comparison of existing data with that obtained by this reference shows that discrepancies exist in flow rate ratio for all flight Mach numbers below approximately 1.7, although good agreement is found for pressure recovery. Reference 50 presents experimental pressure recovery and drag versus flow rate ratio for various types of scoop and flush inlets. The free stream Mach number of this reference varies from 0.55 to 1.3. This range does not encompass all the applications considered herein. References 30 and 51 present the same approach as Reference 49. Since all the documents reviewed have restrictions in their application, a typical scoop inlet and a typical flush inlet used in modern aircraft are considered. Their pressure recovery curves are used for performance analysis. For nose inlets and inlets on engine ducts approximate approaches are used to predict pressure recovery.

An inlet normally is comprised of a mixing section and a diffuser. The function of the mixing region prior to the diffuser is to provide a uniform flow at the diffuser entrance, thus resulting in flow stability at the diffuser exit, and higher pressure recovery in case a thick boundary layer or separated flow exists at the inlet. A theoretical method for determining the optimum length of the mixing region is not well established. A maximum length equivalent to three times the inlet diameter is used in Reference 52. Our studies do not reveal any theoretical approach regarding

optimum diffuser design in a compressible flow field. The diffuser performance is as sensitive to initial boundary layer conditions as it is to diffuser geometry. Diffuser designs nominally are based on experimental data, hence a typical mixing tube and diffuser are discussed. The geometry data are correlated to that of a general inlet to obtain weight and volume estimations.

3.10.3.1 Inlets - Overall performance of inlets and diffusers, and the drag penalties of the inlets are presented. Extrapolation is necessary to obtain pressure recoveries for Mach numbers higher or lower than those shown in the following figures. The pressure recovery values should not be extrapolated beyond a Mach number increment of 0.5 if reasonable accuracy is to be maintained. High flow rate ratios should be used for nose or scoop inlets at supersonic speeds in order to prevent possible flow instabilities. (See Reference 53.)

Pressure Recovery and Area of Flush Inlets - Figure 111 represents a typical pressure recovery map for flush inlets, taken from Reference 54. It is considered applicable to inlets of different sizes having approximately the same width to depth ratio and depth to boundary layer thickness ratio. A flow rate ratio of 0.65 is typical. The pressure recovery versus Mach number, based on the flow rate ratio of 0.65, is shown in Figure 112. Three pressure recovery equations are defined, each representing one segment of the curve:

$$\frac{P_{T1}}{P_{T\infty}} = 0.98, \text{ if } M_\infty < 0.5; \quad (206)$$

$$\frac{P_{T1}}{P_{T\infty}} = 1.055 - 0.15 M_\infty, \text{ if } 0.5 \leq M_\infty \leq 0.90; \quad (207)$$

$$\frac{P_{T1}}{P_{T\infty}} = 1.24 - 0.358 M_\infty, \text{ if } M_\infty > 0.90. \quad (208)$$

The typical flow rate ratio is utilized to determine the inlet area:

$$A_1 = \frac{2.4 W_1}{0.65 \rho_\infty V_\infty^2} \quad (209)$$

Once the inlet area is known, the performance map in Figure 111 is utilized to obtain off-design performance.

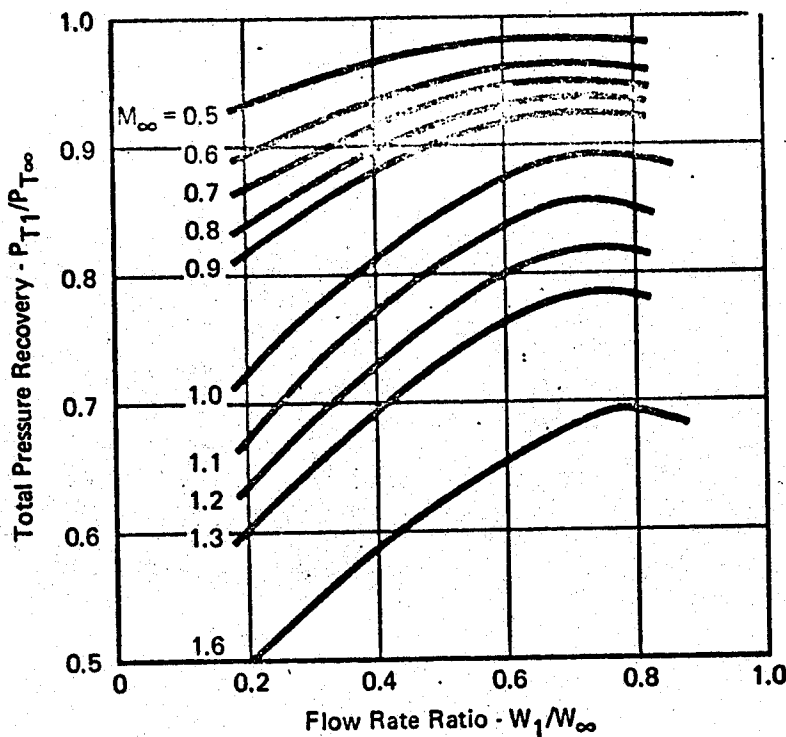


Figure 111 Total Pressure Recovery for Typical Flush Inlet

GP 9416-72

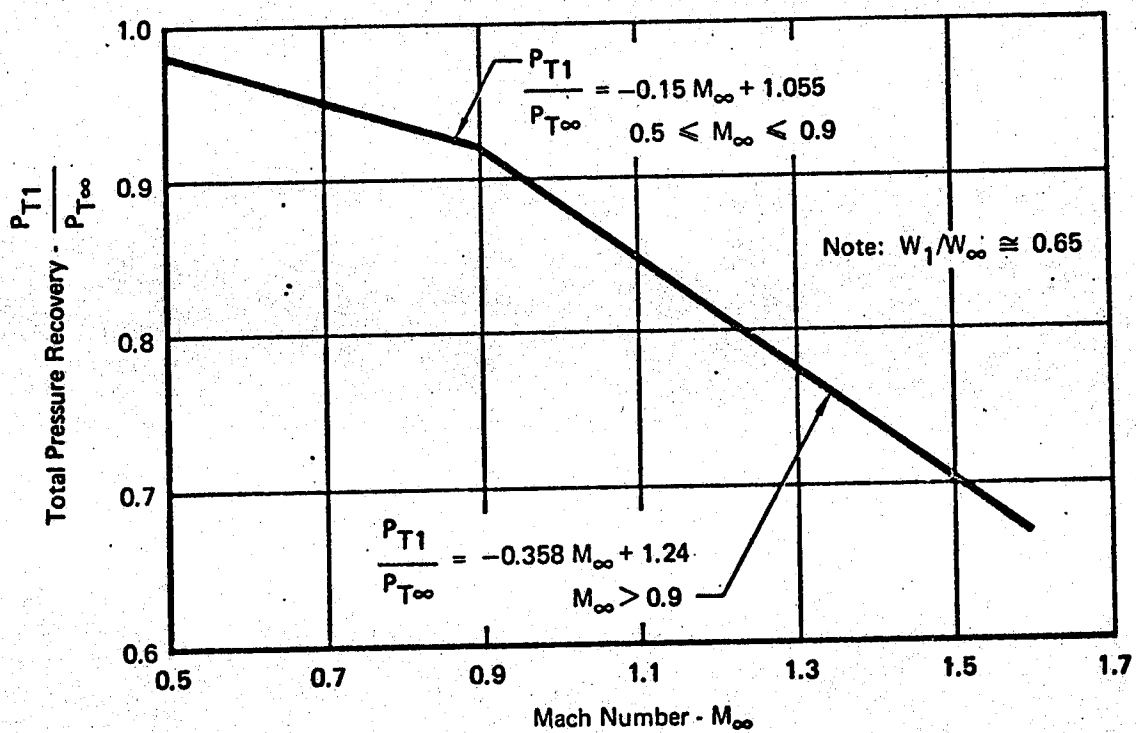


Figure 112 Typical Flush Inlet Pressure Recovery

GP 9416-78

Pressure Recovery and Area of Scoop Inlets - Figure 113 shows typical pressure recovery maps for scoop inlets at subsonic and supersonic flight conditions. The maps are considered applicable to similar types of inlets with different areas but having similar width-to-depth ratios and depth to boundary layer thickness ratios. At flight Mach numbers between 0.4 and 1.0, it is found that W_1/W_{cr} normally is 0.4 to 0.75. At lower Mach numbers, lower values of W_1/W_{cr} are expected. Pressure recoveries range from 0.98 to 0.998 at all subsonic Mach numbers when the typical W_1/W_{cr} are used. Therefore, a mean pressure recovery equal to 0.99 is typical for subsonic flight. At supersonic speeds the pressure recovery is not a strong function of flow rate ratio. A typical W_1/W_∞ of 0.80 is selected. The typical scoop inlet pressure recovery is shown in Figure 114. A smooth curve is constructed in the transonic region. The corresponding equations for typical pressure recovery of scoop inlets are:

$$\frac{P_{T1}}{P_{T\infty}} = 0.99, \text{ if } M_\infty \leq 0.7, \quad (210)$$

$$\frac{P_{T1}}{P_{T\infty}} = 0.99 - 0.0118 M_\infty^{5.40}, \text{ if } 0.7 < M_\infty < 1.5, \quad (211)$$

$$\frac{P_{T1}}{P_{T\infty}} = 1.61 - 0.483 M_\infty, \text{ if } M_\infty \geq 1.5. \quad (212)$$

To determine the inlet area in supersonic flight, the typical W_1/W_∞ of 0.8 is used. If the area is to be determined for subsonic flight, a W_1/W_∞ equal to 0.7 is arbitrarily selected. Thus, the inlet area of a scoop inlet is:

$$A_1 = \frac{2.4 W_1}{0.70 \rho_\infty V_\infty^2} \quad (\text{Subsonic}), \text{ and} \quad (213)$$

$$A_1 = \frac{2.4 W_1}{0.80 \rho_\infty V_\infty^2} \quad (\text{Supersonic}). \quad (214)$$

The applicable performance maps in Figure 113 are used to predict off-design performance.

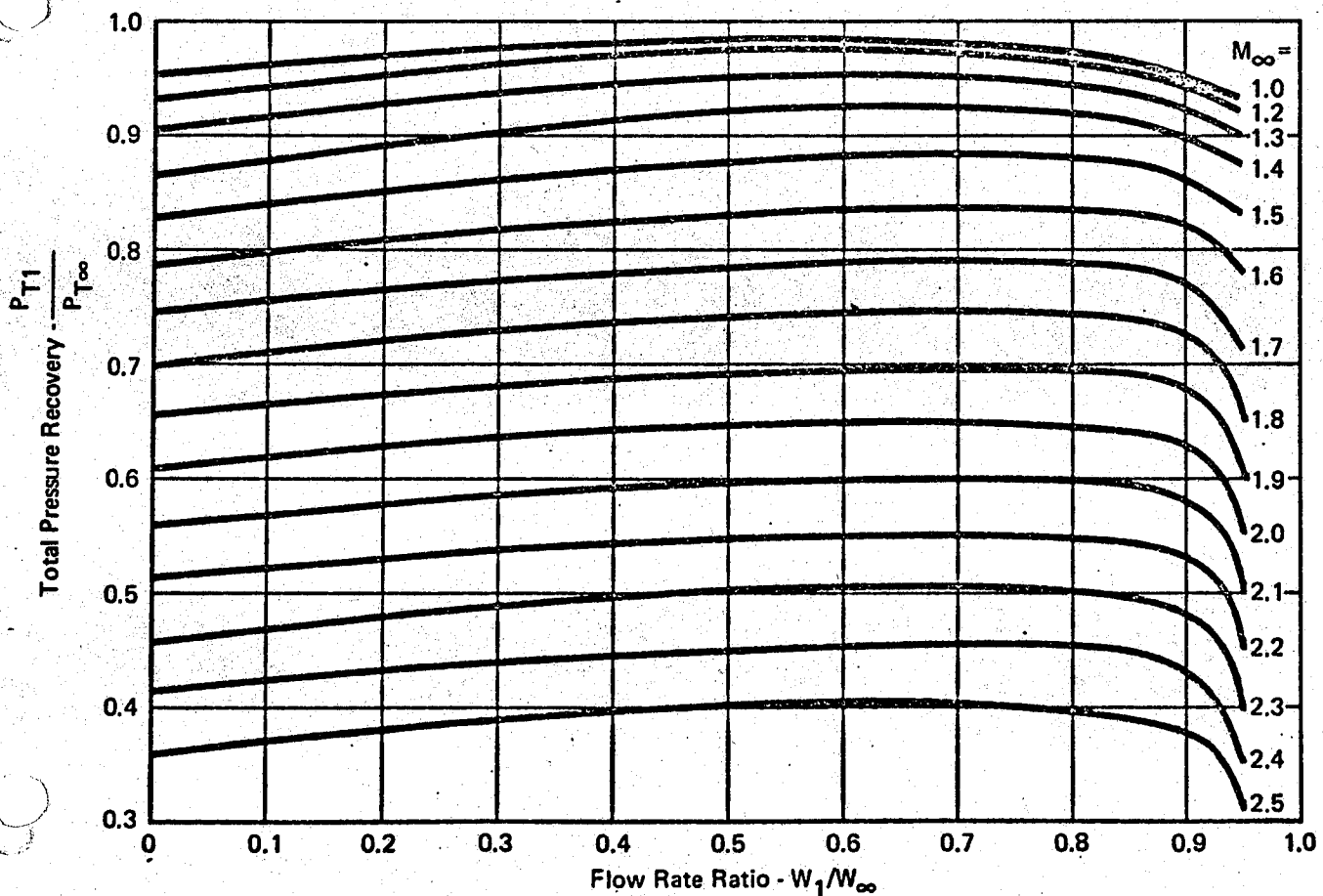
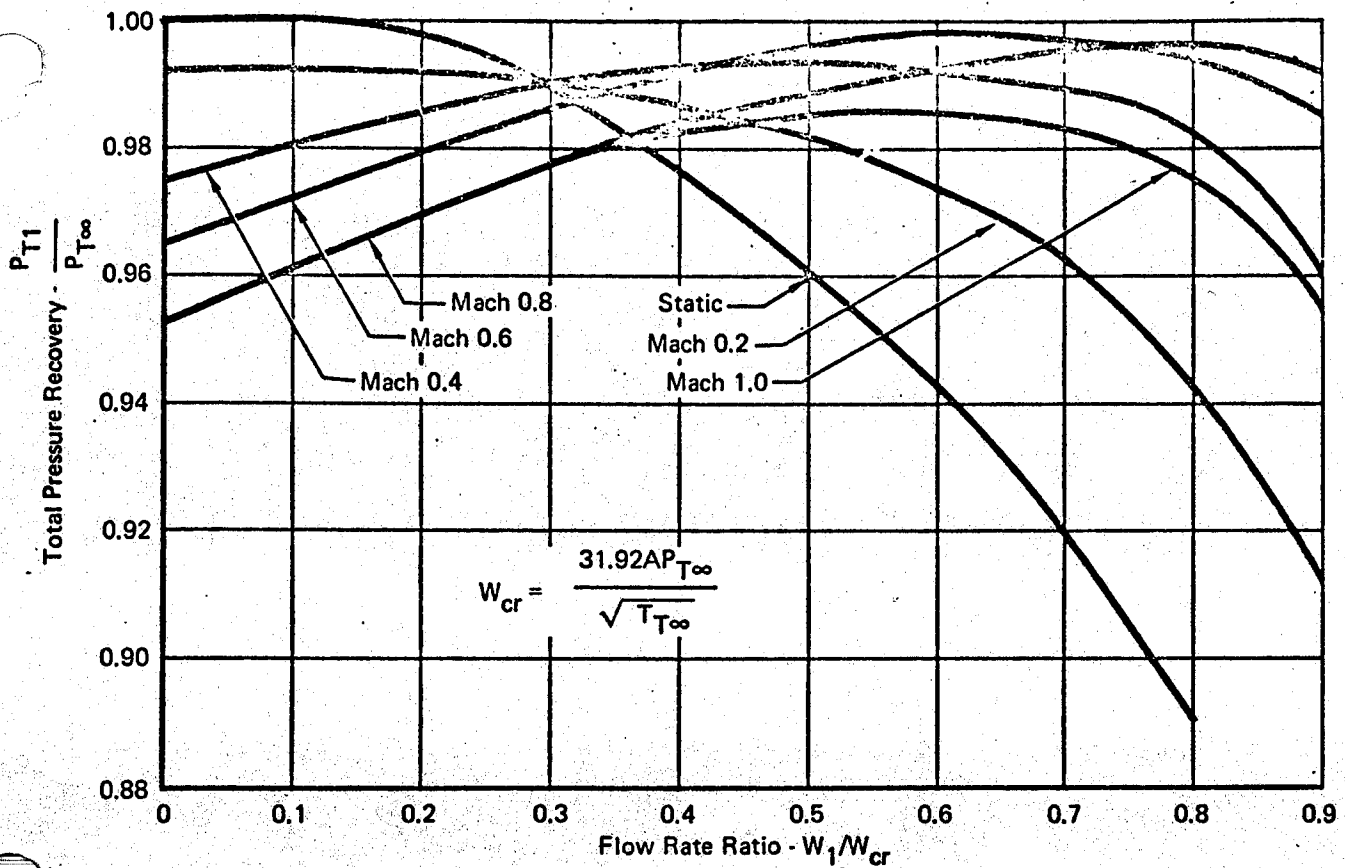


Figure 113 Total Pressure Recovery for Typical Scoop Inlet

GP 9416-77

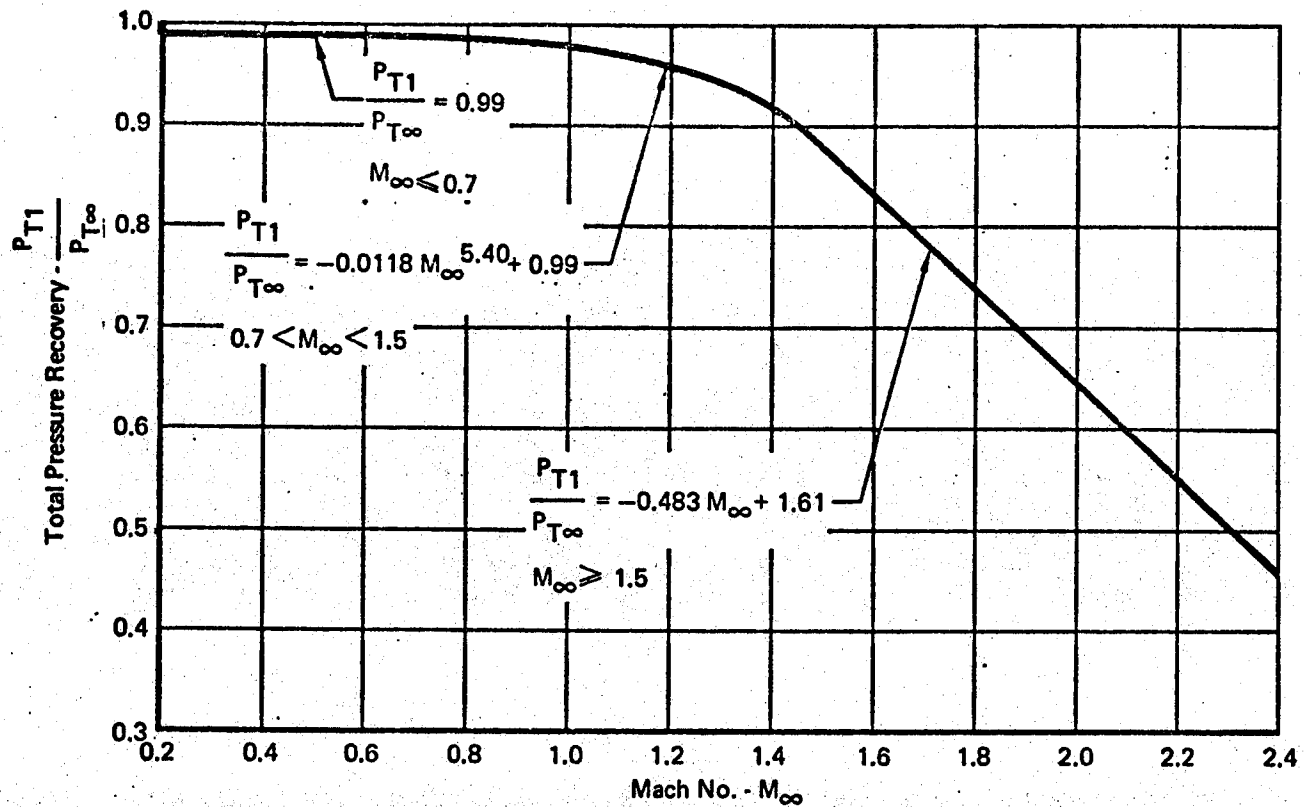


Figure 114 Typical Scoop Inlet Pressure Recovery

GP 9416-74

Pressure Recovery and Area of Inlets on Engine Ducts - An inlet on an engine duct takes ram air from the jet engine diffuser. Some inlets on engine ducts provide air to the ECS at the engine diffuser static pressure (e.g. holes in the diffuser wall). Others provide a stepped inlet around the diffuser periphery (a scoop type inlet) to provide ram air to the ECS (and also engine by-pass air). For simplicity a ram air inlet perpendicular to and flush with the diffuser wall is considered. Thus, the total pressure and temperature at the inlet are the engine diffuser static pressure and total temperature at the inlet opening. Reference 55 provides pressure recovery characteristics for a good engine diffuser design. These determine the total pressure of the engine diffuser exit, where an ECS inlet is located.

$$\frac{P_{T3}}{P_{T\infty}} = 1.0, \text{ if } 0 < M_\infty < 1.0, \text{ and} \quad (215)$$

$$\frac{P_{T3}}{P_{T\infty}} = 1.0 - 0.075 (M_\infty - 1)^{1.35}, \text{ if } 1.0 < M_\infty < 5.0, \quad (216)$$

where P_{T3} is total pressure at the engine diffuser exit.

Local Mach numbers at the engine diffuser exit range from 0.2 to 0.5 (a nominal value of 0.35 may be used to calculate the engine duct static pressure). The total temperature at the engine diffuser exit is the free stream total temperature. An inlet Mach number of 0.3 is typical, and the inlet area is:

$$A_1 = \sqrt{\frac{R}{\gamma g_c}} \sqrt{\frac{T_{T_\infty}}{60M_1^2 P_3}} \left[1 + \frac{1}{2} M_1^2 (\gamma - 1) \right]^{\frac{\gamma+1}{2(\gamma-1)}} \quad (217)$$

Pressure Recovery and Area of Nose Inlets - Nose inlets are located at the nose of a fuselage or at a leading edge, where a boundary layer does not exist. The pressure loss at subsonic speeds is negligible. In supersonic flight a pressure loss occurs, usually due to a normal shock. Additional loss behind the shock is neglected. Therefore, the pressure recovery of the nose inlet is found simply by normal shock relationships. A typical flow rate ratio of 0.8 is assumed in order to determine the inlet area with Equation (214). This typical flow rate ratio is the same as that of a scoop inlet at supersonic speeds. This assumption is justifiable, since both types of inlets attain about the same value of pressure recovery.

Overall Pressure Recovery of Inlet and Diffuser - The inlet total pressure is at the diffuser entrance. Usually the pressure drop of a subsonic diffuser is specified as a total pressure loss coefficient: $(P_{T1} - P_{T2})/q_1$, where P_{T2} is the total pressure at the diffuser exit and q_1 is the dynamic pressure at the diffuser entrance. The total pressure loss coefficient is a function of diffuser geometry as well as boundary layer conditions at the diffuser entrance. (See Reference 53.) It is based largely on experimental data. Typical loss coefficients of well-designed diffusers are 0.05 (for thin diffuser entrance boundary layers) to 0.20 (for thick diffuser entrance boundary layers). (See Reference 30.) Offset and non-symmetrical duct cross-sections, as often found in actual diffusers, incur additional losses. Total pressure loss coefficients ranging from 0.1 to 0.3 are selected as reasonable. The overall pressure recovery of the inlet and diffuser is:

$$\frac{P_{T2}}{P_{T\infty}} = \left[1 - \left(\frac{P_{T1} - P_{T2}}{q_1} \right) \frac{q_1}{P_{T1}} \right] \frac{P_{T1}}{P_{T\infty}} \quad (218)$$

The dynamic to total pressure ratio at the inlet to the diffuser (q_1/P_{T1}) is a function of the Mach number (M_1). An iteration is necessary to obtain this Mach number (M_1).

Inlet Drag - The drag due to the presence of an inlet is approximated by the total momentum loss of the ram air. This correlates with experimental data for flush inlets, but is somewhat discrepant for scoop inlets (especially at low flow rate ratios, where pressure drag of these inlets is high) (See Reference 50.) However, these low flow rate ratios occur at low speeds where the higher pressure drag (relative to momentum drag) is not significant in many mission profiles. Therefore, the inlet drag coefficient is:

$$C_D = \frac{\frac{W_1 V'_\infty}{1/2 \rho_\infty V'_\infty^2 A}}{W_1} = 2 \frac{W_1}{W_\infty} \quad (219)$$

Inlet Weight - The weight of a typical inlet is extrapolated to obtain weight estimates of general inlets. The typical inlet has a mixing length of two inlet hydraulic diameters, and weighs 3.3 pounds. If the same material density, wall thickness and hydraulic diameter to length ratio are used, the weight of a general inlet is directly proportional to the inlet area. If a different material density, a different wall thickness, and the same hydraulic diameter to length ratio are used, the weight of a general inlet is estimated as:

$$W_t = 8\rho t A_1 \quad (220)$$

where ρ is pounds per cubic inch.

Diffuser Weight - A typical diffuser weighs 12 pounds and the divergence angle is twelve degrees. It has an entrance area of 17.0 square inches, an exit area of 84.5 square inches, and an axial length of 26.7 inches. The included divergence angle is based on an assumed equivalent conical diffuser having the same entrance area, exit area, and axial length.

The exit Mach number of the diffuser is assumed to be 0.15. The exit area is:

$$A_2 = \sqrt{\frac{R}{\gamma g}} \frac{\sqrt{T_{T2} W_1}}{P_{T2}} \left[\frac{1 + \frac{\gamma-1}{2} (M_2)^2}{60 M_2} \right]^{\frac{\gamma+1}{2(\gamma-1)}} \quad (221)$$

Knowing the entrance area (A_1), exit area (A_2), and divergence angle, the axial length (L) is:

$$L_d = \frac{\sqrt{\frac{A_2}{\pi}} - \sqrt{\frac{A_1}{\pi}}}{\tan 6^\circ} \quad (222)$$

The lateral surface area of a 6° half angle truncated cone is:

$$S = \sqrt{\pi} (\sqrt{A_1} + \sqrt{A_2}) \frac{L}{\cos 6^\circ} \quad (223)$$

Thus the lateral surface area of the equivalent truncated cone is 661 square inches. If the wall thickness and material density are the same as that of the typical diffuser, the weight is directly proportional to diffuser lateral surface area. If a different material density and a different wall thickness are used, the diffuser weight is:

$$Wt = \rho S \quad (224)$$

where ρ is pounds per cubic inch.

Inlet Volume - The volume of inlet (V_{in}) and diffuser (V_d) are:

$$V_{in} = \frac{8A_1^2}{B} \quad (B \text{ is perimeter of inlet}) \quad (225)$$

$$V_d = \frac{L_d}{3} (A_1 + A_2 + \sqrt{A_1 A_2}) \quad (226)$$

3.10.3.2 Outlets - The performance characteristics of an outlet usually are described in terms of an outlet discharge coefficient as a function of discharge flow rate ratio. The discharge coefficient (K_1) is defined as the ratio of the measured outlet mass flow to the calculated (ideal) outlet mass flow. Reference 30 presents discharge coefficient data for various outlet configurations and free stream Mach numbers. The effects of outlet configuration and flight Mach number on the discharge

coefficient is small. The discharge coefficient in Figure 115, (from Reference 30) for a free stream Mach number of 0.7 and 45° inclined angle square outlet, is typical for many types of outlets at all flight Mach numbers. The discharge coefficient at a design point nominally is high (i.e. > 0.8). The discharge coefficient varies from 0.94 to 0.97 during ground operating conditions. (See Reference 56.) If the exit area is known, the flow rate at off-design conditions is:

$$W_1 = 60 K_1 A_X \frac{P_{TX}}{\sqrt{T_X}} \left[\frac{2g_c \gamma}{R(\gamma-1)} \right]^{1/2} \left[\left(\frac{P_1}{P_{TX}} \right)^{\frac{2}{\gamma}} - \left(\frac{P_1}{P_{TX}} \right)^{\frac{\gamma+1}{\gamma}} \right]^{1/2} \quad (227)$$

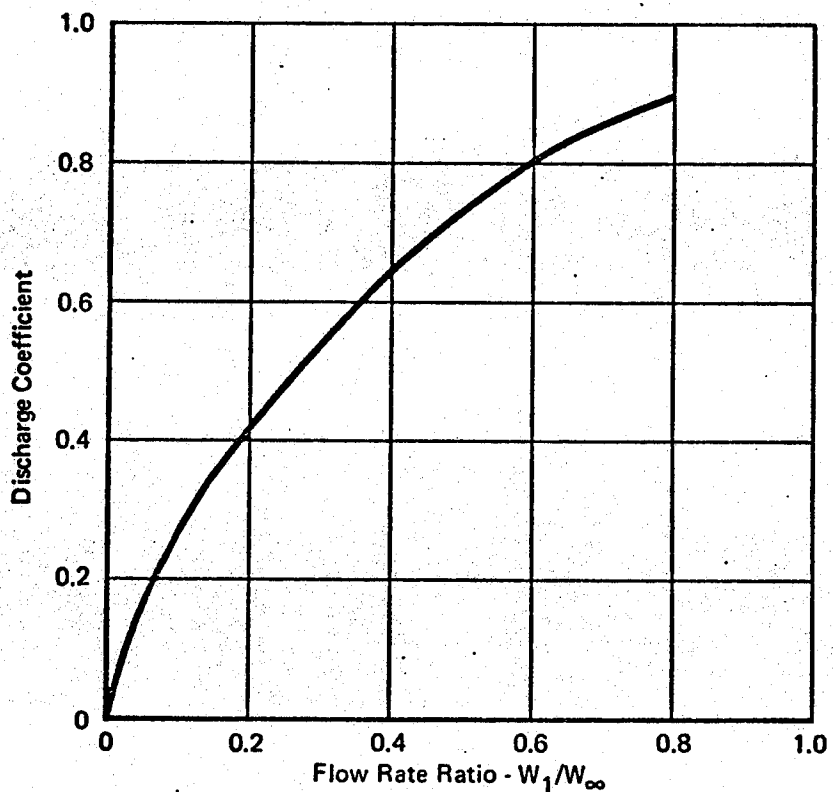


Figure 115 Discharge Coefficient for Typical Outlet

GP 9416-75

The following approach to determine outlet size, weight, and volume applies only to a system without a bleed air ejector in a ram air duct. The performance of a nominal outlet is determined from the data in

Figure 116. Reduced outlet pressure drops (i.e. higher pressure ratio in Figure 116) are obtained with greater exit areas. A typical discharge coefficient is 0.8. The flow rate ratio (W_1/W_∞) is 0.6. W_∞ is determined for the known W_1 , and the exit area is obtained from the continuity equation.

The weight and volume are approximated relative to the following typical outlet. The outlet has a rectangular cross section with length to width ratio of 2, and it has several 45° louvers spaced with a small amount of overlap. The thicknesses of louvers and flanges are assumed to be twice the side wall thickness (t). The mounting flange width is 0.75 inches. The length to height ratio of the outlet is assumed to be 4.0. Based on these assumptions, the weight and volume are calculated by the following equations:

$$W_t = 4.5 \rho t (1 + 1.69 \sqrt{A_x} + 1.20 A_x) \quad (228)$$

$$V = 0.85 A_x^{3/2} \quad (229)$$

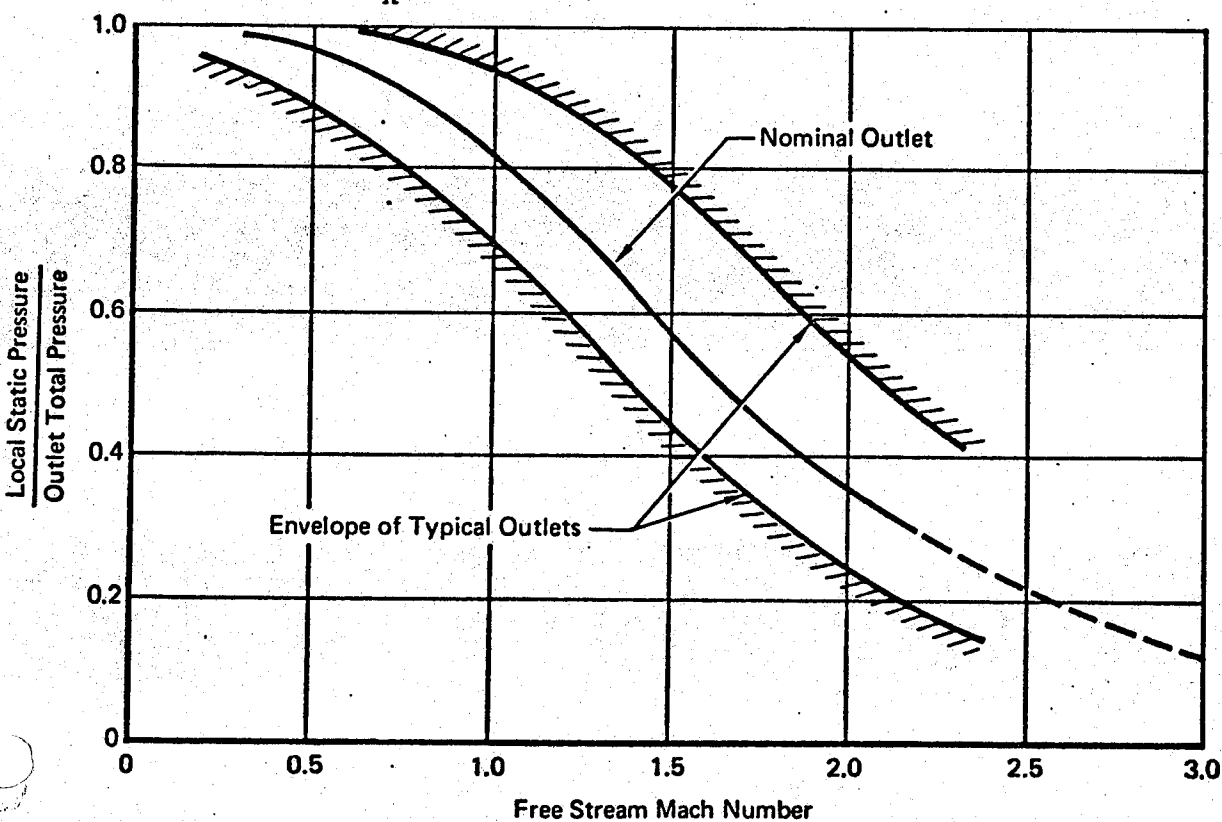


Figure 116 Performance of Typical Outlet

3.10.4 Ejectors - Three types of bleed air ejectors frequently used in aircraft ECS (ram air circuit ejectors, water boiler ejectors, and aspirators) are included herein. The ram air circuit ejector is used for pumping ambient cooling air through a heat exchanger at low flight speeds and ground operating conditions. The function of a water boiler ejector is to create a vacuum in the water boiler so the water evaporates at a lower temperature. The use of an aspirator provides a convenient way to pump the water out of water separators and heat exchangers. All three types of ejectors use bleed air as the primary flow.

A number of documents concerning the performance prediction and sizing of air to air ejectors are available. (See References 30, 57, 58, and 59.) In the latter three references it is assumed that mixing of primary and secondary flow is complete at the end of the mixing region (i.e. the velocity is uniform at the exit of the mixing tube). In Reference 30 the nonuniform velocity profile and pressure distribution at the exit of the mixing tube are accounted for by correction factors determined from experiment, and the ratio of secondary to primary flow areas is 8 or less. This is much less than the area ratios of typical air to air ejectors. Personal correspondence with ejector manufacturers indicates that experimental approaches normally are used. (Empirical parameters, which are proprietary, are obtained from test programs.)

Three existing bleed air ejectors are selected as typical for the three types of ejectors mentioned above. Data representative of these ejectors are used for performance and sizing predictions. General performance maps are utilized to predict performance of the ram air circuit ejectors and aspirators. Weight and volume of a ram air circuit ejector are estimated by scaling the typical unit.

3.10.4.1 Ram Air Ejector - The ram ejector assembly consists of a bleed air line (which contains a shut-off valve) from the main bleed air supply line to the ejector tubing and nozzle assembly, the ejector tubing and nozzle assembly which supplies bleed air to the mixing tubes, and the mixing tube assembly. Performance and sizing of the first two components are determined in the air ducting and valve sections (3.10.1 and 3.10.5). Figure 117 is a typical schematic of a ram air duct with compressor ejector and bleed air ejector for a simple air cycle system.

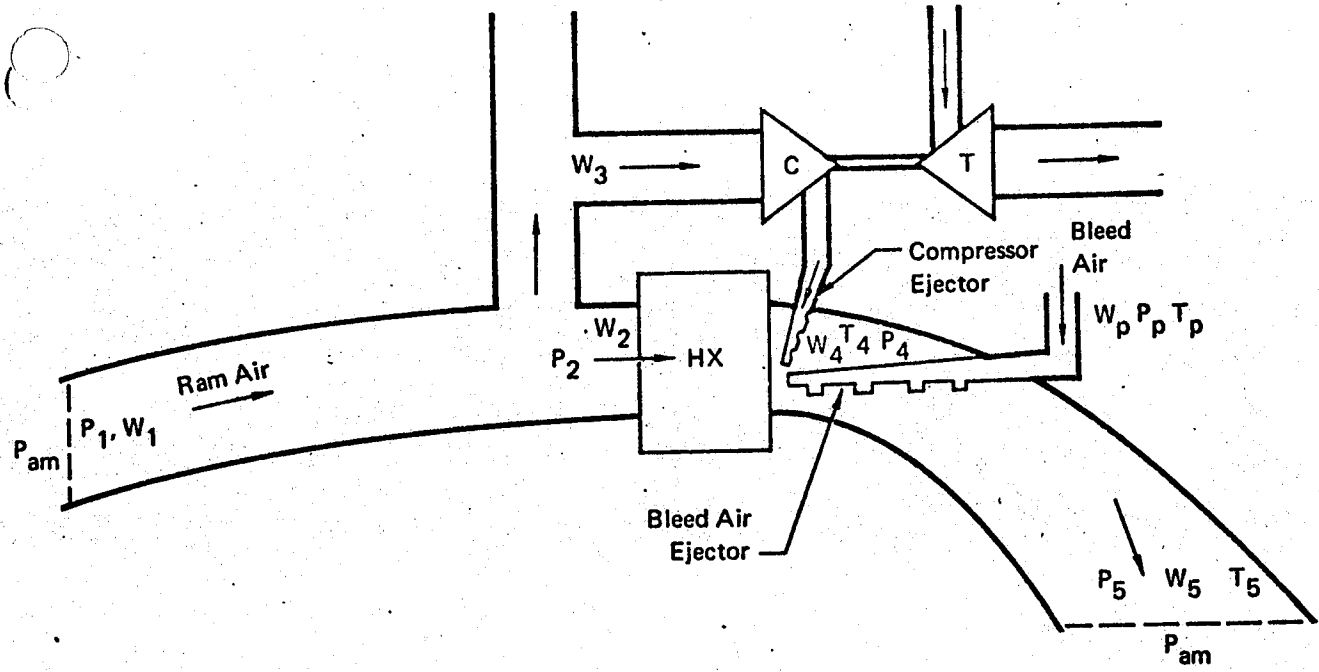
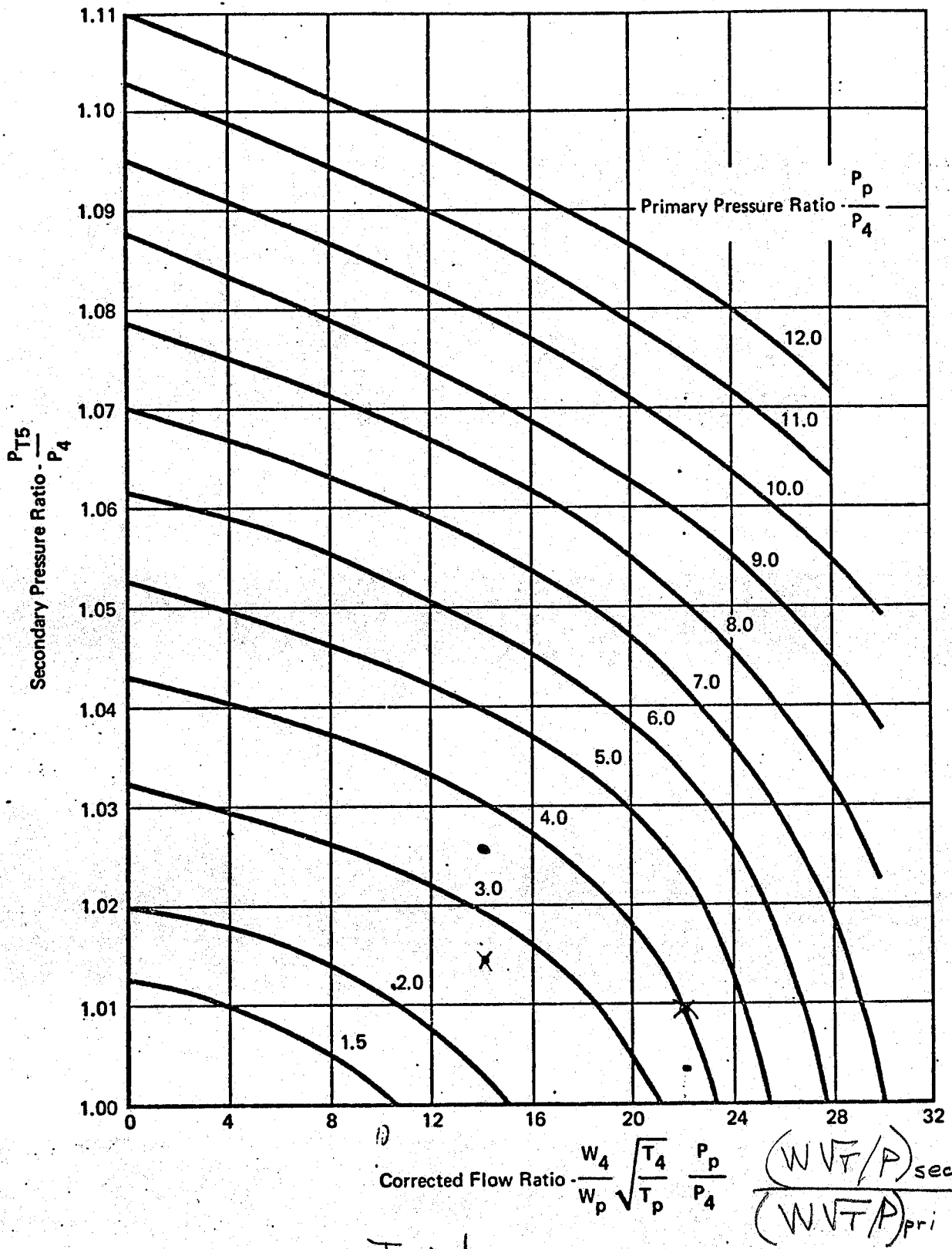


Figure 117 Typical Bleed Air Ejector in a Ram Air Duct

GP 9416-90

Performance - The performance map of a typical ejector that is used to pump ambient air through heat exchangers is shown in Figure 118. This performance is applicable to simple air cycles (shown in Figure 117), bootstrap air cycles (where the compressor is in the bleed air circuit), or ram air circuits utilized in vapor cycle ECS. For the simple air cycle shown in Figure 117 the compressor discharge has little or no pumping effect. Thus, it is assumed that the discharge pressure environment for the compressor ejector is that calculated as the exhaust from the heat exchanger. The primary flow rate (W_p) is calculated with one of the two following equations, depending on whether the flow is choked or not (as indicated by the nozzle pressure ratio). When the flow is choked:

$$W_p = 60 (K_1 A_p) \left[\frac{\gamma g_c}{R} \left(\frac{2}{\gamma + 1} \right)^{\frac{\gamma+1}{\gamma-1}} \right]^{\frac{1}{2}} \sqrt{\frac{P_p}{T_p}} \quad (230)$$



Typical
Figure 118 Ejector Performance

GP 9416-81

where $(K_1 A_p)$ is the effective nozzle area. When the flow is not choked:

$$W_p = 60 (K_1 A_p) \left[\frac{C_{dA}}{\frac{2g_c Y}{R(\gamma-1)}} \right]^{1/2} \left[\left(\frac{P_4}{P_p} \right)^{\frac{2}{\gamma}} - \left(\frac{P_4}{P_p} \right)^{\frac{\gamma+1}{\gamma}} \right]^{1/2} \sqrt{\frac{P_p}{T_p}} \cdot \frac{18}{\sqrt{f_{100}}} \quad (231)$$

$\frac{60(C_{dA})}{144} \left[\frac{4.226}{4.226} \right] \left[\frac{0.391}{0.391} \right] (9) \cdot = .0607 A$

The exit total pressure (P_{T5}) is dependent on T_5 . The temperature T_5 is the mixed temperature of the primary and secondary air flows:

$$T_5 = \frac{W_4 T_4 + W_p T_{px}}{W_4 + W_p} \quad (232)$$

where T_{px} is the static temperature of the primary stream after expansion through the nozzles. This temperature (T_{px}) also depends on whether choked flow occurs or not:

$$T_{px} = \frac{2}{\gamma+1} T_p \quad (\text{choked}); \quad (233)$$

or:

$$T_{px} = T_p \left(\frac{P_4}{P_p} \right)^{\frac{\gamma-1}{\gamma}} \quad (\text{not choked}). \quad (234)$$

The exit total pressure is obtained by assuming that the exit pressure loss of the ram air duct is equal to the dynamic pressure at the exit and that the contraction coefficient of the exit area is equal to one (i.e., the effective area is the same as the actual area).

$$P_{T5} = P_{am} + \frac{1}{2} \frac{\rho V_5^2}{g_c} = P_{am} + 0.02 \frac{R}{g_c} \left(\frac{T_5}{P_{am}} \right) \left(\frac{W_5}{A_5} \right)^2 \quad (235)$$

A typical ratio of primary to secondary flow rates (W_p/W_4) is four.

Sizing of the Bleed Air Ejector - The bleed air ejector is sized through use of a scaling factor referenced to the typical unit. The typical bleed air ejector is related to an actual bleed air ejector having six independent modules. Each module consists of single or multiple subsonic nozzles and one mixing tube. Two of these modules contain four nozzles each and the rest of the modules each have a single nozzle. The mixing tubes are fabricated as a single magnesium casting. The typical unit is assumed to consist of 12 single-nozzle modules having equal lengths of 6.85 inches and equal square cross-

Deal
WRONG

$T_{px} = T_p$
after expns.
back to low
velocity, except
for minor
amt. of work
performed
($M_p < 10\%$)

sectional areas of 5.63 square inches. (The uniform length of the mixing tubes is a weighted area average of the six mixing tube lengths of the actual unit.) The cross-sectional area of each mixing tube of the model is one twelfth of the total cross-sectional area of the actual ejector measured at the mid-section of the mixing tubes. The area ratio and the length to hydraulic diameter ratio of each single-nozzle unit are nearly the same as the average ratios of the actual unit.

The effective nozzle area ($K_1 A_p$) is calculated with Equation (230) if the nozzle flow is choked, or with Equation (231) if the nozzle flow is not choked. The area ratio of the typical ejector ($A_5/K_1 A_p$) is 152, hence the mixing tube area is determined from the effective nozzle area.

The number of single-nozzle ejector modules is:

$$B = \frac{(K_1 A_p)}{0.0371} \quad (236)$$

The effective area of a single nozzle of the typical ejector is 0.0371 in^2 . The number of required modules must be an integer. It is selected from the calculated value of B as follows:

Calculated B	0 to 3.0	3.0 to 5.0	5.0 to 7.0	7.0 to 9.0	etc.
Integer B	2	4	6	8	etc.

(i.e. the minimum number of modules is 2).

Weight - The weight of the ejector mixing tube modules is:

$$Wt = 0.244 (2.5B + 2) \left(\frac{t}{t_r} \right) \left(\frac{\rho}{\rho_r} \right) \quad (237)$$

The reference model wall thickness and density are: $t_r = 0.224$ inch and $\rho_r = 113 \text{ lb/ft}^3$. The wall thickness of the reference is a bulk number which accounts for the total weight of the typical unit (including flanges, stiffeners, etc.). The weight of the typical bleed air tubing and nozzle assembly is about twenty percent of the mixing tube weight.

Volume - Volume is determined by multiplying the number of modules by the volume per module:

$$V = 38.6 B \quad (238)$$

3.10.4.2 Water Boiler Ejector - The performance of the typical water boiler ejector is shown in Equation (13) of Reference 57. Since this equation is derived for low pressure ratio ejector applications, a modification factor (K_1) is introduced to make it applicable to water boiler ejectors which have higher pressure ratios and lower flow rate ratios. The altered equation is:

$$\frac{\Delta P}{2q_p} + K_1 = \frac{1}{K_2} + \frac{K_3^2}{K_4 K_2 (K_2 - 1)} - \frac{(1 + K_3)(1 + \frac{K_3}{K_4}) K_5}{K_2} - \frac{K_3^2}{2K_4 (K_2 - 1)^2}$$
(239)

where:

K_2 = area of mixing section
 effective exit area of primary jet

K_3 = secondary flow rate
 primary flow rate

K_4 = density of secondary flow
 density of primary flow

ΔP = Secondary pressure rise, lb/ft^2

q_p = Dynamic pressure at exit of primary jet, lb/ft^2

K_5 = Flow constant.

Two values of K_1 (-0.043 and 0.054) are obtained from performance data for a typical ejector at sea level and 10,000 feet altitude, respectively. A linear relationship between K_1 and altitude (Z) is assumed:

$$K_1 = (0.097 \times 10^{-4}) Z - 0.043. \quad (240)$$

A typical water boiler ejector has K_2 equal to 3.34. The ratio of diffuser exit area to mixing section area is 1.4. Thus, the flow constant K_5 is 1.0 (Reference 57). To simplify the analysis, the primary flow is assumed to be fully expanded and supersonic at the nozzle exit. Therefore, the effective area of the primary jet is the same as the nozzle exit area.

The primary jet Mach number is:

$$M_p = \left[\frac{\left(\frac{P_p}{P_s} \right)^{\frac{\gamma-1}{\gamma}} - 1}{\frac{\gamma-1}{2}} \right]^{1/2} \quad (241)$$

Equation (239) is utilized to solve for flow rate ratio (K_3). The typical value of K_2 (i.e. 3.34) is used. Assuming choked flow occurs, the nozzle throat area (A^*) is:

$$A^* = \frac{W_p}{60} \left[\frac{\gamma g_c}{R} \left(\frac{2}{\gamma+1} \right)^{\frac{\gamma+1}{\gamma-1}} \right]^{-\frac{1}{2}} \sqrt{\frac{T_p}{P_p}} \quad (242)$$

Having determined the throat area, the off-design performance analysis is accomplished by Equation (239).

The weight of the water boiler ejector is considered to be included in the assembly weight of the water boiler.

3.10.4.3. Aspirator - The performance map for a typical aspirator (water injector) used in fighter and cargo aircraft is shown in Figure 119. The throat area for the primary flow is calculated by Equation (242) for choked flow. At off-design conditions, the performance map is utilized to predict the amount of water the ejector is capable of pumping. From the flow rate ratio obtained from the map, the maximum quantity of water that can be pumped is determined. If the amount of water to be removed is more than that predicted by the performance map for the design, the secondary flow is all-water and the excessive water is accumulated. On the other hand, if the amount of condensate is less than that predicted by the performance map, the secondary flow is a mixture of water and cold air. The cold air removed as well as the bleed air constitutes a penalty for using the aspirator at this condition. For simple evaluations, the amount of cold air is ignored if the condensate to be removed is greater than fifty percent of that predicted by the performance map. If it is less than fifty percent, the amount of cold air removed is assumed twice the primary air flow rate.

The weight of an aspirator is assumed to be included in the heat exchanger or duct assembly weight.

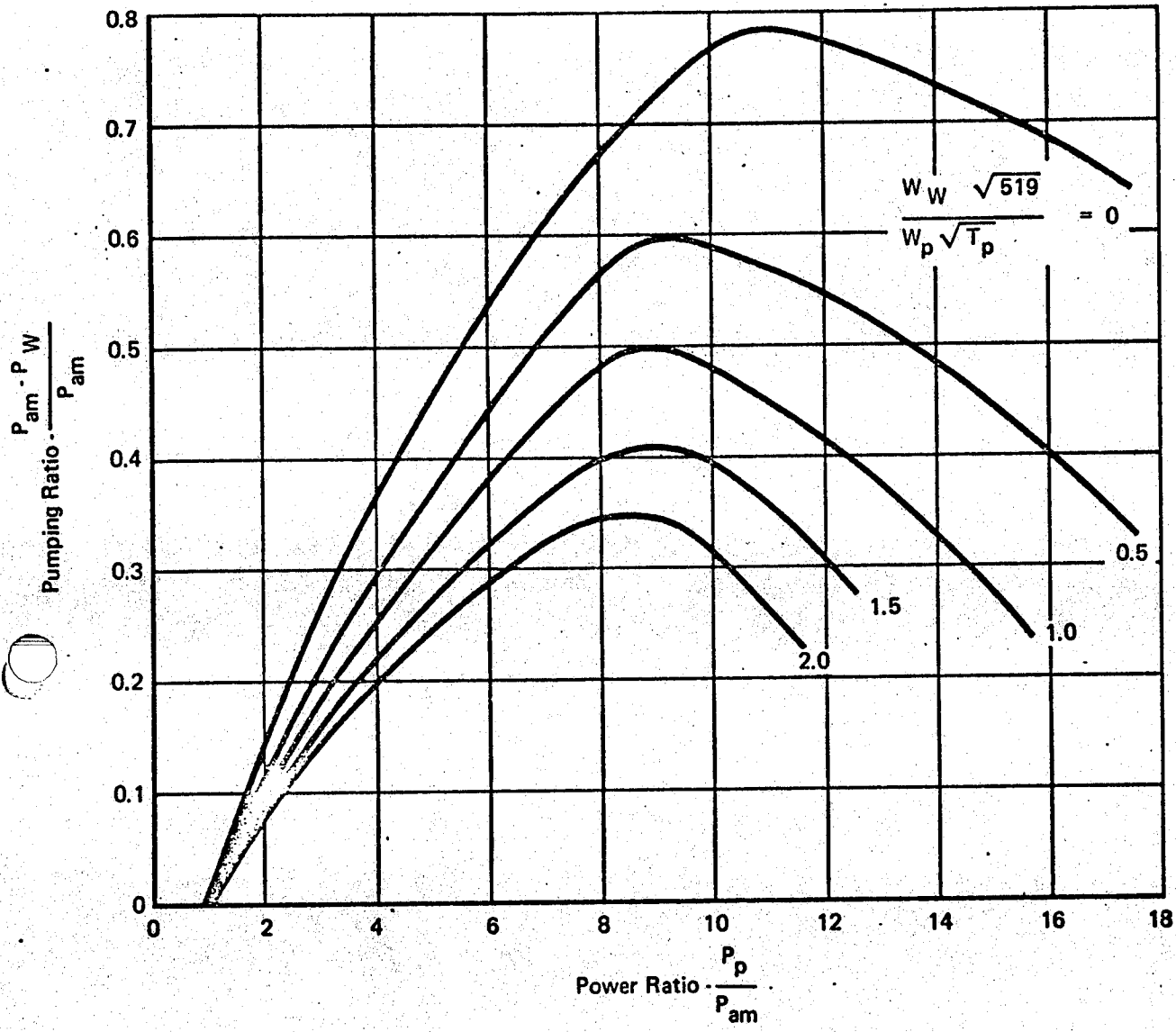


Figure 119 Performance of Typical Aspirator

GP 9416-73

3.10.5 Valves - The types of valves considered include butterfly, poppet, and split flapper check valves. Their functions are flow control, pressure regulation and shutoff, temperature regulation and shutoff, or merely shutoff without regulation. Butterfly and poppet valves considered in this study are pneumatically, electro-pneumatically, or electrically actuated. Manually operated valves are not considered due to their infrequent usage in ECS. Most of the valves considered are made of aluminum or steel depending on the operating temperature, although titanium valves have been proposed. The size of the duct normally dictates the bore diameter of valves.

Pressure Drop - Pressure drop performance at a fully opened position is presented for each type of valve. This represents the minimum pressure loss that a valve has for a given flow rate. At other than fully opened position the valve is performing a function where the downstream pressure is known (e.g. pressure regulator), or it may function as a temperature or flow regulator where the pressure drop is unimportant.

Butterfly valve pressure drop data ($\Delta P_T / P_{T1}$) at fully opened positions from a variety of sources are related to the corrected flow rate ($W \sqrt{T_{T1}} / P_{T1} D^2$). Considerable variance is found in the data. This variance can not be related to bore diameter. Probably it is due to flapper thickness. (See Reference 30.) However, this detail is not available. The upper and lower boundaries of the data are shown in Figure 120. General valve performance is given in Reference 30 in terms of a pressure loss coefficient (K_t):

$$\Delta P_T = K_t [\rho(v')^2 / 2 g_c] \quad (243)$$

The pressure loss coefficients (K_t) of Reference 30 vary from 0.13 to 0.6 depending on the flapper thickness relative to the valve diameter. The above equation is rewritten in terms of the pressure drop ratio and the corrected flow rate:

$$\frac{\Delta P_T}{P_{T1}} = (3.74 \times 10^{-4}) K_t \left(1 + \frac{Y-1}{2} M^2\right)^{\frac{Y-1}{Y-1}} (W \sqrt{T_{T1}} / P_{T1} D^2)^2 \quad (244)$$

A pressure loss coefficient equal to 0.43 (shown in Figure 120) provides good mean correlation at low values of the corrected flow rate, is somewhat high at intermediate values, and is slightly low at the higher corrected flow rates. It is considered typical of current aircraft butterfly valves. Knowing the typical value of K_t , and assuming a typical Mach number as indicated in Section 3.10.1, the pressure drop is evaluated as follows:

$$\Delta P_T = K_t \gamma P M^2 / 2. \quad (245)$$

If the valve diameter (D) is known, the following equation is used for more accurate pressure drop calculation:

$$\Delta P_T = (1.008 \times 10^{-3}) K_t \frac{W^2}{\rho_1 D^4} \quad (246)$$

This equation is obtained by combining the continuity equation and Equation (243). The above two equations also are used for pressure drop calculations of poppet valves and check valves.

Values of K_t for poppet valves are taken from Reference 30. When utilized in Equation (243) to calculate the pressure drop at fully opened conditions,

$K_t = 2.74$ with the stem 45° from line of pipe,

$K_t = 3.40$ with the stem 60° from line of pipe, and

$K_t = 6.50$ with the stem in 90° pipe bend.

The pressure drop for split-flapper check valves is:

$$\Delta P = K_w^2 \quad (247)$$

Variations of K from a number of sources with respect to valve diameter are shown in Figure 121. The mean value of K is represented by the following equation:

$$K = (9.0 \times 10^{-3}) D^{-4} \quad (248)$$

This mean value of K is equivalent to $K_t = 0.68$ in Equation (243).

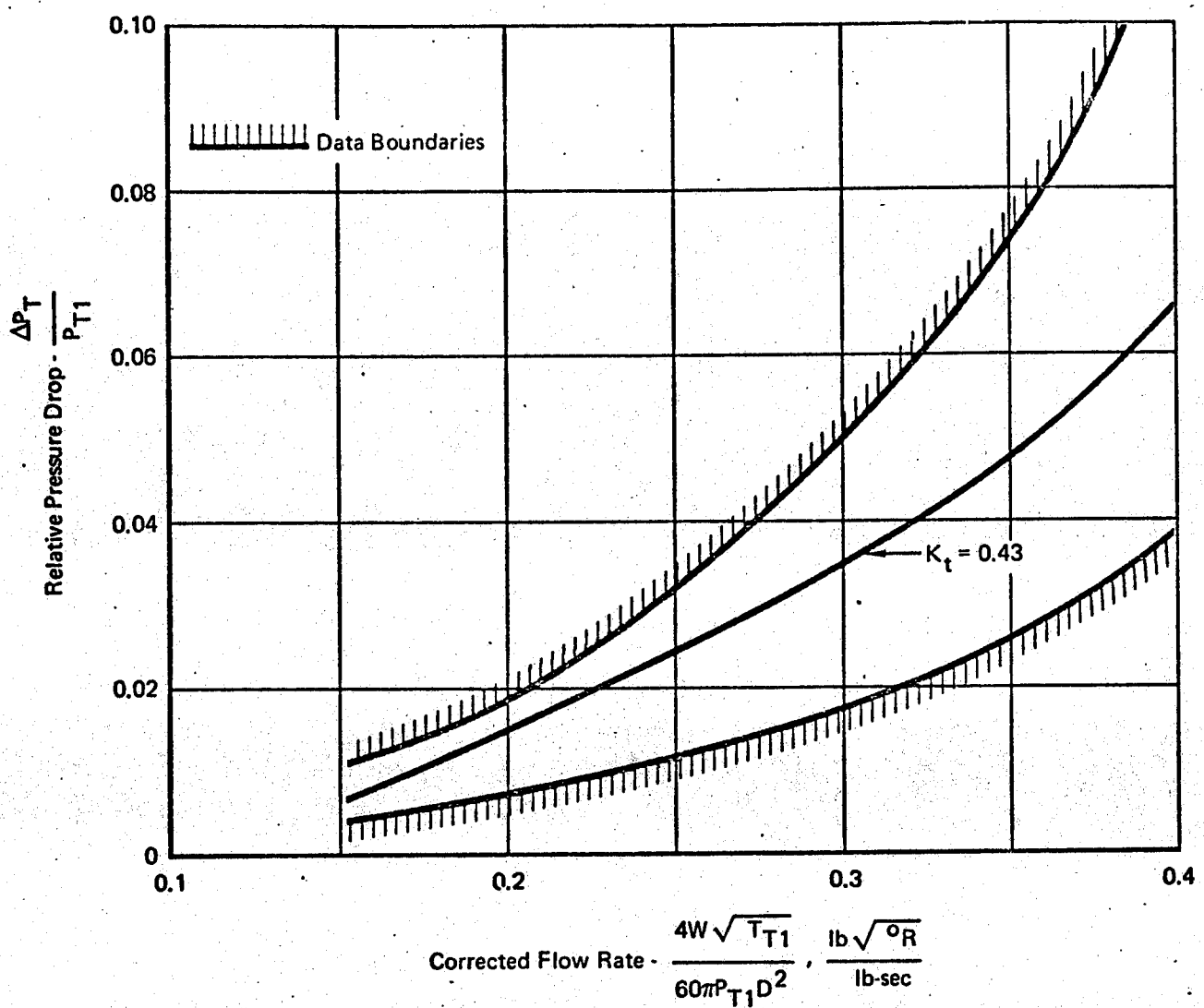


Figure 120 Butterfly Valve Pressure Drop (Fully Opened Position)

GP 9416-89

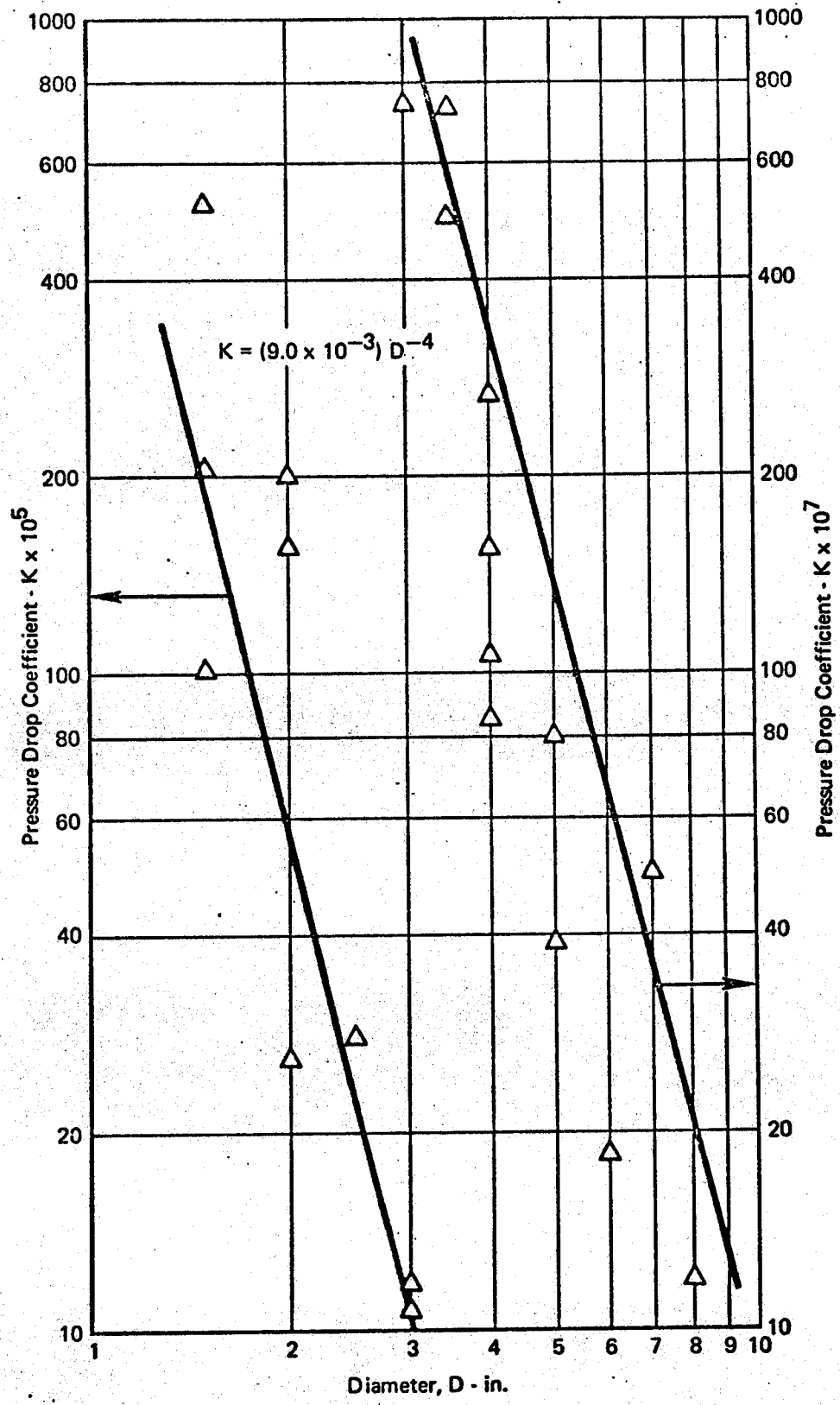


Figure 121 Pressure Drop of Split-Flapper Check Valves

GP 9416-91

Valve Weights - Valve weights for a specific size duct, are very scattered. One reason is design requirements (such as temperature, pressure, life, and leakage) which determine the type of metal used (i.e. various steel and aluminum alloys). Different mechanical requirements (e.g. types of flanges, fittings, mounting provisions, etc.) affect valve weight. Commonality of valves used on a specific aircraft broadens the weight variation (e.g. all bleed air valves on some aircraft use the same actuators even though some valves require modulation and shut-off and others require only the on/off function). All of the weight data are correlated versus inside valve diameter for each of the three valve types (butterfly, poppet, and check).

Steel valves generally are used for operating temperatures of 500°F or above. Aluminum valves are used for lower temperatures. This borderline temperature for steel and aluminum valves is a compromise among different borderline temperatures adopted by different valve manufacturers.

The weights of pneumatically actuated steel and aluminum butterfly valves are shown in Figure 122. The electro-pneumatic and pneumatic actuated valves are considered in the pneumatic category, since the electric portion of the electro-pneumatic actuator is relatively small. The steel valve weights are represented by Equation (249) (with a standard deviation of 35.4%).

$$Wt = 2.68 D - 1.0 \quad (249)$$

The following two equations fit the data for aluminum butterfly valves:

$$Wt = 0.70D + 0.35; \text{ for } D \leq 2.5 \text{ inch (minimum} = 0.5 \text{ lb.)} \quad (250)$$

$$Wt = 1.26D - 1.05; \text{ for } D > 2.5 \text{ inch.} \quad (251)$$

The standard error of this correlation is 33.9%. Weights of typical electric motor actuated butterfly valves are shown in Figure 123. Weight equations for steel and aluminum valves are:

$$Wt = 1.14D + 0.9 \quad (\text{Steel}) \quad (252)$$

$$Wt = 0.56D + 1.1 \quad (\text{Aluminum}) \quad (253)$$

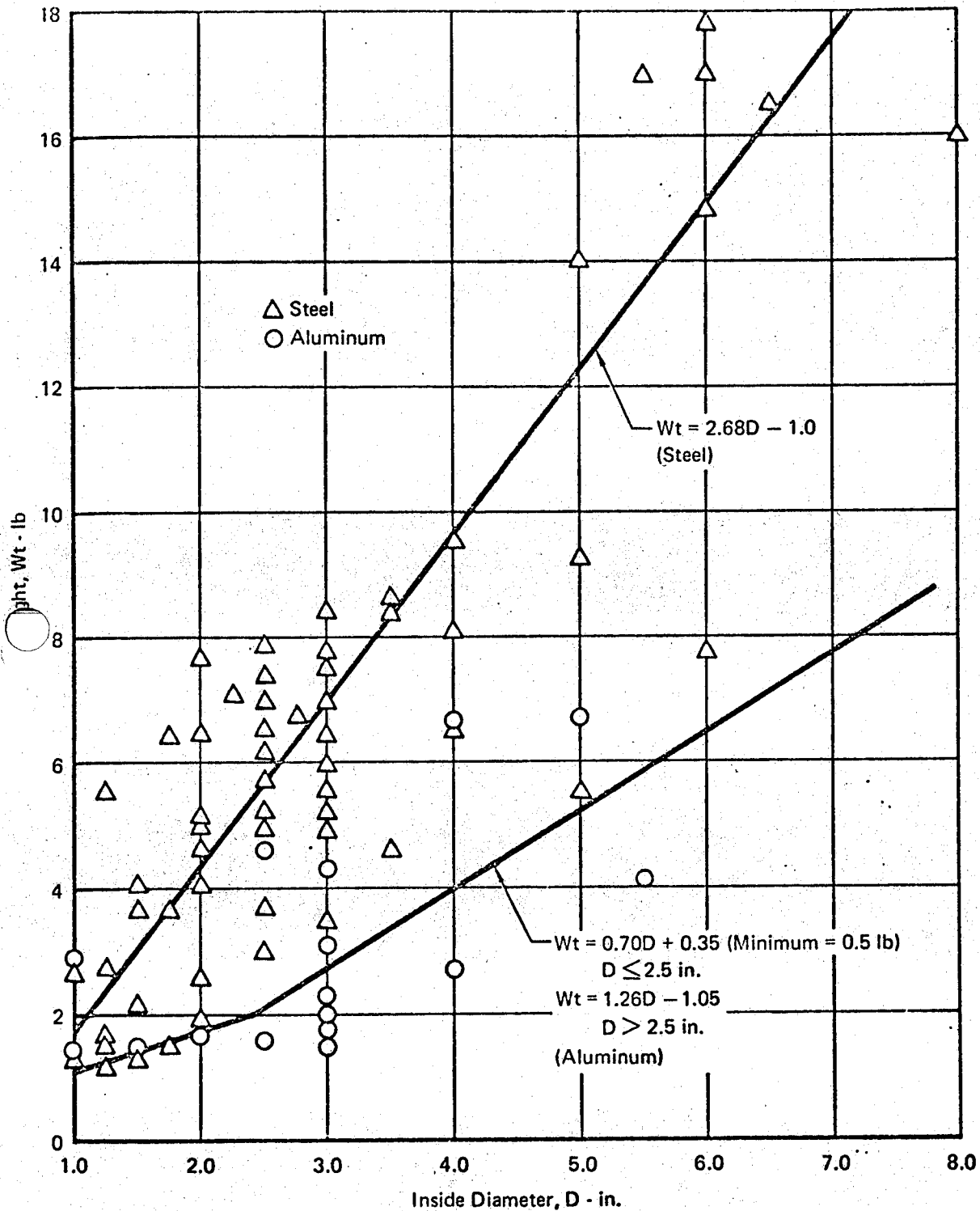


Figure 122 Weights of Pneumatically Actuated Butterfly Valves and Actuators

GP 9416-82

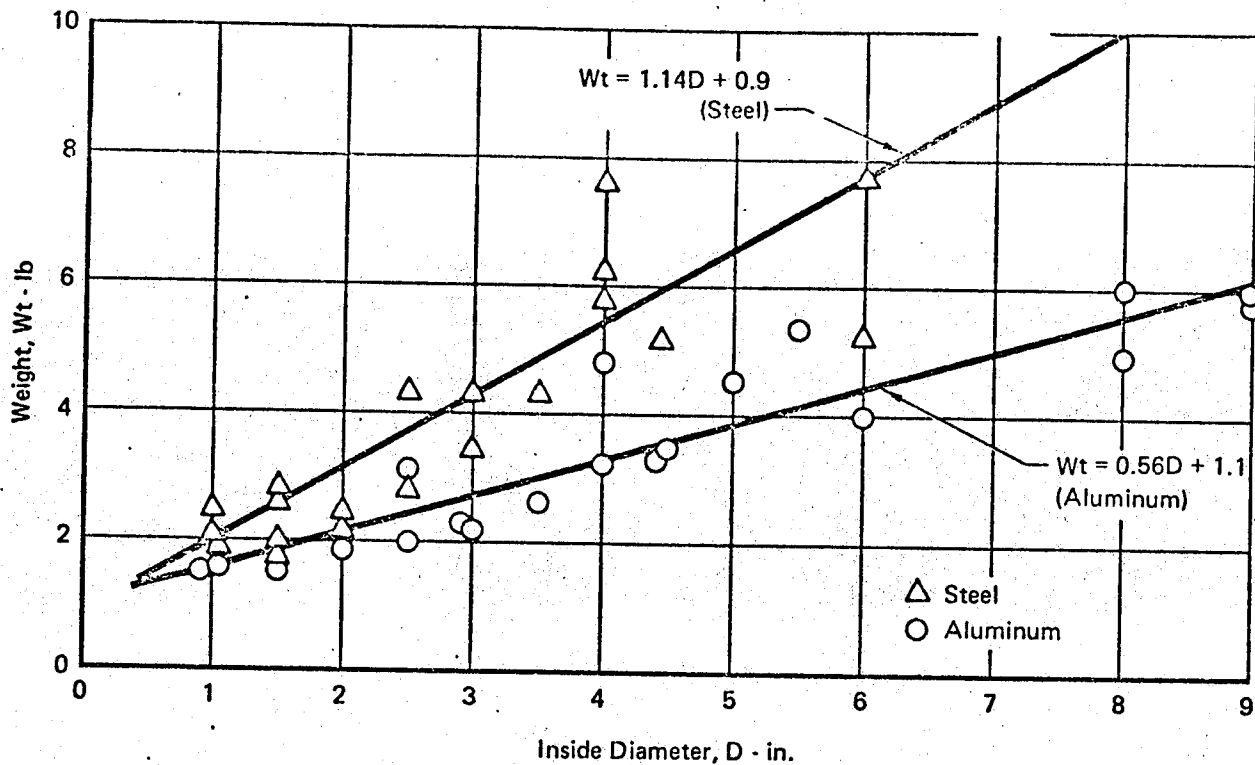


Figure 123 Weights of Electric Motor Driven Butterfly Valves and Actuators

GP 9416-43

Electric motor actuated valves tend to be lighter than the pneumatic actuated valves, as indicated by comparing Figures 122 and 123. The standard error of the electric motor actuated butterfly valves are 20.1% and 17.4%, respectively. The trend is more significant for steel valves than for aluminum valves.

There is no discernible difference in weight between pneumatic and electrical actuated poppet valves. (See Figure 124.) This observation differs from that for the butterfly valves, as is shown in Figures 122 and 123 for diameters above one inch. However, most of the poppet valves are one inch and less, and in this area the butterfly valve data show a converging trend toward the same weight for either type. Thus, at smaller diameters the type of valve actuator has little effect on either butterfly or poppet valve weight. The following two equations represent the weights of steel and aluminum poppet valves:

$$Wt = 2.04D + 0.225 \quad (\text{Steel}) \quad (254)$$

(Standard error = 34.8%)

$$Wt = 0.833D - 0.05 \quad (\text{minimum} = 0.3 \text{ lb}) \quad (\text{Aluminum}) \quad (255)$$

(Standard error = 30.3%)

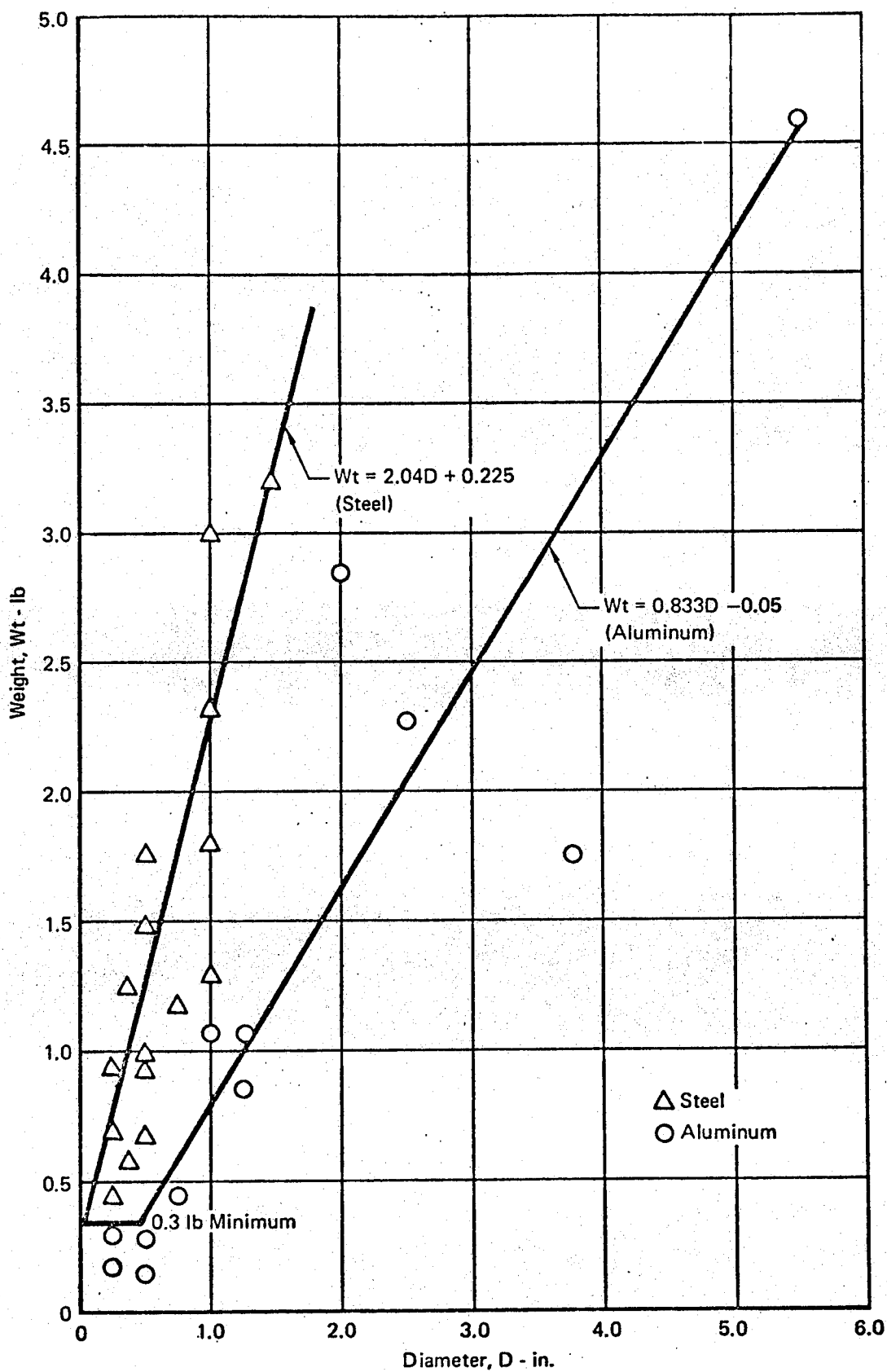


Figure 124 Weights of Poppet Valves and Actuators

GP 9416-93

The variations in the weight of check valves are due primarily to the operating temperature and pressure which determine the thickness of the flapper and valve body. The type of flanges used to accommodate a particular installation also affects the weight. Weights for typical split-flapper check valves are shown in Figure 125. Equations for the weight of steel and aluminum check valves are:

$$Wt = 0.625 D = 0.625 \quad (\text{Steel}) \quad (256)$$

$$Wt = 0.33 D - 0.38 \quad (\text{minimum} = 0.25 \text{ lb}) \quad (\text{Aluminum}) \quad (257)$$

Standard errors of these correlations are 35.9% and 30.0%, respectively.

The valve weight correlations presented herein are typical for many current aircraft. However, the use of titanium and sheet metal fabrication methods result in reduced weights of up to twenty percent for some new and proposed aircraft valves. Further data on ECS valves can be obtained from References 60 and 61, and from other manufacturers of valves for aircraft ECS.

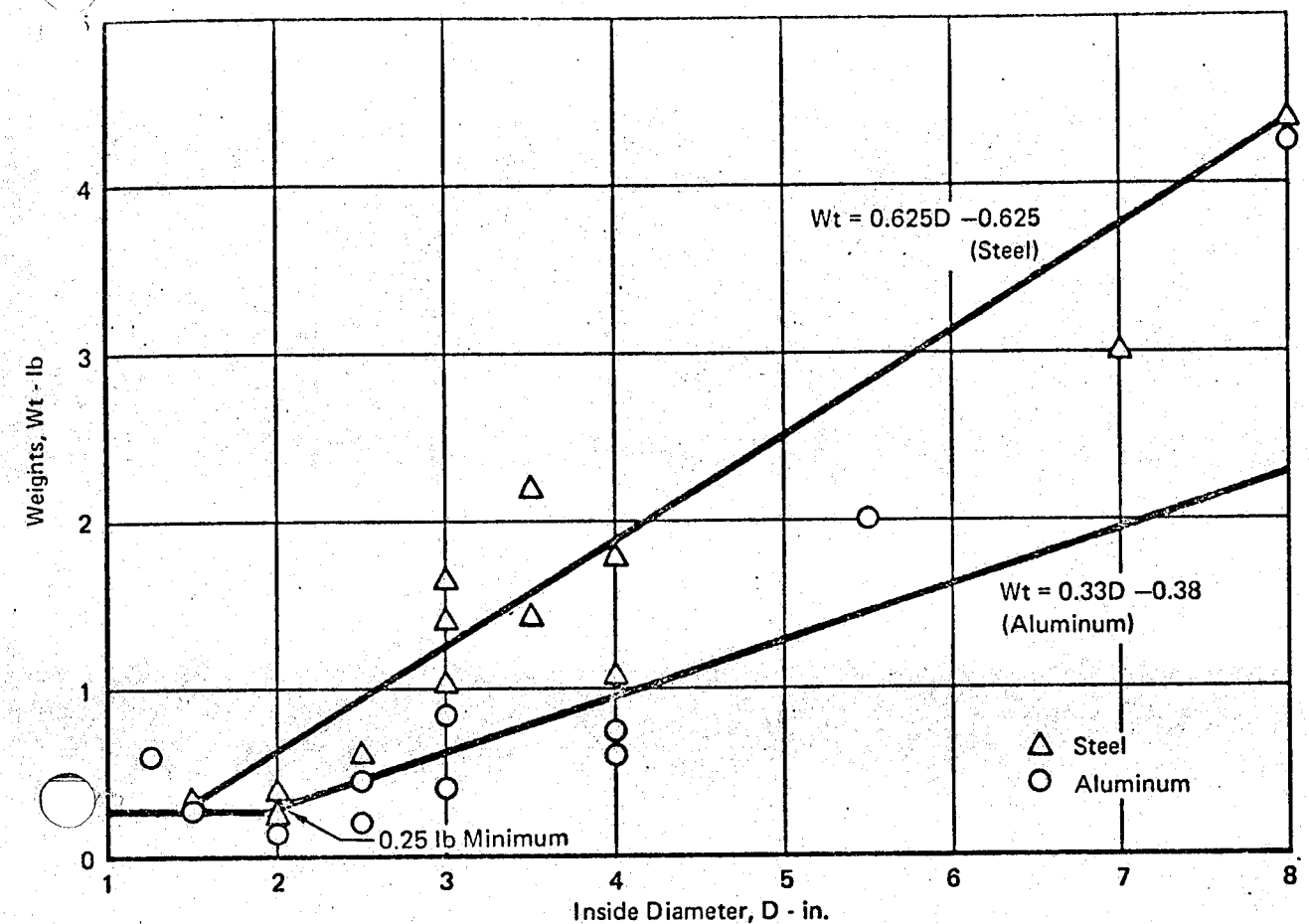


Figure 125 Weights of Split-Flapper Check Valves

GP 9416-92

3.11 Insulation

Design data on ECS ducting insulation and thermal insulations on aircraft compartment surfaces and fuel tanks are discussed in this section.

3.11.1 Ducting Insulations - Requirements for insulation on bleed air ducting and on conditioned air distribution ducting are presented. Data describing insulations which satisfy these requirements are discussed.

3.11.1.1 Bleed Air Duct Insulation - Insulation designs to meet duct insulation requirements are presented.

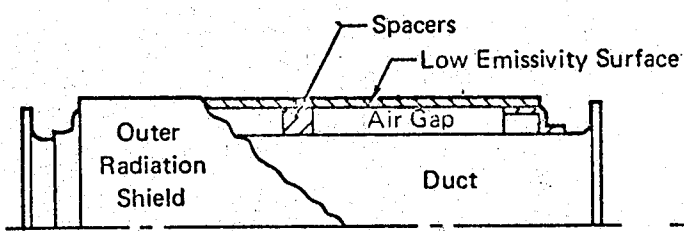
Military specifications applicable to bleed air ducts indicate that duct insulation is recommended for three specific design conditions. Bleed air ducts need not be insulated for other conditions. The conditions requiring insulation are as follows:

- (1) Sufficient insulation is required to prevent the temperature of adjacent structure or hardware from exceeding 250°F due to heat transfer from the bleed air duct. This temperature should be increased in future aircraft using high temperature structural materials. Protection from impingement of hot air from small leaks in bleed air ducts also is required.
- (2) Insulation is required to maintain an external surface temperature below the self-ignition temperature of a flammable fluid to which a duct may be exposed. This temperature is 500°F for still, ambient air. If the air flows past the duct at 6 feet per second or greater an external surface temperature up to 700°F is allowed.
- (3) Insulation is used to reduce the heat load from the bleed air duct in an air conditioned compartment.

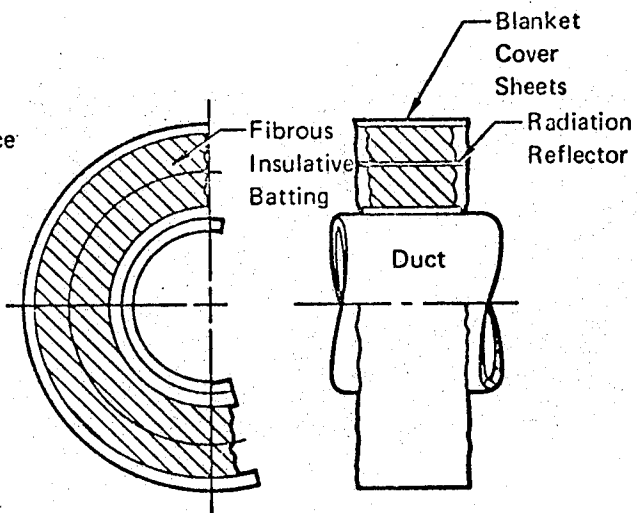
Description - Two basic types of duct insulations are used. The types are a cylindrical "air gap" radiation shield insulation, and an insulating blanket consisting of fibrous insulation batting enclosed in a protective cover material. Sketches of the basic types of duct insulation are shown in Figure 126. The insulations are described relative to cylindrical duct cross-sections. Both integral or removable types of insulation are available. The integral type is a permanent part of the duct assembly. It also strengthens the duct.

Use of the air-gap radiation shield insulation is limited to duct temperatures below about 700°F due to material temperature limitation. It also is limited by the temperature drop attainable across the shield. The outer

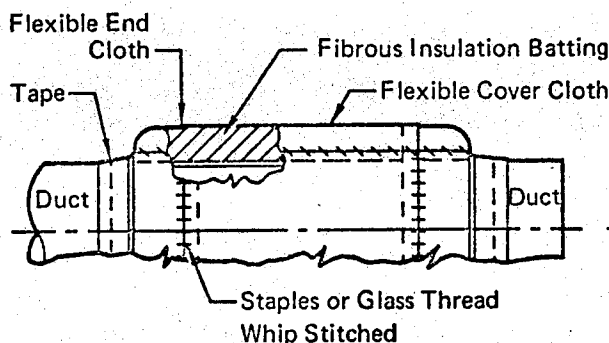
(A) Radiation Shield, Air-Gap Type



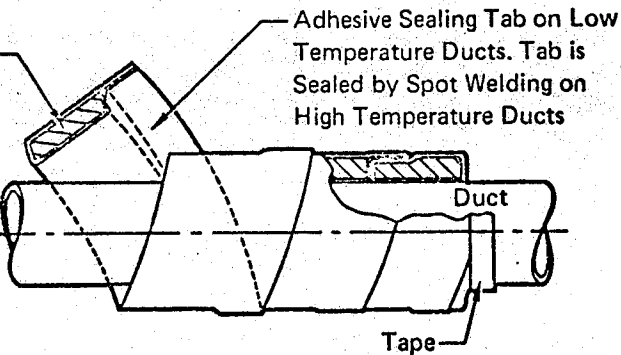
(B) Blanket-Type, Removable, with Radiation Reflector



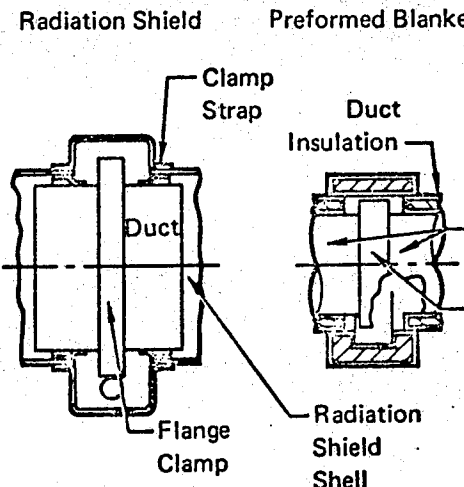
(C) Blanket-Type, Integral



(D) Wrap-Around Type



(E) Duct Flange Clamp Insulation



(F) Expansion Bellows (Flex Section) Insulation

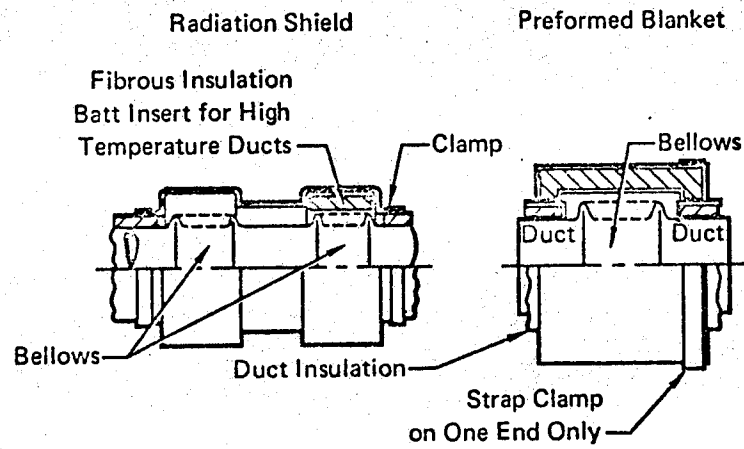


Figure 126 Bleed Air Duct Insulations

GP 9416-3

shell is the radiation shield. (See Figure 126A.) This shield has a low emissivity inner surface, and a high emissivity outer surface. The resultant shell is resilient, and deflects without denting. Dents cause hot spots on the insulation. The shell material may be dimpled or corrugated to improve its rigidity. The air gap is maintained by spacers between the duct and the outer shell. The spacers are made of a high temperature bonded fiberglass, (e.g. silicone impregnated fiberglass). The spacers do not go all the way around, and special cross-sectional geometries are available to minimize heat leak through the spacer. Radiation shield insulations with gap sizes of 1/4, 3/8, and 1/2 inch are available.

The removable type is preformed as two half sections, or as a non-preformed wrap-around insulation. Both of the removable forms are held in place by various fastening techniques. Duct flange latches or clamps, valves, expansion bellows, flexible sections, and compensators generally are insulated with preformed, removable insulation covers. The covers are blanket-type insulations on high temperature ducts (over 700°F). On low temperature ducts the covers are radiation shields made of preformed, elastomer-impregnated fabric.

The blanket insulations are covered. Insulations are available for continuous service above 2000°F duct temperatures, with possible short term operation to about 3000°F.

An extra insulation cover, adjacent to the duct, is required on the removable blanket insulations. A radiation reflector, or shield, can be sandwiched between several layers of insulation in order to minimize the radiative heat transfer through the insulation. (See Figure 126B.)

An integral blanket insulation is shown in Figure 126C. Integral blanket insulation is applicable to duct temperatures up to about 1400°F.

The wrap-around removable insulation is supplied as long tapes, or ribbons, which are wound around the duct along a helical path (Figure 126D), or as a complete wrap-around blanket. Use of the removable, wrap-around insulations generally is limited to straight sections of the duct. An adhesive tab along mating edges of the insulation seals the insulation during application. The adhesive sealant is limited to low duct temperatures. On higher temperature ducts the insulation cover is a metal foil, and the edge tab is spot welded.

Preformed, blanket-type insulation covers for duct assembly expansion bellows and flange clamps are shown in Figures 126E and 126F. The covers are held in place by straps, and the edge flaps of the covers rest on the top of the duct insulation. The blanket-type covers are semi-rigid, and upon heating they expand at a different rate than the rest of the duct assembly. Consequently, the bellows cover generally is strapped down on one end.

Removable radiation shield "boots" of preformed, flexible, impregnated fabrics are used to insulate low temperature duct assembly expansion bellows sections, tolerance compensators, and duct-end flange clamps. (See Figures 126E and 126F.) The inside surface of the fabric has a low emissivity. The edge flaps of the "boot" are strapped down on top of the duct insulation. These light-weight shields also can be used on high-temperature, blanket insulated ducts. The upper temperature application limit of the radiation shield insulation is extended by insertion of a loose layer of fibrous insulation batting between the duct and the shield, as shown in Figure 126F.

Performance and Sizing - The performance of bleed air duct insulation is defined in terms of the outer surface temperature of the insulation. Heat is dissipated from the outer surface of the duct insulation by convective and radiative heat transfer. Heat transfer rates at the three design surface temperatures (i.e. 250°F, 500°F, and 700°F) are shown in Figure 127 for a range of surface to ambient temperature differentials. These heat transfer rates (per unit length of ducting) are dependent on the outer surface diameter of the insulation (D_S). Figure 127 also is applicable to bare (uninsulated) ducts. Radiative heat transfer from the insulation or duct is:

$$q'_r/L = \sigma\pi D_S e [(T_S)^4 - (T_{am})^4] \quad (258)$$

where e is the surface emissivity. Forced convective cooling generally is provided for high surface temperatures (above 500°F). Forced convection heat transfer is estimated by:

$$q'_c/L = 0.066 \pi (\rho V' D_S)^{0.6} (T_S - T_{am}). \quad (259)$$

The forced convection heat transfer rate for the 700°F surface temperature Figure 127 is based on the more complete equations of Reference 62. An

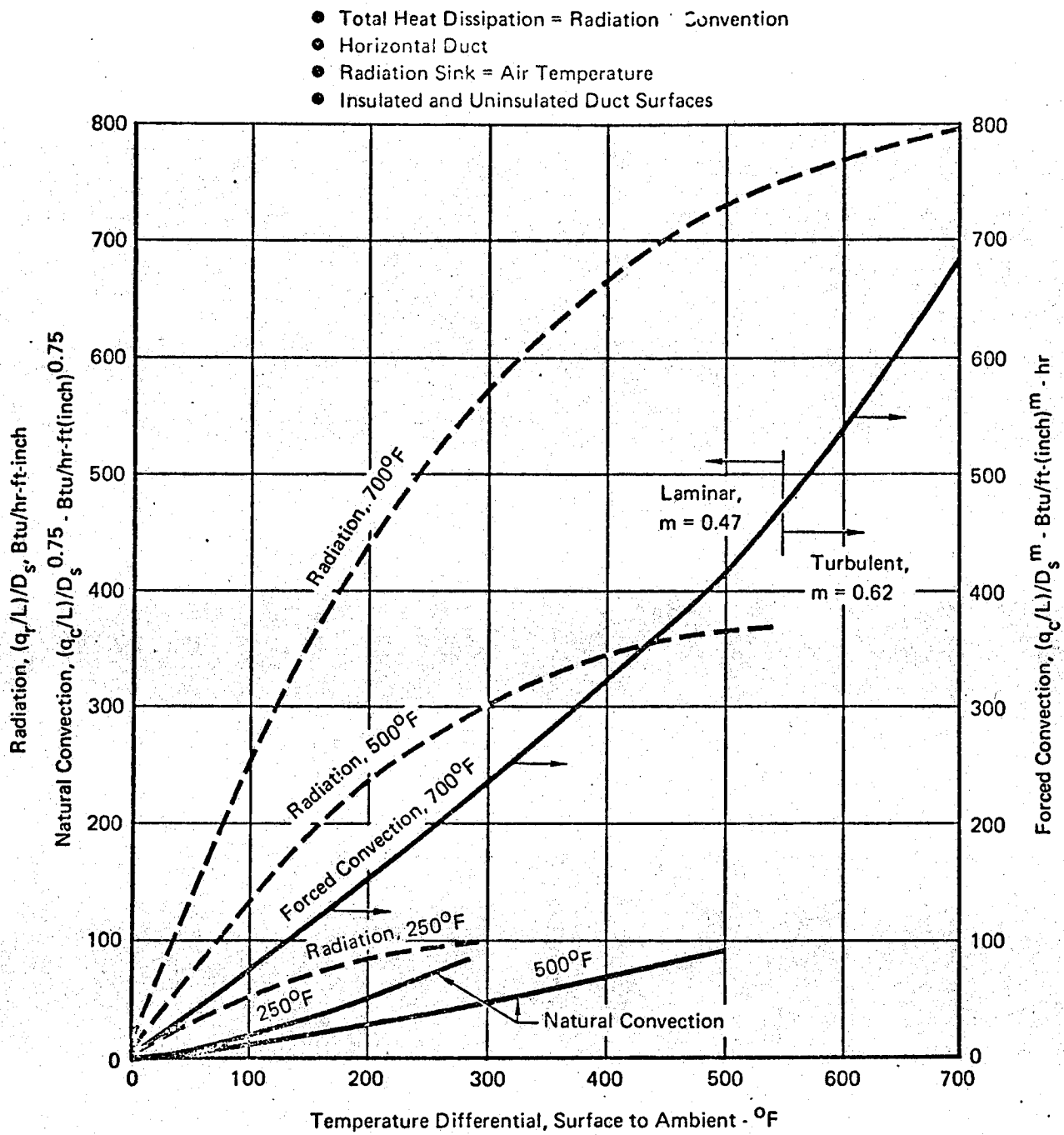


Figure 127 Duct Heat Dissipation

GP 9416-71

estimate for natural convection (from Reference 62) is:

$$q'_c/L = 0.001 \pi D_S^{0.75} \left(\frac{\rho}{\rho_{std}} \right)^{0.5} (T_S - T_{am})^{1.25} \quad (260)$$

Air gap radiation shield duct insulation is used for outer surface temperatures of 250°F. The heat dissipation on the surface of the shield is equated to the heat flow across the air gap. When solved for the surface temperature (T_S), the heat balance equation has the form:

$$T_S = (K_1 T_D + K_2 T_{am}) / (K_1 + K_2). \quad (261)$$

K_2 is a heat transfer parameter for the outside of the radiation shield.

$$K_2 = \frac{D_S}{12} (h_c + h_{rS}) \quad (262)$$

K_1 is a heat transfer parameter for the gap between the duct and the radiation shield.

$$K_1 = (D_D h_{rD} / 12.) + [(2k_{air} + 0.045 w k_{spacer}) / \ln (D_S/D_D)] \quad (263)$$

where w is spacer width. Both heat transfer parameters are functions of T_S , and Equation (261) is solved by iteration. Equation (261) neglects the heat leak through the radiation shield supports at the duct ends and the interface resistances at contact points in the shield assembly. It is assumed that the radiation sink temperature equals the ambient air temperature. The heat dissipation per foot of ducting is:

$$q'/L = (\pi/12) K_1 (T_D - T_S) = (\pi/12) K_2 (T_S - T_{am}) \quad (264)$$

Blanket insulation is used for all three design surface temperatures. The heat dissipation from the insulation surface is equated to the heat flow through the insulation. When solved for the insulation surface temperature (T_S), the heat balance equation is:

$$T_S = (T_{am} + K_4 T_D) / (1 + K_4) \quad (265)$$

where K_4 is a heat transfer parameter defined as follows:

$$K_4 = 24k_i [D_S (h_c + h_{rS}) \ln (D_S/D_D)]^{-1} \quad (266)$$

Since h_{rS} and h_c are dependent upon T_S , Equation (265) is solved by iteration. This equation applies to integral or removable blanket-type insulations. Miscellaneous heat leaks and effects of a radiation shield sandwiched within the insulation are neglected. The heat dissipation per foot of ducting is:

$$q'/L = \pi D_S (h_c + h_r)(T_S - T_{\text{amb}}) = 2\pi k_i (T_D - T_S)/(\ln (D_S/D_D)) \quad (267)$$

Correlation of data shows that both the air gap and blanket insulation thicknesses (t) are estimated by a general equation of the form:

$$t = K_1 (T_D - 460)/(T_S - 0.2 T_D - 416). \quad (268)$$

Values of the constants (K_1) in Equation (268) for a typical three inch diameter, horizontal duct in a 75°F compartment are: for an air gap, $K_1 = 0.06$; for an integral insulation (Figure 126C) of three pounds per cubic foot "AA" fibers in a 0.01 inch fiberglass cover, $K_1 = 0.045$; and for a removable 4.5 pound per cubic foot "AA" fiber insulation with an integral aluminum foil radiation shield (Figure 126B) which is enclosed in 0.002 inch stainless steel foil covers, $K_1 = 0.064$. A correlation of Equation (268) and some typical air gap insulations is shown in Figure 128. (Insulation thickness increments of 1/8 inch are typical.) The estimation is assumed valid up to one inch thickness.

Addition of insulation to ducts with diameters less than a critical duct diameter may result in an increased heat load to a cooled compartment. This problem may occur if the addition of insulation increases the surface area for external heat dissipation. The critical duct diameter is defined in Reference 63.

$$D_D = k/(h_c + h_{rS}) \quad (269)$$

Bleed Duct Insulation Weight - Bleed duct insulation weights are obtained by extrapolating a typical design. Insulation densities are nominally three to nine pounds per cubic foot.

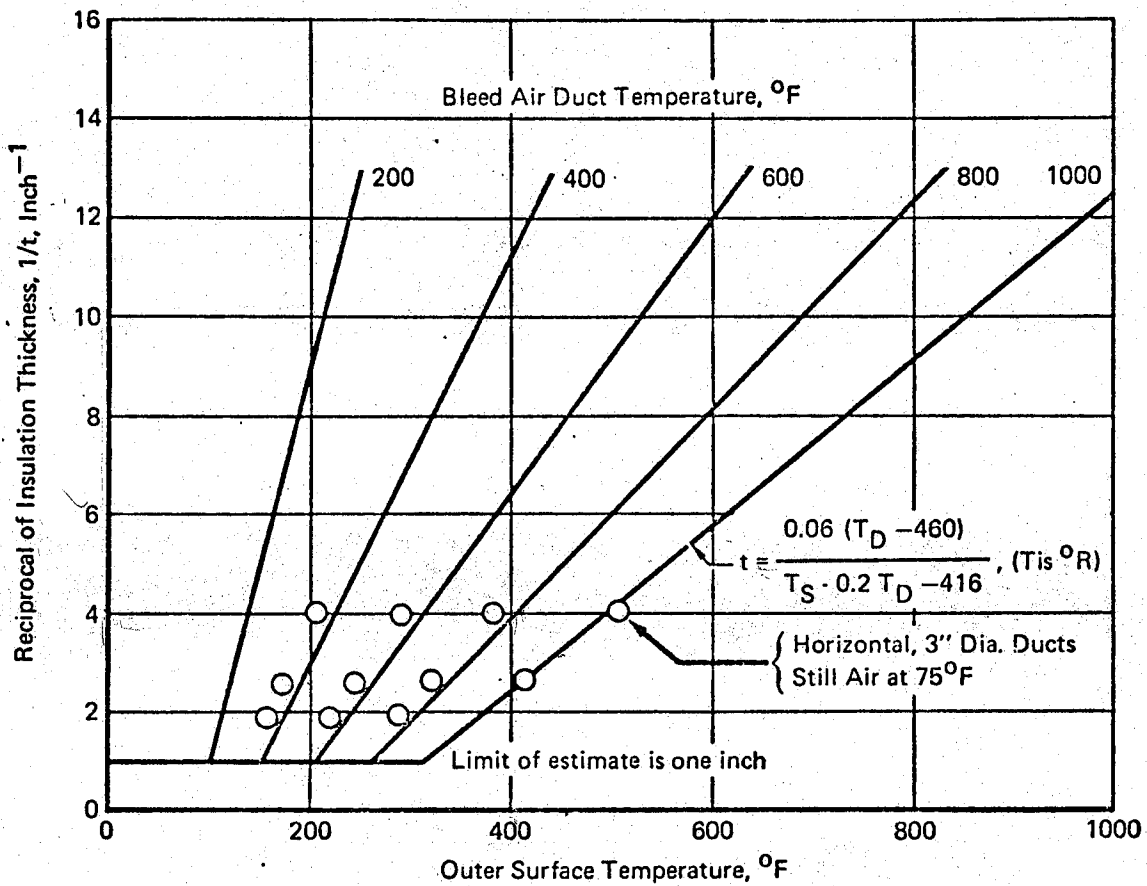


Figure 128 Bleed Air Duct Radiation Shield Air Gap Insulation Thickness

$$\frac{1}{6}$$

$$\frac{1}{t}$$

The weight of air-gap, radiation-shield insulation for a 6-inch diameter bleed air duct with an integral radiation shield is 18 percent of the duct weight. This is used to estimate the weight of air gap radiation shield insulation for gaps of 1/4 inch and 1/2 inch, respectively.

$$Wt/L = (0.0282 D_D + 0.0128)/12 \quad (270)$$

$$Wt/L = (0.0464 D_D + 0.0386)/12 \quad (271)$$

The thickness requirements for 11 air-gap insulation sections were calculated with Equation (268) for 3- to $5\frac{1}{2}$ -inch diameter ducts, and the weight per unit length was determined with Equations (270) and (271). The standard error of these calculated weights is 16.7%. The weight of radiation shield insulation on the flange clamp of a 3.6 inch diameter duct is about 0.08 pounds. Weight for other diameters is:

$$Wt = 0.0153 D_D + 0.0247 \quad (272)$$

Equations (270), (271), and (272) are applicable to duct diameters of about one inch or greater. The weight of radiation shield insulation on the expansion bellows of a 3.6-inch diameter duct is about 0.22 pounds. By extrapolating this value to other duct diameters, the weight is estimated as 6% of the duct diameter (inches).

The estimated weight for removable, blanket type bleed air duct insulation is based on the use of an aluminum foil reflector. The insulation is enclosed on both sides by stainless steel foil. The weights for insulation thickness of 1/4 and 1/2 inch (respectively), a duct diameter greater than 1.5 inches, and various bulk densities (ρ_{bu}) are:

$$Wt/L = \frac{1}{12}[(0.0051 \rho_{bu} + 0.12) D_D + (0.0025 \rho_{bu} + 0.191)] \quad (273)$$

$$Wt/L = \frac{1}{12}[(0.011 \rho_{bu} + 0.12) D_D + (0.0046 \rho_{bu} + 0.422)] \quad (274)$$

The standard error for 9 sections of removable insulations (4.5 pcf) on 3 inch diameter ducting is 5.5%, using the thickness estimated with Equation (268).

The estimated weight for an integral, blanket-type insulation of 3 inches of insulation, with a 0.006 inch thick stainless steel outer cover, and a 0.002 inch thick aluminum radiation reflector is:

$$Wt/L = \frac{1}{12} [(0.066t + 0.0706) D_D + (0.18t - 0.007)] \quad (275)$$

Equation (275) was used to determine the thicknesses of 12 integral insulations (3 and 6 pcf) on 2-1/2 to 5 inch diameter ducting. Using these thicknesses, the standard error of Equation (275) is 14.9%.

The weight of a blanket type duct flange clamp insulative cover, for duct diameters of about one inch or greater, including two attachment straps, is:

$$Wt = 0.0023 D_D^2 + 0.01 D_D = 0.0088 \quad (276)$$

The weight of a blanket type insulative cover for an expansion bellow, for duct diameters of 1.5 inches or greater, and including the weight of one attachment strap, is:

$$Wt = 0.067 D_D + 0.119 \quad (277)$$

3.11.1.2 Conditioned Air Distribution Duct Insulation - Insulation is used on conditioned air distribution ducts which are routed through areas of high or low ambient temperatures relative to the conditioned air to prevent excessive heat gain or loss.

Description - Two basic types of insulation designs are used for conditioned air distribution ducts. These types are classified as external or integral insulations.

The external insulations are applied to the outside of the duct after duct fabrication. The common external insulation used in many aircraft is an insulation blanket which is wrapped around the duct and strapped in place. The insulation designs are similar to the designs for bleed air ducts except lower temperature materials are used. A phenolic-bonded, "B" fiber insulation batting enclosed in a light weight cover material is typical. A bulk density 0.6 pounds per cubic foot is available in standard thicknesses of 3/8, 1/2, and 2 inches. The cover material is a plastic film, reinforced with

synthetic yarn or glass threads, which serves as a vapor barrier. A variation on this design concept is to use a plastic foam instead of fibrous insulation batting. If open cell foam is used, the foam must be enclosed in an impervious film to exclude water and fuel vapors. The foam insulation thickness only needs to be about 2/3 as thick as the fibrous insulation but it is about twice as heavy.

Integral insulation-duct assemblies are an open cell, 2 to 3 pounds per cubic foot plastic foam sandwiched between sheets of fiberglass-resin laminate. (See Figure 129.)

Distribution ducts made of plastics and fiberglass-resin laminate sheeting are somewhat self-insulating due to the low thermal conductivity of the duct material. Flexible ducting made of elastomer-impregnated fiberglass cloth is in the same category. Both types are used extensively.

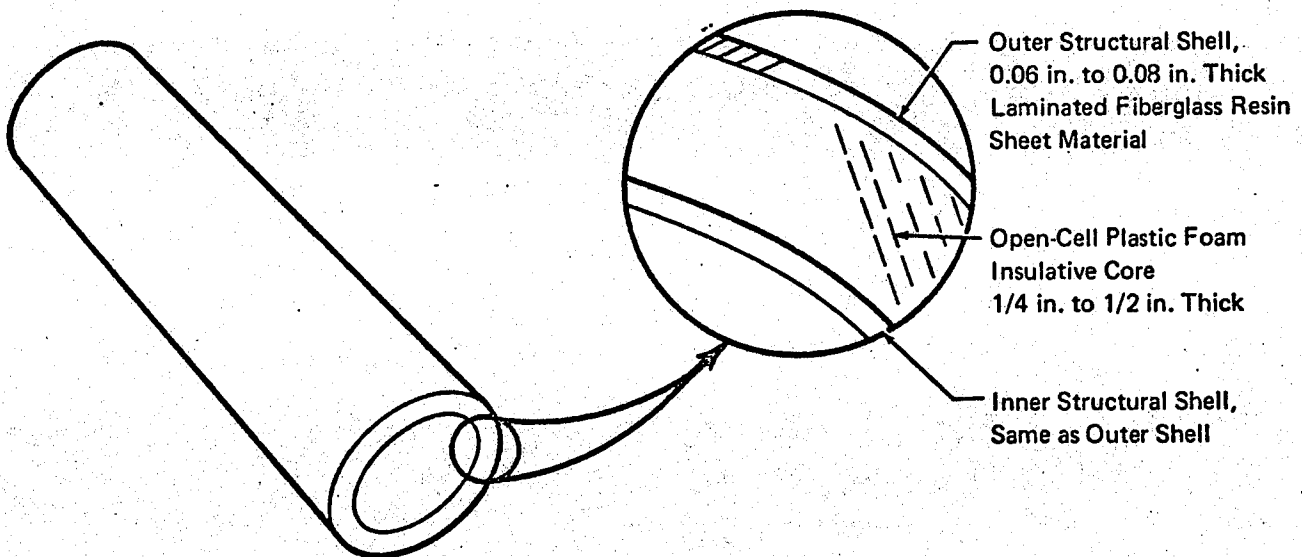


Figure 129 Typical Integral Insulation - Duct Design for Conditioned Air Distribution Duct

GP 9416-34

Performance and Sizing - Performance of blanket insulation is obtained

for cylindrical ducts as a heat leak per foot of duct.

$$q'/L = \frac{2\pi k_i \Delta T}{\ln \frac{D}{D+2t}} \quad (278)$$

$$t = (D/2)(e^m - 1) \quad (279)$$

where:

$$m = 2\pi k_i \Delta T / (q'/L)$$

ΔT is the temperature differential across the insulation. This is estimated as the temperature differential between the conditioned air and the ambient temperature. Several layers of standard batting can be wound onto a duct, if necessary, to achieve the desired thickness. These equations also provide an approximation for the foam thickness on the walls of cylindrical distribution ducts with integral foam-fiberglass laminate configuration. For non-cylindrical distribution ducts an equivalent duct diameter (D_e) is used. The equivalent diameter (D_e) is based on ducts having equal perimeters.

Weight - The weight of removable, blanket type distribution duct insulation is based on an insulation bulk density of 0.6 pounds per cubic foot.

$$Wt/L = \frac{\pi}{12} (D_D + t) [(\rho_S/6.) + 0.00417t] \quad (280)$$

ρ_S is the insulation cover specific weight (lb/ft^2). The total weight of the integral distribution duct is:

$$Wt/L = \frac{1}{12} (D_D + t) (0.1167 + 0.0153t) \quad (281)$$

Based on the accuracy of the weight equations for insulation on bleed air ducts, the error of this equation is estimated as 15%.

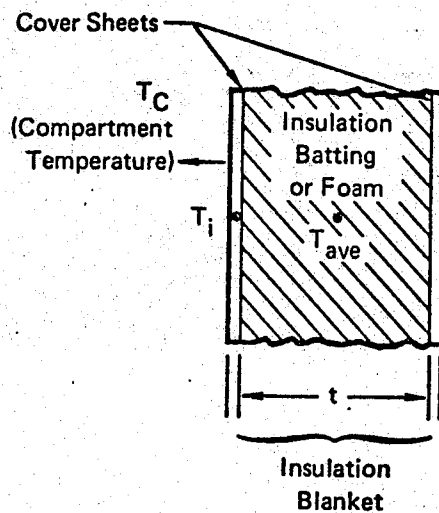
3.11.2 Compartment Insulations - Insulating materials provide thermal and acoustical environmental control of compartments occupied by the crew and passengers, and for some equipment compartments. Only thermal control is provided for cargo compartments. The insulation requirement which exceeds the acoustical requirement is considered herein.

MIL-E-38453 (Reference 3) specifies that the maximum allowable temperature of surfaces which the occupants may "see" during flight shall be 105°F, with no areas cooler than 40°F. MIL-E-18927D(Wep) (Reference 64) specifies that the cabin temperatures in pressurized aircraft shall be maintained in the comfort zone (60° to 80°) during steady state or mild transient aircraft operational conditions. Cabin temperatures during severe transient operations (e.g. combat) are allowed to exceed the comfort zone for brief periods. The cabin temperature comfort zone is 50 to 100°F if the occupants wear pressure suits.

Description - Two aircraft compartment wall thermal insulation designs are presented: insulating blankets, and insulating blankets with an air gap. Typical floor thermal insulation designs are described also.

Blanket insulations are made of fibrous insulation batting which are covered on both sides and stitched together so they can be handled repeatedly without damage. (See Figure 130.) The cover on the cabin side is a vapor barrier. The insulation batting generally is fiberglass fibers bonded with a phenolic or silicone resin. These resins are limited to temperatures below 400°F to 750°F, respectively. Blankets intended for higher temperature applications are made of unbonded fiberglass batting. Most aircraft use 0.6 pound per cubic foot fiberglass insulation batting. The batting is available in thicknesses of 3/8, 1/2, 1, and 2 inches. The insulation batting compresses when the blanket is stitched together. The compression increases the bulk density of the insulation batting and decreases the thermal conductivity.

(A) Insulation Blanket



(B) Insulation Blanket with Air Gap

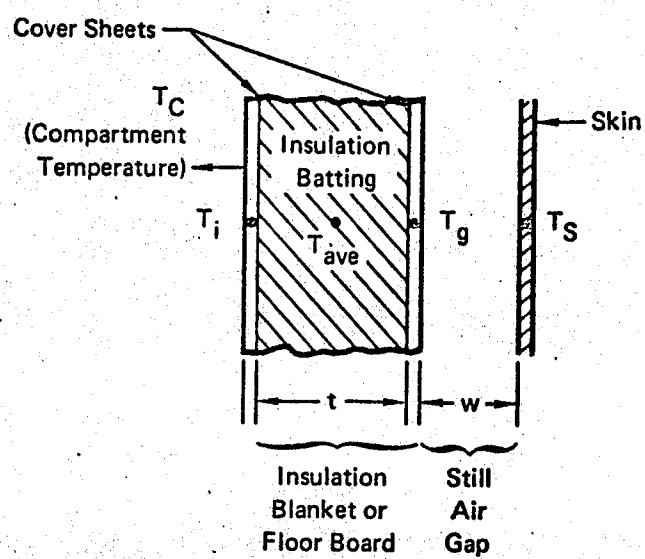


Figure 130 Compartment Thermal Insulation Designs

GP 9416-1

Insulating blankets with an air gap are used on aircraft capable of flight above Mach 3, and on large subsonic aircraft capable of flight at high altitudes. (See Figure 130B.) A reflective cover is used on the air gap side of the insulation to minimize radiative heat transfer.

A typical cabin floor design may include a floor covering (e.g. carpeting) on the floor structure. Heat transfer across the floor contributes significantly to the heat load, especially in large cargo aircraft.

Performance and Sizing - Calculation methods for determining the required insulation blanket thicknesses are outlined in this section. Equilibrium heat transfer for one dimensional heat flow is assumed. Parallel heat flow through wall frames, and similar heat leaks, are accounted for by multiplication factors based upon test data. The standard 0.6 pounds per cubic foot, bonded fiberglass insulation batting is assumed for the insulation blankets. Batting compression during blanket manufacture is allowed.

A six pounds per cubic foot polyurethane foam is assumed for the floor insulation boards.

Calculation of the required thickness (t) of an insulation blanket is based upon Figure 129A. The design temperature differential across the compartment wall or floor insulation ($T_S - T_i$) and the desired insulation blanket inside surface temperature (T_i) are used to determine t . A negative design temperature differential is a heat loss condition. The thermal conductivity of the insulation blanket batting (k) is found at the average temperature across the blanket thickness. The thermal conductivity for "B" fiber, phenolic-bonded fiberglass batt versus the average temperature (T_{ave} in $^{\circ}$ R) and the effective bulk density (ρ_{bu} in pcf) is:

$$k = (0.046 - 0.038 \rho_{bu} + 0.009 \rho_{bu}^2) - (1.78 - 1.91 \rho_{bu} + 0.44 \rho_{bu}^2) \\ (T_{ave} \times 10^{-4}) + (2.58 - 2.43 \rho_{bu} + 0.56 \rho_{bu}^2) (T_{ave}^2 \times 10^{-7}) \quad (282)$$

Equation (282) is valid for bulk densities between 0.5 and 3 pcf, and for average temperatures between 400 to 1000 $^{\circ}$ R. The effective bulk density of the insulation batting is dependent upon the amount the batting is compressed during the manufacture of the insulation blanket. The manufacture compression factor (CF) varies from 0.1 to 1.0 (a nominal CF is 0.5.). The required thickness of insulation batting (t) is:

$$t = 12. L k (T_S - T_i) / (q' T / A) \quad (283)$$

The parallel heat leaks due to the wall frames, to poor installation, and to inservice degradation are approximated by a factor L which varies from 1.25 to 4. The lower value is a very good design for careful fabrication and installation.

The total heat flow per unit area through the insulation blanket is equal to the heat dissipated to the compartment interior by convection and by radiation from the inside surface of the insulation blanket. For crew or passenger compartments a temperature differential of 10 $^{\circ}$ F between the blanket inside surface temperature (T_i) and the average compartment temperature (T_C) is compatible with the temperatures previously recommended. Assumption of a smaller temperature differential requires a lower wall (or floor) heat leak and a heavier insulation design. For cargo compartments a 40 $^{\circ}$ F temperature differential is assumed.

The internal convective heat transfer rate is:

$$q'_c/A = h_c (T_i - T_C) \quad (284)$$

The convection coefficient (h_c) is approximately $(1.5)(P_{am}/14.7)^{1/2}$. The radiative heat transfer is obtained by assuming that the radiation sink temperature is the same as the compartment air temperature:

$$q'_r/A = h_r (T_i - T_C) \quad (285)$$

The radiation coefficient (h_r) is:

$$h_t = \sigma (Fe) (T_i + T_C) (T_i^2 + T_C^2) \quad (286)$$

The inside surface emissivity factor (Fe) varies from 0.8 to 1.0. The required insulation thickness (t) calculated by Equation (283) is for the compressed insulation batting.

The total heat flow per unit area through the blanket (with an air gap) is equal to the heat flows through each blanket surface. This is expressed mathematically for the blanket inside surface, the blanket insulation, and the blanket outside surface.

$$q'_T/A = (h_r + h_c)_i (T_i - T_C) \quad (287)$$

$$= (12 L k/t) (T_g - T_i) \quad (288)$$

$$= (h_r + h_c)_o (T_S - T_g) \quad (289)$$

Equation (287) is solved for q'_T/A by the solutions given for the insulation blanket design. The remaining unknowns are T_g and the blanket thickness (t). Both h_r and h_c for the blanket outside surface are functions of T_g . By substituting the expressions for h_c and h_r in terms of $(T_S - T_g)$ into Equation (289), and by equating Equations (288) and (289), the resulting equation is solved for $(T_S - T_g)$:

$$(T_S - T_g) = 2.24 \pm [5.0 + 13.5 \times 10^{-4} (q'_T/A)]^{1/2} / (-2q'_T/A) \quad (290)$$

A gap width of one inch, flight at 30,000 feet altitude, and an average gap air temperature of 100°F is assumed for Equation (290). The gap film coefficient (h_c) is based on a correlation given in Reference 63 for an effective thermal conductivity for narrow enclosures which is a function of gap width.

The required blanket thickness (t) is:

$$t = \frac{12. L k [(T_s - T_i) - (T_s - T_g)]}{[3.4 \times 10^{-4} (T_s - T_g) + 2.24] (T_s - T_g)} \quad (291)$$

The heat transfer per unit area for a passenger cabin floor is based on a one inch thick honeycomb core covered with a half inch thick carpet and under-pad. The temperature differential in the following equation is between the floor top and bottom surfaces.

$$q'/A = [(5.3 \times 10^{-3}) T_{ave} - 2.3] \Delta T \quad (292)$$

where T_{ave} is the average floor temperature and A is ft^2 . Calculation of the required thickness of an insulation floor board is essentially the same as the procedure for determining insulation blanket thickness. The thermal conductivity of the 6 pounds per cubic foot polyurethane foam is:

$$k = (5.14 \times 10^{-5}) T_{ave} - (5.66 \times 10^{-3}) \quad (293)$$

Weight - Calculations of the weight of compartment thermal insulations use the insulation sizes determined previously. The cover sheet specific weights range from an average of 1.2 ounces/square yard to more than 8 ounces/square yard. A medium-to-heavy sheet of 5 ounces/square yard is used for weight increment calculations. The weight of stitching threads, sealing tapes or staples, and perimeter tabs and tapes for insulation blanket installation are estimated to be about five percent of the insulation blanket weight. The weight per unit area for the thermal insulation designs is:

$$Wt/A = 7.29 \times 10^{-3} [(0.05 t)_{\text{insulation}} + (0.07)] \quad (294)$$

where t is the actual uncompressed thickness of insulation. The estimated error of this equation is 15%.

3.11.3 Fuel Tank Insulations - A simplified technique is presented for sizing the insulation required on the fuel tanks in which the fuel is stored for use as the ECS subsystem heat sink. The limitations on fuel tank insulation, and the variables which control the tank heat gain are discussed.

Limitations - The major source of external heating is aerodynamic heating through the fuel tank walls. For subsonic aircraft insulation is not required. For supersonic aircraft up to Mach 2.5 fuel tank insulation generally is not required. For higher speed supersonic aircraft (above Mach 2.5) fuel tank insulation generally is required. The fuel system is a dynamic subsystem of the aircraft. Its design is dependent on many time dependent parameters of the aircraft (e.g. mission, fuel transfer/recirculation, heat loads other than the ECS, etc.). To estimate the insulation required to protect the fuel (used as an ECS sink) from aerodynamic heating by a single procedure, many simplifications are made. The ECS heat load is dissipated to the fuel in the engine feed line as the fuel is transferred from the fuel tank to the engine. Since the temperature level of the ECS heat sink normally is lower than the other system sinks, the fuel to be used for the ECS sink is stored in a separate fuel tank with more protection than other tanks.

Heat Load - The aircraft mission is approximated by an initial period of no heating, followed by a period of heating, and ended with a period of no heating. The temperature response for the ECS fuel sink during the heating phase is:

$$\Delta T_{fu} = (q'/W_{fu} c_p) \ln [(Wt/W_{fu}) - \theta]^{-1} \quad (295)$$

where: ΔT_{fu} = Fuel temperature rise

q' = Fuel heating rate (assumed constant)

W_{fu} = Fuel flow rate leaving tank (assumed constant during the heating period)

c_p = Fuel specific heat (constant)

Wt = Fuel in tank at the start of the heating period

θ = Duration of the heating period

If ΔT_{fu} represents the maximum allowed temperature rise, the allowed heating rate is:

$$q' = W_{fu} c_p (\Delta T_{fu}) / \ln [(Wt/W_{fu}) - \theta]^{-1} \quad (296)$$

For steady state conduction through the tank wall, the heat flux through the wall is:

$$q' = (T_o - T_i) / [t/kA] + (1/UA) \quad (297)$$

where: T_o = Outer wall average temperature during the heating period

T_i = Inner wall average temperature during the heating period

t = Insulation thickness

k = Insulation thermal conductivity

A = Wall cross sectional area

UA = Wall conduction other than the insulation

Sizing - The two heat fluxes are equated, the outer wall average temperature is assumed to be the equilibrium wall average temperature and the inner wall average temperature is T_{fu} . Thus the required insulation thickness is:

$$t = [kA (T_o - T_{fu}) / W_{fu} c_p (\Delta T_{fu})] \ln [(Wt/W_{fu}) - \theta]^{-1} - (kA/UA) \quad (298)$$

The insulation weight is determined with the above thickness and the technique for an insulating blanket (Section 3.11.2).

3.11.4 Example Insulation Design - Typical examples to determine the insulation for a bleed air duct are presented to illustrate use of the previous information. Insulation weights are determined for a 5-inch diameter duct. The maximum bleed air temperature is 550°F and the maximum surface temperature is to be 250°F. The thickness of air-gap, radiation-shield insulation (Equation 268) is:

$$t = \frac{(0.06)(550)}{710 - (0.2)(1010) - 416} = 0.359 \text{ inch (use } \frac{3}{8} \text{ inch)}$$

The weight per unit length is obtained by interpolating Equations (270) and (271).

$$\frac{Wt}{L} = \frac{(0.0373)(5) + 0.0257}{12} = 0.0177 \text{ lb/in}$$

The thickness of 4.5 pounds per cubic foot removable insulation (Equation 268) is:

$$t = \frac{(0.064)(550)}{710 - (0.2)(1010) - 416} = 0.383 \text{ (use } \frac{3}{8} \text{ inch)}$$

The weight per unit length is obtained by interpolating Equations (273) and (274).

$$\frac{Wt}{L} = \frac{[(0.00805)(4.5) + 0.12](5) + (0.00355)(4.5) + 0.3065}{12}$$
$$= 0.916 \text{ lb/in}$$

3.12 System Controls

Many control systems, for the systems and subsystems described in Section 2.0, can be devised. Discussions of all these possible controls are not presented. Only steady state system performance is considered, hence transient performance of controls is not discussed.

Typical electronic controls are presented for a number of the subsystems in Section 2.0. The approaches for determining the penalties of electronic temperature controls are applicable to pneumatic and electro-pneumatic temperature controls, as well as to water separator anti-ice controls, vapor cycle controls, and other controls which modulate flow. Controls for maintaining cockpit, cabin, and compartment pressures also are discussed. A method for determining thrust recovery from a cabin pressure control valve also is included.

3.12.1 Temperature Control Systems - The temperature control systems considered are either electronic or pneumatic. The electronic system consists of a controller, a selector (optional), one or more sensors, and a valve. The pneumatic system consists of one or more sensors, a controller, and a valve. Pneumatic, electronic, and electro-pneumatic actuated valves, and pneumatic control lines are discussed in Section 3.10.

3.12.1.1 Electronic Temperature Control - The most important component of a temperature control system from a functional standpoint is the controller. The controller is considered to be made up of all solid state electronics. The controller size is observed to be directly related to the number of input and output functions it must perform. Equations for weight and volume of temperature control systems are presented. These equations include factors for the technical difficulty of the control and other special system requirements. This information is presented as system technical and requirements weighting factors, respectively.

Number Inputs and Outputs (NIAO) - The number of functional inputs and outputs of a controller is designated as "NIAO", and is referred to as such throughout this report. The following example typifies the procedure to determine the NIAO. (Refer to Figure 131.)

The number of inputs to the controller consist of the compartment temperature sensor (1 input), high limit sensor (1 input), anticipator (2 inputs - dual sensor), and temperature selector (1 input). The controller output consists of controlling the valve position (2 outputs). The number of outputs for an electric motor valve is two since the motor is

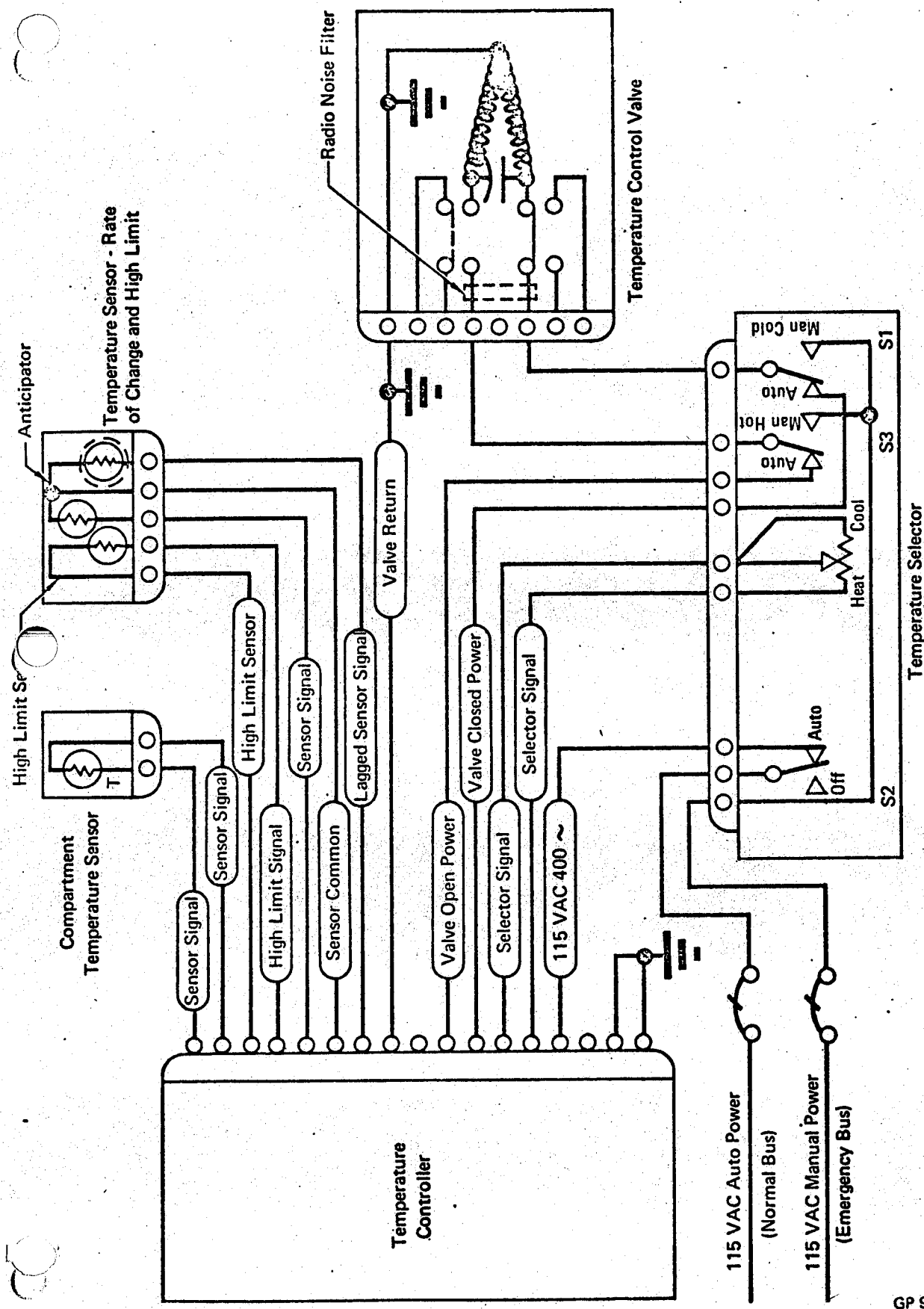


Figure 131 Typical Temperature Control System

GP 9416-203

driven in both directions. Only one output is considered when driving an electro-pneumatic valve. Therefore, the total number of inputs and outputs equals 7. Power inputs, grounds, and return lines from the components are not considered as part of the input and output count. Table XI contains typical values of NIAO for various types of subsystems. Schematics of these subsystems with typical control systems are found in Figures 132 through 138.

Technical Weighting Factor (K_{Te}) - A technical difficulty consideration (such as the "toughness" of the control problem, the stringency of the performance requirements, etc.) also is ascertained. This factor modifies the equations for weight and volume given later. The value of K_{Te} is obtained from Table XI. K_{Te} also is used to modify cost in Section 4.3. For example, the K_{Te} of control for Subsystem 2.3A is 2.5 because dynamically a difficult controls problem exists. Subsystem 6A has a control K_{Te} of 1.3 because typical accuracy and dynamic performance requirements are stringent. K_{Te} is assigned a value of 1.0 if detailed information is lacking.

Requirements Weighting Factor (K_{Re}) - A factor to adjust for special considerations of system requirements is a requirements weighting factor. This factor includes special electromagnetic interference requirements, nuclear hardening requirements, built-in-test-equipment (BITE), high temperature receptacles, speed controls, special packaging requirements, etc. Values of K_{Re} are listed in Table XI. If information is lacking, K_{Re} is assigned a value of 1.0.

Weight - The weight of the controller for numerous aircraft is presented as a function of NIAO:

$$Wt = NIAO/3. \quad (299)$$

The weights of a temperature selector range from 0.19 pound for a simple potentiometer, to 0.6 pound for a unit including auto/manual switching or possibly an integrally lighted panel. Temperature sensor weight is approximately 0.2 pound. Therefore, the total weight of a temperature control system for fighters, light bombers, heavy bombers, or cargo aircraft is:

$$Wt = \frac{NIAO}{3} + Wt_{\text{selector}} + 0.2 (\text{Number of sensors}). \quad (300)$$

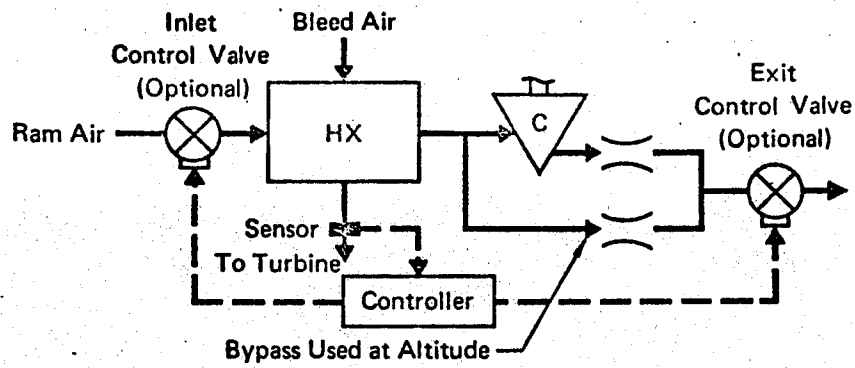
Table XI
Typical Control Inputs and Outputs and Weighting Factors

Subsystem Number*	Sensors	Selector	NIAO(1)	K _T e	K _{Re}	Remarks
2.1A,B,C	1		2	1.2	1	Ram air modulation of inlet or exit.
	1		3	1.3	.1	Ram air modulation of inlet and exit.
2.2A,B	1		2	1.3	1	Control for steam valve. NIAO increased to 3 with ejector.
2.3A	2		4	2.5	1	System dynamics yield "tough" controls problem.
2.3B,C	2		4	1.5	1	Could present difficult dynamics problem if controlled recirculated loop is short.
3.A,B,C (4), D(3), E(3), F(4,5)	1	1	2	1	1	Open system, fixed inlet temperature control.
	1	1	3	1	1	Open system selectable inlet temperature control.
	2	1	3	1	1	Open system selectable inlet temperature control with manual override feature.(2)
	2	1	4	1	1	Closed system, fixed compartment temperature control.
	2	1	4	1.1	1	Closed system, selectable compartment temperature control.
4.A,B,C,D	1		3E	1	1	Closed system selectable compartment temperature control with manual override feature. (2)
5.A,B,C	1		2	1	1	Control inlet temperature only. (2)
	1		2	1.1	1	Coarse temperature control.
	1		2	1.1	1	Fine temperature control
6.A,C,E	1		2	1.3	1	Electronic 35°F water separator control. Pneumatic type controls usually contained within anti-ice valve head.

* Schematics are in Figures 131 through 138.

- (1) Pneumatically driven valves require one output per valve. Electrically driven valves (shown as E) require two outputs per valve.
- (2) If BiTE is used K_{Re} = 1.1.
- (3) Subsystem assumes 1 output to drive valves ganged together. If valves separate, increase output count by 1.
- (4) NIAO between electric heater and controller equals 9 times rated heater power in KW. NIAO of 1 is used above (arbitrarily).
- (5) NIAO is increased by 1 to account for the extra output.

A) Simple Air Cycle for Low Mach Numbers



B) Simple Air Cycle For High Mach Numbers

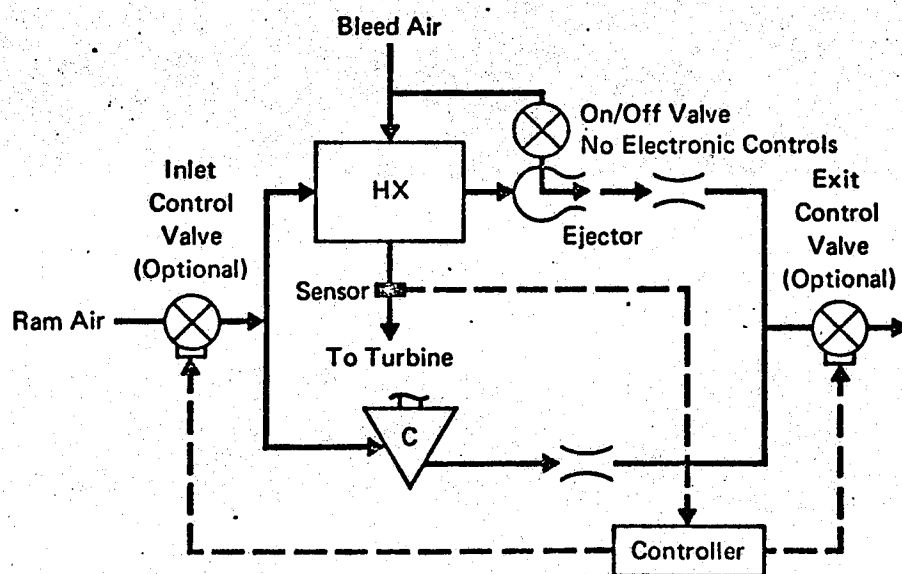
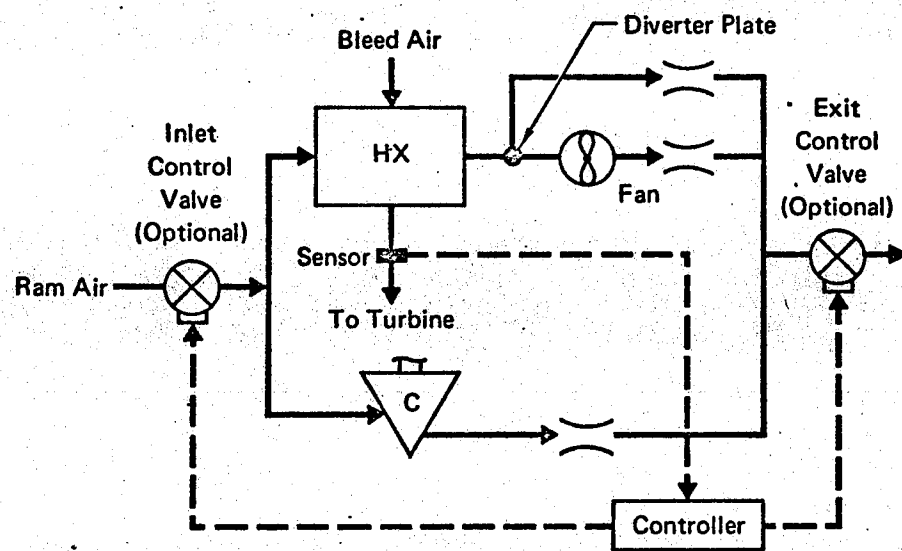


Figure 132A Ram Air Heat Sink Controls for Subsystem 2.1

C) Bootstrap Air Cycle or Vapor Cycle

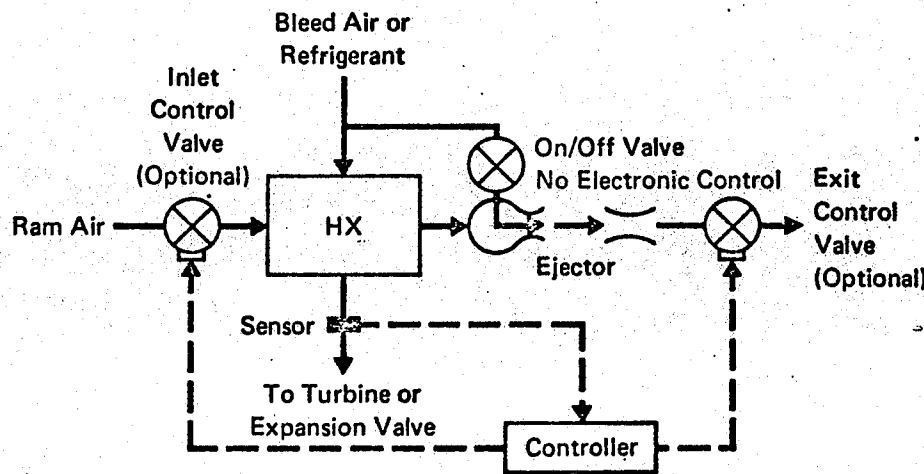
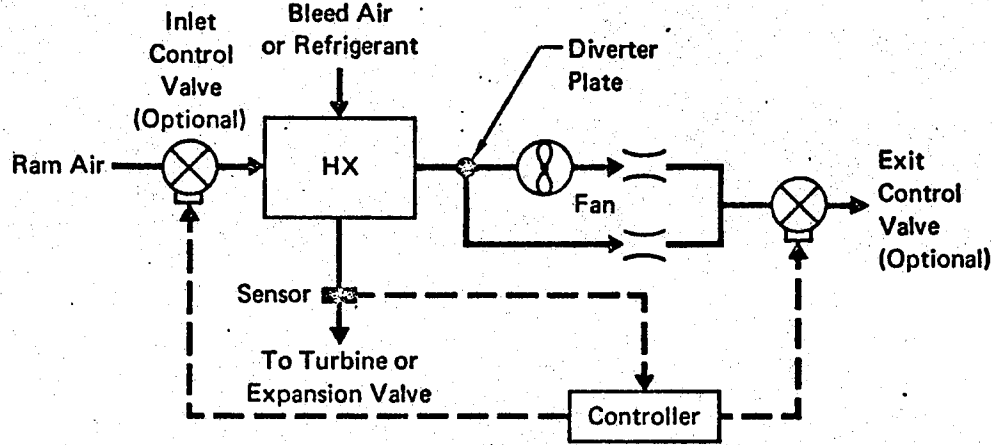
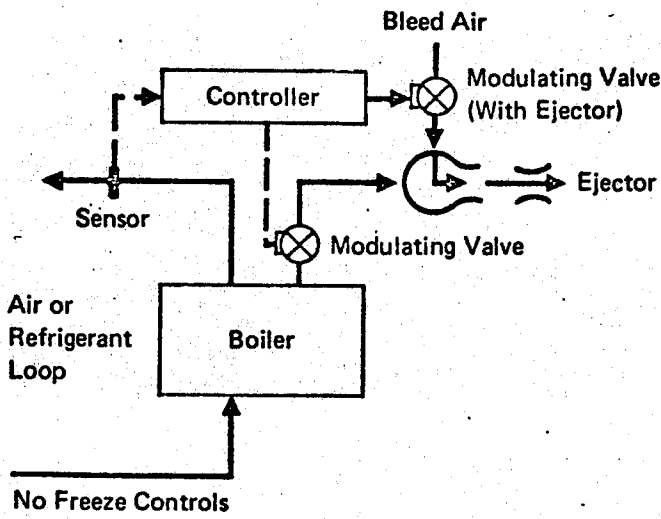


Figure 132B Ram Air Heat Sink Controls for Subsystem 2.1

GP 9416-43

A) Integral Boiler and Reservoir (With or Without Ejector)



B) Separate Boiler and Reservoir (With or Without Ejector)

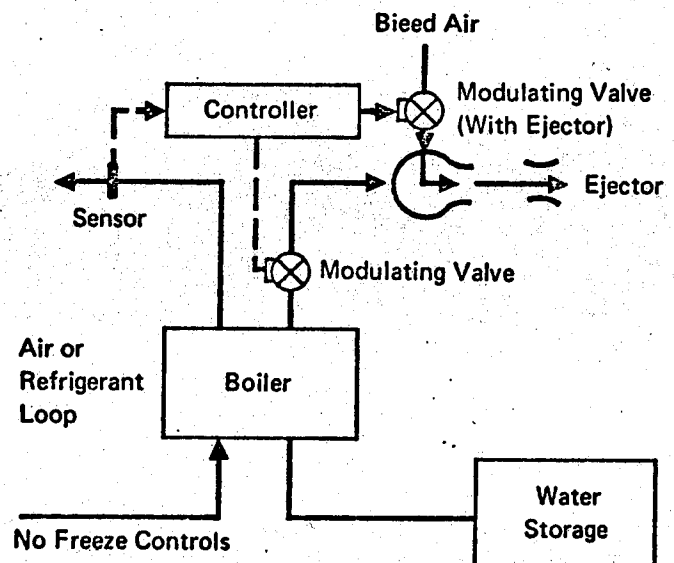
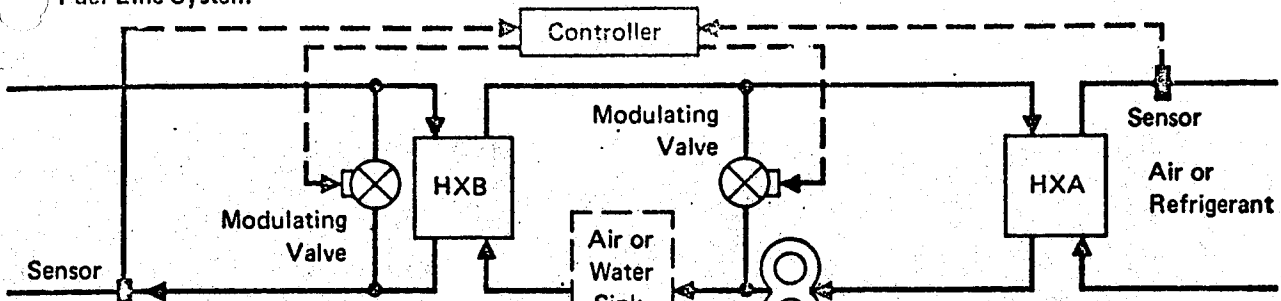


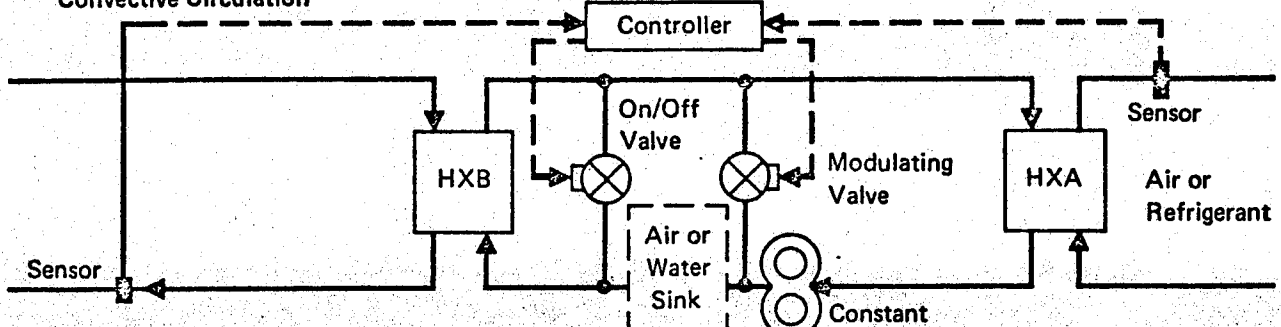
Figure 133 Expendable Water Heat Sink Controls for Subsystem 2.2

GP 9416-48

**A) HXB in Aircraft
Fuel Line System**



**B) HXB in Aircraft Fuel
Tank with Free
Convective Circulation**



**C) HXB in Aircraft
Fuel Tank with
Circulating Pump**

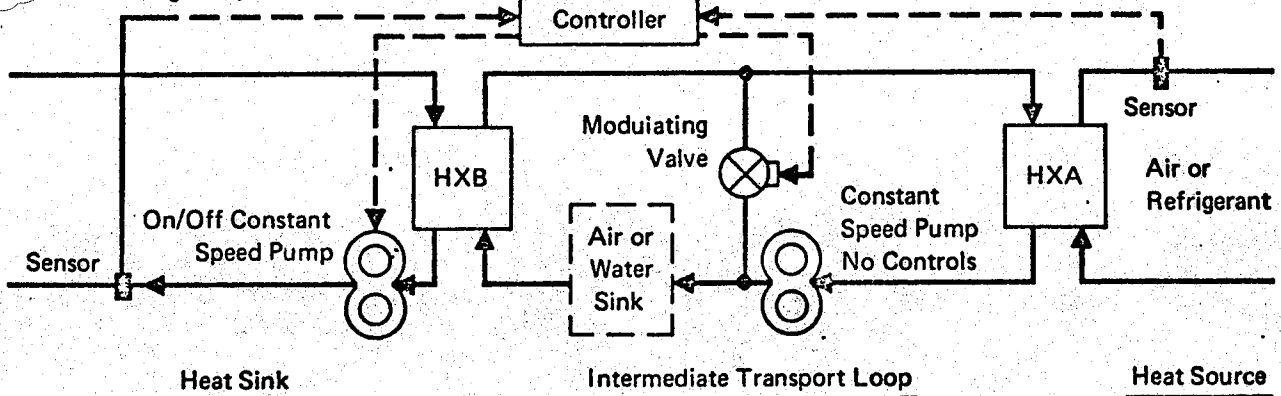
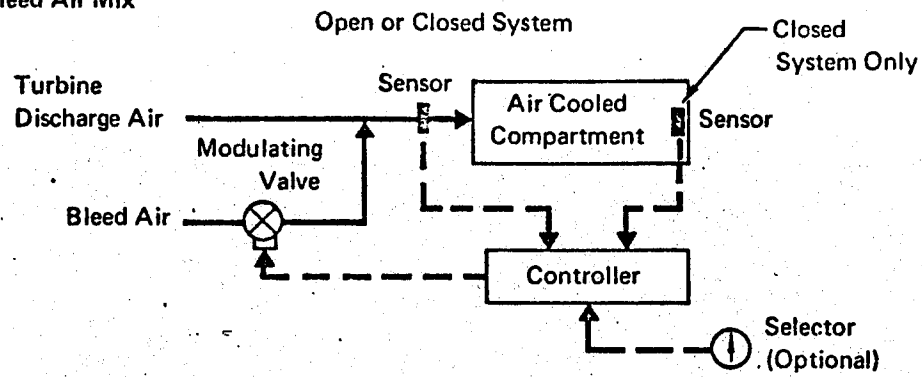


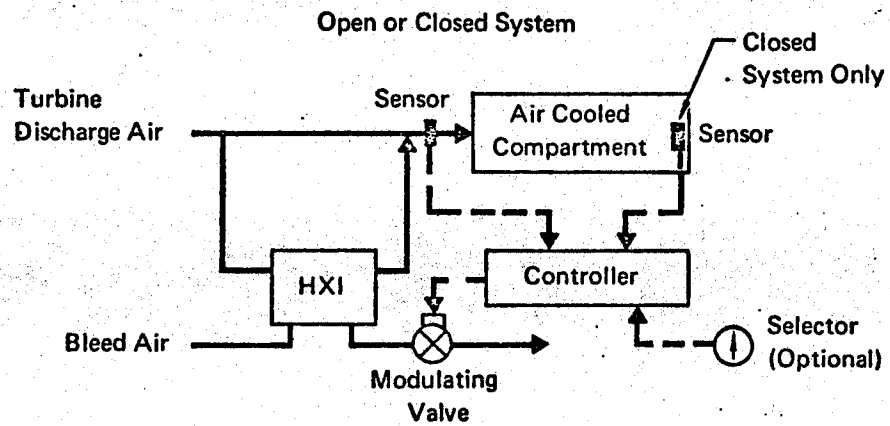
Figure 134 Fuel Heat Sink Controls for Subsystem 2.3

GP 9416-44

A) Bleed Air Mix



B) Temperature Regulation Heat Exchanger - HXI



C) Electric Heater

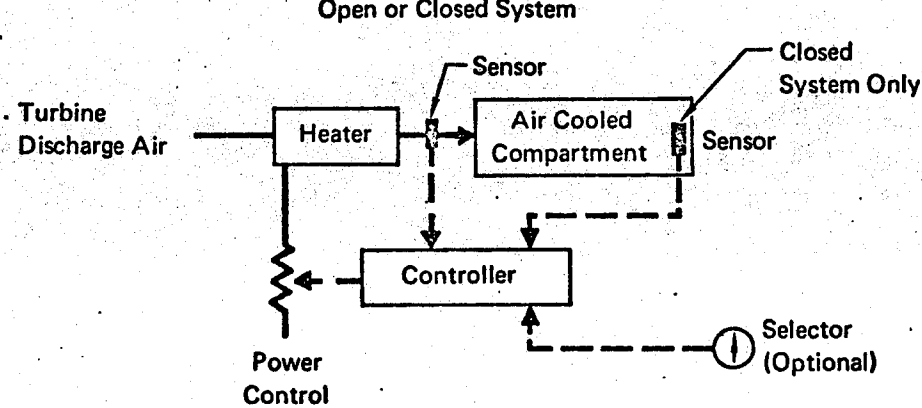
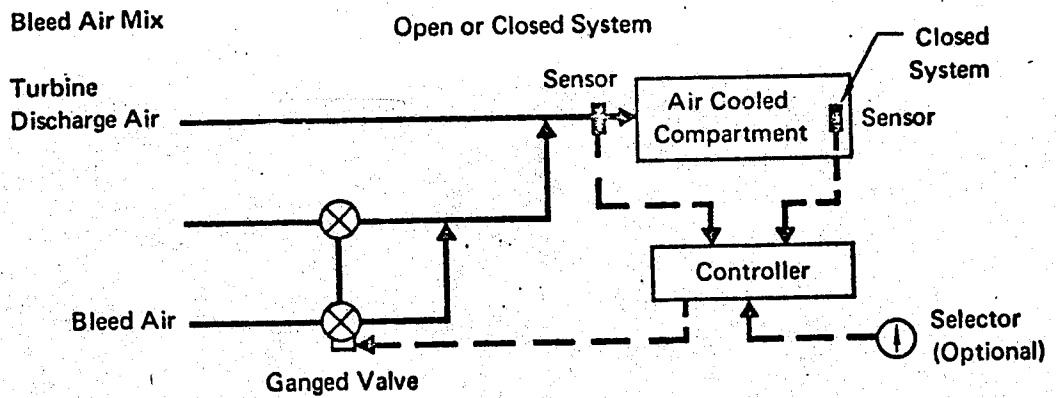


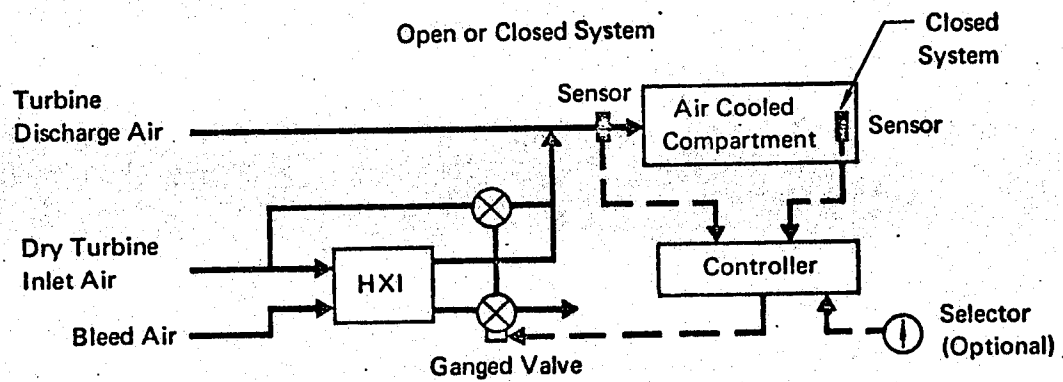
Figure 135A Temperature Control of Cooling Air for Subsystem 3

GP 9416-13

D) Bleed Air Mix



E) Temperature Regulation Heat Exchanger - HXI



F) Electric Heater

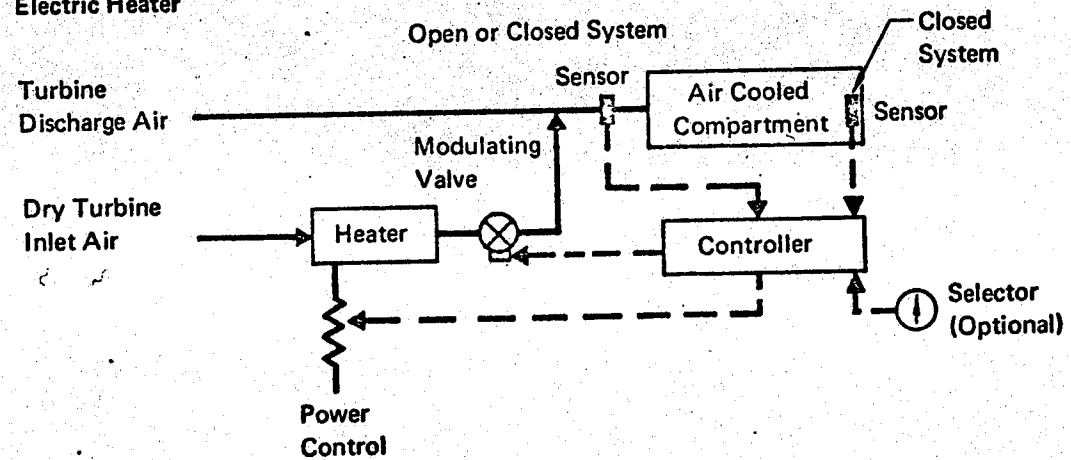


Figure 135B Temperature Control of Cooling Air for Subsystem 3

GP 9416-14

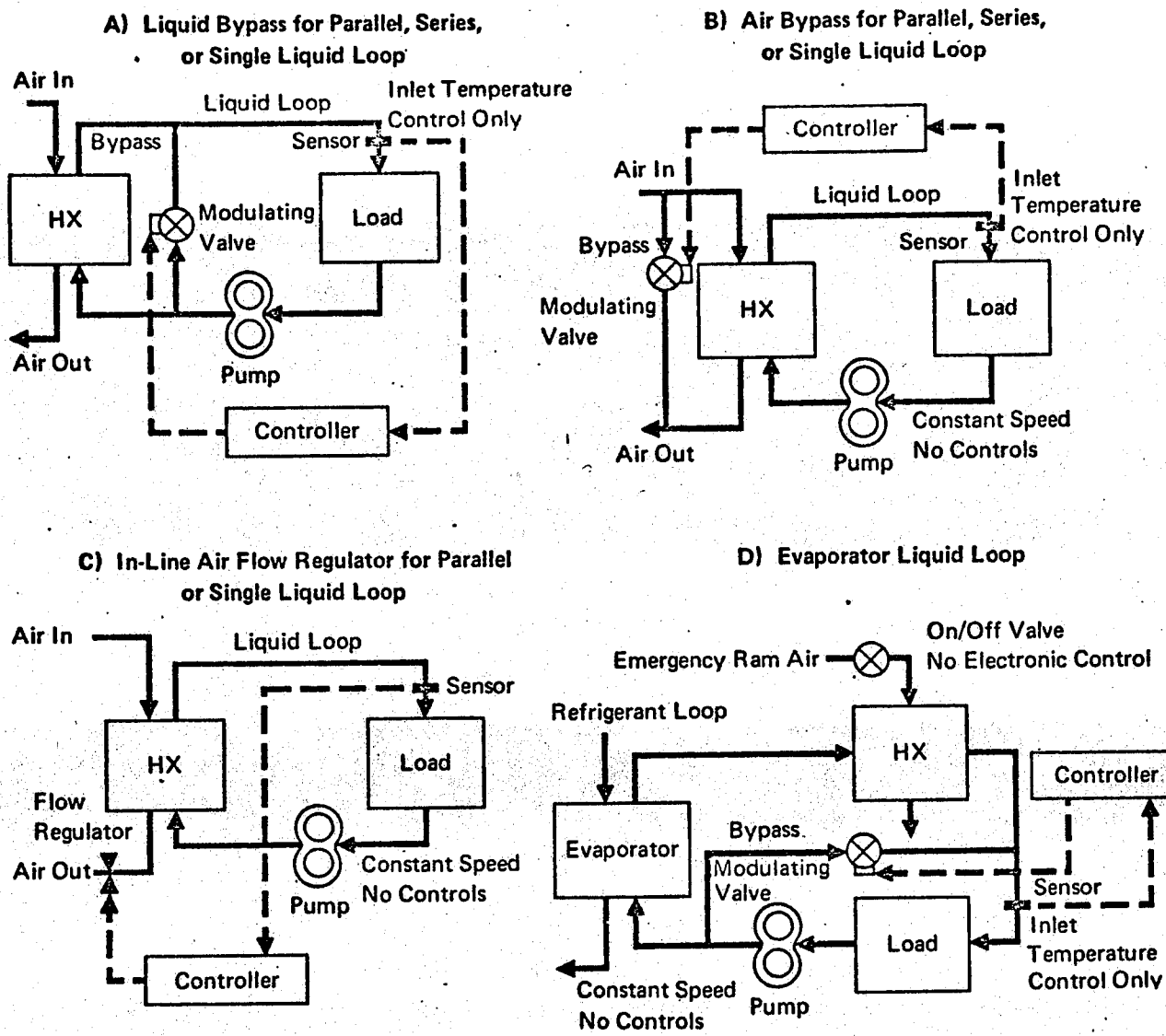


Figure 136 Liquid Loop Controls for Subsystem 4

GP 9416-12

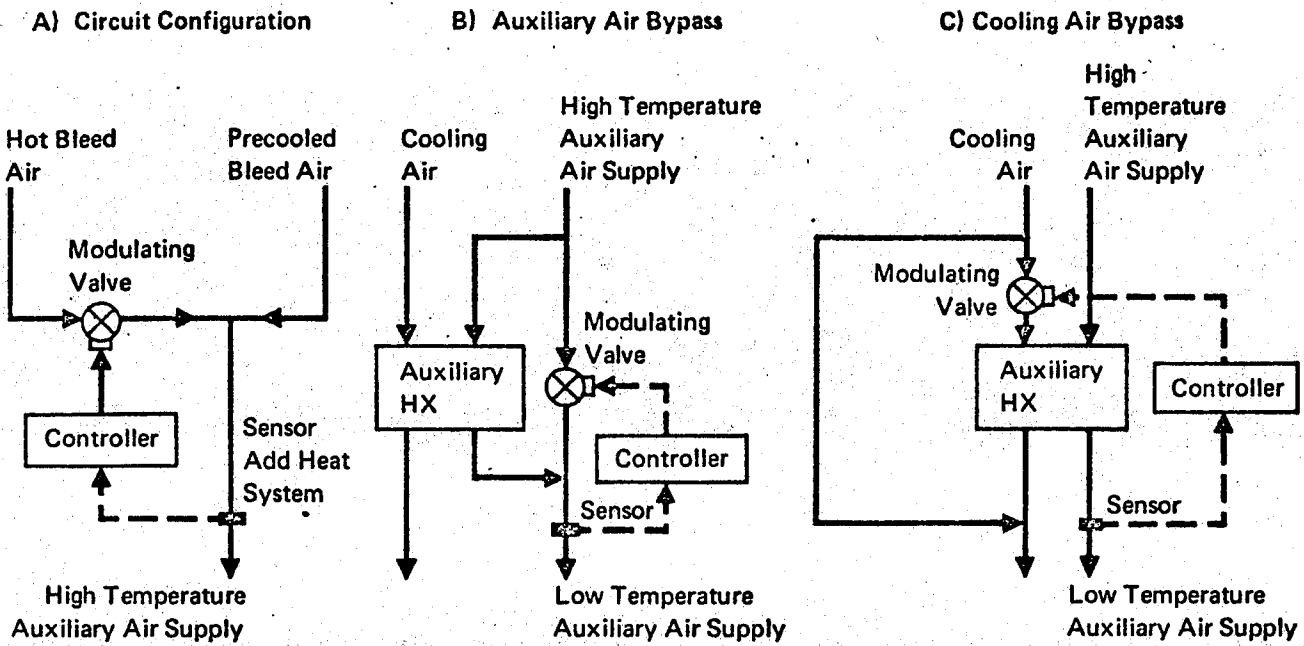
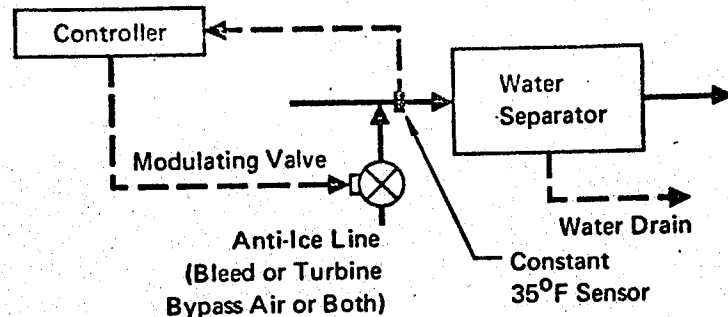


Figure 137 Auxiliary Air Supply Controls for Subsystem 5

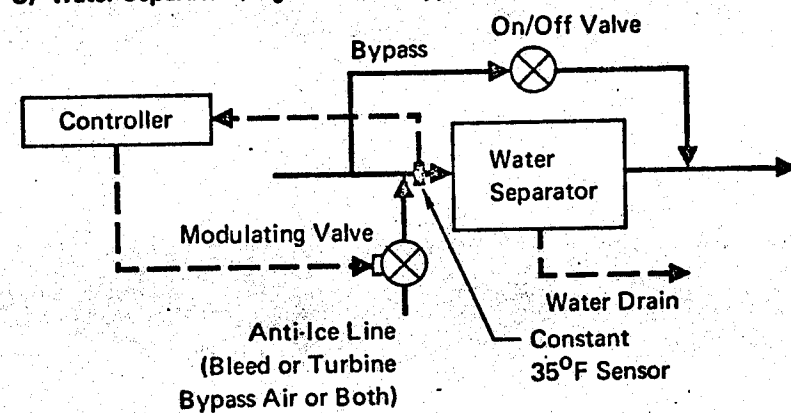
GP 9416-11

A) Water Separator (No High Altitude Bypass) with Anti-Ice Line



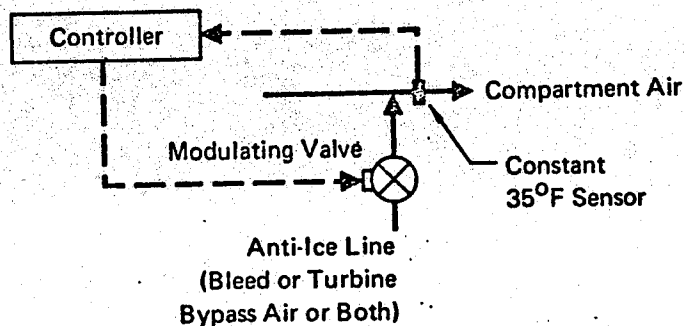
B) Same as (A) without Anti-Ice Line – No Controls

C) Water Separator (High Altitude Bypass) with Anti-Ice Line



D) Same as (C) without Anti-Ice Line – No Controls

E) Anti-Ice Only



F) No Water Separation or Ice Control

Note: 35°F Constant temperature control shown. Screen control and Reference ΔP controls optional.

Figure 138 Water Separator Controls for Subsystem 6

GP 9416-10

Table XII is a compilation of data for weights of fighters and cargo aircraft temperature control system components. Figure 139 (from Reference 65) shows the relationship between controller weight and the number of controller functions. Using the data in Figure 139, the standard error of Equation (300) is 41%.

Volume - The volume for temperature control system is related to the NIAO. An equation for volume is:

$$V = 11.43 \text{ (NIAO)} + 25.71. \quad (301)$$

Table XI presents data for the subsystems and controls described in Figures 132 through 138, with typical technical weighting factors (K_{Te}) and requirements weighting factors (K_{Re}). These factors represent the condition that seems most plausible. If system constraints require other special considerations, appropriate factors should be used. The temperature control system weight and volume is determined by multiplying Equations (300) and (301) by the technical and requirements weighting factors.

$$(Wt \text{ or } V)_{\text{total}} = (Wt \text{ or } V) K_{Te} K_{Re} \quad (302)$$

Example - The following example illustrates the use of information described in this section in order to determine the temperature control system weight and volume. Consider the controls for a ram air heat sink (for Subsystem 2.1A) with modulated inlet and outlet controls as is employed on cargo aircraft. (See Figure 132A.) Assumptions stipulated for this example are:

- (1) The ram inlet and outlet valves are driven electrically.
 - (2) All components of the temperature control system are electronic.
- The system consists of a temperature sensor in the heat exchanger outlet and a controller which receives the sensor input. The controller outputs a signal driving the actuators which position the ram air inlet and outlet valves. The system input/output count consists of the sensor and valves. The number of inputs to the controller is one (the sensor). The number of outputs is four (two outputs per electrically driven valve). The sum of the inputs and outputs (NIAO) equals 5. Since ram air modulation results in controlling both the inlet and outlet, as a function of the dynamics of the

Table XII Temperature Control Component Weights

Component	Aircraft				
	Fighter A Weight (Lb)	Fighter B Weight (Lb)	Cargo A Weight (Lb)	Cargo B Weight (Lb)	Cargo C Weight (Lb)
Controller	2.5	3.23	2.40	2.20	3.8
Selector	0.6	0.60	0.50	0.19	0.6
Sensor*	0.2	0.40	0.45	0.45	0.5

*Based on two sensors.

GP 9416-69

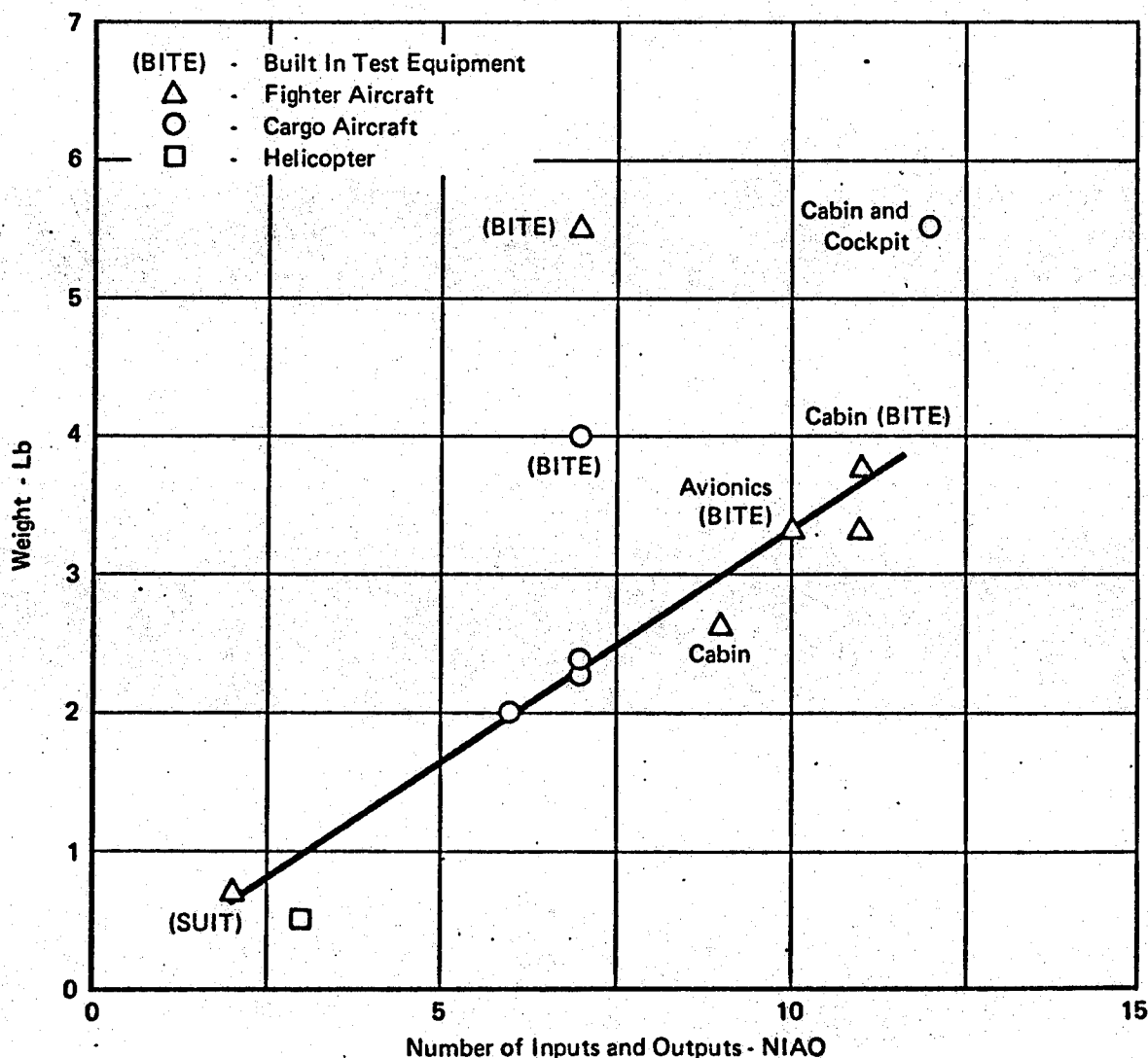


Figure 139 Controller Weight

GP 9416-70

system, a technical weighting factor (K_{Te}) of 1.3 is specified to account for this complexity. The basic temperature control system weight and volume are obtained using Equations (300) and (301). The basic control system weight and volume are:

$$Wt = \frac{NIAO}{3} + Wt_{Selector} + 0.2$$

$$= 5/3 + 0 + (0.2)(1) = 1.87 \text{ pounds}$$

$$\begin{aligned} \text{Volume} &= 11.43 (\text{NIAO}) + 25.71 \\ &= 11.43 (5) + 25.71 = 82.7 \text{ cubic inches.} \end{aligned}$$

Once the basic control system results are obtained they are modified by the weighting factors: $K_{Te} = 1.3$ and $K_{Re} = 1$, in order to obtain the overall system parameters.

$$\text{System Weight} = (1.87)(1.3)(1) = 2.43 \text{ pounds}$$

$$\text{System Volume} = (82.7)(1.3)(1) = 108 \text{ cubic inches}$$

3.12.1.2 Pneumatic Temperature Control - The pneumatic temperature control system is comprised of a temperature sensor, an anticipator, and a valve control head. The valve control head, which usually is an integral part of the valve, normally contains the servomechanism or logic required to control the valve's functions. In most pneumatic temperature control applications a fixed inlet temperature is desired. Therefore, temperature selectors are not considered.

Weight and Volume - The weight and volume of the pneumatic system's control head and sensor are given below. These results are based on detailed investigation of bleed air valves, pressure regulators, and flow control valves used on fighter and cargo aircraft. The control head weight and volume are defined as a function of valve diameter (D). The head weight does not include the "muscle" or actuator weight required to position the valve.

Control Head Weight: $Wt = 0.5D + 1$

(303)

Sensors weigh between 0.5 and 1.0 pounds.

Comparison of Electric, Electro-Pneumatic, and Pneumatic Controls -

A summary of comparisons of basic temperature controls for fighters is discussed in Reference 66. The basic unit of comparison comprises a controller, a sensor, and a valve. The relative weight factors shown below indicate trends between different types of systems for fighter aircraft. Observe that although pneumatic systems may be light, they are not as flexible as electronic systems and they do not provide the same high degree of control performance.

Integral Pneumatic Control Relative Weight = 0.8

Electro-pneumatic Control Relative Weight = 0.668.

Electronic Control Relative Weight = 1.00

3.12.2 Pressure Control Systems - Cabin pressure controls for fighter aircraft are less refined than the cabin pressure controls for cargo aircraft. Types of pressure control systems available for present day aircraft include pneumatic, electro-pneumatic, and electronic.

Fighter Aircraft - The fixed isobaric schedule is used almost exclusively on jet fighter and light bomber aircraft. The cabin remains essentially unpressurized (by following aircraft altitude) until an isobaric altitude is reached. Cabin pressure altitude then is held. As the aircraft climbs further, a ΔP function overrides the isobaric function to control to a constant ΔP . Some aircraft have the capability to change the ΔP limit to reduce differential pressure when operating under combat conditions. The crew and occupants are subjected to high rates of ascent and descent when the aircraft is unpressurized. The isobaric altitude normally is set high enough so that the aircraft lands unpressurized at any air base. This type of system is a simple, lightweight, and reliable control system. There are a minimum of components and no crew action is required during normal operation. The system is implemented with pneumatic controls. The crew members normally are young and healthy, capable of withstanding the high pressurization rates with no serious complications.

The pressure control system comprises a controller, outflow valve, and

safety valve. The controller and outflow valves usually are an integral unit. The outflow valve normally is the poppet type with no thrust recovery capability. The added complexity of a thrust recovery valve is unwarranted since the flow rate is very low.

A comparison of pressure control systems for fighter aircraft indicates that a constant weight and volume are typical. The typical weight is 6 pounds, and the typical volume is 250 cubic inches. (See Reference 67.)

Cargo Aircraft - The variable isobaric pressure control system is available on most large present day jet aircraft. Cabin altitude is controlled to a selected altitude. While changing from one altitude to a new cabin altitude the rate of change is controlled at a selected rate. The system controller also contains a maximum differential pressure limit. The advantage of variable isobaric control over fixed isobaric control is that cabin altitude is kept as low as the cruise altitude will permit. The main disadvantages are the additional complexity of the controller and selector, and the necessity for correct crew action to obtain proper control.

The cabin pressure control system used on cargo aircraft has shifted from the all pneumatic control toward the all electronic control. Probably the main reasons for this shift are the advancements in electronic technology and the addition of a thrust recovery valve. The addition of the thrust recovery valve requires a greater source of power and a more responsive outflow valve. Up to one percent of total aircraft thrust can be recovered. This results in a significant fuel cost saving over the life of the aircraft. A sample calculation to determine thrust recovery is included.

The safety relief valves are pneumatically controlled valves. There are no significant problems in the pressure relief valve designs.

Pressure control systems on cargo aircraft consist of pneumatic, electro-pneumatic, and electronic systems. Representative equations relating system weight and volume as a function of aircraft pressurization air flow rate are presented. The system weight comprises the controller, outflow valve, sensors, selector, and safety valves.

$$W_t = 0.0967 W_{max} + 51.45 \quad (305)$$

$$V = 8.065 W_{max} + 5671.0 \quad (306)$$

If built-in-test-equipment (BITE) is included in a system, the system weight is increased by about 1%. Table XIII shows pressure control system weights for five cargo aircraft. Equation (311) has a standard error of 24% for these five control systems.

Sample Calculation to Determine Thrust Recovery:

Assume: Flight Altitude = 36,000 Ft., $P_{\text{am}} = 3.306 \text{ psia}$,
 $M = 0.82$, $P_C = 8.187 \text{ psig}$, $T_C = 540^\circ\text{R}$.

The total air flow introduced into the pressurized cabin at this flight condition, including air conditioning and floor heating air is 392 lb/min. This amount of airflow, under steady state conditions must leave the pressurized volume as leakage, through a thrust recovery nozzle, or through the pressure regulating valve. Assuming that the airplane has a leakage area with a KA equal to 5.93 in^2 , the flow lost through leakage is:

$$W_L = \frac{31.82 \text{ KA } P_C}{\sqrt{T_C}} \quad (307)$$

$$P_C = P_{\text{am}} + P_C = 3.306 + 8.187 = 11.493 \text{ psia}$$

then:

$$\frac{P_C}{P_{\text{am}}} = \frac{11.493}{3.306} = 3.47;$$

and:

$$W_L = \frac{(31.82)(5.93)(11.493)}{\sqrt{540}} = 91.51 \text{ lb/min}$$

Therefore:

$$W_j = 392 - 91.5 = 300.5 \text{ lb/min (or } 5.01 \text{ lb/sec)}$$

For:

$$\frac{P_C}{P_{\text{am}}} = 3.47; M_j = 1.46,$$

Table XIII Cargo Aircraft Pressure Control Weights

	Aircraft				
	A	B	C	D	E
Flow Rate (lb/min)	500	140	220	450	220
Type System	Electronic	Electro-pneumatic	Pneumatic	Electronic	Electro-pneumatic
Component					
Controller	33	10.5		13.7	
Out Flow Valve Assembly	66	43		83	
Safety Valve*	16	12		16.8	
Total System	115	65.5	40.2	113.5	62

*Safety valves are all pneumatic

GP 9416-94

$$T_X = T_C \left(\frac{1}{3.47} \right)^{\gamma-1/\gamma} = 540 (0.288)^{0.283} = 379^{\circ}\text{R}$$

$$c = 49.04 \sqrt{T_X} = 957 \text{ ft/sec}$$

$$v'_{J} = M_J (c) = 1400 \text{ ft/sec} \quad (308)$$

The theoretical thrust is:

$$Th = \frac{W_1}{g_c} (v'_{J}), \quad (309)$$

hence:

$$Th = \frac{(5.01)(1400)}{32.17} = 218 \text{ lb.}$$

Based on wind tunnel test data, at least 90% of this thrust can be recovered. The actual thrust obtained is:

$$Th_{\text{actual}} = Th (0.9) = 196 \text{ lb.} \quad (310)$$

3.12.3 Water Separator Anti-Ice Control - There are three basic types of control schemes employed in air cycle systems to prevent freezing in the water separator, and to prevent blockage of the conditioned air flow. They are: (1) controlling the inlet temperature of the water separator to a constant temperature a few degrees above freezing using the sensed temperature to position an anti-ice valve; (2) using an icing screen control which is ΔP biased by screen ice accretion to open an anti-ice valve; and (3) using a reference ΔP control which biases water separator outlet pressure against a simulated uniced water separator outlet pressure to position an anti-ice valve. These controls in present day aircraft usually are all pneumatic with the controlling function self-contained within the head of the anti-ice valve. The results of Section 3.12.1 are used for this pneumatic application. The 35°F constant temperature control could be all electronic, with a controller, sensor, and valve. (See Table XI.) The constant temperature anti-ice control is most commonly used in conjunction with a barometric switch to reduce the

ontrol temperature below 32°F at a pre-selected altitude (i.e., moisture contents are greatly reduced at altitude). In a vapor cycle refrigeration system the evaporator is the point of moisture condensation. In order to avoid freezing of this moisture the evaporator discharge air temperature is maintained above freezing. Therefore, no water separator controls are required.

3.12.4 Vapor Cycle Control - It is necessary to make several assumptions about the action of the control system in analyzing the vapor cycle system performance. The necessity for relating the system performance to control system action does not restrict the utility of the analysis. Different methods of providing control result in very similar operating conditions.

Control of a vapor cycle system is by an automatic system controller. A typical controller regulates evaporator discharge temperature by outputting a signal to the speed modulating valve of a turbo-compressor, which controls air flow through the turbine. Therefore, this controls compressor speed. The controller also regulates the ram air through the condenser by controlling the position of an exhaust valve. A comparison between a vapor cycle controller and a temperature controller on an input/output basis indicates a close comparison as to weight and volume. Therefore, vapor cycle controls are determined using the electronic temperature control equations previously obtained.

SECTION 4

PENALTY FACTORS

Environmental control system penalties may be considered in one of two categories - aircraft performance penalties or cost. Of course, the two are not independent.

Component weights and volumes (of major components), and power requirements and drag due to ram air usage (when appropriate) are provided in the previous section. Section 4.1 provides a compilation of the previously derived component weights. Installation weight factors are presented so that total environmental control system weight penalties may be determined.

Aircraft performance penalties due to the environmental control system are a function of the total system weight, the power required by the ECS from other aircraft systems, and other aircraft parameters (e.g. take-off weight, fuel weight, drag, etc.). ECS use of power from other aircraft systems is an additional weight penalty factor which is discussed in Section 4.1. Discussion of the aircraft performance penalty factors will be presented at a later date as part of the computer program description.

Reliability of an environmental control system has a strong influence on the logistics and maintenance cost of an aircraft. A development risk penalty is a measure of the probability and cost to develop a system which will perform as required during the life of the aircraft. A recurring cost penalty represents the unit cost to obtain the system. The reliability, development risk, and recurring cost penalty data presented in this section are relative to the Reference Simple Air Cycle System presented in Section 2.3. Problems involved in obtaining a logistic cost factor are discussed.

4.1 Weights

The weight data developed for the various system components in the previous sections are collected and summarized in this section. This summary is divided into five subsections to provide a breakdown according to application of the various systems and subsystems. In addition to the weight equations of the system components as specific items, weight factors for installation are provided. These factors account for the miscellaneous clamps, end fittings, support brackets, and fasteners required to complete the assembly of the system in the aircraft.

A weight factor for installing most ECS components is based on grouping numerous system components together, and locating each group into a cubic space of the aircraft. The installation weight factor for ECS packages is developed as a function of the sum of the component weights grouped into the package. Installation weights versus the sum of component weights is shown in Figure 140. The installation factor accounts for supports, brackets, and miscellaneous hardware for installing the equipment in the aircraft. The installation factor for ECS packages (shown in Figure 140) is:

$$Wt = 0.205 \sum_{i=1}^N (\text{Wt of each component}) \quad (311)$$

where N is total number of components in the package. Installation factors may be as large as 0.30, depending on the definition of structure which support the ECS.

Installation weight factors for ducting, auxiliary power units, power drives, and control systems are discussed in the following subsections.

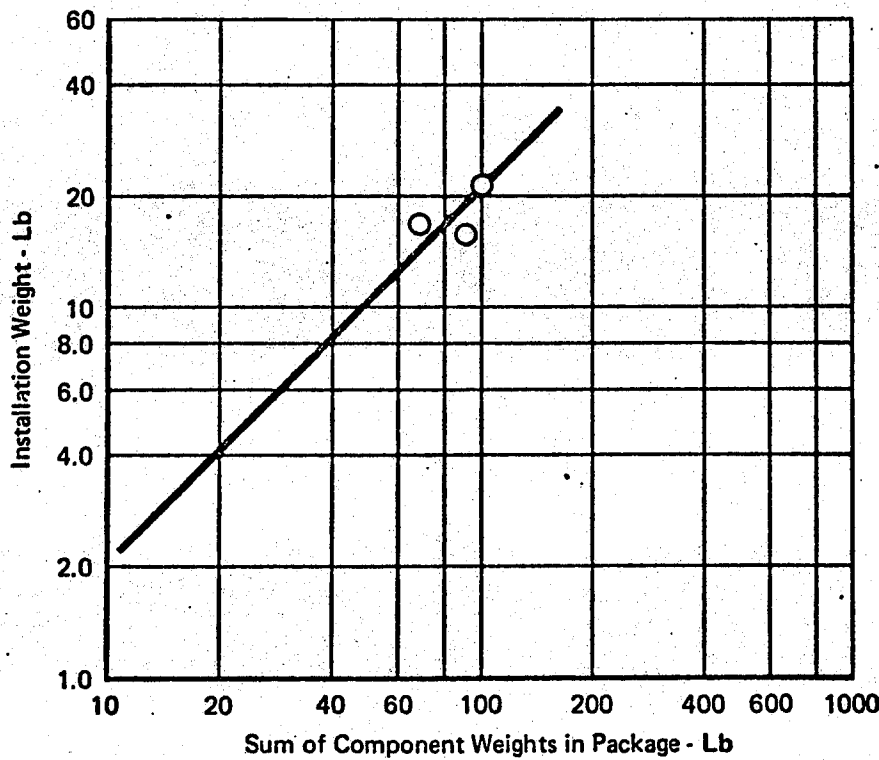


Figure 140 Package Installation Weight

GP 9416-177

4.1.1 Air System Components

Heat Exchangers - (See Section 3.1.) Weight of the heat exchanger core (Heat Transfer Surface) is defined by Equation (63).

$$Wt_{core} = Wt_{FH} + Wt_{FC} + \rho_{metal} (n_H + n_C + 1) L_C L_H t_{SP} \quad (312)$$

The fin weights (Wt_{FH} and Wt_{FC}) are calculated from Equation (56):

$$Wt_{FH} = \rho_{FH} V_H, \text{ and } Wt_{FC} = \rho_{FC} V_C \quad (313)$$

The bulk fin densities (ρ_{FH} and ρ_{FC}) are determined from Equation (58) for triangular fin geometry:

$$\rho_F = \frac{pt_F \rho_{metal} (s + \frac{\pi r \phi}{180})}{b} \quad (314)$$

Equation (60) is for rectangular fins geometry:

$$\rho_F = \frac{t_F p \rho_{metal} [b + 1/p + t_F (2\pi - 9)]}{b} \quad (315)$$

Equation (62) is for rounded fins geometry:

$$\rho_F = pt_F \rho_{metal} [b - t_F + \frac{1}{p} (\frac{\pi}{2} - 1)] \quad (316)$$

The volume of one side of the core is found from Equation (55):

$$V_H = n_H b_{TH} L_C L_H \text{ and } V_C = n_C b_{TC} L_C L_H \quad (317)$$

The separation plate weight is determined from the last term in Equation (63). The product $(n_H + n_C + 1) L_C L_H t_{SP}$ defines the volume of all the separator plates. The separator plate metal density (ρ_{metal}) then determines the separator plate weight.

Equation (64) defines the wrap-up weight of the heat exchanger which includes allowance for headers and miscellaneous supports.

$$Wt_{HX} = K_1 Wt_{core} (V_{core})^{-0.118} \quad (318)$$

Water boiler weight is determined by the summation of Equation (63), the core weight, Equation (70), the water weight:

$$Wt_W = BR(0) \quad (319)$$

and Equation (72), the container weight:

$$Wt_{\text{container}} = 2 (6 V_B^{2/3} t_{\text{metal}} \rho_{\text{metal}}) \quad (320)$$

Resistance heater weight is determined in Section 3.1.4.

$$Wt_{\text{Heater}} = \rho \frac{KW}{25} \quad (321)$$

where:

ρ is obtained from Figure 52

KW = electrical power in kilowatts.

Turbomachinery - (See Section 3.2.) Turbomachinery wheel and housing weight is defined by Equation (104):

$$Wt = 0.40D^2 \quad (322)$$

where:

D = wheel diameter.

Water Separators - (See Section 3.3.) Water separator weight is defined by Equation (119):

$$Wt = 0.0936 W_m \quad (323)$$

where:

W_m is air flow rate at maximum efficiency.

Dust Separators - (See Section 3.4.) Static dust separator weight is calculated from Equation (124):

$$Wt = 0.195 W_m^{0.79} \quad (324)$$

Self-cleaning high pressure dust separator weight is determined from Equation (127):

$$Wt = 0.5 + 0.0346 W, \quad (325)$$

while low pressure dust separator weight is found from Equation (131):

$$Wt = 0.18 + (9.3 \times 10^{-4}) Q \quad (326)$$

Fans - (See Section 3.5.) Electric motor driven fan weight is based on Equation (140):

$$Wt = 0.26 D_T^2 \text{ (for a.c. or d.c. motors)} \quad (327)$$

Hydraulic motor driven fan weight is calculated from Equation (142):

$$Wt = 0.178 D_T^2 \quad (328)$$

Larger fans utilizing shaft drives show weight to be a function of D_T also. Equation (143) describes shaft driven fan weight:

$$Wt = 0.109 D_T^2 \quad (329)$$

Plumbing - (See Section 3.10.1.) High pressure ducting weight is determined from Equation (195):

$$Wt = L t (2.40 D + 1.25) \quad (330)$$

Ducting for refrigeration units weigh 70% of the high pressure ducting weight.

Low pressure aluminum ducting weight is calculated from Equation (196):

$$Wt = 0.34 L t D \quad (331)$$

Low pressure fiberglass ducting weight is found from Equation (197):

$$Wt = 0.40 L t D \quad (332)$$

Flexible ducting, suitable for low pressure applications, weigh:

$$Wt = 0.0149 L D \quad (333)$$

General low pressure ducting (a typical combination of the above three types of ducting) weight is obtained from Equation (198) or (199):

$$Wt = 0.0137 DL, \text{ for } D \leq 3.5 \quad (334)$$

$$Wt = (0.0179 D - 0.0147) L, \text{ for } D > 3.5. \quad (335)$$

Ducting installation factors are based on typical duct runs as installed in actual aircraft. The installation factors are a function of the duct diameter and the duct run length. (See Figure 141.) An allowance for duct assembly installation is:

$$Wt = (3.45 \times 10^{-4}) (DL)^{1.58} \quad (336)$$

This correlation has a standard error of 15.8%.

Pneumatic control line weight is calculated using Equation (203).

$$Wt = 0.3071 (D_o - t) L t \frac{\rho}{\rho_{aluminum}} \quad (337)$$

Inlets and Outlets - (See Section 3.10.3.) The weight of a general inlet is calculated by Equation (220):

$$Wt = 8 \rho t A_1 \quad (338)$$

The cross-sectional area (A_1) of the inlet mixing tube is defined by Equation (217). Equation (224) defines the diffuser weight:

$$Wt = \rho t S \quad (339)$$

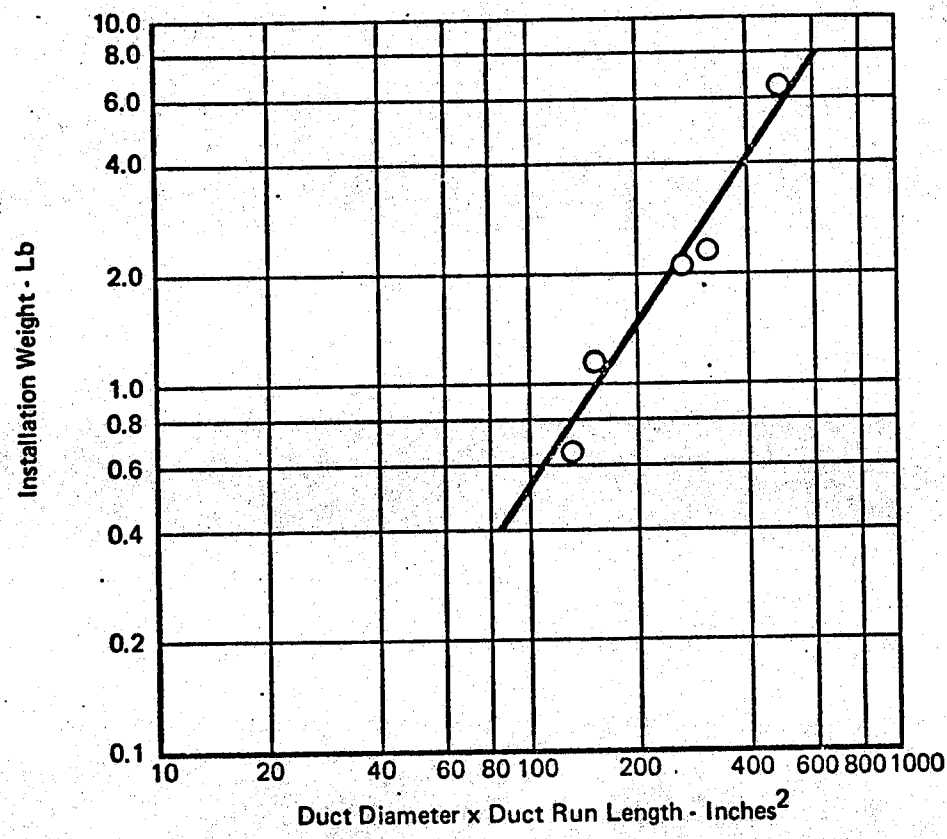


Figure 141 Duct Installation Weight

GP 9416-178

Where S is the surface area of a 12° truncated cone. (See Equation 223.)
Outlet weight (with no ram air ejector) is determined by Equation (228):

$$Wt = 4.5 \rho t (1 + 1.69 \sqrt{A_X} + 1.20 A_X) \quad (340)$$

A_X is the exit area.

Ejectors - (See Section 3.10.4.) Weights of ram air ejectors (with bleed air nozzle assembly and mixing tube) are calculated using Equation (237):

$$Wt = 1.2 [0.244 (2.5 B + 2) \frac{t}{0.244} \frac{\rho}{113}] \quad (341)$$

where the number of single-nozzle ejector modules (B), the material thickness (t), and the material density (ρ) are the factors that determine weight. Water boiler ejector weight is included as part of the water boiler weight.

Valves - (See Section 3.10.5.) Weights for four types of valves are presented; pneumatic butterfly valve equations are (249), (250), and (251):

$$Wt = 2.68 D - 1.0 \quad (\text{steel}) \quad (342)$$

$$Wt = 0.70 D + 0.35 \quad (\text{aluminum for } D < 2.5, \text{ minimum} = 0.5 \text{ lb}), \quad (343)$$

and:

$$Wt = 1.26 D - 1.05 \quad (\text{aluminum for } D > 2.5); \quad (344)$$

motor actuated butterfly valves, Equations (252) and (253),

$$Wt = 1.14 D + 0.9 \quad (\text{steel}), \text{ and} \quad (345)$$

$$Wt = 0.56 D + 1.1 \quad (\text{aluminum}); \quad (346)$$

poppet valves, Equations (254) and (255),

$$Wt = 2.04 D + 0.225 \quad (\text{steel}), \text{ and} \quad (347)$$

$$Wt = 0.833 D - 0.05 \quad (\text{aluminum, minimum} = 0.3 \text{ lb}); \text{ and} \quad (348)$$

check valves, Equations (256) and (257),

$$Wt = 0.625 D - 0.625 \quad (\text{steel}), \text{ and} \quad (349)$$

$$Wt = 0.33 D - 0.38 \quad (\text{aluminum}). \quad (350)$$

A nominal minimum weight for check valves is 0.25 lb.

Insulation - (See Section 3.11.) Bleed duct insulation weights are based on Equations (270) and (271), for radiation air gaps of 1/2 inch and 1/4 inch, respectively (L is feet of length).

$$Wt = L (0.0464 D_D + 0.0386), \quad (1/2" \text{ gap}), \text{ and} \quad (351)$$

$$Wt = L (0.0282 D_D + 0.0128), \quad (1/4" \text{ gap}). \quad (352)$$

Removable, blanket-type bleed duct insulation weights for 1/4 inch and 1/2 inch thickness area found from Equations (273) and (274) respectively (L is feet of length).

$$Wt = L [(0.0051 \rho_{bu} + 0.12) D_D + (0.0025 \rho_{bu} + 0.191)], \quad (1/4" \text{ thick}) \quad (353)$$

$$Wt = L [(0.011 \rho_{bu} + 0.12) D_D + (0.0046 \rho_{bu} + 0.422)], \quad (1/2" \text{ thick}) \quad (354)$$

Removable, blanket-type, distribution duct insulation weight is determined by Equation (280) (L is feet of length).

$$Wt = [\pi (D_D + t) (\rho_s / 6) + 0.00417t]L \quad (355)$$

where ρ_s represents the specific weight of the insulation cover. Compartment theoretical insulation weight is calculated using Equation (294).

$$Wt = 7.29 \times 10^{-3} [(0.05t)_{\text{insulation}} + (0.07)_{\text{covers}}]A \quad (356)$$

This weight represents the insulation material and its associated cover. The above equation is also used to calculate fuel tank insulation weight.

4.1.2 Liquid Subsystem Components

Pump Package - (See Section 3.6.) Vane or gear pump and electric motor drive weight is determined from Equation (147):

$$Wt = 10.63 \left(\frac{1728Q}{N} \right)^{2/3} \quad (357)$$

If the quantity $\left(\frac{1728Q}{N} \right) < 0.088$, $Wt = 2.1$ lb. Centrifugal pump and electric motor weight is defined by Equation (148):

$$Wt = 22.92 \left(\frac{1728Q}{N} \right)^{2/3} \quad (358)$$

If the quantity $\left(\frac{1728Q}{N} \right) < 0.028$, $Wt = 2.1$ lb.

Reservoir weight is computed with Equation (149):

$$Wt = 0.131 V_d^{2/3} \quad (359)$$

where V_d is the fluid volume of the system.

Filter weight is calculated from Equation (150):

$$Wt = 0.55 + 0.128 (W') \quad (360)$$

Weight of the pump package (i.e. pump, drive, filter, bypass valve, reservoir, miscellaneous lines) is 10% to 15% more than the sum of the components weight.

Heat Exchanger - (See Section 3.1.) Liquid heat exchanger weight calculations are outlined in Section 4.1.1. Note that the weight of liquid in the core is accounted for by using Equation (55) and the density of the liquid.

Plumbing - (See Section 3.10.) Coolant or liquid line weight is the sum of the line and liquid weight.

$$Wt = Wt_{line} + Wt_{co} \quad (361)$$

Line weight is defined by Equation (203).

$$Wt_{line} = 0.3071 (D_o - t) L t \frac{\rho}{\rho_{aluminum}} \quad (362)$$

The weight of the liquid is found by Equation (204).

$$Wt_{co} = \frac{\pi}{4} D_i^2 L \rho_{co} \quad (363)$$

where ρ_{co} is the specific weight of the coolant or liquid.

Valves - (See Section 3.10.) Since liquid system line diameters are small ($D < 1.0$) the control valve weight (Equation (253)) is estimated as a constant:

$$Wt = 1.1 \quad (364)$$

4.1.3 Vapor Cycle Components

Compressors - (See Section 3.7.) Vapor cycle centrifugal compressor weight is one half of the weight of the motor needed to drive the compressor.

Evaporators and Condensors - (See Section 3.7.) Evaporator and condenser weight is calculated using the method described in Section 4.1.1.

Refrigerant - (See Section 3.7.) The refrigerant charge weight is:

$$Wt = (1.15/\text{ton}) + 0.04/(\text{ton}/L), \quad (365)$$

where L is the separation of the evaporator and condenser in feet, and (ton) is the system cooling capacity. An alternate method for determining refrigerant charge weight is:

$$Wt = 1.50 [0.20 \rho_R V_{\text{evaporator}} + 0.40 \rho_R V_{\text{condensor}} + 0.002 Q] \quad (366)$$

where Q is the vapor volumetric flow rate at the compressor inlet.

Receiver - (See Section 3.7.) The receiver weight is:

$$Wt = \rho_{bu} (1.20 V_R) \quad (367)$$

where $\rho_{bu} = 0.01 \text{ lb/in}^3$ and V_R is the refrigerant charge volume.

Plumbing - (See Section 3.10.) Refrigerant line weight is:

$$Wt = 01. Wt_B + 0.01 Wt_B L \quad (368)$$

The basic weight (W_{t_B}) represents the combined weights of the evaporator, condenser, reservoir, and pump. The separation weight (L) is the distance between the condenser and evaporator.

4.1.4 Auxiliary Air Sources and Power Drives

Auxiliary Power Units - (See Section 3.8.) Installed weight for APU's providing bleed air and shaft power is calculated from Equation (170):

$$W_t = \frac{EHP}{(4.215 \times 10^{-4})(EHP) + 0.159} \quad (369)$$

Bare APU's are approximately 39.8% of the installed weight.

Auxiliary Compressors - (See Section 3.8.) Weight of an auxiliary compressor wheel and housing is defined by Equation (104):

$$W_t = 0.4D^2 \quad (370)$$

The weight of associated clutch and gearing equals the compressor weight.

Power Drives - (See Section 3.9.) Equations (177) and (180) define the weights for a.c. and d.c. powered electric motors, respectively.

$$W_t = 2.0 + 2.3 (HP)^{5/6} (N \times 10^{-4})^{-1.25} \text{ for a.c. power, and} \quad (371)$$

$$W_t = 1.5 + 3.83 (HP)^{5/6} (N \times 10^{-4})^{-1.25} \text{ for d.c. power.} \quad (372)$$

Hydraulic motor drive weight is computed by Equation (181):

$$W_t = 11.37 \left(\frac{1728Q}{N} \right)^{1/2} \quad (373)$$

This equation does not account for gearing. If gearing is included:

$$W_t = 17.055 \left(\frac{1728Q}{N} \right)^{1/2} \quad (374)$$

Pneumatic drive weight is computed from Equation (104) to account for the turbine wheel and its housing:

$$W_t = 0.40D^2. \quad (375)$$

Power Drive Installation - An additional ECS weight penalty is incurred because use of an electric or a hydraulic power drive increases the size of the electrical generator or the hydraulic pump.

The electric system penalty includes additional weight for the generator, wiring, and busses. Nominally the maximum electrical load is 60% of the generating system capacity (i.e., the generators are not 100% redundant), and two or more generators are used.

Present generating systems (generator and busses) of 60 to 90 KVA capacity have a penalty of 2.0 lb/KW. Present designs include a constant speed drive (CSD). Older generating systems used a variable speed constant frequency (VSCF) design which are heavier (50% or more). (See Reference 41.) Wire weight is assessed as 0.007 lb/KW per foot of run. Typical efficiencies at high load factors are 85% or greater.

Hydraulic power is provided by an engine or APU shaft driven pump. Based on a maximum delivered fluid power to the ECS power drive, a 0.5 lb/HP penalty is assessed. This value accounts for the sizing effects on the hydraulic pump, reservoir, valves, and pressure regulator. This weight penalty assumes a 90% pump and line efficiency based on pump loads above the rated capacity. An additional penalty of 0.045 lb/HP per foot of line run is typical for low power (HP < 10) hydraulic lines.

4.1.5 Controls

Temperature Controls for Air and Liquid Systems - (See Section 3.12.) Total weight for electronic control systems is defined by Equation (302):

$$Wt = \left[\frac{NIAO}{3} + Wt_{\text{Selector}} + 0.2 \times (\text{Number of Sensors}) \right] K_{Te} K_{Re} \quad (376)$$

where K_{Te} is the technical weighing factor and K_{Re} is the requirements weighting factor. Pneumatic control system weight is the control head weight (Equation (303)) and the sensor weight, modified by weighting factors:

$$Wt = [0.5 D + 1.0 + Wt_{\text{Sensor}}] K_{Te} K_{Re} \quad (377)$$

Sensor weight is between 0.5 to 1.0 pound. Electro-pneumatic controls are considered to weigh 66.8% of the electronic controls weight. The additional weight of BITE is included in the K_{Re} .

Pressure Controls for Compartments - (See Section 3.12.) Weight of the pressure control system (controller, outflow valve, sensors, selector, and safety valves) is determined by Equation (305):

$$Wt = 6.0 \text{ (for fighter aircraft)} \quad (378)$$

$$Wt = 51.45 + 0.0967 W \text{ (for cargo/bomber aircraft)} \quad (379)$$

The pressure control system weight is increased by 1.0% to account for BITE. Installation weight is estimated at 30% of the sum of the component weights.

4.2 Reliability

The inherent reliability of an ECS is dependent on the detail design of the components and the selection of components assembled into a system. The reliability actually realized from an ECS also is dependent on other considerations such as the environment in which the ECS will operate, the frequency of needed maintenance and the probability of actually getting it, the ease of maintenance from the accessibility and human factors point-of-view, and the complexity of maintenance procedures. All these considerations affect reliability predictions, but are unknowns early in a program.

Reliability of component designs is achieved by utilizing the best design methods available. Reliability must be considered a design tradeoff as are performance, weight, or cost. Maximum reliability is obtained when it is considered as an important tradeoff parameter. If components are designed to meet a minimum reliability requirement, few of them will. Components should be designed toward a reliability goal much larger than the minimum. This "overdesign" results in increased weight and cost in many cases, but it is necessary if most of the components are to attain the minimum reliability.

Reliability of the system is determined primarily by the complexity of the system and by the type of subsystems used. Without a major advance in the state-of-the art it is unreasonable to expect a system that is sophisticated in performance and construction to have an inherent reliability greater than a system of less sophistication. The following analyses assess the reliability of ECS based on its complexity and sophistication.

4.2.1 Air Systems - The item causing the greatest reliability penalty in cycle systems almost always is the turbomachine assembly. The greatest

improvement in system reliability will be realized by making reliability the number one priority in turbomachine design and development. The state-of-the-art is such that considerable time and effort must be applied to turbomachine design and development before maximum reliability can be attained. (This may have been done for the new simple-bootstrap turbomachine (3 wheel) used in current large subsonic aircraft.)

ECS that use auxiliary subsystems not directly related to equipment cooling (e.g. bleed air for anti-icing) have a higher reliability penalty. This penalty must be outweighed by some other consideration before the use of such subsystems is warranted. Air cycle system components receive a great deal of contamination through the bleed air system. Attention must be given during detail design to eliminate areas where the contaminants may lodge and affect component operation. Icing also is a problem. Prevention of ice build-up in the system and protection of internal components (such as sensors and limit switches) from ice is essential. Components should be oriented in such a manner that condensation does not accumulate in areas that will cause corrosion and system failure.

A significant increase in reliability can be obtained if the ratio of system operating time to flight time is reduced. This ratio may vary from less than 1 to greater than 4. A reduction can be accomplished through use of an independent shut-off device which allows the system to operate only when necessary.

4.2.2 Liquid Subsystems - Liquid subsystems pose an additional problem not present in the air systems. This is leakage. An air system can tolerate some leakage with no drastic effects. Leakage in a liquid system becomes catastrophic because of a limited fluid supply.

Some liquid coolants are susceptible to water contamination and must be changed periodically. Water causes the liquid to precipitate solids which can jam valves and clog filters. A potential problem to be avoided is a pressurized liquid reservoir with a precharge gas volume and pressure which are so low that normal checking of the gas pressure with an external gage depletes the precharge. Pump cavitation then results followed by pump failure.

4.2.3 Vapor Cycle Systems - Vapor cycle systems reliability (presently used in cargo aircraft) are comparable to air cycle system reliability. Contributing to better reliability is reduced complexity and contamination (because it is a closed system).

Many vapor cycle systems are removed as a package from the aircraft for repair, so there are little data available on component failures. However, as in the air cycle system, the compressor is the least reliable component. Most compressors are of the centrifugal type, driven by turbines or electric motors. The electric motor driven compressors appear to be more reliable than the turbine driven types, but considerable variations have been reported.

Future systems should have provisions to check and service refrigerant charge without requiring removal of system components. Such provisions should help eliminate maintenance induced failures and false reports of corrective action to components.

4.2.4 Controls - Air cycle valves, sensors, limiters, and controllers in pneumatic subsystems tend to be more reliable than those in electrical control subsystems. Although little data are available, it appears that fluidic controls will be more reliable than their electrical and pneumatic counter-parts merely because of their structural simplicity and lack of moving parts. Contamination of the fluid could prove to be a significant problem however.

Little data are available on components of vapor cycle temperature control systems. The systems, however, are more reliable than those of air cycle systems.

The order of preference for maximum reliability of anti-ice controls is:

1. Icing screen
2. Reference ΔP
3. Constant 35°F

The most reliable anti-ice control is utilized in the vapor cycle system. Since the evaporator discharge air temperature is maintained above freezing, no control system is required.

All types of pressure controls are expected to be approximately equal in reliability. Controls in heavy bombers and cargo aircraft seem to be more reliable than those in fighters and light bombers. The difference is probably attributable to the greater cycles per flight hour in the fighters and light bombers.

4.2.5 Reliability Index - The reliability of components and systems often is expressed as the Mean Time Between Failures (MTBF). The failure rate (failures per unit of time) is the reciprocal of MTBF. The failure rates of the components of an ECS may be summed to obtain the system failure rate, and hence the system MTBF (i.e., the reciprocal of the system failure rate).

A Reliability Index is defined by the following equation:

$$RI = \frac{10^6}{(MTBF)K_1} \quad (380)$$

where: RI = Reliability Index

MTBF = Mean Time Between Failures in operating hours.

Components with the low RI Numbers are the more reliable components. The Reliability Index of the Reference Simple Air Cycle System is set equal to 1.00000. The failure rates of all the components used in this reference system were summed. The MTBF of the Reference Simple Air Cycle System is approximately 175 hours, hence the constant K_1 in Equation (380) is equal to 5726.58.

Reliability Index Numbers of ECS components and subsystems are found in Table XIV. The RI Numbers in this table are obtained by first determining what basic design features affect the gross reliability of a component. An application factor also is considered for turbomachine designs. A fighter or light bomber turbine is less reliable than a turbine in a bomber or cargo aircraft because of the larger and more frequent changes in flight conditions with corresponding changes in input conditions to the turbine. Failure rates are obtained from the following sources: 1) AFM 66-1 (Air Force F-4), 2) Navy Maintenance and Material Management Reporting System (Navy F-4), 3) MDC data, 4) FARADA (Aircraft Source Codes), and 5) vendor estimates.

This RI approach provides for comparisons of subsystems and complete systems. RI Numbers for each component in the system are added together. If BITE is used, the total RI of the controls is approximately 5% higher. The system with the lowest total Reliability Index Number has the greatest MTBF.

Table XIV Sheet I
Reliability Index Numbers

<u>COMPONENT</u>	<u>RI NUMBER</u>
Heat Exchanger	
Air/Air, Single Pass	0.00256
Air/Air, Double Pass	0.01973
Liquid/Air	0.00328
Water Boiler	0.02165
Liquid/Liquid	0.00106
Electric Heaters	0.01109
Turbomachines	
Simple Cycle	
Bomber/Cargo	0.04575
Fighter/Light Bomber	0.06793
Bootstrap Cycle	
Bomber/Cargo	0.00929
Fighter/Light Bomber	0.05136
Simple-Bootstrap Cycle (3 Wheel)	0.00794
Water Removal/Dust Separators	
Collector, Water	0.00175
Separator, Water	0.00285
Separator, Dust	0.04135
Fans	
Electric	0.00546
Hydraulic	0.01162
Pneumatic	0.00707
Pumps	
Liquid Coolant, Electric Drive	0.04016
Liquid Coolant, Hydraulic Drive	0.02322
Liquid Coolant, Pneumatic Drive	0.06891
Vapor Cycle Components	
Motor-Compressor	0.00873
Turbine-Compressor	0.02567
Compressor Oil Pump	0.00918
Evaporator	0.00216
Condenser	0.00306
Expansion Valve	0.00760
Receiver	0.00513
Auxiliary Compressors	
Bleed Air Turbine Driven	0.07072
Electric Motor Driven	0.01976
Hydraulic Motor Driven	0.00780
Shaft Driven	0.00072
APU	0.24971
Ducts	
Bleed Air	0.01164
Bleed Air, Wye	0.04005
Bleed Air Manifold	0.07098
Conditioned Air	0.00291
Bleed Ejector	0.00177
Drain Line	0.00285

Table XIV Sheet 2
Reliability Index Numbers

<u>COMPONENT</u>	<u>RI NUMBER</u>
Reservoirs	
Bladder	0.01310
Piston	0.12486
Diaphragm	0.00873
Plain Tank	0.00707
Valves	
Butterfly, Electric Motor, Open-Close Cycle	0.04820
Butterfly, Electric Motor, Modulating Cycle	0.07649
Butterfly, Pneumatic, Open-Close Cycle	0.00943
Butterfly, Pneumatic, Modulating Cycle	0.04610
Poppet, Solenoid	0.00262
Gate, Electric Motor	0.03065
Flow Control, Bleed Air	0.02267
Pressure Regulating, Single Schedule, Hot Air	0.00529
Pressure Regulating, Double Schedule, Hot Air	0.08731
Pressure Regulating, Suit	0.02331
Pressure Regulating, Cabin	0.10373
Pressure Relief, Duct	0.00135
Pressure Relief, Cabin	0.04645
Bypass, Vernatherm	0.00571
Pressure Relief, Liquid	0.00219
Butterfly, Electric Motor with Brake, Modulating Cycle	0.77708
Ram Air Shutoff	0.00536
Bleed Air Check	0.05710
Ram Air Check	0.00181
Bleed Air Shutoff, Pneumatic	0.05291
Diverter	0.00999
Controllers	
Selector, Temperature	0.00213
Pneumatic, Temperature	0.00582
Electrical, Single Output with Relay	0.43656
Electrical, Single Output, Solid State	0.04628
Electrical, Dual Output with Relays	0.48545
Electrical, Dual Output, Solid State	0.15280
Cabin Pressurization, Solid State	0.09430
Cabin Pressurization Amplifier	0.01205
Sensors/Limiters	
Switch, Low Air Temperature Limit	0.01317
Switch, High Air Temperature Limit	0.02498
Sensor, Electrical, Temperature, Air	0.03781
Sensor, Pneumatic, Temperature, Air	0.04069
Limiter, Pneumatic	0.00498
Sensor, Cooling Effect with Heater	0.02030
Sensor, Liquid Temperature	0.00291
Switch, High Temperature Limit, Liquid	0.01259
Anticipator, Temperature, Pneumatic	0.02532

4.3 Cost Factors

The following environmental control system cost factors are discussed: development risks, recurring costs, and logistic costs.

4.3.1 Development Risk Factors - The procedures for developing an environmental control system and its many components vary according to the requirements of the load, the flight environments to be encountered (i.e. aircraft mission), and the relative importance of development costs, system performance, and maintainability (as determined by the cognizant procuring agency). Hence ECS development risks may be related to the type of system and its intended use (e.g. temperature, speed, etc.), and to the aircraft system development plan. The latter is not considered herein.

Each of the ECS component types is assigned a relative development risk factor. Arbitrarily, a development risk factor (DR) of 1.0 is assigned to each of the types of components in the Reference Simple Air Cycle of Section 2.3. The development risk factor of an ECS is defined as the product of the component DR's and a system DR. The system DR relates the development risks involved in utilizing the numerous ECS components in any integrated system compared to that of a Simple Air Cycle.

The development risk factors are intended for comparisons of environmental control systems to be used in the same aircraft application only.

Component development risk factors are discussed first. This is followed by comments on system development risk factors.

4.3.1.1 Component Development Risk Factors - Component development risk factors are assigned a value of 1.0 if their development is present state-of-the-art design. Components may have higher or lower development risk factors (but greater than zero). Development risk factors of components are not varied according to the type of aircraft in which they are used, the aircraft mission, or the environment surrounding the component (e.g. vibration, shock mounting, location in aircraft, etc.). The component development risk factors also are modified by the steady state fluid properties and other component properties (e.g. speed). For example, a check valve used in the conditioned air duct of an existing aircraft has a DR of 1.0, and a check valve used in the bleed air duct of this aircraft also has a DR of 1.0, because each valve (individually) is designed with present state-of-the-art concepts. As would be expected, therefore, future state-of-the-art component designs have a DR greater than 1.0.

Component development risk factors are discussed in the same order as in Section 3.0.

Heat Exchangers - The DR of air-to-air heat exchangers is assigned a value of 1.0 if the fluid inlet temperature is equal to or less than 1300°F and the pressure is less than 300 psig. New materials are required above 1300°F. Plate-fin designs are impractical above 300 psig. For air temperatures above 1300°F the DR is greater than 1.0. At an air temperature of 1600°F the DR is estimated as 50% greater than at 1300°F, with a parabolic increase of the DR above 1300°F. Similarly, a DR of 1.5 at an air pressure of 500 psig is selected. These two factors are considered as additive, hence the development risk of air-to-air heat exchangers is:

$$\text{DR} = 1.0 \quad \text{at } T \leq 1300^{\circ}\text{F}, \quad P \leq 300 \text{ psig} \quad (381)$$

$$\text{and: } \text{DR} = 1.0 + \left(\frac{T-1300}{425}\right)^2 + \left(\frac{P-300}{283}\right)^2 \quad (382)$$

$$\text{at } T > 1300^{\circ}\text{F}, \quad P > 300 \text{ psig}$$

The critical factor in heat exchangers containing a liquid (other than a water boiler) is the temperature and pressure condition at which vaporization occurs. If the liquid becomes a vapor, the heat exchanger may be damaged (e.g. headers or core inlets). Thus the development risk factor is very large. An increase in the DR also occurs at 300 psig. Thus, for heat exchangers containing a liquid:

$$\text{DR} = 1.0 + \left(\frac{P-300}{283}\right)^2 \quad (383)$$

The development risk factor for water boiler heat exchangers is assigned a value of 1.15 times as high as an air-to-liquid heat exchanger, since few water boiler heat exchangers have been used previously.

Air Cycle Machines - A simple air cycle turbomachine, as is used for the Reference Simple Air Cycle System, is assigned a DR of 1.0. Since it is necessary to design this simple cycle turbomachine for high overspeed conditions, a bootstrap air cycle turbomachine is assigned a DR which is 0.8 times that of a simple air cycle machine. The simple-bootstrap (3-wheel) air cycle machine is relatively new. Three large 3-wheel turbomachines

have been developed, and one small machine recently went into service. The simple-bootstrap air cycle turbomachine is assigned a DR which is 1.05 times that of a simple cycle turbomachine.

The air temperature, blade tip speed, and rotational speed are factors which affect the development of air cycle machines. Present maximum air temperatures are about 1000°F. A parabolic increase of the DR is considered above 1000°F, with a DR of 2.0 at 2000°F. Designs for keeping a wheel intact, and for providing containment should it fail, are related to the wheel tip speed. A maximum tip speed of 1500 feet per second is considered state-of-the-art, hence turbomachines with a tip speed equal to or less than 1500 feet per second have a DR of 1.0. A parabolic increase in the DR, at tip speeds above 1500 feet per second, to a DR of 1.5 at 2000 feet per second, is selected. Oil bearings are used up to a maximum rotational speed of about 60,000 rpm, and air bearings designs are degraded at speeds less than about 60,000 rpm. A DR of 1.0 is considered up to a maximum rotational speed of 60,000 rpm. A DR of 1.5 at 90,000 rpm is assumed for oiled bearings, with a parabolic variation above 60,000 rpm. A DR of 1.05 is assumed for air bearings at 50,000 rpm, with a parabolic variation below 60,000 rpm.

The temperature, tip speed, and rotational effects are assumed to be independent, thus the following equations are used:

$$DR = 1.0 \quad (384)$$

If: $T_{c,out}$ and $T_{t,in} \leq 1000^{\circ}\text{F}$

$$U'_{T} \leq 1500 \text{ ft/sec}$$

$$N_{oil} \leq 60,000 \text{ rpm or } N_{air} \geq 60,000 \text{ rpm}$$

$$\text{and: } DR = \left[1 + \frac{T-1000}{1000} \right]^2 \left[1 + \frac{(U'-1500)^2}{707} \right] \left[1 + \left(\frac{N_{oil}-60,000}{42,500} \right)^2 \right] \quad (385)$$

If: $T > 1000^{\circ}\text{F}$, $U' > 1500 \text{ ft/sec}$,

and $N_{oil} > 60,000 \text{ rpm}$.

For air bearings at $N_{air} < 60,000$ rpm, the latter term in Equation (385)

is: $[1 + (\frac{60,000-N}{45,000})^2]$

Water Separators - The development risk factor of water separators located downstream of an expansion turbine is 1.0 (they are state-of-the-art). A high pressure water separator (heat exchanger) has an assumed DR which is 1.2 times that of a heat exchanger. This assumption is made to account for the phase change which takes place, and the few units which have been built.

Fans - A large number of air circulation and distribution fans, or ram air fans, have been developed. These designs should be adequate in the future, hence fans are assigned a DR of 1.0. Although electric motor fan drives are used most often, the development risk of fans using other types of drives should not be affected.

Vapor Cycle - Vapor cycle system designs generally are considered as present state-of-the-art. Air cooled vapor cycle condensers have the same development risk factor as do liquid heat exchangers having air on one side. Evaporators used for air cooled heat loads have a DR which is higher than that condensers because of the moisture condensation on the air side. Few liquid cooling evaporators have been developed, hence their development risk also is high. Hence evaporators are assigned a DR which is 1.2 times that of a simple heat exchanger. Electric or hydraulic motor driven compressors have a DR of 1.0 (i.e. the development is equivalent to a simple air cycle machine). Turbine driven compressors are assigned a DR of 1.15 times that of a simple cycle machine.

Auxiliary Air Sources - The development risk factor of an APU is influenced by the shaft power requirements, the accuracy of the gear box speed control, and the turbine inlet temperature. High turbine inlet temperatures are usually the result of trying to reduce weight or to keep weight to a minimum. Two spool machines also would have a higher development risk. An APU is assigned a DR of 1.15, but if the shaft power is greater than 150 HP (i.e. greater than many present designs), a DR of 1.20 is used. If accurate speed control is included the DR is 1.25, and if a high performance APU is used the DR is 1.35.

The development risk factor for an auxiliary compressor is the same as for a simple air cycle machine. A staged compressor would have a higher development risk.

Power Drives - Electric, hydraulic, and shaft types of power drives have a DR of 1.0 since they are commonly used. The pneumatic power drive development risk is the same as that of a simple air cycle machine.

Plumbing - Aluminum, fiberglass, and steel ducting have a present state-of-the-art relative development risk factor of 1.0. The DR of titanium ducting is higher.

Valves - Development problems in valve designs are to prevent chatter (poppet and check valves) and to provide adequate lubrication. These factors are partially related to pressure and temperature. The upper pressure and temperature limits for a DR of 1.0 are selected as 350 psig and 1000°F. At 1200°F the development risk factor is selected as 1.2, with a parabolic variation above 1000°F. A DR of 1.2 is assigned for a pressure of 550 psig using a 3/2 exponential variation. The pressure and temperature effects are considered independently, hence;

$$DR = 1.0$$

$$\text{if } T \leq 1000^{\circ}\text{F}, P \geq 350 \text{ psig}$$

(386)

$$\text{and: } DR = 1.0 + \left(\frac{T-1000}{450}\right)^2 + \left(\frac{P-350}{385}\right)^{1.5} \quad (387)$$

$$\text{if } T > 1000^{\circ}\text{F}, P > 350 \text{ psig}$$

Insulation - Insulations are available for use above 2000°F, hence a DR of 1.0 is used. If the compartment has a transpiration cooled insulation design (such as was in the experimental XB-70 bomber), a DR of 1.2 is selected.

Controls - Development risk factors for controls are the product of the Technical Weighing Factor and the Requirements Weighing Factor. (See Section 3.12.) Temperature control systems for fighter cockpits and equipment compartments normally are of the single-zone type; while for cargo aircraft multiple-zone controls may be used. Each of these is considered as having a development risk of 1.0. Controls for modulating the ram air flow are affected by external flow conditions, hence they have a

DR of 1.05. The DR for controlling the steam flow from a water boiler is selected as 1.1 since few have been developed. Controls on the intermediate transfer loop for a fuel heat sink are present state-of-the-art, hence it has a DR of 1.0. If the fuel flow also is modulated a DR of 1.2 should be used. Water separator anti-ice controls presently in use have a DR of 1.0, and a development risk of 1.1 is suggested for an improved water separator anti-ice control. Vapor cycle control techniques are varied, and few aircraft use vapor cycle systems, hence, a DR of 1.1 is suggested for vapor cycle controls.

Fixed isobaric compartment pressure controls typically are used in fighters, and proportional or variable isobaric plus rate pressure controls are used for cargo aircraft. Hence a development risk of 1.0 is used for these types of pressure controls on the respective types of aircraft. A development risk of 1.1 is recommended for a fixed isobaric plus fixed rate pressure control system on fighters, and a DR of 1.2 is recommended for a proportional or variable isobaric plus rate control on a fighter.

4.3.1.2 System Development Risk Factors - The development risks of the subsystems and systems of Section 2 are related to the arrangements of components in the systems or unique factors dependent on the aircraft in which the systems are used. Except for a few component arrangements, the DR's of the systems are 1.0, because the development risk factors related to most arrangements are included as a DR for one or more of the components. (For example, the arrangement of components for use of a high pressure water separator does not increase the system DR because the high pressure water separator DR is 1.2.) A fuel heat sink subsystem arrangement must be integrated with the engine fuel subsystem. Since few aircraft presently use fuel as an ECS heat sink, a DR of 1.05 is recommended. Several of the systems (i.e., Systems S2, B2, B3, and B5) allow for optional use of a regenerative heat exchanger. A system DR of 1.05 is suggested for any system arrangement which includes a regenerative heat exchanger because major use of the concept is in aircraft presently being developed. The hybrid vapor cycle-air cycle system (V3) is untried. It is assigned a DR of 1.2 because of potential complexities of flow rate and power balancing for the air loop turbine driven refrigerant compressor.

System development risks related to the aircraft include effects of the flight envelope, locations of the system or components in the aircraft,

and use of two or more systems in parallel or in series. Qualitatively these factors increase the development risks. Development problems of ECS in aircraft which fly higher and faster will be encountered. Requirements to shape some components to available aircraft space can cause development problems. Increased development risks are incurred if two or more different systems are to be used for different loads, but with commonalities between them. However, the DR is 1.0 if parallel identical systems are used (e.g. as in commercial aircraft). The reader should choose a development risk factor greater than one if he feels the aircraft imposes ECS development problems.

Numerous arrangements of the subsystems in the systems of Section 2.2 are possible. A subsystem development risk factor would represent potential complexities of the component arrangements of the subsystem.

4.3.2 Recurring Cost Factors - Relative recurring cost factors are presented for ECS components using the cost of the Reference Simple Air Cycle System (Section 2.3) as a cost base. The recurring cost of this Reference Simple Air Cycle System is defined as 1000 cost units (CU). This represents the summation of the component costs. The recurring costs do not include handling, system assembly, and installation into an aircraft since these vary depending on the component locations in the aircraft and aircraft manufacturer's practices for obtaining components and systems. The component cost data presented in this report are based on costs from References 68 and 69, and from vendors of environmental control systems and components. Hence, costs are based on present state-of-the-art designs. Some vendor cost data are considered proprietary and are not presented in detail. However, this information is used to obtain estimated cost trends.

The basis for the cost of the Reference Simple Air Cycle System is found in Table XV. Federal Stock Numbers are indicated when applicable. The sum of the estimated component costs of this system is \$20,196. Using this system cost, one cost unit (CU) represents \$20.196. Considerable scatter exists for some of the cost comparisons. This is probably due to detailed component requirements (e.g., vibration, ambient environment, shape, etc.) which are not encompassed by this general study, or to inconsistent quantity and dates for the costs of References 68 and 69 data. Other cost data are based on a 1970 economy and quantity sets of 100.

Table XV Reference Simple Air Cycle System

Component List

Item No.	Name	FSN	Remarks	Weight (lb)
1	Duct (2), Engine Manifold		3.0D	25 ea.
2	Valve (2), Check, Bleed Air	4820-182-8978	4.5D	2.35 ea.
3	Duct, Wye, Bleed Air		4.5D	28
4	Valve, Shutoff, Bleed Air	4810-443-1691	4.5D (Butterfly)	16.9
5	Duct, Bleed Air		4D, 15 ft	66.7
6	Duct, Bleed Air		2.5D, 12 ft	21.5
7	Heat Exchanger, Air-to-Air	1660-793-5801	2 pass	38
8	Valve, Shutoff, Ejector	1660-089-3544	1D (Butterfly)	2.2
9	Duct, Bleed Air		1D, 3 ft (Tubing)	2
10	Ejector, Compressor Air/Bleed Air		Part of No. 7	
11	Duct, Outlet, Heat Exchanger		2D, 2.5 ft	2.1
12	Valve, Pressure Regulating and Shutoff	1660-909-1473	2D (Butterfly)	6.5
13	Duct, T Section		Valve on Turbine Inlet, Part of No. 12	
14	Turbine	1660-793-6951		13.3
15	Compressor			
16	Duct, Bypass, Hot Air T Section		1.25D	0.1
17	Valve, Modulating, Anti-Ice	1660-831-5321	1.25D (Butterfly)	1.7
18	Duct, Bypass, Muff and T Section			1.1
19	Sensor, Temperature, Anti-Ice	6685-794-4951		0.12
20	Controller, Temperature	1660-805-9105		2
21	Duct, Bypass, Temperature Control		Part of No. 16	
22	Duct, Turbine Outlet		2.5D, 3 ft	3.3
23	Water Separator	1660-610-9651		3.5
24	Water Line		5/16D, 2 ft	0.05
25	Valve, Bypass, Hot Air	1600-089-3550	1.5D (Butterfly)	2.25
26	Duct, Hot Air		1.5D, 3 ft	1.6
27	Controller, Temperature	6685-115-9606		2
28	Duct, Delivery Air		3D, 12 ft	8.8
29	Sensor, Temperature	6685-211-4149		0.1
30	Switch, Limit, Temperature	5930-950-0693		0.44
31	Inlet, Ram Air		Casting	10.2
32	Diffuser, Ram Air		Casting	5.2
33	Outlet, Ram Air		Casting	7.8
34	Duct, Bypass, Ram Air		(3D, 1.5 ft) Part of No. 7	
35	Valve, Shutoff Emergency Ram Air	1660-795-2615	2.5D (Butterfly)	1.6
36	Valve, Check, Ram Air	1660-796-0243	2.5D	0.5
37	Duct, Ram Air		(3D) Part of No. 22	
38	Duct, Compressor Outlet		(2.5D, 1 ft) Part of No. 7	
39	Insulation, Duct		1/2 thick	14

GP 9416-61

Heat Exchangers - Relative costs of twenty heat exchangers are indicated in Figure 142. These values are based on costs of five FSN parts (1660-798-3183, -063-4871, -251-1097, -830-3066, and -794-9053) and costs from other sources for fifteen units. These heat exchangers are representative of fighters, fighter-bomber, and cargo aircraft. The estimated cost equation is:

$$CU = (2.08) (Wt) \quad (388)$$

This equation is representative of plate fin construction. Cost does not seem to be a strong function of material or brazing method. The data indicated in Figure 142 averages out the effects of different assembly techniques of the manufacturers.

Turbomachinery - Relative cost of ten turbomachines are represented in Figure 143. Four of these are costs of FSN parts (1660-793-6951, -135-9566, -961-6325, and -766-6147) and six represent unit costs obtained from other sources. The estimated cost equation is:

$$CU = (5.5) (Wt) \quad (389)$$

The above equation is representative of centrifugal and mixed flow wheel designs. Axial wheel designs are evaluated with the same equation although no cost data for axial components were available.

Water Separators - Relative costs of ten low pressure water separators (i.e. located downstream of the expansion turbine) are indicated in Figure 144. These costs are taken from References 68 and 69. The following parts are used: FSN's 1660-610-9651, -859-1702, -627-9136, -601-6455, -060-5514, -461-8661, -450-5208, -735-5517, -056-1394. These water separators are used in fighters, bombers, and cargo aircraft. The data show no trend for higher or lower cost according to the type of aircraft in which the water separator is used. The least mean squared equation for these costs is:

$$CU = 18.82 + (2.08) (Wt). \quad (390)$$

High pressure water separator costs are considered as heat exchanger costs. Cost for water collectors in ducts are estimated at 5 to 8 CU.

Dust Separators - Costs of static dust separators is estimated as:

$$CU = 5.4 + (0.71) (Wt). \quad (391)$$

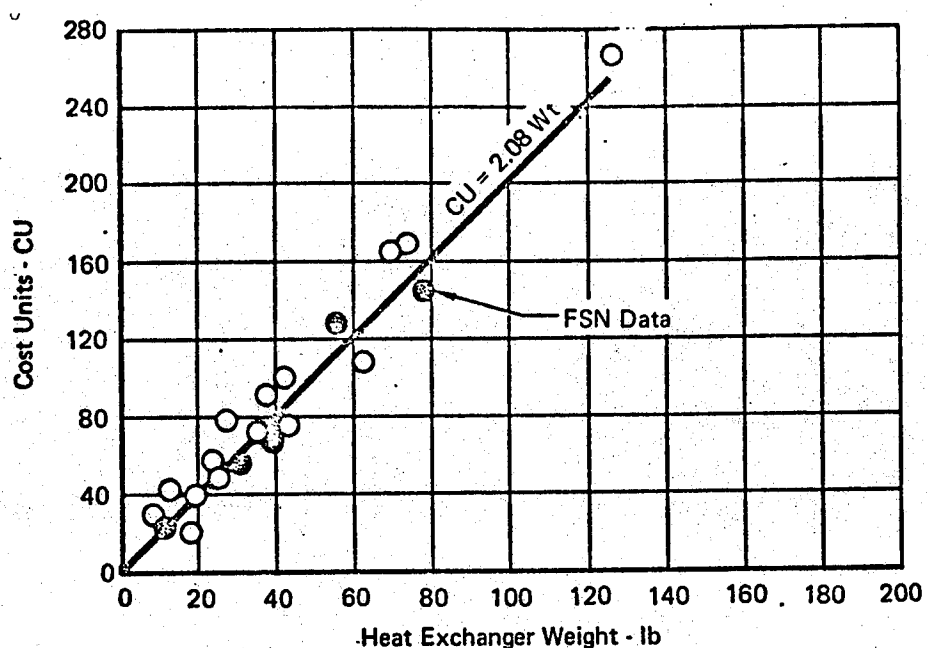


Figure 142 Heat Exchanger Costs

GP 9416-206

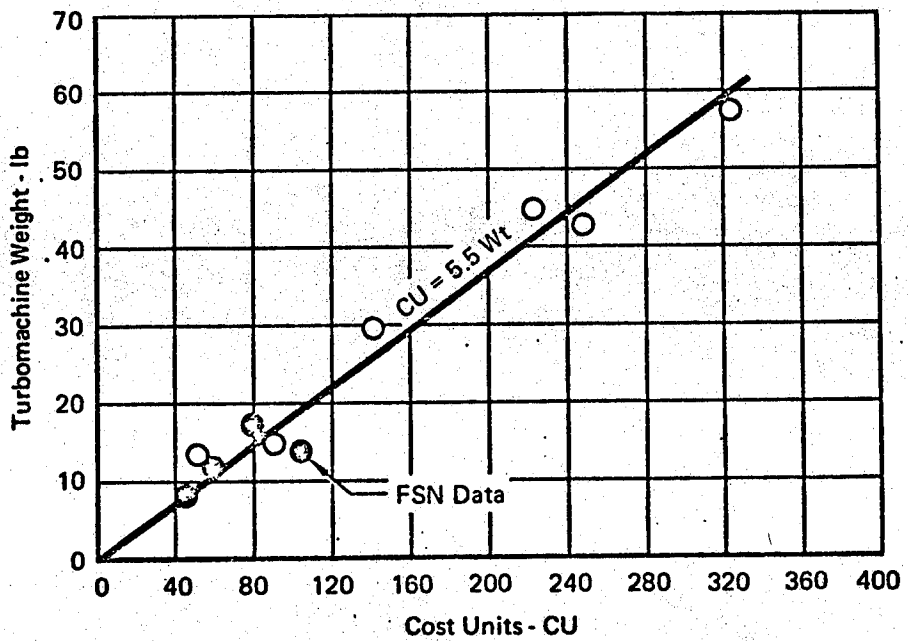
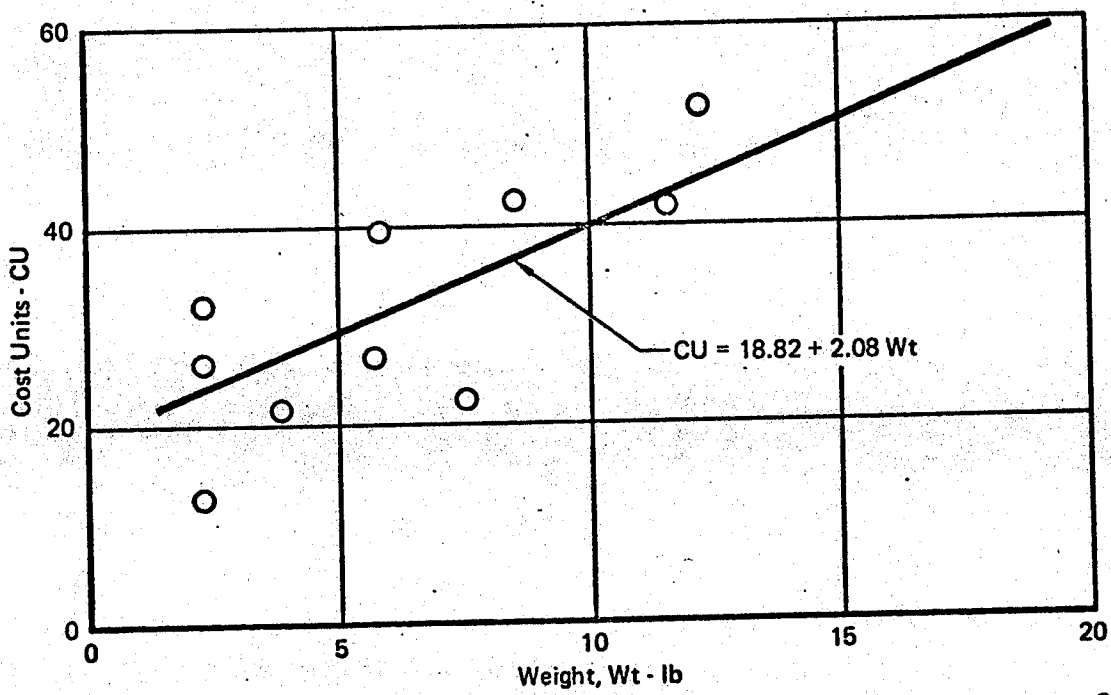


Figure 143 Turbomachinery Costs

GP 9416-207



GP 9416-59

Figure 144 Water Separator Costs

This equation is considered applicable to tee-type and rectangular shaped static filters. Costs of self-cleaning high pressure dust separators are based on rough estimates, since only a few are available. The estimated cost equation is:

$$CU = 9.11 + (1.07) (Wt). \quad (392)$$

Self-cleaning ambient dust separators are expected to have a lower cost than is indicated by this equation.

Fans - Costs of electric motor driven axial fans are shown in Figure 145. Vendor and References 68 and 69 costs are included. The following parts from the latter reference are used: FSN's 1660-564-5986, -786-2928, -788-5969, -757-4437, -116-2158, -106-0997, -717-5277, -073-9167, -051-2620, -983-1597, -099-7858, -309-1511; 1680-862-3128; and 4140-119-5855, -787-1576, -967-0027, -720-1836, -988-7329. The type of aircraft in which the fans are used is not known for all the data points shown, and the aircraft for which the application is known are cargo aircraft. The large data scatter probably are due to detail requirements beyond the scope of this study and inconsistencies in the quantity base for the cost. The least mean squared equation for the a.c. motor driven fans is:

$$CU = 14.29 + (0.46) (Wt), \quad (393)$$

and for the d.c. motor driven fans:

$$CU = 4.87 + (0.76) (Wt). \quad (394)$$

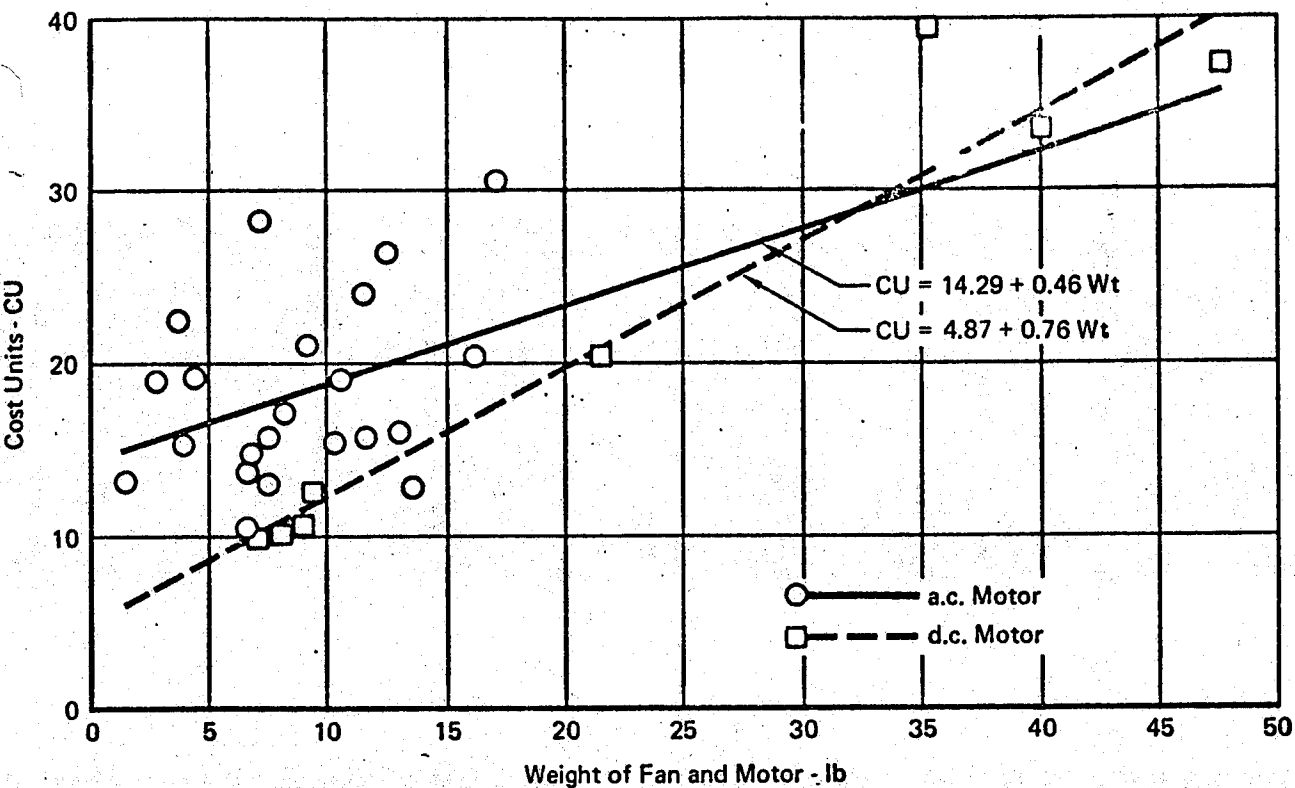


Figure 145 Axial Fan Costs

GP 9416-62

These different cost trends possibly are due to lower cost for small a.c. motor, and higher costs of large d.c. motors compared to a.c. motors.

Hydraulic motor driven fans are more expensive than electric motor driven fans on a equal fan plus motor weight basis. However, hydraulic motors are lighter than electric motors (except for the small motor sizes). Data on costs of hydraulic motor driven fans are not adequate to obtain cost trends, except that they are approximately 3-1/2 to 4 times the cost of electric motor driven fans for the same fan plus motor weight.

Pump Packages - The pump package includes a pump and motor, accumulator, filter, and miscellaneous valves (e.g., relief, temperature control, etc.). An estimated cost for pump packages is:

$$CU = 81.2 + (1.05) (Wt). \quad (395)$$

This recurring cost factor is based on a medium size unit.

Vapor Cycle Components - Costs of condensers (with an air heat sink) and of evaporators (which cool air loads) are shown in Figure 146. (Data are estimated information for commercial aircraft.) The correlating cost equation for condensers and evaporators is:

$$CU = 29.7 + (2.72) (Wt). \quad (396)$$

The estimated equation for motor driven centrifugal compressor costs is:

$$CU = 34.7 + (17.3) (Wt). \quad (397)$$

Little data are available to substantiate these cost trends. Other miscellaneous vapor cycle component costs (except controls) are approximated by:

$$CU = 14.85 + (10.9) (\text{tons}), \quad (398)$$

where (tons) is tons of refrigeration.

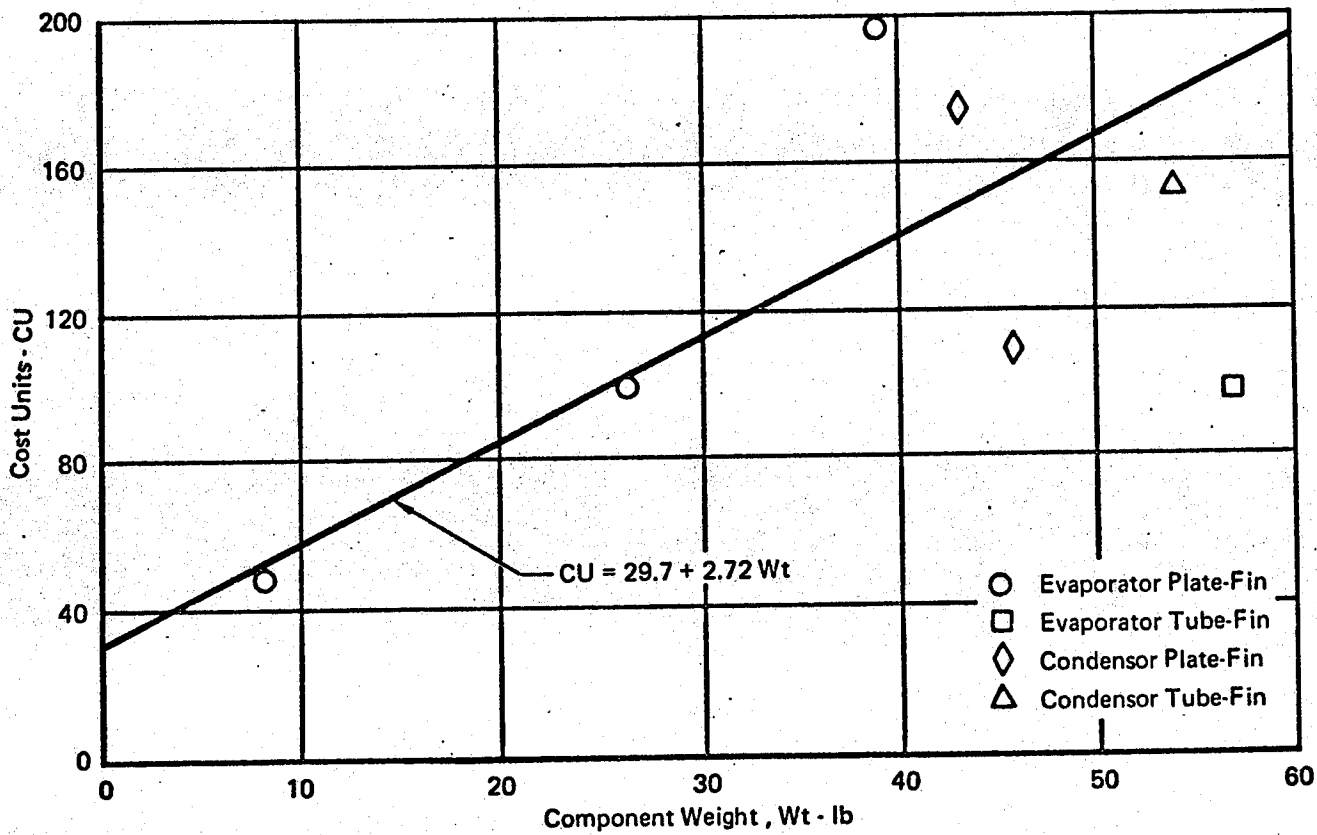


Figure 146 Air/Refrigerant Heat Exchanger Costs

GP 9416-60

Auxiliary Air Sources - The correlation of the costs of auxiliary power units is based on data for eleven APU's. (Actual costs considered are based on vendor proprietary information, hence they must be contacted for details.) The correlation equation for bare APU costs is:

$$CU = (7.3) (EHP). \quad (399)$$

Auxiliary compressor costs are estimated with Equation (389).

Power Drives - Alternating current electric motor costs are approximated by the equation:

$$CU = 4 + (0.6) (Wt), \quad (400)$$

and direct current motor costs are approximately:

$$CU = 3 + (Wt) \quad (401)$$

No costs for hydraulic motors used in ECS are available. Costs for several hydraulic motors used for other than environmental control systems (from References 68 and 69) follow the trend:

$$CU = 17 + (4.57) (Wt). \quad (402)$$

Pneumatic drive costs are estimated by Equation (389).

Ducting - High pressure bleed air ducting cost data for each diameter group in Table VII are shown in Figure 147.

$$\frac{CU}{L} = 0.103D + 0.026, D \leq 2.5 \quad (403)$$

$$\frac{CU}{L} = 0.231D - 0.295, D > 2.5 \quad (404)$$

Low pressure ducting cost data are determined for aluminum, fiberglass, and flexible rubber ducting. Actual cost data are used for a duct diameter of 1.75 inches. Standard MCAIR techniques are used to scale the data to larger duct sizes. (See Figure 148.)

Aluminum tubing -

$$\frac{CU}{L} = 0.0097D + 0.0199, D \leq 3.5 \text{ in.} \quad (405)$$

$$\frac{CU}{L} = 0.029D - 0.0477, D > 3.5 \text{ in.} \quad (406)$$

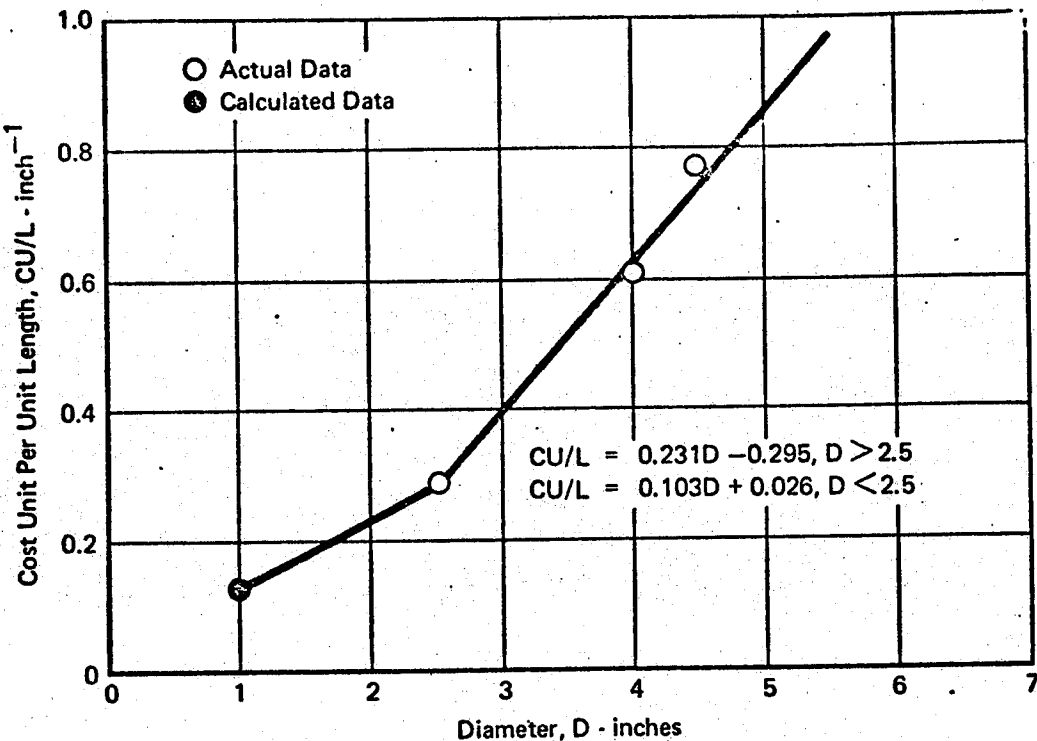


Figure 147 High Pressure Bleed Air Ducting Costs

GP 9416-201

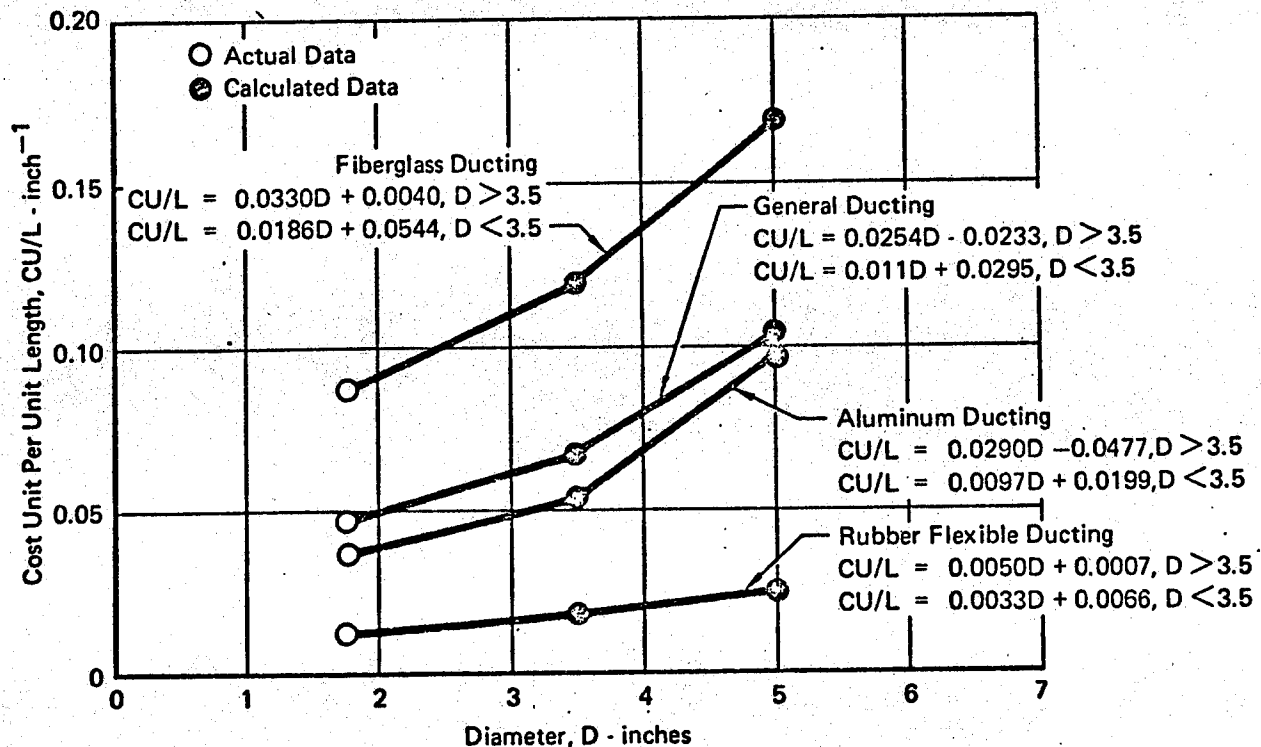


Figure 148 Low Pressure Ducting Costs

GP 9416-200

Fiberglass ducts -

$$\frac{CU}{L} = 0.0186D + 0.0544, D \leq 3.5 \text{ in.} \quad (407)$$

$$= 0.033D + 0.0040, D > 3.5 \text{ in.} \quad (408)$$

Flexible rubber ducts -

$$\frac{CU}{L} = 0.00326D + 0.00658, D \leq 3.5 \text{ in.} \quad (409)$$

$$= 0.00495D + 0.00073, D > 3.5 \text{ in.} \quad (410)$$

A typical cost of general low pressure ducting using all three types of materials is:

$$\frac{CU}{L} = 0.0110D + 0.0295, D \leq 3.5 \text{ in.} \quad (411)$$

$$= 0.0254D - 0.0233, D > 3.5 \text{ in.} \quad (412)$$

The above aluminum tubing cost equations are applicable for low and high pressure ducting made of tubing. They also are applicable for all liquid and pneumatic control lines (typical diameters are less than one inch).

Inlets, Outlets and Ejectors - Cost data for typical inlets and outlets are utilized to obtain the equation for cost estimation. The equation is:

$$CU = 13.0 + (0.139) (Wt)^{1.65} \quad (413)$$

The cost data are based on cast magnesium structures.

Cost of bleed air ejectors in a ram air circuit is the sum of outlet (mixing tube) cost, given by the above equation, and the cost of bleed air tubing assembly. The tubing assembly cost is estimated as:

$$CU = 4.96 + (5.36) (Wt)^{0.64} \quad (414)$$

Combining this equation with the one for outlet cost results in the following equation for costs of ram air circuit ejectors.

$$CU = 17.96 + (5.36) (Wt)^{0.64} + (0.139) (Wt)^{1.65} \quad (415)$$

Cost of water boiler ejector is estimated as 9.2 CU. Since the inherent size of water boiler ejectors is small, it is reasonable to assume that water boiler ejector cost is independent of size and weight. An aspirator (water injector) is included as part of a heat exchanger. Cost is included in that package.

Valves - Relative cost for butterfly valves, poppet valves, and split flapper check valves are shown in Figures 149, 150 and 151. Most cost data are from References 68 and 69. The following parts are used: FSN's 1660-684-6857, -630-5044, -664-1069, -612-3569, -089-3544, -906-9339, -529-3414, -513-4471, -670-3256, -056-9244, -486-6293, -056-9266, -305-4423, -337-4593, -887-3291, -796-0243, -627-9887, -305-4419, -794-1333, -798-0235, -326-6172; 1650-884-7571, -533-2474, -694-7461; 2995-590-9608; 2835-682-5352; 4810-760-4136; and 2995-761-2851. No cost variations due to different types of actuators and fabrication materials are apparent. The number of functions for butterfly valves does not appear to be a cost trend factor. The large data scatter probably are due to design requirements, and inconsistencies in the quantity base for the cost. The cost equations are:

Butterfly valves:

$$CU = 27.0, \text{ for } (D \text{ Wt}) \leq 17.5 \quad (416)$$

$$CU = 1.13 (D \text{ Wt})^{1.11}, \text{ for } (D \text{ Wt}) > 17.5 \quad (417)$$

Poppet valves:

$$CU = 5.4, \text{ for } (D \text{ Wt}) \leq 0.1 \quad (418)$$

$$CU = 8.4 (D \text{ Wt})^{0.192}, \text{ for } (D \text{ Wt}) > 0.1 \quad (419)$$

Split flapper check valves:

$$CU = 2.37, \text{ for } (D \text{ Wt}) \leq 0.1 \quad (420)$$

$$CU = 3.7 (D \text{ Wt})^{0.193}, \text{ for } (D \text{ Wt}) > 0.1 \quad (421)$$

Bleed Air Duct Insulation - Estimates of the cost of $1/4$ inch insulation on a 3 inch diameter bleed duct are as follows:

Type Insulation	CU
Bellows or Flex Section	0.5 to 0.75
Flange Clamp	0.2 to 0.4
90° Elbow	0.75 to 1.0
Straight (per foot)	0.25 to .5
Wye Section	2.5 to 3.0

For other duct diameters it is estimated that 15% of the above costs are proportional to weight. Insulation clamps and brackets are an additional 25% of total cost. A estimate for the costs of general bleed air duct

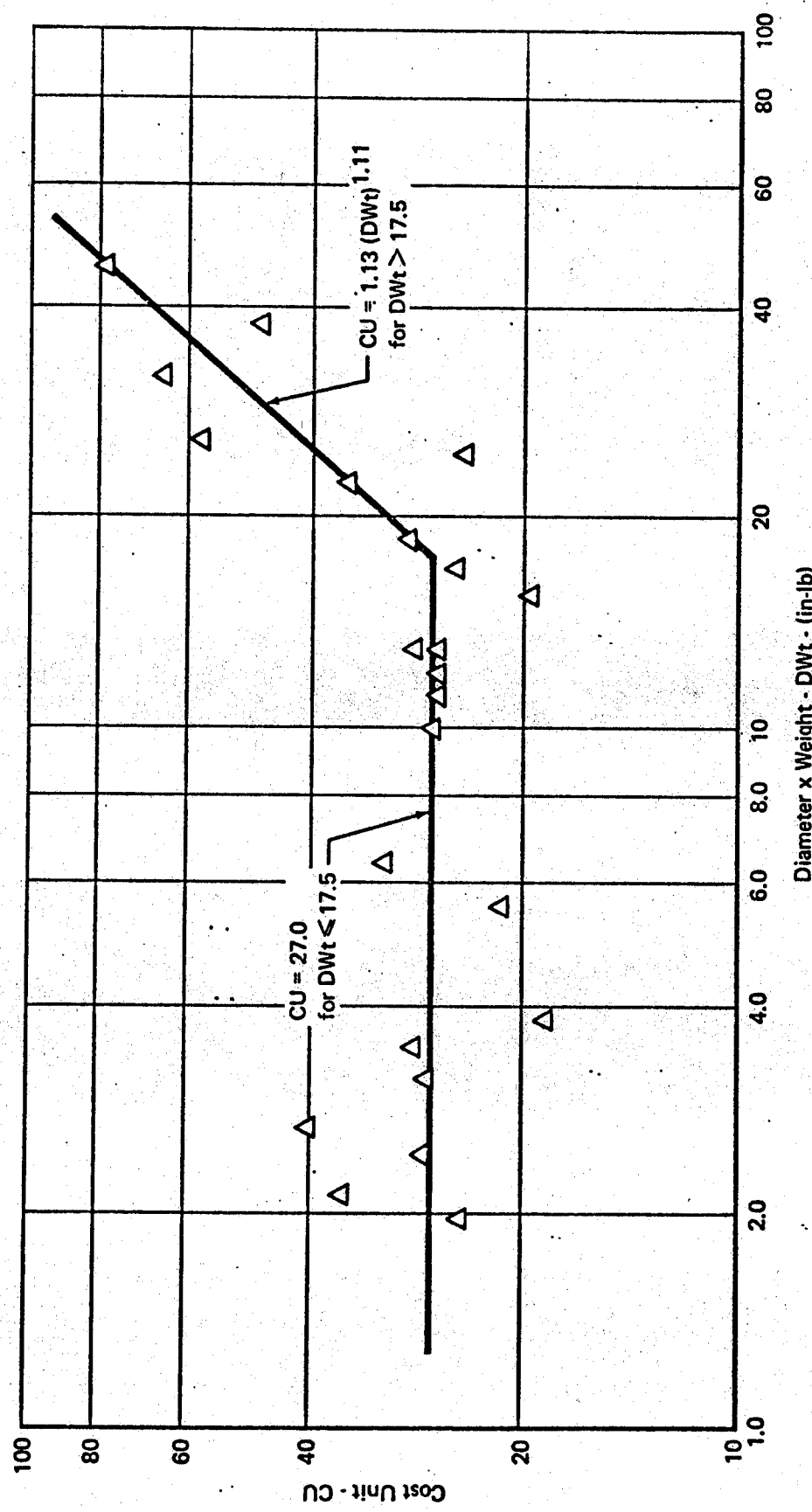


Figure 149 Butterfly Valve Costs

GP 9416-182

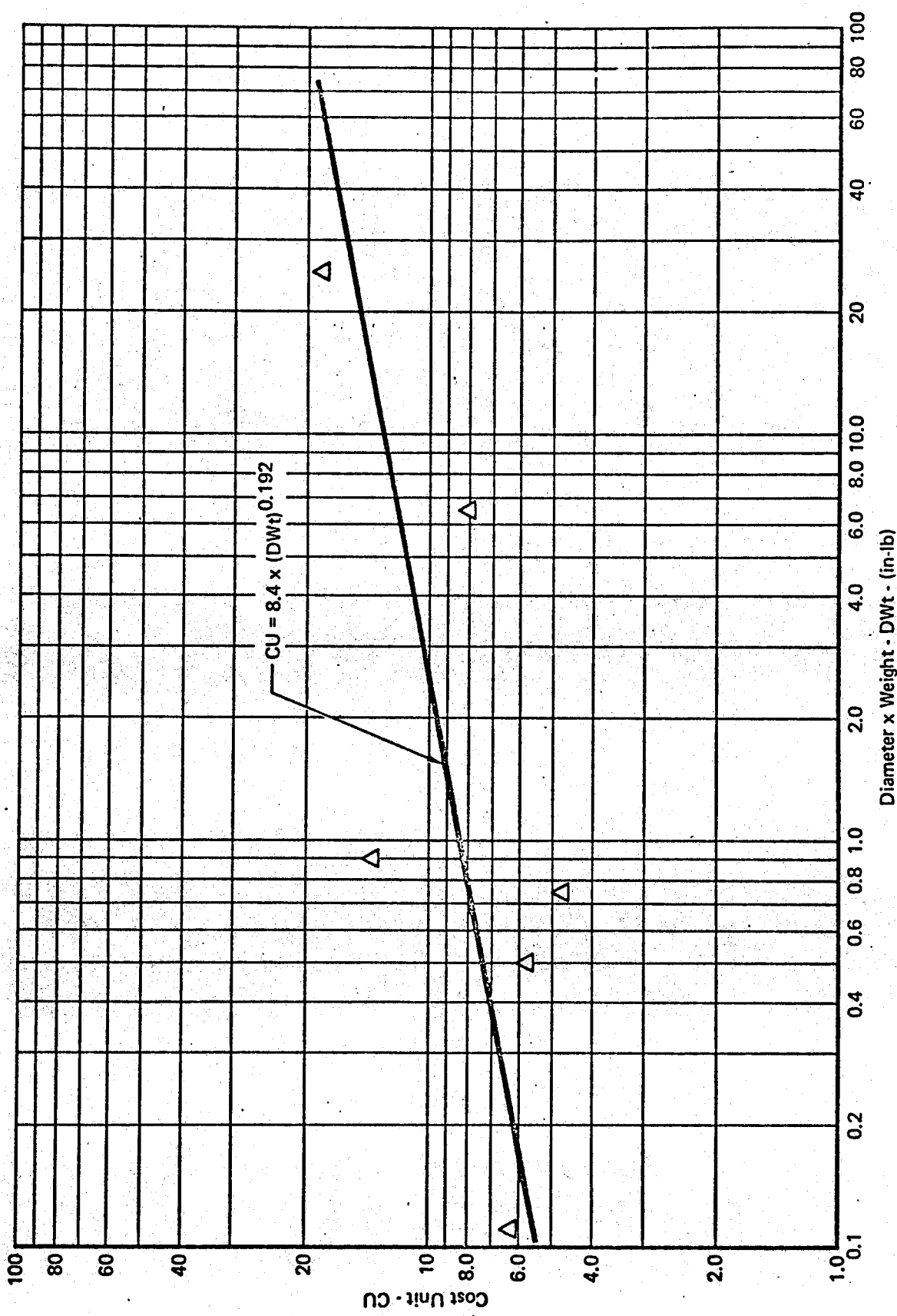


Figure 150 Poppet Valve Costs

GP 9416-180

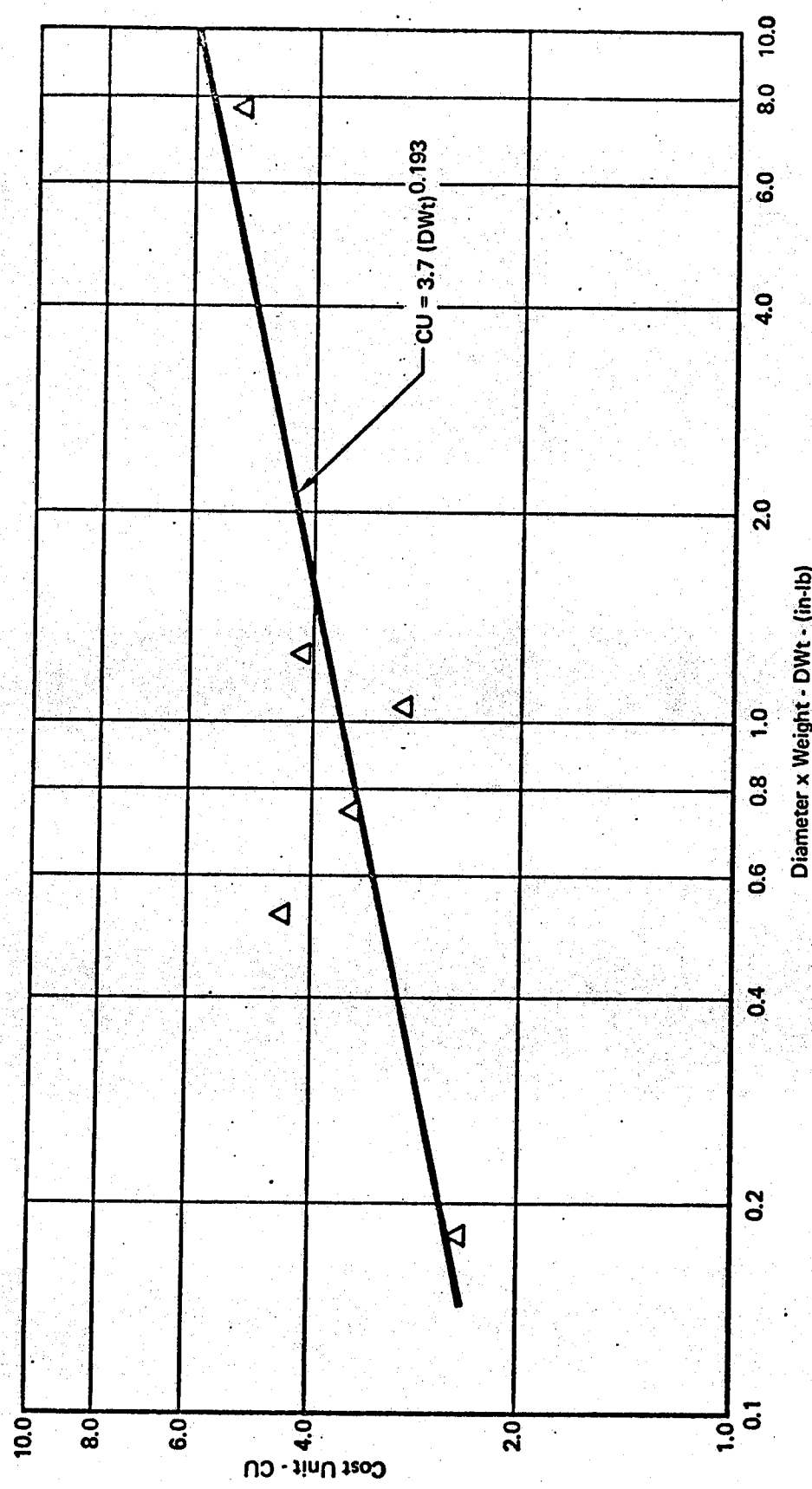


Figure 151 Split-Flapper Check Valve Costs

GP 9416-181

insulation per foot of length (L) is:

$$CU = L [0.115t(D+t) + 0.531] \quad (422)$$

Compartment Insulation - The primary cost of small insulation blankets is the fabrication cost to put the insulation batting into shapes, with covers, for handling. The costs of small insulation blankets (approximately 1 ft²) is estimated as 0.109 CU. Cost of larger blankets (approximately 4 ft²) is dependent on blanket thickness also:

$$CU = 0.10 + 0.0114t \quad (423)$$

Control Systems - Costs of temperature control systems depend on the type of control used (i.e. pneumatic or electronic) and the type of aircraft in which they are used. Proportional pneumatic temperature control system costs for control heads are:

$$CU/lb = 4.95; \quad (424)$$

and for sensors:

$$CU/lb = 17.3, \text{ (which is based on 0.5 lb sensors).} \quad (425)$$

Components used in fighter and cargo aircraft are considered for these costs.

Electronic temperature control system costs depend on the number of inputs and outputs (NIAO) of the controls. Table XVI shows costs of several temperature control components. Electronic temperature controls are cheaper for fighter/light bomber aircraft compared to heavy bomber/cargo aircraft, as is shown by the following correlations:

$$CU/lb = 14.6 + (0.545)(NIAO) \quad 426
(for fighter/light bomber aircraft)$$

and:

$$CU/lb = 14.85 + (1.04)(NIAO) \quad 427
(for heavy bomber/cargo aircraft)$$

Table XVI Temperature Control Component Costs

Component	Aircraft									
	Fighter A		Fighter B		Cargo A		Cargo B		Cargo C	
	Weight (Lb)	Cost Units								
Controller	2.5	13.37	3.32	46.90	2.40	55.9	2.20	79.20	3.8	74.30
Selector	0.6	9.16	0.60	5.45	0.50	17.1	0.19	8.17	0.6	7.43
Sensor*	0.2	2.57	0.40	9.90	0.45	22.8	0.45	23.80	0.5	19.10

*Based on two sensors.

GP 9418-119

The temperature control system costs are directly proportional to the Technical Weighting Factor (K_{Te}) and the Requirements Weighting Factor (K_{Re}). Typical values for these factors are shown in Table XI.

A relative cost comparison trend of the controller, sensors, and valves of three types of temperature systems for heavy bomber/cargo aircraft is:

Electronic = 1.00

Electro-pneumatic = 1.03

Integral pneumatic = 1.045

Note that this comparison includes an integral pneumatic control, which is different from the proportional pneumatic control discussed above.

Pneumatic pressure controls for compartments are typically used in fighter and light bomber aircraft. These control systems provide a fixed isobaric schedule. The cost of these pneumatic pressure control systems (controller, outflow valve, and safety valve) is essentially constant at 49.5 CU.

Heavy bomber and cargo aircraft normally use a variable isobaric compartment pressure control system. Table XVII shows cost data on five cargo aircraft pressure control systems. The cost estimate for variable isobaric pressure control systems is related to the flow rate:

$$CU/lb = 6.45 + 0.0176W.$$

(428)

This cost applies to pneumatic, electro-pneumatic, and electronic pressure controls. It includes the controller, outflow valve, safety valve, selector, and sensors.

Table XVII Cargo Aircraft Pressure Control System Costs

	Aircraft									
	A		B		C		D		E	
Flow Rate (lb/min)	500		140		220		450		220	
Type System	Electronic		Electro-pneumatic		Pneumatic		Electronic		Electro-pneumatic	
Component	Weight (lb)	Cost Units	Weight (lb)	Cost Units	Weight (lb)	Cost Units	Weight (lb)	Cost Units	Weight (lb)	Cost Units
Controller	3		10.5	221			13.7			
Out Flow Valve Assy	66		43.0	282			83.0			
Safety Valve*	16		12.0	91			16.8			
Total System	115	1490	65.5	594	40.2	248	113.5	1490	62	891

*Safety valves are all pneumatic

GP 9416-95

Temperature control systems for a vapor cycle, or of an electronic 35°F water separator anti-ice control are considered as having the same cost as the previously discussed electronic temperature controls. The previously discussed pneumatic temperature control cost are adequate for pneumatic water separator anti-ice controls which: (1) provide 35°F inlet temperatures, (2) control to the pressure drop across a screen, and (3) control to a reference pressure at the water separator outlet.

The use of built-in-test-equipment (BITE) increases the cost of temperature control systems by 10% and of pressure controls by 4%.

Example of System Relative Cost - An example of computing the relative cost of the bootstrap air cycle ECS of the C-9A Aeromedical Transport is presented in Volume II.

4.3.3 Logistic Cost Factors - A Logistic Cost Factor (LCF) encompasses those ECS costs which occur after aircraft delivery. The total ECS logistic support costs include costs of spare parts, maintenance costs, costs for repairing the ECS at several levels, costs of ground support equipment for the ECS, costs of special tools and facilities for maintenance and repair of the ECS, and costs to prepare technical data describing the maintenance and repair procedures. Logistic cost factors of an environmental control system are an important part of the total ECS cost. The determination of relative logistic cost factors is a lengthy and complex process. Hence, a brief discussion of one aspect of the LCF - maintenance manhours per flight hour - is presented.

Examination of available maintenance data indicates that similar ECS configurations installed in the same series of aircraft exhibit large variations in maintenance penalties. One factor is that the same series of aircraft are used for different primary missions. In addition to the variable operational characteristics imposed on the ECS by these different primary missions, a variety of geographical environments are encountered.

The development of Logistic Cost Factors is considered as a desirable factor to be used in evaluating aircraft ECS. Development of LCF for environmental control systems should consider the physical, operational, and environmental characteristics of the ECS. The importance of the ECS to total aircraft operations is shown by USAF data for the F-4D/E aircraft. During 1969, the ECS of the F-4D/E aircraft was the highest single contributor to the inflight abort rate.

Detailed historical maintenance data are required to assess the maintenance penalty properly. The use of maintenance manhours per flight hour as a maintenance penalty is not necessarily a true assessment of maintenance requirements. For example, maintainability penalties such as accessibility, removals to facilitate other maintenance, or checks with no defects are results of peculiar installation designs, troubleshooting procedures, etc. These factors preclude a true assessment of maintenance costs, and should be included when historical maintenance data are evaluated.

Historical data for the total ECS and the auxiliary systems to which the ECS provides pressurized air are summarized for some fighter, cargo, and commercial aircraft. The total ECS maintenance manhours per 1000 flight hours (MMH/1000 FH) for seven fighters varies from 198 to 938, with an average of 400. Maintenance data on bomber aircraft is not readily available. The total

ECS MMH/1000 FH for four cargo aircraft varies from 85 to 288, with an average of 188. The total ECS MMH/1000 FH for four commercial aircraft varies from 35 to 110, with an average of 70. The above data show an expected trend: reduction in the severity of the aircraft operational environment decreases the maintenance penalty.

Data for three components of fighter ECS also are presented. The MMH/1000 FH for the air cycle machines varies from 2.7 to 116.3, with an average of 24.7; and for the heat exchangers the MMH/1000FH varies from 0.07 to 12.3, with an average of 3. The average MMH/1000 FH for three fighter water separators (which must be checked regularly for clogging) is 47.3.

The average MMH/1000 FH of these same three components of cargo and commercial aircraft shown a different trend. The average MMH/1000 FH of these components of cargo aircraft are: air cycle machines = 8; heat exchangers = 2.7; and water separators = 7.3. The average MMH/1000 FH of these components of commercial aircraft are: turbomachines (air cycle and vapor cycle) = 7.3; heat exchangers = 4.7; and water separators = 3. As expected, the dynamic components require more maintenance.

The use of environmental control system logistic cost factors is an important part of the total ECS cost. Valid determinations of the LCF requires further evaluations of the detailed design and operational characteristics of the individual ECS. The development of ECS logistic cost factors is recommended as a study area for future efforts.

SECTION 5

REFERENCES

1. "Development of Integrated Environmental Control System Designs for Aircraft, Oral Presentation: System Schematics and Controls," MDC Report A0470, 3 June 1970.
2. Krantweiss, G., "Survey of Aircraft Thermal Control Systems," AFFDL-TR-66-44, November 1966.
3. MIL-E-38453 (USAF), "General Specification for Aircraft and Aircraft Launched Missiles. Environmental Control, Environmental Protection, and Engine Bleed Air Systems," 9 September 1966 and Amendment 1, 4 May 1967.
4. Diaguila, A. J. and Livingood, J. N. B., "Rapid Determination of Core Dimensions of Crossflow Gas-to-Gas Heat Exchangers," NACA TN 3891, 1956.
5. Shah, R. K. and London, A. L., "Offset Rectangular Plate-Fin Surfaces -- Heat Transfer and Flow Friction Characteristics" Stanford University Technical Report No. 66, 1 September 1967.
6. U.S. Naval Air Development Center, "Design Manual for Methods of Cooling Electronic Equipment," NAVWEPS 16-1-532, February 1965.
7. "Design Manual for Heat Exchangers," United Aircraft Products, Inc.
8. "Heat Exchanger/Water Separator Catalog," Hamilton Standard B213.
9. "Plate and Fin Heat Exchanger Design," Hamilton Standard.
10. Kays, W. M. and London, A. L., Compact Heat Exchangers, McGraw-Hill, 2nd ed., 1964.
11. Shepherd, D. G., Principles of Turbomachinery, The Macmillan Company, 1956.
12. Balje, O. E., "A Study on Design Criteria and Matching of Turbomachines, Part A and Part B," Journal of Engineering for Power, January 1962, pp. 83 through 114.
13. Balje, O. E., "Turbine Performance Prediction: Optimization Using Fluid Dynamic Criteria," Rocketdyne Report R-6805, 1 December 1966.
14. Rosenberg, H. N., Coombs, M. G., and Stockwell, G., "Thermal Control of Pod-Mounted Electronic Systems," AFFDL-TR-70-19, Volume I, Part I, March 1970.
15. Rohlik, H. E., "Analytical Determination of Radial Inflow Turbine Design Geometry for Maximum Efficiency," NASA TN D-4384, February 1968.
16. Wood, H. J., "Current Technology of Radial-inflow Turbines for Compressible Fluids," Transactions of ASME, January, 1963, pp. 72 through 83.

17. Hasinger, S., "Water-Mist Separation in Cabin Air Conditioning Systems," WADC TR 53-324, November 1953.
18. MIL-STD-21CA, "Climatic Extremes for Military Equipment," 30 November 1958.
19. Guzdar, A. R., Harvey, A. C., and Erickson, A. J., "Development of An Improved Water Separator for Use in Aircraft Having An Air Cycle Refrigeration System," AFFDL-TR-69-13, May 1969.
20. "Air-Moisture Separators," Stratos Division
21. "Air Conditioning and Heat Transfer Equipment," AiResearch Manufacturing Company Catalog.
22. MIL-A-83116 (USAF), "Air Conditioning Subsystems, Air Cycle, Aircraft and Aircraft-Launched Missiles, General Specification For," 3 February 1969.
23. Aircraft Porous Media, Inc., "Tee-Type Filter Assemblies," Bulletin A4A.
24. Farr Company, "F/S Air Filter," Bulletin B-1302-1A
25. Pinchak, A. C., "A Review of the State of the Art of Cyclone-Type Separators," ARL 67-0047, March 1967.
26. Brookman, R. S., Phillipi, J. L., and Maisch, C. L., "Small-Diameter Cyclones," Chemical Engineering Progress, November 1963, Vol. 59, No. 11, pp. 66-69.
27. Thomas, G. E., "Effectiveness of an Inertial Air Cleaner in Extending Gas Turbine Life In a Dusty Environment," Southwest Research Institute AR643, March 1968.
28. Kawa, M. M., "Development of Particle Separator Engine Air Induction System for the OH-58A Light Observation Helicopter," Ninth Annual National Conference on Environmental Effects on Aircraft and Propulsion Systems, 1 September 1969.
29. Stephenson, C. D. and Shohet, H. N., "CH-54A Engine Inlet Air Particle Separator," AHS Paper 117, May 1967.
30. SAE Aerospace Applied Thermodynamics Manual, Society of Automotive Engineers, 2nd ed., 1969.
31. "Vaneaxial Flow Blowers," Dynamic Air Engineering, Inc.
32. "Fans for Airborne and Ground Equipment Applications," AiResearch Manufacturing Company.
33. "Aircraft and Electronic Fans," Joy Manufacturing Company.

4. "Turbomachinery Catalog," Task Corporation.
5. "Coolant Pumps for Various Fluids," Catalog 6068, Hydro-Aire Division.
6. "Heat Transfer Systems and Related Components for Cooling Electronics," Report Number 69-5353, The Garrett Corporation.
7. Martin, J. J., "Thermodynamic Properties of Dichloretetrafluorethane," Journal of Chemical and Engineering Data, Vol. 5, No. 3, pp. 334-336, 1960.
8. "Thermodynamic Properties of "Freon-11" Refrigerant," E. I. duPont de Nemours and Company, Wilmington, Delaware, 1965.
9. Martin, J. J., "Correlations and Equations Used in Calculating the Thermodynamic Properties of Freon Refrigerants", ASME Symposium on Thermal Properties, Thermodynamic and Transport Properties of Gases, Liquids and Solids, pp. 110-122, 1959.
10. Nicholls, B. H., "Auxiliary Power System Study for 1975 Fighter Aircraft," AFAPL-TR-67-135, January 1968.
11. Lee, C. H. and Chirgwin, K. M., "Investigation and Development of New Concepts for Improvement of Aircraft Electrical Power Systems," AiResearch Manufacturing Division Report 68-4176.
12. Arinuskkin, L. S., Abramovich, R. B., et.al., "Aircraft Centrifugal Pump Units," USAF (FTD) - MT-24-407-68, 1967.
13. "Aerospace Fixed Displacement Piston Type Hydraulic Motors," Bulletin A-5205-B, Vickers Incorporated.
14. "Hydraulic Motor Curves," Abex Corporation.
15. "Hydraulic Product Line," Hydro-Aire Division
16. MIL-B-81365(WP) "General Specification for Bleed Air Systems," 4 April 1966.
17. Binder, R. C., Fluid Mechanics, Prentice-Hall, Inc., 4th ed., 1962.
18. "Flow of Fluids through Valves, Fittings, and Pipes" Technical Paper No. 410, Crane Company, 1965.
19. Simon, P. C., and Kowalski, K. L., "Charts of Boundary-Layer Mass Flow and Momentum for Inlet Performance Analysis, Mach Number Range, 0.2 to 5.0," NACA TN 3583, November 1955.
20. Dennard, J. S., "The Total Pressure Recovery and Drag Characteristics of Several Auxiliary Inlets at Transonic Speeds," NASA Memo 12-21-58L.
21. Shatzer, W. T., et.al, "Cooling System Study for Supersonic Bomber," WADC TR 57-68, February 1969.

Unclassified
Security Classification

DOCUMENT CONTROL DATA - R & D

(Security classification of title, body of abstract and indexing annotation must be entered when the overall report is classified)

ORIGINATING ACTIVITY (Corporate author)

McDonnell Aircraft Company
St. Louis, Missouri

2a. REPORT SECURITY CLASSIFICATION

Unclassified

2b. GROUP

N/A

3 REPORT TITLE

Development of Integrated Environmental Control System Designs for Aircraft
Volume I, ECS Design

4. DESCRIPTIVE NOTES (Type of report and inclusive dates)

Final Report March 1970 - January 1972

5. AUTHOR(S) (First name, middle initial, last name)

Richard R. Dieckmann
Alvin C. Watson
Sherril F. Glover

6. REPORT DATE

May 1972

7a. TOTAL NO. OF PAGES

319

7b. NO. OF REFS

69

8a. CONTRACT OR GRANT NO.

F33615-70-C-1235

9a. ORIGINATOR'S REPORT NUMBER(S)

b. PROJECT NO.

6146

9b. OTHER REPORT NO(S) (Any other numbers that may be assigned
this report)

c.

AFFDL-TR-72-9, Volume I

d.

10. DISTRIBUTION STATEMENT

Distribution limited to U.S. Government agencies only; test and evaluation; statement applied April 1972. Other requests for this document must be referred to Air Force Flight Dynamics Laboratory (FEE), Wright-Patterson Air Force Base, Ohio 45433

11. SUPPLEMENTARY NOTES

None

12. SPONSORING MILITARY ACTIVITY

Air Force Flight Dynamics Laboratory (FEE)
Air Force Systems Command
Wright-Patterson AFB, Ohio 45433

13. ABSTRACT

This report presents the results of a study of environmental control system (ECS) designs for aircraft. The study was performed for the Air Force Flight Dynamics Laboratory. ECS design information is presented for arrangements of components which make up the systems, for performance of the components of the systems, and for penalty factors incurred by an aircraft using these systems. Ten system arrangements for simple and bootstrap air cycles and vapor cycles are presented. Subsystems which are common to many of these systems are discussed. Typical performances of the many components utilized by these systems are presented. Penalty factors of weight, volume, and relative reliability and cost of these components are related to the design features of these system components.

The ECS design information presented in this volume is included in the digital computer program described in Volume II. The ECS Computer Program will provide system performance, sizing, and penalty factor information. Volume II includes sample problems for the rough performance and sizing analyses of three Air Force aircraft, and the detailed performance and sizing of one Air Force aircraft. Volume III is the IECS Computer Program Users Manual. It contains a complete description of sample problems for rough performance and sizing analyses, and detailed performance analysis. Volume IV presents the laboratory demonstration ECS setup and results, and the computer program setup and results of detailed performance and sizing analyses to represent this ECS.

KEY WORDS	LINK A		LINK B		LINK C	
	ROLE	WT	ROLE	WT	ROLE	WT
Aircraft Equipment Air Conditioning Equipment Environmental Control Systems Cooling Systems Heat Exchangers Turbomachinery Centrifugal Compressors Water Separators Dust Filters Fans Liquid Cooling Coolant Pumps Evaporators Refrigerant Condensers Refrigerant Compressors Auxiliary Power Units Electric Motors Hydraulic Motors Ducts Butterfly Valves Poppet Valves Check Valves Inlets Outlets Ejectors Insulation Pneumatic Temperature Control Electronic Temperature Control Pressure Control Reliability						